

AMES

NASA Contractor Report 177343 - Vol - 2

Propulsion and Airframe Aerodynamic Interactions of Supersonic V/STOL Configurations

Volume II: Wind Tunnel Test Force and Moment Data Report

D.E. Zilz

**CONTRACT NAS2-10791
SEPTEMBER 1985**

(NASA-CR-177343-Vol-2) PROPULSION AND
AIRFRAME AERODYNAMIC INTERACTIONS OF
SUPERSONIC V/STOL CONFIGURATIONS. VOLUME 2:
WIND TUNNEL TEST FORCE AND MOMENT DATA
REPORT (McDonnell Aircraft Co.) 328 p

N88-22867

Unclas
G3/C2 0142915

Date for general release: August 1987.

NASA

NASA Contractor Report 177343

Propulsion and Airframe Aerodynamic Interactions of Supersonic V/STOL Configurations

Volume II: Wind Tunnel Test Force and Moment Data Report

D.E. Zilz
McDonnell Aircraft Company
St. Louis, Missouri



Prepared for
Ames Research Center
under Contract NAS2-10791
September 1985



National Aeronautics and
Space Administration

Ames Research Center
Moffett Field, California 94035

FORWORD

This report was prepared by McDonnell Aircraft Company (MCAIR), a component of McDonnell Douglas Corporation, St. Louis, Missouri, for the National Aeronautics and Space Administration, Ames Research Center. The study was performed under NASA Contract NAS2-10791, "Propulsion and Airframe Aerodynamic Interactions of Supersonic V/STOL Configurations". The work was performed from October 1980 through September 1985 with R. O. Bailey as the NASA ARC Technical Representative. The program was accomplished under the direction of P. E. Hiley, Program Manager and H. W. Wallace, Technical Study Manager.

Acknowledgement is also given to S. C. Smith and J. B. Gustie of NASA ARC for their efforts during the calibrations, wind tunnel tests, and data analysis at the NASA ARC Unitary Plan 11-Foot Transonic Wind Tunnel.

This report was prepared by D. E. Zilz of MCAIR. The author is indebted to the following MCAIR personnel for their assistance during the study: M. R. Mraz, P. A. Devereaux, A. V. Arena, and M. E. Booher of Propulsion and Thermodynamics.

The author also commends J. C. Poole, W. Cerski, and C. C. Smithson of the MCAIR Aerodynamics and Propulsion Laboratories for their efforts in the design and testing of the wind tunnel models.

Special acknowledgements are also due K. H. Token and D. W. Esker of MCAIR (Propulsion and Thermodynamics), who, in their supervisory positions, have made valuable contributions to the program and this report.

This report was submitted in four volumes by the authors in September 1985.

PRECEDING PAGE BLANK NOT FILMED

TABLE OF CONTENTS

| <u>Section</u> | | <u>Page</u> |
|----------------|---|-------------|
| 1. | INTRODUCTION | 1 |
| 2. | TEST ARTICLE DESCRIPTION | 4 |
| 2.1 | TEST MODES | 11 |
| 2.1.1 | Common Model Support System and Metric Arrangement | 12 |
| 2.1.2 | CMAPS Mode | 18 |
| 2.1.3 | Jet-Effects Mode | 22 |
| 2.1.4 | Flow-Through Mode | 22 |
| 2.2 | INLET/EXHAUST SYSTEMS | 26 |
| 2.2.1 | Inlet Systems | 26 |
| 2.2.2 | Exhaust Systems | 29 |
| 2.3 | TEST CONFIGURATIONS | 30 |
| 2.3.1 | Common Baseline Configuration | 31 |
| 2.3.2 | Nozzle Extension Configuration | 33 |
| 2.3.3 | Nozzle Extension Baseline Configuration | 33 |
| 2.3.4 | Simulated Aircraft Configuration | 34 |
| 3. | FACILITIES, INSTRUMENTATION AND DATA REDUCTION PROCEDURES | 35 |
| 3.1 | FACILITY | 35 |
| 3.2 | INSTRUMENTATION | 35 |
| 3.2.1 | Force and Moment Balance and Thermal Control System | 37 |
| 3.2.2 | Model Pressure Instrumentation | 40 |
| 3.2.2.1 | ALBEN Surface Static Pressures | 42 |
| 3.2.2.2 | Seal and Cavity Pressures | 42 |
| 3.2.2.3 | Model Total Pressure Instrumentation | 43 |
| 3.2.2.4 | Internal Nozzle Static Pressures | 46 |
| 3.2.3 | Model Temperature Instrumentation | 46 |
| 3.2.4 | Miscellaneous Instrumentation | 46 |
| 3.2.5 | Facility/CMAPS Instrumentation | 48 |

TABLE OF CONTENTS (Concluded)

| <u>Section</u> | <u>Page</u> |
|---|-------------|
| 3.3 CALIBRATIONS | 50 |
| 3.3.1 Force Balance Calibrations | 50 |
| 3.3.2 Airflow Calibrations | 57 |
| 3.4 DATA REDUCTION PROCEDURES | 60 |
| 3.4.1 Inlet Airflow Calculation | 60 |
| 3.4.2 Inlet Stream Thrust and Ram Drag | 62 |
| 3.4.3 Force Balance Data Reduction | 62 |
| 3.4.4 Nozzle Pressure Ratio Calculation | 62 |
| 4. REFERENCES | 68 |
| APPENDIX A WIND TUNNEL TEST RESULTS: FORCE AND MOMENT DATA | 70 |
| A.1 ANGLE-OF-ATTACK SWEEPS | 70 |
| A.2 NPR SWEEPS | 74 |
| A.3 CANARD ROOT BENDING MOMENT | 75 |
| APPENDIX B TEST MATRICES | 77 |
| APPENDIX C DATA REDUCTION PROCEDURE | 78 |

LIST OF ILLUSTRATIONS

| <u>Figure</u> | | <u>Page</u> |
|---------------|--|-------------|
| 1-1 | Compact Multimission Aircraft Propulsion Simulator (CMAPS) | 1 |
| 1-2 | Aerodynamic Characteristics of Study Concepts . . . | 3 |
| 2-1 | Air-to-Air Model Installed on NASA-Ames Transonic Wind Tunnel | 4 |
| 2-2 | Test Model Characteristics | 5 |
| 2-3 | Common Support System and Metric Arrangement . . . | 6 |
| 2-4 | Comparison of Test Configurations | 7 |
| 2-5 | Canard Geometric Description | 8 |
| 2-6 | Wing Geometry Description | 9 |
| 2-7 | Vertical Tail Geometric Description | 10 |
| 2-8 | Inlet/Nozzle Combinations Tested in Each Mode . . . | 10 |
| 2-9 | Interchangeable Nacelle Core Hardware | 11 |
| 2-10 | Core Support Hardware | 12 |
| 2-11 | Model Installation in NASA/Ames Eleven-by-Eleven Foot Unitary Plan Wind Tunnel | 13 |
| 2-12 | Model Support Sting | 14 |
| 2-13 | Core Hardware | 15 |
| 2-14 | Core Hardware with Simulator | 16 |
| 2-15 | Core Hardware with Flow-Through Duct | 16 |
| 2-16 | Core Hardware on Sting | 17 |
| 2-17 | Metric Seal Arrangement | 18 |
| 2-18 | Propulsion Simulator Installed in Left Hand Engine Nacelle | 19 |
| 2-19 | CMAPS Instrumentation Planes | 19 |
| 2-20 | CMAPS Model Nacelle Core Hardware | 20 |
| 2-21 | Simulator Internal Flow Paths | 21 |

LIST OF ILLUSTRATIONS (Continued)

| <u>Figure</u> | | <u>Page</u> |
|---------------|---|-------------|
| 2-22 | Jet-Effects Mode Nacelle Core Hardware | 23 |
| 2-23 | Flow-Through Mode Nacelle Core Hardware | 24 |
| 2-24 | Flow-Through Mode with Nozzle Extensions Internal Flow Path and Exit Chokes | 25 |
| 2-25 | Ejector Apparatus Connected to Nozzle Extensions . | 26 |
| 2-26 | Flowing Inlet System with 0° Cowl Lip Rotation . . | 27 |
| 2-27 | Flowing Inlet System with 45° Cowl Lip Rotation . . | 27 |
| 2-28 | Faired Inlet System on Test Vehicle | 28 |
| 2-29 | Untested Inlet for Alternate Configuration | 29 |
| 2-30 | Unvectored A/B ALBEN System on Test Vehicle | 30 |
| 2-31 | Nozzle Extension System on Test Vehicle | 31 |
| 2-32 | Test Summary | 32 |
| 2-33 | Nozzle Extension Configuration with Wing Flaps Deflected 30° | 33 |
| 3-1 | NASA-Ames Unitary Plan Wind Tunnels | 36 |
| 3-2 | Instrumentation Requirements Jet-Effects and Flow- Through Model Configuration | 37 |
| 3-3 | Model Balance | 38 |
| 3-4 | Balance Thermal Control System | 39 |
| 3-5 | Heater Blanket Power Density | 40 |
| 3-6 | Location of Model External Pressure Instrumen- tation | 41 |
| 3-7 | Fuselage Interior | 42 |
| 3-8 | ALBEN External Pressure Instrumentation | 43 |
| 3-9 | Location of Aft Metric Break Seal Pressure Instrumentation | 44 |
| 3-10 | Location of Cavity Pressure Instrumentation | 44 |

LIST OF ILLUSTRATIONS (Continued)

| <u>Figure</u> | | <u>Page</u> |
|---------------|--|-------------|
| 3-11 | Location of Model Total Pressure Instrumentation . | 45 |
| 3-12 | Location of Flow-Through Choke Throat Static Pressure Instrumentation | 47 |
| 3-13 | Simulator Instrumentation Summary | 49 |
| 3-14 | Isolated Balance Loading Schedule | 50 |
| 3-15 | Installed Balance Loading Fixture | 51 |
| 3-16 | Pressurized Inlet Duct Seal Calibration Setup . . . | 52 |
| 3-17 | Installation and Inlet Duct Seal Pressurization Corrections to Aircraft Balance in Axial Direction | 53 |
| 3-18 | Duct Seal Pressure Effect on Balance, Simulator Mode | 54 |
| 3-19 | Duct Seal Pressure Effect on Balance, Conventional Mode | 54 |
| 3-20 | Definition of Balance Output Correction Terms Due to Installation Effects | 55 |
| 3-21 | CMAPS Inlet Airflow Calibration Set-Up | 57 |
| 3-22 | MCAIR Mass Flow Calibration Facility (MFCF) | 58 |
| 3-23 | Instrumentation Used with Choke/ALBEN Calibration . | 59 |
| 3-24 | Calibration Installation and Instrumentation . . . | 60 |
| 3-25 | Typical CMAPS Operating Map In Terms of Turbine Discharge Pressure | 61 |
| 3-26 | Example of Inlet Stream Thrust, Ram Drag, and MFR Calculations | 63 |
| 3-27 | Variation of Stream Thrust and Ram Drag Coefficients, CMAPS Mode Mach 0.4 | 64 |
| 3-28 | Variation of Stream Thrust and Ram Drag Coefficients, CMAPS Mode Mach 0.9 | 65 |
| 3-29 | Variation of Stream Thrust and Ram Drag Coefficients, CMAPS Mode Mach 1.4 | 66 |

LIST OF ABBREVIATIONS AND SYMBOLS

| <u>Symbol</u> | <u>Definition</u> |
|---------------|---|
| A/B | Afterburning power setting on nozzle |
| A_c | Inlet capture area (35.23cm ²) |
| AF | Axial Force |
| A_o | Total inlet captured stream tube area (cm ²) |
| ALBEN | Aerodynamically Load Balanced Exhaust Nozzle |
| ALPHA, ALPHAM | Model angle of attack (Deg) |
| A_{TH} | Nozzle throat area |
| b_c | Model canard span (52.49cm) |
| b_w | Model wing span (130.30cm) |
| B.L. | Model butt line |
| \bar{c}_c | Mean aerodynamic canard chord (19.60cm) |
| CD | Total aircraft drag coefficient (CDA + CDNOZ) |
| CDA | Metric airframe drag coefficient |
| CDNOZ | Exhaust nozzle drag coefficient (2 nozzles) |
| CL | Total aircraft lift coefficient (CLA + CLNOZ) |
| CLA | Metric airframe lift coefficient |
| CLNOZ | Exhaust nozzle lift coefficient (2 nozzles) |
| CM | Total aircraft pitching moment coefficient |
| CMO | Total aircraft pitching moment coefficient at zero lift |
| CMA | Metric airframe pitching moment coefficient |
| CMNOZ | Exhaust nozzle pitching moment coefficient (2 nozzles) |
| CMCRB | Canard root bending moment coefficient (MCRB/($S_c b_s Q$)) |
| \bar{c}_w | Mean aerodynamic wing chord (41.70cm) |
| C_p | Pressure coefficient [($P_L - P_o$)/ Q_o] |

LIST OF ABBREVIATIONS AND SYMBOLS (CONTINUED)

| <u>Symbol</u> | <u>Definition</u> |
|---------------|--|
| CMAPS | Compact Multimission Aircraft Propulsion Simulator |
| DELCR | Right hand canard deflection angle, positive leading edge up (Deg) |
| DELCL | Left hand canard deflection angle, positive leading edge up (Deg) |
| DPDS | Static pressure differential across inlet duct seal |
| Dry | Dry power setting on nozzle |
| ES | Engine station |
| F/T, FT | Flow-Through test mode |
| FS | Fuselage Station |
| J/E, JE | Jet-Effects test mode |
| Mach, M | Free stream Mach number |
| MCAIR | McDonnell Aircraft Company |
| MCRB | Canard root bending moment |
| MFR, MFRA | Average of left and right Inlet Mass Flow Ratios based on calibration correlated to CMAPS turbine exit pressure for Simulator Mode or at nozzle exit chokes for Flow-Through Mode, [A^O/A_c] |
| MS | Model Station |
| N | CMAPS Rotor speed (RPM) |
| NPR, NPRA | Average of left and right Nozzle Pressure Ratios [P_{T_J}/P_o] |
| NRP | Percent of sea-level referenced design rotor speed, $(N/75185) \times \theta \times 100$ |
| P, P_o | Free Stream static pressure |
| P2 | Average static pressure at compressor face |
| P_L | Local Static Pressure |

LIST OF ABBREVIATIONS AND SYMBOLS (CONTINUED)

| <u>Symbol</u> | <u>Definition</u> |
|----------------|--|
| Plane 2 | Compressor face |
| Plane 4 | Turbine inlet |
| Plane 8 | Exhaust Nozzle Duct |
| Plane 15 | Compressor discharge |
| Plane 57 | Turbine discharge |
| PS57 | Turbine discharge static pressure |
| P_T, P_{T_0} | Free stream total pressure |
| P_{T_2} | Average total pressure at compressor face, left or right |
| P_{T_8} | Average total pressure at exhaust nozzle |
| $P_{T_{max}}$ | Maximum value of total pressure of compressor face |
| $P_{T_{min}}$ | Minimum value of total pressure at compressor face |
| P_{T_J} | Total pressure of jet exhaust at nozzle exit |
| Q, Q_0 | Free stream dynamic pressure |
| R _____ | "R" preceeding any parameter indicates Reference value for all points in a given run; usually the value measured at $\alpha = 0^\circ$ |
| REC1R | Total pressure recovery at right hand compressor face, $[P_{T_2}/P_{T_0}]$ |
| SIM | Simulator test mode |
| T_{T_2} | Total Temperature at Plane 2 |
| T_{T_8} | Total Temperature at Plane 8 |
| W2 | Inlet Mass Flow Rate |
| W8 | Nozzle Mass Flow Rate |
| WL | Model water line |
| WTAP | Mass Flow function $(WB \sqrt{TT_8}/(PTB * A_{TH}))$ |

LIST OF ABBREVIATIONS AND SYMBOLS (CONCLUDED)

| <u>Symbol</u> | <u>Definition</u> |
|---------------|---|
| α | ALPHA |
| θ | Sea-level standard day temperature correction $\sqrt{((T_{T2} + 460)/518.67)}$ |
| δ_c | DELCR or DELCL |
| δ_f | Wing flap deflection angle, positive trailing edge down (Deg) |
| δ_n | Nozzle thrust vectoring angle, positive trail- ing edge down (Deg) |

SUMMARY

A wind tunnel model of a supersonic V/STOL fighter configuration has been tested to measure the aerodynamic interaction effects which can result from geometrically close-coupled propulsion system/airframe components. The approach was to configure the model to represent two different test techniques. One was a conventional test technique composed of two test modes. In the Flow-Through mode, absolute configuration aerodynamics are measured, including inlet/airframe interactions. In the Jet-Effects mode, incremental nozzle/airframe interactions are measured. The other test technique is a propulsion simulator approach, where a sub-scale, externally powered engine is mounted in the model. This allows proper measurement of inlet/airframe and nozzle/airframe interactions simultaneously.

Comparison of the measured aerodynamic characteristics between the two test techniques is a direct indication of the extent to which inlet and nozzle flowfields are coupled together. If significant coupling does exist, there will be disagreement between the two data sets. The simulator test technique may then be required in the future to properly measure the aerodynamic characteristics of compact fighter configurations.

Measurement of these propulsion/airframe interaction effects was carried out in a three phase experimental program, sponsored by the NASA-Ames Research Center. Conceptual model design was accomplished in Phase 1, detailed model design and fabrication in Phase 2, and high speed testing in Phase 3.

The aerodynamic configuration tested was a canard/wing concept designed for high transonic maneuverability, employing non-axisymmetric, vectorable exhaust nozzles located near the wing trailing edge.

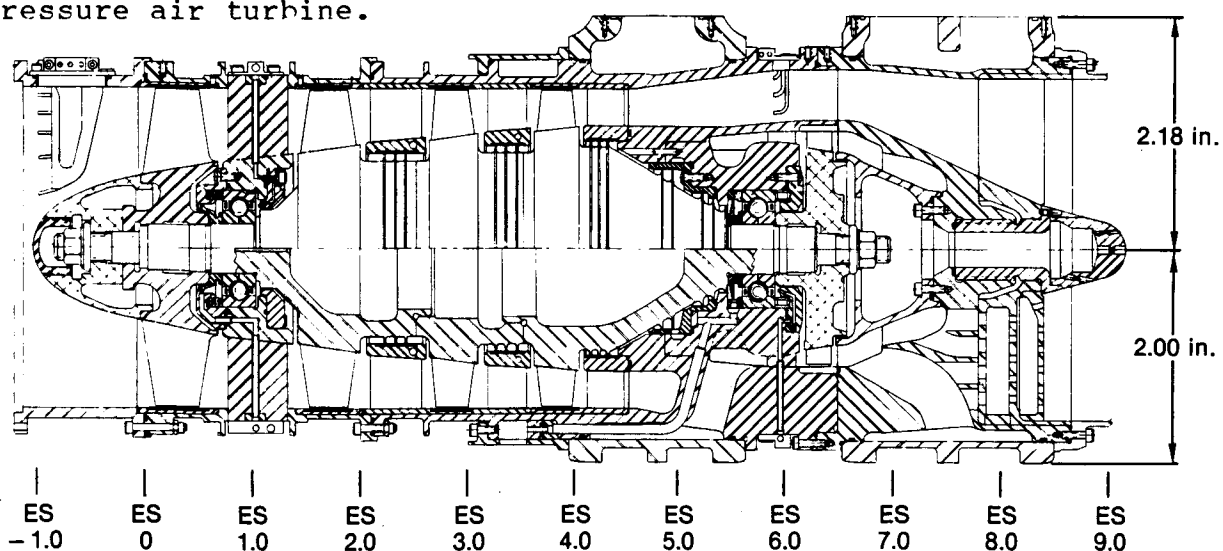
PRECEDING PAGE BLANK NOT FILMED

The overall character of the aerodynamic flowfield, including the interactions due to inlet/nozzle coupling, were quantified by comparing force balance data between the different test modes, and by comparing static pressure distributions over the entire model surface. The purpose of this Volume II report is to document the basic force and moment data in detail. The Volume I report documents the pressure data, Reference 1. All of the analysis for both pressure and force and moment data is presented in the Volume III Test Analysis Report, Reference 2.

1. INTRODUCTION

Many of the configurations proposed for advanced supersonic V/STOL aircraft are very compact in nature. This results primarily from the design goal to minimize control forces and forward lift engine size by concentrating the major components of the aircraft near the center of gravity. Integration of the propulsion system with the airframe for these configurations can result in potentially significant aerodynamic flowfield interactions. These interactions may arise from geometrically close-coupled inlet/nozzle arrangements arising from minimum length nacelles. The problem can be further complicated if the configuration includes movable canards and vectorable nozzles located near the wing.

The data obtained with conventional wind tunnel test techniques can be questionable in the presence of large flowfield interactions, since these techniques cannot achieve simultaneous simulation of all of the flowfields involved. Proper simulation can be achieved with the compact Multi-Mission Aircraft Propulsion Simulator (CMAPS), developed by the Air Force Aeropropulsion Laboratory (AFAPL), Reference 3. The CMAPS, Figure 1-1, is a miniature, low bypass ratio turbofan engine powered by a high pressure air turbine.



GP53-0871-19-R

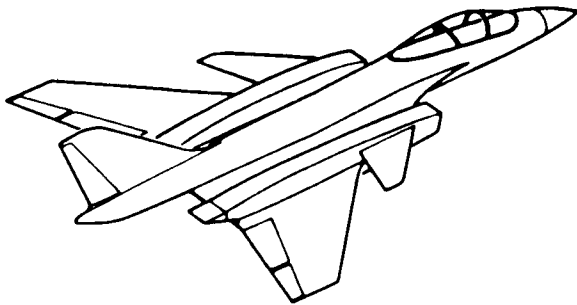
Figure 1-1. Compact Multimission Aircraft Propulsion Simulator (CMAPS)

The most beneficial application of the CMAPS will obviously be on those aircraft that have potentially large flowfield interactions between the inlet, nozzle, and airframe. Since testing a CMAPS equipped model may be more complex than testing a conventional model (Flow-Through and Jet-Effects), the need to identify the types of configurations which require CMAPS evaluation is critical. An aerodynamically close-coupled V/STOL configuration represents an effective means of evaluating the requirement for simultaneous inlet and exhaust nozzle flow simulation, and thus the potential need for the CMAPS testing technique.

Based on the foregoing considerations, a three phase NASA program was initiated in October, 1980 to measure airframe/propulsion system interactions of close-coupled supersonic V/STOL configurations. Both propulsion simulator and conventional model techniques were used. An equally important objective was to continue development of installation and test techniques for wind tunnel models equipped with propulsion simulators. This program represented the first time that twin CMAPS had been tested in a wind tunnel model of a full configuration aircraft. Previous programs have tested only single simulators in simple body/nacelle models, Reference 4.

The approach to accomplish these objectives was to design, fabricate, and test two model configurations characterized by close-coupled airframe/propulsion arrangements, each in simulator and conventional test modes. Key characteristics of the two test configurations are shown in Figure 1-2. The external airframe components of the basic model were provided by the Air Force. This basic configuration was developed under prime contract to the Air Force Wright Aeronautical Laboratories (AFWAL) by MCAIR in the Advanced Nozzle Concepts (ANC) program, Reference 4. The alternate configuration is a derivative of the basic configuration with the inlet/nozzle length shortened and the canard removed. At this time, only the basic configuration has been tested. However, the hardware has been fabricated to model the alternate configuration.

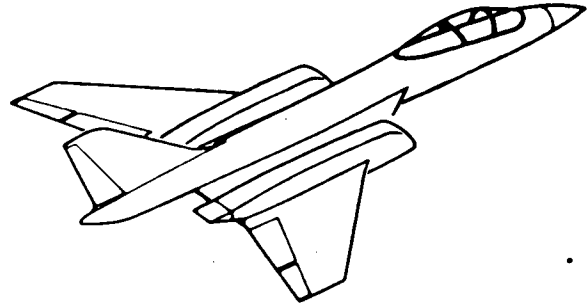
Basic Design



Air-to-Air Concept

- 2-D ALBEN Vectorable Nozzles (AR 4)
- 2-D Normal Shock Inlet With Droop Lip
- Wide-Spaced Poddled Nacelles
- Close-Coupled, All Movable Canards
- Advanced Maneuvering Wing

Alternate Design



Changes for Alternate

- Round Short Inlet With Lower Slot
- Canards Removed
- Inner Wing Extension Shortened

GP53-0871-18-R

Figure 1-2. Aerodynamic Characteristics of Study Concepts

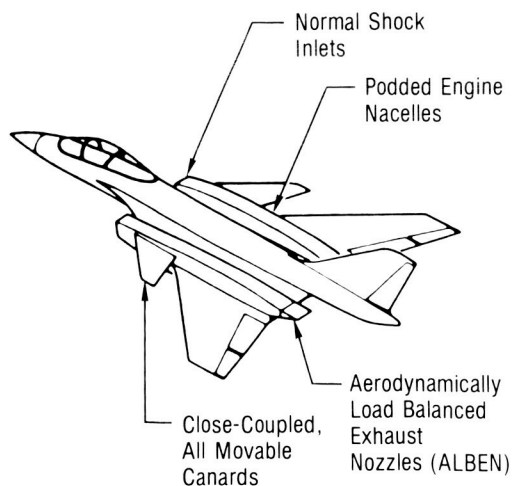
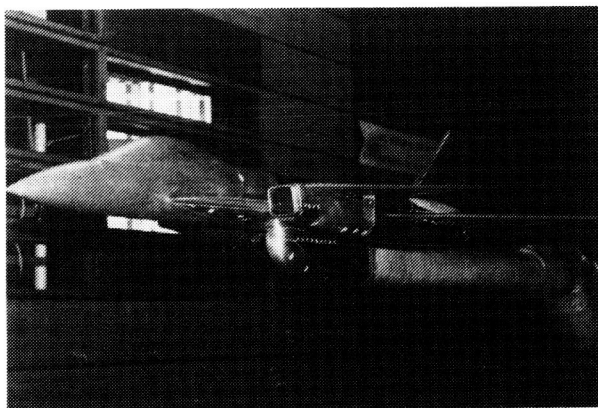
Conceptual design of the test model was completed in Phase 1 during the first seven months of the program, Reference 5. Detailed design and model fabrication were accomplished in Phase 2, as reported in Reference 6.

The results of the Phase 3 wind tunnel tests and analysis are presented in a series of four NASA Contractor Reports (CRs). The pressure data is reported in Volume I of the Wind Tunnel Data Report, (Reference 1). The force and moment data and data reduction procedures are reported in this document, Volume II. The detailed data analysis and executive summary are presented in the Test Analysis Report and Final Report, respectively (References 2 and 7).

The following sections include a description of the test article, facility, instrumentation and other data reduction procedures. The force and moment data is presented graphically in Appendix A of this volume.

2. TEST ARTICLE DESCRIPTION

The test vehicle was a 9.62% scale model of a supersonic V/STOL aircraft with twin, podded engine nacelles. The nacelles incorporated normal shock inlets and vectorable Aerodynamically Load Balanced Exhaust Nozzles (ALBENs), designed by General Electric. The model installed in the NASA-Ames 11x11-ft transonic wind tunnel is shown in Figure 2-1. Testing was performed at speeds from Mach 0.4 to 1.4 and through the angle-of-attack range from -2° to 20° .



Model Geometry

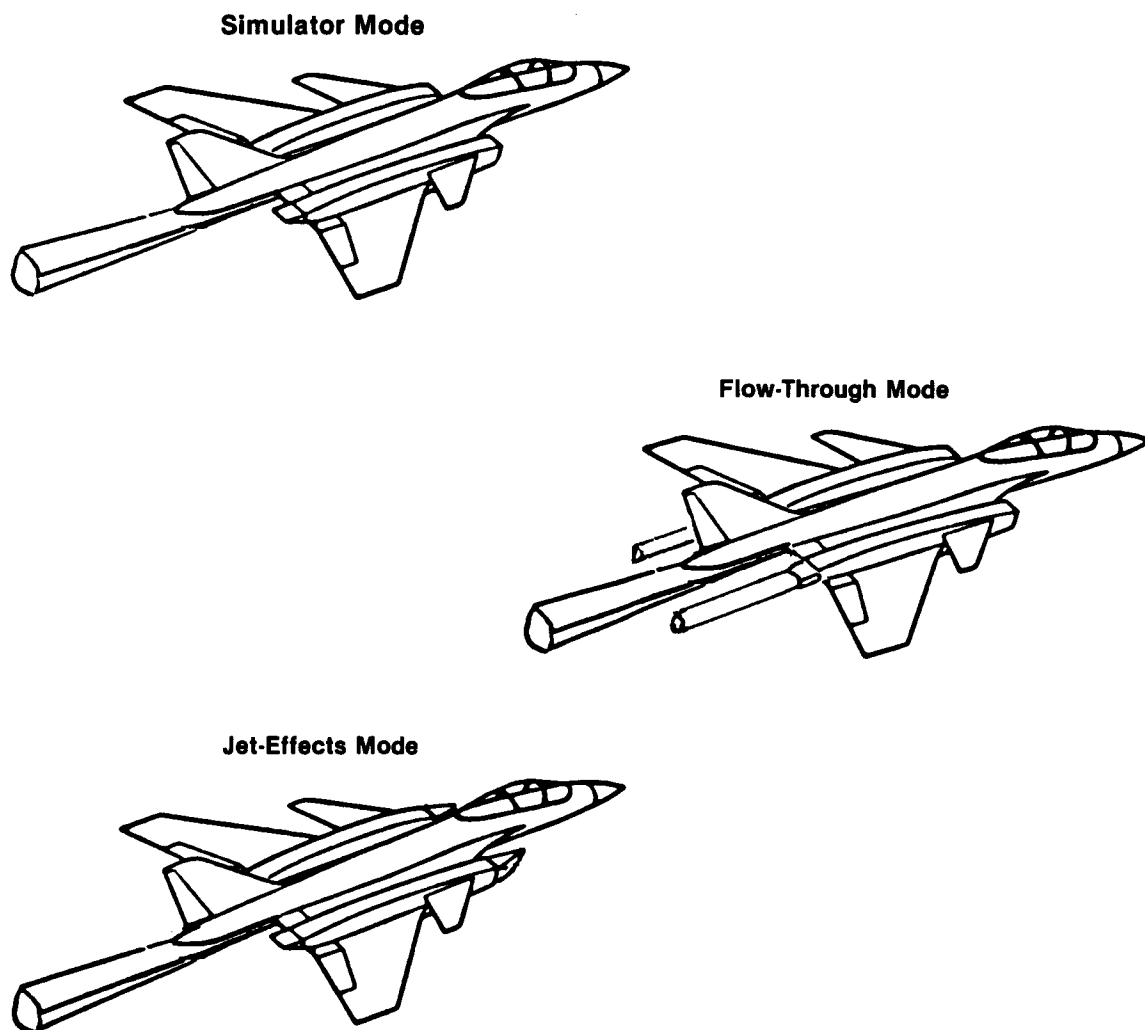
| | |
|---------------------------|--|
| Fuselage Length: | 1.79 m (5.88 ft) |
| Nacelle Length: | 0.86 m (2.83 ft) |
| Wing Span: | 1.30 m (4.28 ft) |
| Wing Area: | 0.48 m ² (5.22 ft ²) |
| Canard Area: | 0.09 m ² (1.02 ft ²) |
| Inlet Capture Area: | 35.23 cm ² (5.46 in. ²) |
| Nacelle Max Area: | 116.14 cm ² (18 in. ²) |
| Nozzle Throat Area (Dry): | 19.42 cm ² (3.01 in. ²) |
| Nozzle Throat Area (A/B): | 33.23 cm ² (5.15 in. ²) |

GP53-0871-42-R

Figure 2-1. Supersonic V/STOL Wind Tunnel Model Installed in NASA-Ames Transonic Tunnel

**ORIGINAL PAGE IS
OF POOR QUALITY**

The model was tested in three different modes; the conventional Jet-Effects and Flow-Through modes, and the propulsion simulator (CMAPS) mode. A schematic of the three modes, each in its characteristic configuration, is shown in Figure 2-2. A common support system and metric arrangement were maintained for all three test modes as shown in Figure 2-3.



GP53-0871-17-R

Figure 2-2. Test Mode Characteristics

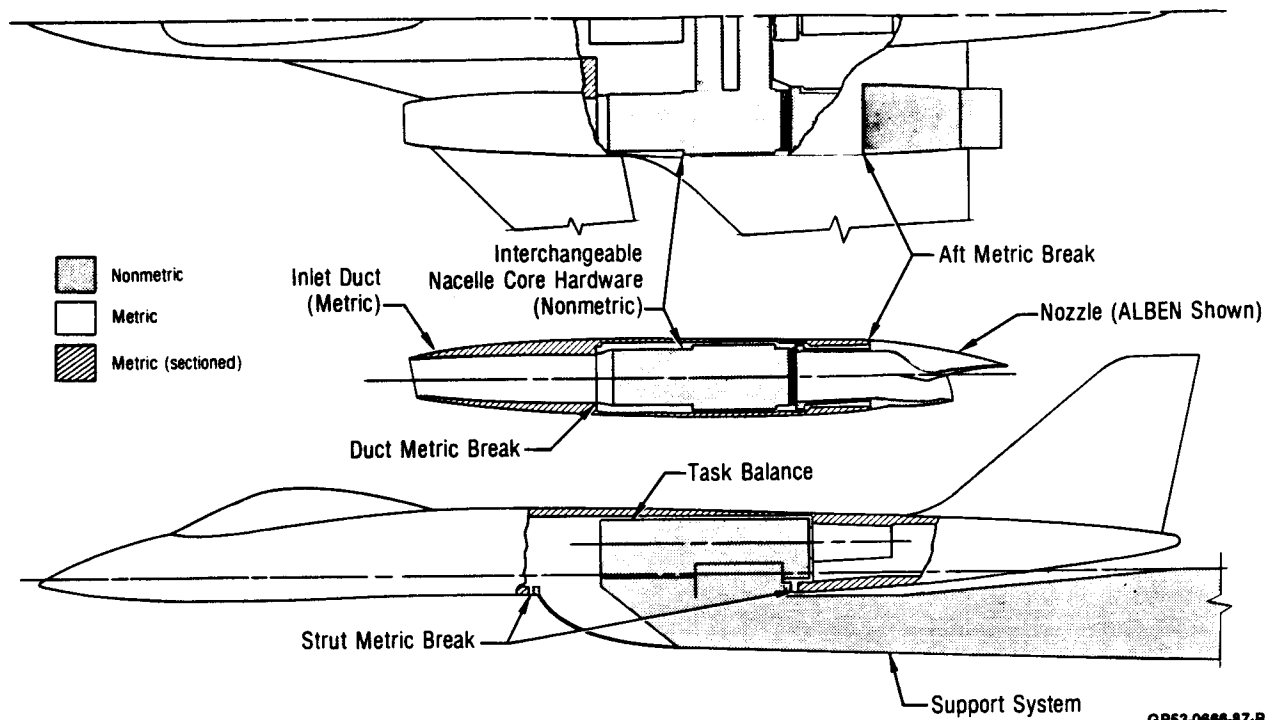


Figure 2-3. Common Support System and Metric Arrangement

Within the three test modes, a matrix of two inlet and two exhaust system configurations was tested. The inlet was configured as either flowing or faired. The exhaust system incorporated either ALBENs or nozzle extension ducts with chokes installed. Four aerodynamically different test configurations were derived from the two inlet and two exhaust configurations. These configurations were termed: 1) Common Baseline, 2) Nozzle Extension, 3) Nozzle Extension Baseline, and 4) Simulated Aircraft. The external differences in these configurations were only in the nacelle geometry, Figure 2-4; all other external model features were common, including canards, wings, and vertical tail, Figures 2-5 through 2-7. A matrix of the modes, inlet/nozzle combinations, and test configurations is shown in Figure 2-8. The Common Baseline configuration was tested in each mode as a tie-in for the three separate model build-ups and used to account for any bias errors created between tunnel entries. The Nozzle Extension configuration used the extension ducts to displace the exhaust plume from the vicinity of the airframe such

that inlet mass flow ration (MFR) effects could be measured independent of jet-induced effects. The Nozzle Extension Baseline configuration was used to account for the effects of the extension ducts on the metric airframe as compared to the ALBEN installation. Of the four configurations tested, the Simulated Aircraft configuration is the best representation of an aircraft in flight.

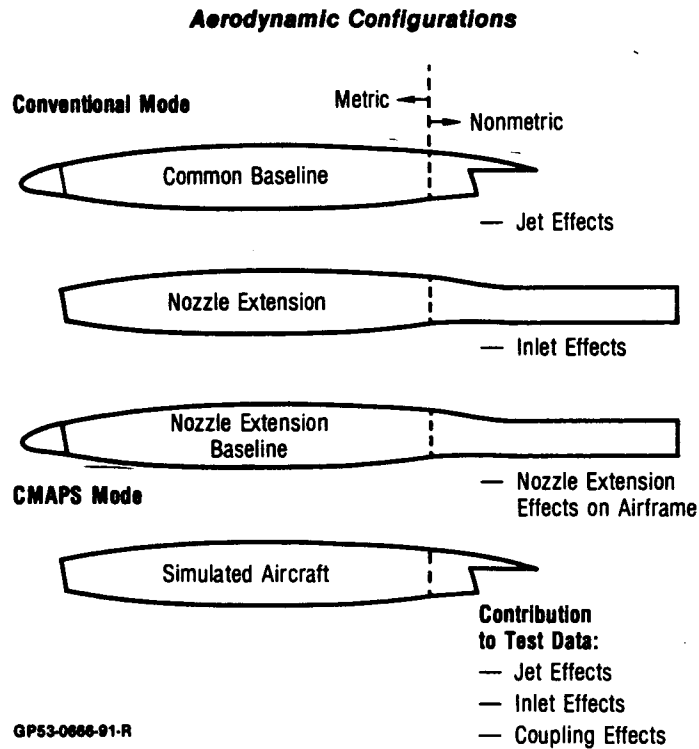


Figure 2-4. Comparison of Test Configuration

Model Geometry

$s = 0.0919 \text{ m}^2$ (0.989 ft²), Exposed

$b = 0.5249 \text{ m}$ (1.722 ft)

Aspect Ratio = 3.0

$\tau = 0.25$

$c_R = 28.000 \text{ cm}$ (11.02 in.)

$c_T = 7.00 \text{ cm}$ (2.76 in.)

MAC = 19.60 cm (7.72 in.)

$\Lambda_{LE} = 45 \text{ deg}$

Airfoil Sections

BL 79.5: NACA 64A006

BL 177.54: NACA 64A003.5

Deflection

$\delta_c = -20 \text{ to } 10 \text{ deg}$

δ_c Is Positive for
Leading Edge Up

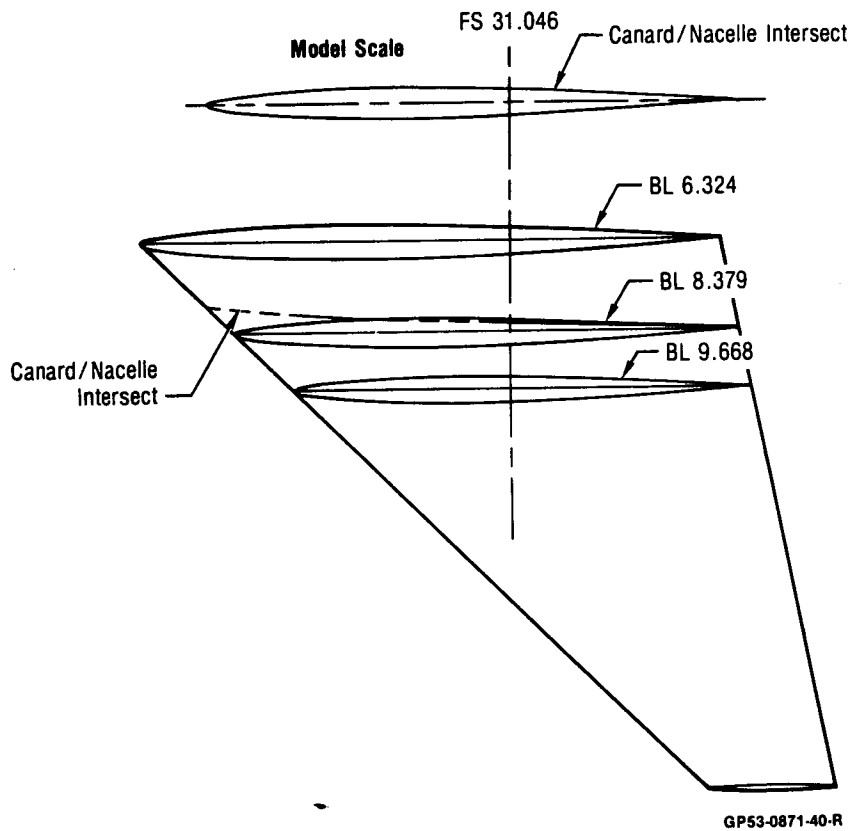


Figure 2-5. Canard Geometry Description

Model Geometry

$s = 0.4851 \text{ m}^2$ (5.221 ft²)

$b = 1.3031 \text{ m}$ (4.275 ft)

Aspect Ratio = 3.5

$\tau = 0.25$

$c_R = 59.564 \text{ cm}$ (23.45 in.)

$c_T = 14.890 \text{ cm}$ (5.86 in.)

MAC = 41.697 cm (16.42 in.)

$\Delta_{L_E} = 45 \text{ deg}$

Airfoil Sections

BL 20.000: NACA 64A004.6

BL 41.000: NACA 64A004.6

BL 104.000: NACA 64A005.5

BL 243.350: NACA 64A003.0

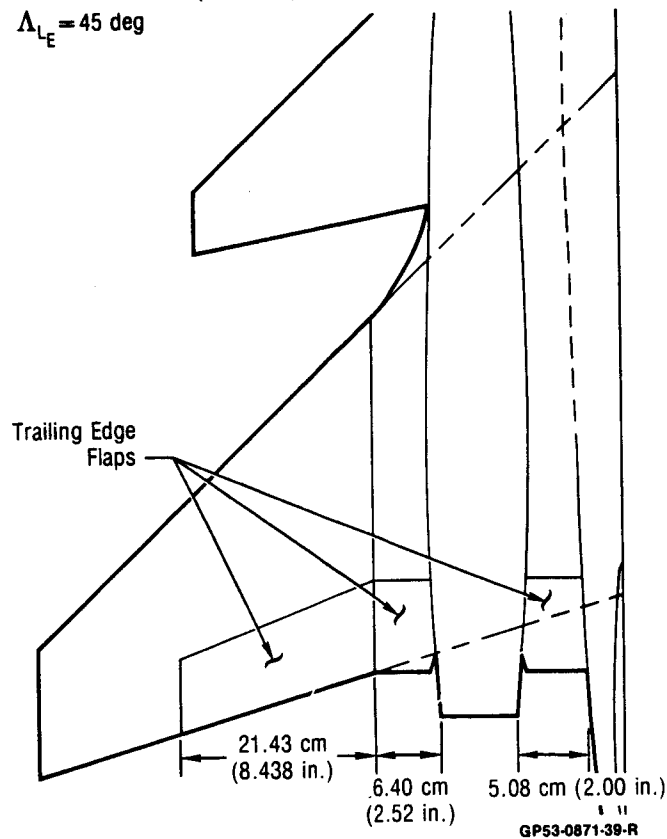


Figure 2-6. Wing Geometry Description

Model Geometry

$s = 0.0630 \text{ m}^2 (0.678 \text{ ft}^2)$, Exposed

$h = 25.09 \text{ cm} (9.88 \text{ in.})$

Aspect Ratio = 3.5

$\tau = 1.0$

$\lambda = 0.333$

$c_R = 37.64 \text{ cm} (14.82 \text{ in.})$

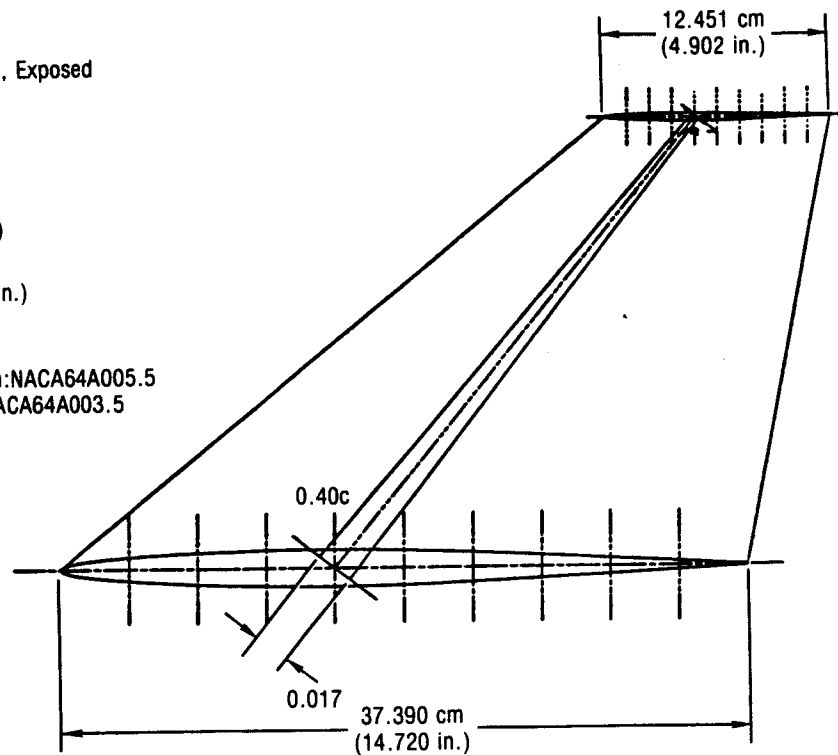
$c_T = 12.55 \text{ cm} (4.94 \text{ in.})$

MAC = 27.18 cm (10.70 in.)

$\Delta_{LE} = 50 \text{ deg}$

Fuselage/Tail Intersection: NACA64A005.5

Highest Tail Waterline: NACA64A003.5



GP53-0871-38-R

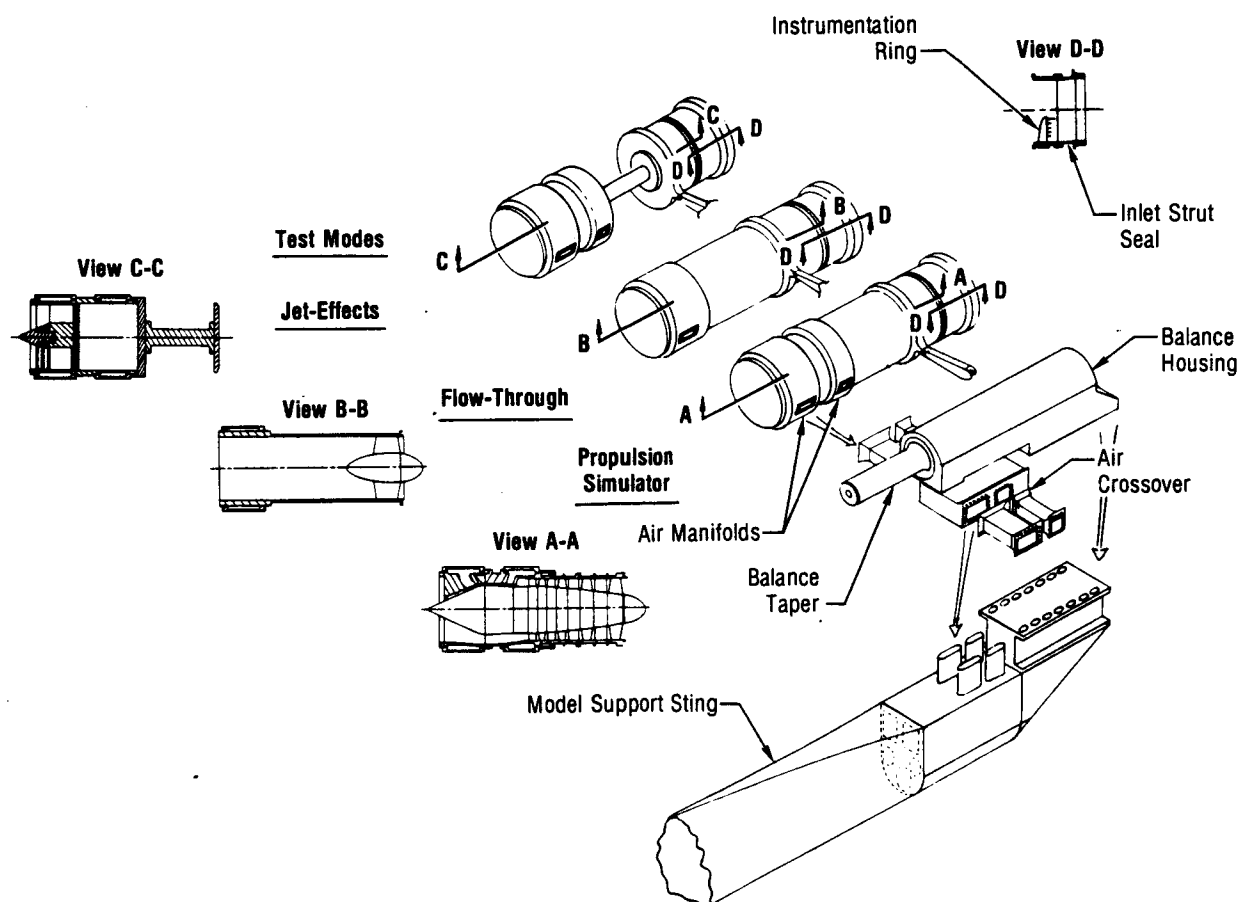
Figure 2-7. Vertical Tail Geometry Description

| Test Configuration | Propulsion System Configuration | | Test Mode | | |
|---------------------------|---------------------------------|------------|-------------|--------------|-------|
| | Inlet | Nozzle | Jet-Effects | Flow-Through | CMAPS |
| Common Baseline | Faired | ALBEN | X | X | X |
| Nozzle Extension | Flowing | Extensions | | X | X |
| Nozzle Extension Baseline | Faired | Extensions | | X | |
| Simulated Aircraft | Flowing | ALBEN | | | X |

GP53-0666-55-R

Figure 2-8. Inlet/Nozzle Combinations Tested in Each Mode

2.1 TEST MODES - Each of the three test modes (CMAPS, Jet-Effects, and Flow-Through) represented a different wind tunnel test technique. A major program objective was to eliminate bias errors due to test technique differences. Therefore, a common support system and a common metric arrangement were used for all three test modes (Figure 2-3). The internal flow hardware was unique to each test mode but interchangeable between the three modes, as shown in Figure 2-9. The flow path through the nacelle could be changed by installing a simulator, a jet-effects plenum, or a flow-through duct, depending on the test mode desired.



GP53-0871-37-R

Figure 2-9. Interchangeable Nacelle Core Hardware

In this section, the common hardware is further described, as well as the individual test modes.

2.1.1 Common Model Support System and Metric Arrangement -

The support system and metric arrangement were common between the three test modes to eliminate test technique bias errors. The model support system and core hardware provided the model-to-facility interface for airflows and instrumentation and the structural support for both the metric and non-metric components of the model. The support and core hardware consisted of the sting, balance housing, air crossover, air manifolds, nozzle support, front simulator mount, retainer, and transition duct. These components are shown in Figure 2-10. The optional front simulator mount was designed to remove torsional loads during the CMAPS mode, but was flexible in the axial direction to allow limited movement due to thermal growth. The front mount was not used in this program in order to provide more space for instrumentation lines. The nozzle support was used to react to axial loads and nozzle vectoring loads.

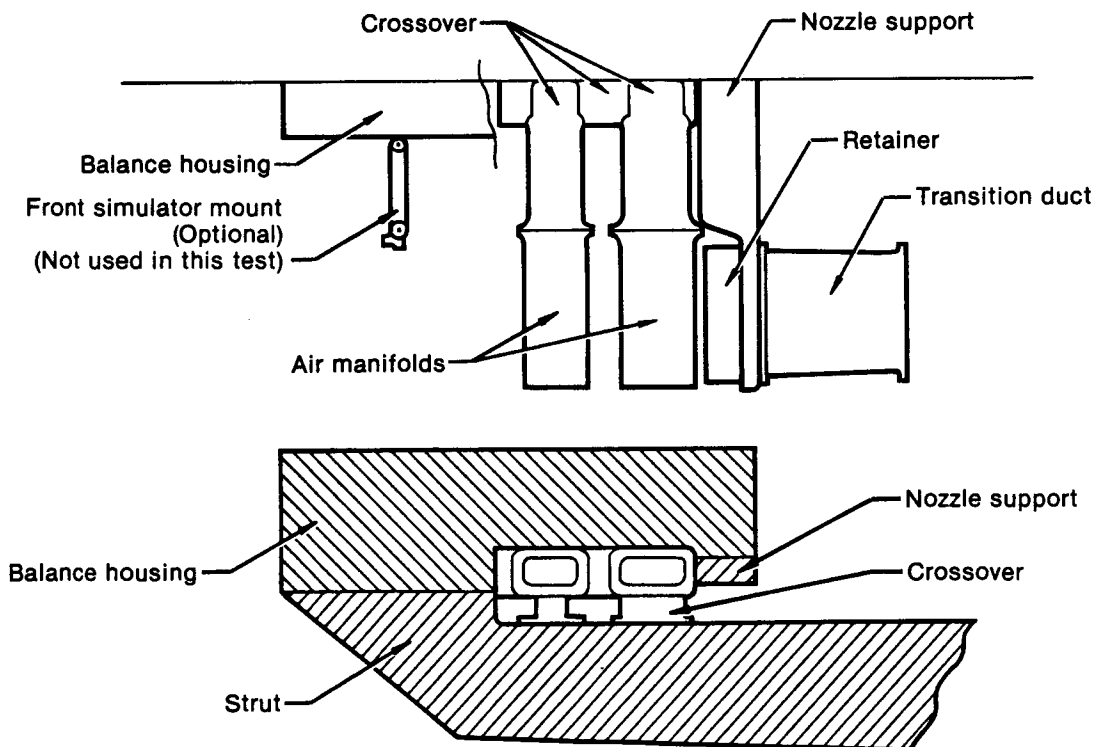


Figure 2-10. Core Support Hardware

GP53-0871-62-R

The retainer and transition duct served to deliver the air from the interchangeable nacelle components to the exhaust system. The retainer was firmly attached to the nacelle component and connected to the transition duct with a no-load seal. This seal isolated the interchangeable nacelle components from the exhaust system loads.

In each test mode, the model was supported by a single sting which extended from the center of the lower fuselage to the wind tunnel offset adapter. A schematic of the tunnel installation and support system is shown in Figure 2-11. This sting was selected as a compromise between a rear entry sting design and lower fuselage mounted "hockey stick" design. This selection is detailed in Reference 3.

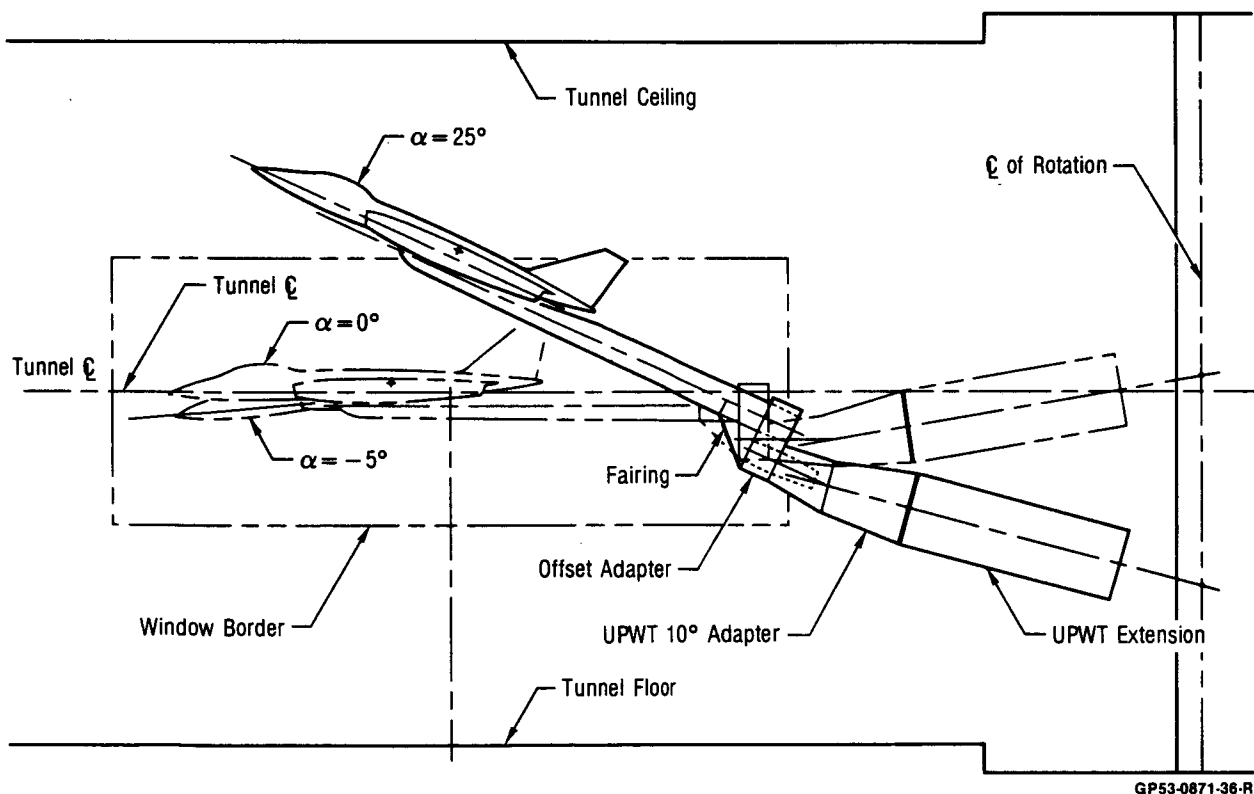
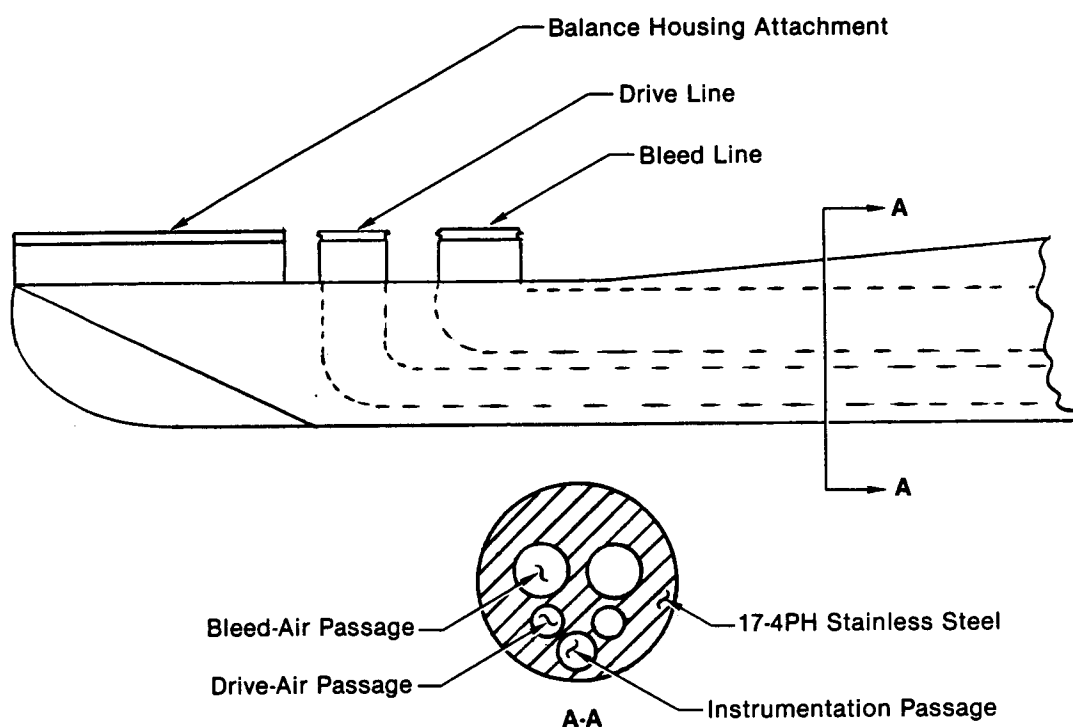


Figure 2-11. Model Installation in NASA-Ames 11 ft x 11 ft Unitary Plan Wind Tunnel

Four high pressure air passages, two for the CMAPS drive air and two for the bleed air, were contained in the sting along with a passage for model instrumentation lines. These passages, shown in Figure 2-12, were machined out of the solid 17-4PH stainless steel sting and sized to accommodate the airflow requirements of the propulsion simulators. At the offset adapter, these air lines, and the model instrumentation, connect with air supply lines and the instrumentation lines from the facility.

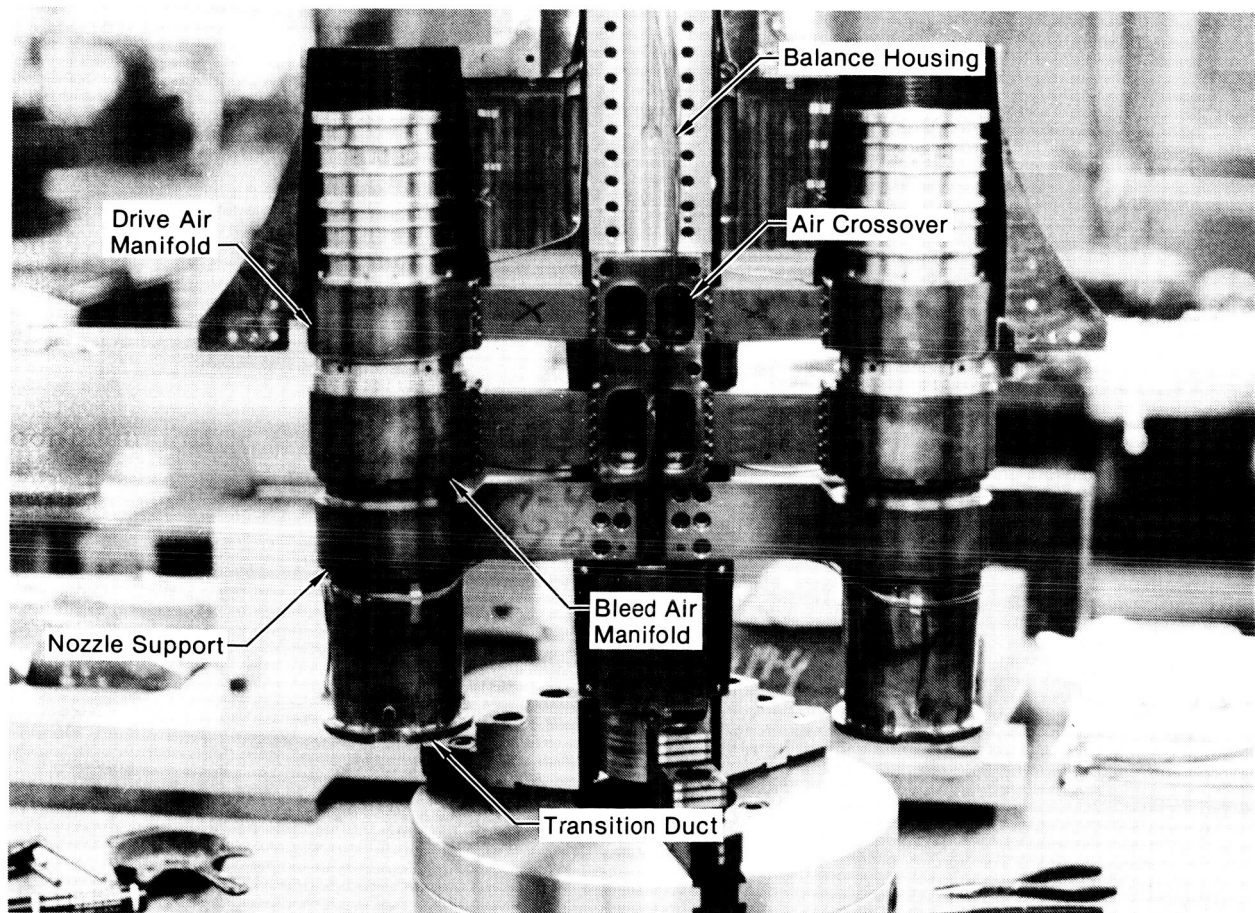


GP53-0871-8-R

Figure 2-12. Model Support Sting

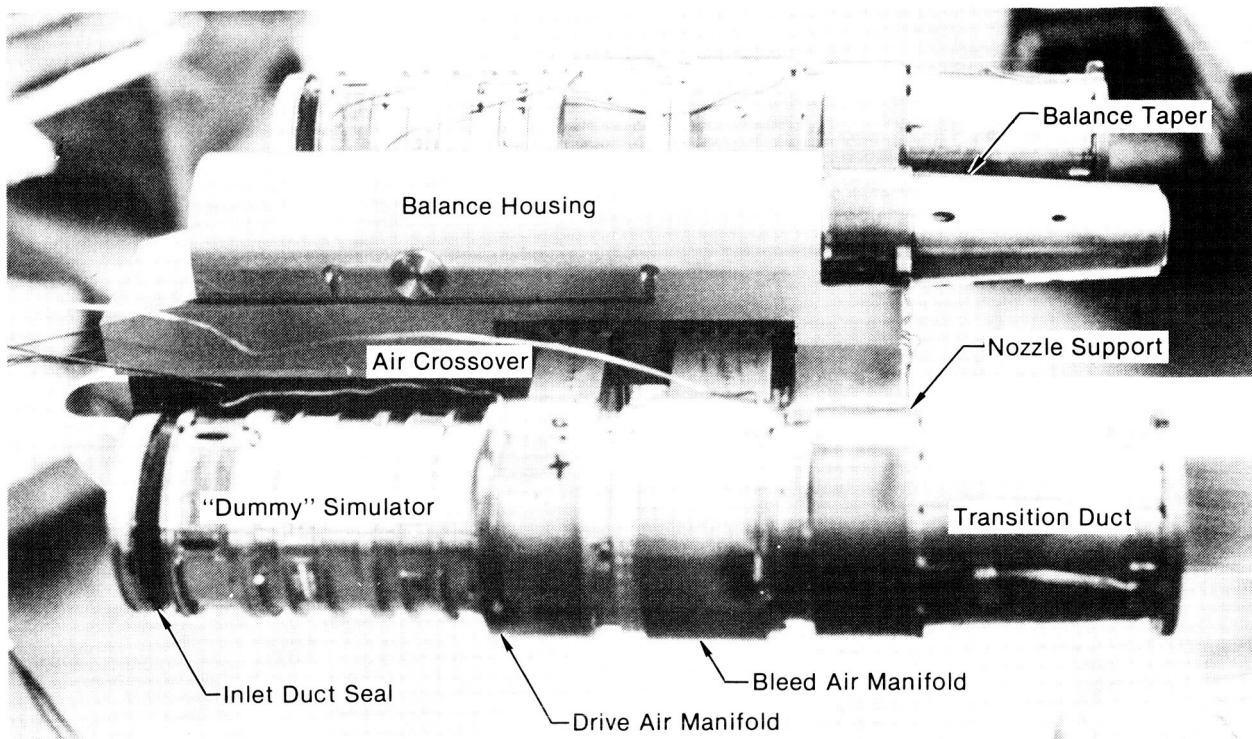
Photographs taken during model assembly show the support system and core hardware. The assembled core hardware supporting the transition duct and "dummy" simulator is shown in Figure 2-13. A sideview of the same assembly with the balance installed is shown in Figure 2-14. The flow-through duct hardware supported by the bleed-air manifold is shown in Figure 2-15. The assembly of the core hardware onto the sting is shown in Figure 2-16.

ORIGINAL PAGE IS
OF POOR QUALITY



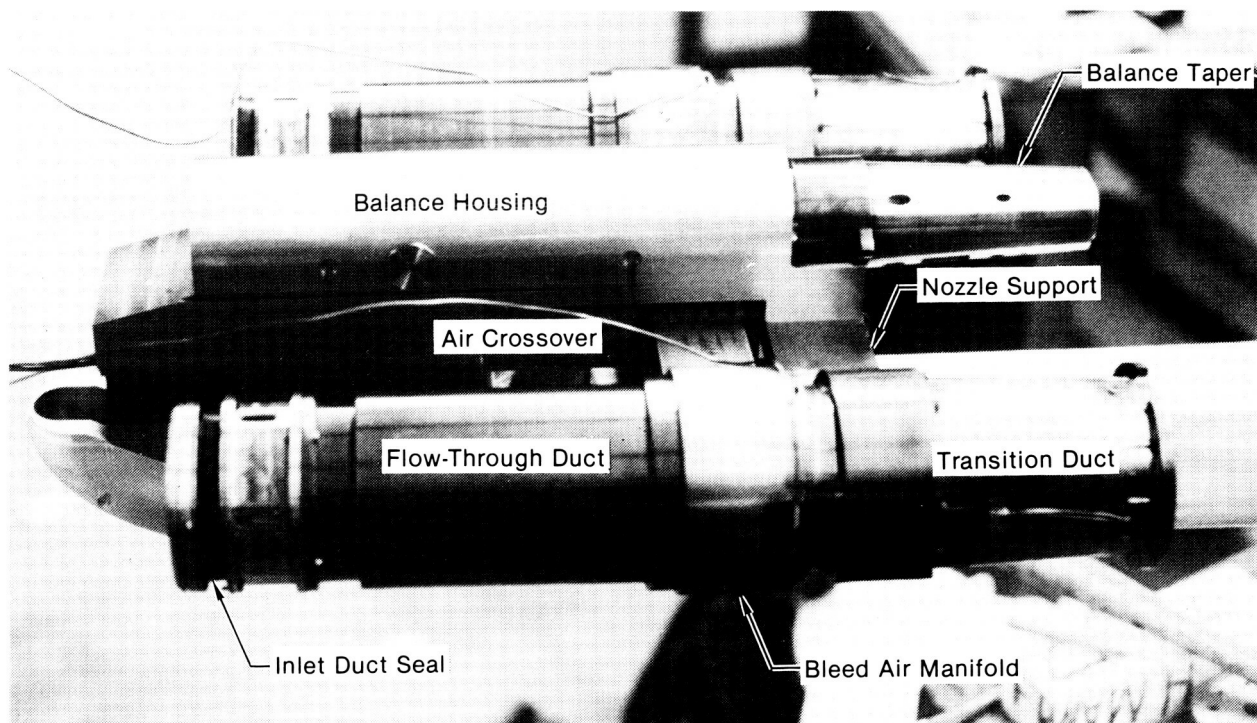
GP53-0871-61-R

Figure 2-13. Core Hardware



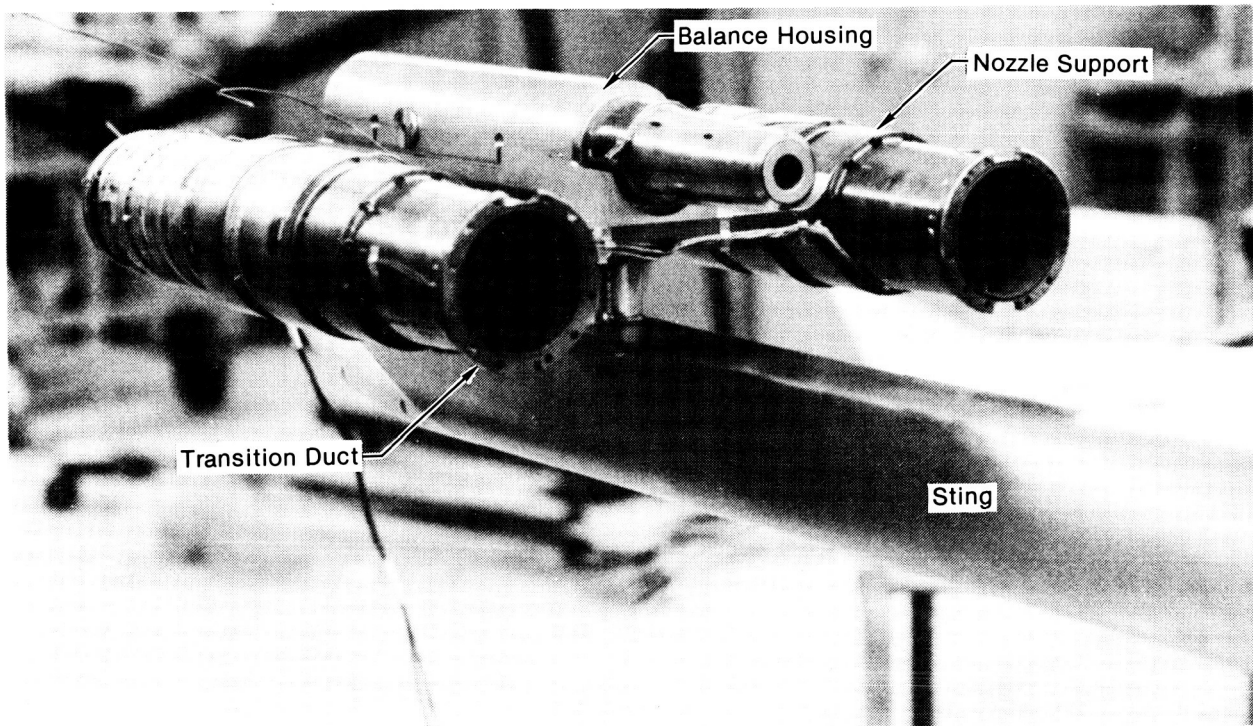
GP53-0871-59-R

Figure 2-14. Core Hardware With Simulator



GP53-0871-60-R

Figure 2-15. Core Hardware With Flow-Through Duct

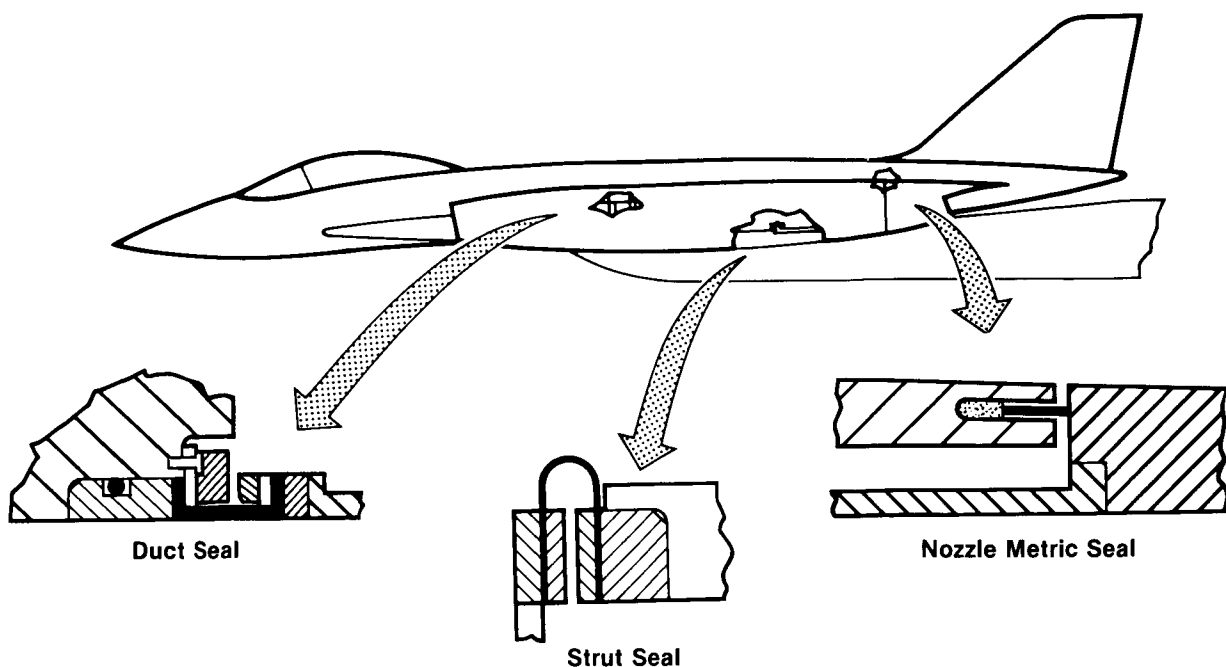


GP53-0871-58-R

Figure 2-16. Core Hardware on Sting

A common metric break seal arrangement was used for all three test modes. This arrangement consisted of three different seals: the nozzle metric break seal, the inlet duct seal, and the strut support seal, Figure 2-17.

The nozzle metric break seal was designed to prevent free movement of air into or out of the cavity. Therefore, a uniform cavity pressure was maintained and easily measured. The nozzle metric seal consisted of a stiff Teflon strip 1.067 cm (0.42 in.) long and 0.076 cm (0.030 in.) inches thick inserted into a slot in the nacelle shell 0.203 cm (0.080 in.) wide with four small coil springs in the shell applying a small axial force on the Teflon strip. This seal and spring arrangement allowed movement of the nozzle relative to the nacelle shell in the axial direction and in rotation while still keeping the seal flush against the nozzle.



GP53-0871-20-R

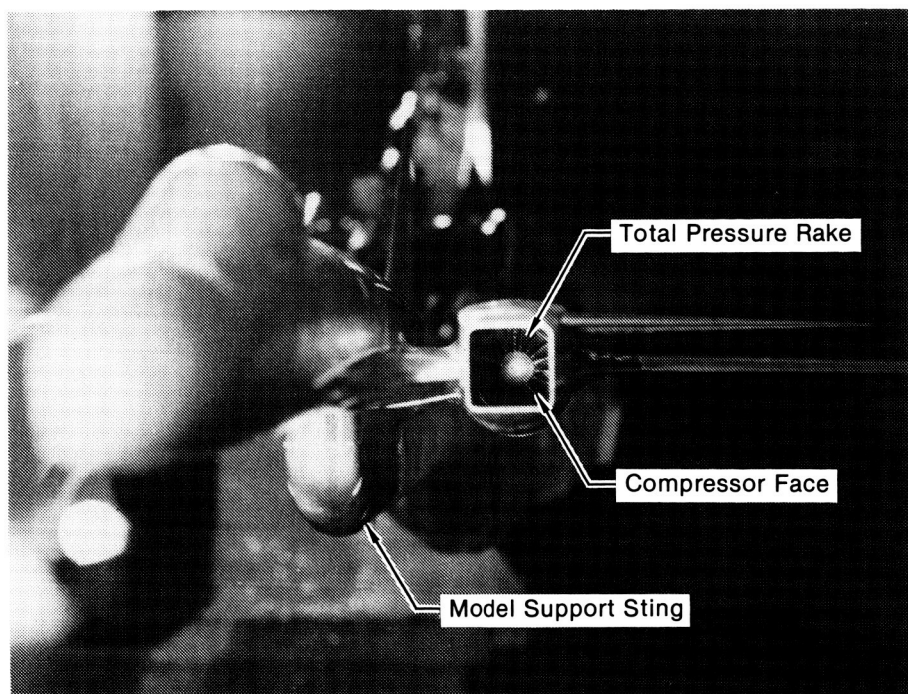
Figure 2-17. Metric Seal Arrangement

The strut seal function was to prevent the external flow from causing non-uniform pressures in the model cavity. The strut seal was a thin race track shaped, pliable silicone rubber strip. This created an airtight, flexible seal around the bottom of the model between the non-metric strut and the metric model.

The inlet duct seal provided a leak-proof airflow transition between the metric inlet duct and the non-metric instrumentation ring. The instrumentation ring was the common component attached to the front of either the simulator, flow through duct, or jet-effects plenum hardware. The seal was a pliable, butyl rubber, flanged tube which allowed normal and axial direction movement while exerting predictable forces on the model.

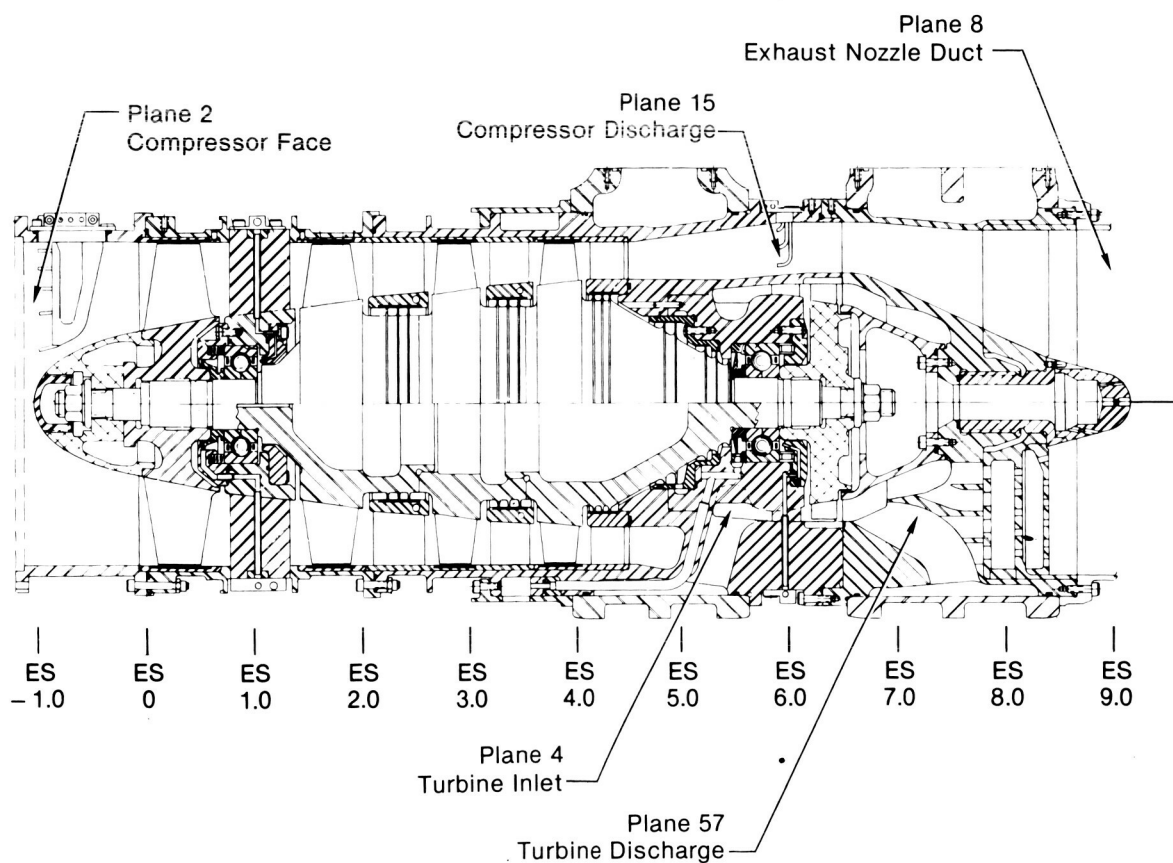
2.1.2 CMAPS Mode - Propulsion simulators were installed in the engine nacelles for all the CMAPS mode testing. The engine face (Plane 2) total pressure rake and simulator compressor face can be seen behind the close-coupled inlet in Figure 2-18. The location of the CMAPS instrumentation planes is defined in Figure 2-19. A schematic of the nacelle hardware for the CMAPS mode is shown in Figure 2-20.

ORIGINAL PAGE IS
OF POOR QUALITY



GP53-0871-35-R

Figure 2-18. Propulsion Simulator Installed in Left Hand Engine Nacelle



GP53-0871-16-R

Figure 2-19. CMAPS Instrumentation Planes

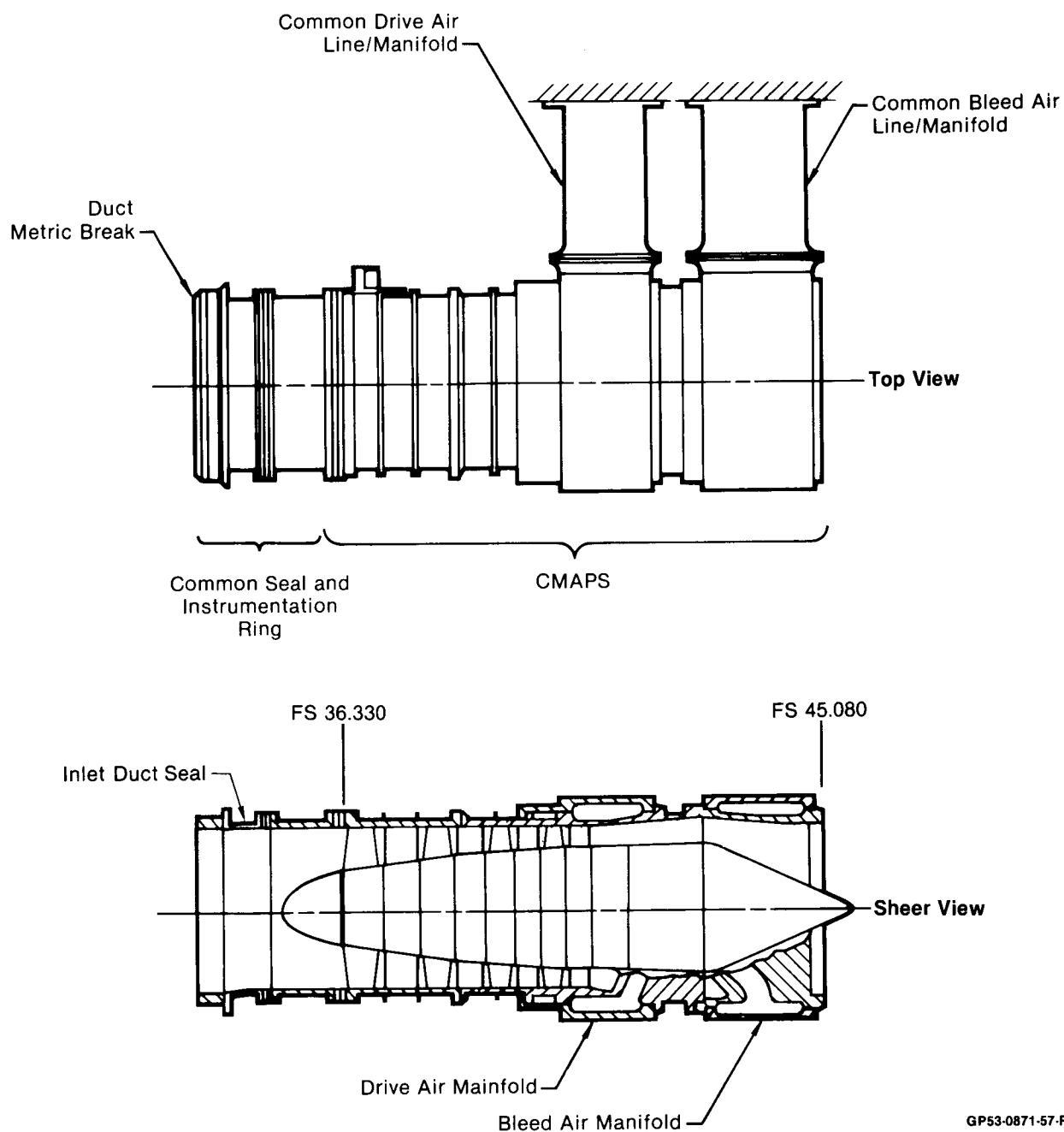


Figure 2-20. CMAPS Mode Nacelle Core Hardware

Independent control of the high pressure air through the drive and bleed lines in the support sting allowed the simulator to produce desired combinations of inlet and nozzle flow conditions independently. A schematic of the simulator flow path is shown in Figure 2-21.

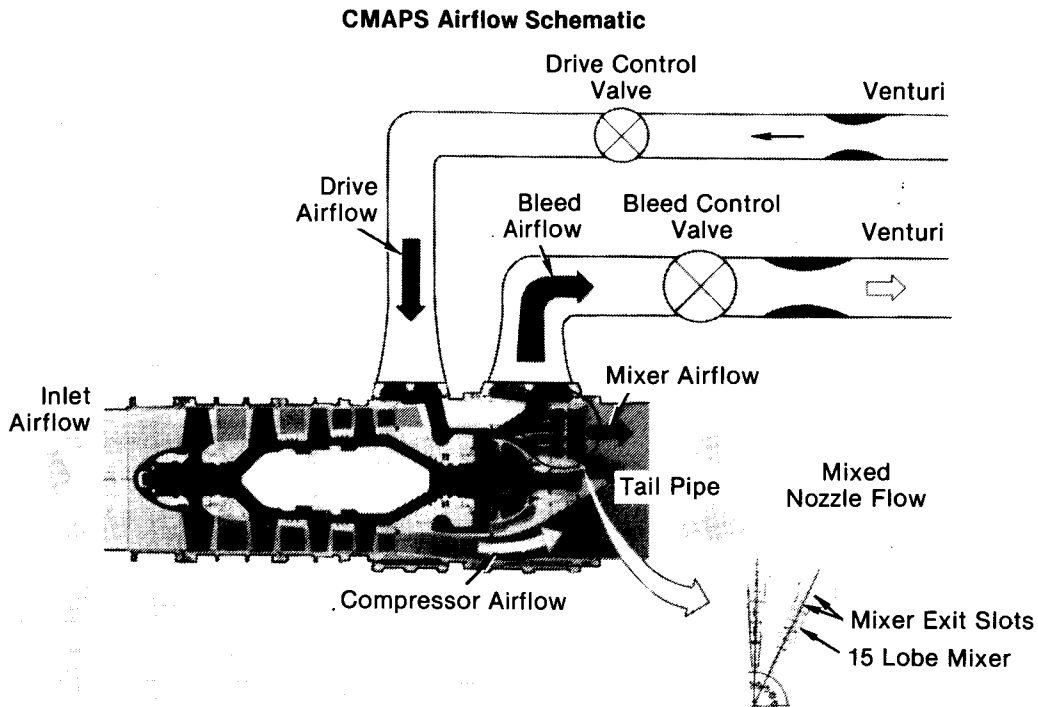


Figure 2-21. Simulator Internal Flow Paths

The Simulated Aircraft and the Nozzle Extension configurations, as well as the Common Baseline configuration, were all tested in the CMAPS mode. Data was acquired for the Simulated Aircraft configuration in the form of angle-of-attack (AOA) sweeps and engine pressure ratio (EPR) sweeps. The Nozzle Extension configuration data was taken for AOA sweeps at various canard angles and mass flow ratios (MFRs). Only the largest exit area chokes were used in the Nozzle Extension configuration for the CMAPS mode. MFR was controlled solely by the simulators. The Common Baseline configuration was tested in each test mode to isolate tunnel induced effects due to separate tunnel entries. A complete run matrix for the CMAPS mode is included in Appendix B.

2.1.3 Jet-Effects Mode - Plenum chambers replaced the simulators in the engine nacelles during the Jet-Effects mode testing. The nacelle hardware for the Jet-Effects mode is shown in Figure 2-22. The drive and bleed lines in the support sting were used to provide two independently controlled high pressure air sources to the plenum. The air was then mixed in the plenum and exhausted through the ALBEN's. This dual-flow plenum design was intended to duplicate the internal airflow paths and resultant pressure and temperature patterns encountered in the CMAPS mode. Although not required, the inlet duct seal was retained during the Jet-Effects mode in order to maintain a common seal arrangement between the three test modes.

Only the Common Baseline configuration was tested in this mode. Data was acquired with jet-on and jet-off AOA sweeps and nozzle pressure ratio (NPR) sweeps. A complete run matrix for the Jet-Effects mode is included in Appendix B.

2.1.4 Flow-Through Mode - Flow-through ducts were interchanged with the plenum chambers or simulators to build-up the Flow-Through mode. The non-metric duct units, Figure 2-23, were designed to model the propulsion simulators with respect to the internal inlet flow, particularly at the simulated engine face. Therefore, the Plane 2 total pressure rakes, inlet duct seals, and compressor face hubs were identical for Flow-Through and Simulator modes. Therefore, the Plane 2 total pressure rakes, inlet duct seals, and compressor face hubs were identical for Flow-Through and Simulator modes.

The Nozzle Extension configuration and the Nozzle Extension Baseline, as well as the Common Baseline, were tested in this mode. Inlet MFR was controlled in the Nozzle Extension configuration with four nozzle chokes sized as follows: 12.49 cm², 18.74 cm², 26.11 cm², and 34.25 cm². The internal flow path and exit choke geometry is shown in Figure 2-24. An ejector system was

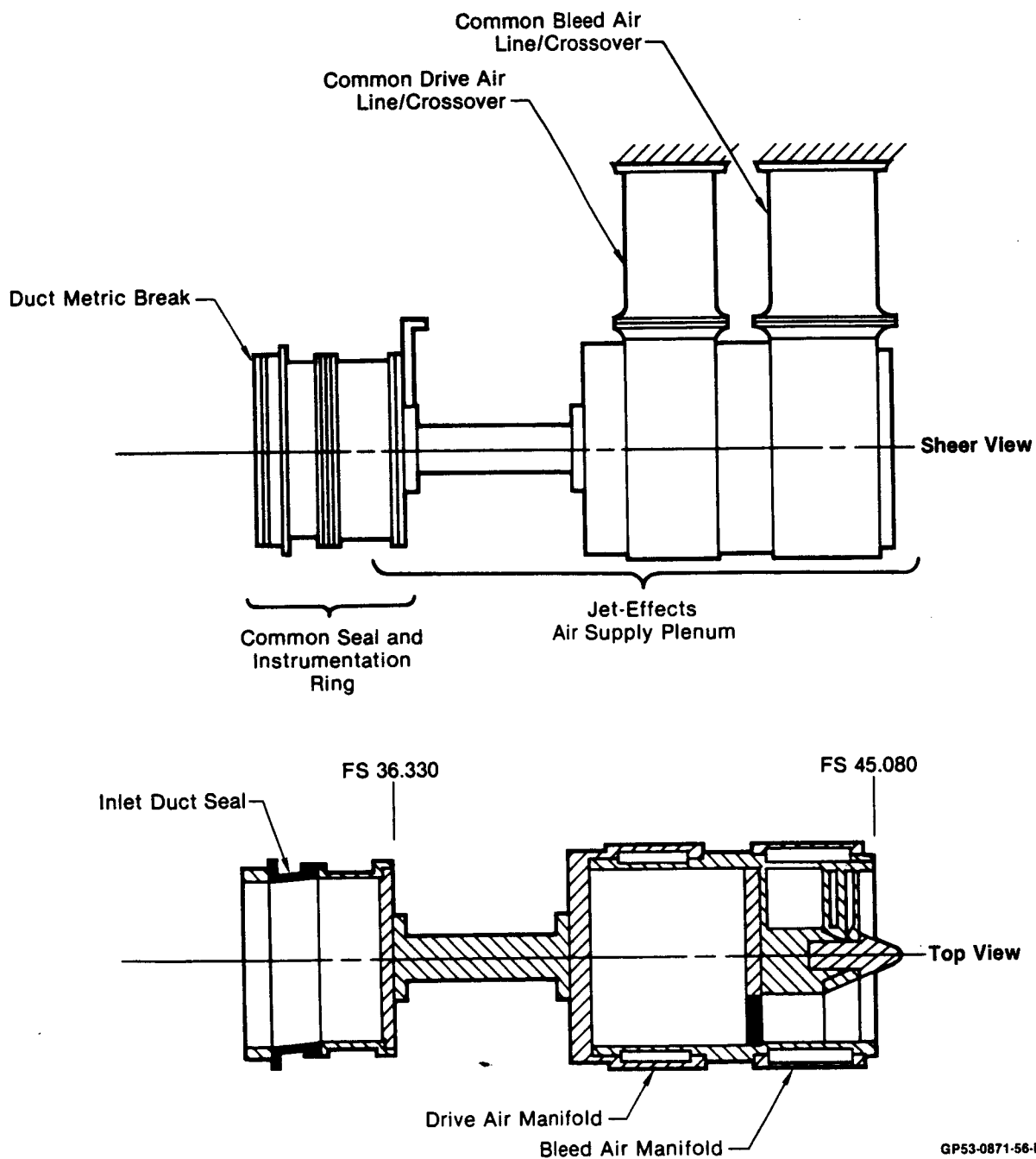
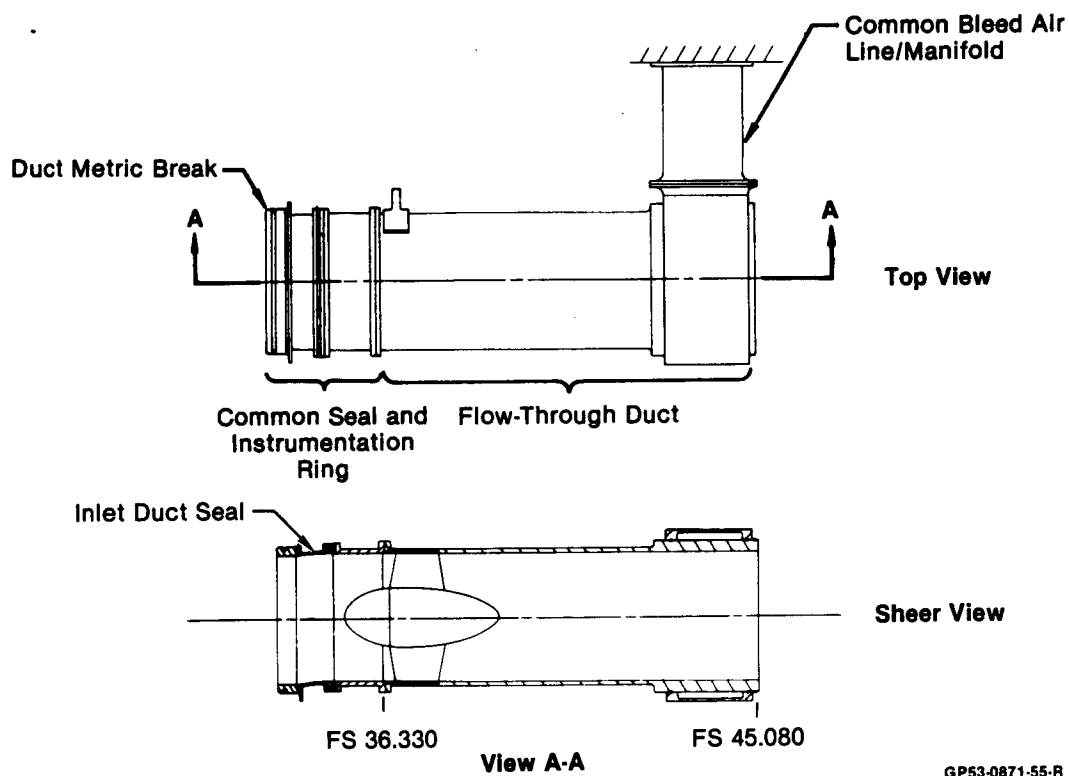
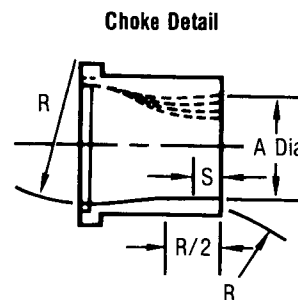
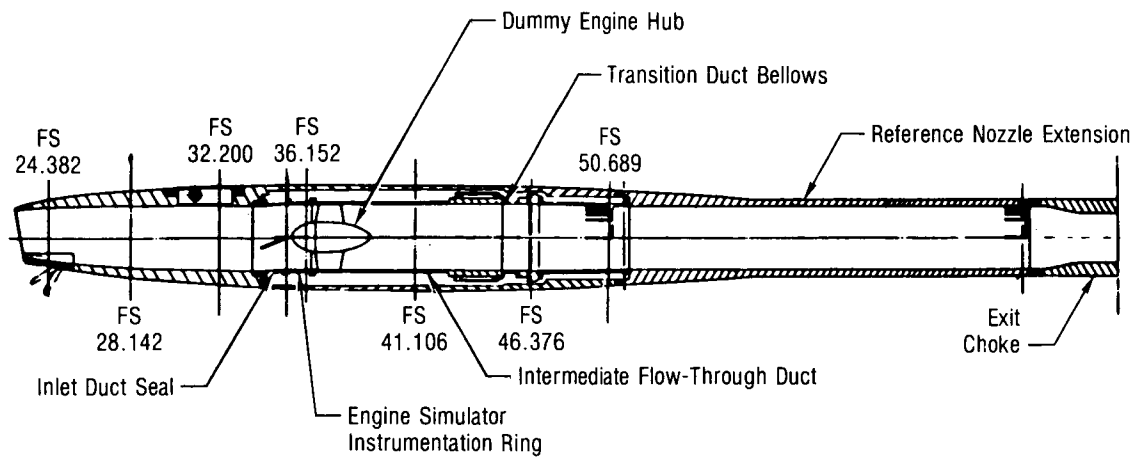


Figure 2-22. Jet-Effects Mode Nacelle Core Hardware



GP53-0871-55-R

Figure 2-23. Flow-Through Mode Nacelle Core Hardware



Convergent Choke Geometry

| Drawing | A | A/2 | A _{throat} | R | S |
|------------------|-------------------------|-------------------------|---|--------------------------|-------------------------|
| 254-4452-5, -6 | 6.604 cm (2.600 in.) | 3.302 cm (1.300 in.) | 34.252 cm ² (5.309 in. ²) | 12.637 cm (4.975 in.) | 1.651 cm (0.650 in.) |
| 254-4452-7, -8 | 5.766 cm (2.270 in.) | 2.883 cm (1.135 in.) | 26.110 cm ² (4.047 in. ²) | 8.273 cm (3.257 in.) | 1.440 cm (0.567 in.) |
| 254-4452-9, -10 | 4.887 cm (1.924 in.) | 2.443 cm (0.962 in.) | 18.755 cm ² (2.907 in. ²) | 6.711 cm (2.642 in.) | 1.234 cm (0.486 in.) |
| 254-4452-11, -12 | 3.988 cm (1.570 in.) | 1.994 cm (0.785 in.) | 12.490 cm ² (1.936 in. ²) | 6.005 cm (2.364 in.) | 0.996 cm (0.392 in.) |

GP53-0871-34-R

Figure 2-24. Flow-Through Mode With Nozzle Extensions
Internal Flow Path and Exit Chokes

connected to the extension assemblies for Mach 0.4 and 0.6 testing, since the ram air was not sufficient to provide maximum airflow. The ejector installation is shown in Figure 2-25. The data was acquired with AOA sweeps at constant canard angles and inlet MFRs as shown in Appendix B.

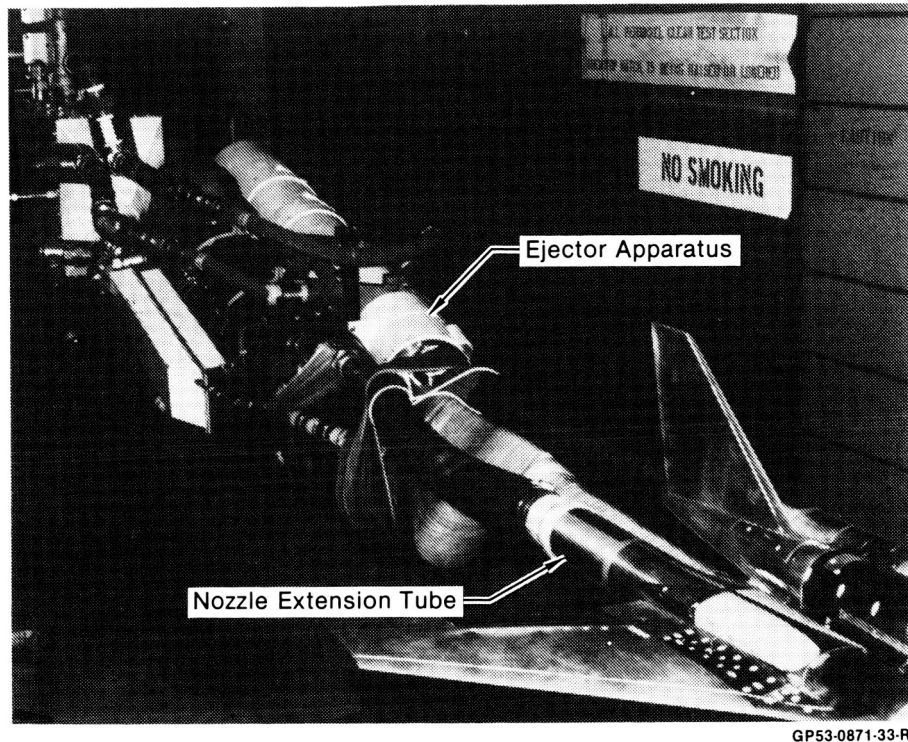
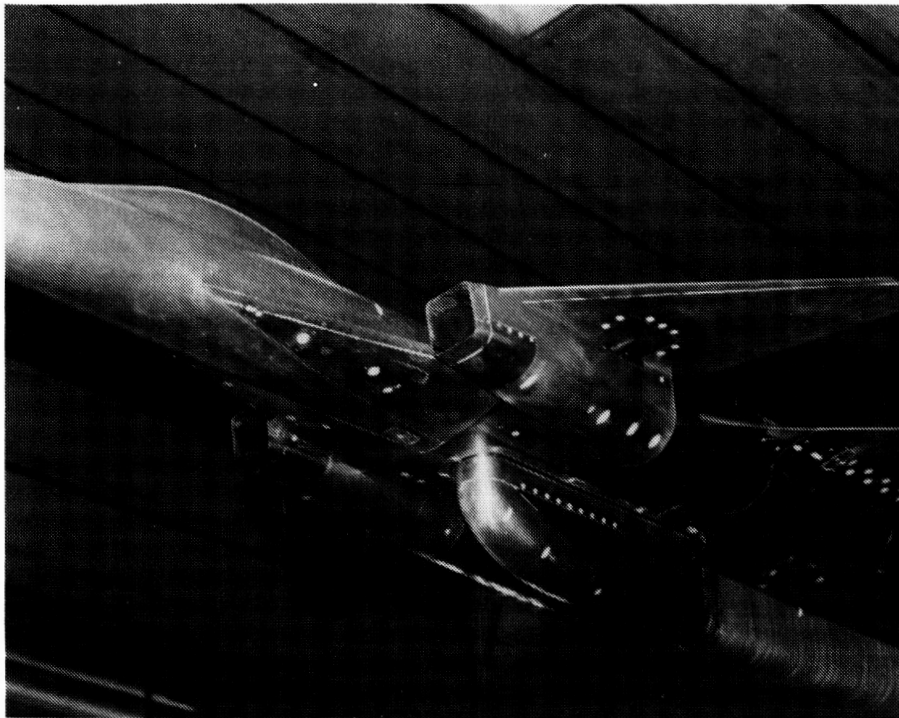


Figure 2-25. Ejector Apparatus Connected to Nozzle Extensions

2.2 INLET/EXHAUST SYSTEMS - Two inlet and two exhaust systems were tested on the twin podded engine nacelles.

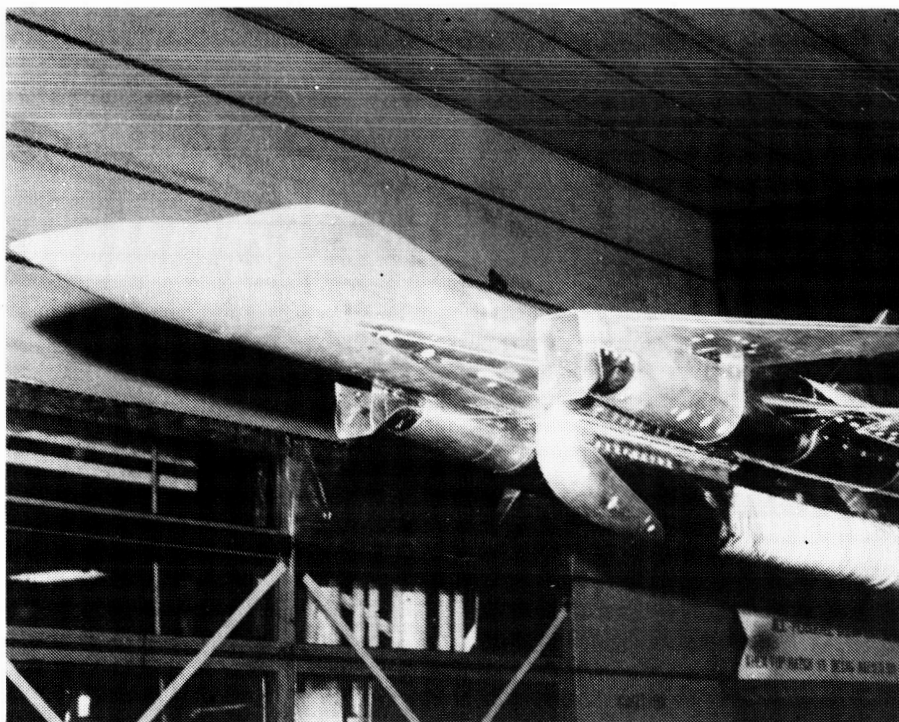
2.2.1 Inlet Systems - The inlet was tested in both a flowing and a faired configuration. The flowing inlet was a rectangular, normal shock design with 15° scarf angle and a rotating lower cowl lip. The flowing inlet system with 0° and 45° cowl lip rotations is shown in Figures 2-26 and 2-27 respectively. The cowl lip rotation is to reduce flow separation around the lip at high angle-of-attack conditions. However, only a limited amount of testing was performed on the 45° lip rotation configuration.

ORIGINAL PAGE IS
OF POOR QUALITY



GP53-0871-26-R

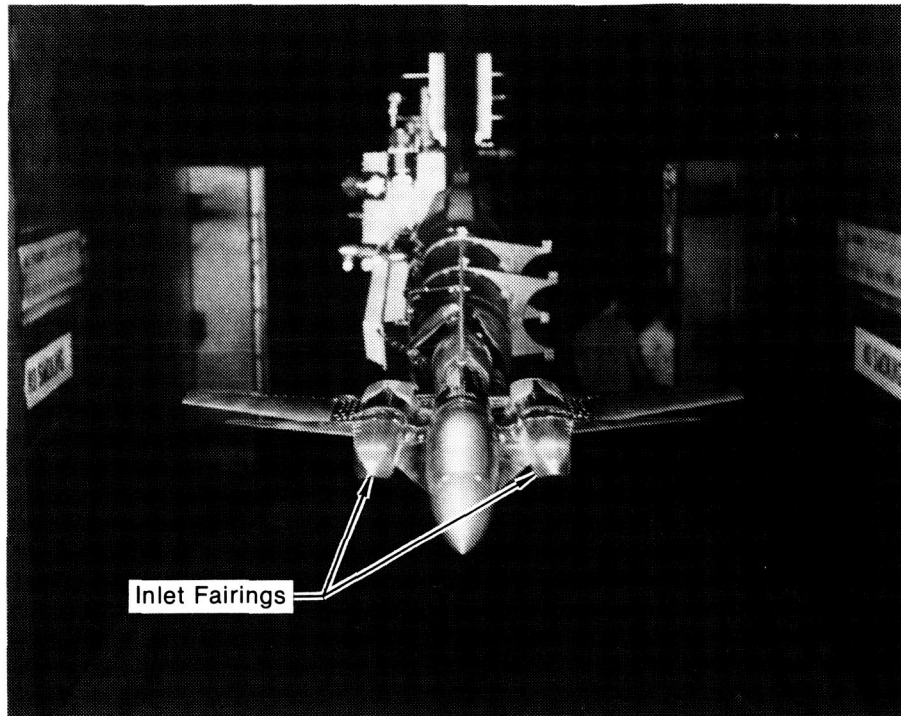
Figure 2-26. Flowing Inlet System With 0° Cowl Lip Rotation



GP53-0666-60-R

Figure 2-27. Flowing Inlet System With 45° Cowl Lip Rotation

The faired inlet configuration was formed by installing pyramidal fairings to the flowing inlets with 0° lip rotation. The fairing shapes represented simple forward extensions of the local cowl moldlines. The model with the faired inlet system is shown in Figure 2-28.

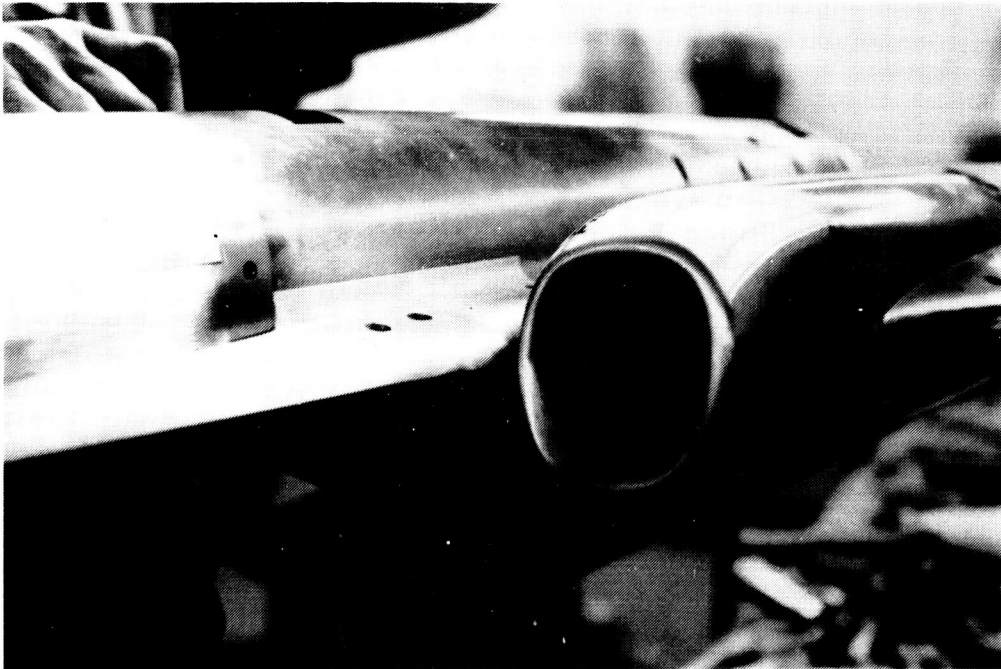


GP53-0871-32-R

Figure 2-28. Faired Inlet System on Test Vehicle

A second flowing inlet system was also fabricated for use on the alternate aircraft configuration (see Figure 1-2). However, it was never tested due to time constraints. This inlet was a circular design with a 13° reverse scarf angle, Figure 2-29.

The detailed design of these inlet systems is presented in Reference 7.

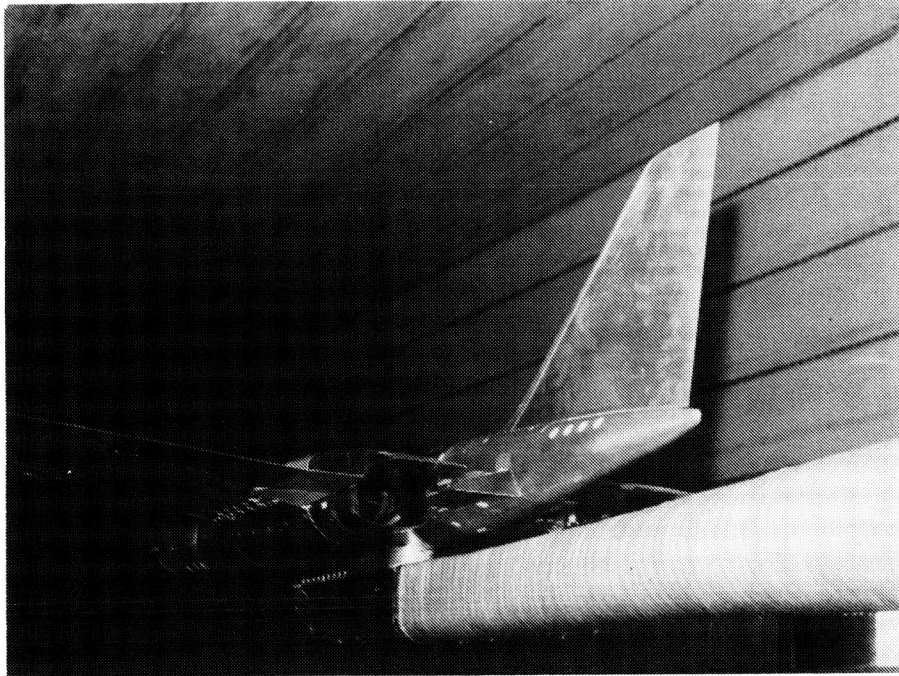


GP53-0871-14-R

Figure 2-29. Untested Inlet for Alternate Configuration

2.2.2 Exhaust Systems - The exhaust system was tested with both ALBENS and nozzle extension tubes. The ALBEN and nozzle extension systems were both non-metric to the internal aircraft balance. Both were pressure instrumented to obtain their external aerodynamic characteristics. The metric break and common station for the airframe/ exhaust system interface was at model station 50.689.

The ALBEN model was designed to simulate various power settings and thrust vectoring angles. The model configured with the ALBENS is shown in Figure 2-30. Two different power settings (dry and afterburning) were tested by interchanging the lower flap components, which change the throat and exit areas. Interchangeable upper flap components were used to configure the ALBENS for 0°, 20°, or 30° of thrust vectoring (vector angle measured from nominal horizontal reference plane, positive trailing edge down).



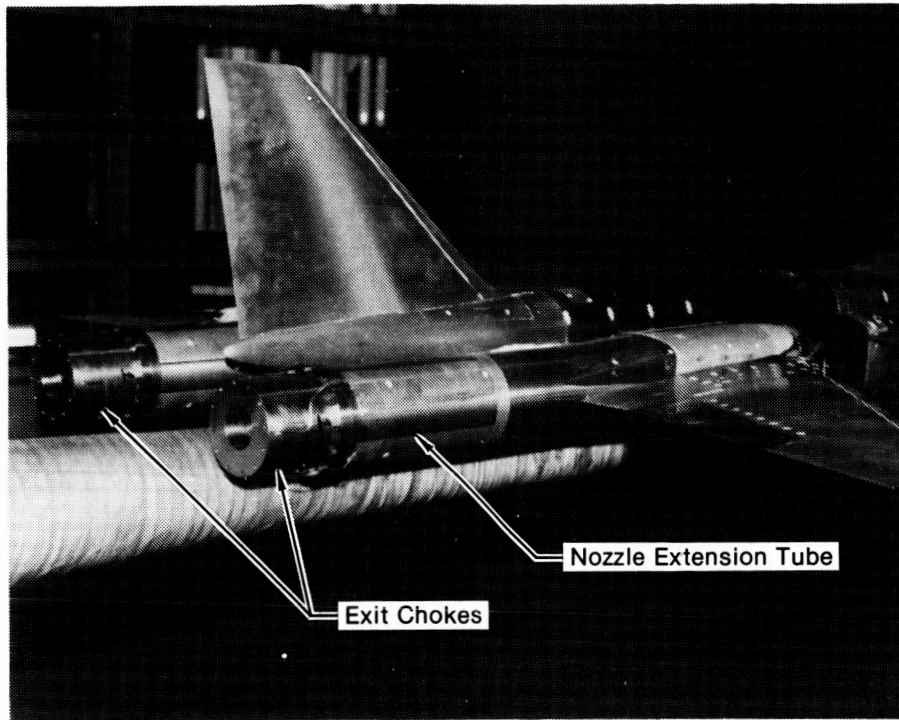
GP53-0871-31-R

Figure 2-30. Unvectored A/B ALBEN System on Test Vehicle

Nozzle extension assemblies replaced the ALBENS in order to isolate the flowing inlet effects from those associated with the exhaust plume. The extension tubes were sized such that the exhaust plume and base area effects would not be felt on the metric surfaces of the model. The nozzle extension installation is shown in Figure 2-31. Exit chokes were attached to the extension tubes to control inlet mass flow ratio (MFR). Four interchangeable chokes were used in the Flow-Through mode to cover the operating MFR range of the propulsion simulator.

2.3 TEST CONFIGURATIONS - The four test configurations (Figure 2-4) were used to identify the presence of flowfield coupling and measure the net effect. These configurations were tested in the three test modes as summarized in Figure 2-32.

ORIGINAL PAGE IS
OF POOR QUALITY



GP53-0871-30-R

Figure 2-31. Nozzle Extension System on Test Vehicle

2.3.1 Common Baseline Configuration - The Common Baseline configuration is defined with faired inlets and the ALBEN exhaust system. This configuration, with unvectored A/B ALBENS in the jet-off condition, was tested in all three test modes to isolate any bias errors due to the separate tunnel entries.

The unvectored dry power ALBENS and vectored A/B ALBENS were also tested but only in the Jet-Effects mode. The A/B ALBEN system was tested at 0°, 20°, and 30° thrust vectoring. The 30° vectoring case was different from all other Jet-Effects configurations in that the wing flaps were also deflected 30°. This build-up, tested only at Mach 0.4, simulated the vehicle in a high-lift low-speed mode.

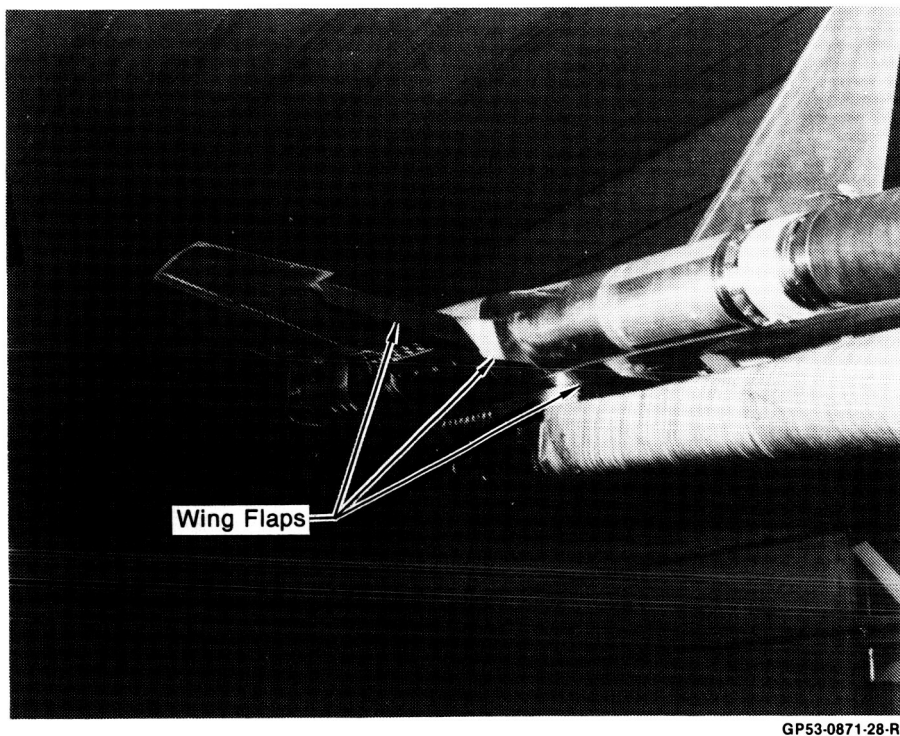
| Configuration | Test Mode | Mach | MFR | NPR | α (deg) | δ_c (deg) |
|--|-----------|------|-----------|------------|----------------|------------------|
| Common Baseline $\delta_N = 0^\circ$ $\delta_F = 0^\circ$ A/B ALBEN | F/T | 0.4 | N/A | 1.0 | -1 → 18 | +5 → -15 |
| | | 0.6 | | | | |
| | | 0.9 | | | | |
| | | 1.2 | | | -1 → 10 | +5 → -10 |
| | | 1.4 | | | -1 → 9 | |
| | J/E | 0.4 | N/A | 1.0 → 4.0 | -1 → 18 | +5 → -15 |
| | | 0.6 | | 1.0 → 6.0 | | -5 |
| | | 0.9 | | 1.0 → 8.5 | | -5 |
| | | 1.2 | | 1.0 → 11.0 | -1 → 6 | 0 |
| | | 1.4 | | 1.0 → 14.0 | -1 → 6 | 0 |
| | CMAPS | 0.4 | N/A | 1.0 | -1 → 16 | +5 → -15 |
| | | 0.6 | | | | -5 |
| | | 0.9 | | | | -5 |
| | | 1.2 | | | -1 → 6 | 0 |
| | | 1.4 | | | | 0 |
| Common Baseline $\delta_N = 20^\circ$ $\delta_F = 0^\circ$ A/B ALBEN | J/E | 0.4 | N/A | 1.0 → 4.0 | -1 → 20 | -5 |
| | | 0.6 | | 1.0 → 6.0 | -1 → 22 | -5 |
| | | 0.9 | | 1.0 → 8.0 | -1 → 18 | 0 → -15 |
| | | 1.2 | | 1.0 → 12.0 | -1 → 7 | 0 |
| Common Baseline $\delta_N = 30^\circ$ $\delta_F = 0$ A/B ALBEN | J/E | 0.4 | N/A | 1.0 → 4.0 | -1 → 20 | +5 → -5 |
| Common Baseline $\delta_N = 0^\circ$ $\delta_F = 0^\circ$ Dry ALBEN | J/E | 0.4 | N/A | 1.0 → 6.0 | -1 → 9 | 0, -5 |
| | | 0.6 | | 1.0 → 6.0 | | -5 |
| | | 0.9 | | 1.0 → 6.0 | | 0, -5 |
| Nozzle Extension Baseline | F/T | 0.4 | N/A | 1.0 | -1 → 21 | -5 |
| | | 0.6 | | | | |
| | | 0.9 | | | | -5, -15 |
| | | 1.2 | | | -1 → 6 | 0 |
| | | 1.4 | | | | |
| Nozzle Extension | F/T | 0.4 | 0.5 → 1.2 | N/A | -1 → 22 | +5 → -15 |
| | | 0.6 | 0.3 → 0.9 | | | 0 → -15 |
| | | 0.9 | 0.3 → 0.9 | | | 0 → -15 |
| | | 1.2 | 0.3 → 0.9 | | -1 → 6 | 0 → -10 |
| | | 1.4 | 0.3 → 0.9 | | | 0 → -10 |
| | CMAPS | 0.4 | 0.5 → 1.2 | N/A | -1 → 17 | +5 → -15 |
| | | 0.6 | 0.3 → 0.9 | | | 0 → -10 |
| | | 0.9 | 0.3 → 0.9 | | | 0 → -10 |
| | | 1.2 | 0.3 → 0.9 | | -1 → 7 | 0 → -10 |
| | | 1.4 | 0.3 → 0.9 | | | 0 → -5 |
| Simulated Aircraft | CMAPS | 0.4 | 0.7 → 1.2 | 1.0 → 3.5 | 0 → 17 | 0 → -15 |
| | | 0.6 | 0.3 → 0.9 | 1.0 → 4.0 | 0 → 17 | 0 → -10 |
| | | 0.9 | 0.4 → 0.9 | 1.0 → 5.0 | 0 → 18 | 0 → -10 |
| | | 1.2 | 0.3 → 0.8 | 1.0 → 7.5 | 0 → 6 | 0, -5 |
| | | 1.4 | 0.3 → 0.8 | 1.0 → 9.5 | 0 → 7 | 0, -5 |

GP53-0871-29-R

Figure 2-32. Test Summary

ORIGINAL PAGE IS
OF POOR QUALITY

2.3.2 Nozzle Extension Configuration - The Nozzle Extension configuration is defined as having the flowing inlet system and the nozzle extension exhaust system. The inlet was tested with both the 0° and 45° cowl lip rotations. Most of the 45° lip cases were tested with the wing flaps deflected 30° as shown in Figure 2-33.



GP53-0871-28-R

Figure 2-33. Nozzle Extension Configuration With Wing Flaps Deflected 30°

This configuration models the flowing inlet effects on the airframe independent of the exhaust effects.

2.3.3 Nozzle Extension Baseline Configuration - The Nozzle Extension Baseline configuration is defined as having the faired inlet system and the nozzle extension exhaust system. In this configuration, only one canard angle was tested for each Mach number. The purpose of this build-up was to account for the nozzle extension effects on the airframe as compared to the ALBEN installation.

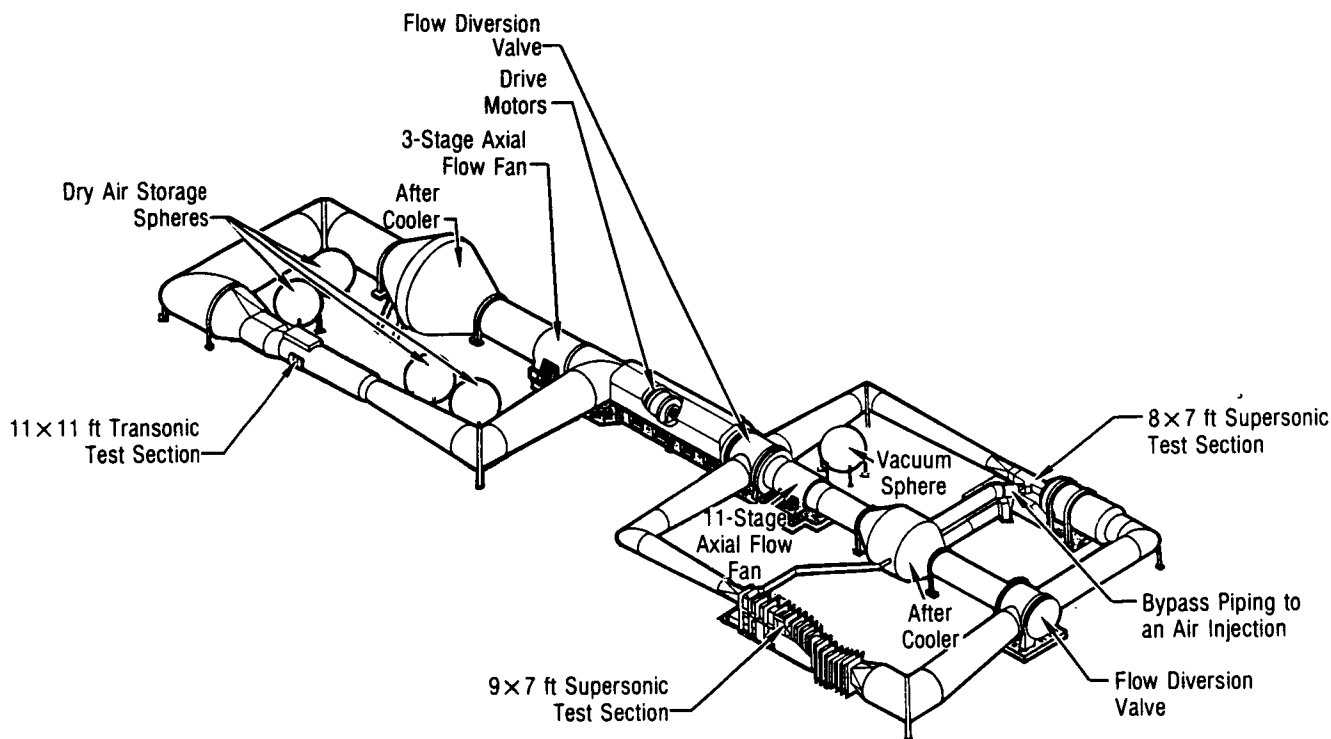
2.3.4 Simulated Aircraft Configuration - The Simulated Aircraft configuration is defined with flowing inlets and the ALBEN exhaust system. This configuration was tested with only the flowing inlets at 0° lip rotation and the ALBENS in the afterburning (A/B) position with 0° thrust vectoring. This configuration closely models an aircraft in flight, with jet effects, inlet effects, and coupling effects measured simultaneously.

3. FACILITIES, INSTRUMENTATION AND DATA REDUCTION PROCEDURES

The nature of testing with propulsion simulators requires unique data acquisition and data reduction techniques. Even the Jet-Effects and Flow-Through modes were configured in slightly unconventional metric arrangements to reduce bias errors between test techniques (see Section 2.1). The facilities, instrumentation and data reduction used during this program are described in this section.

3.1 FACILITY - All testing was performed at NASA-Ames Research Center in the Eleven-by-Eleven-Foot Transonic Wind Tunnel (Moffett Field, California). This facility is a closed-return, variable density tunnel. It employs a fixed geometry, ventilated throat and a single-jack flexible nozzle. Airflow is produced by a three-stage/axial-flow compressor which is powered by four wound-rotor, variable-speed induction motors. The closed test section measures 11.0 feet high, 11.0 feet wide and 22.0 feet long. Flow speeds up to Mach 1.4 with corresponding Reynolds numbers of 9.4 million per foot are possible. The 11 ft. tunnel is one of three wind tunnels in the NASA-Ames Unitary Plan Wind Tunnel Complex. A schematic of the unitary complex and corresponding operating characteristics is shown in Figure 3-1.

3.2 INSTRUMENTATION - The model was instrumented to obtain the aerodynamic characteristics of the airframe and the nozzles. These characteristics were based on measurements of model forces and moments, pressures, temperatures, canard angle, and angle of attack. The airflow through the model was also calculated. A list of the instrumentation which is common to the three test modes is presented in Figure 3-2. Each propulsion simulator contained additional instrumentation to monitor its health and performance.



Major Components of the Unitary Plan Wind Tunnels

| Unitary Test Sections | Height and Width (ft) | Speed Range (Mach) | Stagnation Pressure (atm) | Stagnation Temperature (°R) | Reynolds Number (ft) | Dynamic Pressure (lb/ft ²) | Special Features |
|-----------------------|-----------------------|--------------------|---------------------------|-----------------------------|-------------------------|--|-------------------------------|
| 11 ft Transonic | 11×11 | 0.70 - 1.4 | 0.5 - 2.25 | 580 | $1.7 - 9.4 \times 10^6$ | 250 - 2,000 | Slotted Test Section, 4 Watts |
| 9×7 ft Supersonic | 7×9 | 1.55 - 2.5 | 0.3 - 2.0 | 580 | $1.5 - 6.5 \times 10^6$ | 200 - 1,450 | |
| 8×7 ft Supersonic | 8×7 | 2.45 - 3.5 | 0.3 - 2.0 | 580 | $1.0 - 5.0 \times 10^6$ | 200 - 1,000 | |

GP53-0871-23-R

Figure 3-1. NASA-Ames Unitary Plan Wind Tunnels

| 1) Forces and Moments | | | |
|--|----------------------------|---------------------------------|------------------------------|
| Measurands | Components | Balance | |
| Aircraft Balance Forces and Moments | 6 (NF, AF, SF, PM, RM, YM) | Task Mark XXXII 2.5 in. Balance | |
| 2) Pressure Instrumentation | | | |
| | Number | Range | Sensor |
| Inner Wing Surface Static Pressures | 14 | ± 15 psid | Internal Scanivalve |
| Outer Wing Surface Static Pressures | 27 | ± 15 psid | Internal Scanivalve |
| Centerline Surface Static Pressures | 10 | ± 15 psid | Internal Scanivalve |
| Nacelle Surface Static Pressures | 45 | ± 15 psid | Internal Scanivalve |
| Nozzle Boattail Surface Static Pressures | 50 | ± 15 psid | Internal Scanivalve |
| Internal Cavity Pressures | 16 | ± 15 psid | Internal Scanivalve |
| Nacelle/Nozzle Seal Pressures | 8 | ± 15 psid | Internal Scanivalve |
| Nozzle Total Pressures | 18 | ± 15 psid | Internal Scanivalve |
| Nozzle Static Pressures | 8 | ± 15 psid | Internal Scanivalve |
| Transition Duct Total Pressures | 8 | 0 – 50 psia | |
| 3) Temperature Instrumentation | | | |
| Balance Housing Temperature | 10 | 60° – 200°F | Iron/Constantan Thermocouple |
| Transition Duct Total Temperature | 4 | 60° – 400°F | Iron/Constantan Thermocouple |
| 4) Miscellaneous | | | |
| Canard Deflection | 2 | – 10° to + 20° | Potentiometer |
| Angle-of-Attack | 1 | – 10° to + 40° | Internal Angle-of-Attack |
| Nozzle Mass Flow Rate | 4 | 0 to 7 lb/sec | Venturi Flowmeter |
| Canard Root Bending Moment | 1 | ± 1,500 in.-lb | Strain Gage |

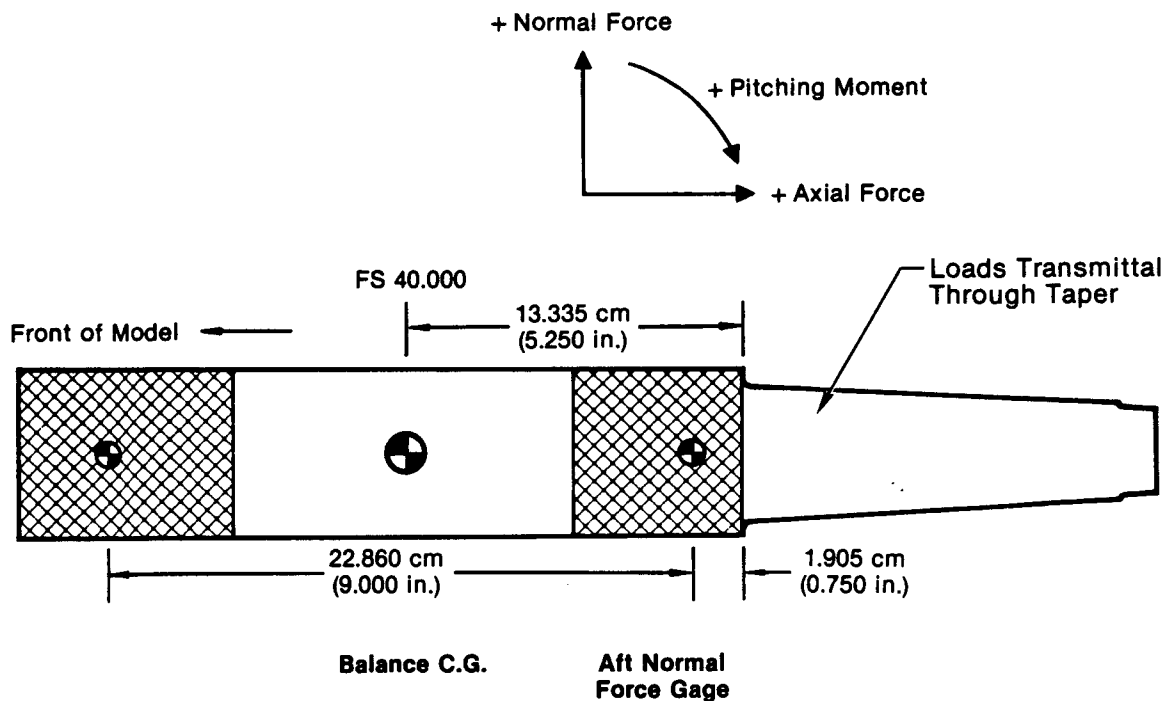
GP53-0909-3-R

Figure 3-2. Model Instrumentation Common to All Test Modes

Only the instrumentation required for the force and moment data acquisition is described in this section. The external pressure instrumentation is fully described in Volume I of this report (Reference 1).

3.2.1 Force and Moment Balance and Thermal Control System -

The external aerodynamic loads were measured with a Task MK XXXII strain gage balance unit. The six component balance measured all forces and moments, except those on the ALBEN or nozzle extension assemblies. The aerodynamic loads are transmitted to the 6.350 cm (2.5 in.) diameter balance through the balance taper and taper adapter. The balance physical dimensions and orientation are shown in Figure 3-3. This non-standard balance installation with the taper loaded, resulted from the required locations of the drive and bleed air lines inside the model.

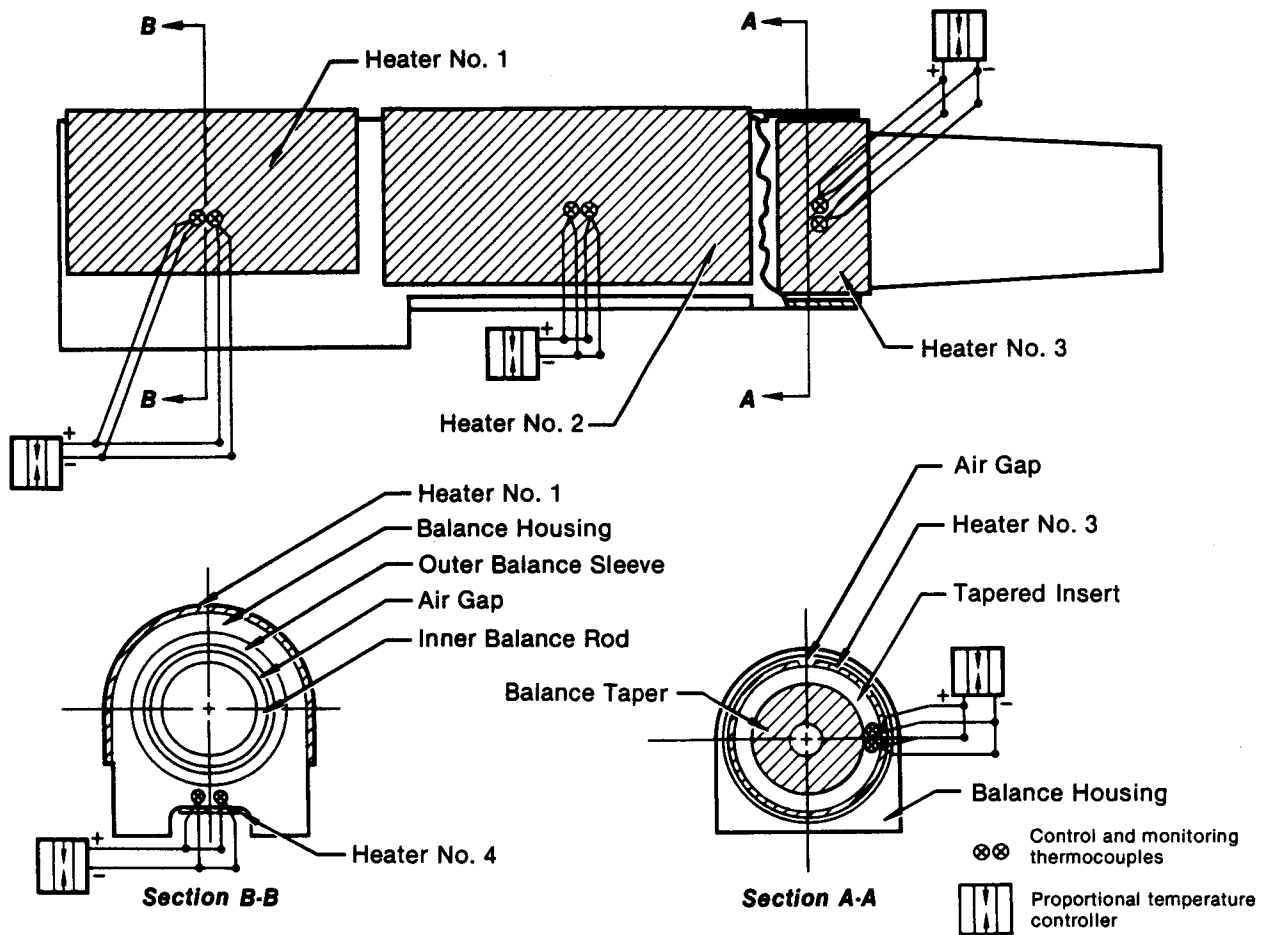


GP53-0871-53-R

Figure 3-3. Model Balance

Since the force balance was subjected to a wide range of temperature environments in the three test modes, a balance thermal control system was provided to maintain the balance at a constant and uniform selected temperature. This was to prevent bias errors in the force balance output due to thermal gradients and levels.

The balance housing was divided into four heating zones, each with a heater blanket, controller and thermocouple feedback loop. The balance thermal control system configuration is shown in Figure 3-4. The thermal control system was designed to limit temperature gradients to about 1.5°C at an operating temperature of 71°C (160°F). The heater power density for steady state operation at selected tunnel conditions is given in Figure 3-5.



GP53-0871-54-R

Figure 3-4. Balance Thermal Control System

| Test Condition | Heater Number | Power Density (watts/cm ²) | Power (watts) |
|---------------------------------------|---------------|--|---------------|
| System Start-Up | 1 | 0.178 | 35.35 |
| • T _{tunnel} = 26.67°C | 2 | 0.197 | 36.61 |
| • 1 hr Required to Reach Steady State | 3 | 0.716 | 37.34 |
| | 4 | 1.184 | 37.34 |
| Flow-Through Mode ⁽¹⁾ | 1 | 0.037 | 7.45 |
| • M _{tunnel} = 1.4 | 2 | 0.059 | 13.86 |
| | 3 | 0.454 | 34.05 |
| | 4 | 0.581 | 19.22 |
| Simulator Mode ⁽¹⁾ | 1 | 0.031 | 6.09 |
| • M _{tunnel} = 1.4 | 2 | 0.019 | 4.54 |
| • T _{drive} = 93.33°C | 3 | 0.426 | 31.92 |
| • T _{bleed} = 73.89°C | 4 | 0.532 | 17.56 |
| Simulator Mode ⁽¹⁾ | 1 | 0.033 | 6.55 |
| M _{tunnel} = 1.4 | 2 | 0.036 | 8.24 |
| • T _{drive} = 93.33°C | 3 | 0.414 | 31.08 |
| • T _{bleed} = 10°C | 4 | 0.544 | 17.97 |

Notes:

(1) Steady state operation

(2) The area of each heater is as follows

| Heater no. | Area |
|------------|---|
| 1 | 198.09 cm ² (30.7 in. ²) |
| 2 | 234.85 cm ² (36.4 in. ²) |
| 3 | 74.85 cm ² (11.6 in. ²) |
| 4 | 32.91 cm ² (5.1 in. ²) |

GP53-0871-22-R

Figure 3-5. Heater Blanket Power Density

3.2.2 Model Pressure Instrumentation - A total of 226 pressures were measured on the model, including external static pressures, internal total pressures, seal and cavity pressures, and Scanivalve reference and calibrate pressures. The overall external surface tap layout is presented in Figure 3-6 and further detailed in Volume I of this report, Reference (5).

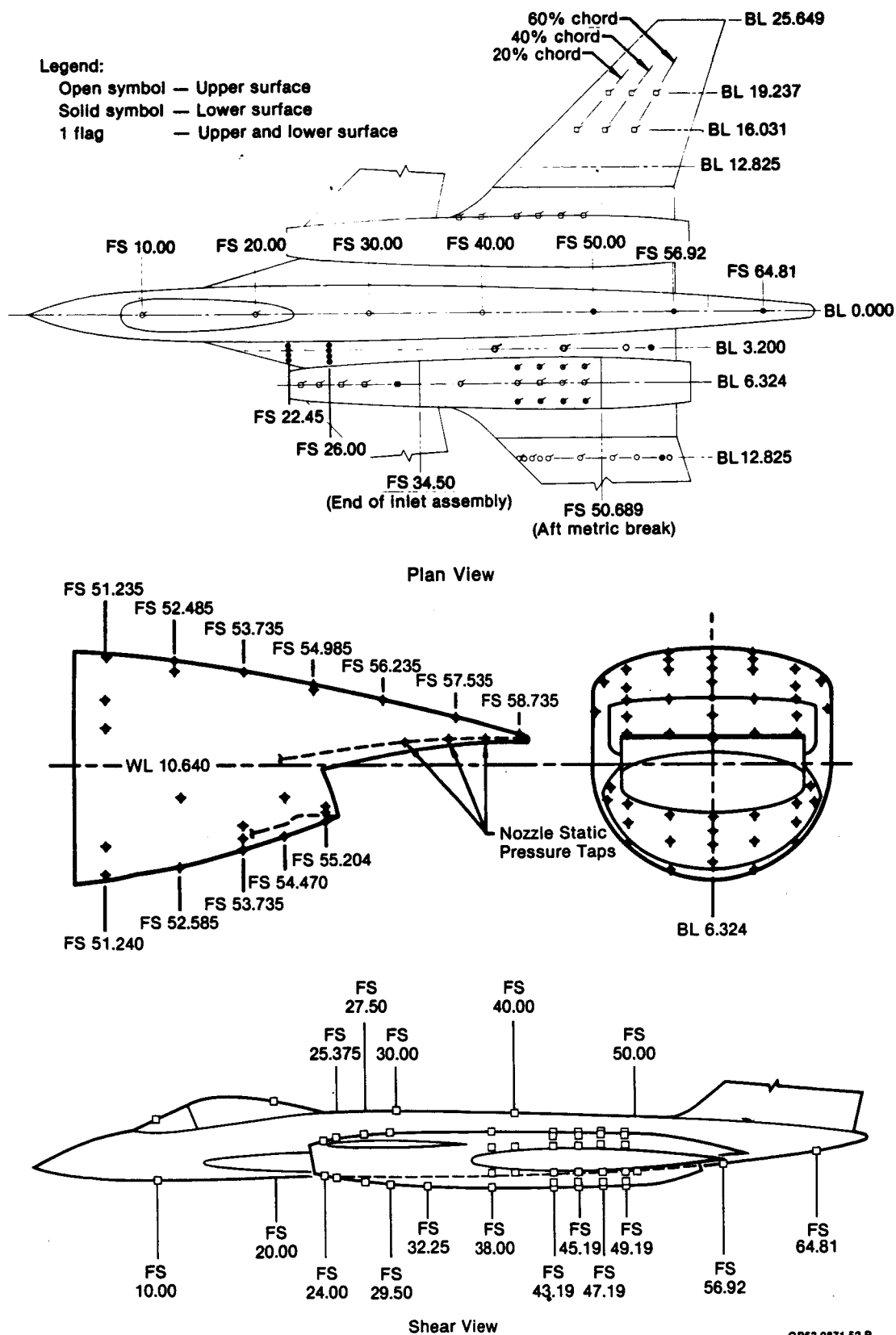


Figure 3-6. Location of Model External Pressure Instrumentation

Six Scanivalve modules were used to measure the model pressures. A four module, S-type Scanivalve was located in the forward fuselage and a two module, S-type Scanivalve was located in the aft fuselage as shown in Figure 3-7. Each Scanivalve was a synchronous, 48-port unit using a 15 psid transducer. The Scanivalves and transducers were provided by NASA-Ames.

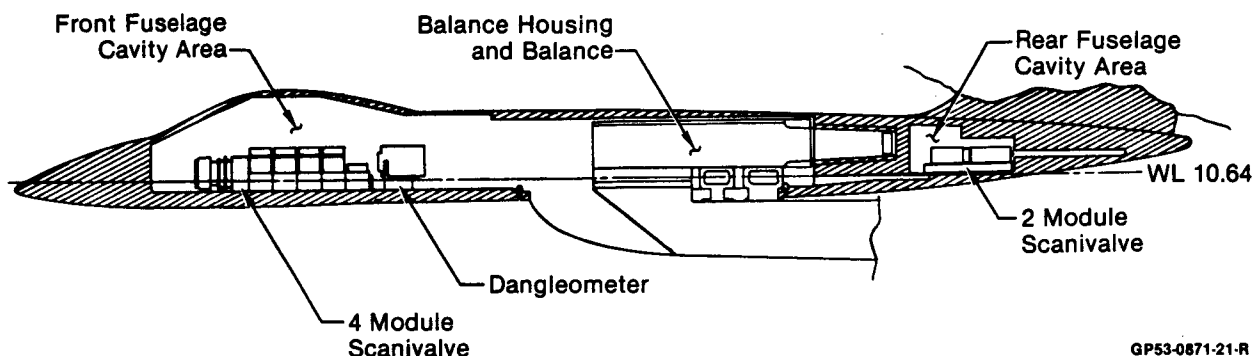
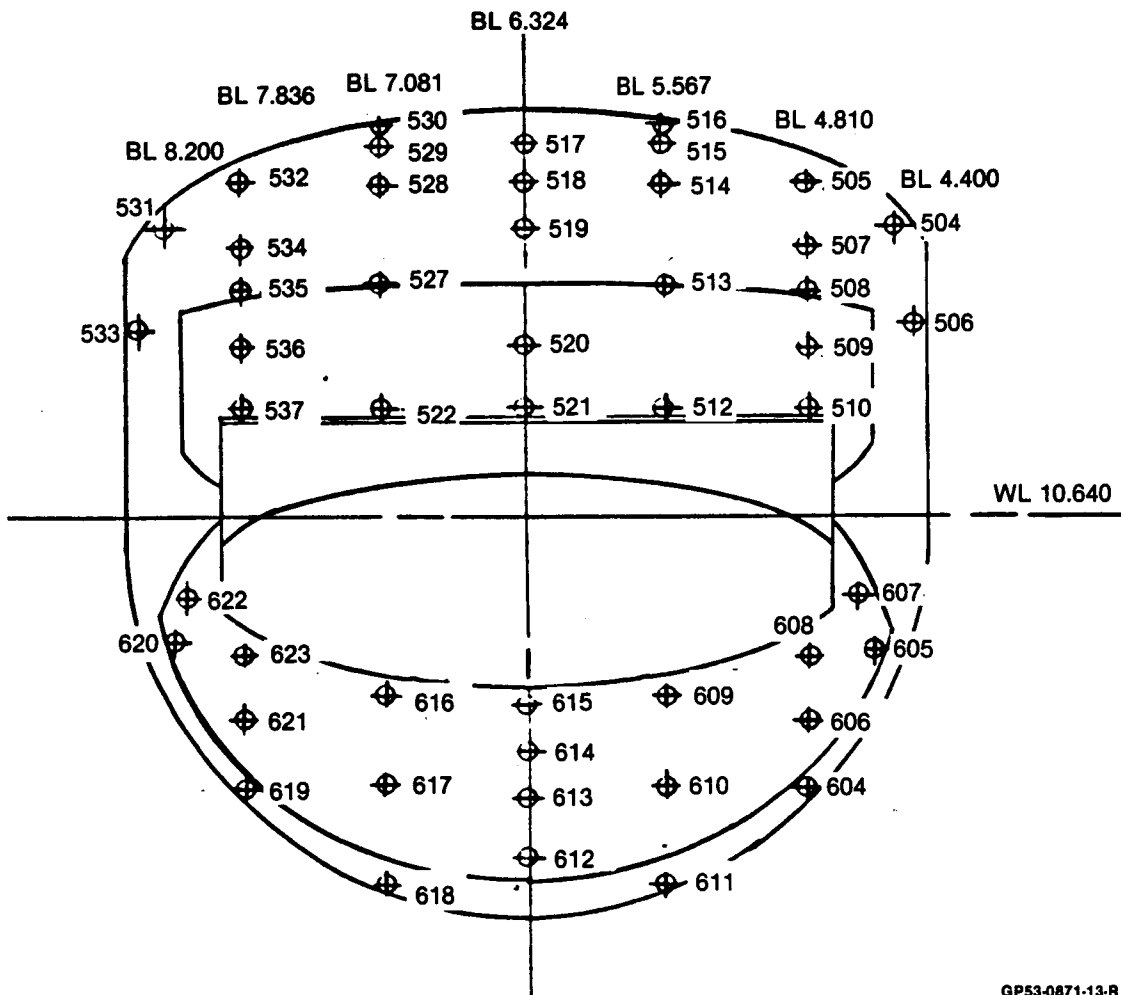


Figure 3-7. Fuselage Interior

Those pressure measurements requiring a larger transducer range than available at the Scanivalves were routed through the sting to a NASA supplied transducer housed in a temperature controlled pod.

3.2.2.1 ALBEN Surface Static Pressures - The non-metric ALBEN was instrumented with 49 surface taps. The tap layout across the ALBEN is shown in Figure 3-8. This large number of taps was used to perform a pressure-area integration from which lift, drag, and pitching moment on the nozzles were calculated.

3.2.2.2 Seal and Cavity Pressures - Eight static pressure orifices were distributed around the outside of the aft metric break seal on the left hand nacelle. The location of these orifices is shown in Figure 3-9. A pressure-area integration was performed with these measurements to calculate the axial force and pitching moment tares acting on this metric base area. The aircraft balance outputs were corrected for these tares.

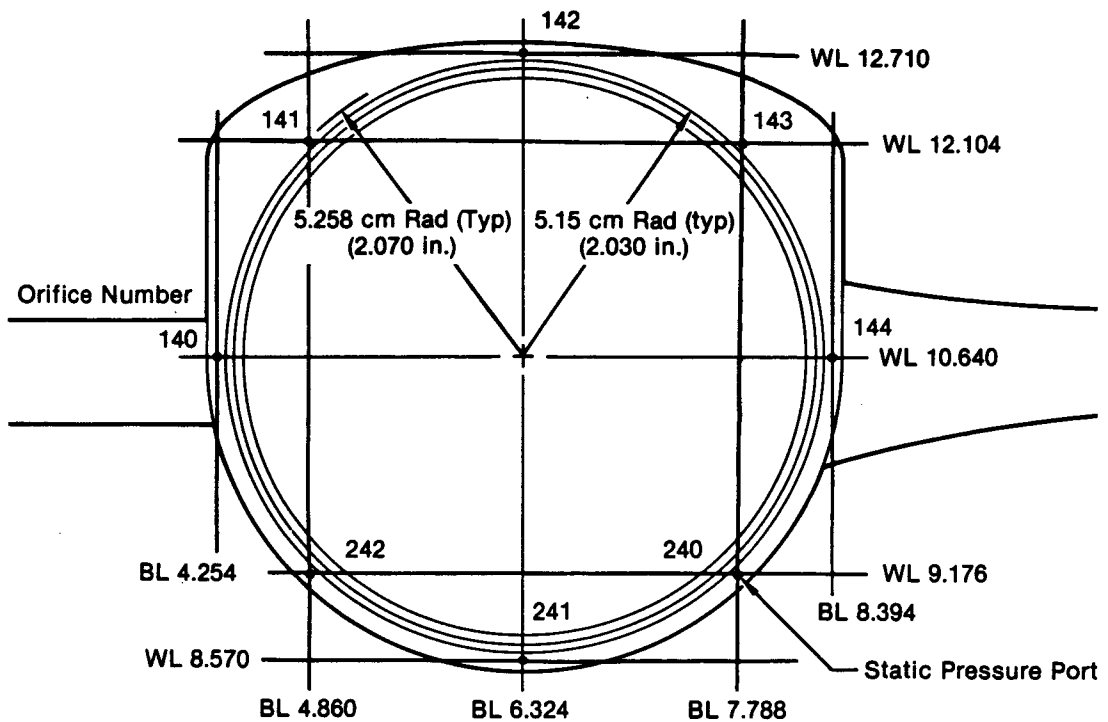


GP53-0871-13-R

Figure 3-8. ALBEN External Pressure Instrumentation

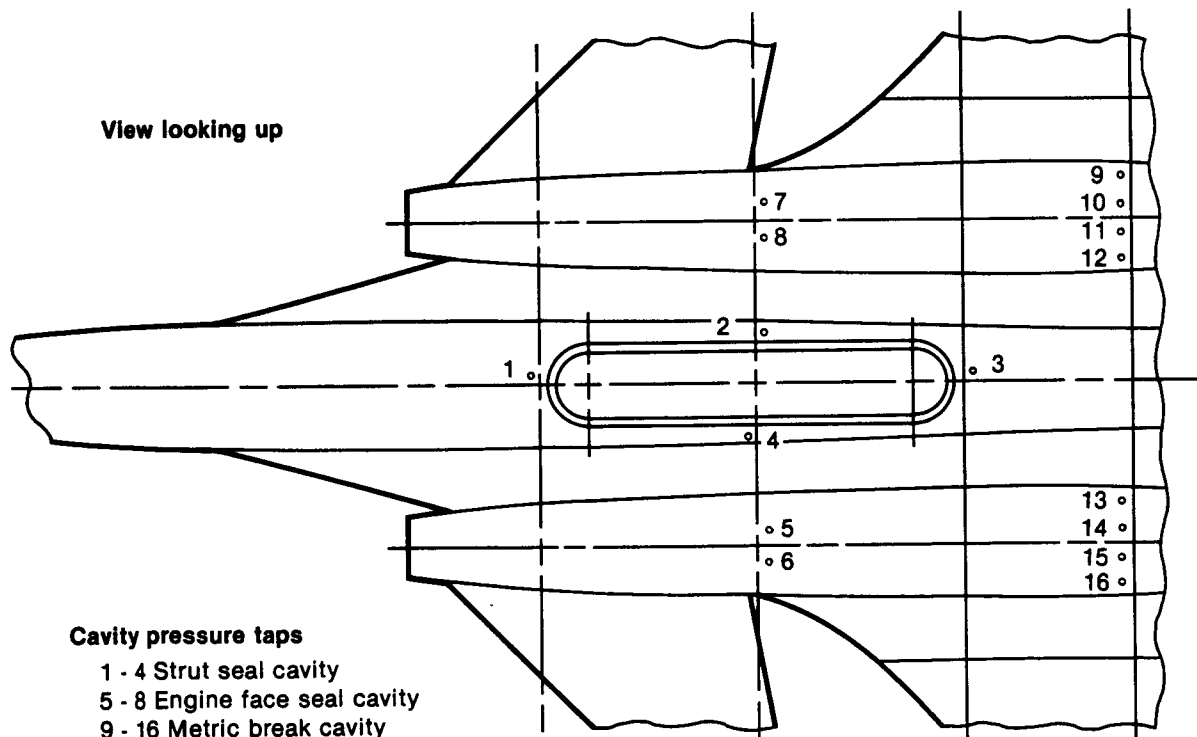
Sixteen pressure tubes were routed throughout the model to monitor cavity pressure. The location of these tubes is shown in Figure 3-10. These measurements were used to compute pressure-differential tares across the cavity seals, and were applied to the balance output as a correction term.

3.2.2.3 Model Total Pressure Instrumentation - Model total pressure instrumentation was used to measure airflow and to determine the engine pressure ratio and nozzle pressure ratio.



GP53-0871-43-R

Figure 3-9. Location of Aft Metric Break Seal Pressure Instrumentation
FS 50.689



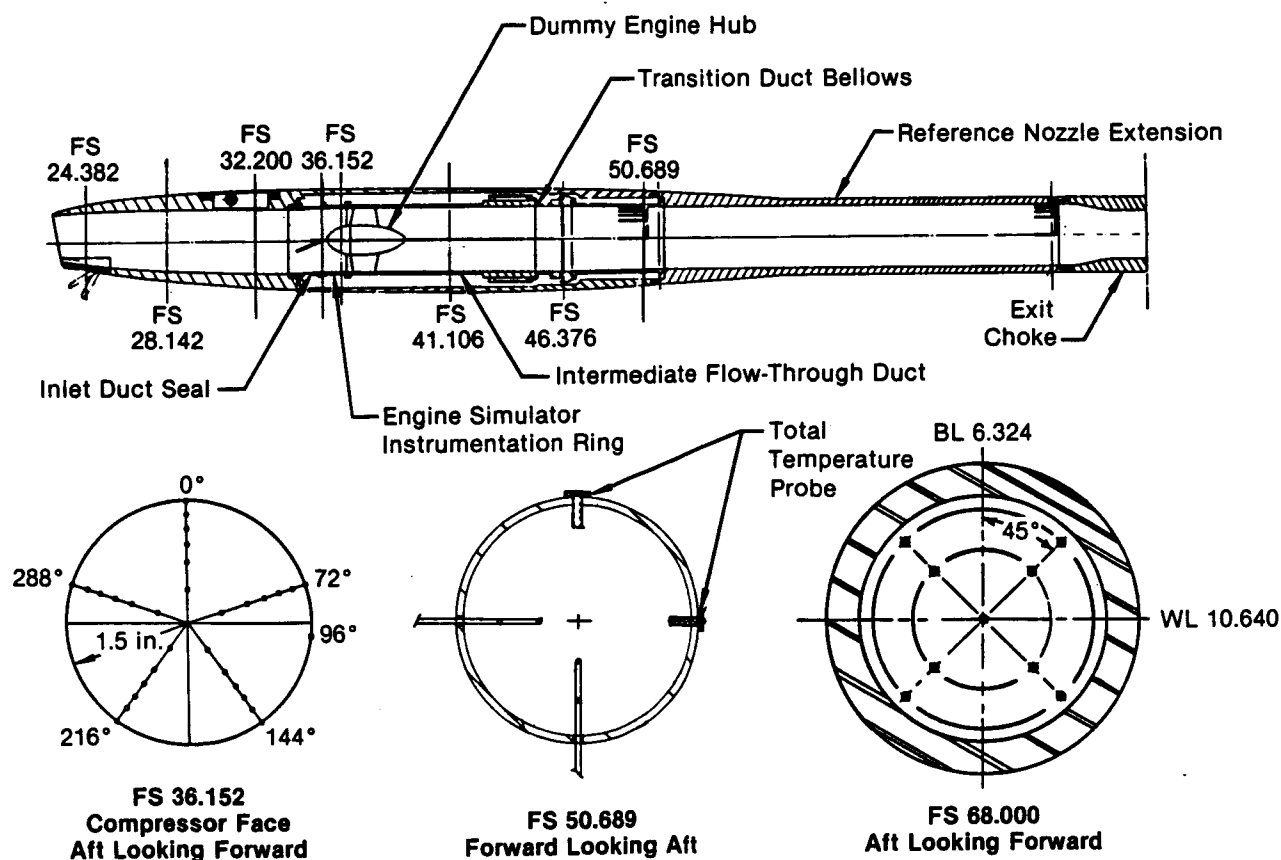
GP53-0871-44-R

Figure 3-10. Location of Cavity Pressure Instrumentation

Thirty-five (35) total pressure probes were located at the engine face, Plane 2. There were ten active probes on the left hand engine face rake and twenty-five (25) probes on the right hand engine face rake. A full description of the engine face pressure instrumentation is included in Volume I of this report.

The transition ducts each had four total pressure probes used in the calculation of nozzle pressure ratio and airflow. The total pressure probe locations are shown in Figure 3-11.

Each nozzle extension used during the Flow Through mode, also had a 9 probe total pressure rake. This rake was located at FS 68.000 as shown in Figure 3-11.



GP53-0871-51-R

Figure 3-11. Location of Model Total Pressure Instrumentation

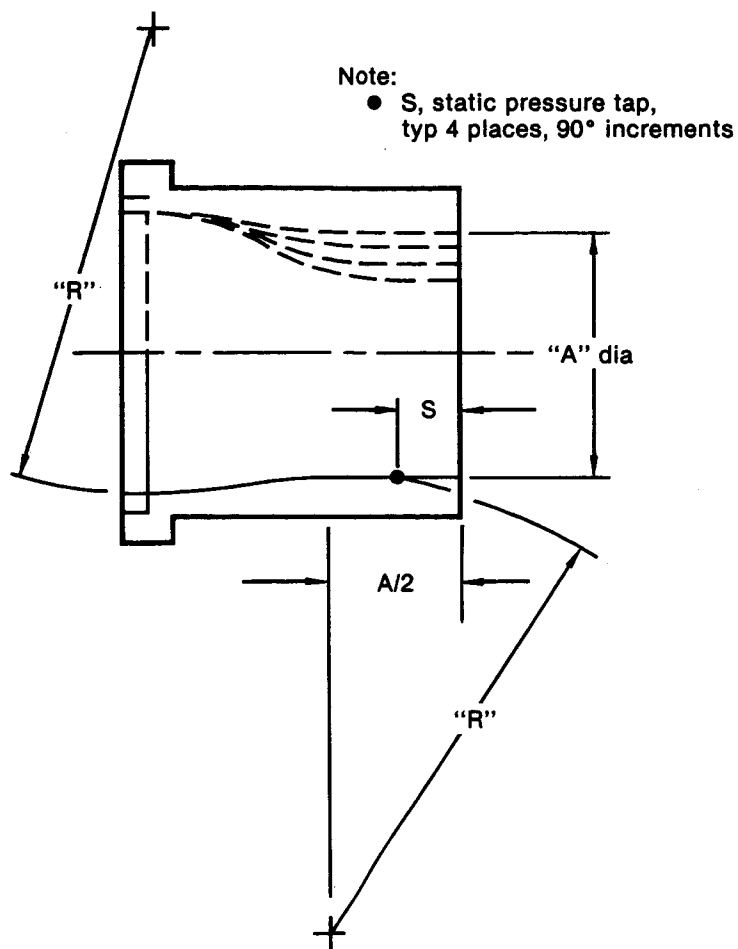
3.2.2.4 Internal Nozzle Static Pressures - Each of the chokes and ALBEN models was instrumented with static pressure taps. The choke nozzles had four throat static pressure taps utilized in determining nozzle airflow. The pressure tap locations are shown in Figure 3-12. The ALBEN had three static pressure taps located on the expansion ramp as shown in Figure 3-6.

3.2.3 Model Temperature Instrumentation - Model temperature instrumentation was used for control of balance housing temperature and to measure nozzle duct total temperature.

The model balance housing was instrumented with eight iron/constantan thermocouples. Four of the thermocouples connected directly to the heater blanket controllers. The remaining four thermocouples measured the balance housing temperature at each heating zone for recording in the data system. Two additional thermocouples were attached directly to the balance, one at the taper base and one at the electrical connector housing. The location of thermocouples on the balance housing is shown in Figure 3-4.

The transition duct assembly had two iron/constantan thermocouples in each nacelle used in the calculation of duct airflow. The location of these thermocouples is shown in Figure 3-11.

3.2.4 Miscellaneous Instrumentation - Instrumentation was installed on the model to measure angle-of-attack, canard deflection angle and canard root bending moment. The instrumentation for these measurements is listed in Figure 3-2.



Flow-through choke data table

| Configuration | Drawing | "A" | A/2 | A _{throat} | "R" | "S" |
|---------------|------------------|-------------------------|-------------------------|---|--------------------------|-------------------------|
| 1, 5 | 254-4452-5, -6 | 6.604 cm (2.600 in.) | 3.302 cm (1.300 in.) | 34.252 cm ² (5.309 in. ²) | 12.637 cm (4.975 in.) | 1.651 cm (0.650 in.) |
| 2, 6 | 254-4452-7, -8 | 5.766 cm (2.270 in.) | 2.883 cm (1.135 in.) | 26.110 cm ² (4.047 in. ²) | 8.273 cm (3.257 in.) | 1.440 cm (0.567 in.) |
| 3, 7 | 254-4452-9, -10 | 4.887 cm (1.924 in.) | 2.443 cm (0.962 in.) | 18.755 cm ² (2.907 in. ²) | 6.711 cm (2.642 in.) | 1.234 cm (0.486 in.) |
| 4, 8 | 254-4452-11, -12 | 3.988 cm (1.570 in.) | 1.994 cm (0.785 in.) | 12.490 cm ² (1.936 in. ²) | 6.005 cm (2.364 in.) | 0.996 cm (0.392 in.) |

GP53-0871-50-R

Figure 3-12. Location of Flow-Through Choke
 Throat Static Pressure Instrumentation

Two separate angle-of-attack measurements were made. A dangleometer mounted in the model forebody, Figure 3-7, provided one measurement of angle-of-attack. An angle-of-attack measurement was also provided which was external to the model on the support sting. The angle-of-attack based on the support sting angle required a calibration to account for elastic and thermal bending in the sting.

A potentiometer was installed in each canard drive assembly to measure the canard deflection of each of the two independently controlled canards. The potentiometers measured the canard deflection angles directly at the canard support shaft.

A strain gauge was installed in the upper surface of the left hand canard to measure the bending moment at the root.

3.2.5 Facility/CMAPS Instrumentation - Significant instrumentation was provided by the facility for measurement of airflow rates to and from the model, angle-of-attack, CMAPS health, and basic tunnel operating parameters.

In the CMAPS mode, high pressure air was delivered to the model through the drive-air passage in the sting and removed from the model through the bleed-air passage. The mass flow through each of these passages was measured with a critical flow venturi. The drive and bleed valves, operated from the simulator control console, were used to regulate the airflow.

In the Jet-Effects mode, high pressure air was delivered to the model through both the drive and the bleed passages. The drive passage airflow was also measured with a venturi. The bleed passage airflow was measured with a choked orifice flow-meter.

An apparatus called the Knuckle-Sleeve assembly which was used to measure the inclination of the support sting. These measurements were in turn used to calculate the model angle-of-attack.

Each propulsion simulator was instrumented to measure pressure, temperature, rotor thrust, vibration, and rotor speed. The simulator instrumentation was required for a combination of health monitoring and operating control. A summary of simulator instrumentation and functional use is given in Figure 3-13.

| Symbol | Definition | Quantity | Connects To | Function |
|-----------|----------------------|----------|-------------------|---|
| TBF-1 | Fwd Brng Temp | 1 | Controller | Health/Diagnostic |
| TBF-2 | Fwd Brng Temp | 1 | Backup | Health/Diagnostic |
| N1 | Rotor Speed | 1 | Controller | Health/Diagnostic |
| N2 | Rotor Speed | 1 | Backup | Health/Diagnostic |
| TBA1,2 | Aft Brng Temp | 2 | Controller/Backup | Health/Diagnostic |
| RT | Rotor Thrust | 1 | Controller | Health/Diagnostic |
| PS-57 | Mixer Press | 1 | Controller | Health/Diagnostic/ Airflow Correlation |
| PSK15 | Comp Disch Dyn Press | 1 | Controller | Health/Diagnostic |
| TT-4 | Turbine Inlet Temp | 1 | Controller | Health/Diagnostic |
| PS, PT-15 | Comp Disch Press | 2 | Controller | W ₂ (Corrected) |
| TT-15 | Comp Disch Temp | 1 | Controller | W ₂ (Corrected) |
| PT-4 | Turbine Inlet Press | 1 | Controller | Health/Diagnostic |
| V1B | Vibration | 1 | Controller | Health/Diagnostic |

GP53-0871-25-R

Figure 3-13. Simulator Instrumentation Summary
Per Simulator

Standard facility pressure and temperature instrumentation was provided to calculate tunnel operating conditions. These conditions included the tunnel static and total pressure, dynamic pressure, Mach number, Reynold's number, and total temperature.

3.3 CALIBRATIONS - Complete calibrations of the installed force balance, inlet mass flow measurement, and CMAPS systems were conducted at NASA-Ames and MCAIP. These calibrations are briefly discussed in this section. A detailed description of all of the model calibrations is presented in the Phase II-Final Report, Reference 7. The CMAPS calibrations are described in References 9 and 10.

3.3.1 Force Balance Calibrations - The force balance was calibrated both isolated and installed in the model. The installed calibration results were compared with those of the isolated calibration to ensure that fouling or improper metric bridging did not occur. Pressurized loadings were also performed during the installed calibration to obtain the balance correction due to the inlet duct seal.

The isolated balance calibration was used to determine sensitivities and interactions of the six component balance to applied forces and moments. This calibration was performed by statically loading the aircraft balance at ambient pressure and temperature and at operating temperature (71°C) over the specified ranges shown in Figure 3-14. The non-standard model installation was simulated during this calibration at NASA-Ames by holding the sleeve of the balance in a non-metric support structure and applying loads to the taper end.

| Gage Loaded | Range of Loadings | Increment |
|-------------------|---|-----------------------|
| Axial | -113.4 - 113.4 kgf (-250 - 250 lb) | 22.7 kgf (50 lb) |
| Normal, N1 and N2 | -1,361 - 1,361 kgf (-1,361 - 1,361 lb) | 272.2 kgf (600 lb) |

GP53-0871-9-R

Figure 3-14. Isolated Balance Loading Schedule

The balance was then calibrated installed in the model to account for the effects of instrumentation lines and the three sets of seals (strut seal, inlet duct seal, and nozzle metric break seal). A loading fixture, shown in Figure 3-15, was attached to the upper surface of the center fuselage to which normal force, pitching moment, and axial force components were applied. Note that the model was rolled to an inverted position for the application of these loadings. Throughout the calibrations, the balance was maintained at 71°C (160°F) (the same temperature maintained during the test).

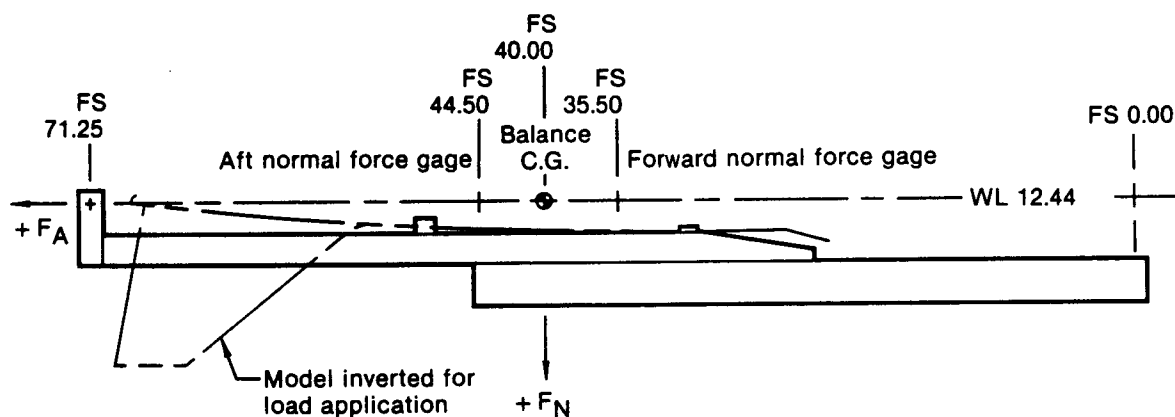
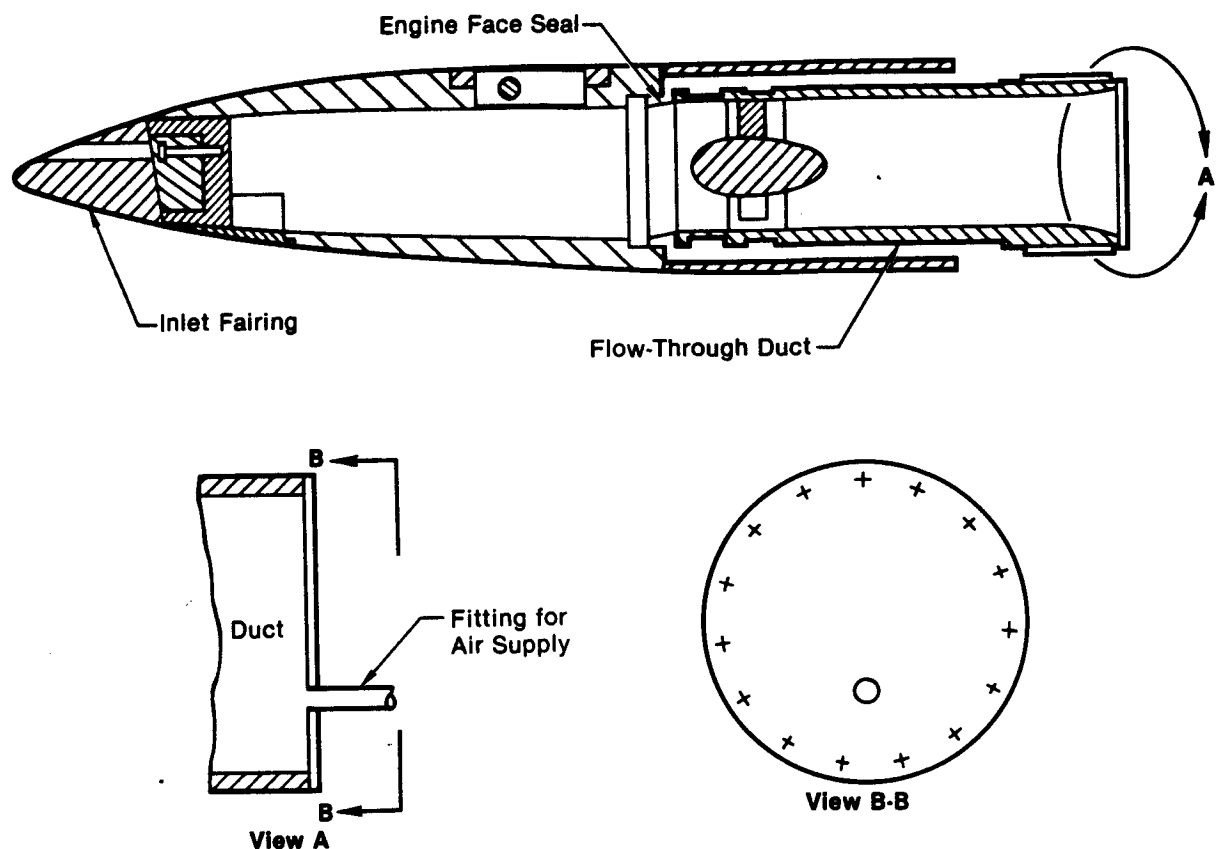


Figure 3-15. Installed Balance Loading Fixture

The installed calibrations were performed with and without a pressure differential applied across the inlet duct seal. The hardware to pressurize the inlet duct seal is shown in Figure 3-16. Small, but repeatable effects of the installation and inlet duct seal pressurization were identified by comparing the isolated and installed calibration results. An example of the intercept change and slope change which were identified in this comparison is shown in Figure 3-17.



GP53-0871-48-R

Figure 3-16. Pressurized Inlet Duct Seal Calibration Setup

The change in intercept was caused by a deformation of the inlet duct seal when subjected to a pressure differential. The deformed seal exerted a force on the metric portion of the model. This force was removed from the calculated balance outputs as a tare. The contributions of this tare to axial force and pitching moment were termed FSEALA and MSEALA, respectively. The variations of these terms with the pressure differential across the duct seal (DPDS) are shown in Figures 3-18 and 3-19 for both simulator and conventional modes. The contribution to normal force was zero.

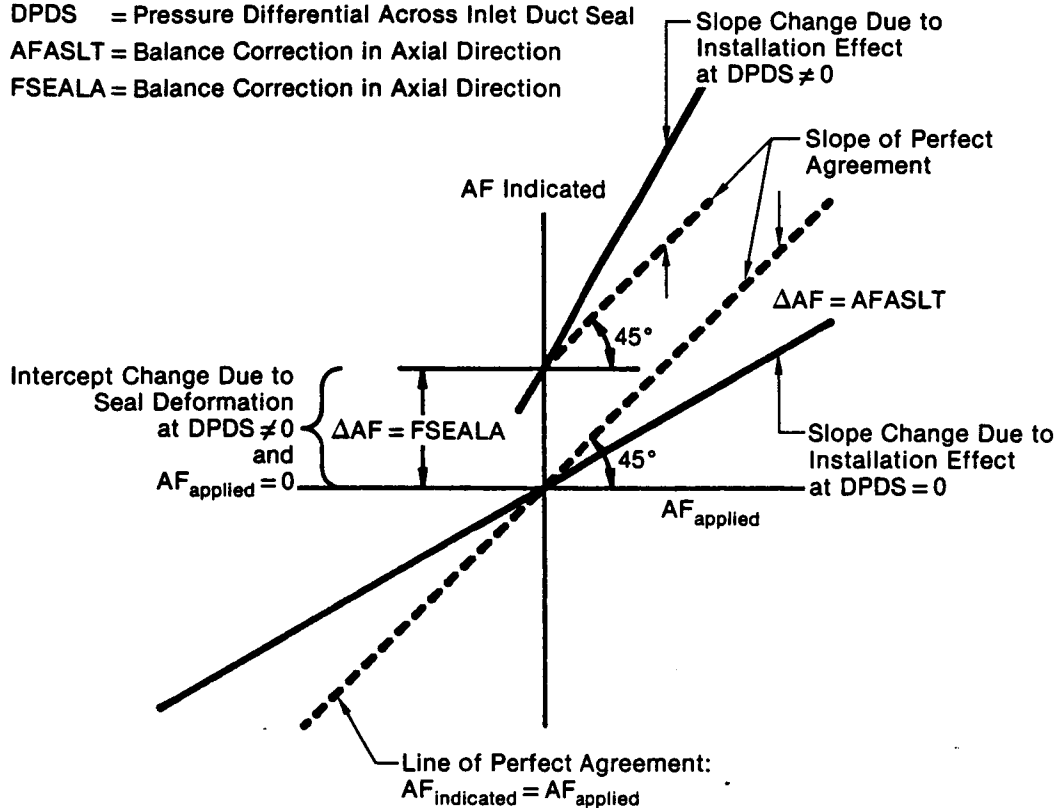
Nomenclature:

AF = Force in Axial Direction

DPDS = Pressure Differential Across Inlet Duct Seal

AFASLT = Balance Correction in Axial Direction

FSEALA = Balance Correction in Axial Direction

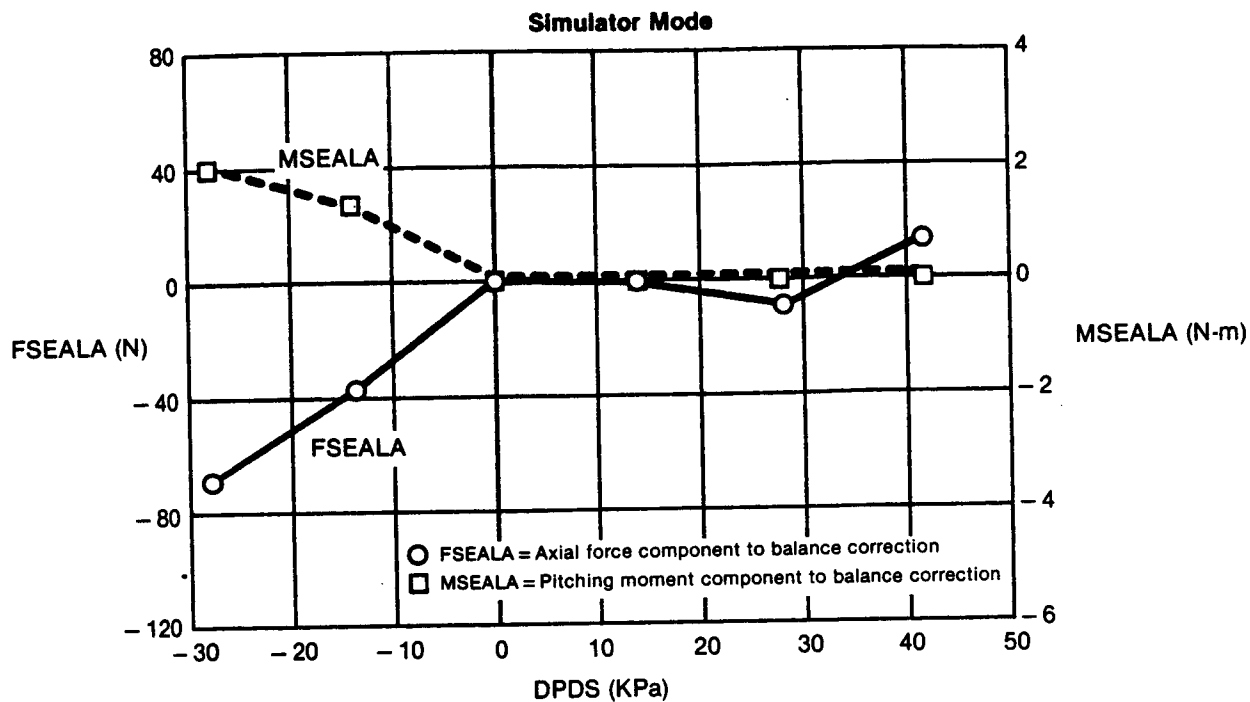


Note: Similar corrections were calculated for normal force and pitching moment

GP53-0871-7-R

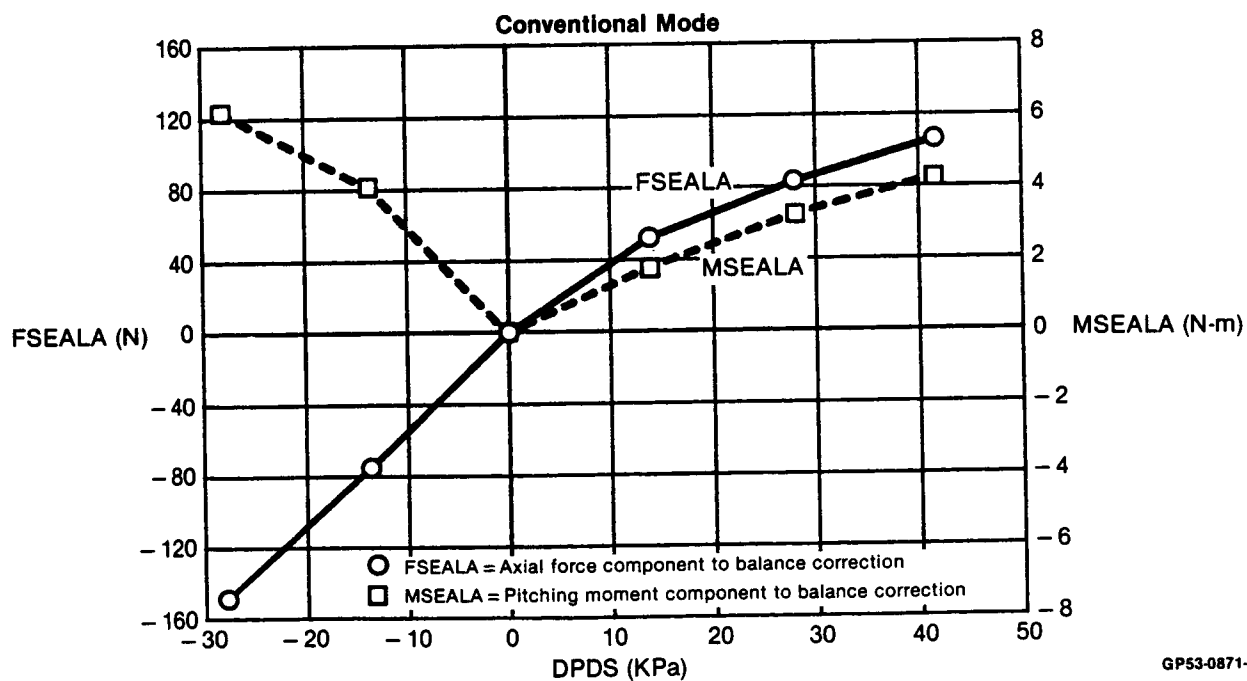
Figure 3-17. Installation and Inlet Duct Seal Pressurization Corrections to Aircraft Balance in Axial Direction

The change in slope was due to the non-ideal effects of the metric seals and installation. The metric break seals and instrumentation lines which bridged the metric breaks exerted small but predictable forces on the metric portion of the model which varied with the applied load and the inlet duct seal pressure differential (DPDS). Correction terms were applied to the calculated balance outputs to account for these effects. These correction terms were labeled AFNSLT, AFASLT, and APMSLT for the contributions to normal force, axial force, and pitching moment. They are defined in Figure 3-20.



GP53-0871-6-R

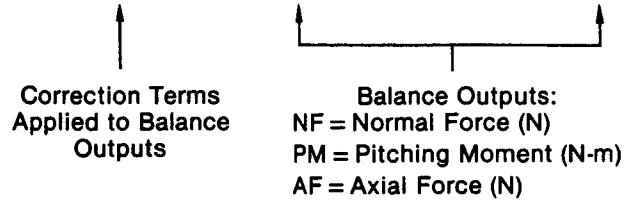
Figure 3-18. Duct Seal Pressure Effect on Balance Simulator Mode



GP53-0871-5-R

Figure 3-19. Duct Seal Pressure Effect on Balance Conventional Mode

Normal Force: $AFNSLT = KST28 \cdot NF + KST29 \cdot PM + KST30 \cdot AF$
 Axial Force: $AFASLT = KST31 \cdot NF + KST32 \cdot PM + KST33 \cdot AF$
 Pitching Moment: $APMSLT = KST34 \cdot NF + KST35 \cdot PM + KST36 \cdot AF$



Where Values for KST Are Tabulated Below:
CMAFS Mode: Nozzle Extension Configuration (Runs 1 - 86)

| | DPDS (KPa) = $P_{duct} - P_{cav}$ | | | |
|-----------------|-----------------------------------|-----------|-----------|-----------|
| | - 27.58 | 0 | 13.79 | 27.58 |
| KST28 (N/N) | - 0.00289 | - 0.00063 | 0.00480 | 0.00581 |
| KST29 (N/N-m) | 0.03615 | 0.02995 | 0.04517 | 0.05311 |
| KST30 (N/N) | 0 | 0 | 0 | 0 |
| KST31 (N/N) | 0.01097 | 0.00464 | 0.00641 | 0.01010 |
| KST32 (N/N-m) | - 0.03556 | - 0.04369 | - 0.04248 | - 0.03963 |
| KST33 (N/N) | 0.00741 | 0.00591 | 0.00882 | 0.01731 |
| KST34 (N-m/N) | - 0.00932 | - 0.00315 | 0.00367 | - 0.00003 |
| KST35 (N-m/N-m) | 0.0589 | 0.00626 | 0.00820 | 0.00857 |
| KST36 (N-m/N) | 0 | 0 | 0 | 0 |

CMAFS Mode:
 Simulated Aircraft and Common Baseline Configurations (Runs 87 - 293)

| | DPDS (KPa) | | | |
|-----------------|------------|-----------|-----------|-----------|
| | - 27.58 | 0 | 13.79 | 27.58 |
| KST28 (N/N) | - 0.00324 | - 0.00098 | 0.00445 | 0.00546 |
| KST29 (N/N-m) | 0.02471 | 0.01850 | 0.03373 | 0.04165 |
| KST30 (N/N) | 0 | 0 | 0 | 0 |
| KST31 (N/N) | 0.00885 | 0.00252 | 0.00428 | 0.00798 |
| KST32 (N/N-m) | - 0.03732 | - 0.04544 | - 0.04423 | - 0.04137 |
| KST33 (N/N) | 0.01143 | 0.00993 | 0.01284 | 0.02133 |
| KST34 (N-m/N) | - 0.00661 | - 0.00044 | 0.00638 | 0.00241 |
| KST35 (N-m/N-m) | 0.0361 | 0.00399 | 0.00593 | 0.00629 |
| KST36 (N-m/N) | 0 | 0 | 0 | 0 |

**Figure 3-20. Definition of Balance Output Correction Terms
Due to Installation Effects**

Flow-Through Mode:
Common Baseline Configuration (Runs 66 - 95)

| | DPDS (KPa) | | | |
|-----------------|------------|----------|----------|----------|
| | - 27.58 | 0 | 13.79 | 27.58 |
| KST28 (N/N) | 0.01810 | 0.02412 | 0.02515 | 0.02899 |
| KST29 (N/N-m) | 0.03976 | 0.04773 | 0.05550 | 0.06137 |
| KST30 (N/N) | 0 | 0 | 0 | 0 |
| KST31 (N/N) | 0.00387 | 0.00016 | -0.00029 | 0.00430 |
| KST32 (N/N-m) | -0.03392 | -0.03972 | -0.04130 | 0.04523 |
| KST33 (N/N) | 0.01311 | 0.01352 | 0.01848 | 0.02078 |
| KST34 (N-m/N) | -0.03864 | -0.02260 | -0.00991 | -0.00453 |
| KST35 (N-m/N-m) | 0.0690 | 0.00673 | 0.01079 | 0.01191 |
| KST36 (N-m/N) | 0 | 0 | 0 | 0 |

Flow-Through Mode:
Nozzle Extension and Nozzle Extension Baseline Configurations
(Runs 96 - 236)

| | DPDS (KPa) | | | |
|-----------------|------------|----------|----------|----------|
| | - 27.58 | 0 | 13.79 | 27.58 |
| KST28 (N/N) | 0.01091 | 0.01693 | 0.01796 | 0.02180 |
| KST29 (N/N-m) | 0.03585 | 0.04382 | 0.05160 | 0.05747 |
| KST30 (N/N) | 0 | 0 | 0 | 0 |
| KST31 (N/N) | 0.00813 | -0.00436 | -0.00584 | 0.00922 |
| KST32 (N/N-m) | -0.00907 | -0.01084 | -0.01132 | -0.01252 |
| KST33 (N/N) | 0.00824 | 0.00865 | 0.01361 | 0.01591 |
| KST34 (N-m/N) | -0.03654 | -0.02050 | 0.00781 | -0.00243 |
| KST35 (N-m/N-m) | 0.0563 | 0.00546 | 0.00952 | 0.01064 |
| KST36 (N-m/N) | 0 | 0 | 0 | 0 |

Jet-Effects Mode:
Common Baseline Configuration (Runs 237 - 321)

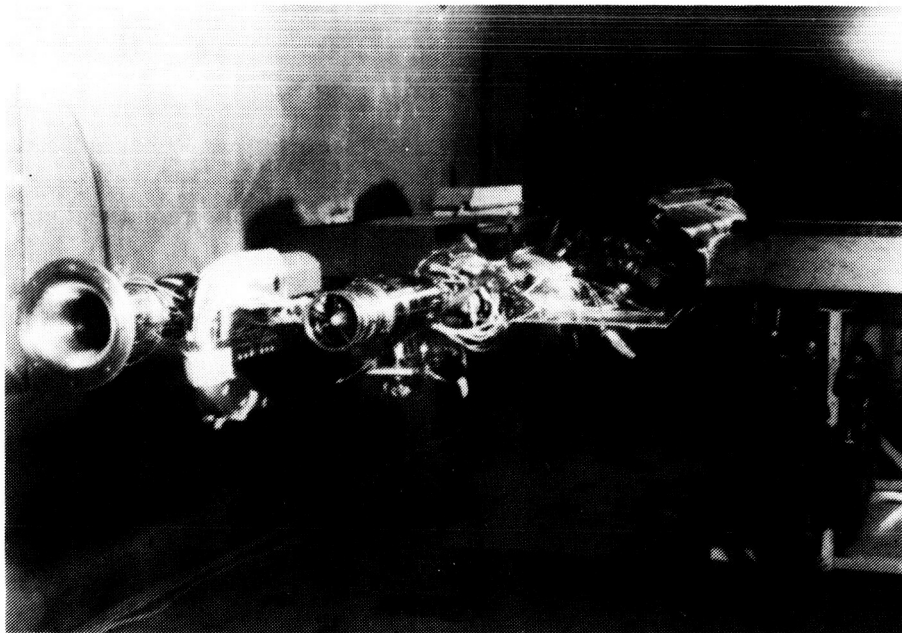
| | DPDS (KPa) | | | |
|-----------------|------------|----------|----------|----------|
| | - 27.58 | 0 | 13.79 | 27.58 |
| KST28 (N/N) | -0.00306 | 0.00296 | 0.00399 | 0.00783 |
| KST29 (N/N-m) | 0.04169 | 0.04966 | 0.05744 | 0.06331 |
| KST30 (N/N) | 0 | 0 | 0 | 0 |
| KST31 (N/N) | -0.00117 | -0.00498 | -0.00543 | -0.00084 |
| KST32 (N/N-m) | -0.02457 | -0.03037 | -0.03195 | -0.03589 |
| KST33 (N/N) | 0.01179 | 0.01220 | 0.01716 | 0.01946 |
| KST34 (N-m/N) | -0.00443 | 0.01161 | 0.02431 | 0.02969 |
| KST35 (N-m/N-m) | 0.0974 | 0.00957 | 0.01363 | 0.01475 |
| KST36 (N-m/N) | 0 | 0 | 0 | 0 |

GP53-0871-12-R

**Figure 3-20. (Continued) Definition of Balance Output Correction Terms
Due to Installation Effects**

3.3.2 Airflow Calibrations - The airflow through the model was used to correct the balance outputs for axial stream thrust at Plane 2, as well as to determine inlet MFR and ram drag. The airflow calculations were based on a series of calibrations conducted by NASA-Ames and MCAIR. NASA-Ames was responsible for calibration of the CMAPS and standard facility instrumentation. MCAIR calibrated the ALBEN and nozzle extension exit chokes.

The CMAPS calibrations were conducted by NASA-Ames in their nine-by-seven-foot supersonic wind tunnel. A photo of both simulators mounted on the support sting during the static freestream airflow calibrations is shown in Figure 3-21. A bellmouth inlet, shown on the right hand CMAPS in Figure 3-21, was used to calculate the reference airflow. The bellmouth inlet was calibrated at the Colorado Engineering Experiment Station, Inc. (CEESI), as described in Reference 10. Details of the CMAPS calibration are discussed in References 9 and 10.



GP53-0866-65-R

Figure 3-21. CMAPS Compressor Airflow Calibration Set-Up

The ALBEN and nozzle extension exit chokes were both calibrated at the MCAIR Propulsion Subsystem Test Facility (PSTF) located in St. Louis, Missouri. The PSTF houses the Mass Flow Calibration System (MFCS) used in the calibration, Figure 3-22.

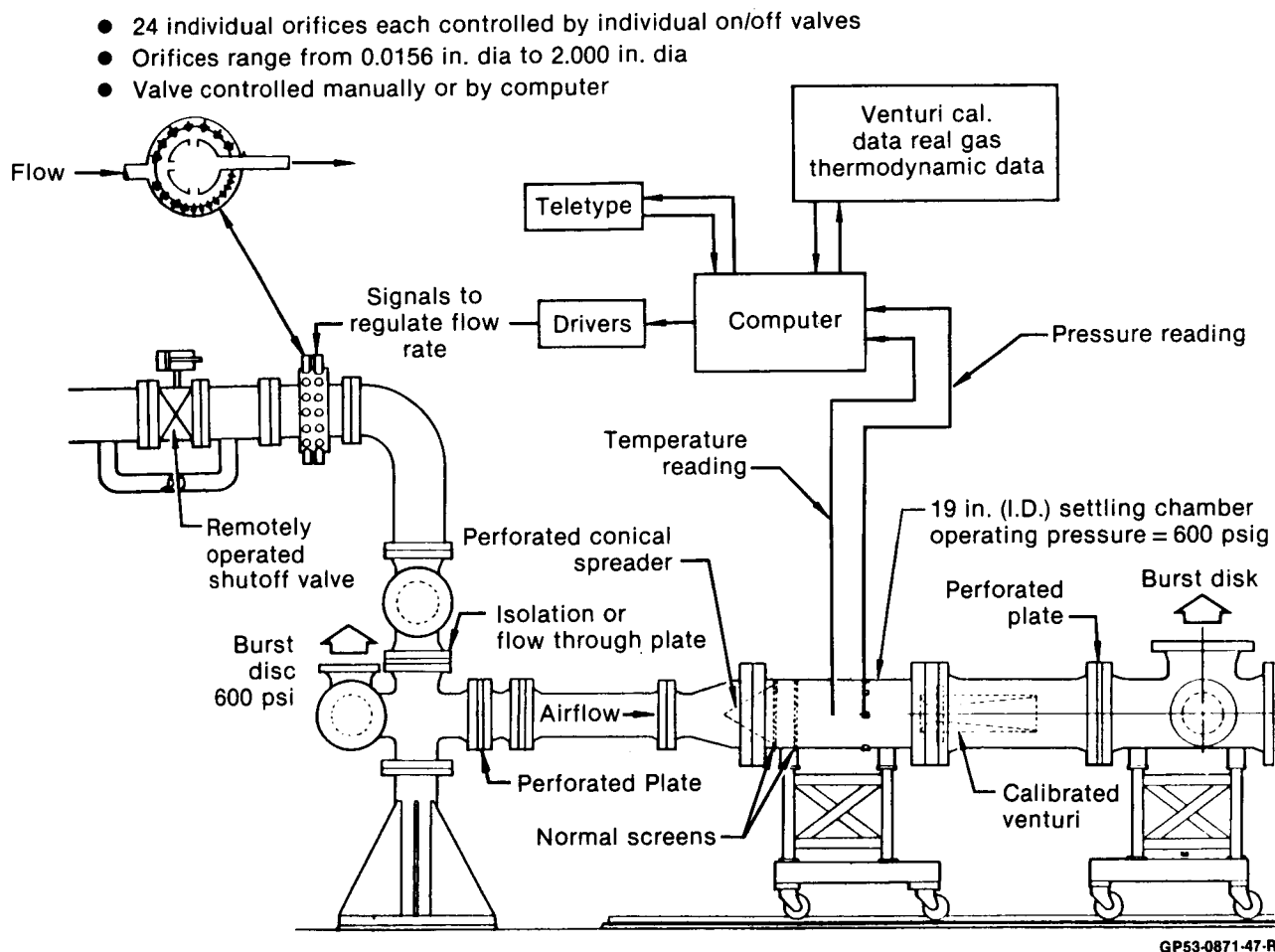


Figure 3-22. MCAIR Mass Flow Calibration Facility (MFCF)

The instrumentation for the ALBEN calibration included four total pressure probes in the transition duct, one total temperature and total pressure in the upstream plenum, and three static pressures on the variable external expansion ramp (VEER) of the ALBEN.

The instrumentation for the exit chokes included the four total pressure readings in the transition duct, nine total pressure readings in the nozzle extension tube and four static pressures from the choke throat. The instrumentation for both the ALBEN and chokes is shown in Figures 3-23 and 3-24.

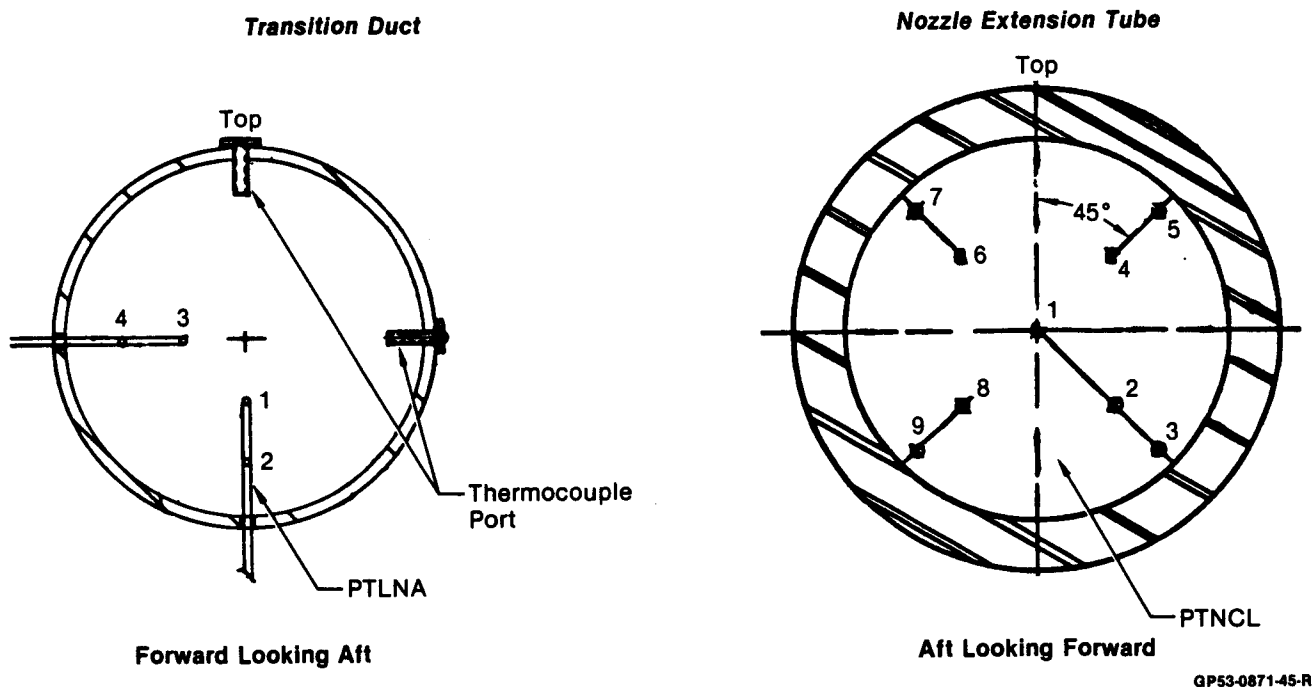
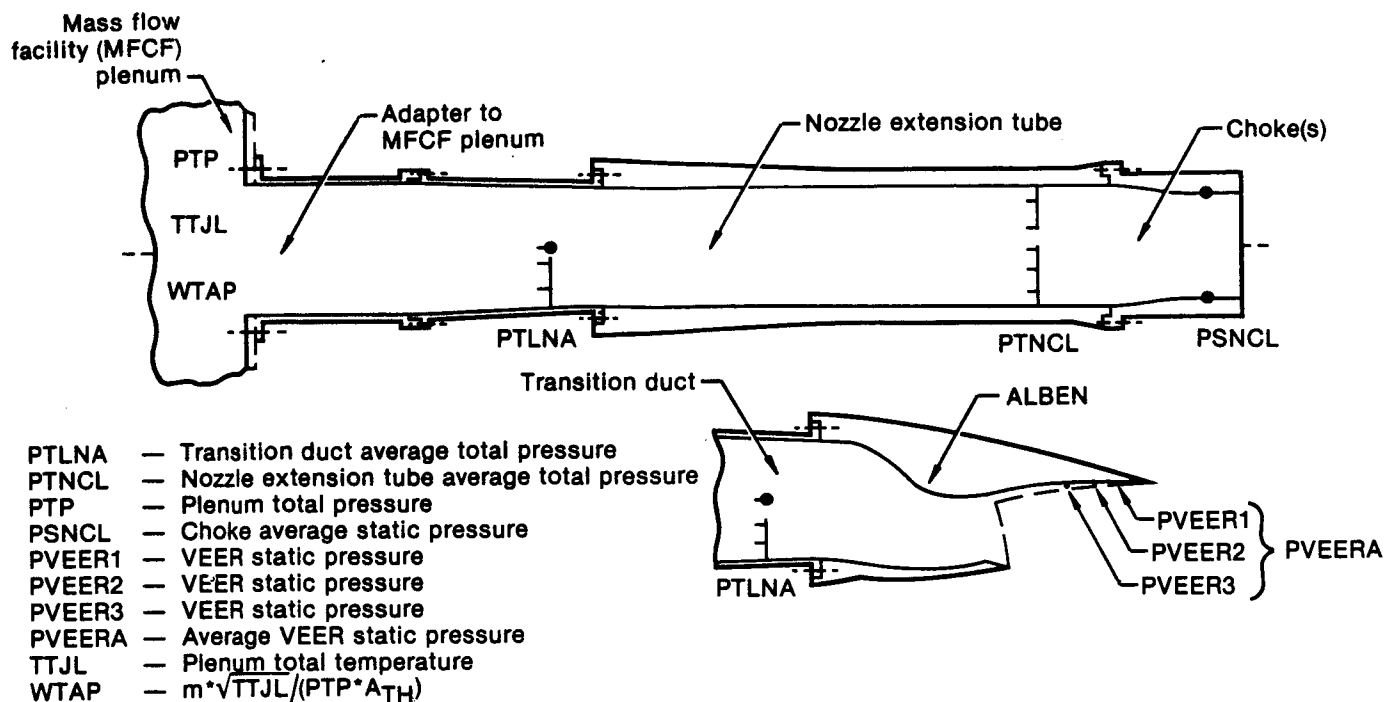


Figure 3-23. Instrumentation Used With Choke/ALBEN Calibration

Correlation of the airflow data for both ALBEN and chokes was in the form of a mass flow parameter (WTAP, Figure 3-24) versus pressure ratio. The pressure ratio for the chokes was the total pressure measured in the extension tubes divided by the static throat pressure measured in the chokes. The ALBEN correlation was based on the ratio of the transition duct total pressure and the static pressure measured by the first pressure tap on the ALBEN VEER. All airflow calibration data are presented in detail in Reference 7.



GP53-0871-48-R

Figure 3-24. Calibration Installation and Instrumentation

During the wind tunnel tests, mass flow to and from the model was measured with facility provided venturi and orifice flowmeters (see Section 3.2.5). NASA-Ames was responsible for the standard laboratory calibration of these flowmeters.

3.4 DATA REDUCTION PROCEDURES - The data reduction effort concentrated on the calculation of aerodynamic and propulsion system performance parameters. The unique elements of the data reduction are described herein. Further discussion is presented in Reference 7. A list of the data reduction equations is included herein as Appendix C.

3.4.1 Inlet Airflow Calculation - During the Flow-Through mode testing, inlet airflow was based on measurements made in the exhaust nozzle duct (Plane 8). An indirect method of airflow calculation based on turbine discharge (Plane 57) pressure was used in the CMAPS mode.

The Plane 8 method was based on total temperature and total and static pressure measurements at the exit chokes. These measurements were used in the one-dimensional, isentropic, compressible flow equations to directly calculate an ideal airflow at Plane 8. Flow coefficients, obtained during pre-test calibrations, were then applied to these ideal calculations to obtain the actual inlet airflow.

The Plane 57 method used in the CMAPS test mode is an indirect calculation based on a correlation of rotor speed and static pressure in the turbine discharge flow. In other words, a modified form of the engine operating map was used to determine corrected inlet airflow. The instrumentation for this pressure measurement is located in the mixer as shown in Figure 2-11. An example of corrected inlet airflow variation with rotor speed and corrected turbine discharge static pressure (PS57) is shown in Figure 3-25. Plots of this type formed the basis for the empirical correlation. This method was developed by S. C. Smith of NASA-Ames (Reference 9).

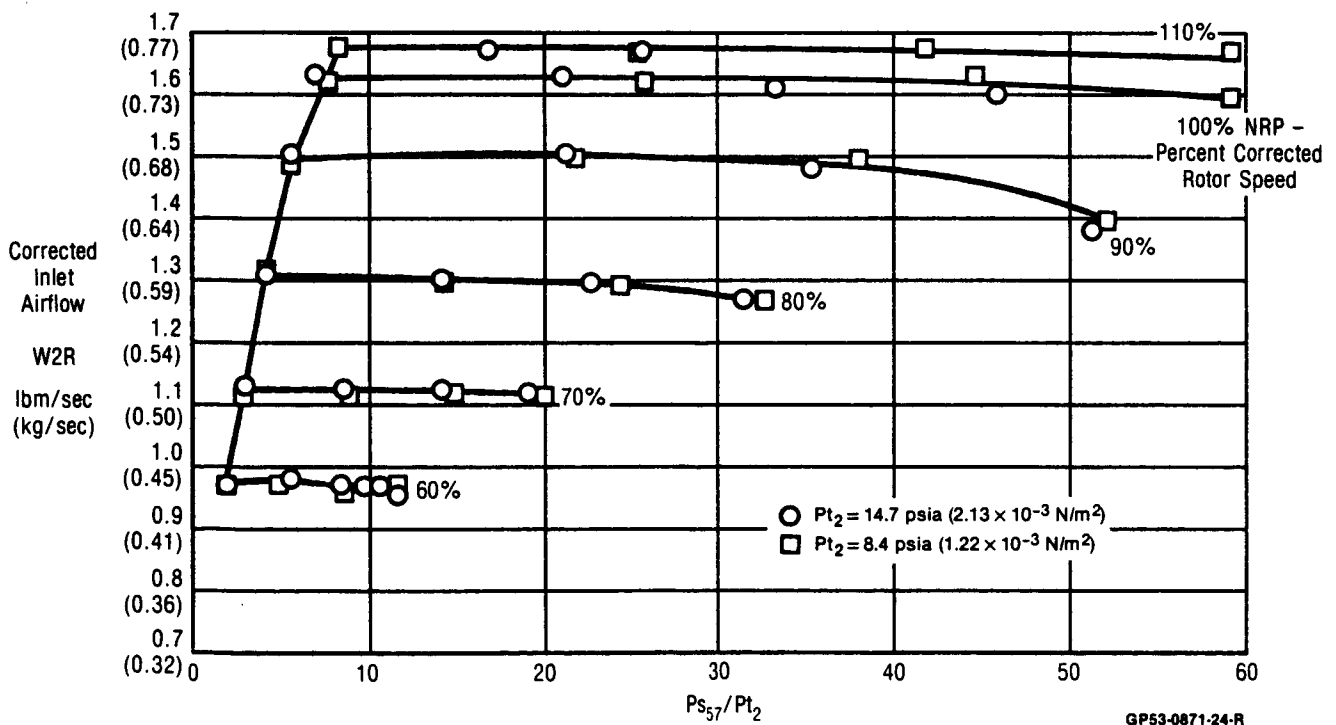


Figure 3-25. Typical CMAPS Operating Map In Terms of Turbine Discharge Pressure

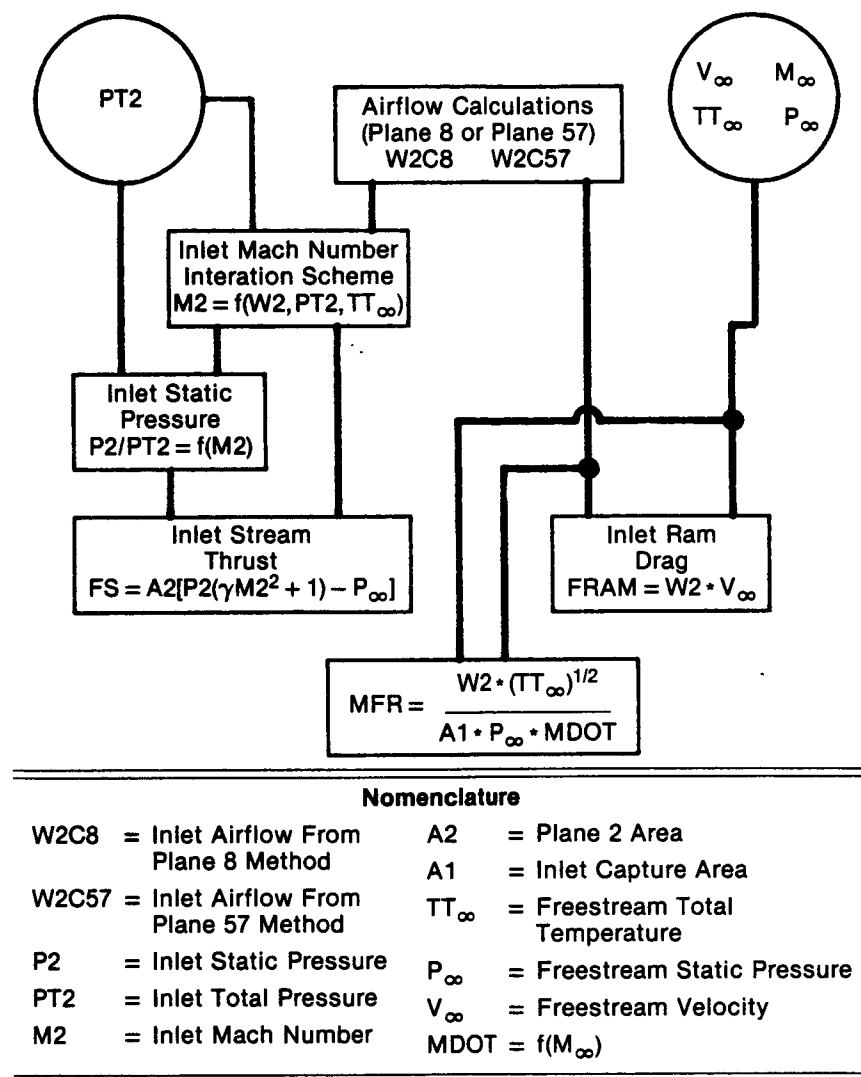
Other methods of CMAPS inlet airflow calculation were also investigated based on measurements at the engine face (Plane 2) and at the compressor discharge (Plane 15). There was also a form of the Plane 8 method investigated for the CMAPS mode. However, the Plane 57 airflow calculation was clearly shown to have the lowest uncertainty. The four methods are discussed further in Reference 2.

3.4.2 Inlet Stream Thrust and Ram Drag - The airflow calibration results were used to correct the balance output for the axial stream thrust at Plane 2, as well as the MFR and ram drag. The value of Plane 2 stream thrust/ram drag was based on the Plane 8 airflow method in the Flow-Through mode and the Plane 57 method in the CMAPS mode. An example of this calculation is shown in Figure 3-26. The variations of stream thrust and ram drag coefficients with angle-of-attack, MFR, and Mach number are shown in Figures 3-27 through 3-29.

3.4.3 Force Balance Data Reduction - Standard NASA-Ames procedures were employed to compute the basic, balance-indicated forces (normal, side, and axial) and moments (roll, pitch, and yaw).

Additional procedures were used to correct the axial force, normal force, and pitching moment outputs of the balance for seal, cavity, base, stream thrust, and ram drag tares. The application of these corrections is summarized in Appendix C.

3.4.4 Nozzle Pressure Ratio Calculation - The calculation of nozzle pressure (NPR) was based on the airflow through the nozzle for both CMAPS and Jet-Effects modes. Failures in the ALBEN total pressure instrumentation (PT7) prohibited direct measurement of NPR. Total airflow to each nozzle was defined as the sum of net airflow into the model from the support sting and inlet airflow.



GP53-0871-4-R

Figure 3-26. Example of Inlet Stream Thrust, Ram Drag, and MFR Calculation

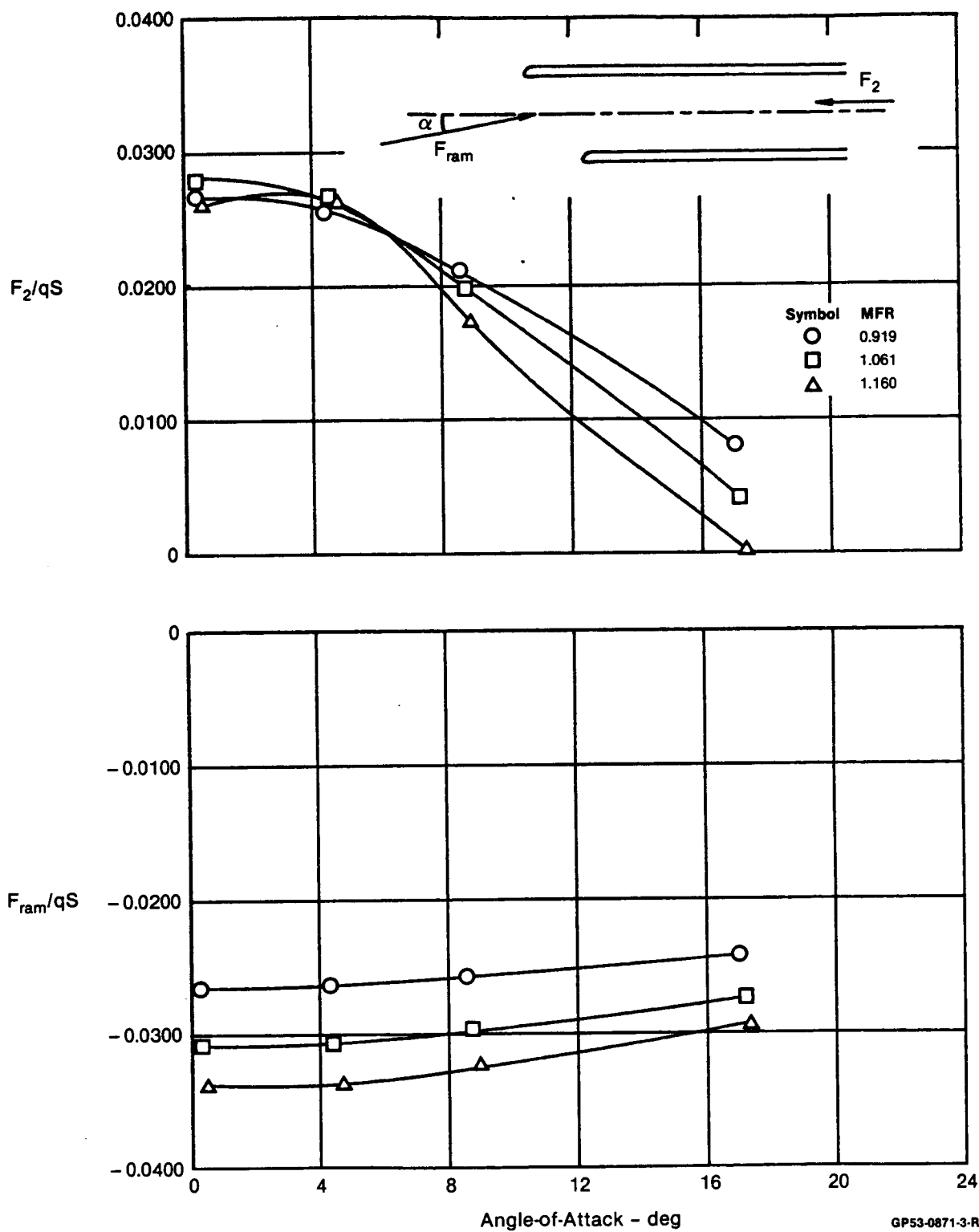
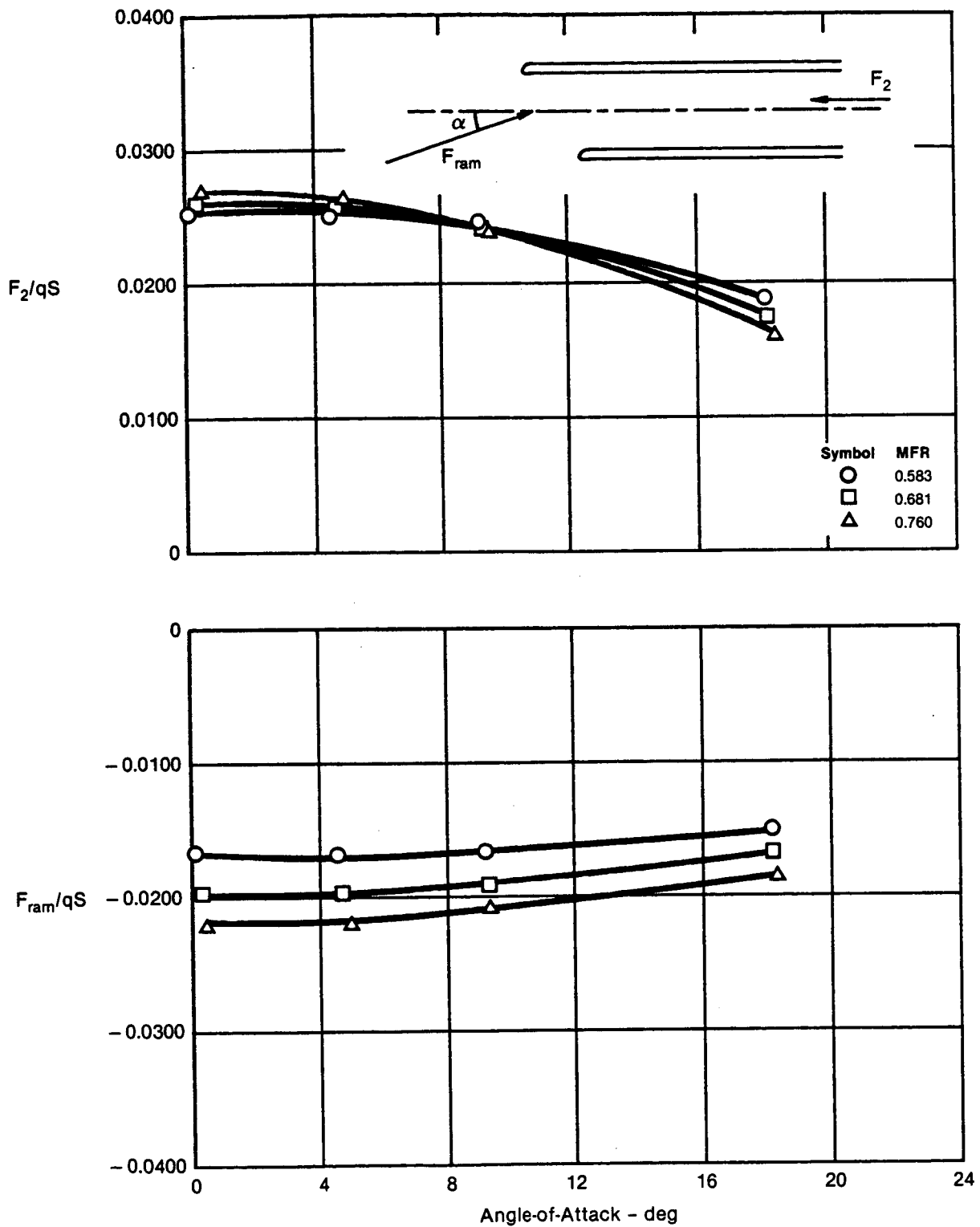


Figure 3-27. Variation of Stream Thrust and Ram Drag Coefficients
CMAPS Mode Mach 0.4



GP53-0871-2-R

Figure 3-28. Variation of Stream Thrust and Ram Drag Coefficients
CMAPS Mode Mach 0.9

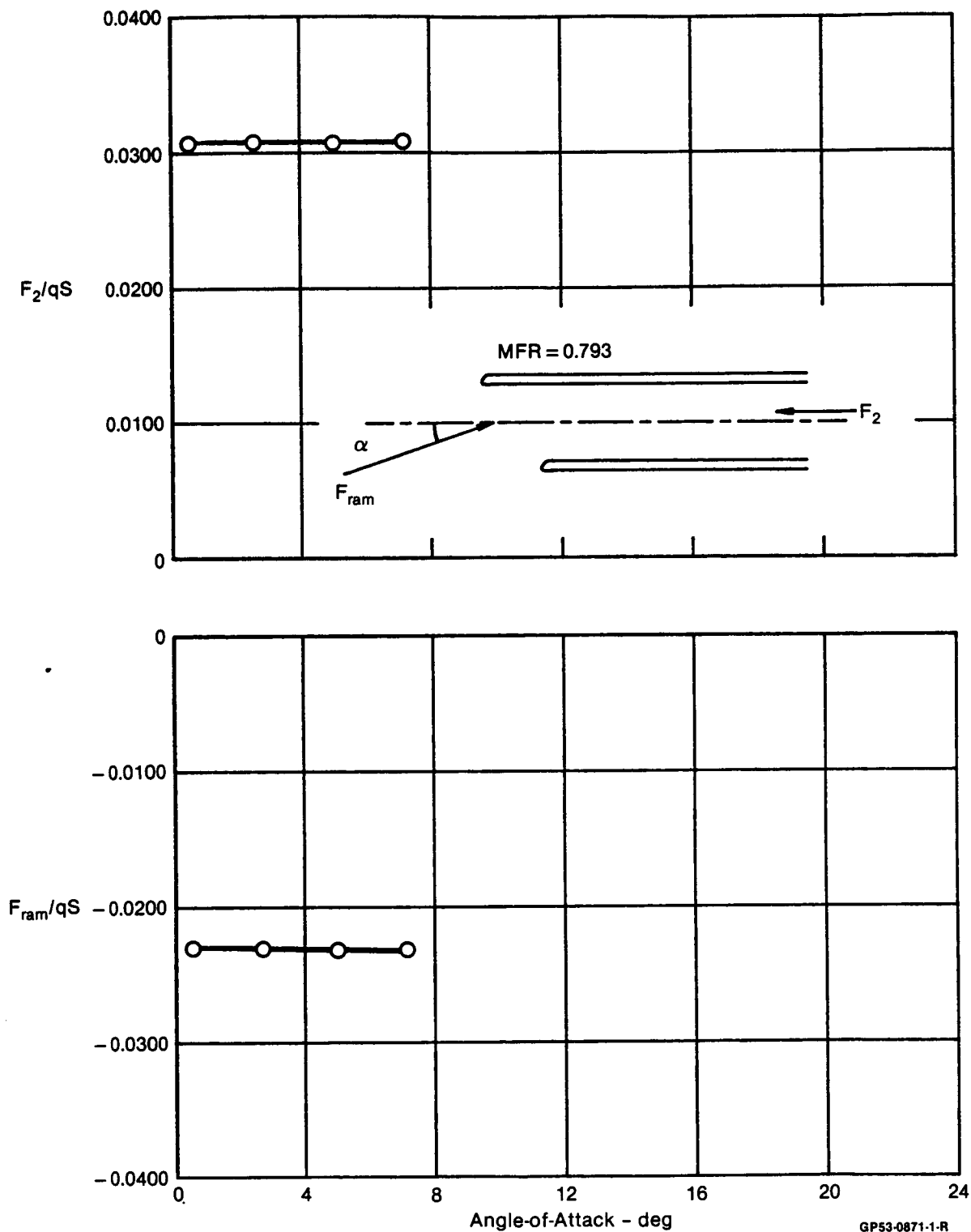


Figure 3-29. Variation of Stream Thrust and Ram Drag Coefficients
 CMAPS Mode Mach 1.4

For the CMAPS mode, the net airflow through the sting was the difference between the drive-line and bleed-line airflows, measured with critical flow venturi flowmeters. The value used for inlet airflow was based on the Plane 57 method described in Section 3.4.1.

For the Jet-Effects mode, total nozzle airflow was defined as the sum of drive-line and bleed-line airflows. (There is, of course, no inlet flow in the Jet-Effects mode.) The drive-line airflow was again measured with a venturi. The bleed-line airflow was based on an empirical correlation. Failure of the bleed-line airflow metering system early in the Jet-Effects mode test necessitated such a correlation. Airflow measurements made prior to the instrumentation failure were correlated with corresponding manifold pressure and total temperature. These correlation equations were then used to calculate bleed-line airflow. This predicted airflow was used for all the Jet-Effects runs as the bleed-line contribution to the total nozzle airflow. The correlation equations are included in Appendix C.

The pre-test airflow calibrations performed on the ALBEN by MCAIR and the total temperature measurements in the transition duct provided the means of calculating NPR from nozzle airflow. The calibration curves are presented in Reference 7.

4. REFERENCES

1. Zilz, D.E. and Devereaux, P.A., "Propulsion and Airframe Aerodynamic Interactions of Supersonic V/STOL Configurations - Volume I: Wind Tunnel Test Pressure Data Report", NASA CR-177343, September 1985.
2. Zilz, D. E.; Wallace, H. W.; and Hiley, P. E.; Propulsion and Airframe Aerodynamic Interactions of Supersonic V/STOL Configurations - Volume III: Wind Tunnel Test Data Analysis Report", NASA CR-177343, September.
3. Eigenmann, M. F. and Devereaux, P. A., Compact Multi-Mission Propulsion Simulator Development", AFWAL-TR-82-2040, September 1982.
4. Eigenmann, M. F.; Bear, R. L.; and Chandler, T. C.; "Turbine Engine Multi-Mission Propulsion Simulator Wind Tunnel Demonstration", AFAPL-TR-76-73, November 1976.
5. Hiley, P. E.; Wallace, H. W.; Booher, M.E.; and Reinsberg, J. G.; "Advanced Nozzle Concepts Program Volume III - Nozzle Integration for Air Superiority Fighter Application", AFWAL-TR-81-3165, Volume III, January 1982.
6. Mraz, M. R. and Hiley, P.E., "Propulsion and Airframe Aerodynamic Interactions of Supersonic V/STOL Configurations: Phase I - Final Report", NASA CR-177369, September 1985.
7. Booher, M.E., "Propulsion and Airframe Aerodynamic Interactions of Supersonic V/STOL Configurations: Phase II - Final Report", NASA CR-177370, September 1985.

8. Zilz, D. E.; Wallace, H. W.; and Hiley, P. E.; "Propulsion and Airframe Aerodynamic Interactions of Supersonic V/STOL Configurations - Volume IV: Final Report - Summary", NASA CR-177343, September 1985.
9. Smith, S.C., "Determining Compressor Inlet Airflow in the Compact Multimission Aircraft Propulsion Simulators in Wind Tunnel Applications", AIAA Paper 83-1231, June 1983.
10. Bailey, R.O., "Propulsion Simulation Test Technique for V/STOL Configurations", SAE Paper 83-1427, October 1983.
11. Smith, S.C., "Airflow Calibration of a Bellmouth Inlet for Measurement of Compressor Airflow in Turbine Powered Propulsion Simulators," NASA TM-84399.

APPENDIX A

WIND TUNNEL TEST RESULTS: FORCE AND MOMENT DATA

The basic force and moment data is presented graphically as lift, drag, and pitching moment coefficients. These coefficients are plotted in a manner which reflects the main variable during each run. Since most of the runs consisted of angle-of-attack (AOA) sweeps, the general plot format is to present C_L versus C_D , AOA, and C_M . The data which was acquired during nozzle pressure ratio (NPR) sweeps is presented as C_L , C_D and C_M versus NPR. The following plots of lift, drag, and pitching moment coefficients are therefore presented in two categories either angle-of-attack sweeps or nozzle pressure ratio sweeps.

The lifting characteristics of the canard are also presented here graphically. The left-hand canard was instrumented with a single strain gage near the root, Figure A-1, which was calibrated to measure a spanwise bending moment. The canard root bending moment coefficient ($C_{m_{CRB}}$) is an indirect indication of the canard's lifting properties.

A.1 ANGLE-OF-ATTACK SWEEPS - The force and moment plots are grouped to show the effects of various inlet, nozzle and control surface configurations over an angle-of-attack range. Each of these configurations is presented in a series of three plots. These three plots are as follows:



- (1) C_L -vs- C_D
- (2) C_L -vs- AOA
- (3) C_L -vs- C_M

The forces on the nozzle extensions were not included in the total lift, drag, and pitching moment coefficients. Therefore, the plots which include the Nozzle Extension or Nozzle Extension



Baseline Configurations are based on the airframe lift, drag, and pitching moment coefficients denoted here as CLA, CDA, and CMA.

Following is an index of the force and moment plots from the angle-of-attack sweeps.

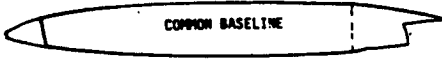
Inlet Mass Flow Ratio Effects

| Configuration | Test Mode | Mach | NPR | δ_c | Pages |
|--|-----------|------|-----|------------|---------|
|  NOZZLE EXTENSION COWL LIP = 0° $\delta_F = 0^\circ$ | F/T | 0.4 | N/A | -5° | 78-79 |
| | | 0.6 | ↓ | ↓ | 80-81 |
| | | 0.9 | ↓ | ↓ | 82-83 |
| | | 1.2 | ↓ | ↓ | 84-85 |
| | | 1.4 | ↓ | ↓ | 86-87 |
| COWL LIP = 45° $\delta_F = 30^\circ$ | F/T | 0.4 | N/A | 0° | 88-89 |
| COWL LIP = 0° $\delta_F = 0^\circ$ | CMAPS | 0.4 | N/A | 0° | 90-91 |
| | | 0.6 | ↓ | ↓ | 92-93 |
| | | 0.9 | ↓ | ↓ | 94-95 |
| | | 1.2 | ↓ | ↓ | 96-97 |
| | | 1.4 | ↓ | ↓ | 98-99 |
|  SIMULATED AIRCRAFT ALBEN A/B $\delta_N = 0^\circ$ | CMAPS | 0.4 | 1.3 | 0° | 100-101 |
| | | 0.9 | 2.0 | 0° | 102-103 |

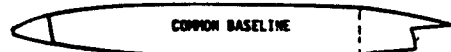
Nozzle Pressure Ration Effects

| Configuration | Test Mode | Mach | MFR | δ_c | Pages |
|---|-----------|------|------|------------|---------|
|  COMMON BASELINE ALBEN DRY $\delta_N = 0^\circ$ | J/E | 0.4 | N/A | -5° | 104-105 |
| | | 0.6 | ↓ | ↓ | 106-107 |
| | | 0.9 | ↓ | ↓ | 108-109 |
| ALBEN A/B $\delta_N = 0^\circ$ | J/E | 0.4 | N/A | -5° | 110-111 |
| | | 0.6 | ↓ | -5° | 112-113 |
| | | 0.9 | ↓ | -5° | 114-115 |
| | | 1.2 | ↓ | 0° | 116-117 |
| | | 1.4 | ↓ | 0° | 118-119 |
|  SIMULATED AIRCRAFT ALBEN A/B $\delta_N = 0^\circ$ | CMAPS | 0.4 | 1.15 | 0° | 120-121 |
| | | 0.6 | 0.92 | -5° | 122-123 |
| | | 0.9 | 0.75 | -5° | 124-125 |
| | | 1.2 | 0.69 | 0° | 126-127 |
| | | 1.4 | 0.72 | 0° | 128-129 |


NPR Effects With Thrust Vectoring

| Configuration | Test Mode | Mach | MFR | δ_c | Pages |
|--|-----------|------|-----|------------|---------|
|  COMMON BASELINE ALBEN A/B $\delta_N = 20^\circ$ | J/E | 0.4 | N/A | -5° | 130-131 |
| | | 0.6 | ↓ | -5° | 132-133 |
| | | 0.9 | | -5° | 134-135 |
| | | 1.2 | | 0° | 136-137 |
| $\delta_N = 30^\circ$ ALBEN A/B $\delta_F = 30^\circ$ | J/E | 0.4 | N/A | -5° | 138-139 |


Nozzle Vectoring Effects

| Configuration | Test Mode | Mach | NPR | δ_c | Pages |
|---|-----------|------|-----|------------|---------|
|  COMMON BASELINE $\delta_N = 0^\circ$ - vs - $\delta_N = 20^\circ$ | J/E | 0.4 | 4.1 | -5° | 140-141 |
| | | 0.6 | 4.2 | ↓ | 142-143 |
| | | 0.9 | 6.2 | -5° | 144-145 |
| $\delta_N = 0^\circ$ - vs - $\delta_N = 30^\circ$ $\delta_F = 0^\circ$ - vs - $\delta_F = 30^\circ$ | J/E | 0.4 | 4.1 | -5° | 146-147 |



Power Setting Effects

| Configuration | Test Mode | Mach | NPR | δ_c | Pages |
|--|-----------|------|-----|------------|---------|
|  COMMON BASELINE Dry-vs-A/B | J/E | 0.6 | 4.2 | -5° | 148-149 |
| | | 0.9 | 6.7 | -5° | 150-151 |


Canard Rotation Effects

| Configuration | Test Mode | Mach | MFR | NPR | Pages |
|---|-----------|------|------|-----|---------|
|  NOZZLE EXTENSION COWL LIP = 0° $\delta_F = 0^\circ$ | F/T | 0.4 | 1.20 | N/A | 152-153 |
| | | 0.6 | 0.92 | ↓ | 154-155 |
| | | 0.9 | 0.87 | | 156-157 |
| | | 1.2 | 0.89 | | 158-159 |
| | | 1.4 | 0.93 | | 160-161 |


Standard Rotation Effects (Continued)

| Configuration | Test Mode | Mach | MFR | NPR | Pages |
|--|-----------|------|------|-----|---------|
|  COMMON BASELINE ALBEN A/B $\delta_N = 0^\circ$ | F/T | 0.4 | N/A | 1.0 | 162-163 |
| | | 0.6 | ↓ | ↓ | 164-165 |
| | | 0.9 | ↓ | ↓ | 166-167 |
| | | 1.2 | ↓ | ↓ | 168-169 |
| | | 1.4 | ↓ | ↓ | 170-171 |
|  SIMULATED AIRCRAFT ALBEN A/B $\delta_N = 0^\circ$ | CMAPS | 0.4 | 1.15 | 2.8 | 172-173 |
| | | 0.6 | 0.91 | 3.8 | 174-175 |
| | | 0.9 | 0.75 | 5.4 | 176-177 |
| | | 1.2 | 0.75 | 7.5 | 178-179 |
| | | 1.4 | 0.79 | 9.6 | 180-181 |



Wing Flap and Cowl Lip Deflection Effects

| Configuration | Test Mode | Mach | MFR | NPR | δ_C | Pages |
|--|-----------|------|------|-----|------------|---------|
|  NOZZLE EXTENSION | F/T | 0.4 | 1.11 | N/A | 0° | 182-183 |


Cowl Lip Deflection Effects

| Configuration | Test Mode | Mach | MFR | NPR | δ_C | Pages |
|---|-----------|------|------|-----|------------|---------|
|  NOZZLE EXTENSION | F/T | 0.6 | 0.85 | N/A | -5° | 184-185 |
| | | 0.9 | 0.85 | ↓ | ↓ | 186-187 |

Nozzle Extension Effects

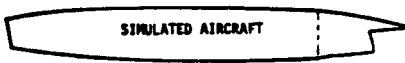
| Configuration | Test Mode | Mach | MFR | NPR | δ_C | Pages |
|--|-----------|------|-----|-----|------------|---------|
|  NOZZLE EXTENSION BASELINE — vs — | F/T | 0.4 | N/A | N/A | -5° | 188-189 |
| | | 0.6 | ↓ | ↓ | -5° | 190-191 |
| | | 0.9 | ↓ | ↓ | -5° | 192-193 |
| | | 1.2 | ↓ | ↓ | 0° | 194-195 |
| | | 1.4 | ↓ | ↓ | 0° | 196-197 |
|  COMMON BASELINE | | | | | | |

Common Baseline Comparison

| Configuration | Test Mode | Mach | MFR | NPR | δ_c | Pages |
|--|---------------|------|-----|-----|------------|---------|
|  ALBEN A/B $\delta_N = 0^\circ$ | FT, JE, CMAPS | 0.4 | N/A | 1.0 | -5° | 198-199 |
| | | 0.6 | ↓ | ↓ | -5° | 200-201 |
| | | 0.9 | | | -5° | 202-203 |
| | | 1.2 | | | 0° | 204-205 |
| | | 1.4 | | | 0° | 206-207 |

A.2 NPR SWEEPS - The throttle dependent effects on lift, drag, and pitching moment are presented in this section. Nozzle and total configuration force and moment data is plotted versus nozzle pressure ratio.

Inlet Mass Flow Ratio Effects

| Configuration | Test Mode | Mach | δ_c | α | Pages |
|---|-----------|------|------------|--------------|---------|
|  ALBEN A/B $\delta_N = 0^\circ$ | CMAPS | 0.6 | -5° | 0° | 208-209 |
| | | | | 4.5° | 210-211 |
| | | | | 9° | 212-213 |
| | | | | 17.5° | 214-215 |
| | | | | | |

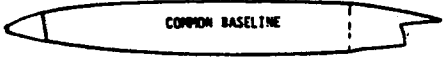
Angle of Attack Effects

| Test Mode | Mach | δ_c | MFR | Pages |
|-----------|------|------------|------|---------|
| CMAPS | 0.6 | -5° | 0.91 | 216-217 |


Canard Rotation Effects

| Test Mode | Mach | MFR | α | Pages |
|-----------|------|------|--------------|---------|
| CMAPS | 0.6 | 0.69 | 0° | 218-219 |
| | | 0.91 | 0° | 220-221 |
| | | 0.61 | 17.5° | 222-223 |
| | | 0.75 | 17.5° | 224-225 |

Nozzle Vectoring Effects



| Configuration | Test Mode | Mach | δ_C | | Pages |
|---|-----------|------|------------|----|---------|
|  ALBEN A/B | J/E | 0.4 | -5° | 0° | 226-227 |
| | | 0.6 | -5° | ↓ | 228-229 |
| | | 0.9 | -5° | ↓ | 230-231 |
| | | 1.2 | 0° | ↓ | 232-233 |

Power Setting Effects



| Configuration | Test Mode | Mach | δ_C | | Pages |
|---|-----------|------|------------|----|---------|
|  ALBEN A/B vs ALBEN Dry | J/E | 0.4 | -5° | 0° | 234-235 |
| | | 0.6 | ↓ | ↓ | 236-237 |
| | | 0.9 | ↓ | ↓ | 238-239 |

A.3 CANARD ROOT BENDING MOMENT - The effects of canard deflection angle, MFR, and NPR variations on the canard root bending moment ($C_{m_{CRB}}$) are presented in this section. All of the plots are in the form of $C_{m_{CRB}}$ versus angle-of-attack.



Canard Rotation Effects

| Configuration | Test Mode | Mach | MFR | NPR | Pages |
|---|-----------|------|------|-----|-------|
|  ALBEN A/B $\delta_N = 0^\circ$ | FT | 0.4 | N/A | 1.0 | 240 |
| | | 0.6 | ↓ | ↓ | 241 |
| | | 0.9 | ↓ | ↓ | 242 |
| | | 1.2 | ↓ | ↓ | 243 |
| | | 1.4 | ↓ | ↓ | 244 |
| | FT | 0.4 | 1.10 | N/A | 245 |
| | | 0.6 | 0.92 | ↓ | 246 |
| | | 0.9 | 0.87 | ↓ | 247 |
| | | 1.2 | 0.89 | ↓ | 248 |
| | | 1.4 | 0.92 | ↓ | 249 |
|  ALBEN A/B $\delta_N = 0^\circ$ | CMAPS | 0.4 | 1.15 | 2.8 | 250 |
| | | 0.6 | 0.91 | 3.8 | 251 |
| | | 0.9 | 0.75 | 5.4 | 252 |
| | | 1.2 | 0.75 | 7.5 | 253 |
| | | 1.4 | 0.79 | 9.6 | 254 |

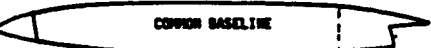
Mass Flow Ratio Effects

| Configuration | Test Mode | Mach | NPR | δ_c | Pages |
|---|-----------|------|-----|------------|-------|
|  NOZZLE EXTENSION COWL LIP = 0° $\delta_F = 0^\circ$ | FT | 0.4 | N/A | -5° | 255 |
| | | 0.6 | ↓ | -5° | 256 |
| | | 0.9 | | -5° | 257 |
| | | 1.2 | | 0° | 258 |
| | | 1.4 | | 0° | 259 |
|  SIMULATED AIRCRAFT ALBEN A/B $\delta_N = 0^\circ$ | CMAPS | 0.4 | 1.3 | 0° | 260 |
| | | 0.9 | 4.4 | 0° | 261 |

Nozzle Pressure Ratio Effects

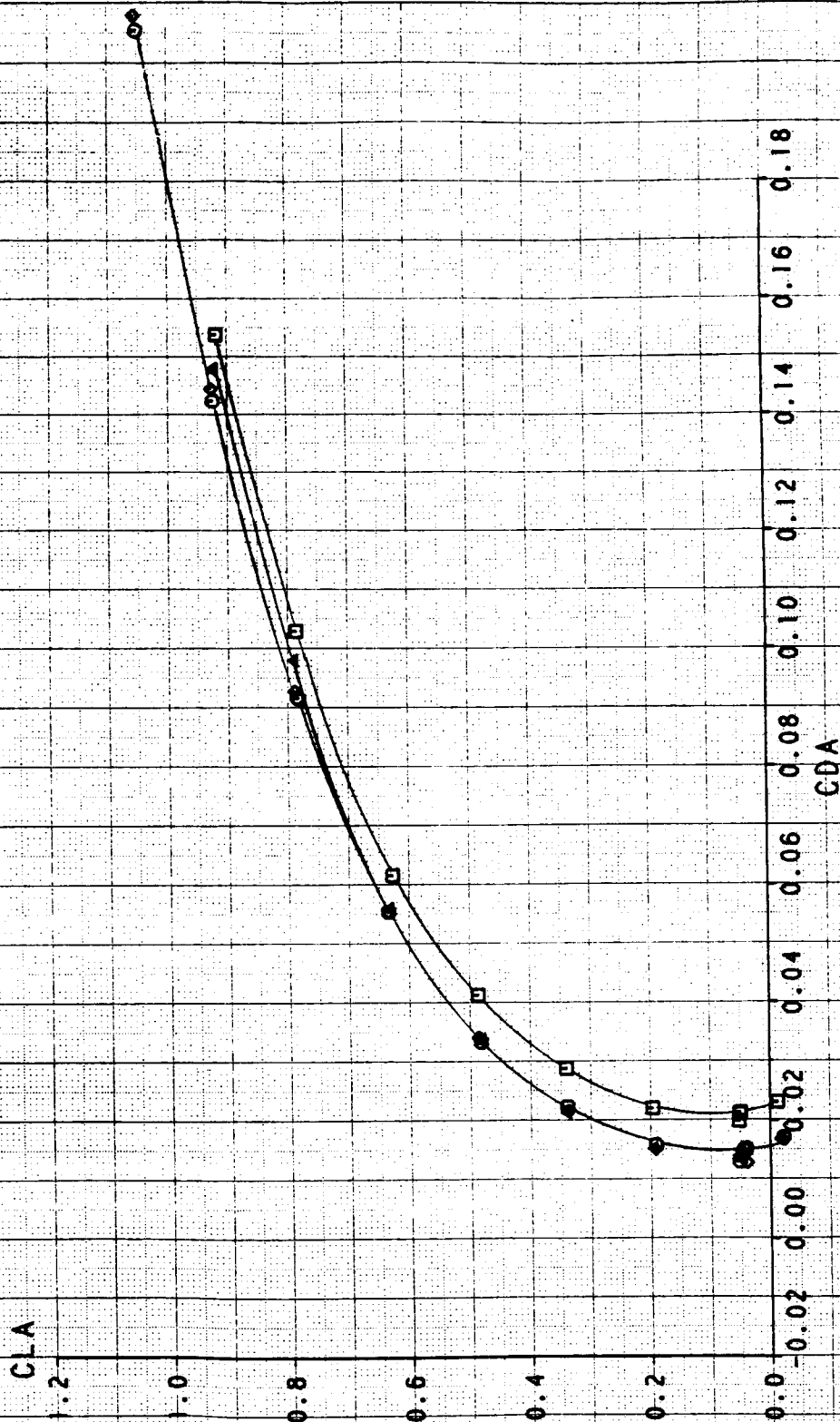
| Configuration | Test Mode | Mach | MFR | δ_c | Pages |
|---|-----------|------|------|------------|-------|
|  COMMON BASELINE ALBEN A/B $\delta_N = 0^\circ$ | JE | 0.4 | N/A | -5° | 262 |
| | | 0.6 | ↓ | -5° | 263 |
| | | 0.9 | | -5° | 264 |
| | | 1.2 | | 0° | 265 |
| | | 1.4 | | 0° | 266 |
|  SIMULATED AIRCRAFT ALBEN A/B $\delta_N = 0^\circ$ | CMAPS | 0.4 | 1.16 | -5° | 267 |
| | | 0.6 | 0.92 | 0° | 268 |
| | | 0.9 | 0.76 | -5° | 269 |
| | | 1.2 | 0.69 | 0° | 270 |
| | | 1.4 | 0.72 | 0° | 271 |

Nozzle Vectoring Effects

| Configuration | Test Mode | Mach | NPR | δ_c | Pages |
|---|-----------|------|-----|------------|-------|
|  COMMON BASELINE ALBEN A/B $\delta_N = 0^\circ$ -vs- $\delta_N = 20^\circ$ | JE | 0.4 | 4.0 | -5° | 272 |
| | | 0.6 | 4.2 | -5° | 273 |
| | | 0.9 | 6.2 | -5° | 274 |

INLET MASS FLOW RATIO EFFECTS ON CLA VS CDA FLOW-THROUGH MODE WITH NOZZLE EXTENSIONS

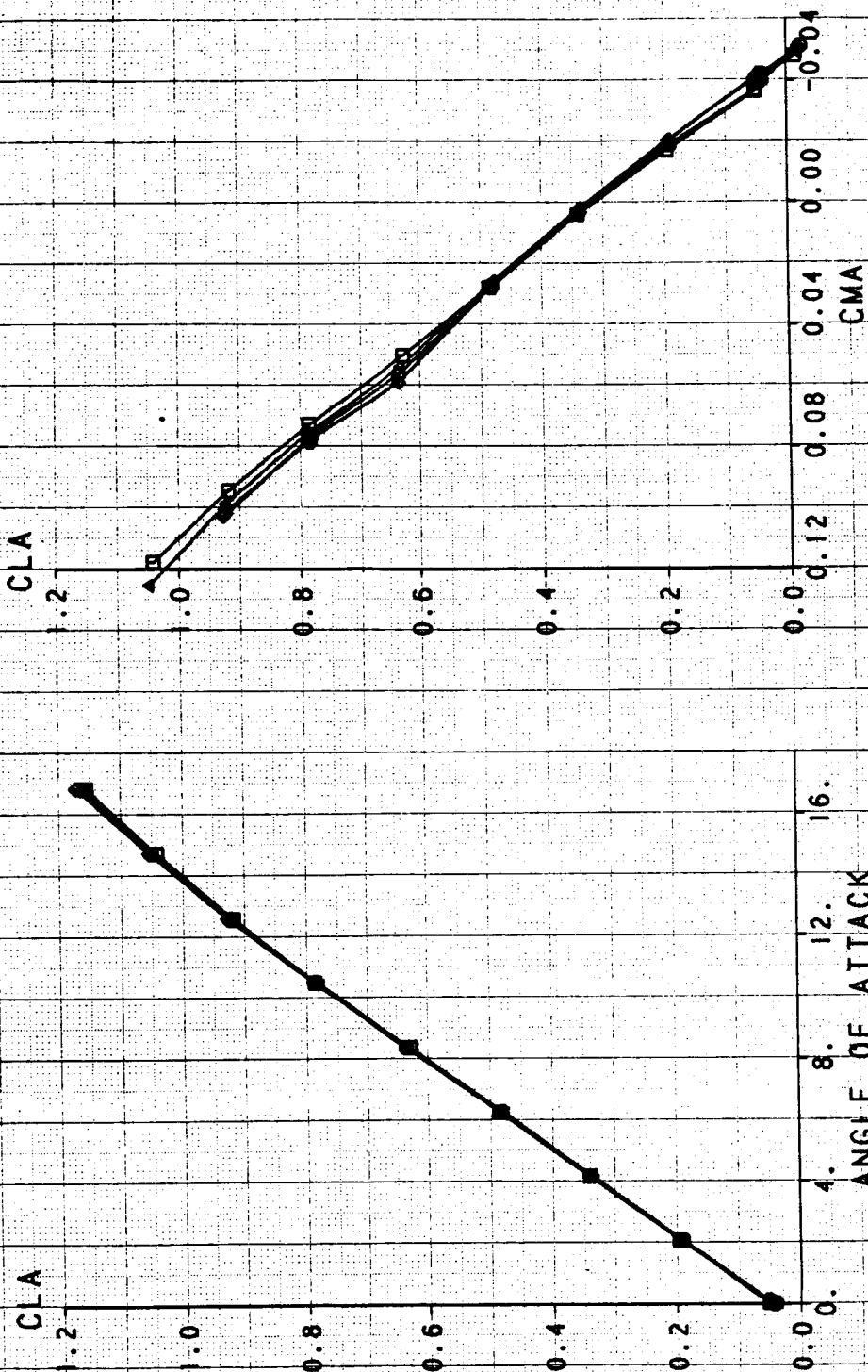
| SYM | TEST | RUN | RMACH | RMFR | RDELCL |
|-----|------|-----|--------|--------|---------|
| □ | 514 | 188 | 0.3999 | 0.5546 | -4.9989 |
| △ | 514 | 206 | 0.3982 | 0.6216 | -4.9948 |
| ◇ | 514 | 178 | 0.3988 | 1.1164 | -4.9726 |
| ○ | 514 | 167 | 0.4016 | 1.1343 | -4.9956 |



ORIGINAL PAGE IS
OF POOR QUALITY

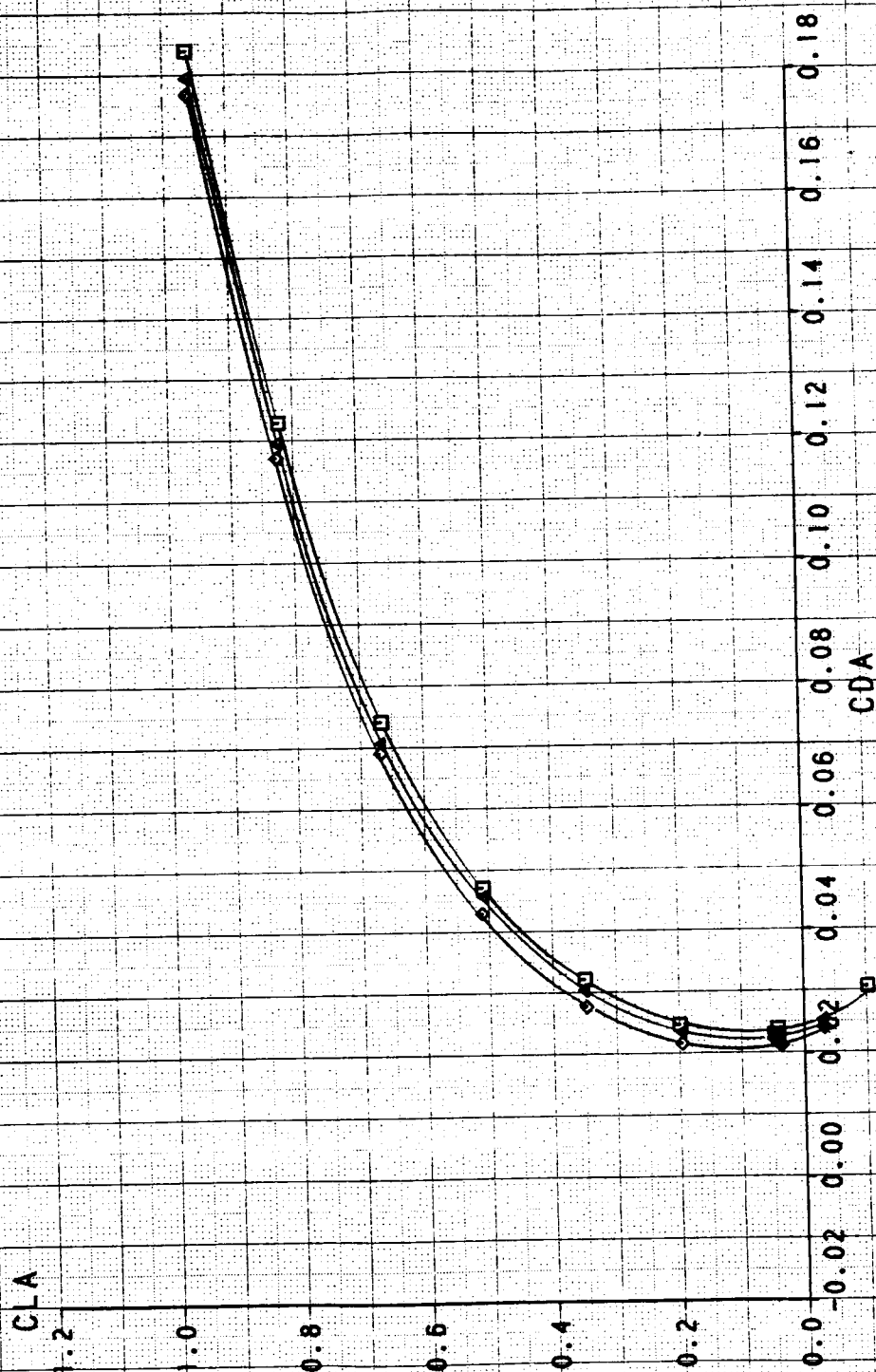
INLET MASS FLOW RATIO EFFECTS ON CLA VS AOA AND CMA

| SYM | TEST | RUN | RMACH | RWER | RDELCL |
|-----|------|-----|--------|--------|---------|
| □ | 514 | 188 | 0.3999 | 0.5546 | -4.9989 |
| △ | 514 | 206 | 0.3982 | 0.8216 | -4.9948 |
| ◇ | 514 | 178 | 0.3988 | 1.1164 | -4.9728 |
| ○ | 514 | 167 | 0.4016 | 1.1343 | -4.9956 |



INLET MASS FLOW RATIO EFFECTS ON CLA VS CDA

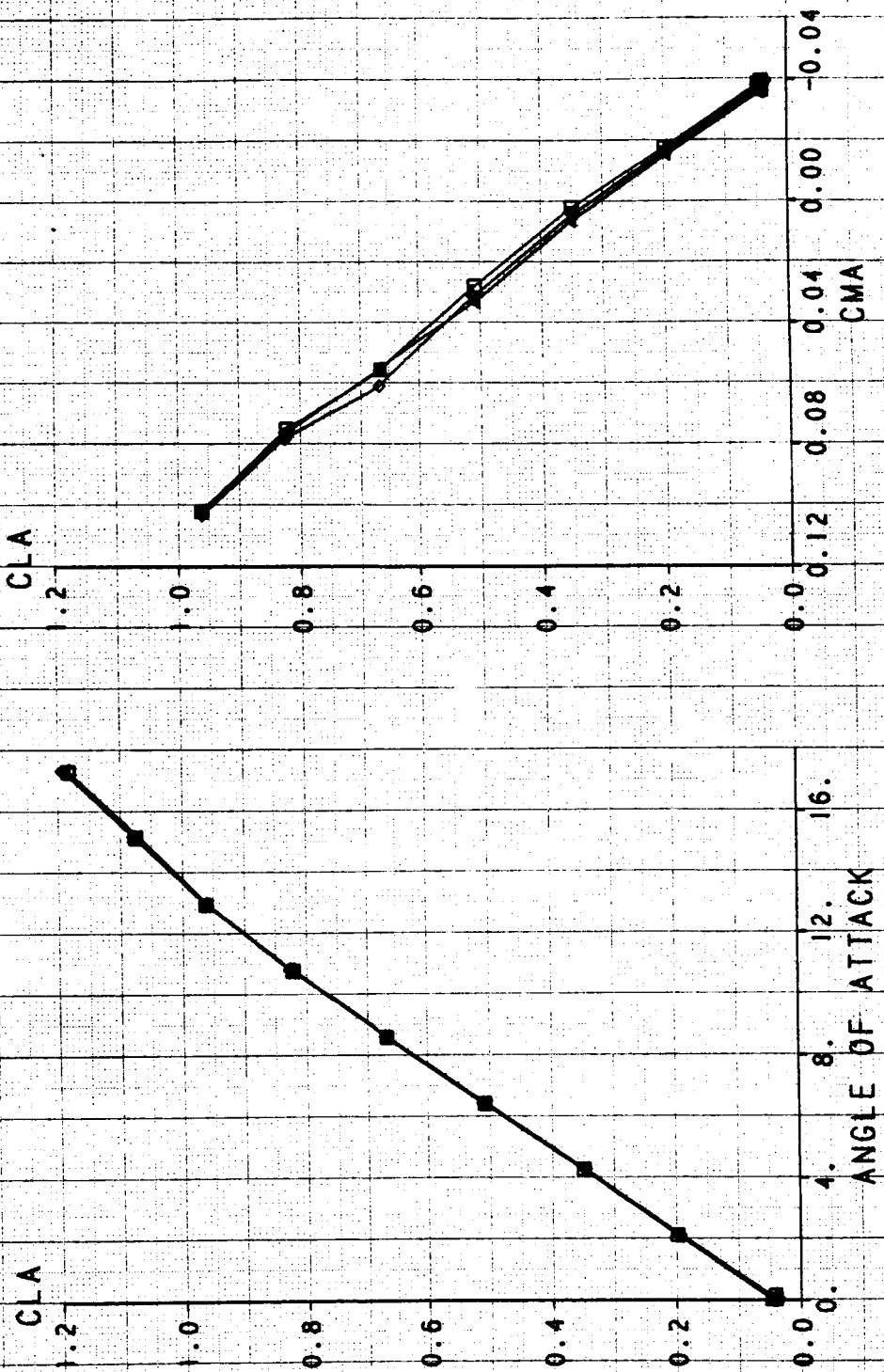
| SYM | TEST | RUN | RMACH | RMFR | RDELCL |
|-----|------|-----|--------|--------|---------|
| □ | 514 | 112 | 0.5970 | 0.3531 | -4.9087 |
| △ | 514 | 137 | 0.5997 | 0.3265 | -4.9685 |
| ◇ | 514 | 152 | 0.5987 | 0.7036 | -4.9599 |



INLET MASS FLOW RATE EFFECTS ON CLA VS AOA AND CMA

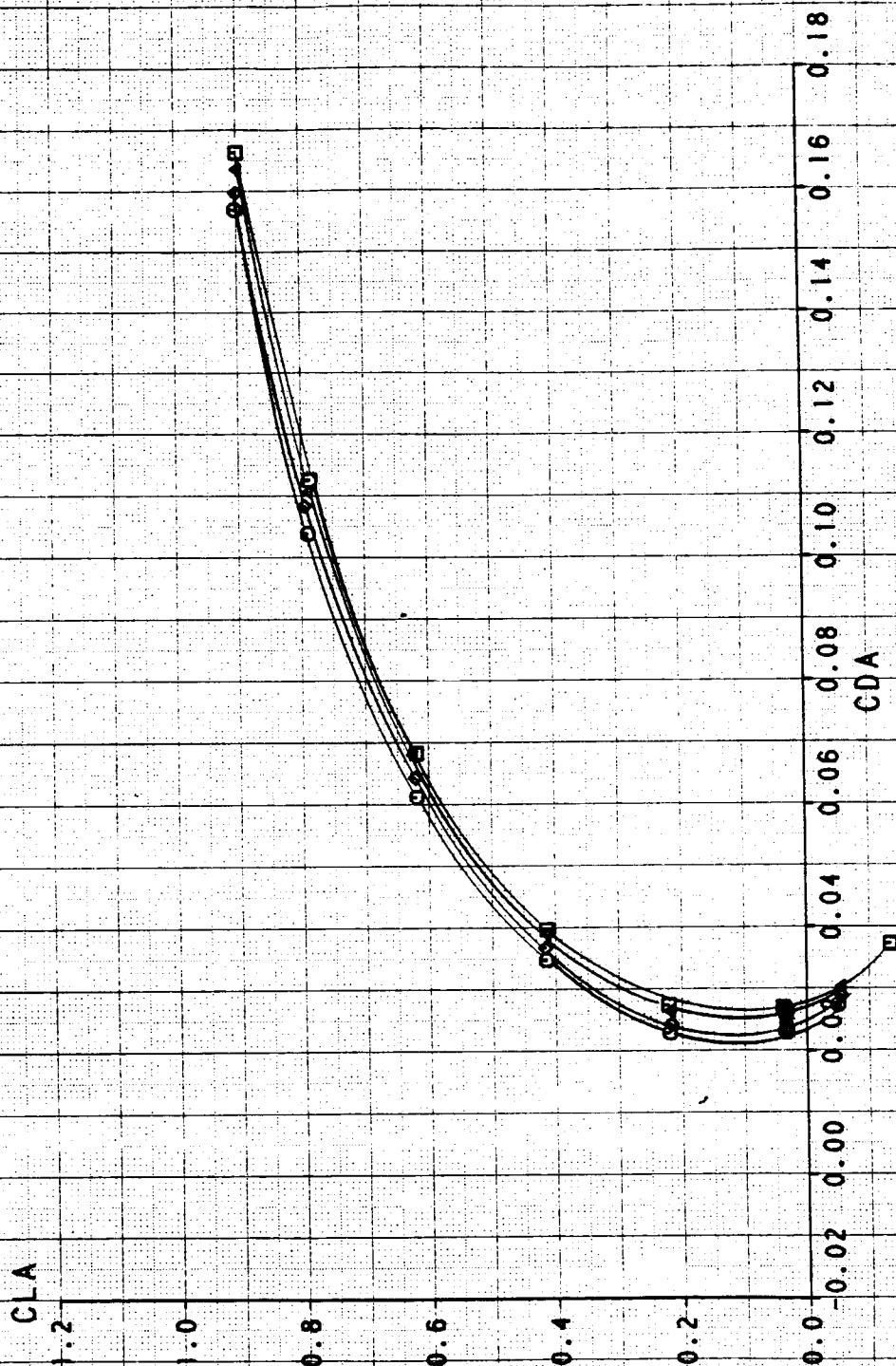
FLOW-THROUGH MODE WITH NOZZLE EXTENSIONS

| SYM | TEST | RUN | RMACH | RMFR | RDELCL |
|-----|------|-----|--------|--------|---------|
| □ | 514 | 112 | 0.5970 | 0.3531 | -4.9087 |
| △ | 514 | 137 | 0.5997 | 0.5265 | -4.9685 |
| ◇ | 514 | 152 | 0.5987 | 0.7036 | -4.9599 |



INLET MASS FLOW RATIO EFFECTS ON CLA VS CDA FLOW-THROUGH MODE WITH NOZZLE EXTENSIONS

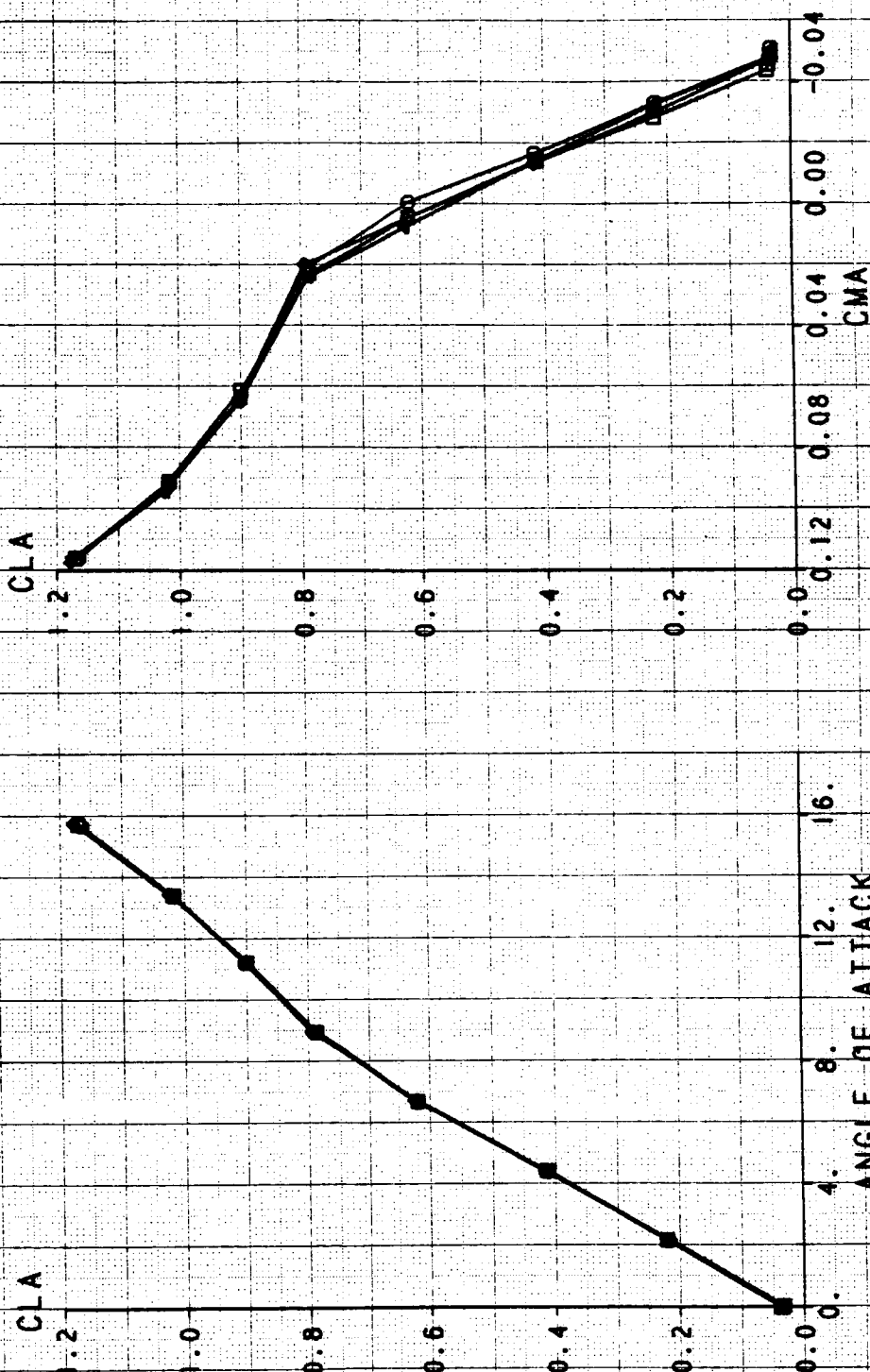
| SYM | TEST | RUN | RMACH | RNER | RDELCL |
|-----|------|-----|--------|--------|---------|
| □ | 514 | 117 | 0.9000 | 0.3485 | -4.9149 |
| △ | 514 | 133 | 0.9018 | 0.5176 | -4.9635 |
| ◇ | 514 | 147 | 0.9018 | 0.7063 | -4.9854 |
| ⊙ | 514 | 156 | 0.9022 | 0.8692 | -4.9921 |



INLET MASS FLOW RATE EFFECTS ON CLA VS ADA AND CMA

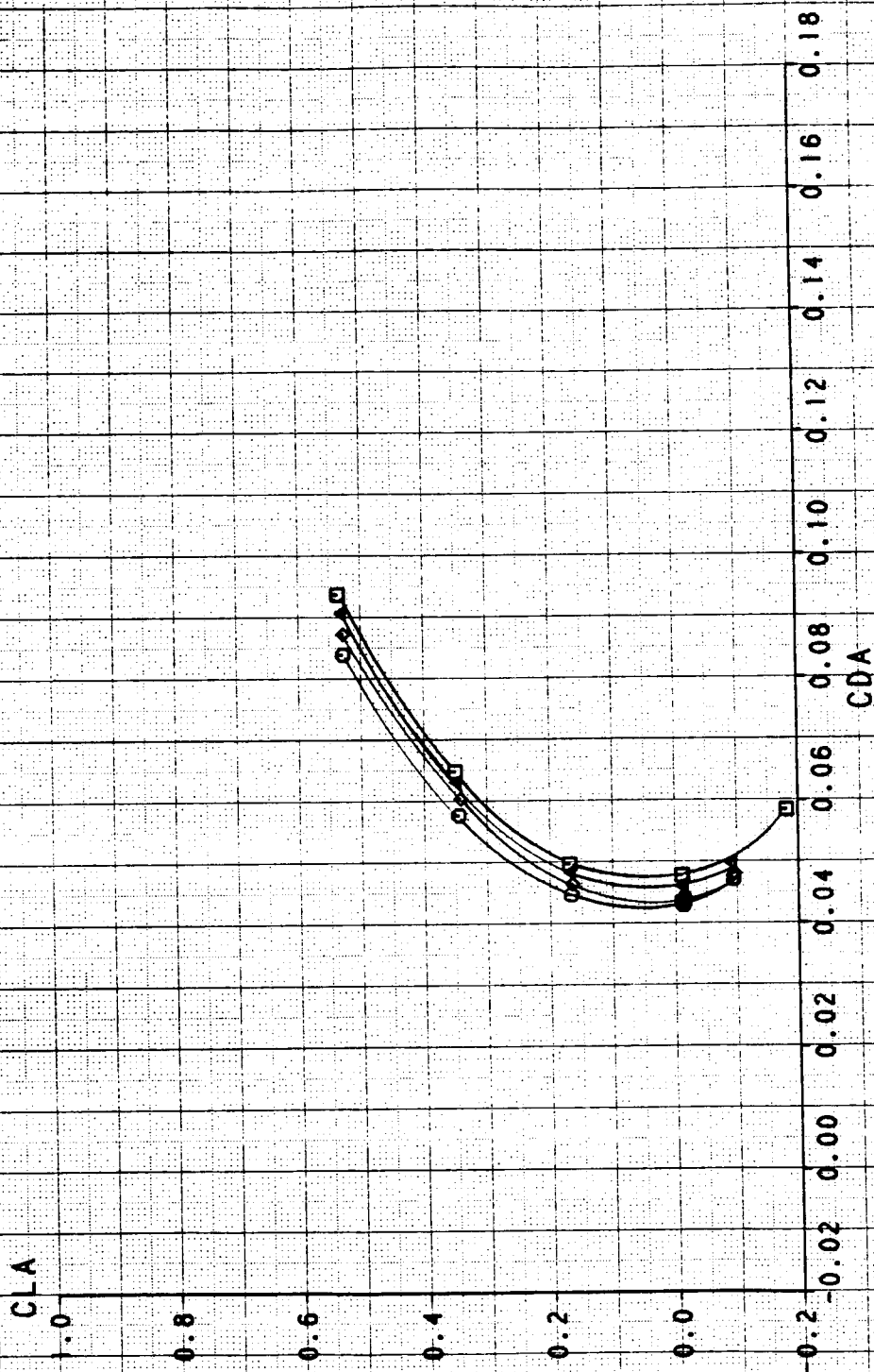
FLOW-THROUGH MODE WITH NOZZLE EXTENSIONS

| SYM | TEST | RUN | RMACH | RNFR | RDELCL |
|-----|------|-----|--------|--------|---------|
| □ | 514 | 117 | 0.9000 | 0.3485 | -4.9149 |
| △ | 514 | 133 | 0.9018 | 0.5176 | -4.9635 |
| ◇ | 514 | 147 | 0.9018 | 0.7063 | -4.9854 |
| ⊙ | 514 | 156 | 0.9022 | 0.8692 | -4.9921 |



INLET MASS FLOW RATIO EFFECTS ON CLA VS CDA FLOW-THROUGH MODE WITH NOZZLE EXTENSIONS

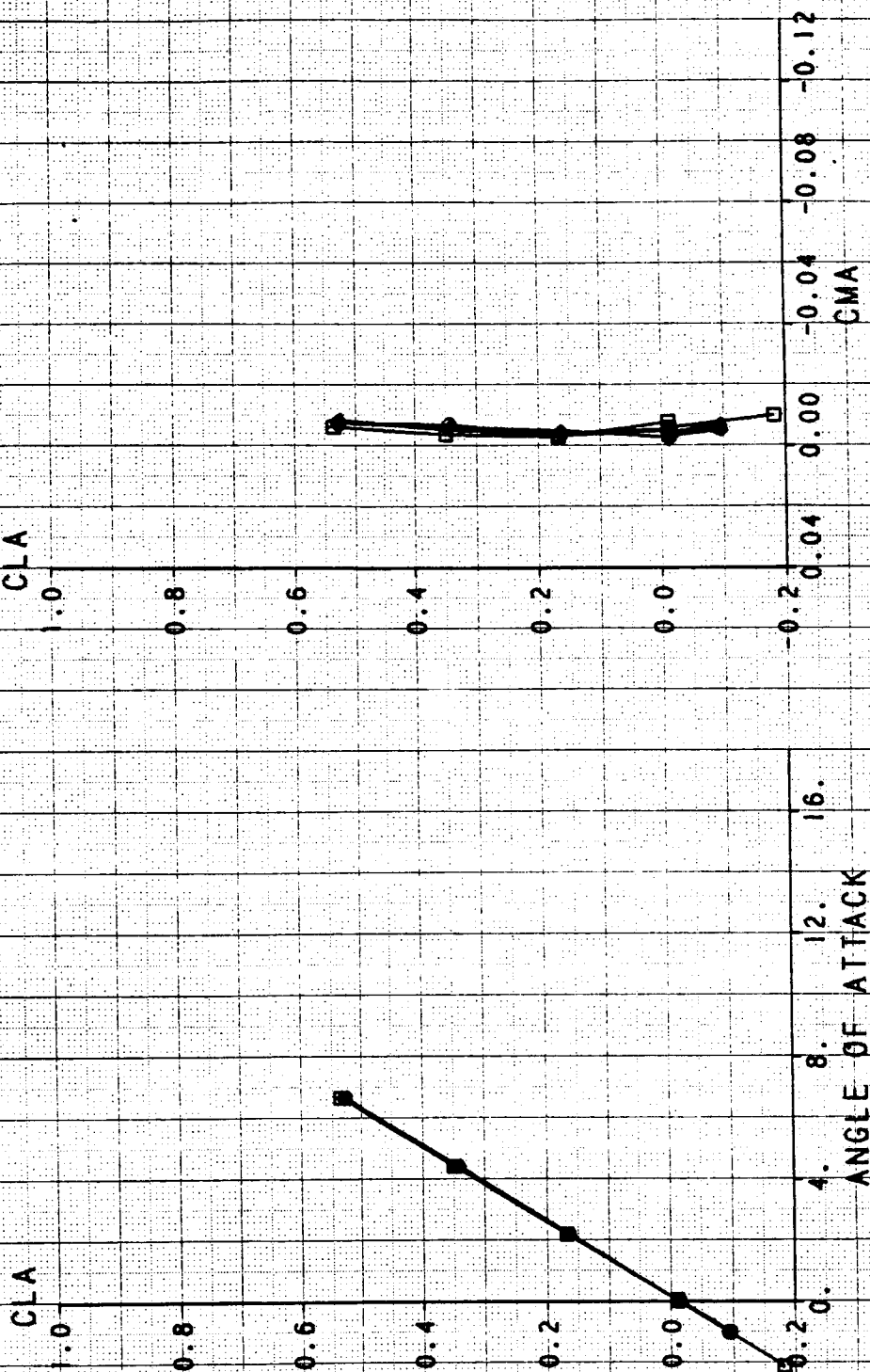
| SYM | TEST | RUN | RMACH | RMFR | RDELCL |
|-----|------|-----|--------|--------|---------|
| □ | 514 | 120 | 1.2012 | 0.3525 | -4.9670 |
| △ | 514 | 130 | 1.1985 | 0.3223 | -4.9605 |
| ◇ | 514 | 144 | 1.1979 | 0.7103 | -4.9762 |
| ○ | 514 | 159 | 1.1977 | 0.8895 | -4.9745 |



INLET MASS FLOW RATIO EFFECTS ON CLA VS AOA AND CMA

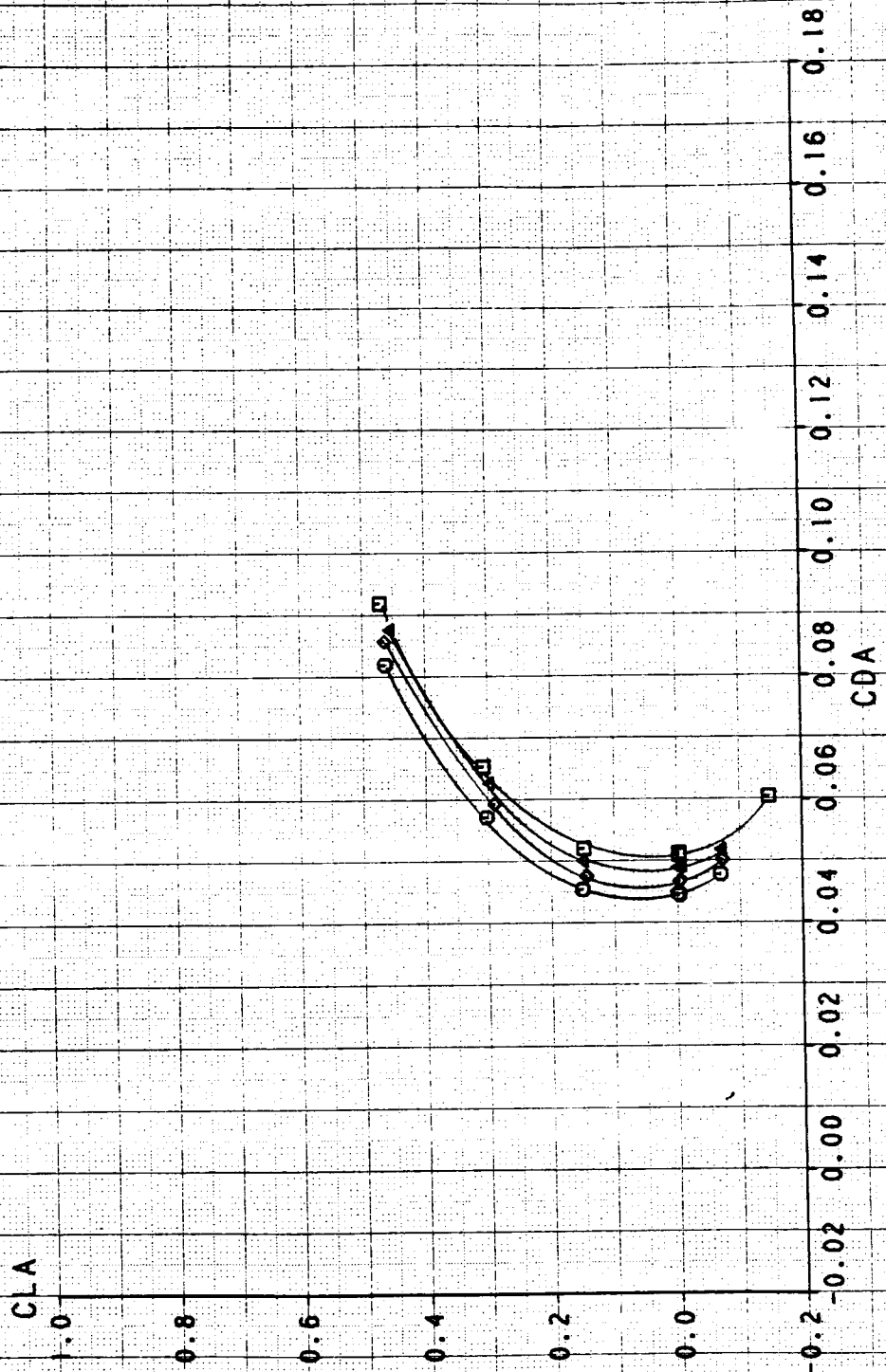
FLOW-THROUGH MODE WITH NOZZLE EXTENSIONS

| SYM | TEST | RUN | RMACH | RUEF | RDELCL |
|-----|------|-----|--------|--------|---------|
| □ | 514 | 120 | 1.2012 | 0.3525 | -4.9670 |
| △ | 514 | 130 | 1.1985 | 0.3223 | -4.9605 |
| ◇ | 514 | 144 | 1.1979 | 0.7103 | -4.9762 |
| ○ | 514 | 159 | 1.1977 | 0.8895 | -4.9745 |



INLET MASS FLOW RATE EFFECTS ON CLA VS CDA FLOW-THROUGH MODE WITH NOZZLE EXTENSIONS

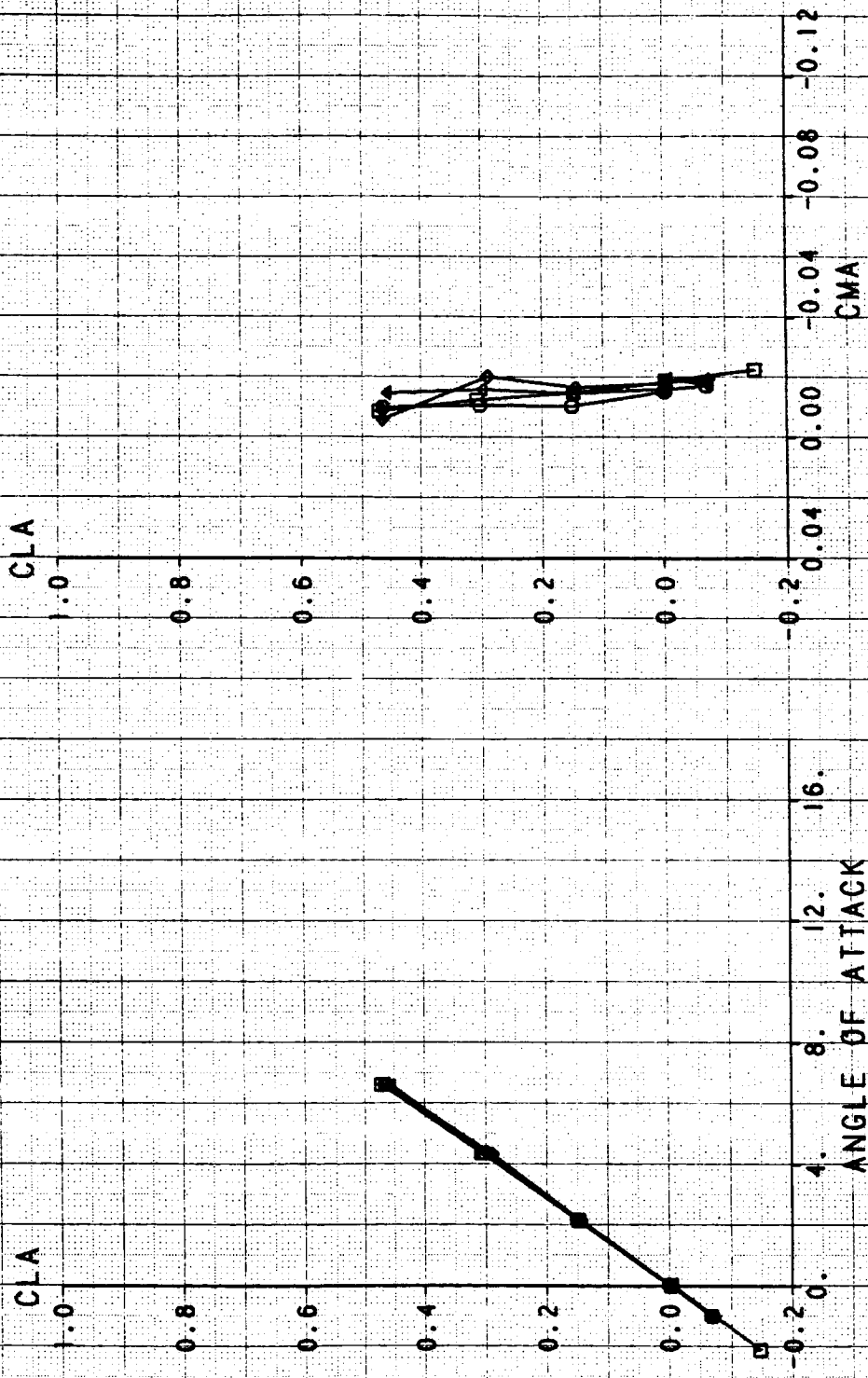
| SYM | TEST | RUN | RMACH | RWER | ROELCL |
|-----|------|-----|--------|--------|----------|
| □ | 514 | 123 | 1.3879 | 0.3651 | -4.96636 |
| △ | 514 | 127 | 1.3944 | 0.5440 | -4.9658 |
| ◇ | 514 | 143 | 1.3977 | 0.7424 | -4.9978 |
| ○ | 514 | 162 | 1.3939 | 0.9261 | -4.9931 |

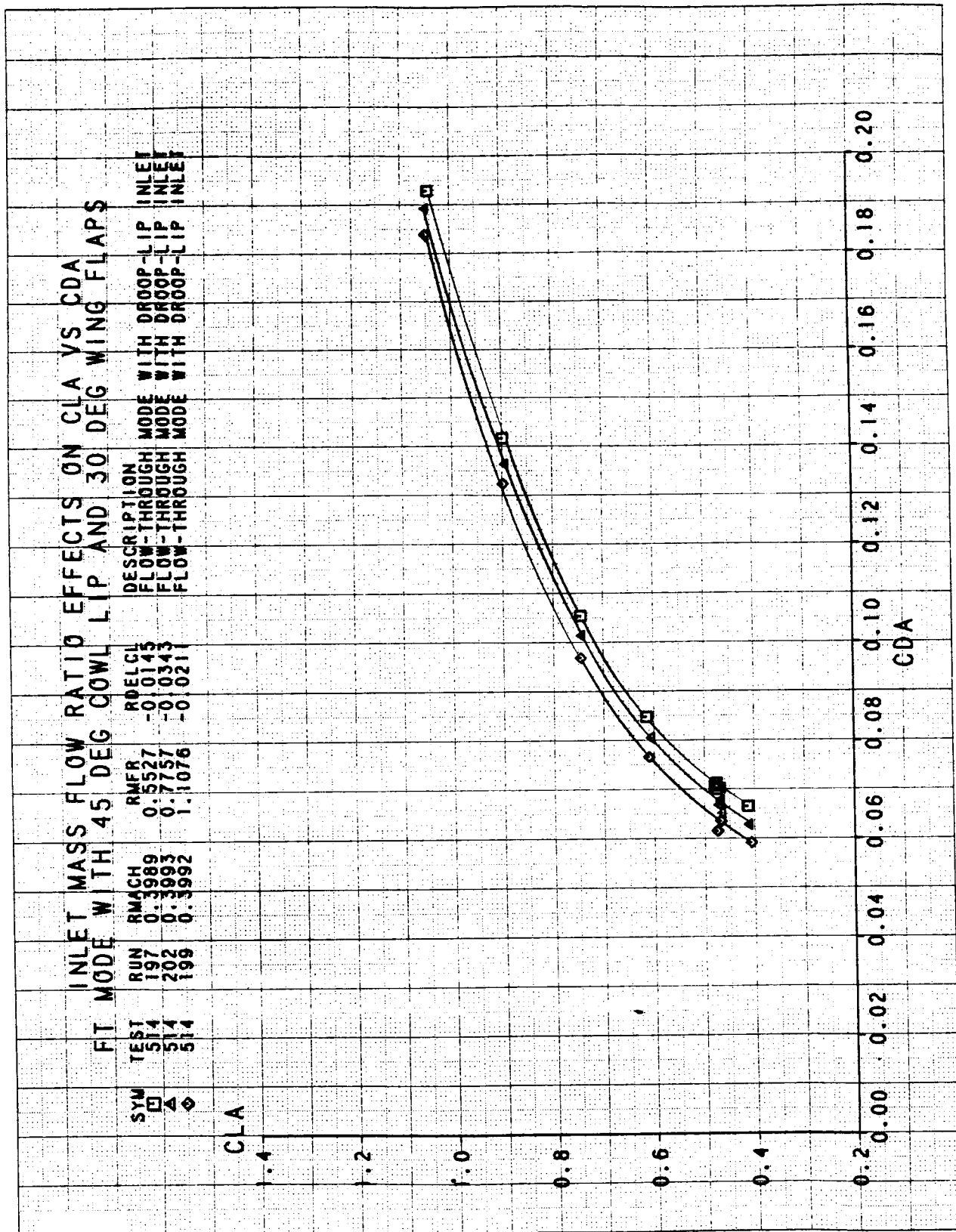


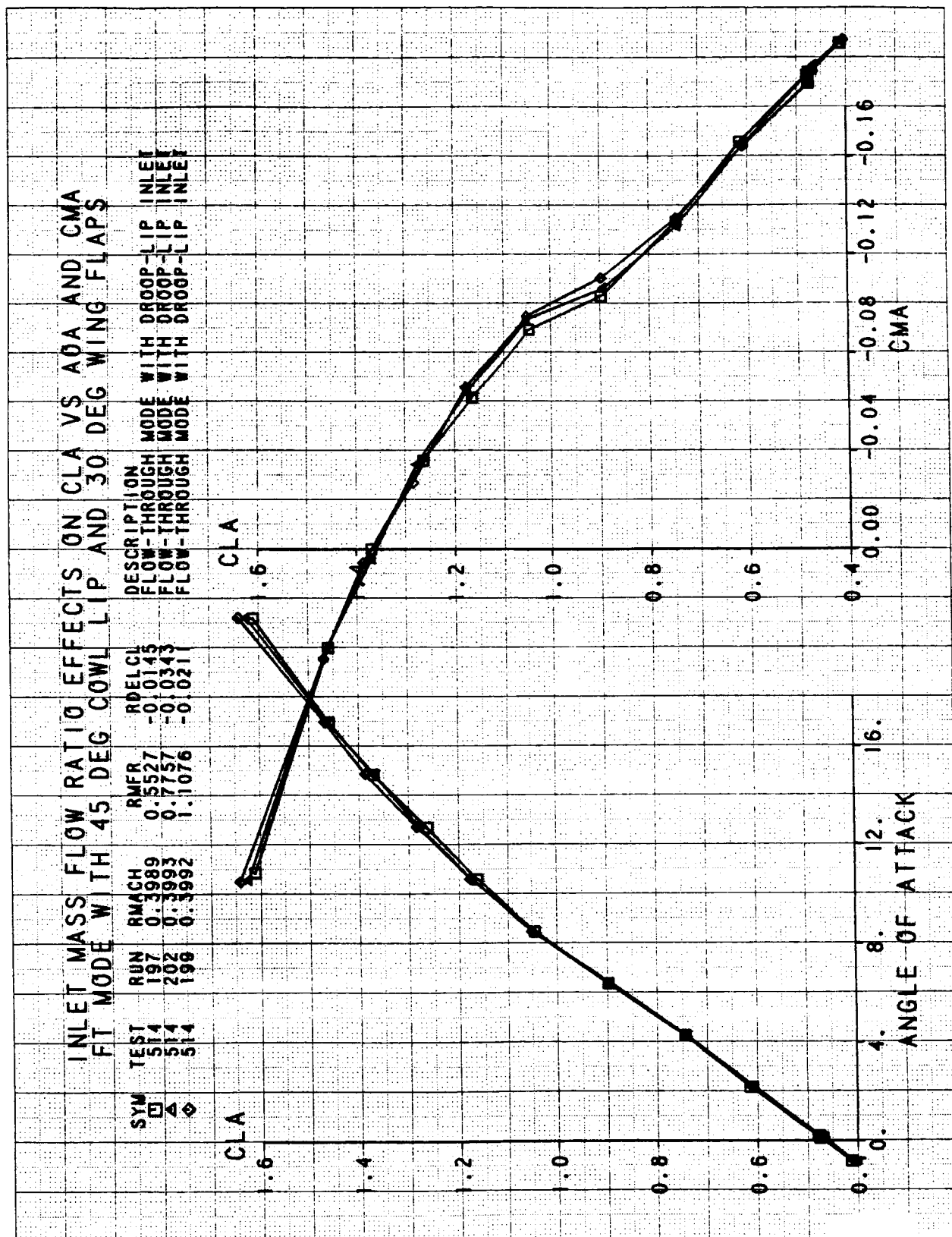
INLET MASS FLOW RATE EFFECTS ON CLA VS AOA AND CMA

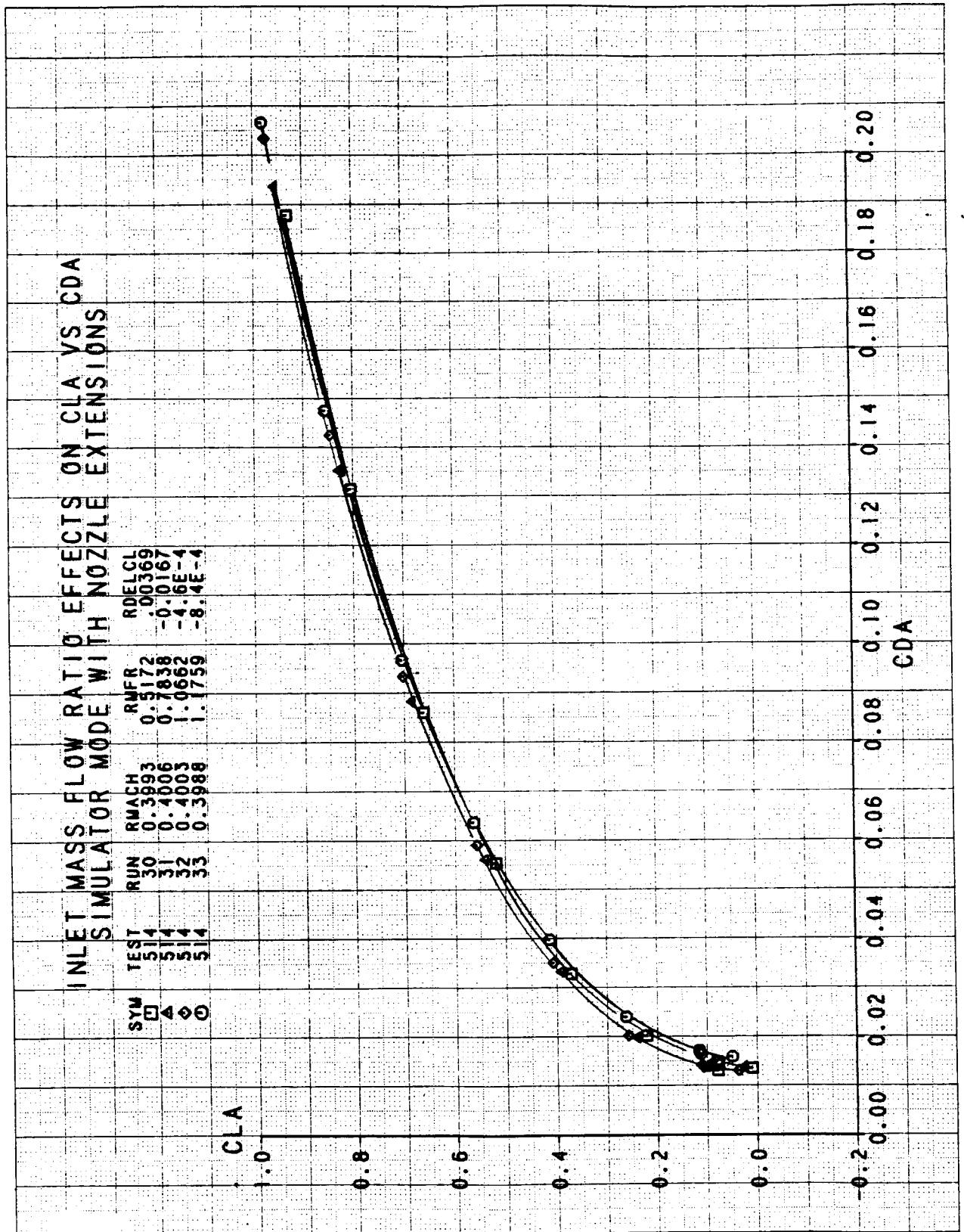
FLOW-THROUGH MODE WITH NOZZLE EXTENSIONS

| SYM | TEST | RUN | RMACH | RNFR | ROELCL |
|-----|------|-----|--------|--------|---------|
| □ | 514 | 123 | 1.3879 | 0.3651 | -4.9636 |
| △ | 514 | 127 | 1.3944 | 0.5440 | -4.9658 |
| ◇ | 514 | 143 | 1.3977 | 0.7424 | -4.9978 |
| ○ | 514 | 162 | 1.3939 | 0.9261 | -4.9931 |



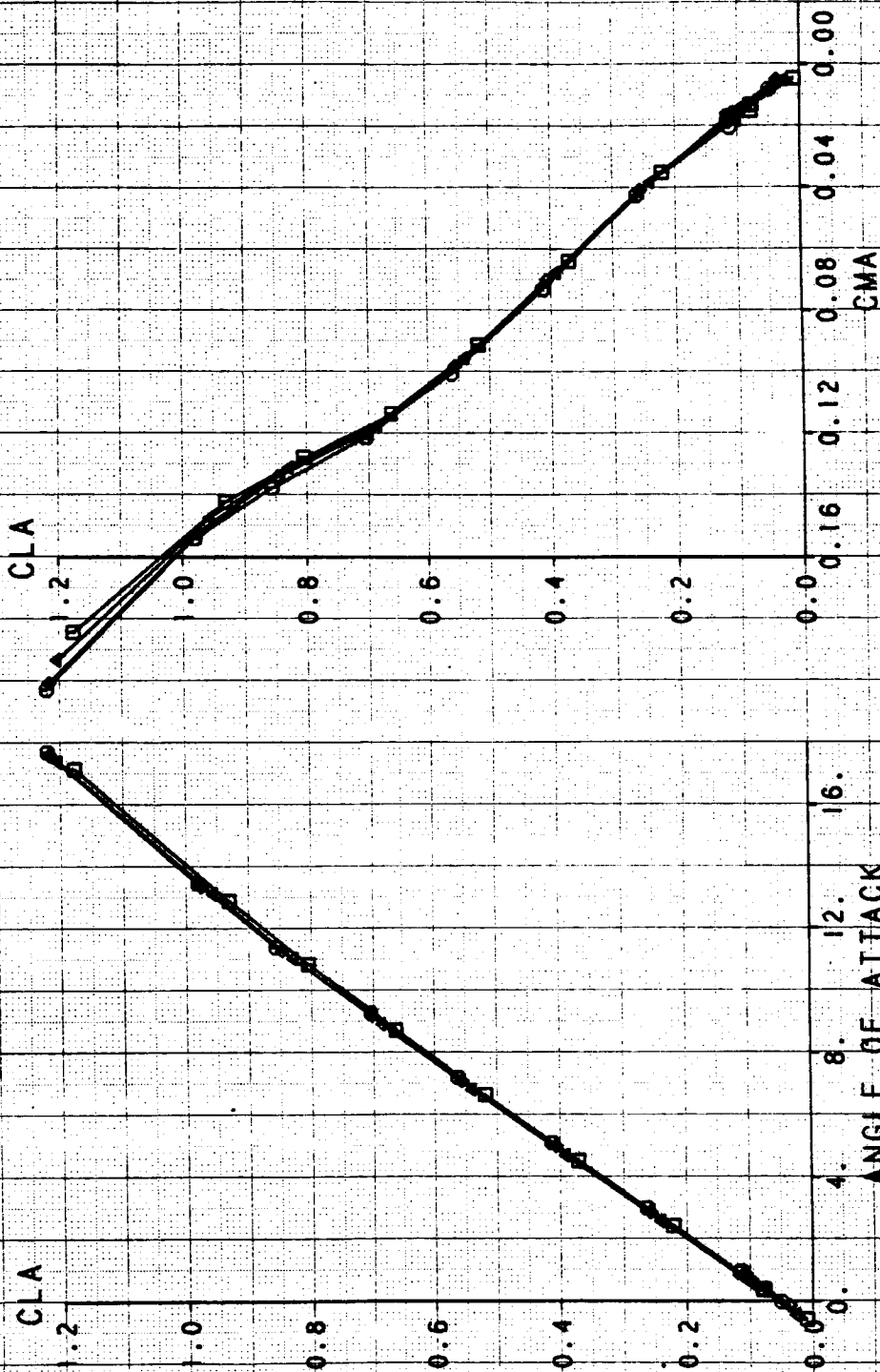






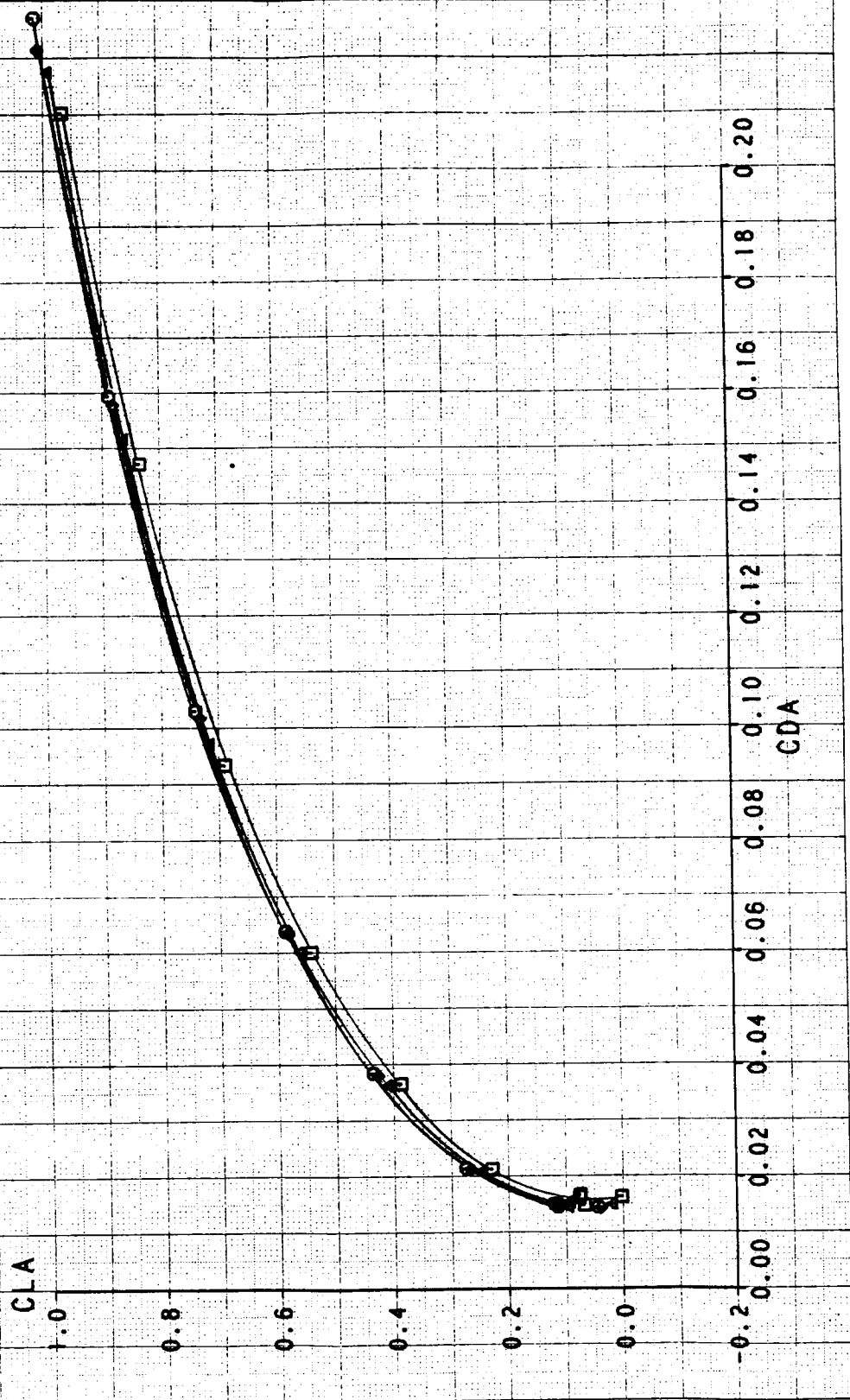
INLET MASS FLOW RATIO EFFECTS ON CLA VS AOA AND CMA

| SYM | TEST | RUN | RMACH | RMFR | RDELCL |
|-----|------|-----|--------|--------|----------|
| □ | 514 | 30 | 0.3993 | 0.5172 | 0.00369 |
| △ | 514 | 31 | 0.4006 | 0.7838 | -0.0167 |
| ◇ | 514 | 32 | 0.4003 | 1.0652 | -4.16E-4 |
| ○ | 514 | 33 | 0.3988 | 1.1759 | -8.4E-4 |



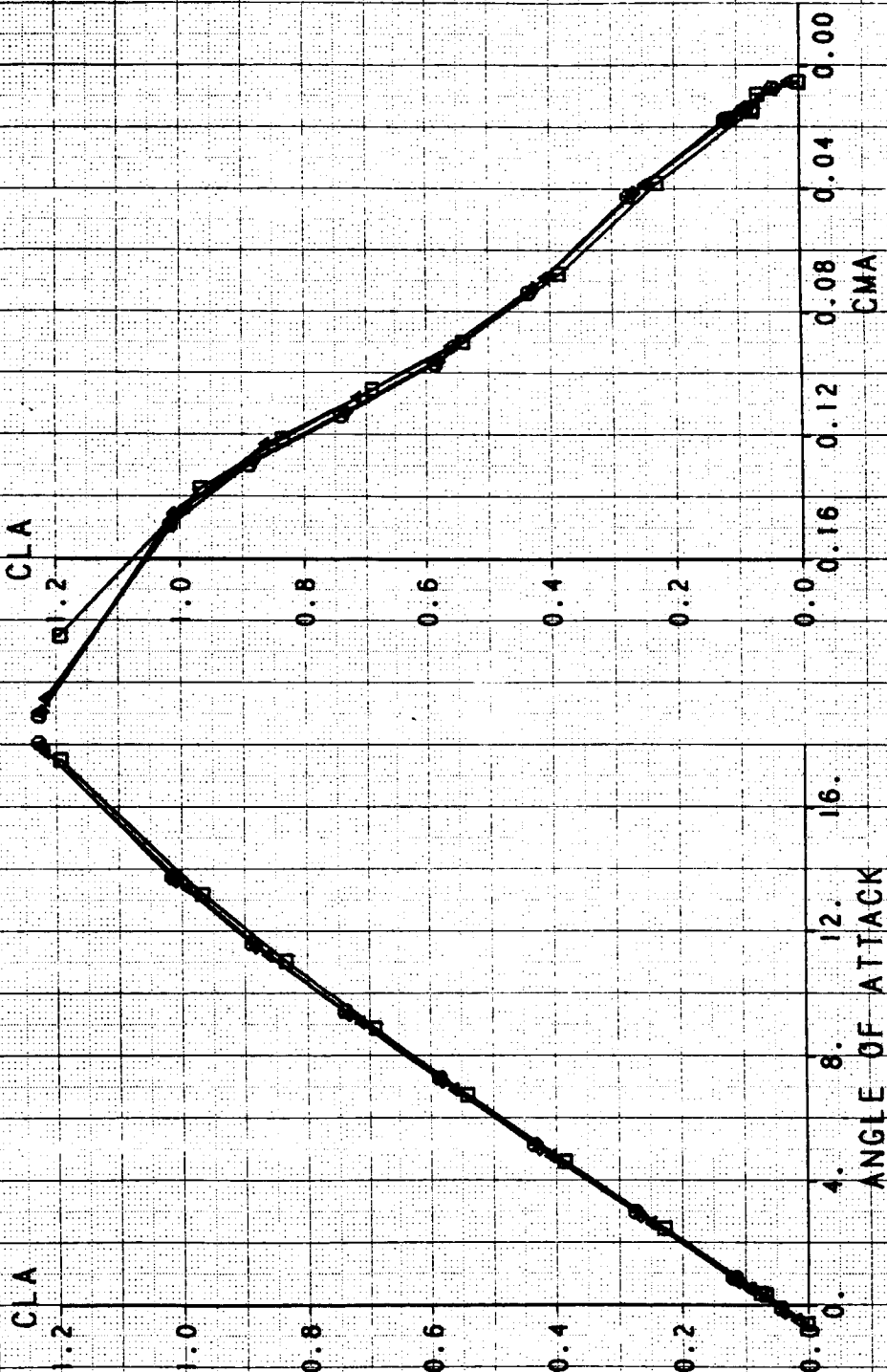
INLET MASS FLOW RATIO EFFECTS ON CLA VS CDA SIMULATOR MODE WITH NOZZLE EXTENSIONS

| SYM | TEST | RUN | RMACH | RMFR | RDELCL |
|-----|------|-----|--------|--------|---------|
| □ | 514 | 47 | 0.5993 | 0.3851 | .00859 |
| △ | 514 | 52 | 0.5999 | 0.5868 | 2.19E-4 |
| ◇ | 514 | 53 | 0.6004 | 0.8067 | -.00348 |
| ○ | 514 | 54 | 0.5994 | 0.9176 | -.00725 |



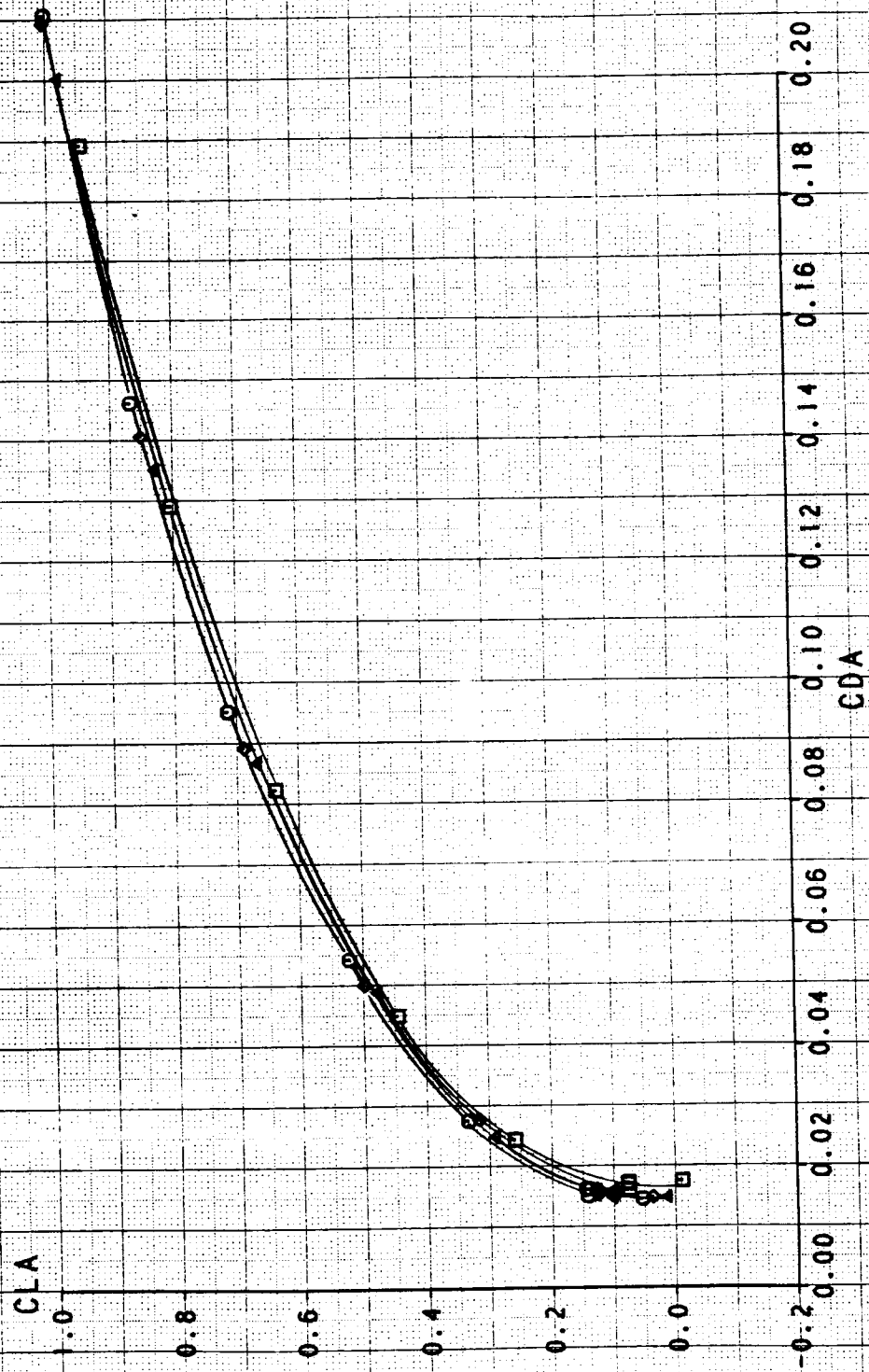
INLET MASS FLOW RATIO EFFECTS ON CLA VS AOA AND CMA

| SYM | TEST | RUN | RMACH | RUEFR | ROELCL |
|-----|------|-----|--------|--------|---------|
| □ | 514 | 47 | 0.5993 | 0.3851 | .00859 |
| △ | 514 | 52 | 0.5999 | 0.3868 | 2.9E-4 |
| ◇ | 514 | 53 | 0.6004 | 0.3867 | -.00348 |
| ○ | 514 | 54 | 0.5994 | 0.9176 | -.00725 |



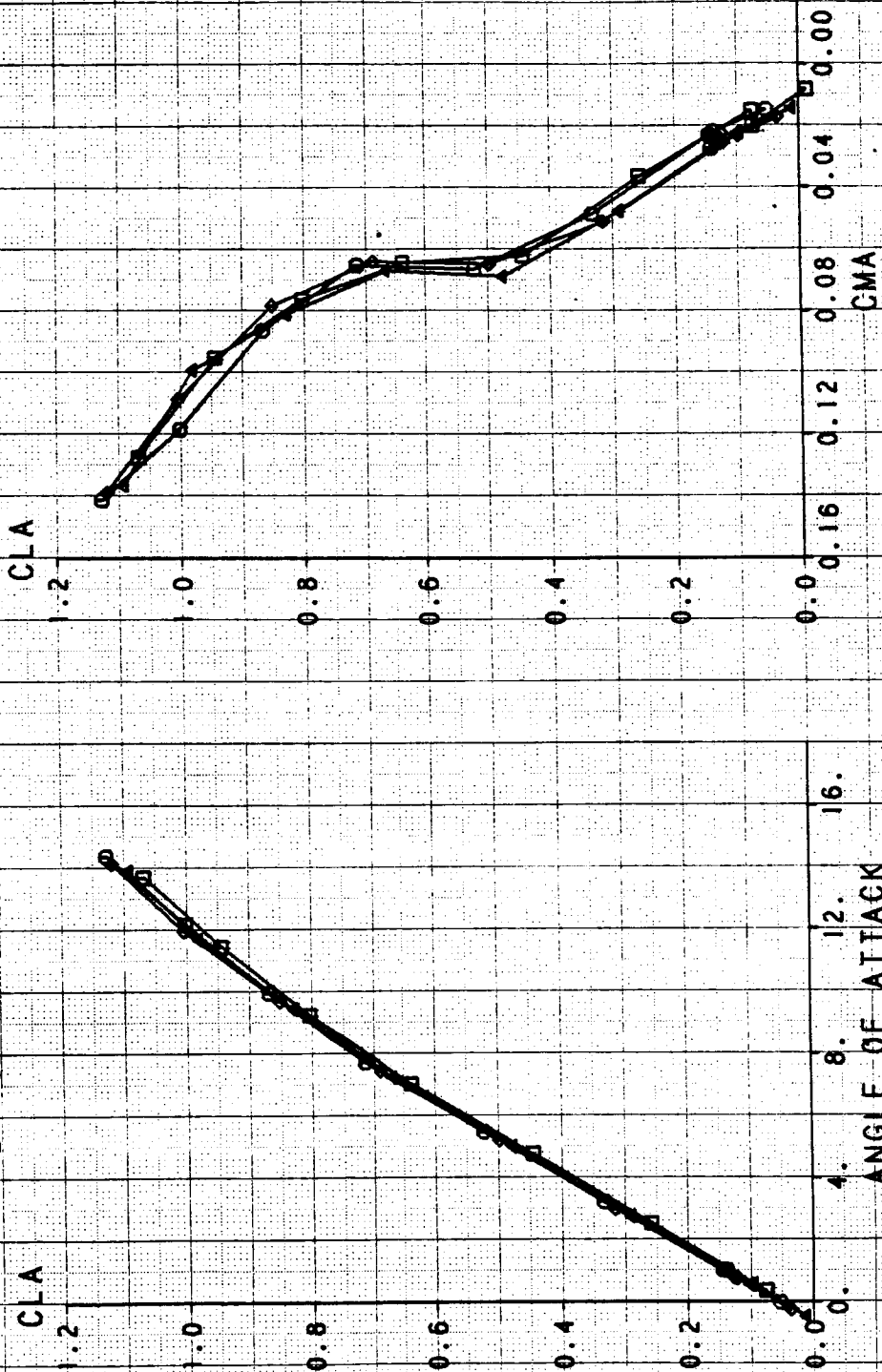
INLET MASS FLOW RATIO EFFECTS ON CLA VS CDA SIMULATOR MODE WITH NOZZLE EXTENSIONS

| SYM | TEST | RUN | RMACH | RNFR | RDELCL |
|-----|------|-----|--------|--------|---------|
| □ | 514 | 59 | 0.8980 | 0.3235 | -0.0136 |
| △ | 514 | 60 | 0.8959 | 0.4953 | -0.0809 |
| ◇ | 514 | 61 | 0.9030 | 0.6834 | -0.0120 |
| ○ | 514 | 62 | 0.9032 | 0.8687 | -0.0289 |



INLET MASS FLOW RATIO EFFECTS ON CLA VS AOA AND CMA

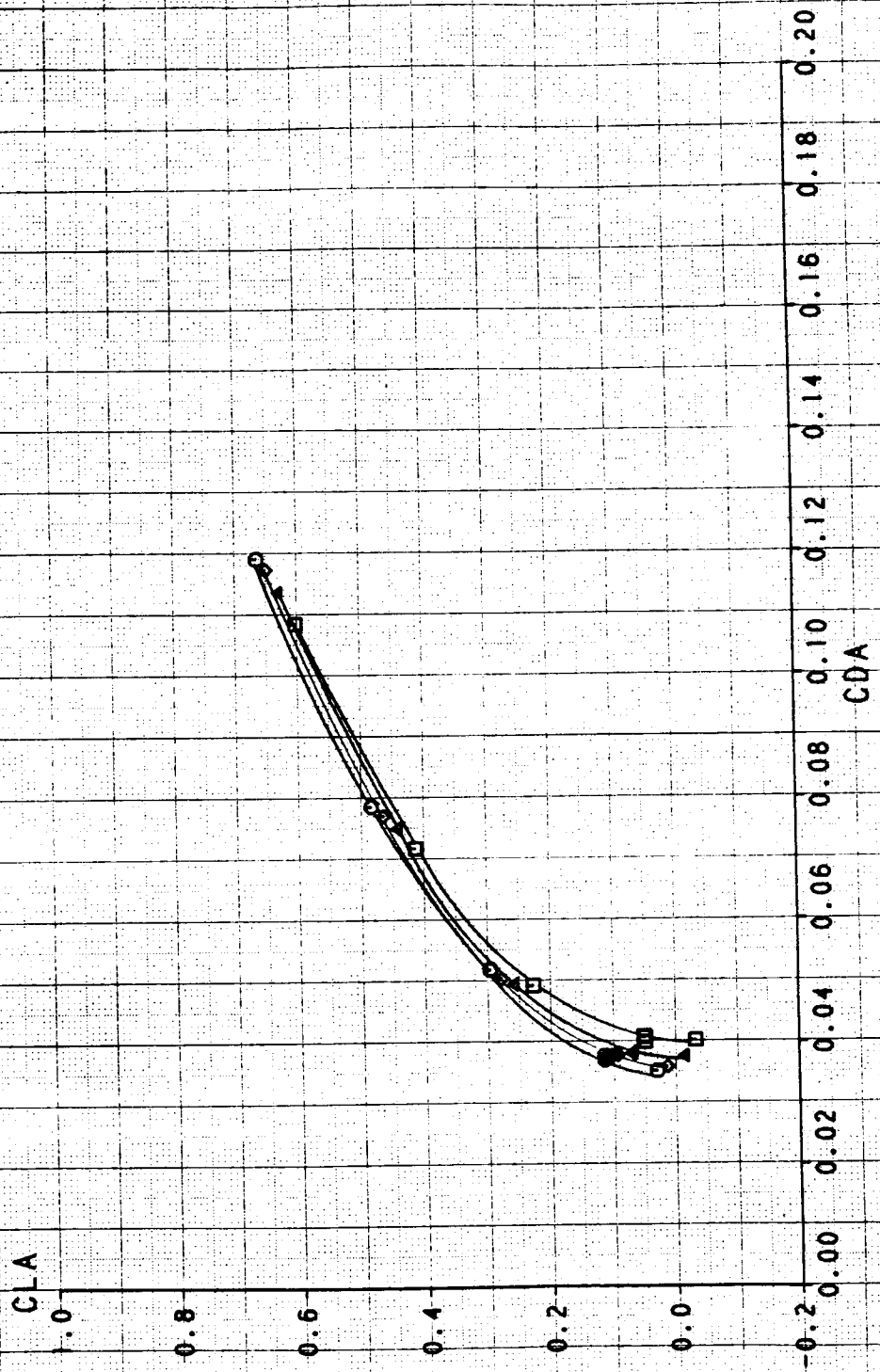
| SYM | TEST | RUN | RWACH | RWFR | RDELCL |
|-----|------|-----|--------|--------|---------|
| □ | 514 | 59 | 0.8980 | 0.3255 | -0.0136 |
| △ | 514 | 60 | 0.8959 | 0.4953 | -0.0809 |
| ◇ | 514 | 61 | 0.9030 | 0.6834 | -0.0120 |
| ⊙ | 514 | 62 | 0.9032 | 0.8687 | -0.0289 |



INLET MASS FLOW RATIO EFFECTS ON CLA VS CDA

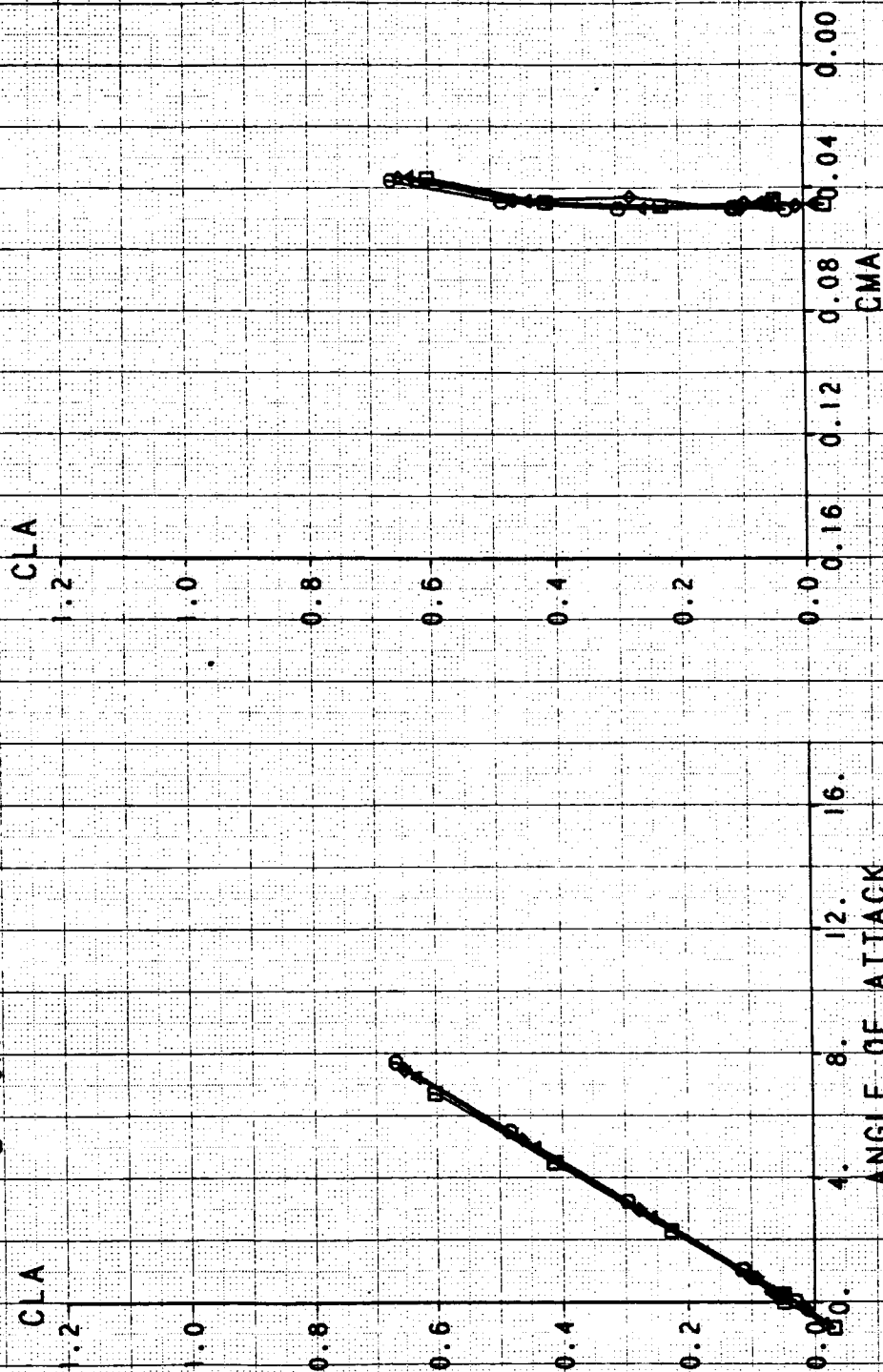
SIMULATOR MODE WITH NOZZLE EXTENSIONS

| SYM | TEST | RUN | RWACH | RWER | RDELCL |
|-----|------|-----|--------|--------|----------|
| □ | 514 | 71 | 1.1954 | 0.3316 | 0.0152 |
| △ | 514 | 72 | 1.1965 | 0.5032 | -0.00222 |
| ◇ | 514 | 73 | 1.1953 | 0.6928 | -0.00509 |
| ○ | 514 | 74 | 1.1951 | 0.8779 | -0.00617 |



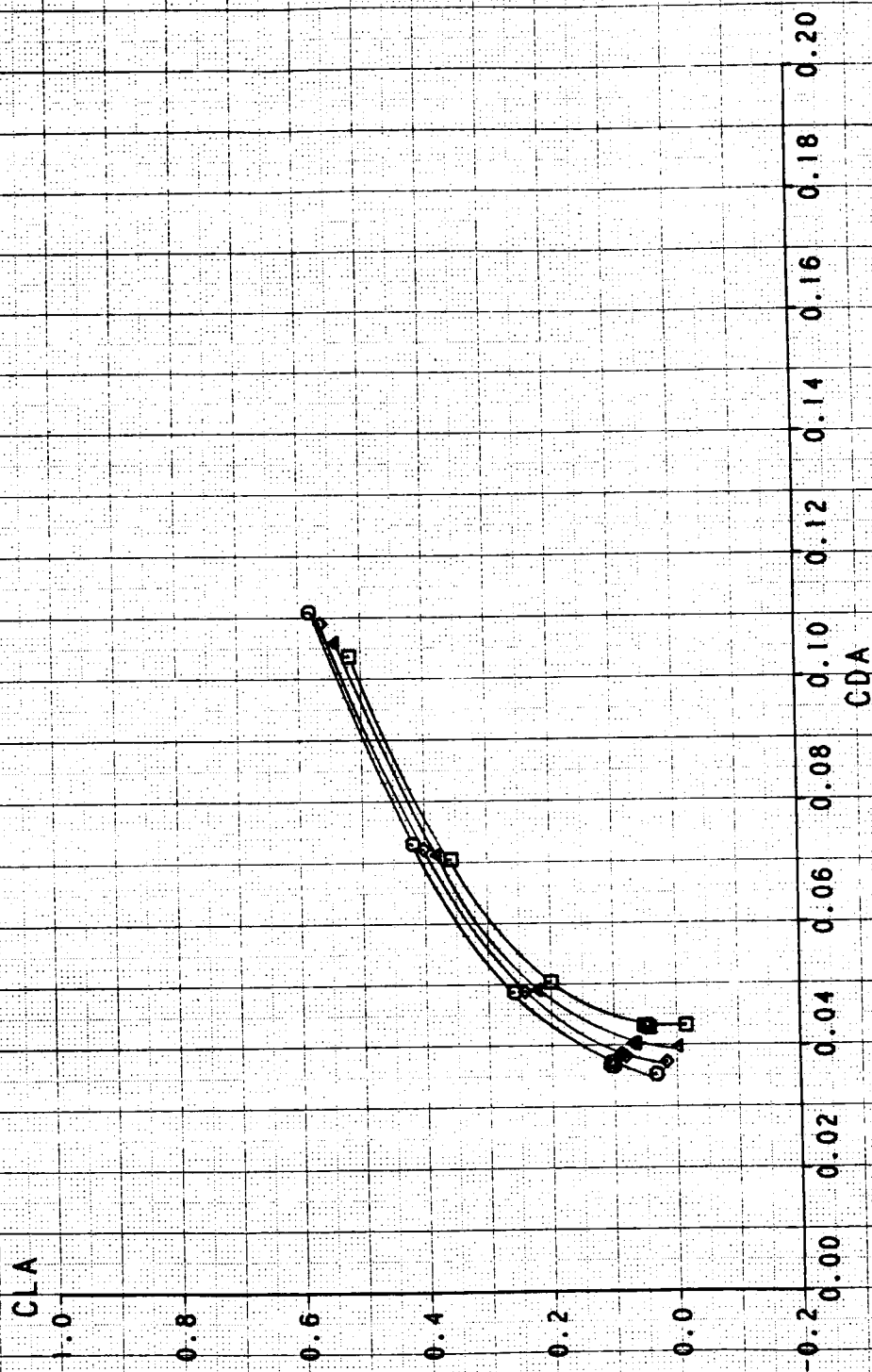
INLET MASS FLOW RATIO EFFECTS ON CLA VS AOA AND CMA

| SYM | TEST | RUN | RMACH | RMFR | RDELCL |
|-----|------|-----|--------|--------|----------|
| □ | 514 | 71 | 1.1954 | 0.3316 | 0.0152 |
| △ | 514 | 72 | 1.1965 | 0.5032 | -0.00222 |
| ◇ | 514 | 73 | 1.1933 | 0.6928 | -0.00509 |
| ○ | 514 | 74 | 1.1931 | 0.8779 | -0.00617 |



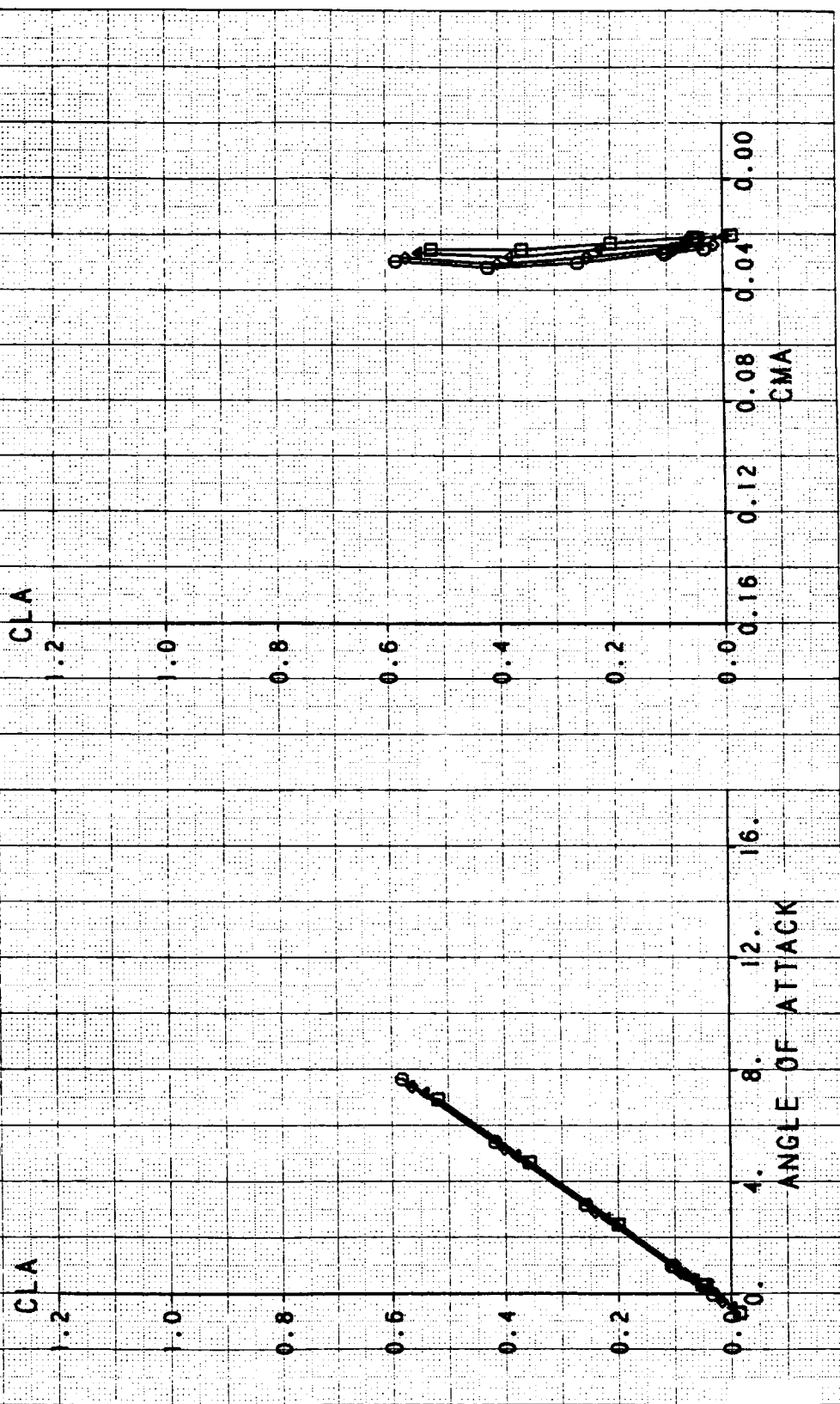
INLET MASS FLOW RATIO EFFECTS ON CLA VS CDA SIMULATOR MODE WITH NOZZLE EXTENSIONS

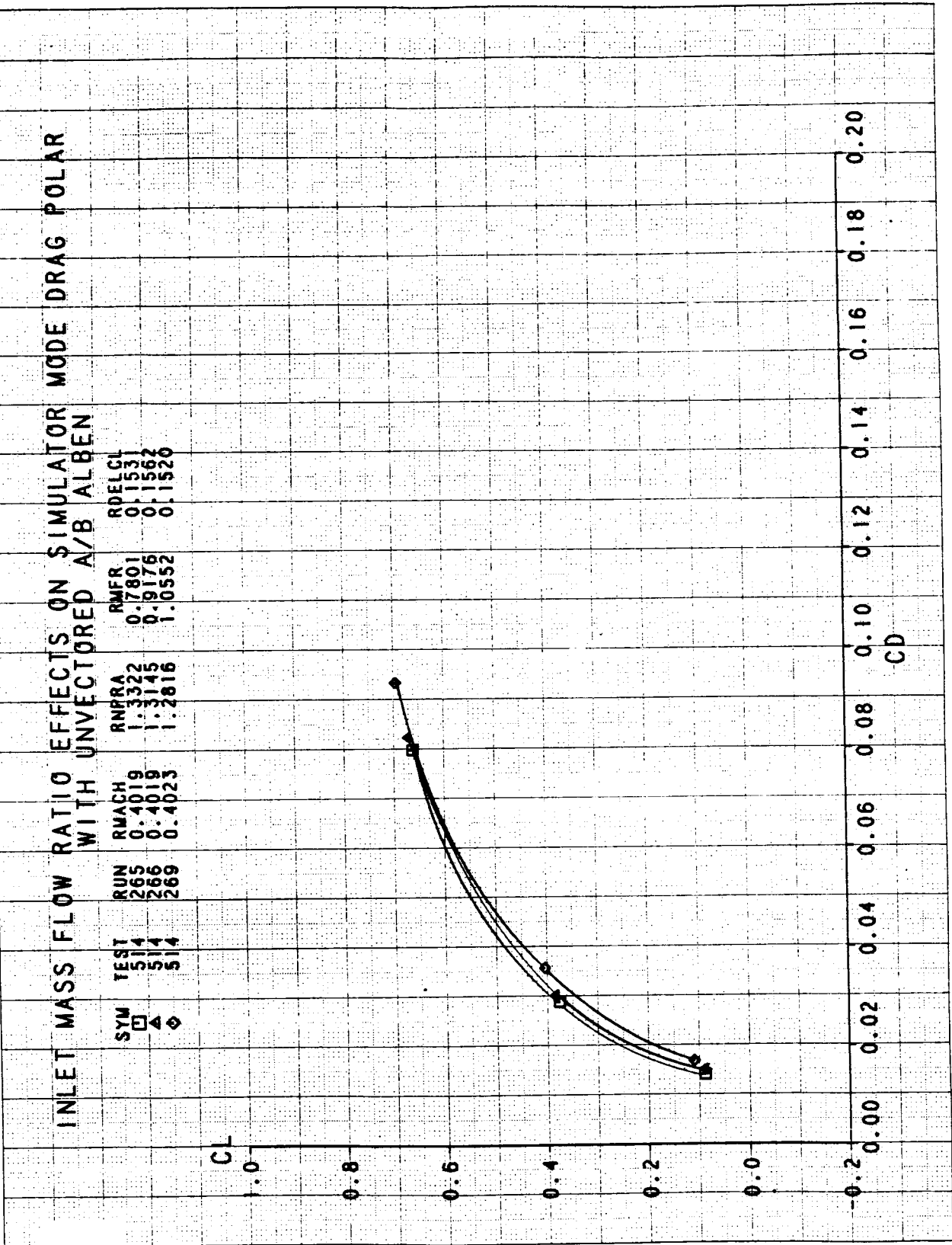
| SYM | TEST | RUN | RMACH | RMFR | RDELCL |
|-----|------|-----|--------|--------|----------|
| □ | 514 | 79 | 1.4023 | 0.3477 | -0.0322 |
| △ | 514 | 80 | 1.4014 | 0.3283 | -0.0204 |
| ◇ | 514 | 81 | 1.4016 | 0.7284 | -0.0157 |
| ○ | 514 | 82 | 1.4012 | 0.9303 | -0.00617 |



INLET MASS FLOW RATE EFFECTS ON CLA VS AOA AND CMA

| SYM | TEST | RUN | RMACH | RMFR | RDELCL |
|-----|------|-----|--------|--------|---------|
| □ | 514 | 79 | 1.4023 | 0.3477 | -0.0322 |
| △ | 514 | 80 | 1.4014 | 0.5283 | -0.0204 |
| ◇ | 514 | 81 | 1.4016 | 0.7284 | -0.0157 |
| ○ | 514 | 82 | 1.4012 | 0.9303 | -0.0067 |

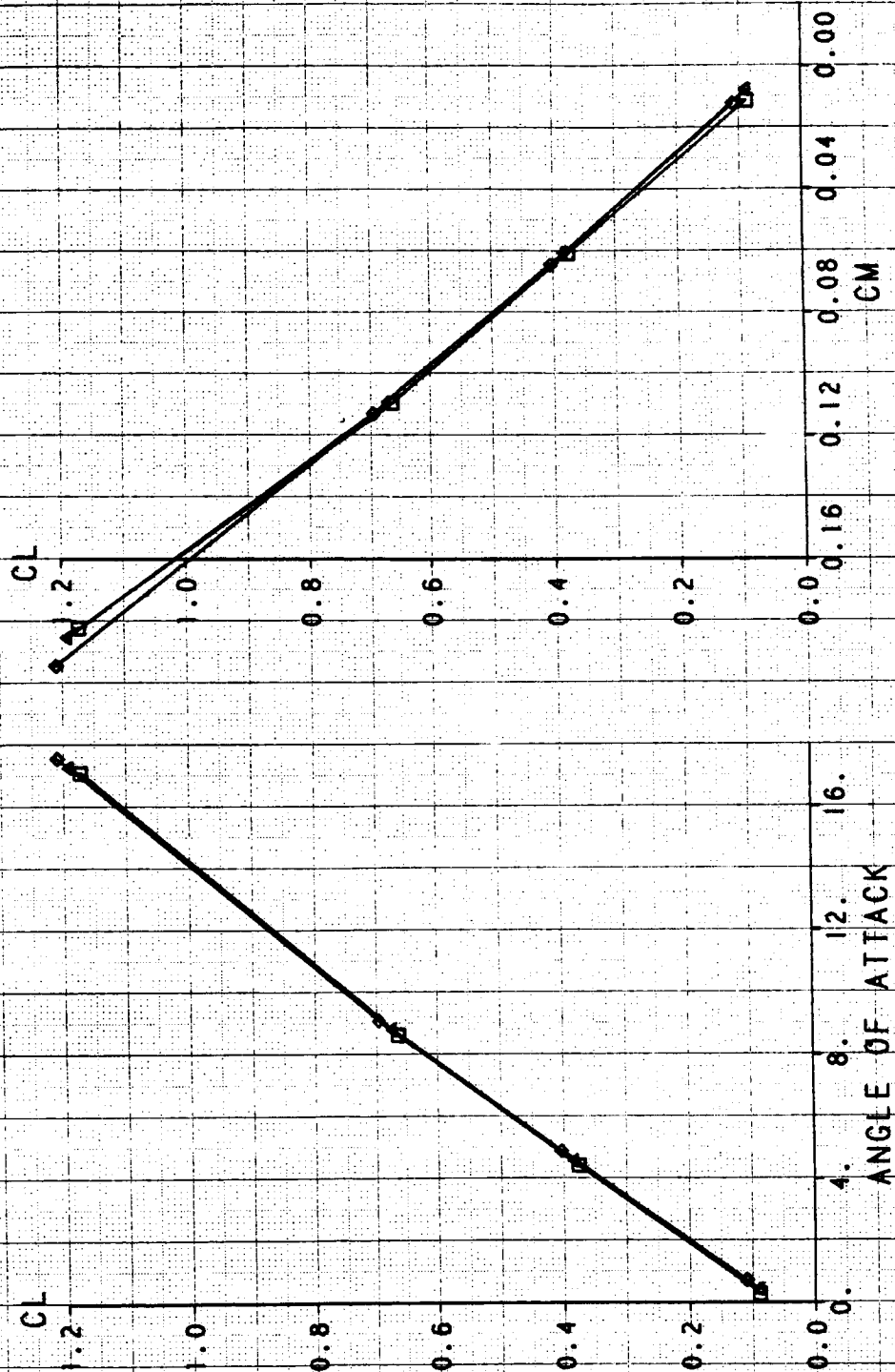




INLET MASS FLOW RATIO EFFECTS ON CL VS AOA AND CM

SIMULATOR MODE WITH UNVECTORED A/B ALBEN

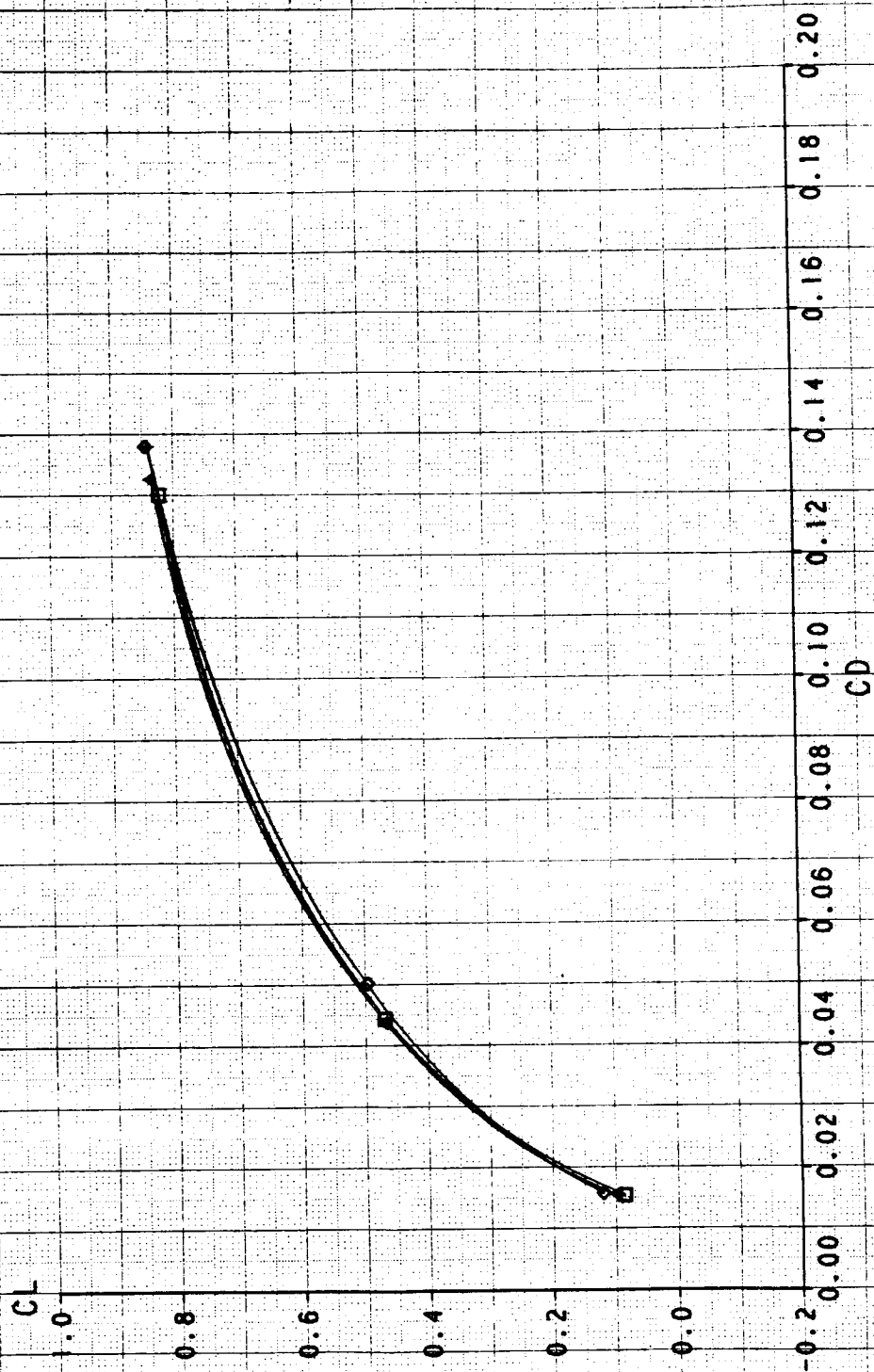
| SYM | TEST | RUN | RMACH | RNPRA | RMFR | RDELCL |
|-----|------|-----|--------|--------|--------|--------|
| □ | 514 | 265 | 0.4019 | 1.3322 | 0.7801 | 0.1531 |
| △ | 514 | 266 | 0.4019 | 1.3145 | 0.9176 | 0.1562 |
| ◇ | 514 | 269 | 0.4023 | 1.2816 | 1.0552 | 0.1520 |



INLET MASS FLOW RATIO EFFECTS ON SIMULATOR MODE DRAG POLAR

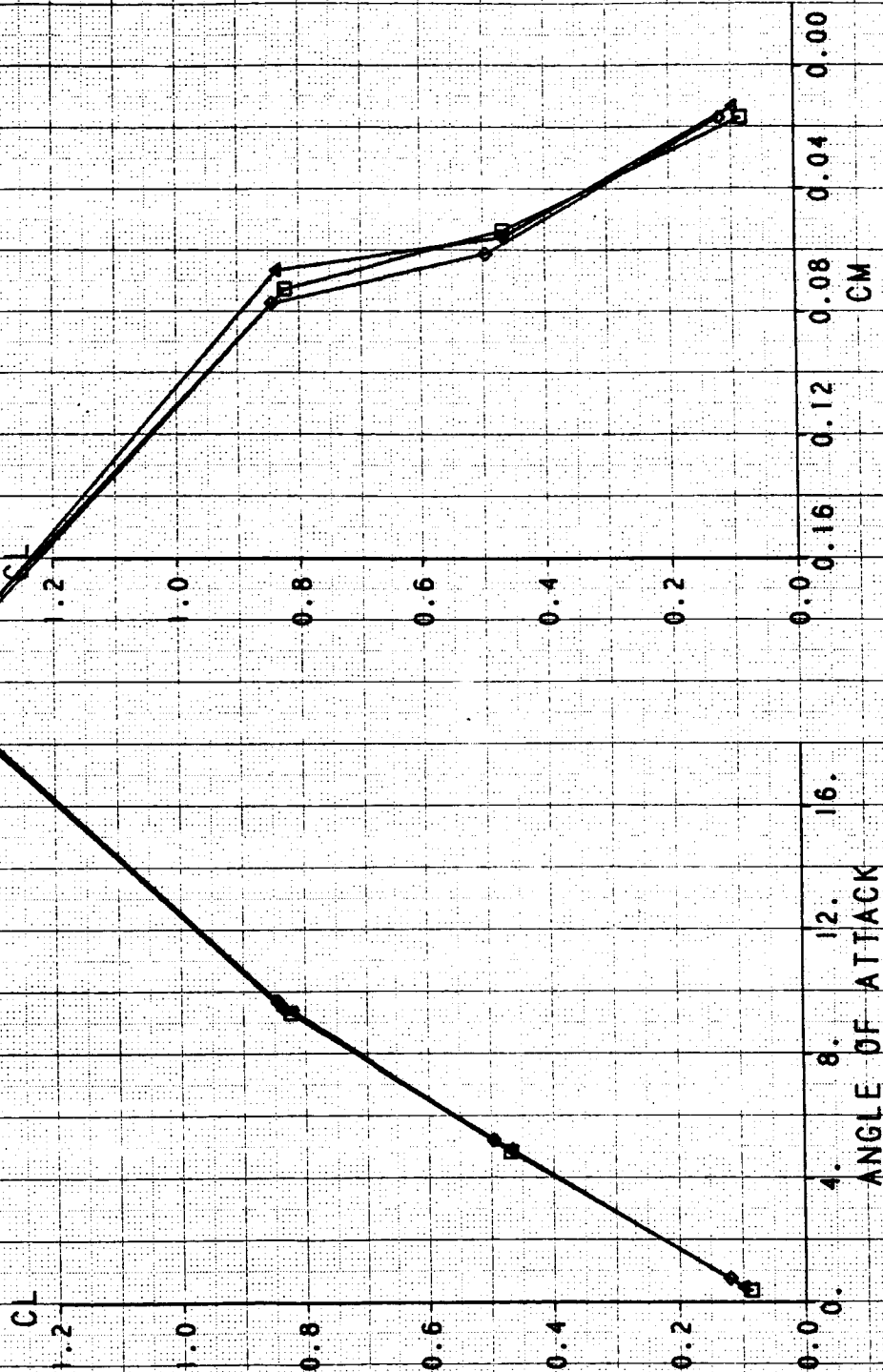
WITH UNVECTORED A/B ALBEN

| SYM | TEST | RUN | RMACH | RNPRA | RMFR | RDELCL |
|-----|------|-----|--------|--------|--------|--------|
| □ | 514 | 192 | 0.9021 | 4.4266 | 0.6751 | 0.1239 |
| △ | 514 | 196 | 0.9042 | 4.3951 | 0.7568 | 0.0938 |
| ◇ | 514 | 200 | 0.9052 | 4.2850 | 0.8685 | 0.1250 |



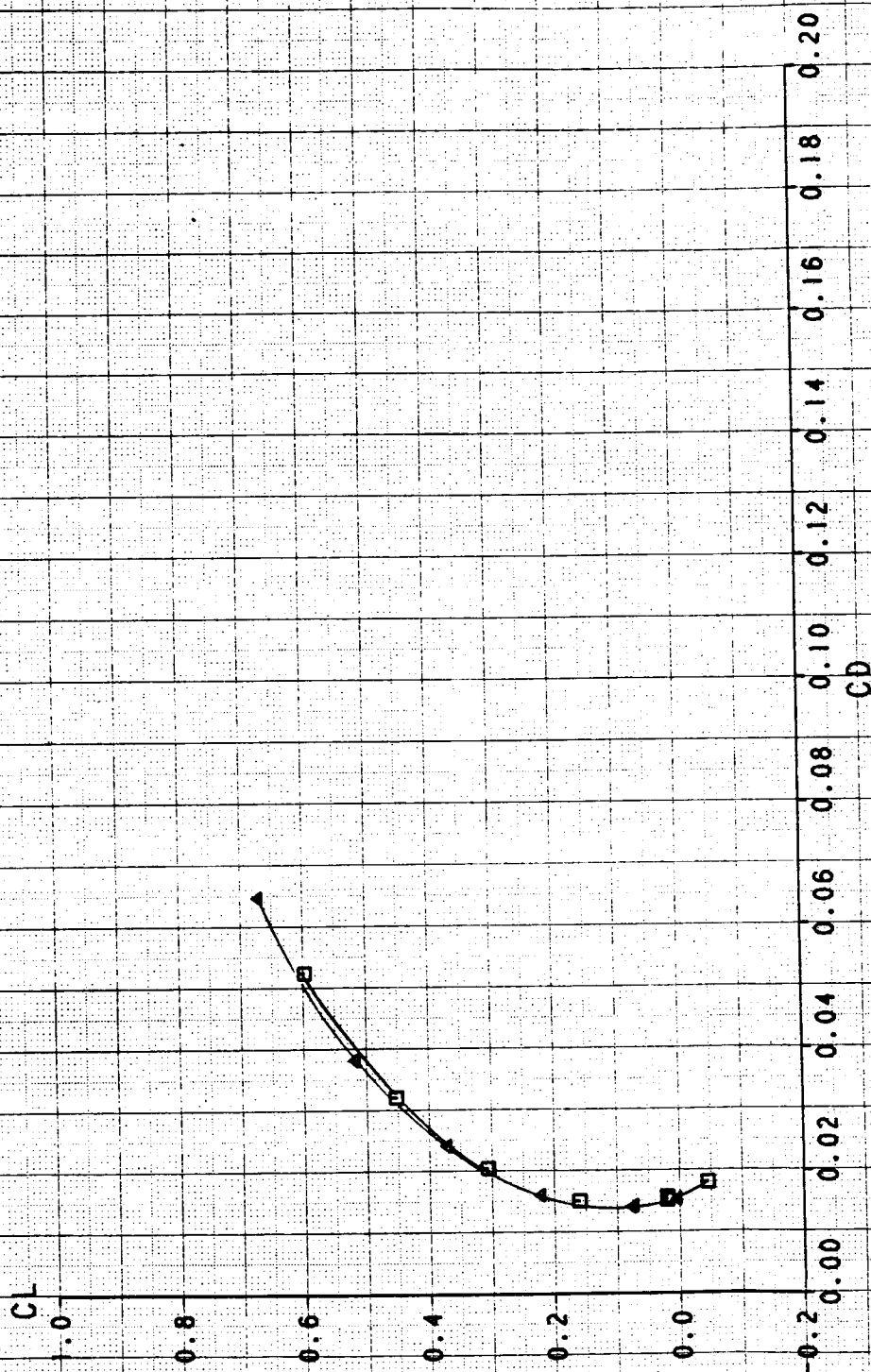
INLET MASS FLOW RATIO EFFECTS ON CL VS AOA AND CM

| SYM | TEST | RUN | RMACH | RNPRA | RMFR | RDELCL |
|-----|------|-----|--------|--------|--------|--------|
| □ | 514 | 192 | 0.9021 | 4.1266 | 0.6751 | 0.1239 |
| △ | 514 | 196 | 0.9042 | 4.3951 | 0.7568 | 0.0938 |
| ◇ | 514 | 200 | 0.9052 | 4.2850 | 0.8685 | 0.1250 |



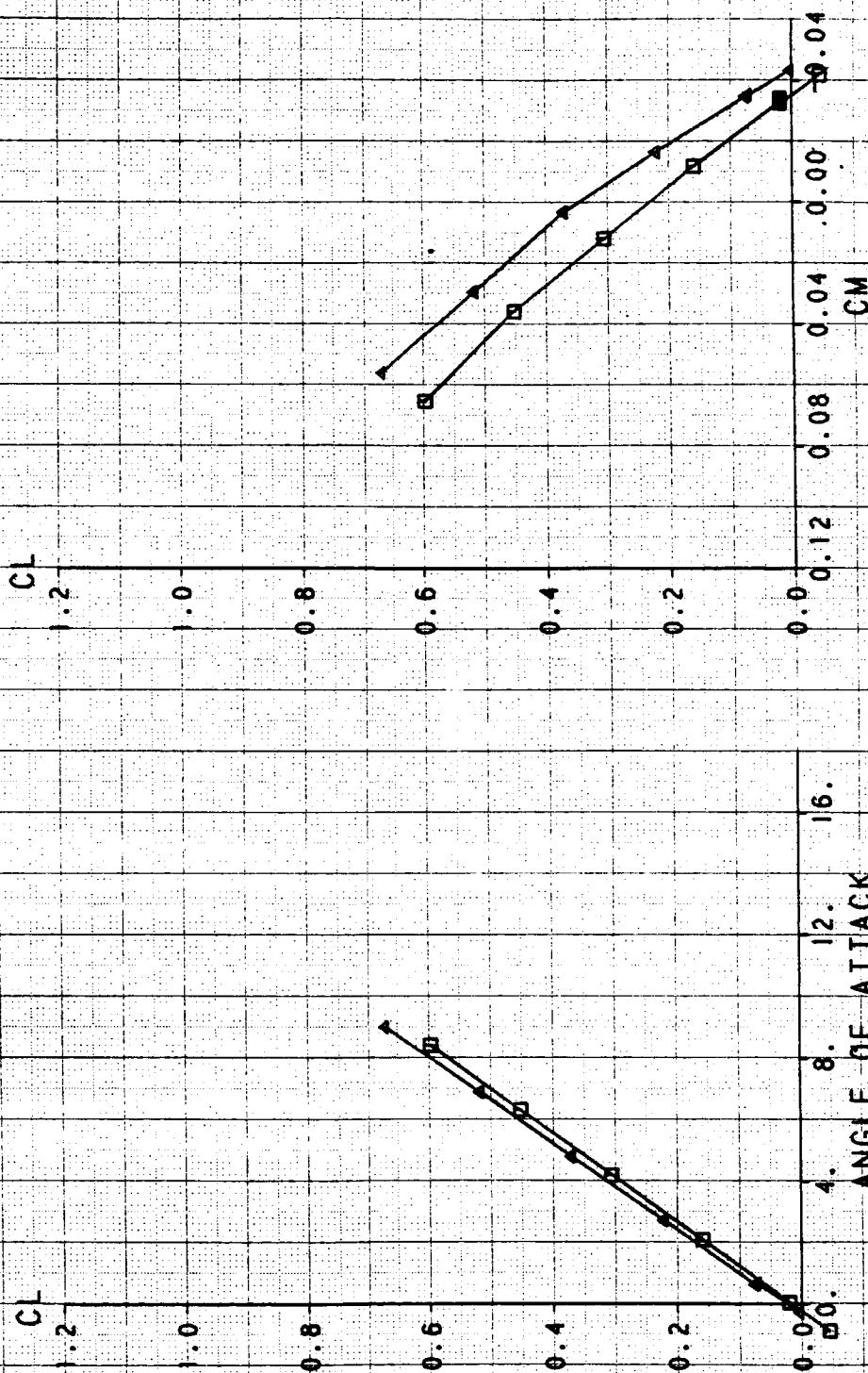
NOZZLE PRESSURE RATIO EFFECT ON DRAG POLAR JET-EFFECTS MODE WITH UNVECTORED DRY ALBEN

| SYM | TEST | RUN | RWACH | RNPRA | RDELCL |
|-----|------|-----|--------|--------|---------|
| □ | 514 | 303 | 0.3977 | 0.1022 | -5.0162 |
| △ | 514 | 305 | 0.3985 | 6.9133 | -4.9686 |



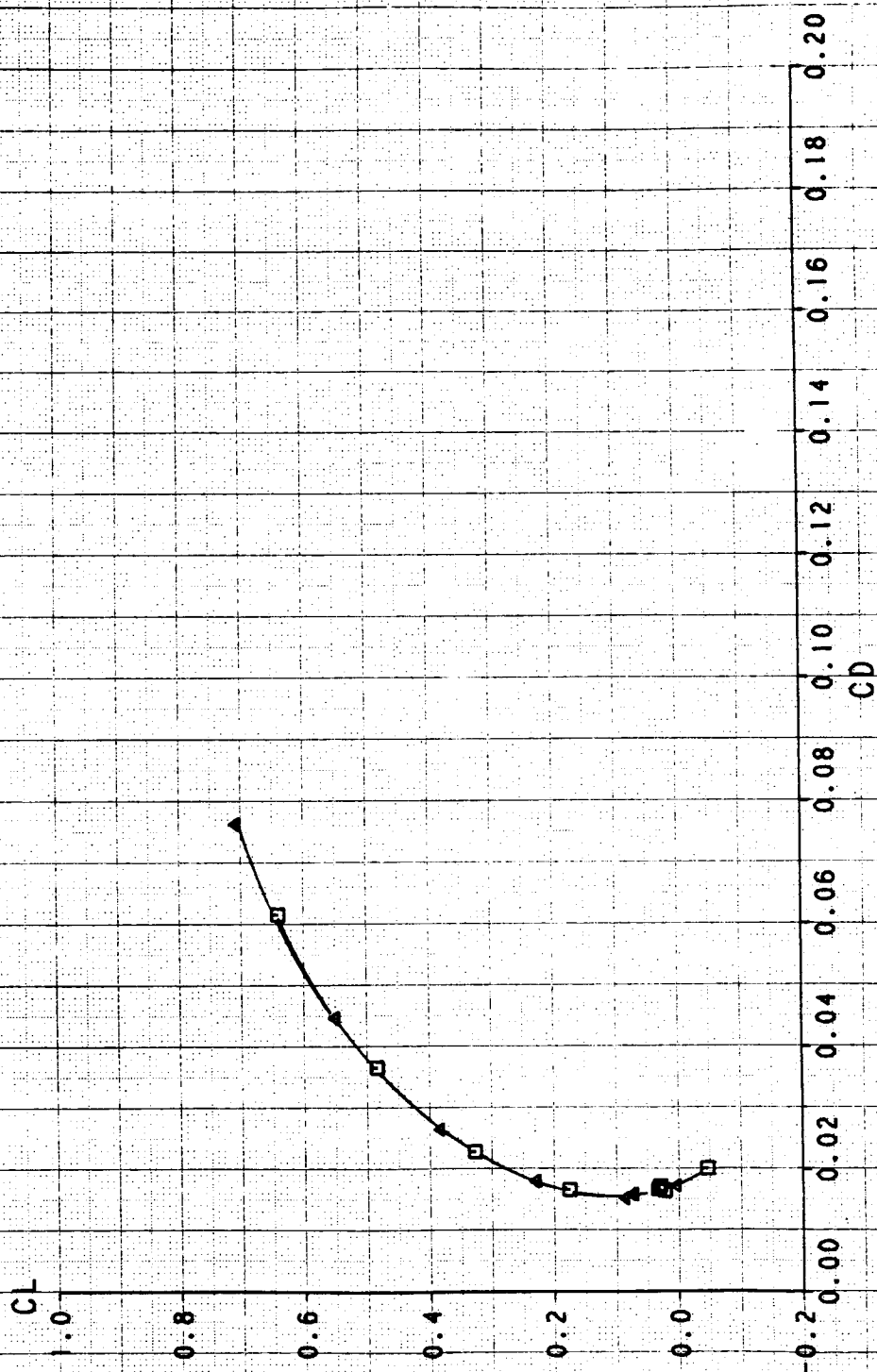
NOZZLE PRESSURE RATIO EFFECT ON CL VS AOA AND CM

SYM TEST RUN RMACH BNPR RDELCL
 □ 514 303 0.3977 0.1022 -5.0162
 ▲ 514 305 0.3985 6.9133 -4.9686



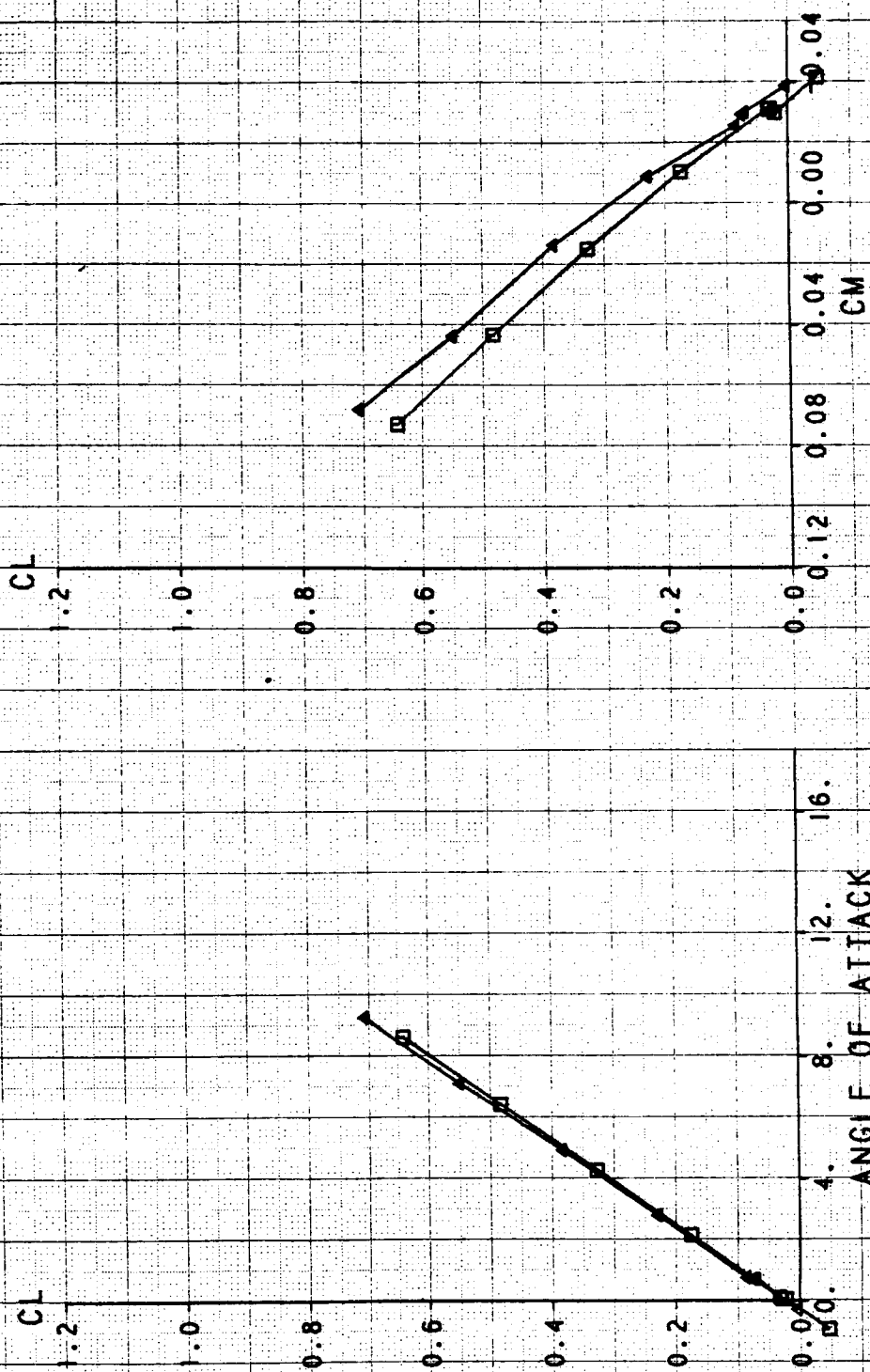
NOZZLE PRESSURE RATIO EFFECT ON DRAG POLAR JET-EFFECTS MODE WITH UNVECTORED DRY ALBEN

| SYM | TEST | RUN | RMACH | RNPRA | RDELCL |
|-----|------|-----|--------|--------|---------|
| □ | 514 | 312 | 0.5997 | 0.1435 | -4.9709 |
| △ | 514 | 314 | 0.6001 | 4.6697 | -4.9617 |



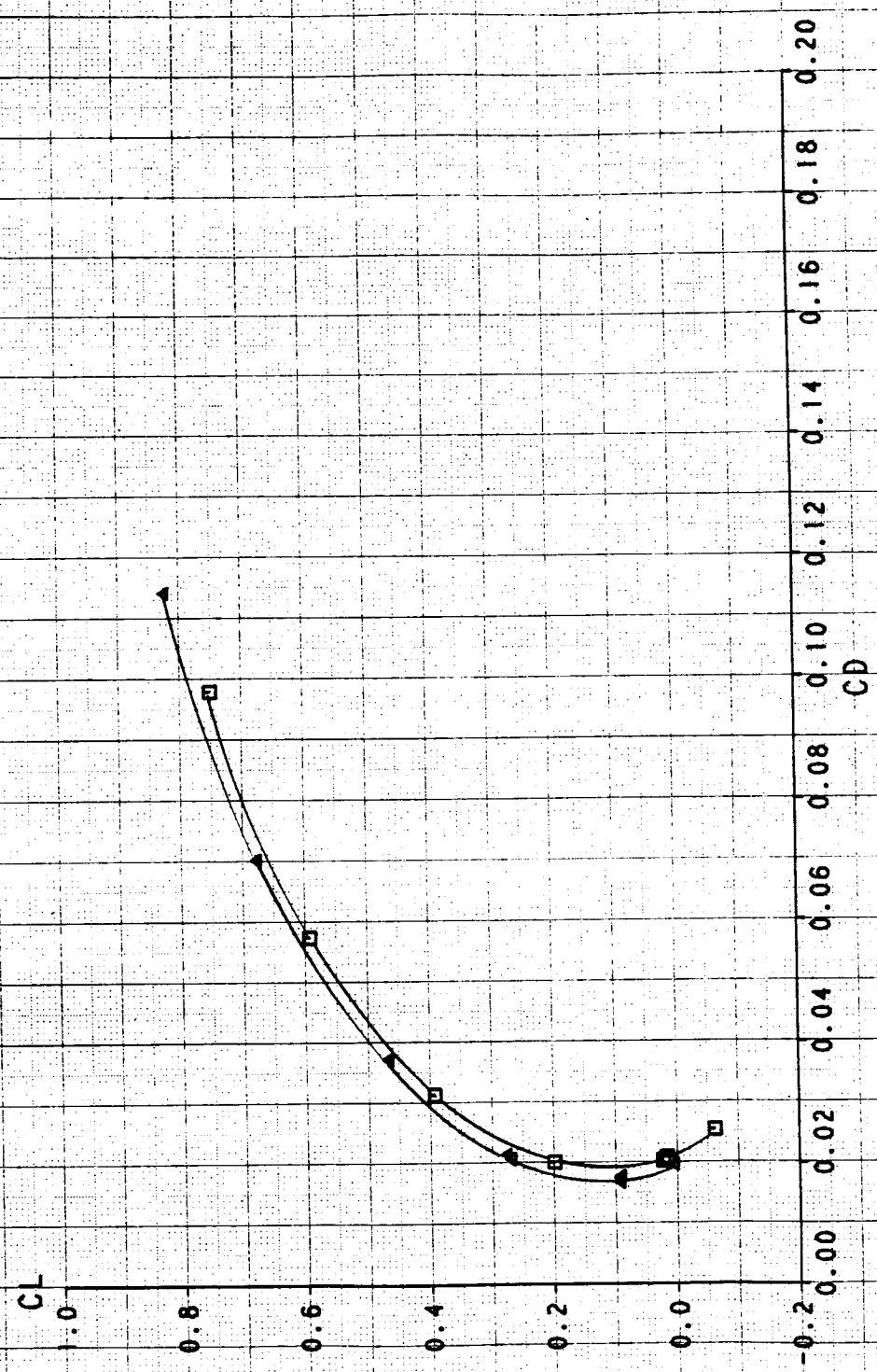
NOZZLE PRESSURE RATIO EFFECT ON CL VS AOA AND CM

SYM TEST RUN RMACH RNPRA RDELCL
 □ 514 312 0.5997 0.1435 -4.9709
 ▲ 514 314 0.6001 4.6697 -4.9617



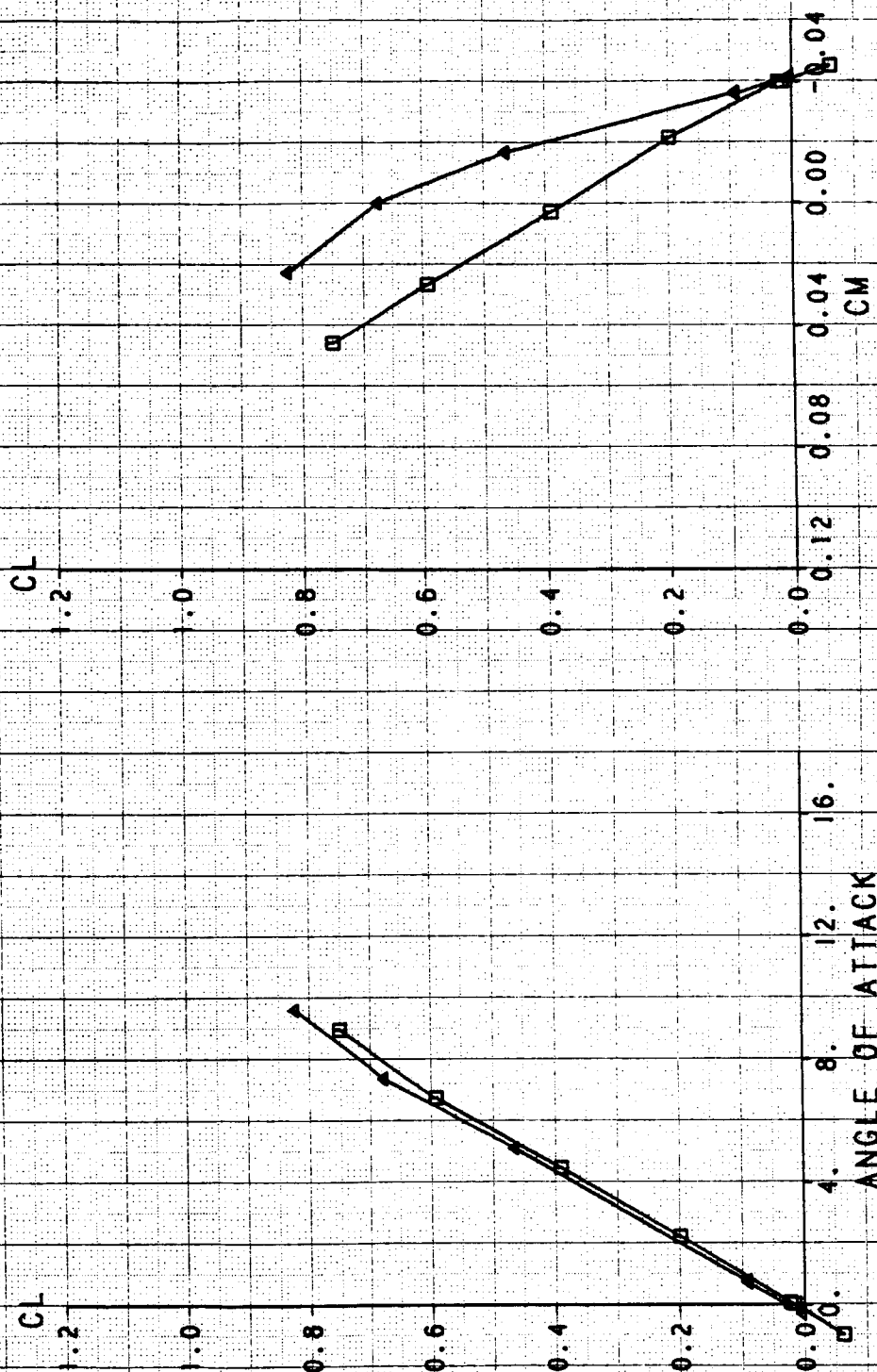
NOZZLE PRESSURE RATIO EFFECT ON DRAG POLAR JET-EFFECTS MODE WITH UNVECTORED DRY ALBEN

| | | | | | |
|-----|------|-----|--------|--------|---------|
| SYM | TEST | RUN | RMACH | RNPRA | RDELCL |
| □ | 514 | 319 | 0.9002 | 0.2180 | -4.9679 |
| △ | 514 | 315 | 0.8992 | 5.7075 | -4.9260 |



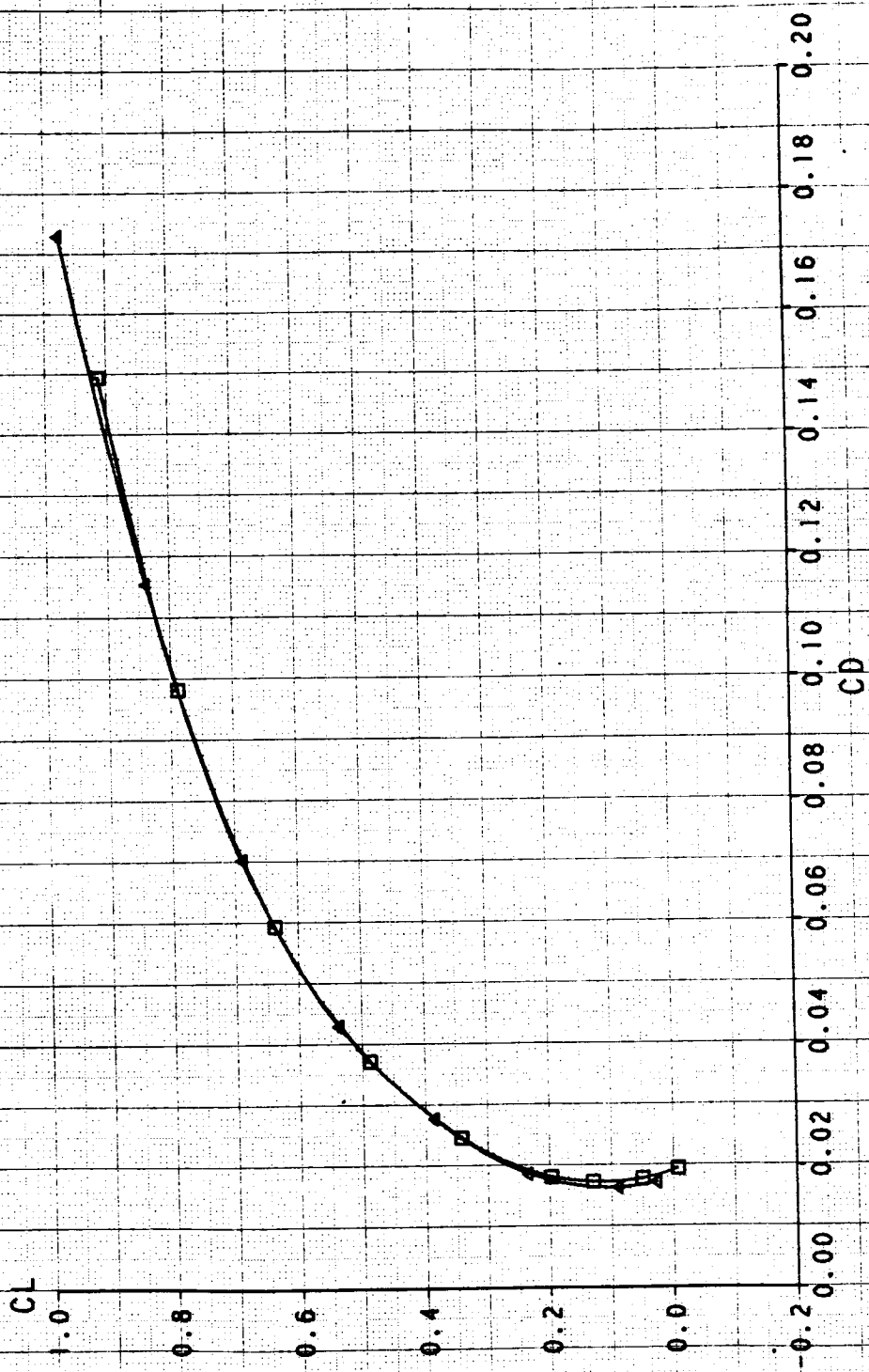
NOZZLE PRESSURE RATIO EFFECT ON CL VS AOA AND CM

JET-EFFECTS MODE WITH UNVECTORED DRY ALBEN
 SYM TEST RUN RMACH RNPRA ROELCL
 □ 514 319 0.9002 0.2180 -4.9679
 ▲ 514 315 0.8992 6.7075 -4.9260



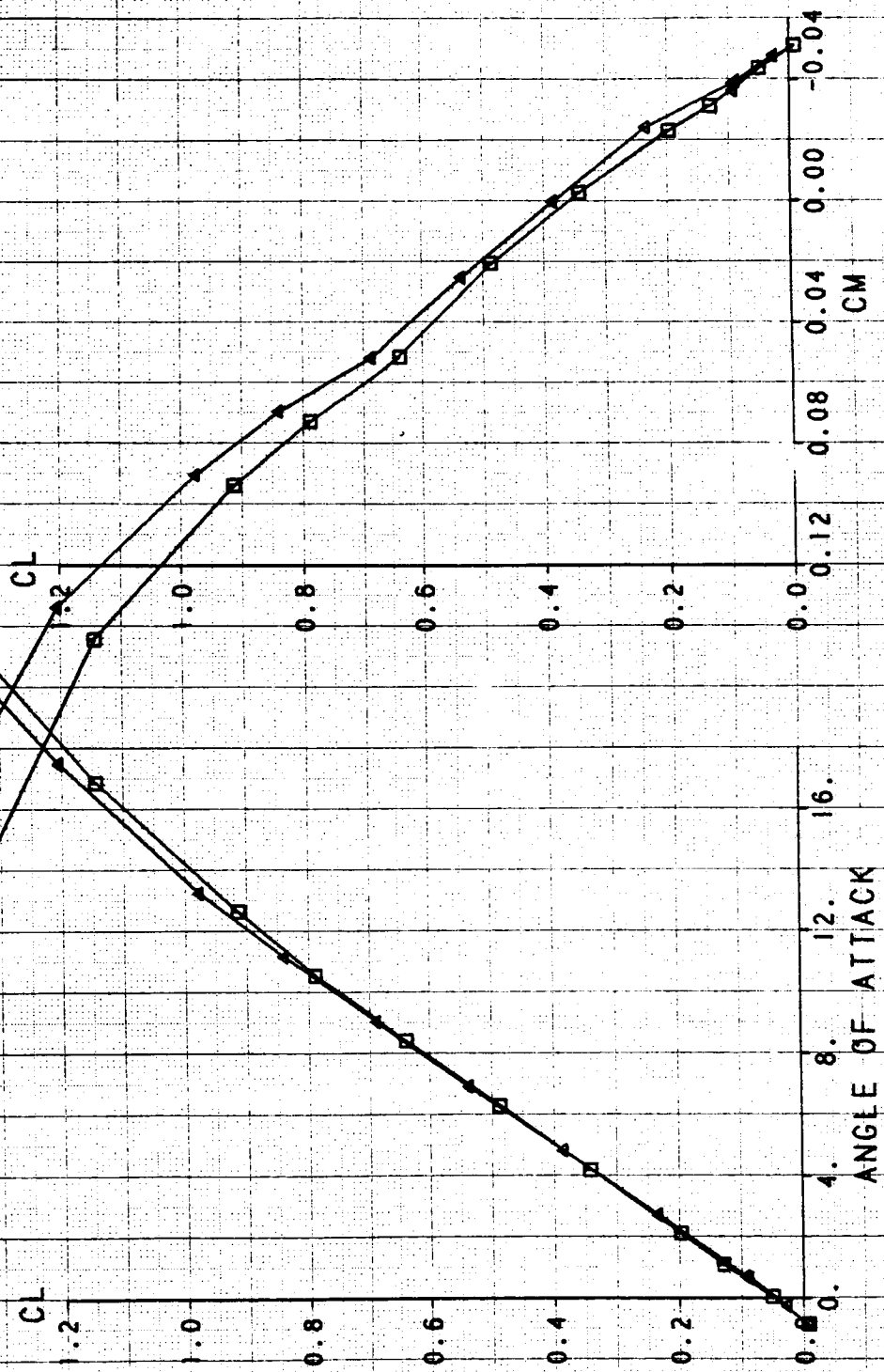
NOZZLE PRESSURE RATIO EFFECT ON DRAG POLAR JET-EFFECTS MODE WITH UNVECTORED A/B ALBEN

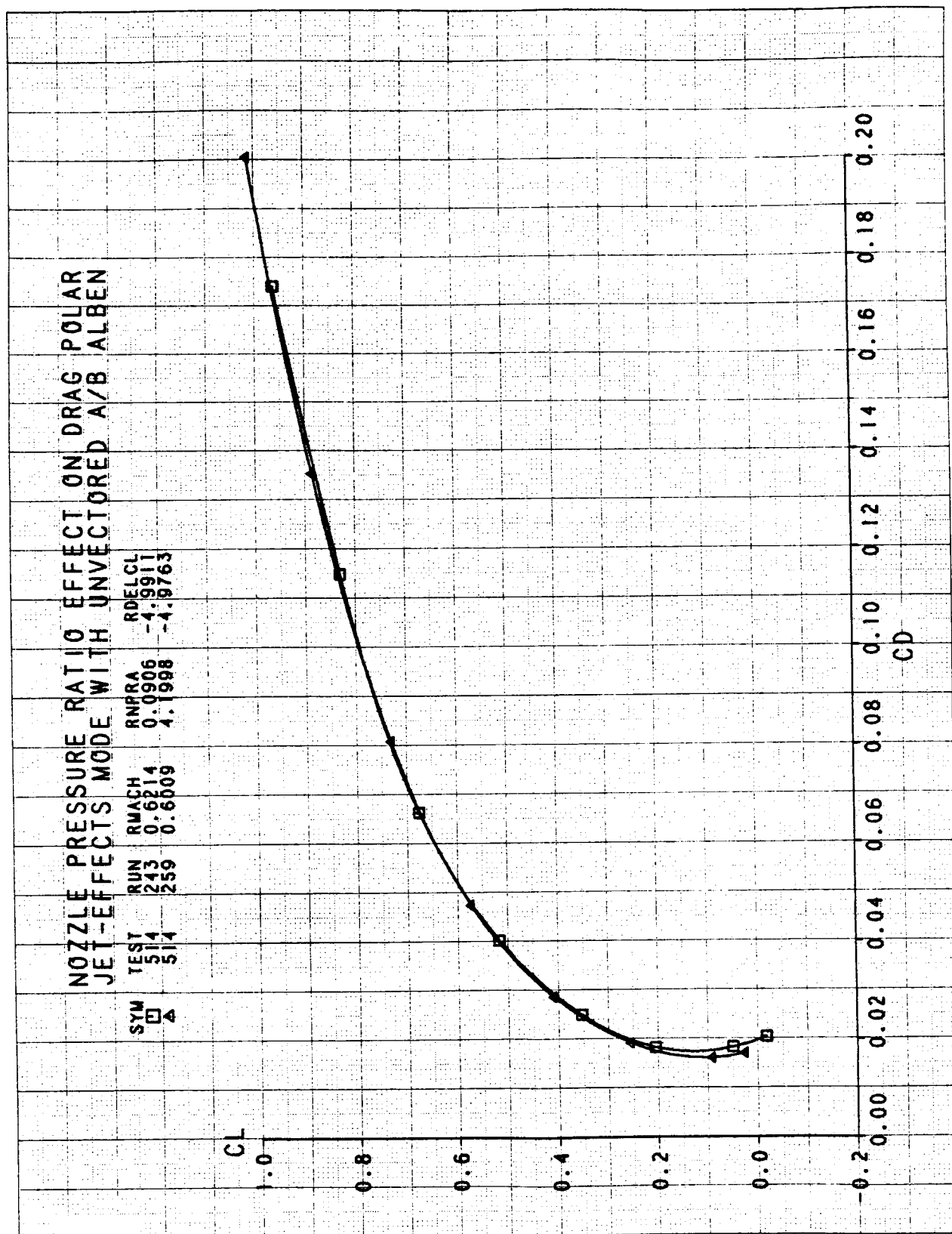
SYM TEST RUN RMACH RNPRA RDELCL
 □ 514 238 0.3989 0.0637 -4.9629
 △ 514 258 0.3992 4.0334 -5.0064



NOZZLE PRESSURE RATIO EFFECT ON CL VS AOA AND CM

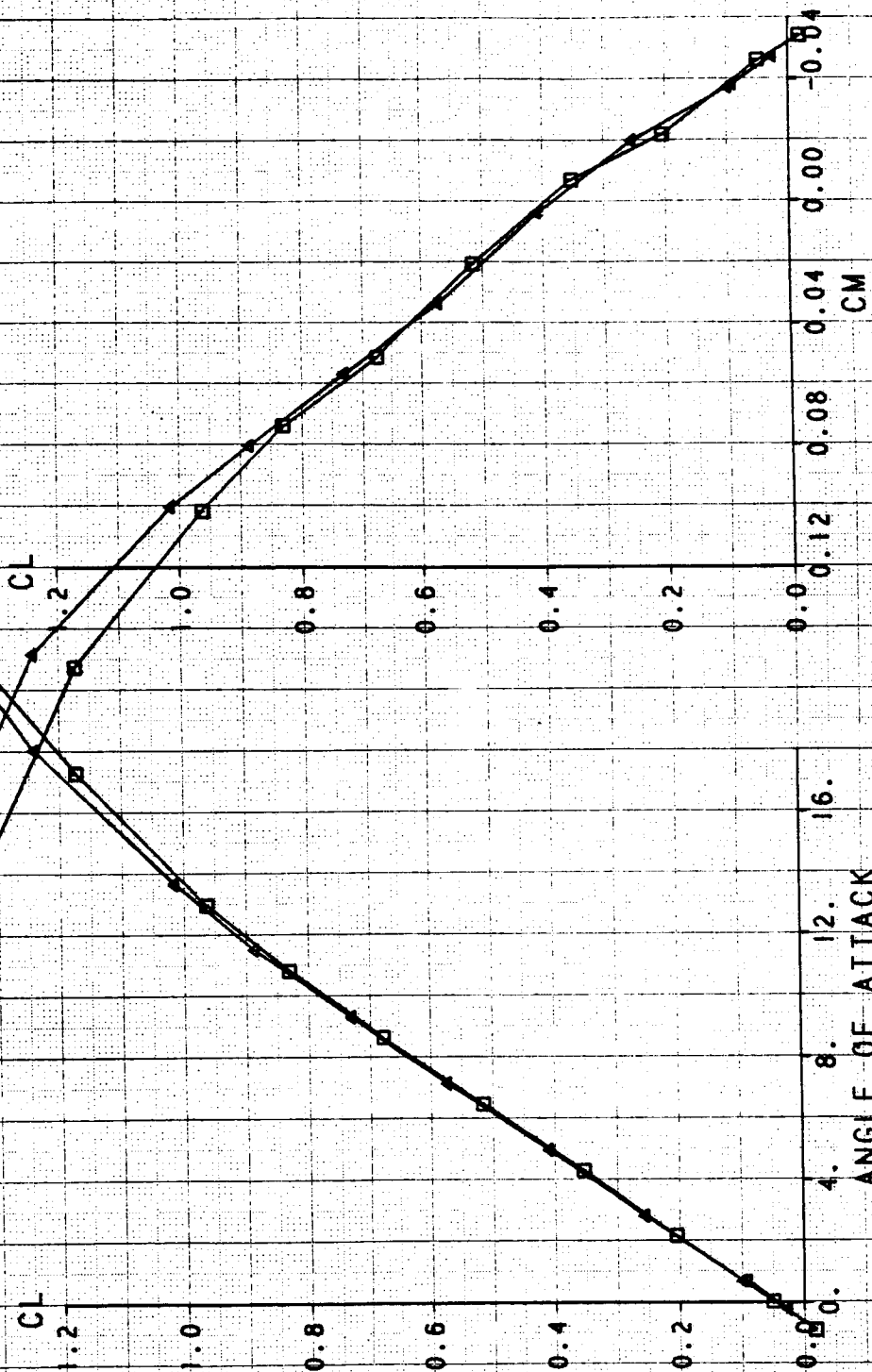
TEST RUN RWACH RNPRA RDELCL
 514 238 0.3989 0.0637 -4.9629
 514 258 0.3992 4.0334 -5.0064





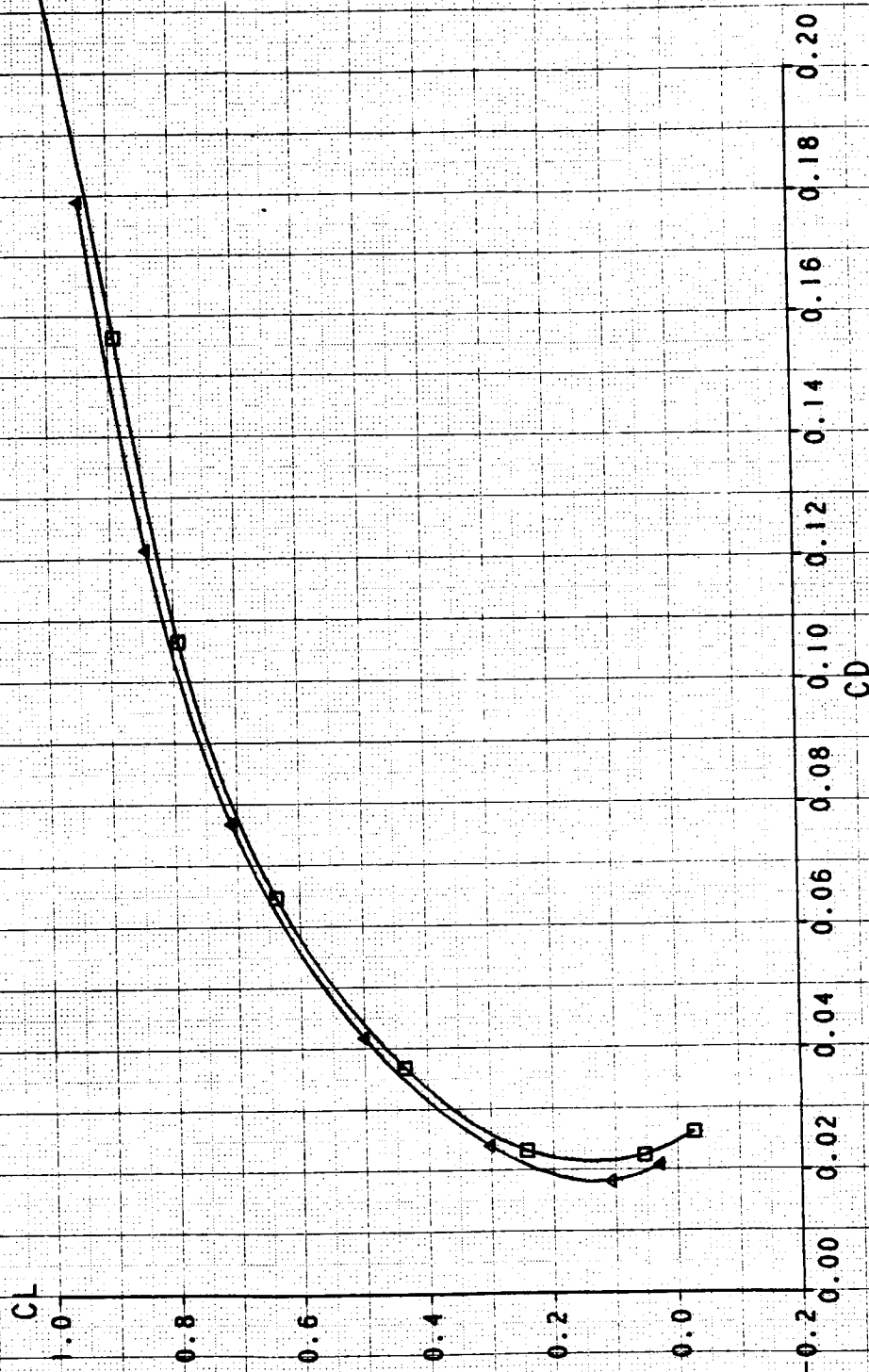
NOZZLE PRESSURE RATIO EFFECT ON CL VS AGA AND CM JET-EFFECTS MODE WITH UNVECTORED A/B ALBEN

| SYM | TEST | RUN | RMACH | RNPR | RDELCL |
|-----|------|-----|--------|--------|---------|
| □ | 514 | 243 | 0.6214 | 0.0906 | -4.9911 |
| △ | 514 | 259 | 0.6009 | 4.998 | -4.9763 |



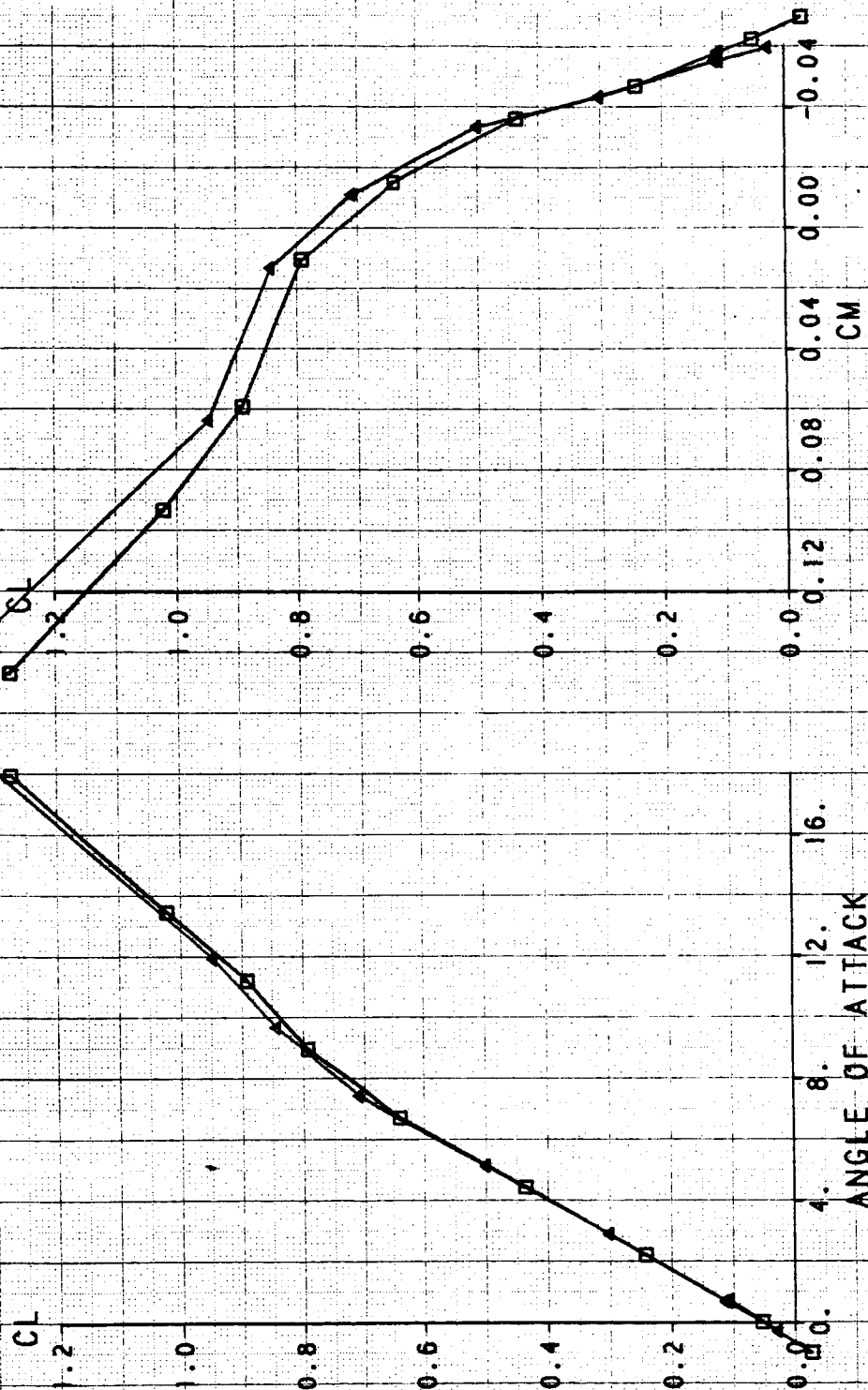
NOZZLE PRESSURE RATIO EFFECT ON DRAG POLAR JET-EFFECTS MODE WITH UNVECTORED A/B ALBEN

| | | | | | |
|-----|------|-----|--------|--------|---------|
| SYM | TEST | RUN | RMACH | RNPRA | RDELCL |
| □ | 514 | 244 | 0.9022 | 0.1384 | -4.9674 |
| △ | 514 | 262 | 0.9019 | 6.0982 | -4.9891 |



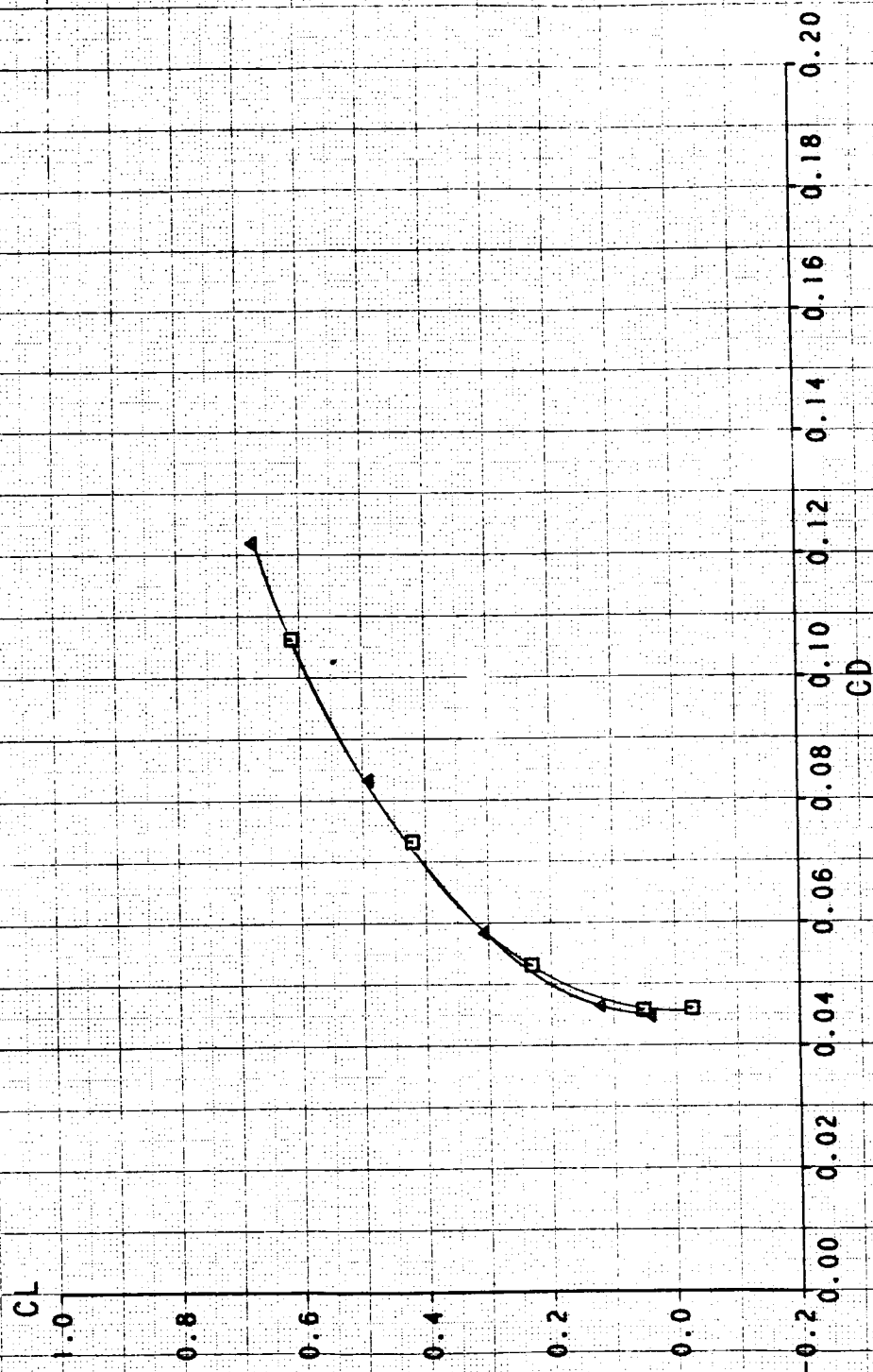
NOZZLE PRESSURE RATIO EFFECT ON CL VS AOA AND CM JET-EFFECTS MODE WITH UNVECTORED A/B ALBEN

| SYM | TEST | RUN | RMACH | RNPRA | RDELCL |
|-----|------|-----|--------|--------|---------|
| □ | 514 | 244 | 0.9022 | 0.1384 | -4.9674 |
| ▲ | 514 | 262 | 0.9019 | 6.0982 | -4.9891 |



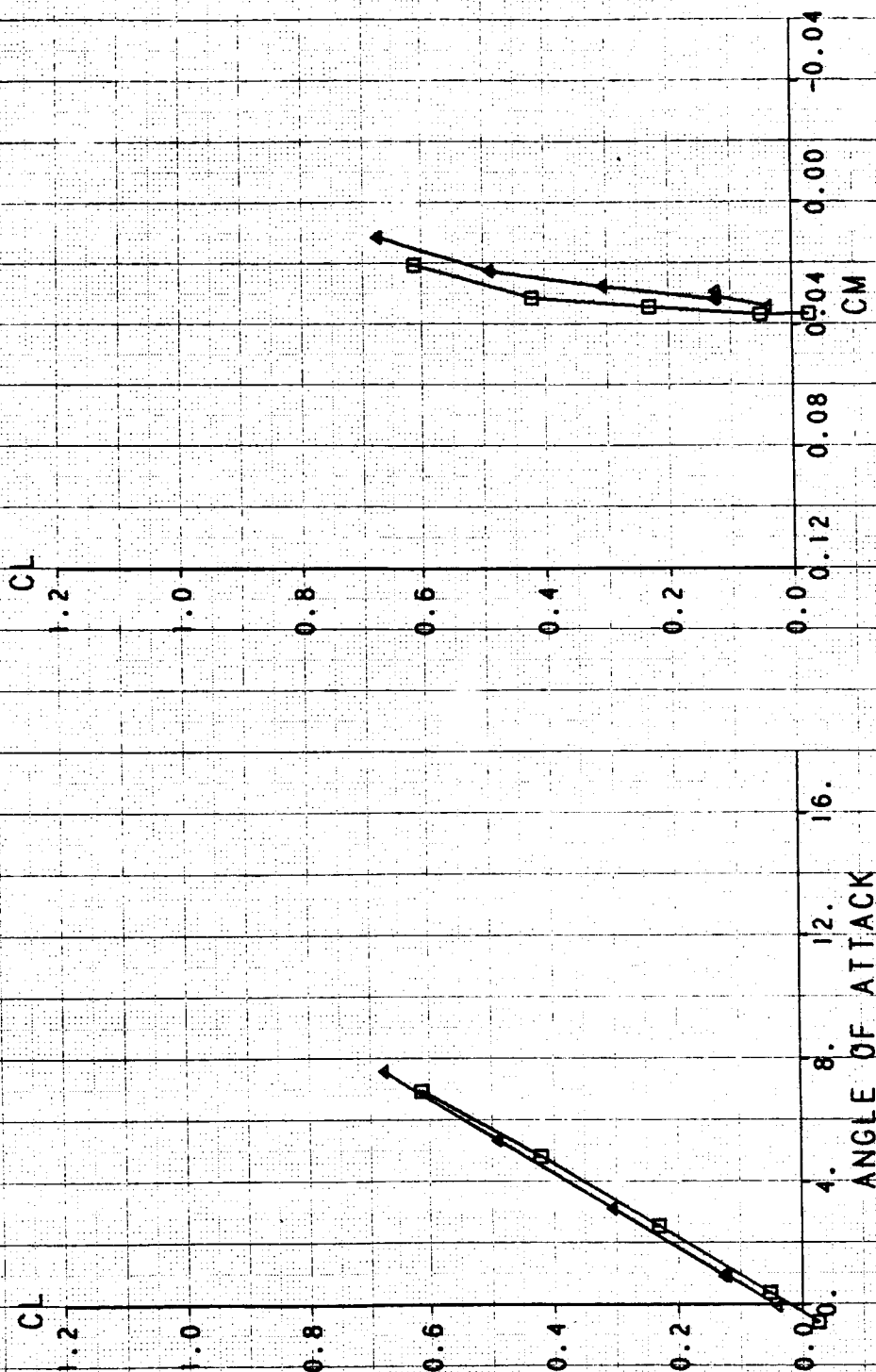
NOZZLE PRESSURE RATIO EFFECT ON DRAG POLAR JET-EFFECTS MODE WITH UNVECTORED A/B ALBEN

SYM TEST RUN RMACH RNPRA RDELCL
 □ 514 245 1.1772 0.1893 -0.1056
 ▲ 514 252 1.1940 9.0806 -0.0448



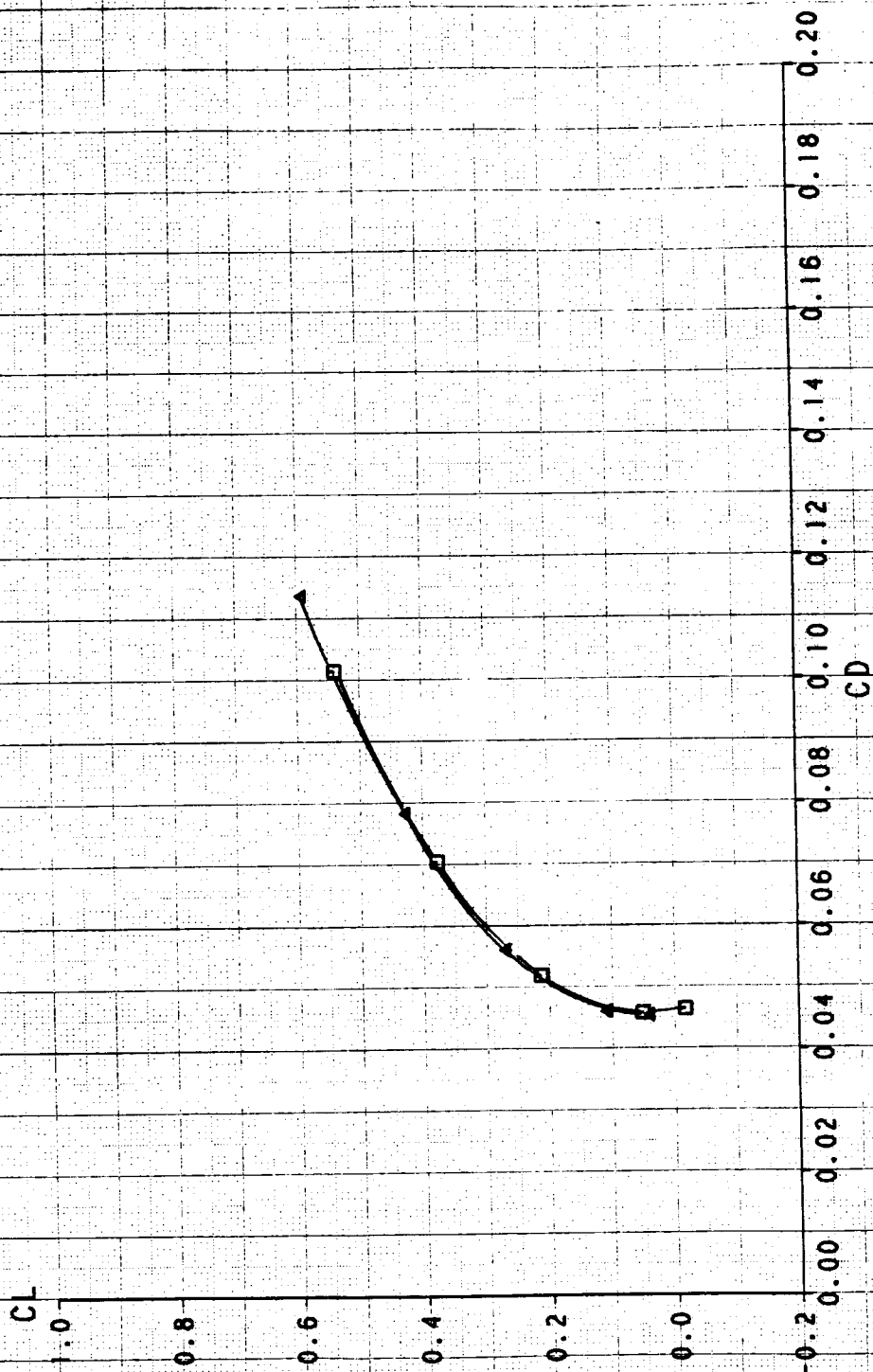
NOZZLE PRESSURE RATIO EFFECT ON CL VS AOA AND CM JET-EFFECTS MODE WITH UNVECTORED A/B ALBEN

| SYM | TEST | RUN | RMACH | RNPRA | RDELCL |
|-----|------|-----|--------|--------|---------|
| □ | 514 | 245 | 1.1772 | 0.1893 | -0.1056 |
| △ | 514 | 252 | 1.1940 | 9.0806 | -0.0448 |



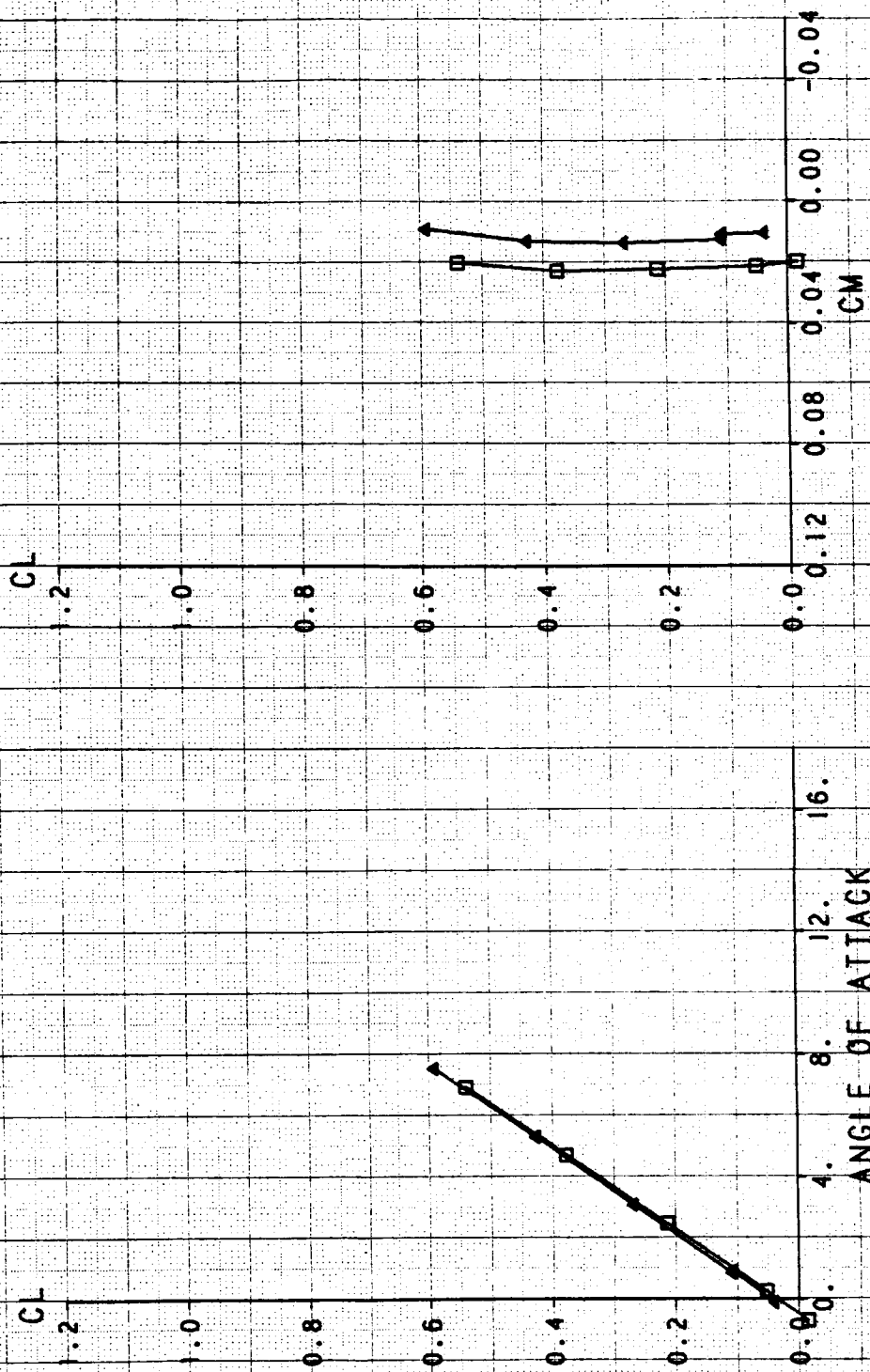
NOZZLE PRESSURE RATIO EFFECT ON DRAG POLAR JET-EFFECTS MODE WITH UNVECTORED A/B ALBEN

SYM TEST RUN RMACH RNPRA RDELCL
 □ 514 246 1.3548 0.2345 .00883
 △ 514 254 1.3859 10.389 -0.0460



NOZZLE PRESSURE RATIO EFFECT ON CL VS AOA AND CM JET-EFFECTS MODE WITH UNVECTORED A/B ALBEN

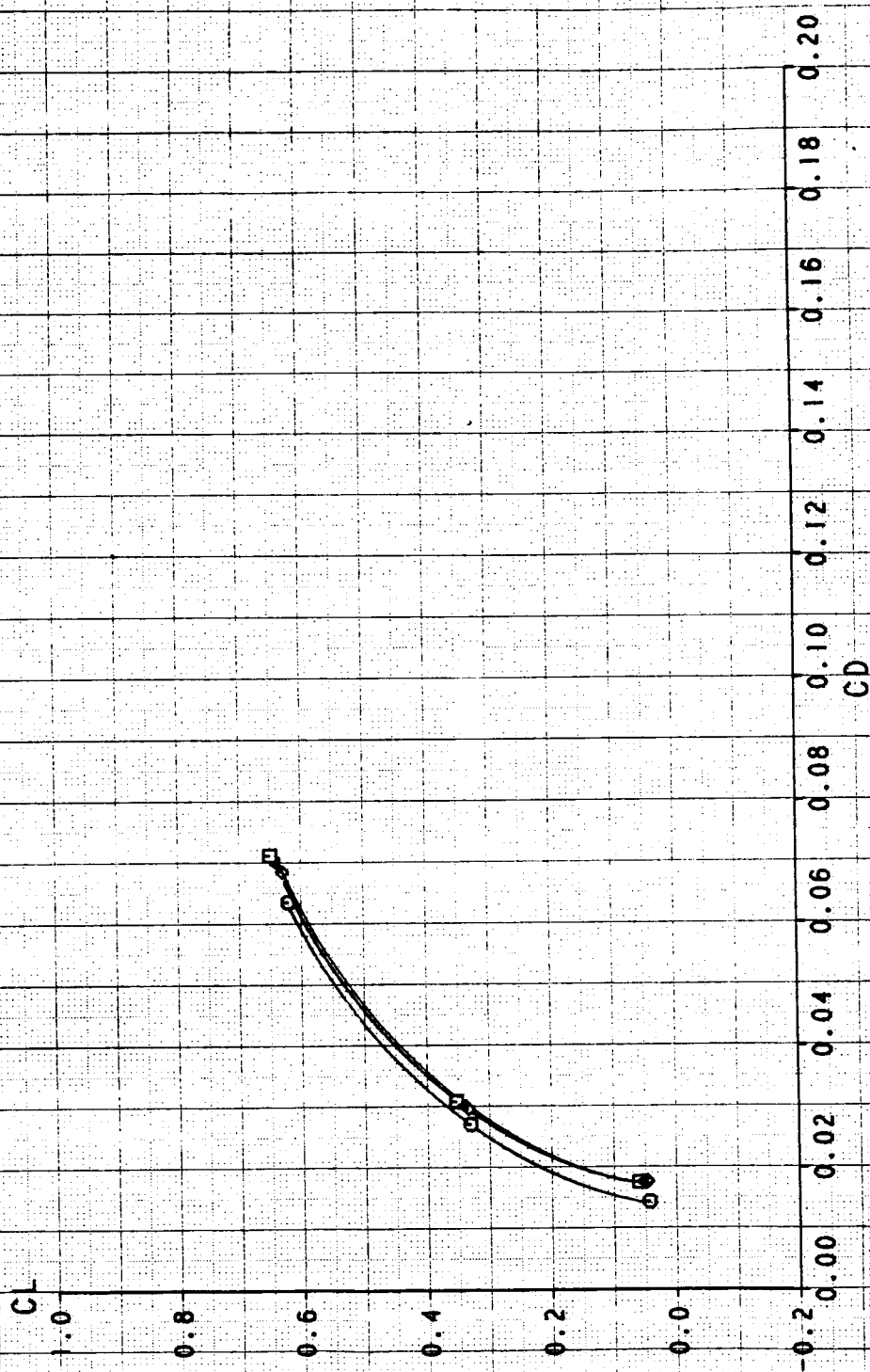
| SYM | TEST | RUN | RWACH | RNPRA | RDELCL |
|-----|------|-----|--------|--------|---------|
| □ | 514 | 246 | 1.3548 | 0.2345 | .00883 |
| △ | 514 | 254 | 1.3859 | 10.389 | -0.0460 |



NOZZLE PRESSURE RATIO EFFECT ON DRAG POLAR

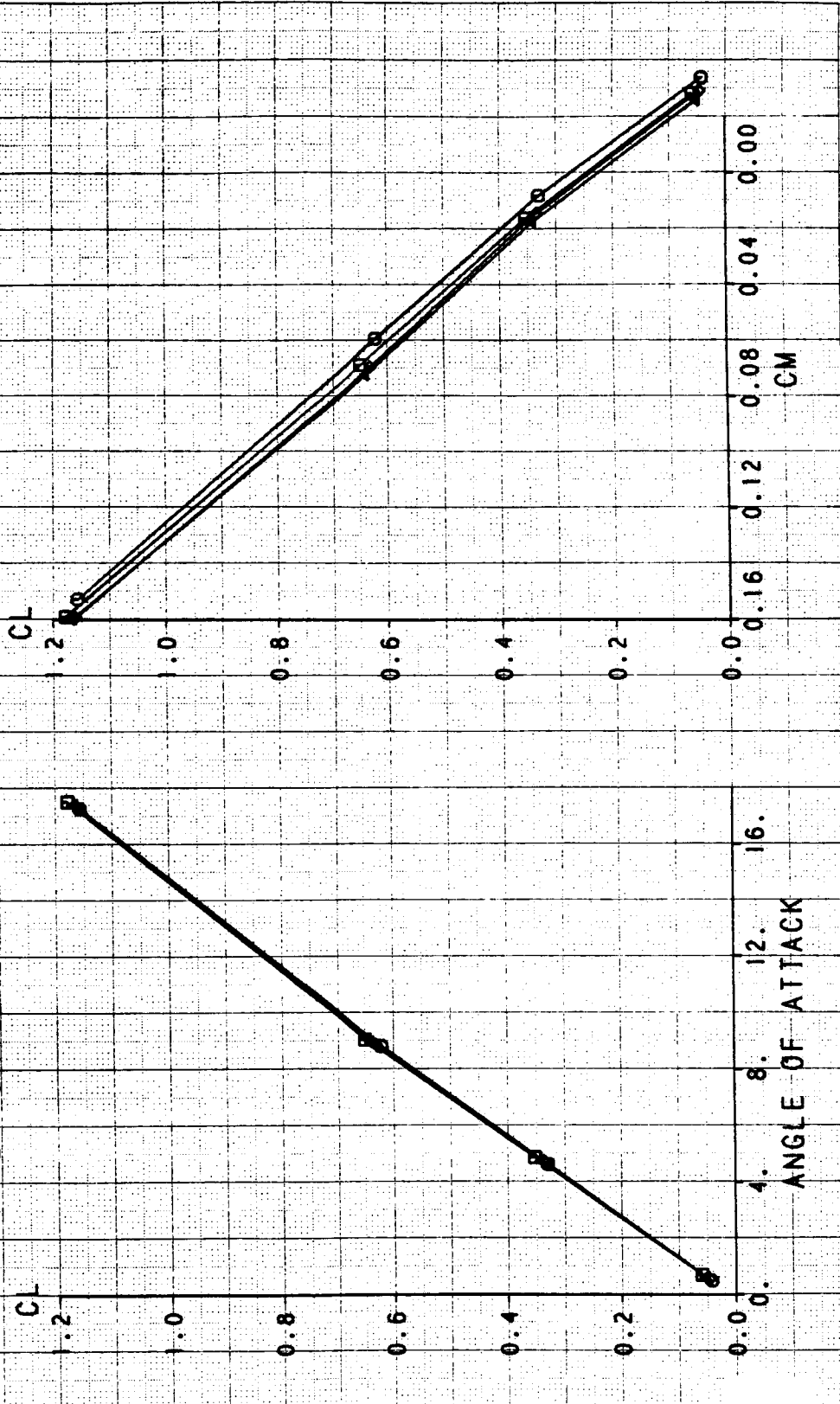
SIMULATOR MODE WITH A/B ALBEN

| SYM | TEST | RUN | RMACH | RMFRA | RMFR | RDELCL |
|-----|------|-----|--------|--------|---------|---------|
| □ | 514 | 283 | 0.4017 | 1.6483 | 1.11604 | -5.0039 |
| △ | 514 | 284 | 0.4014 | 1.9882 | 1.11603 | -5.0028 |
| ◇ | 514 | 285 | 0.4019 | 2.4178 | 1.11571 | -4.9983 |
| ○ | 514 | 288 | 0.4032 | 3.3566 | 1.11353 | -5.0263 |



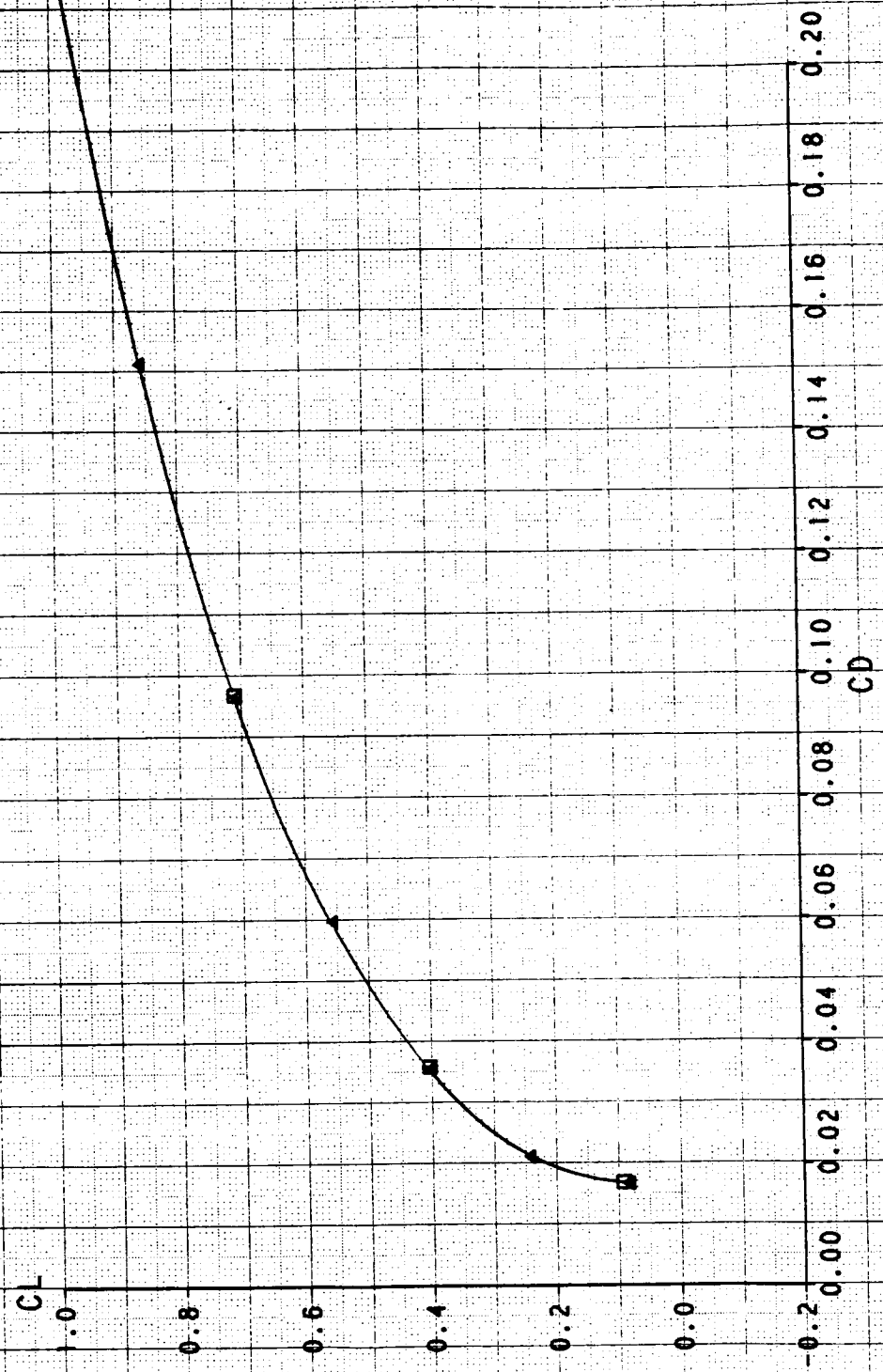
NOZZLE PRESSURE RATIO EFFECT ON CL VS AOA AND CM

| SYM | TEST | RUN | RMACH | RNPR | RMFR | RDELCL |
|-----|------|-----|--------|--------|--------|---------|
| □ | 514 | 283 | 0.4017 | 1.6483 | 1.1604 | -5.0039 |
| △ | 514 | 284 | 0.4014 | 1.9882 | 1.1603 | -5.0028 |
| ◇ | 514 | 285 | 0.4019 | 3.4178 | 1.1571 | -4.9983 |
| ○ | 514 | 288 | 0.4032 | 3.3566 | 1.1353 | -5.0263 |



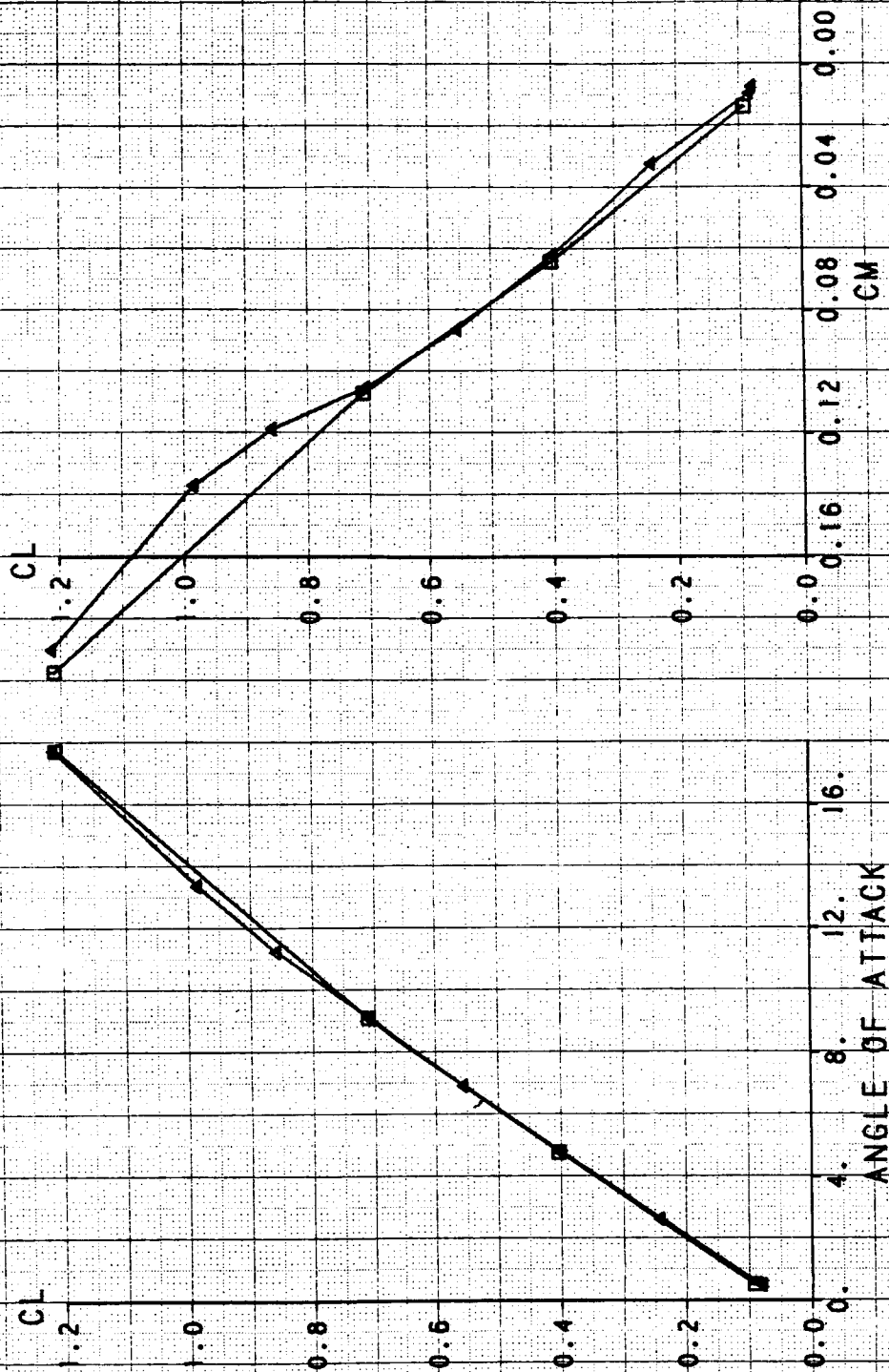
NOZZLE PRESSURE RATIO EFFECT ON DRAG POLAR SIMULATOR MODE WITH A/B ALBEN

SYM TEST RUN RMACH RNPRA RMFR RDELCL
 514 175 3.2903 0.9202 0.1480
 514 178 0.6009 0.9161 0.1001



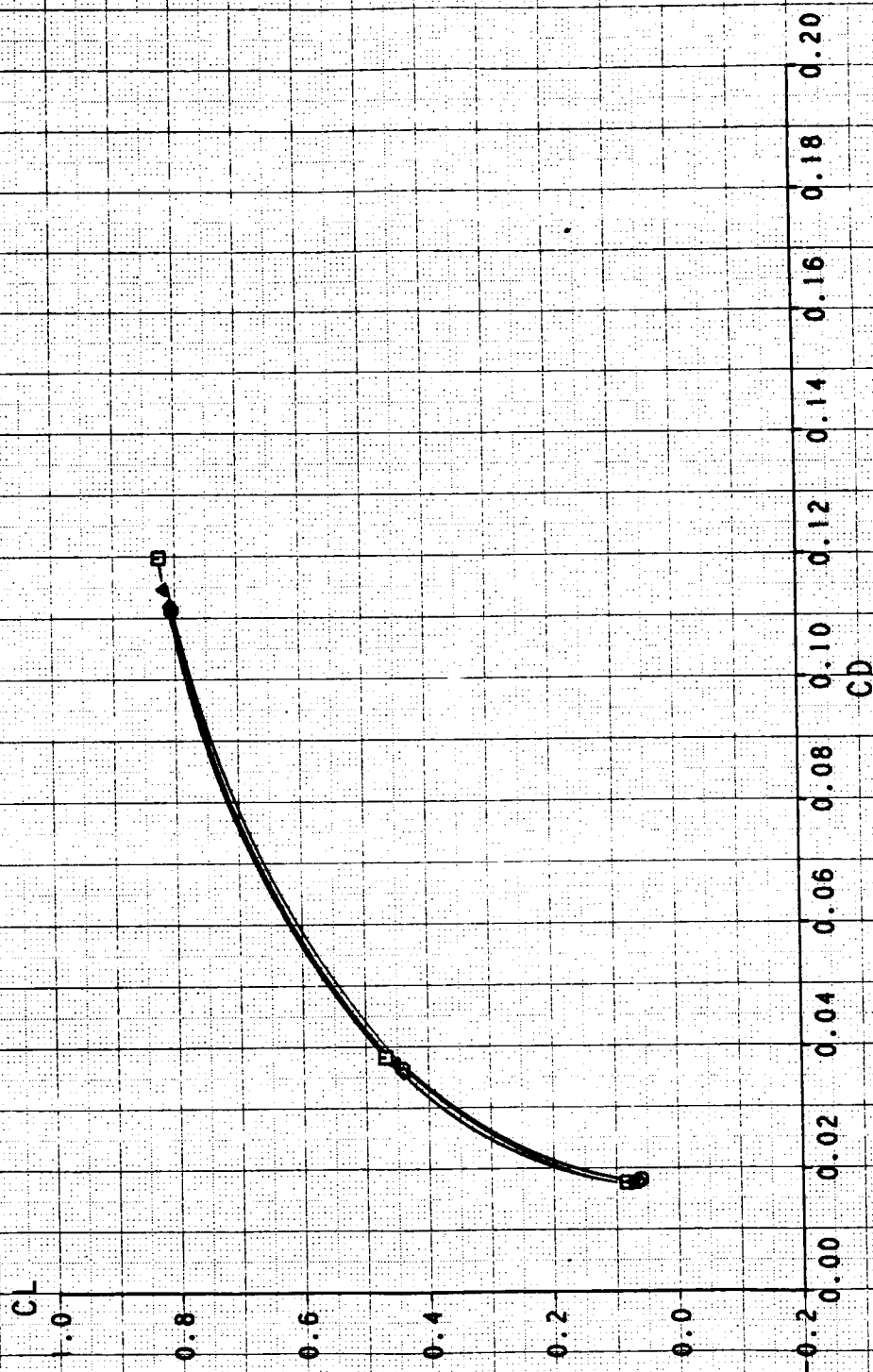
NOZZLE PRESSURE RATIO EFFECT ON CL VS AOA AND CM

SYM TEST RUN RMACH RNPR RDELCL
 □ 514 175 0.5892 3.2903 0.1480
 ▲ 514 178 0.6009 3.8301 0.100



NOZZLE PRESSURE RATIO EFFECT ON DRAG POLAR SIMULATOR MODE WITH A/B ALBEN

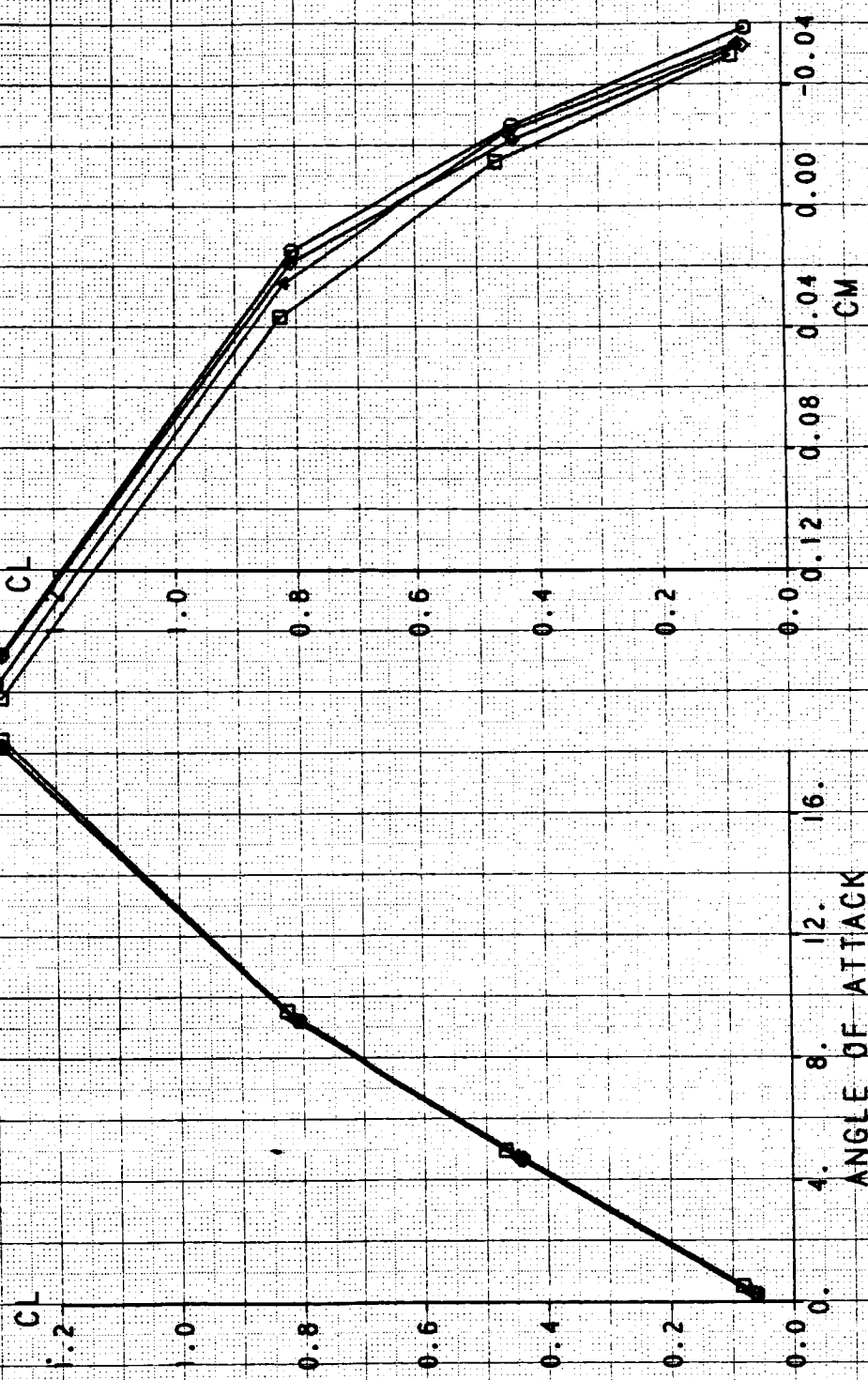
| SYM | TEST | RUN | RMACH | RNPR | RMFR | RDELCH |
|-----|------|-----|--------|--------|--------|---------|
| □ | 514 | 211 | 0.8966 | 2.4771 | 0.7627 | -4.9703 |
| ◇ | 514 | 213 | 0.8953 | 3.6541 | 0.7639 | -4.9849 |
| ◇ | 514 | 214 | 0.8987 | 4.3555 | 0.7595 | -4.9849 |
| ○ | 514 | 215 | 0.8964 | 5.3011 | 0.7534 | -4.9623 |



NOZZLE PRESSURE RATIO EFFECT ON CL VS AOA AND CM

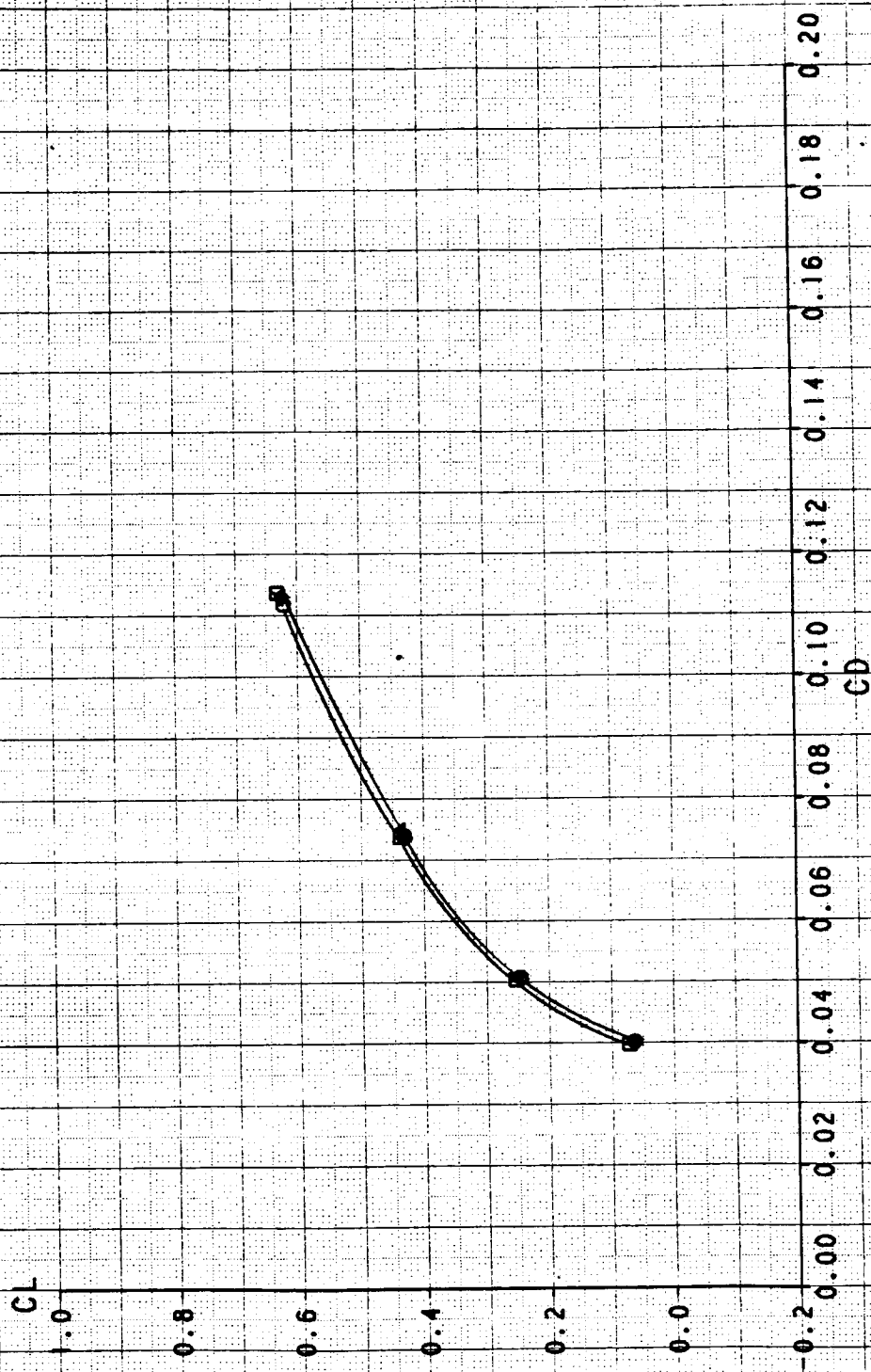
SIMULATOR MODE WITH A/B ALBEN

| SYM | TEST | RUN | RMACH | RNPRA | RMFR | RDELCL |
|-----|------|-----|--------|--------|--------|---------|
| □ | 514 | 211 | 0.8966 | 2.4771 | 0.7627 | -4.9703 |
| △ | 514 | 213 | 0.8953 | 3.6541 | 0.7539 | -4.9849 |
| ◇ | 514 | 214 | 0.8987 | 4.3555 | 0.7595 | -4.9849 |
| ○ | 514 | 215 | 0.8964 | 5.3011 | 0.7534 | -4.9625 |



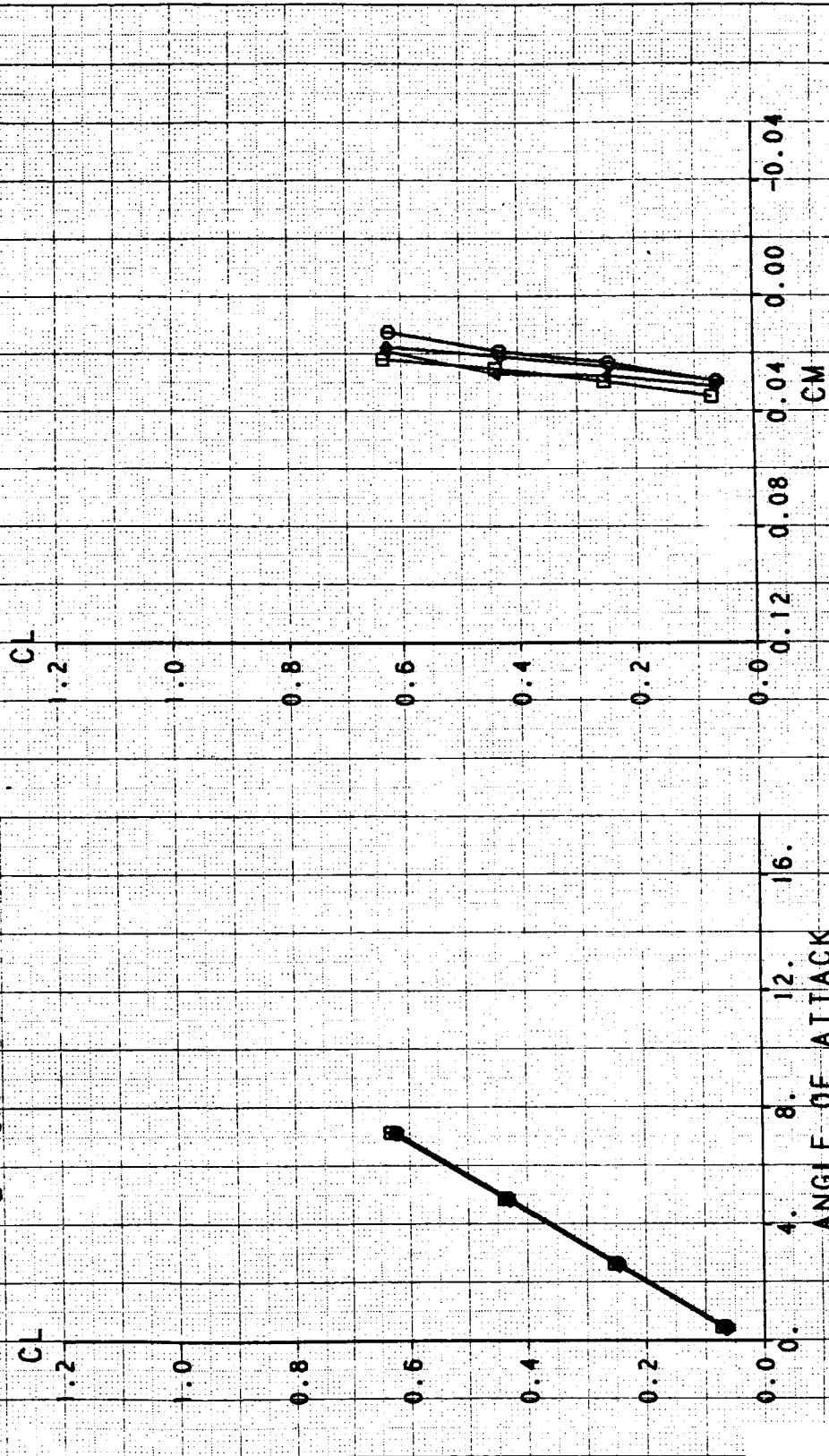
NOZZLE PRESSURE RATIO EFFECT ON DRAG POLAR SIMULATOR MODE WITH A/B ALBEN

| SYM | TEST | RUN | RMACH | RNPR | RMFR | RDELCL |
|-----|------|-----|--------|--------|--------|--------|
| □ | 514 | 239 | 1.1834 | 4.2464 | 0.6863 | 0.1042 |
| △ | 514 | 240 | 1.1896 | 5.2134 | 0.6841 | 0.1033 |
| ◇ | 514 | 241 | 1.1903 | 6.1521 | 0.6803 | 0.1125 |
| ○ | 514 | 242 | 1.1906 | 7.5840 | 0.7579 | 0.1042 |



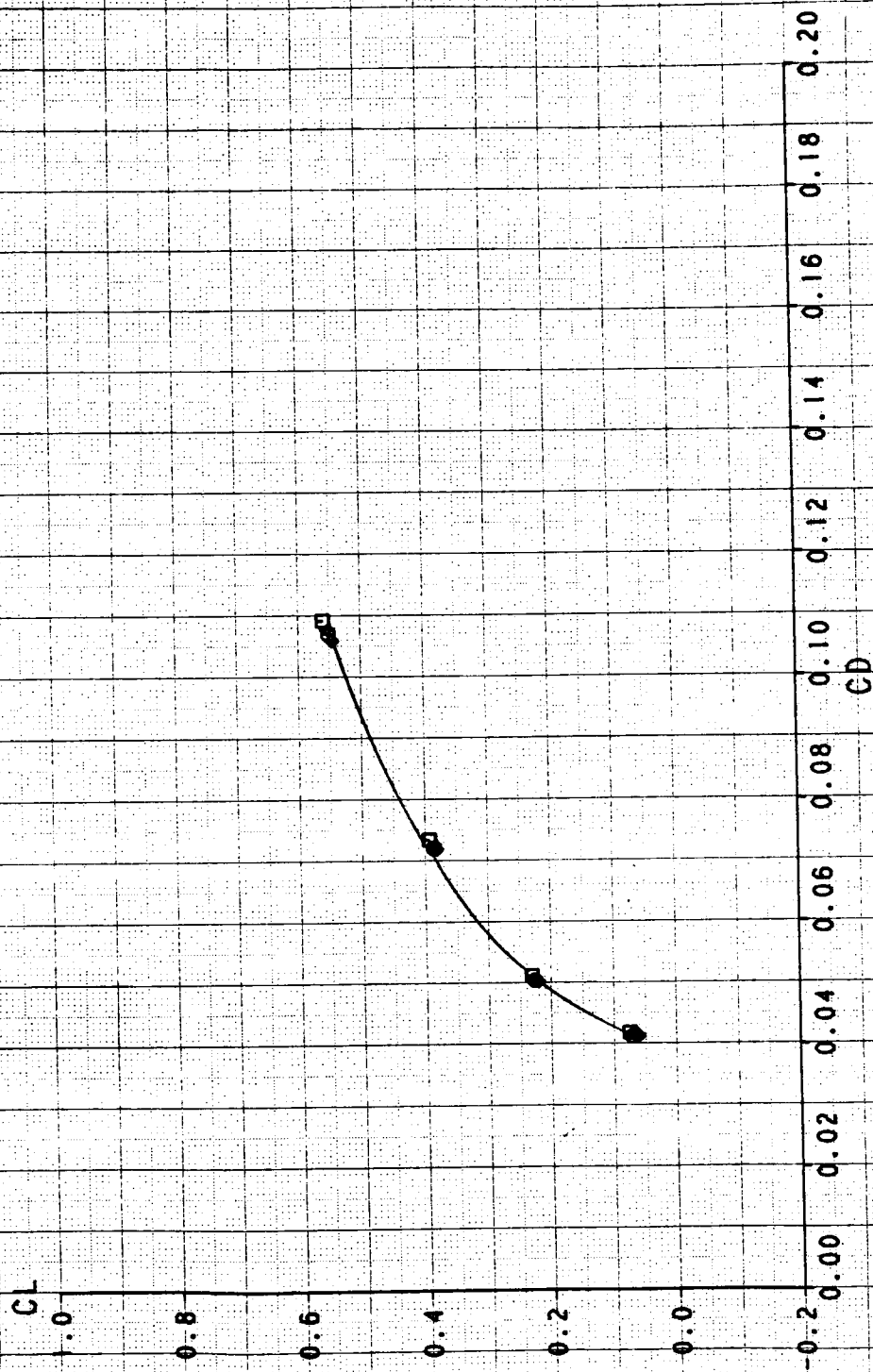
NOZZLE PRESSURE RATIO EFFECT ON CL VS AOA AND CM

| SYM | TEST | RUN | RMACH | RNPRA | RMFR | RDELCL |
|-----|------|-----|--------|--------|--------|--------|
| □ | 514 | 239 | 1.1834 | 4.2464 | 0.6863 | 0.1042 |
| △ | 514 | 240 | 1.1896 | 5.2134 | 0.6841 | 0.1083 |
| ◇ | 514 | 241 | 1.1903 | 6.1521 | 0.6803 | 0.1125 |
| ○ | 514 | 242 | 1.1906 | 7.9840 | 0.7579 | 0.1042 |



NOZZLE PRESSURE RATIO EFFECT ON DRAG POLAR SIMULATOR MODE WITH A/B ALBEN

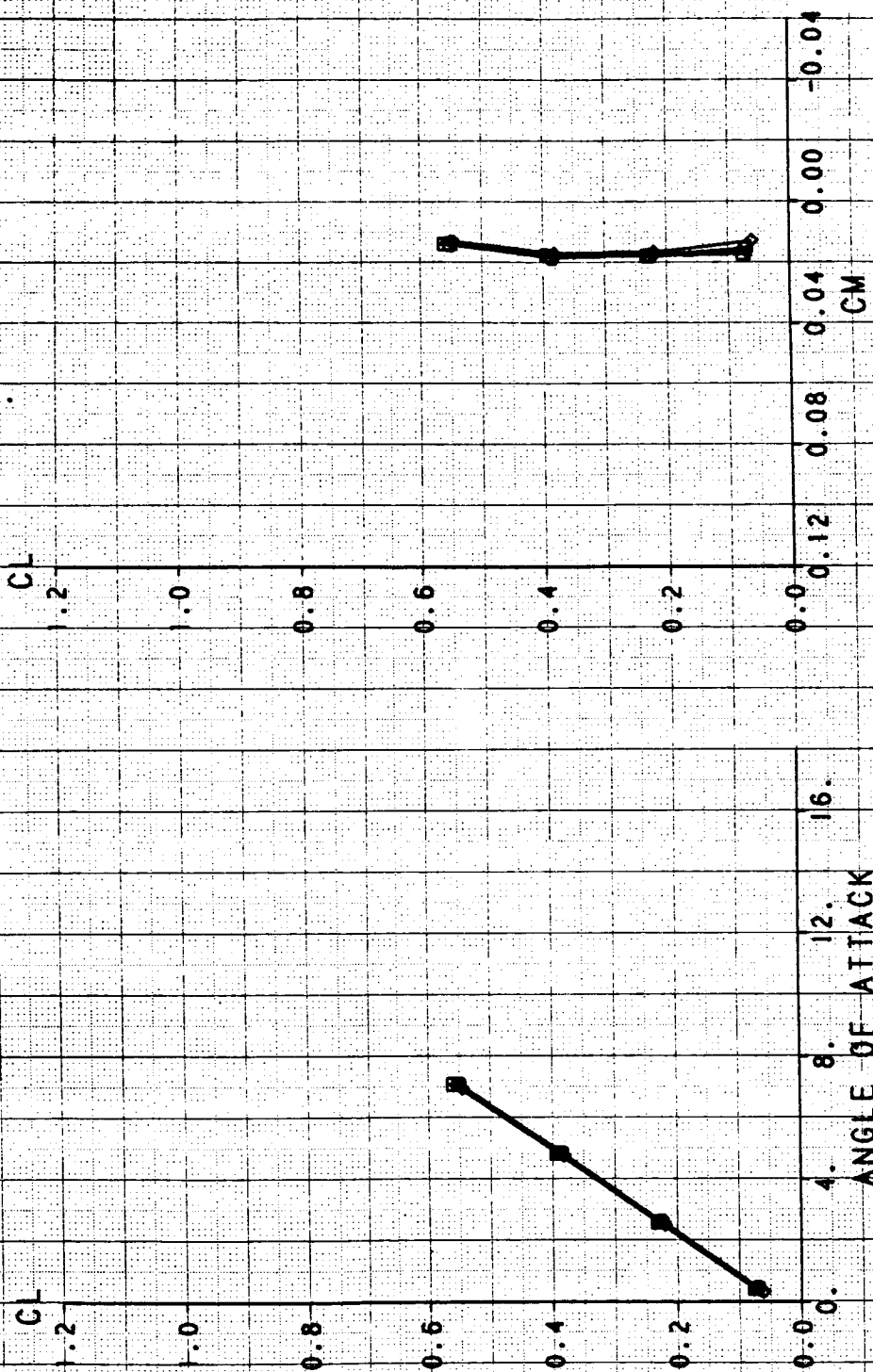
| SYM | TEST | RUN | RMACH | RNPRA | RMFR | RDELCL |
|-----|------|-----|--------|--------|--------|--------|
| □ | 514 | 253 | 1.3958 | 5.4634 | 0.7198 | 0.1281 |
| △ | 514 | 254 | 1.3978 | 6.6757 | 0.7203 | 0.1229 |
| ◇ | 514 | 255 | 1.3966 | 7.8725 | 0.7118 | 0.1323 |
| ○ | 514 | 256 | 1.3969 | 9.5970 | 0.7929 | 0.1083 |

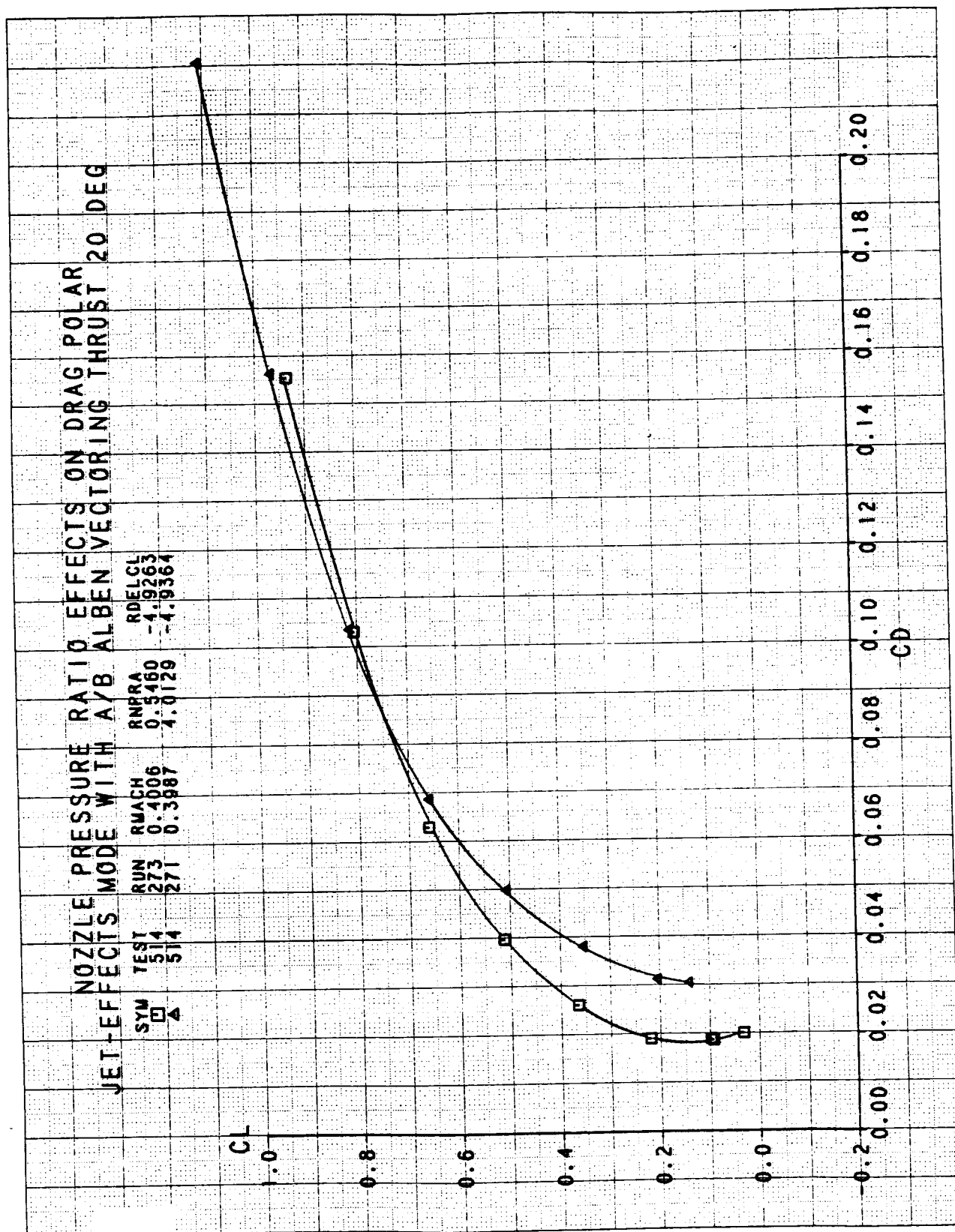


NOZZLE PRESSURE RATIO EFFECT ON CL VS AOA AND CM

SIMULATOR MODE WITH A/B ALBEN

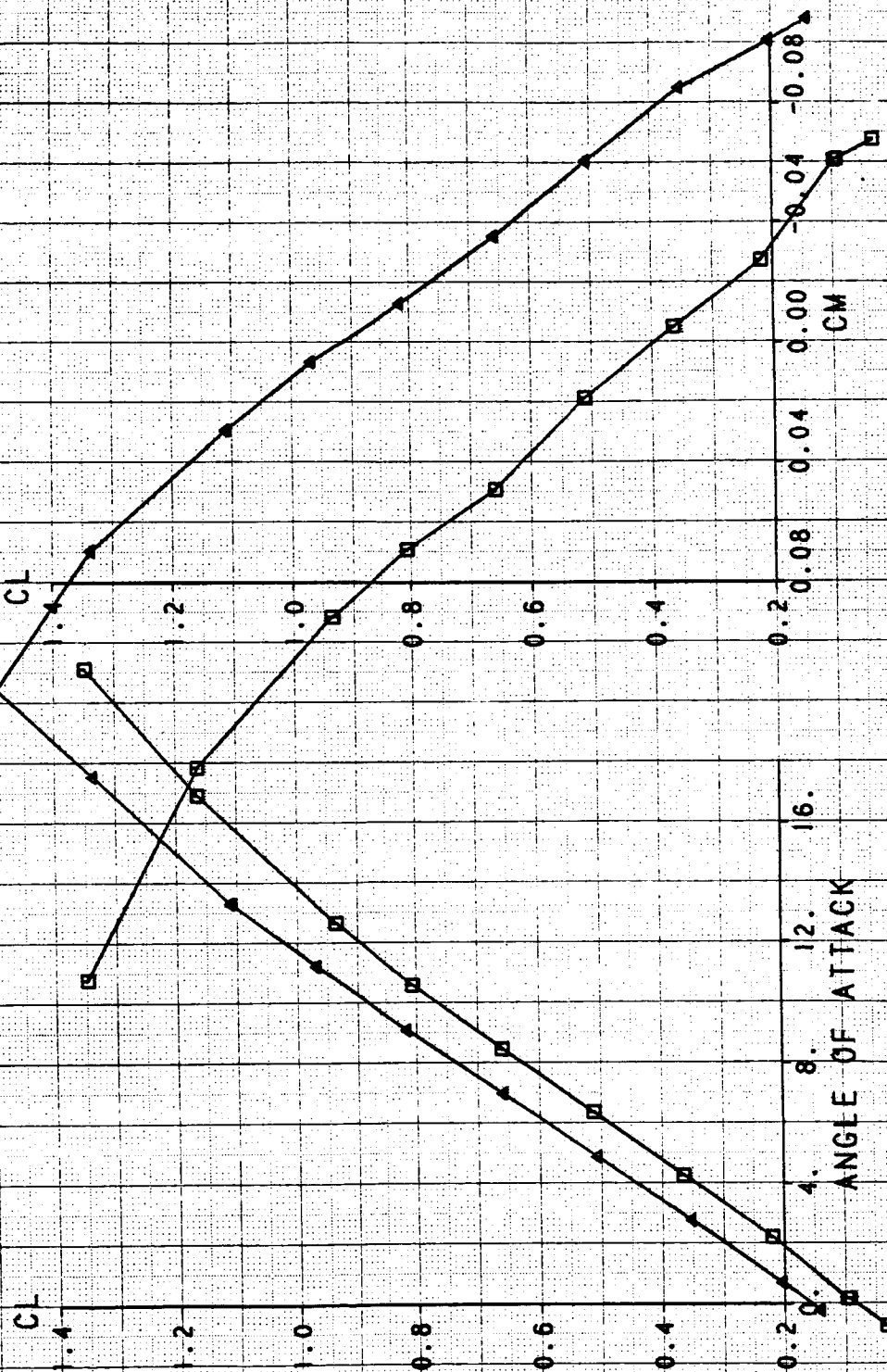
| SYM | TEST | RUN | RMACH | RNPRA | RNFR | RDELCL |
|-----|------|-----|--------|--------|--------|--------|
| □ | 514 | 253 | 1.3958 | 5.4634 | 0.7198 | 0.1281 |
| △ | 514 | 254 | 1.3978 | 6.6757 | 0.7203 | 0.1229 |
| ◇ | 514 | 255 | 1.3966 | 7.8725 | 0.7118 | 0.1322 |
| ○ | 514 | 256 | 1.3969 | 9.3970 | 0.7929 | 0.1083 |

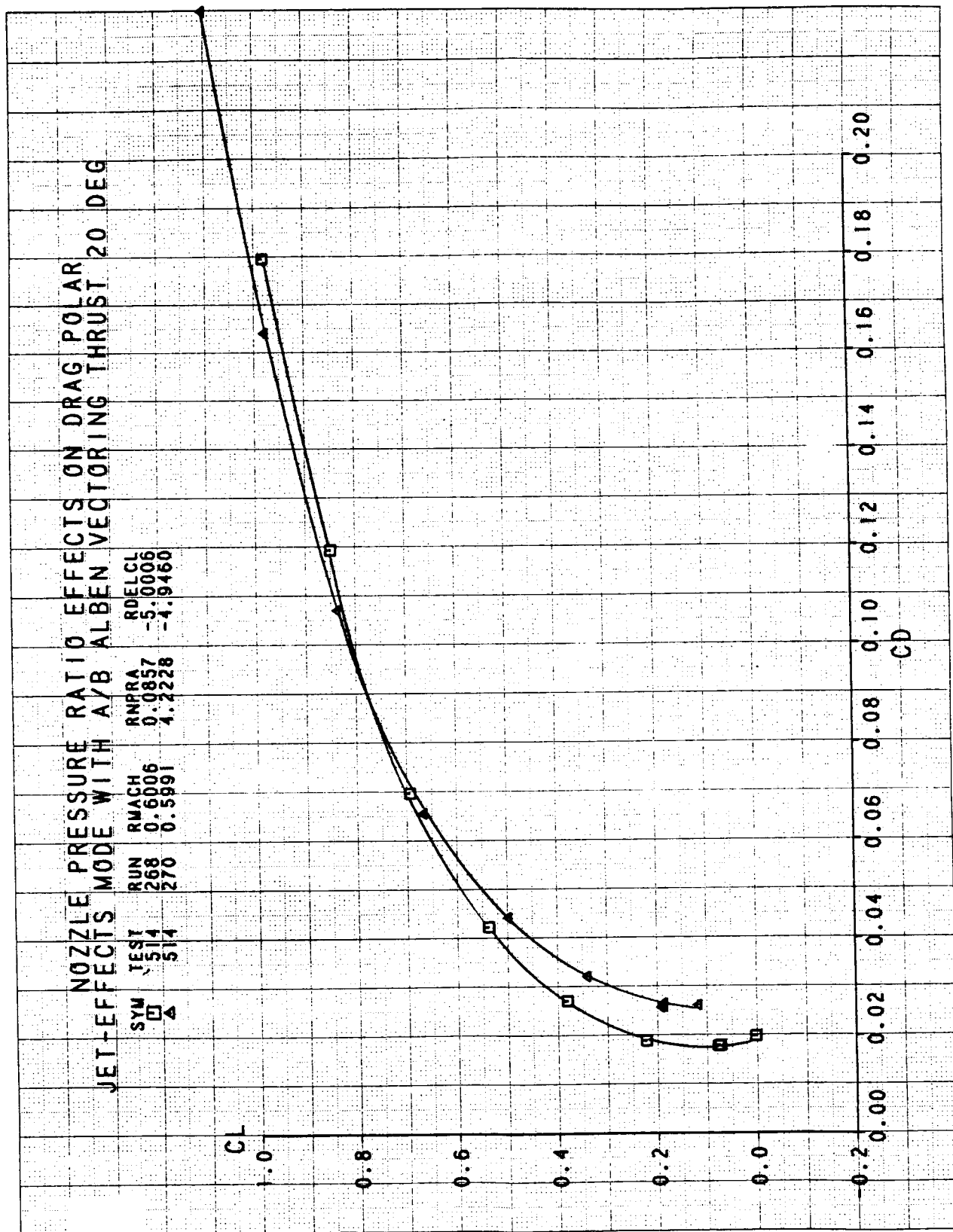




NOZZLE PRESSURE RATIO EFFECT ON CL VS AOA AND CM JET-EFFECTS MODE WITH A/B ALBEN VECTORED THRUST 20 DEG

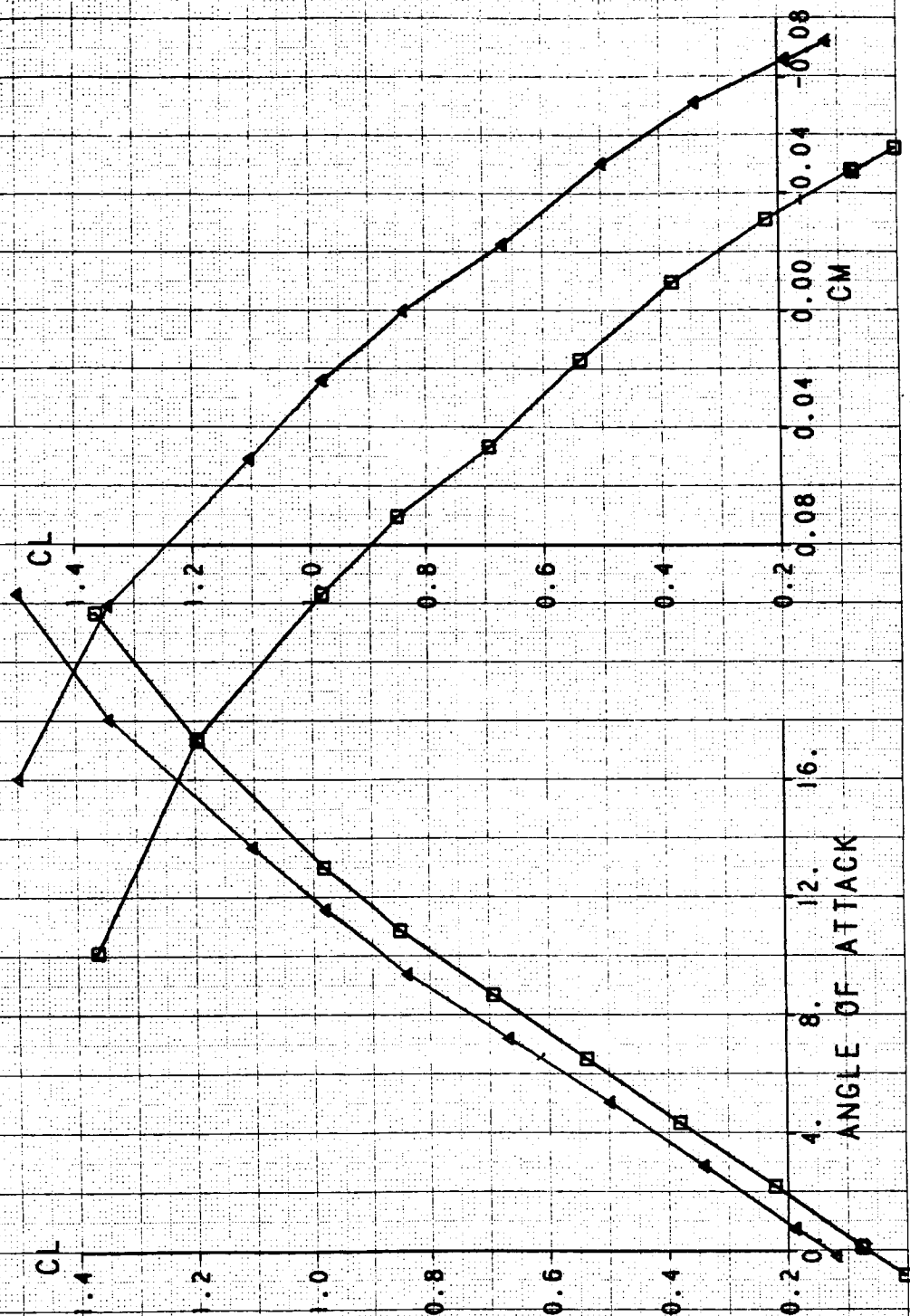
| SYM | TEST | RUN | RMACH | RNPRA | RDELCL |
|-----|------|-----|--------|--------|---------|
| □ | 514 | 273 | 0.4006 | 0.5460 | -4.9263 |
| △ | 514 | 271 | 0.3987 | 4.0129 | -4.9364 |

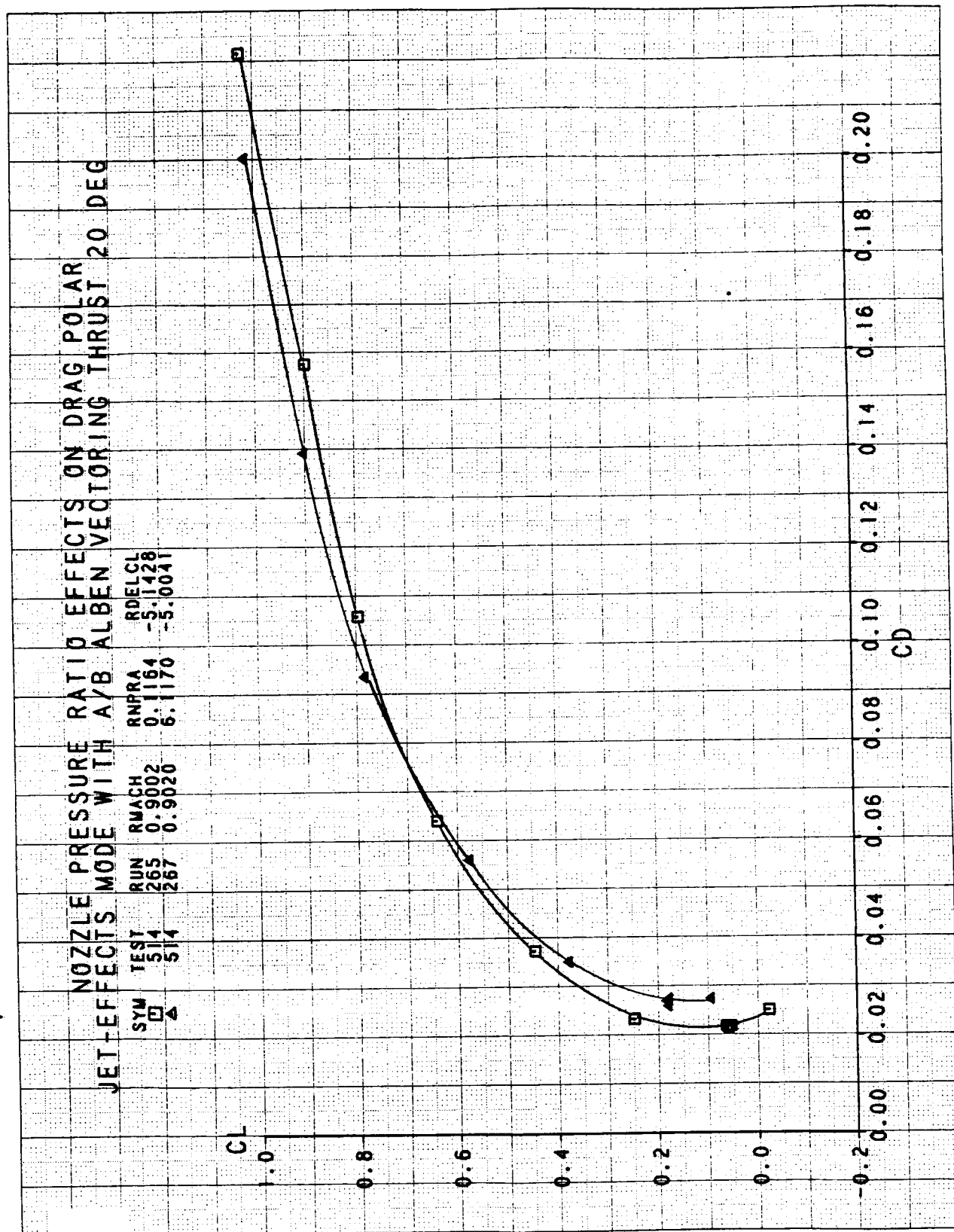




NOZZLE PRESSURE RATIO EFFECT ON CL VS AOA AND CM JET-EFFECTS MODE WITH A/B ALBEN VECTORING THRUST 20 DEG

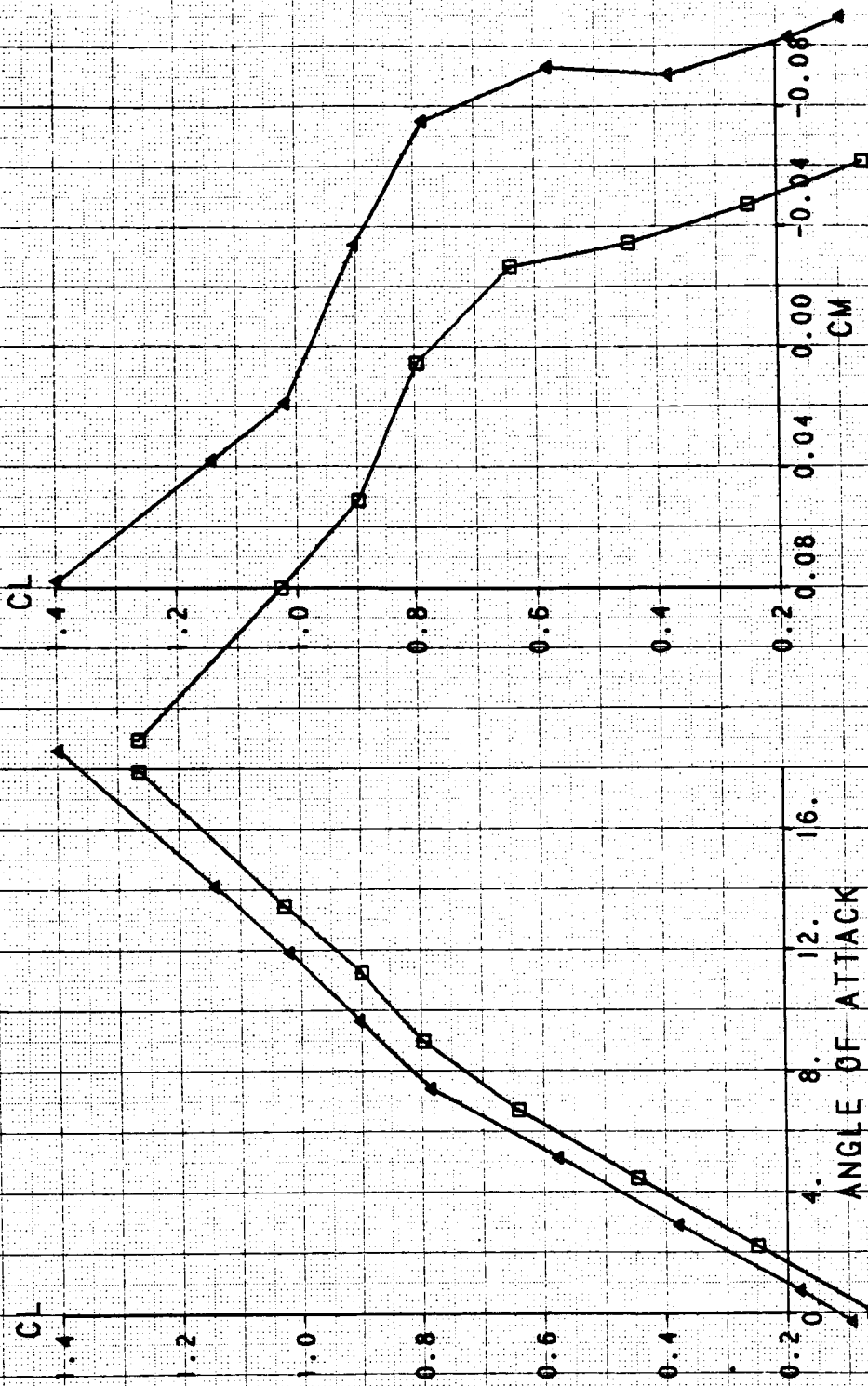
| SYM | TEST | RUN | RMACH | RNPRA | RDELCL |
|-----|------|-----|--------|--------|---------|
| □ | 514 | 268 | 0.6006 | 0.0857 | -5.0006 |
| △ | 514 | 270 | 0.5991 | 4.2228 | -4.9460 |

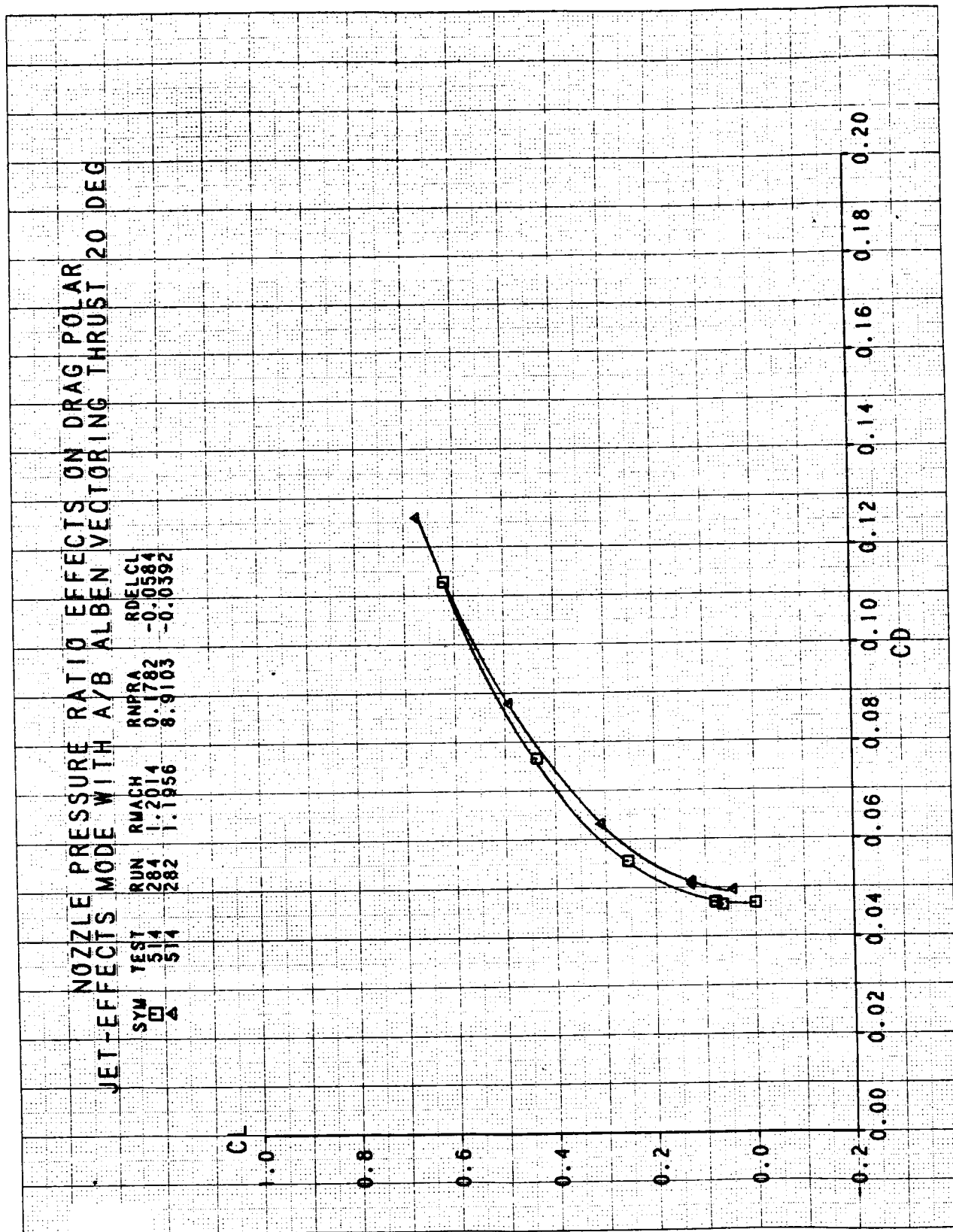




NOZZLE PRESSURE RATIO EFFECT ON CL VS AOA AND CM JET-EFFECTS MODE WITH A/B ALBEN VECTING THRUST 20 DEG

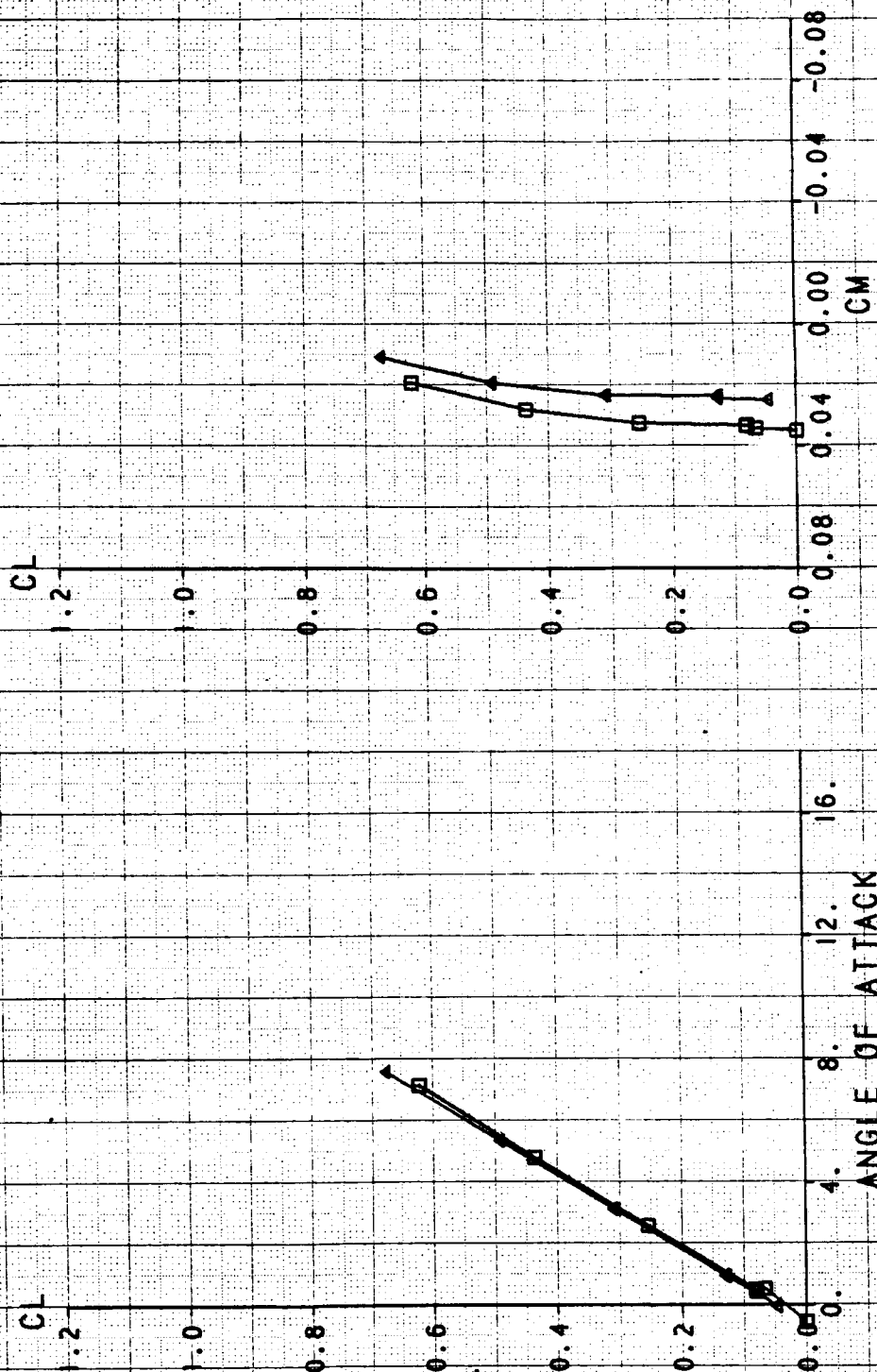
| SYM | TEST | RUN | RMACH | RNPRA | RDELCL |
|-----|------|-----|--------|--------|---------|
| □ | 514 | 265 | 0.9002 | 0.1164 | -5.1428 |
| ▲ | 514 | 267 | 0.9020 | 6.1170 | -5.0041 |

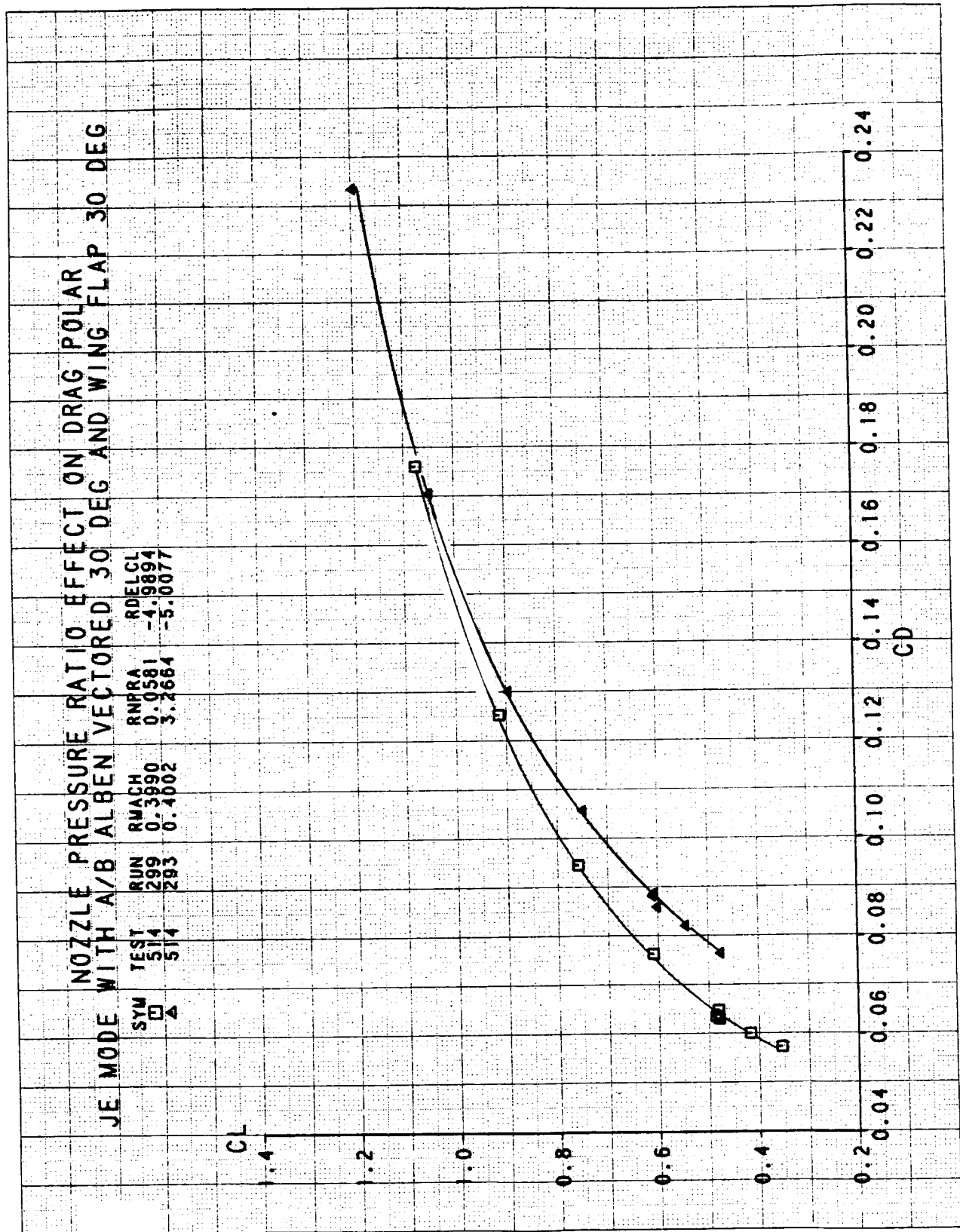




NOZZLE PRESSURE RATIO EFFECT ON CL VS AOA AND CM JET-EFFECTS MODE WITH A/B ALBEN VECTORIZING THRUST 20 DEG

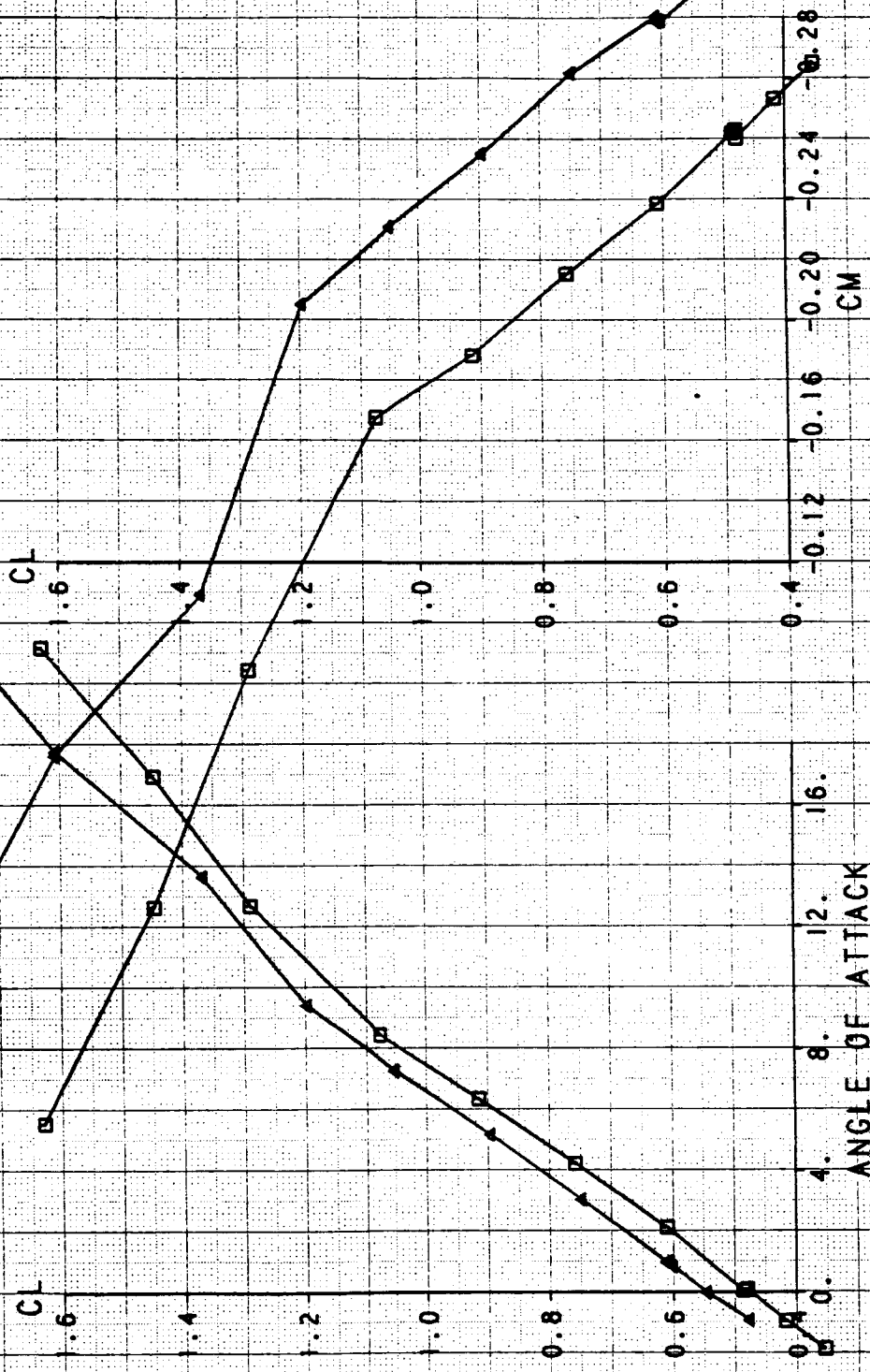
SYM TEST RUN RWACH RNPRA RDELCL
□ 514 284 1.2014 0.1782 -0.0584
△ 514 282 1.1956 8.9103 -0.0392

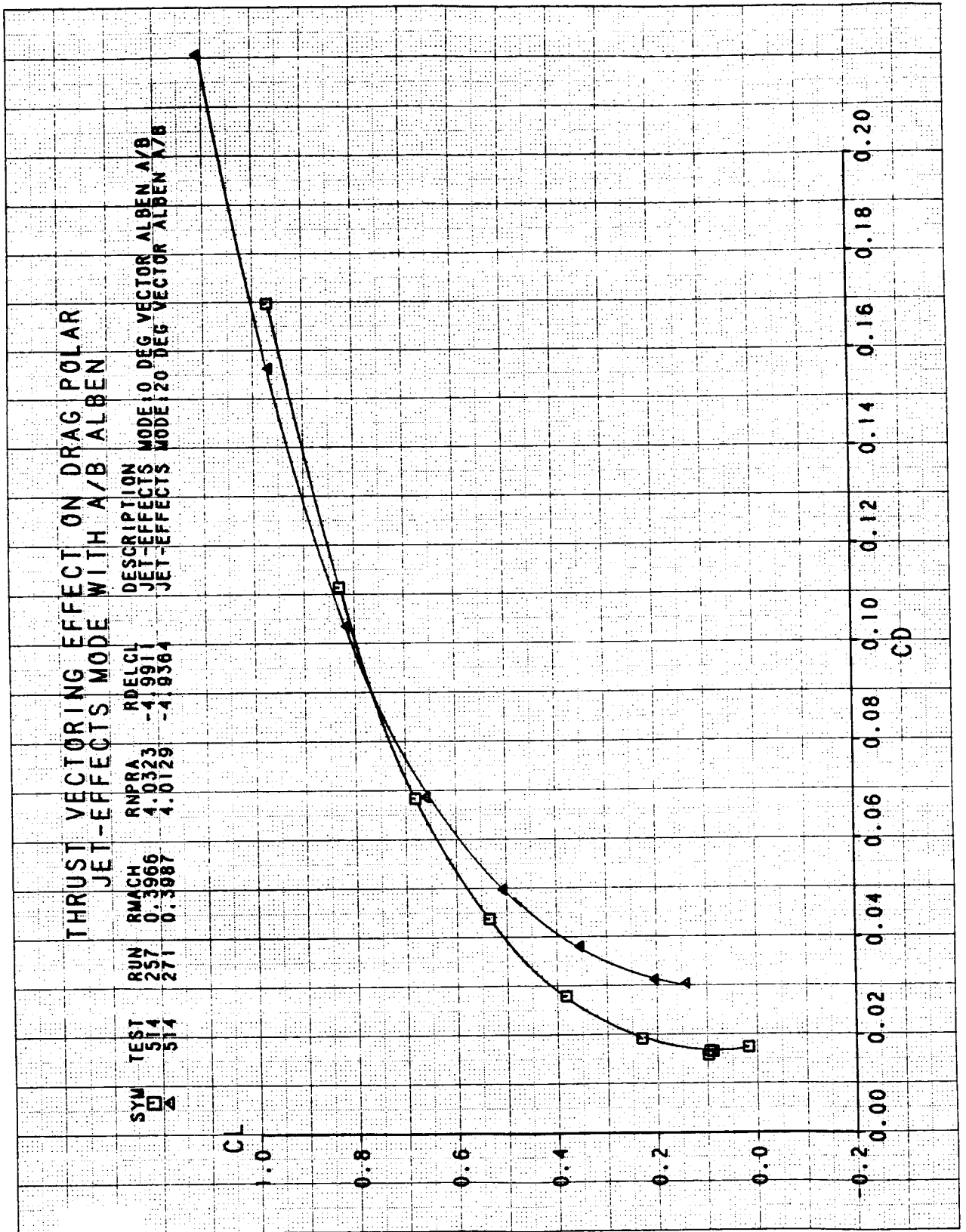




NOZZLE PRESSURE RATIO EFFECT ON CL VS AOA AND CM JE MODE WITH A/B ALBEN VECTORED 30 DEG AND WING FLAP 30 DEG

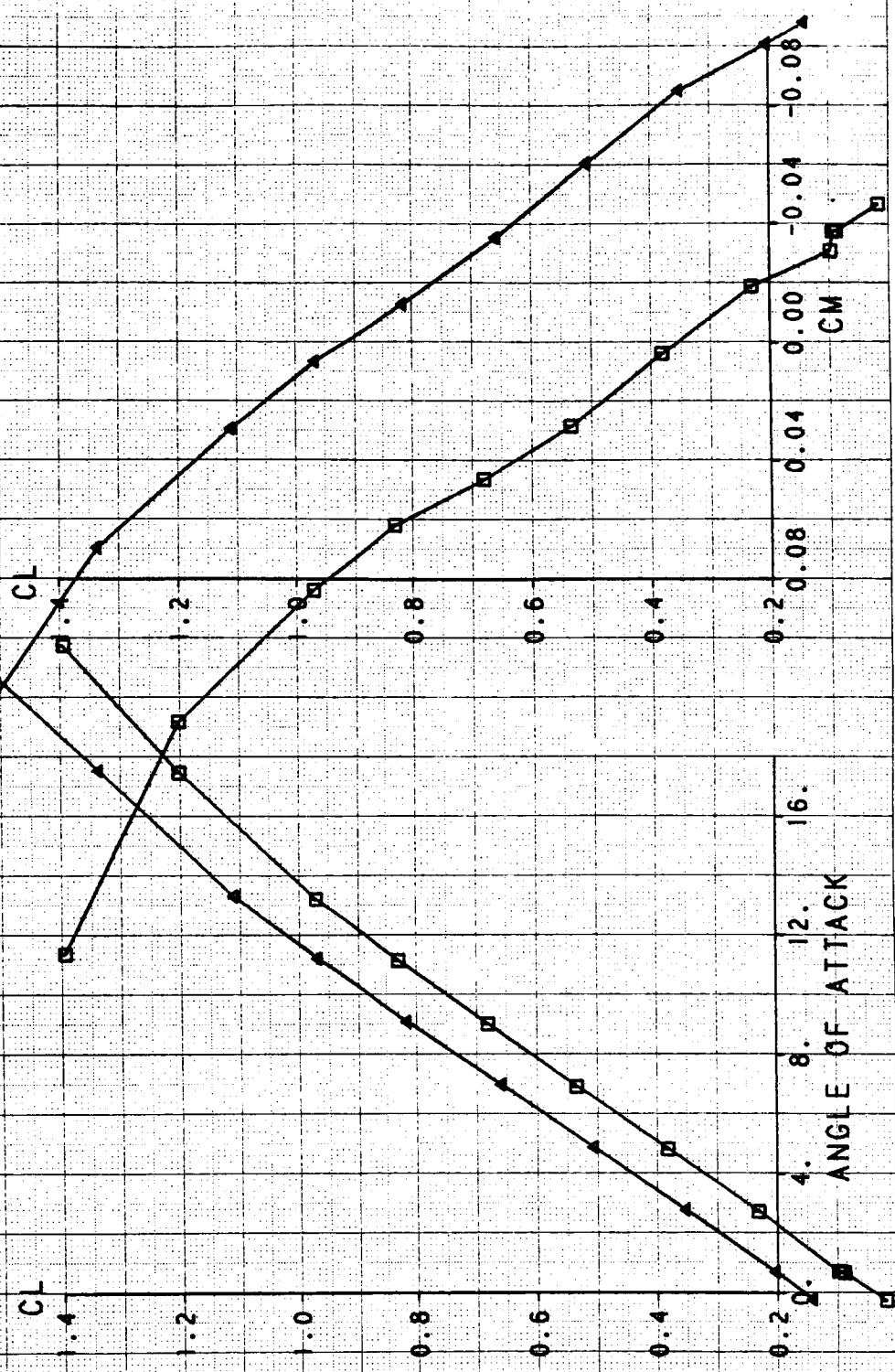
SYM TEST RUN RMACH RNPRA RDELCL
 514 299 0.3990 0.0581 -4.9894
 514 299 0.4002 3.2654 -5.0077

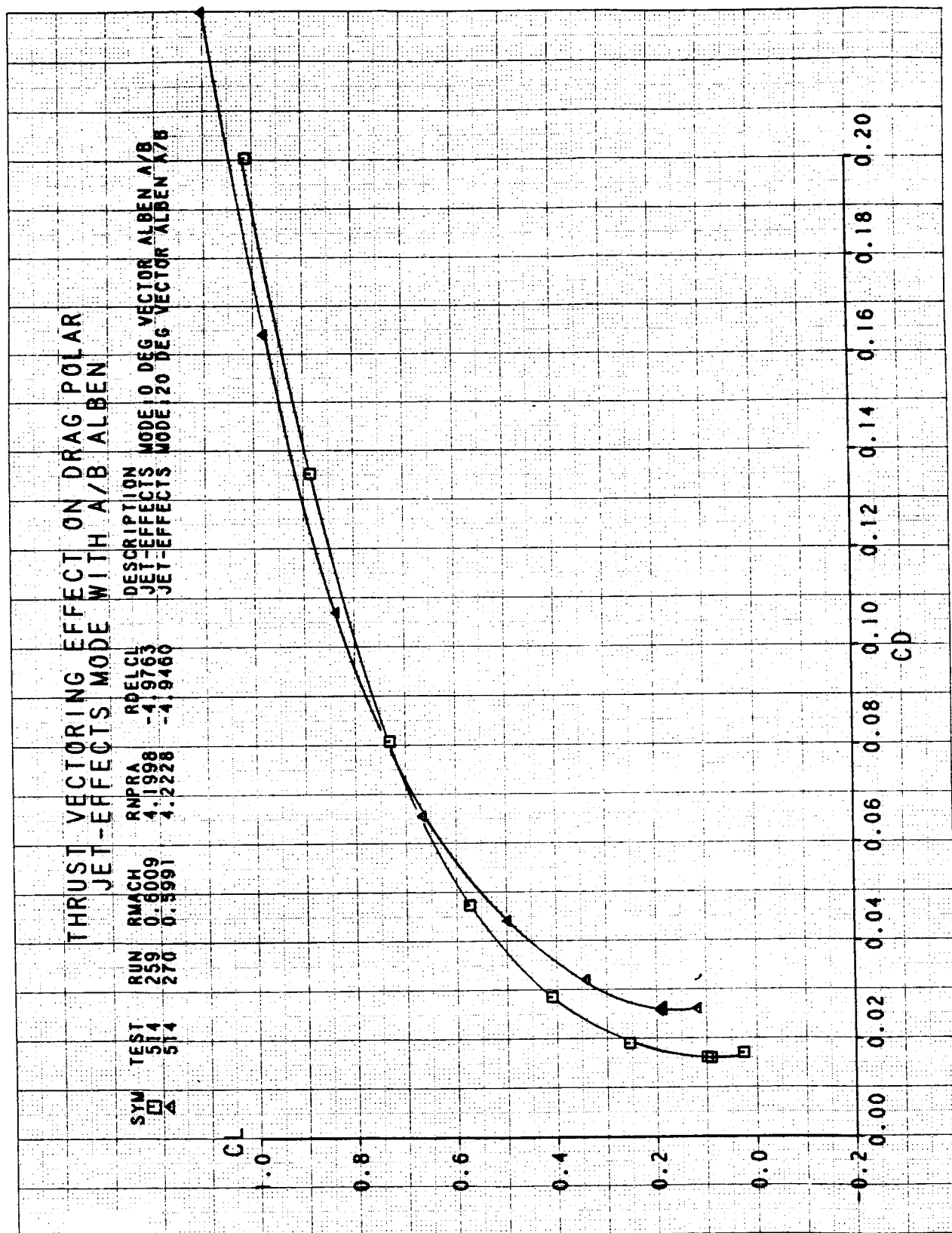




THRUST VECTORIZING EFFECT ON CL VS AOA AND CM

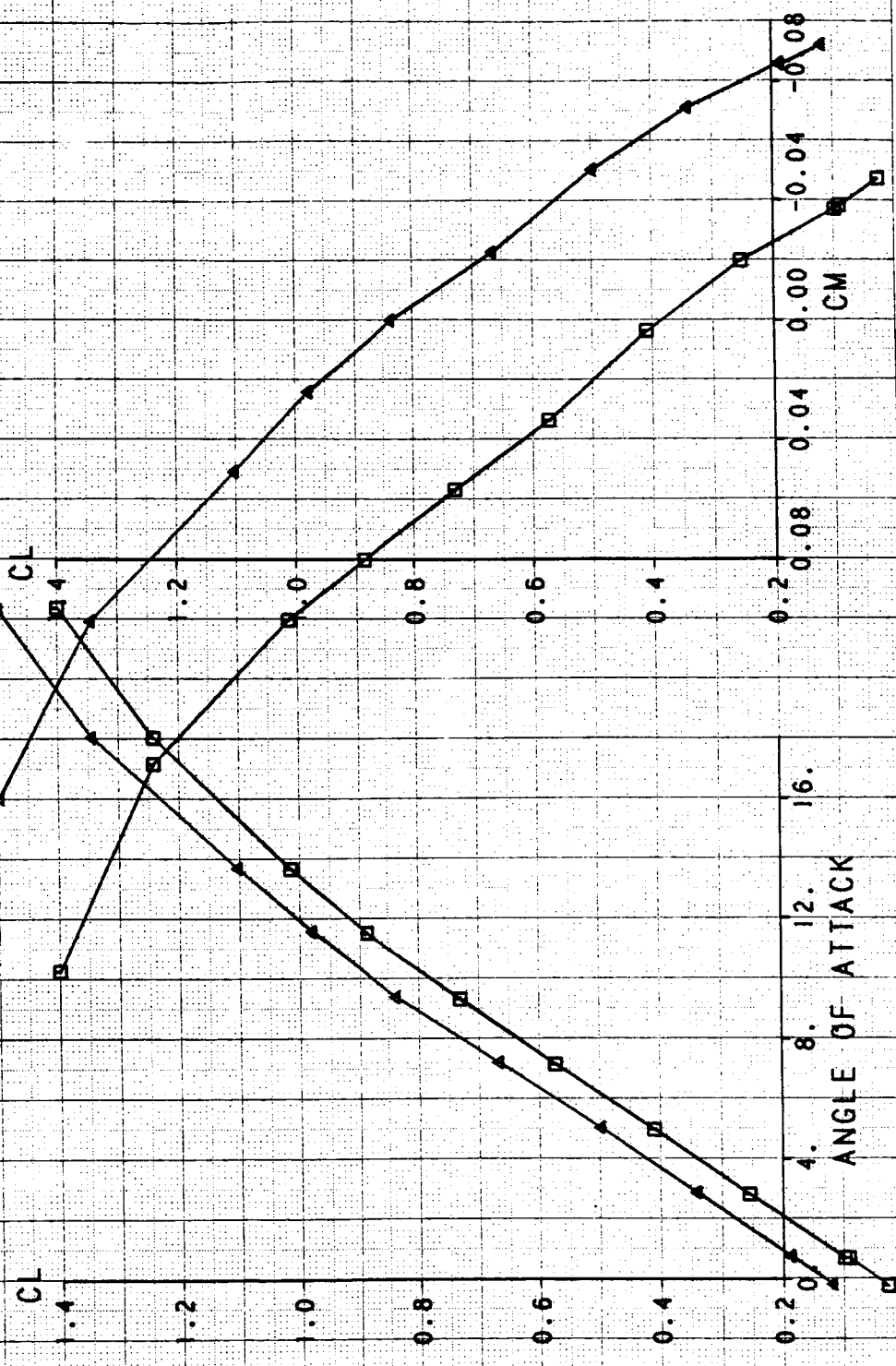
TEST 514
 SYM □
 RUN 257
 RMACH 0.3966
 RNPRA 4.0323
 RDELCL -4.9911
 DESCRIPTION
 JET-EFFECTS
 JET-EFFECTS
 MODE 0 DEG VECTOR ALBEN A/B
 MODE 20 DEG VECTOR ALBEN A/B

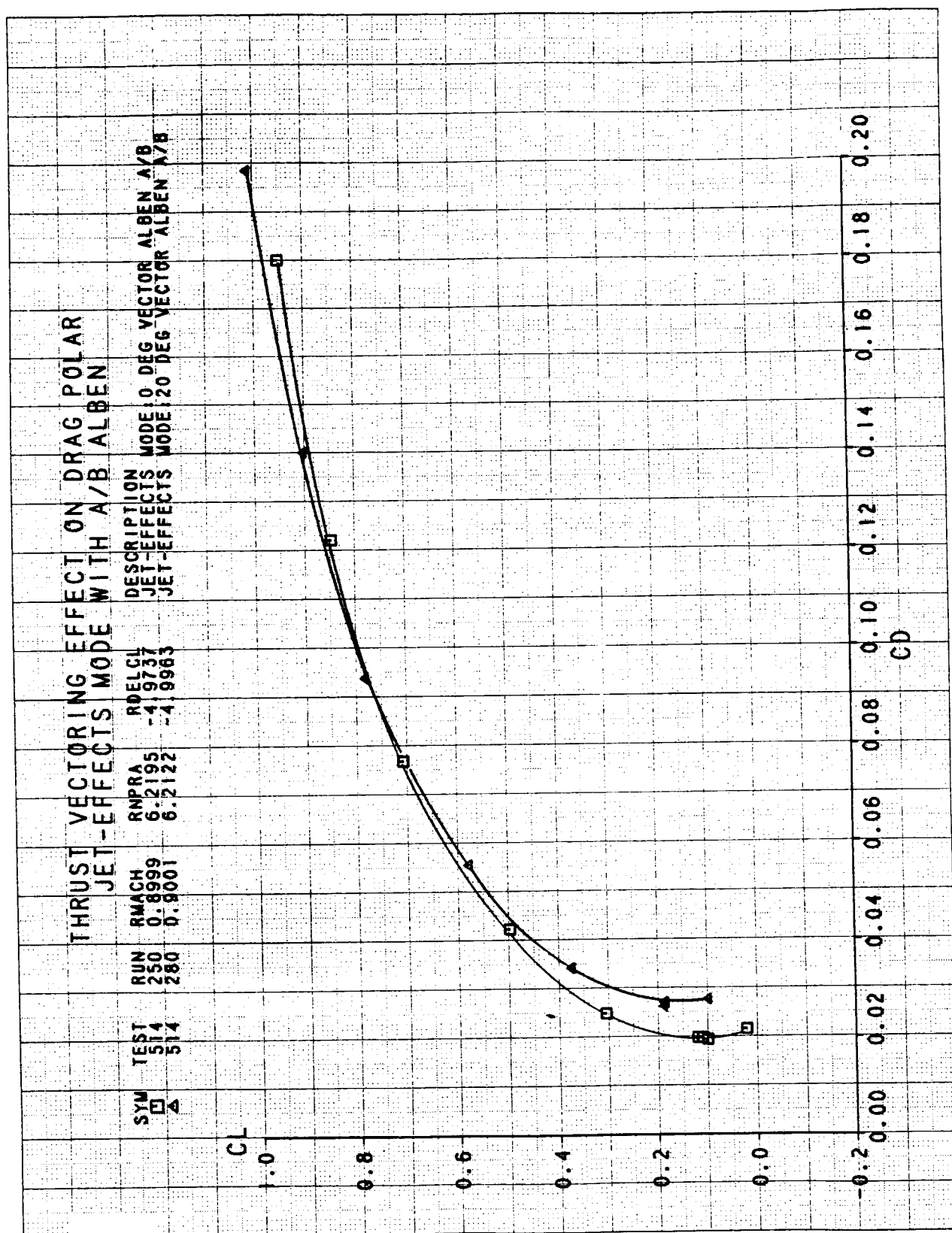




THRUST VECTORIZING EFFECT ON CL VS AOA AND CM

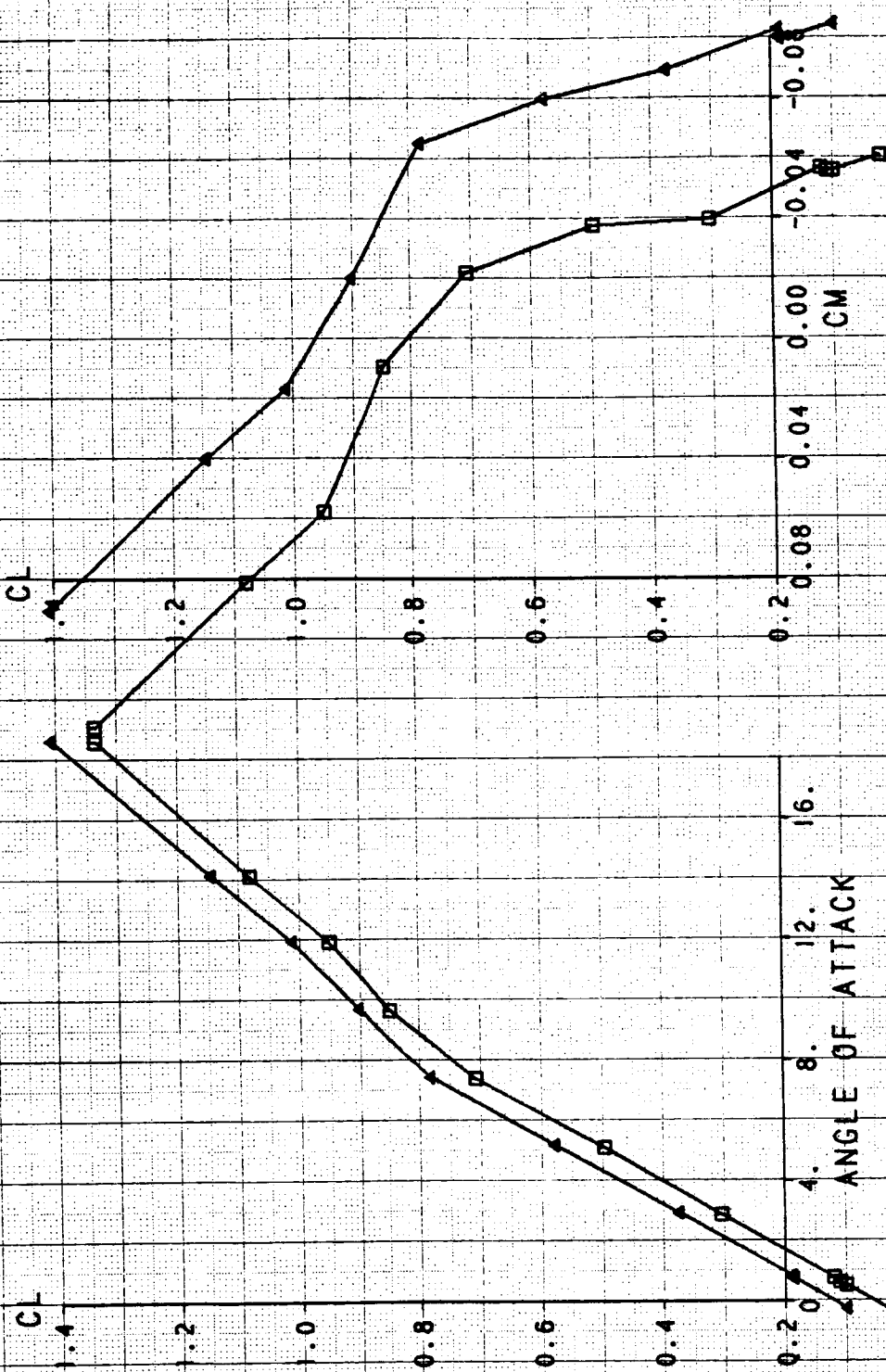
SYM TEST RUN RMACH RNPRA RDELCL DESCRIPTION
 □ 514 259 0.6009 4.1998 -4.9763 JET-EFFECTS MODE: 0 DEG VECTOR ALBEN A/B
 △ 514 270 0.5991 4.2228 -4.9460 JET-EFFECTS MODE: 20 DEG VECTOR ALBEN A/B

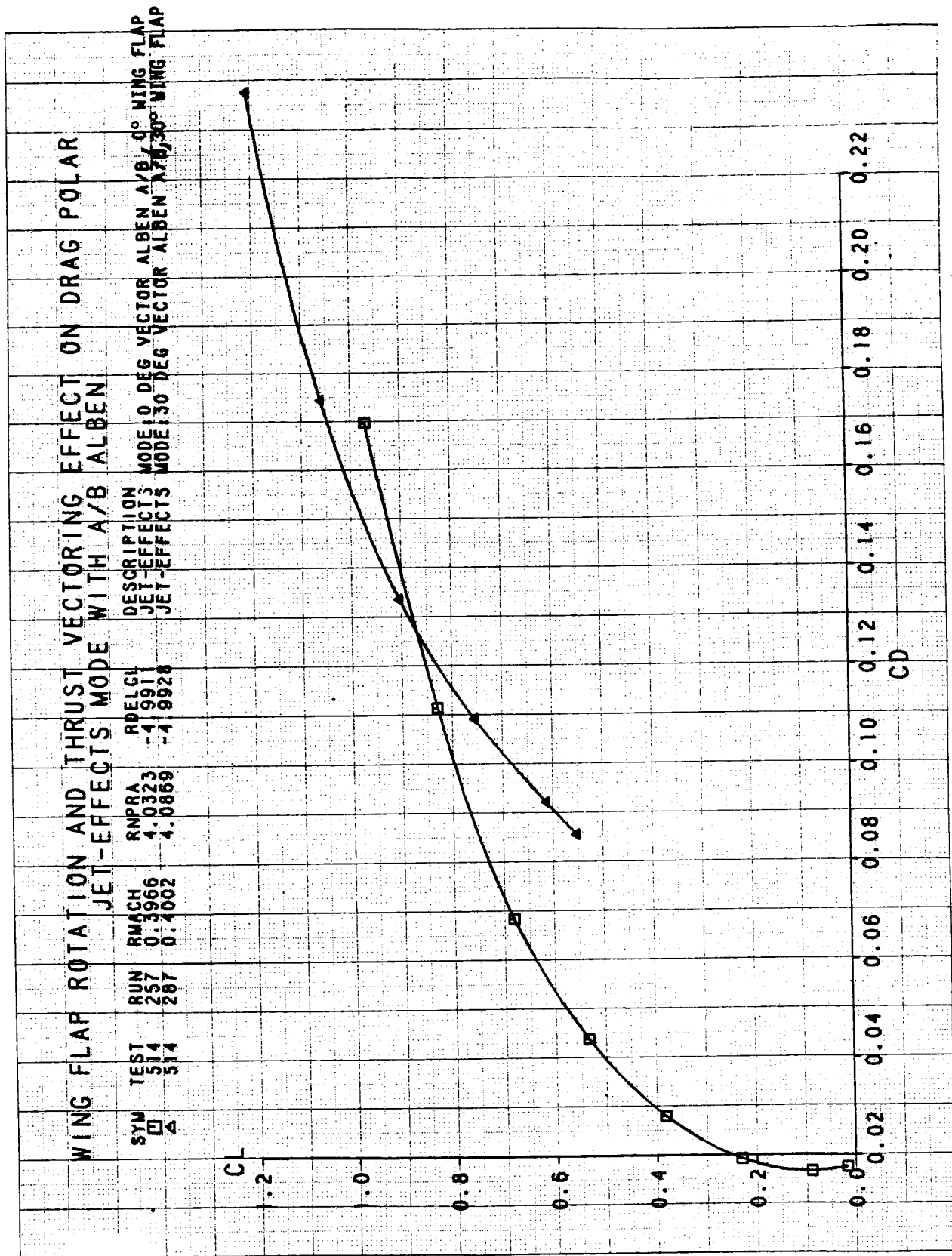




THRUST VECTORIZING EFFECT ON CL VS AOA AND CM

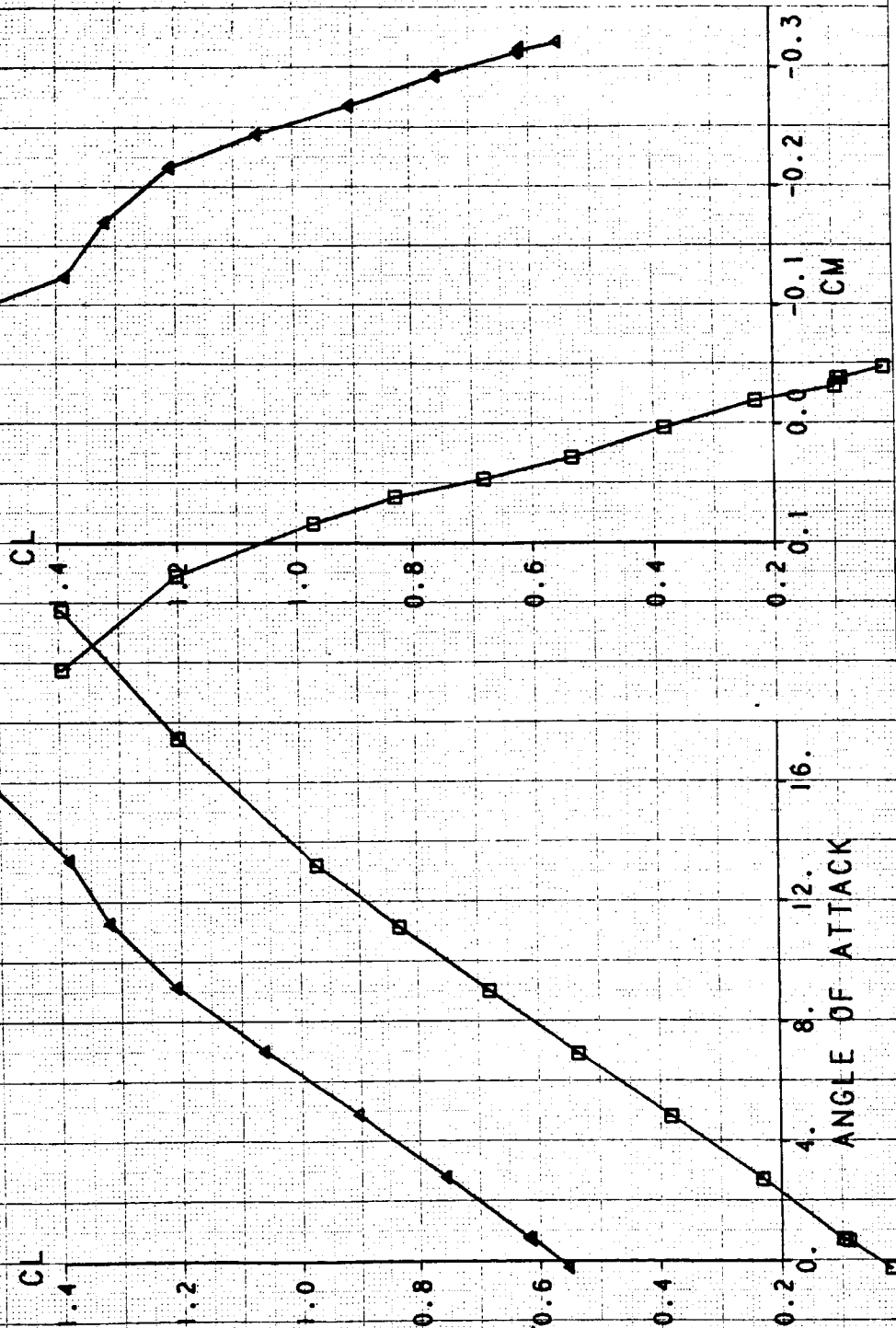
SYM TEST RUN RMACH RNPRA RDELCL DESCRIPTION MODE: 0 DEG VECTOR ALBEN A/B
 □ 514 250 0.8999 6.2195 -4.9737 JET-EFFECTS
 △ 514 280 0.9001 6.2122 -4.9963 JET-EFFECTS MODE: 20 DEG VECTOR ALBEN A/B

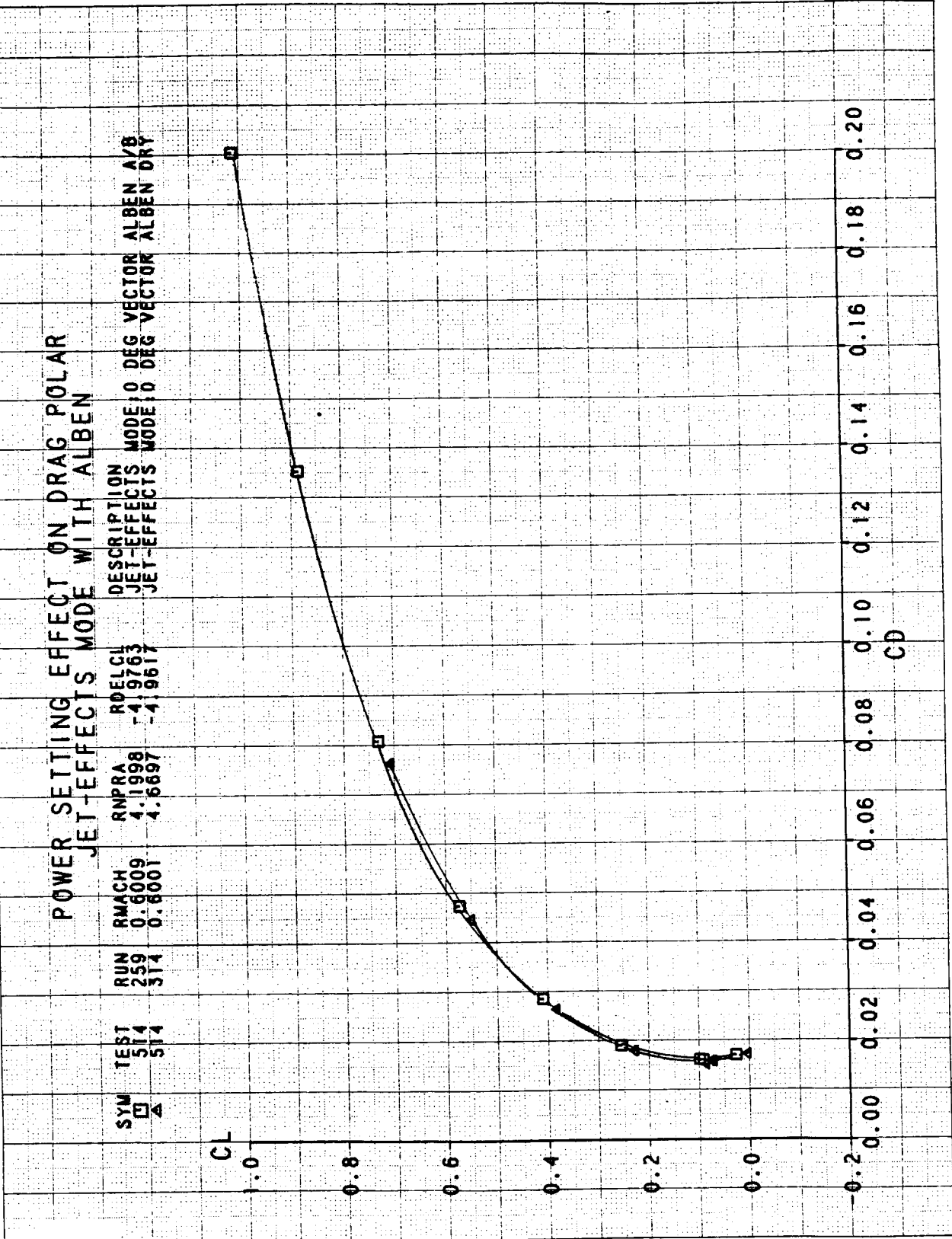




WING FLAP ROTATION AND THRUST VECTORING EFFECT ON CL VS AOA & CM

SYM TEST RUN RMACH RNPRA RDELCL DESCRIPTION
 514 257 0.3966 4.0323 -4.9911 JET-EFFECTS
 514 287 0.4002 4.0869 -4.9928 JET-EFFECTS
 MODE: 0 DEG VECTOR ALBEN A/B, 0° WING FLAP
 MODE: 30 DEG VECTOR ALBEN A/B, 30° WING FLAP

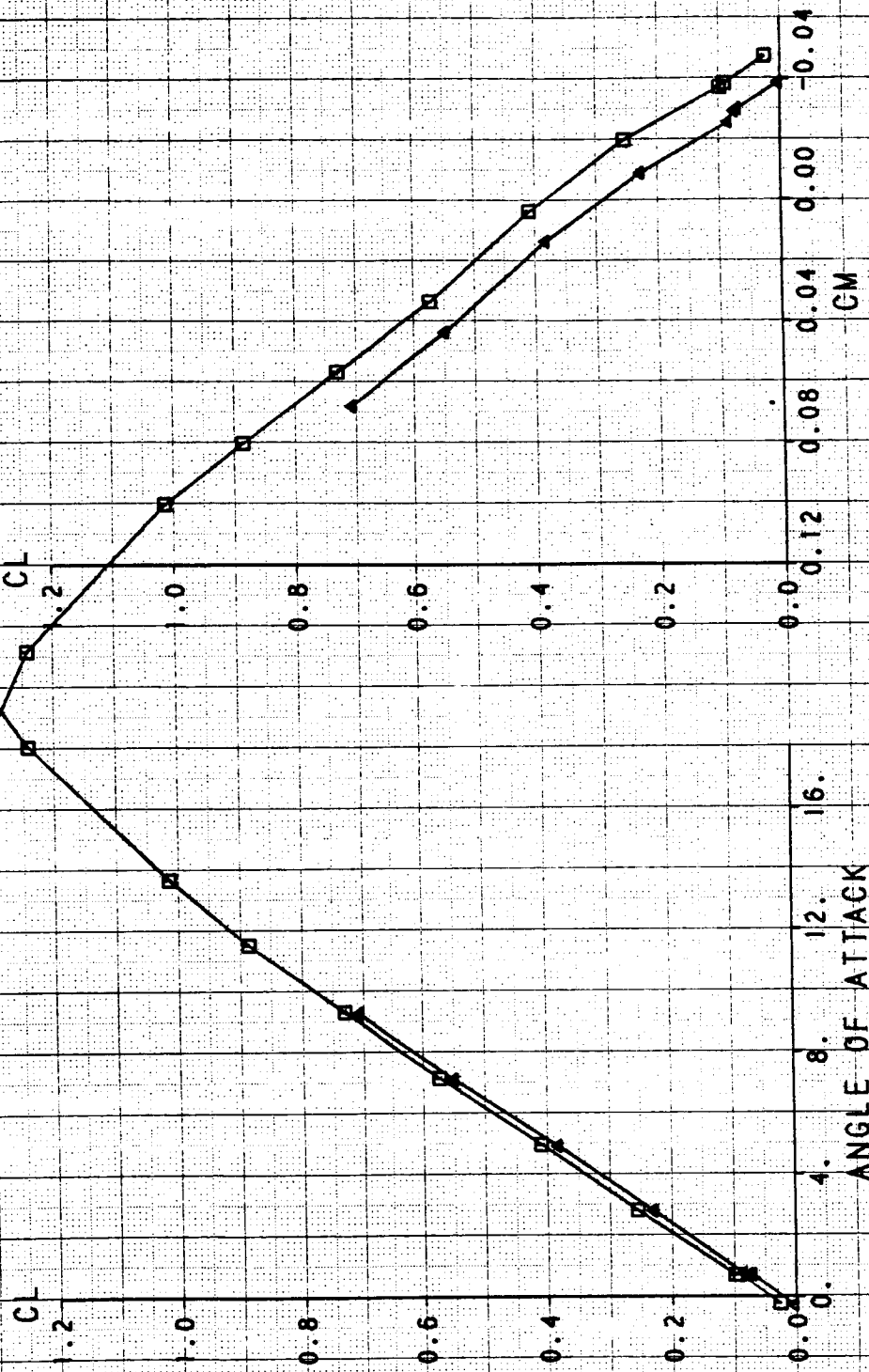


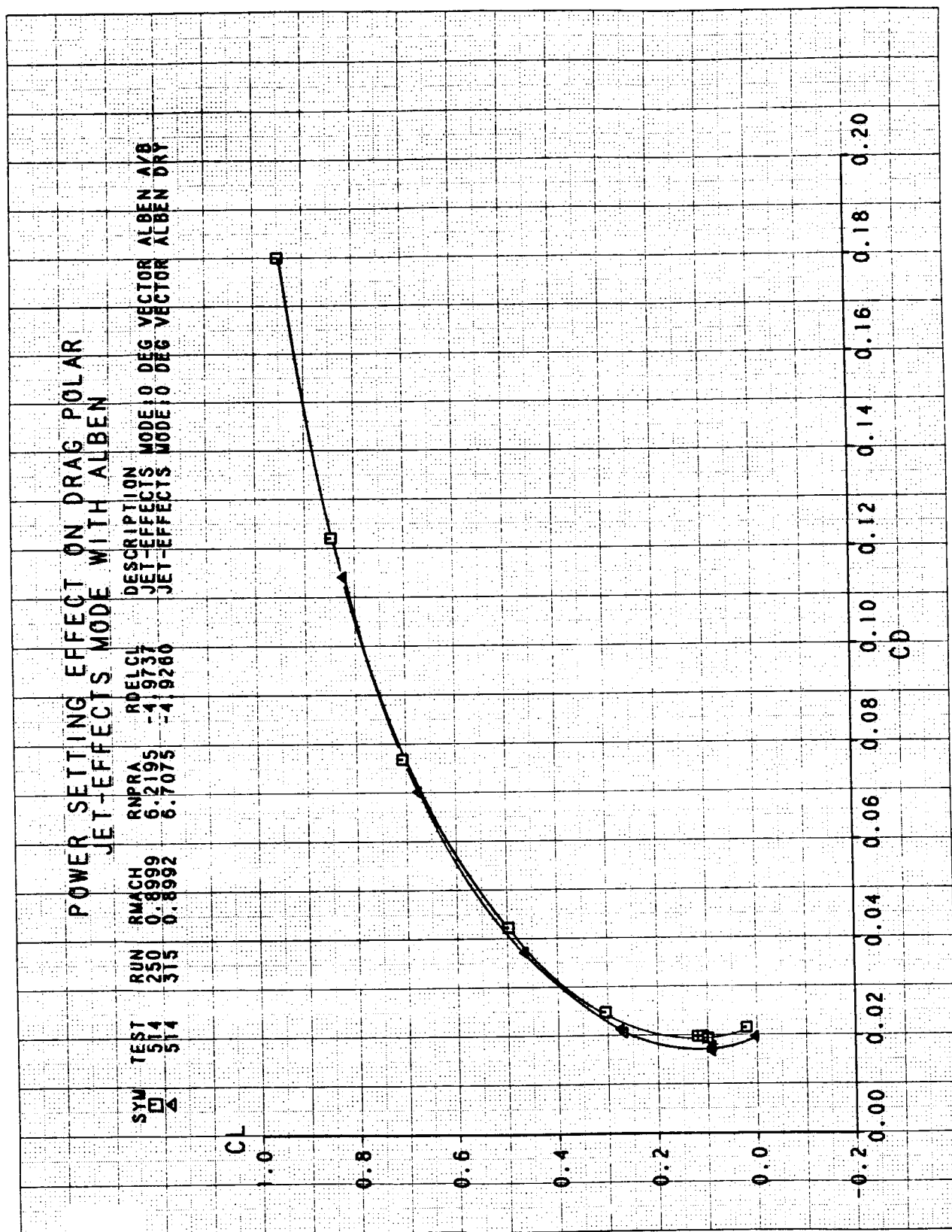


POWER SETTING EFFECT ON CL VS AOA AND CM

JET-EFFECTS MODE WITH ALBEN

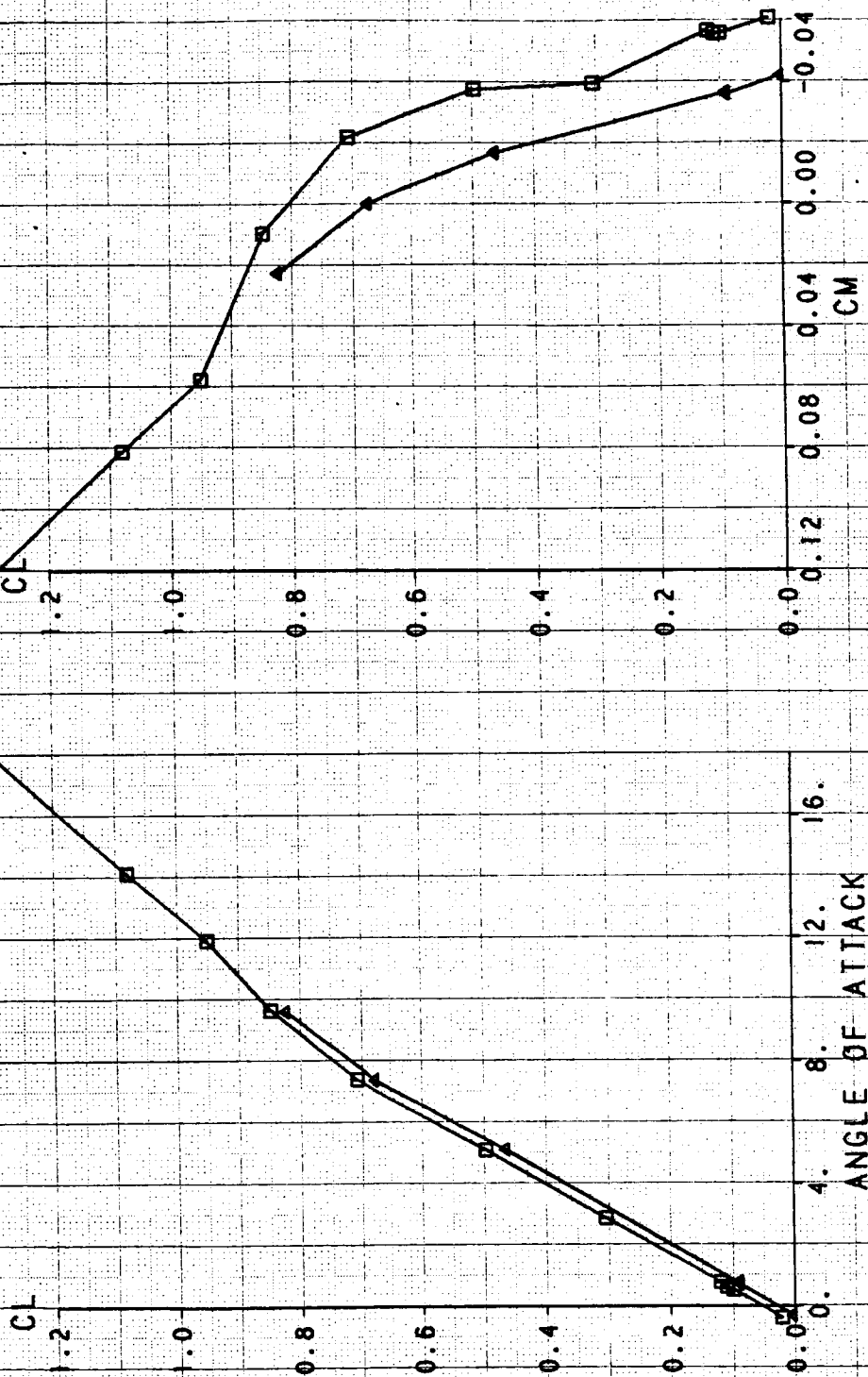
| SYM | TEST | RUN | RMACH | RNPRA | RDELCL | DESCRIPTION | MODE | 0 DEG VECTOR | ALBEN A/B |
|-----|------|-----|--------|--------|---------|-------------|--------|--------------|-----------|
| □ | 514 | 259 | 0.6009 | 4.1998 | -4.9763 | JET-EFFECTS | MODE 0 | 0 DEG VECTOR | ALBEN A/B |
| △ | 514 | 314 | 0.6001 | 4.8667 | -4.9617 | JET-EFFECTS | MODE 0 | 0 DEG VECTOR | ALBEN DRY |





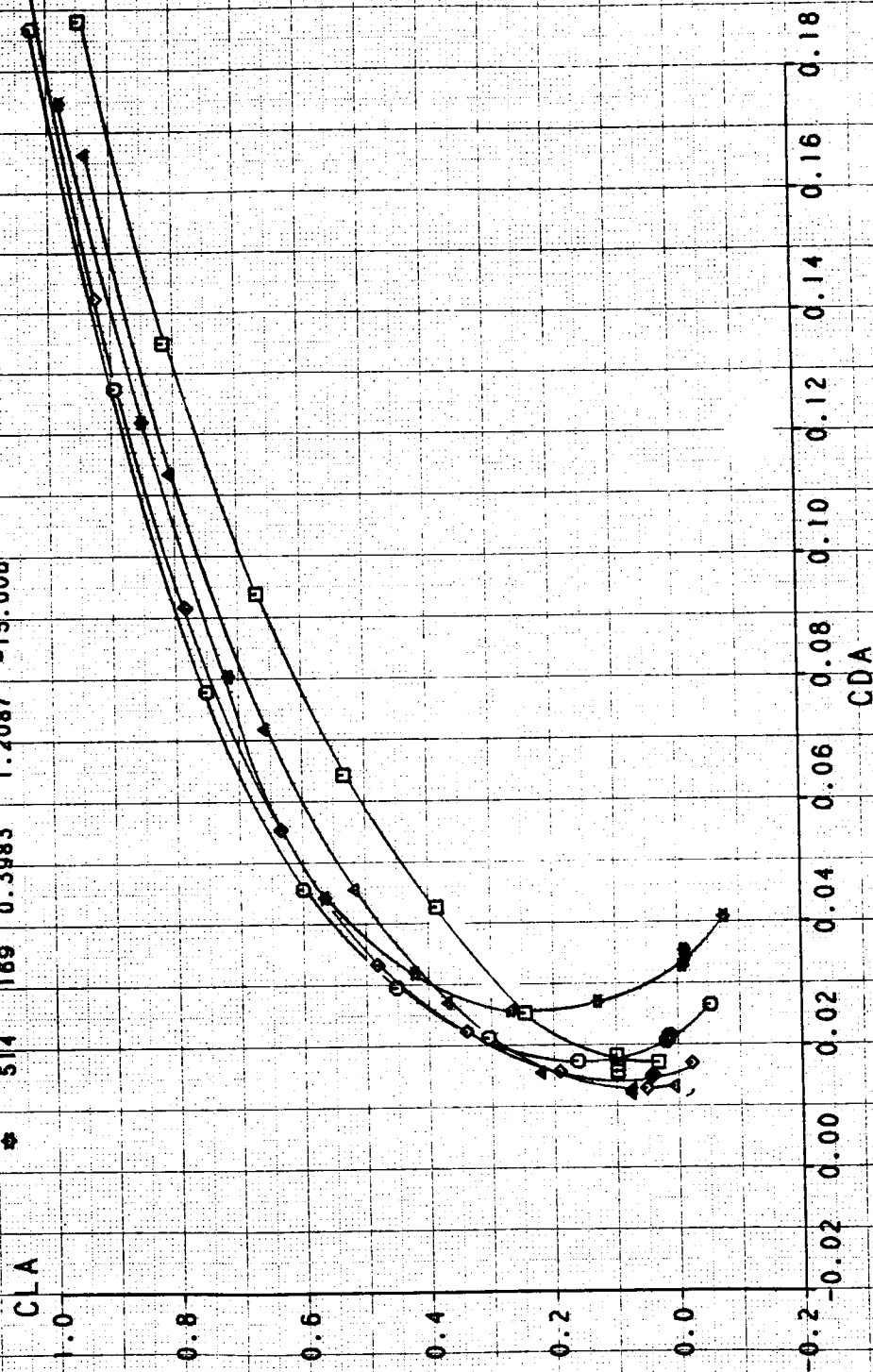
POWER SETTING EFFECT ON CL VS AOA AND CM

SYM TEST RUN RMACH RNPRA RDELCL DESCRIPTION MODE:0 DEG VECTOR ALBEN A/B
 514 250 0.8999 6.2195 -4.9737 JET-EFFECTS MODE:0 DEG VECTOR ALBEN DRY
 514 315 0.8992 6.7075 -4.9260 JET-EFFECTS



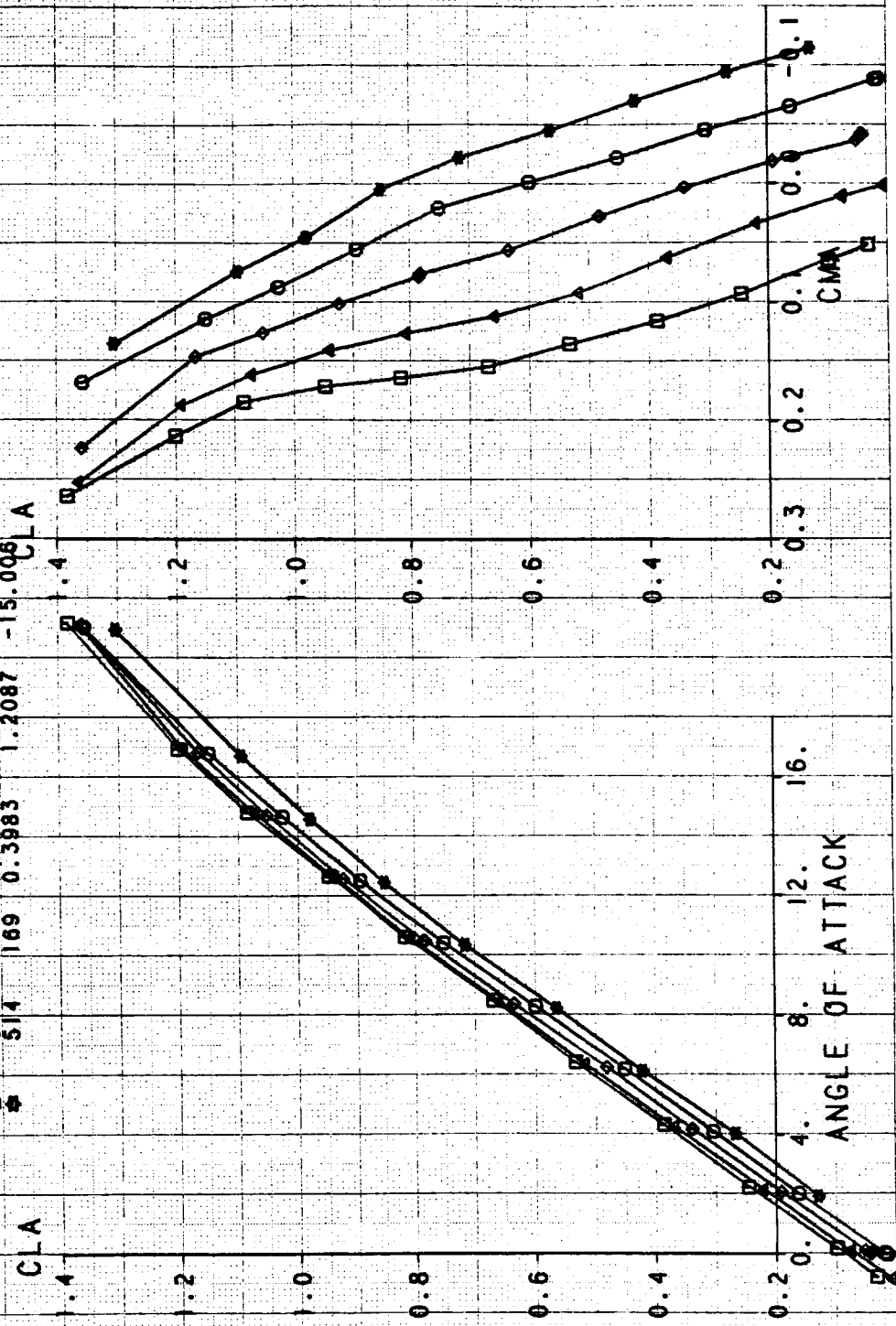
CANARD ROTATION EFFECTS ON CLA VS CDA FLOW-THROUGH MODE WITH NOZZLE EXTENSIONS

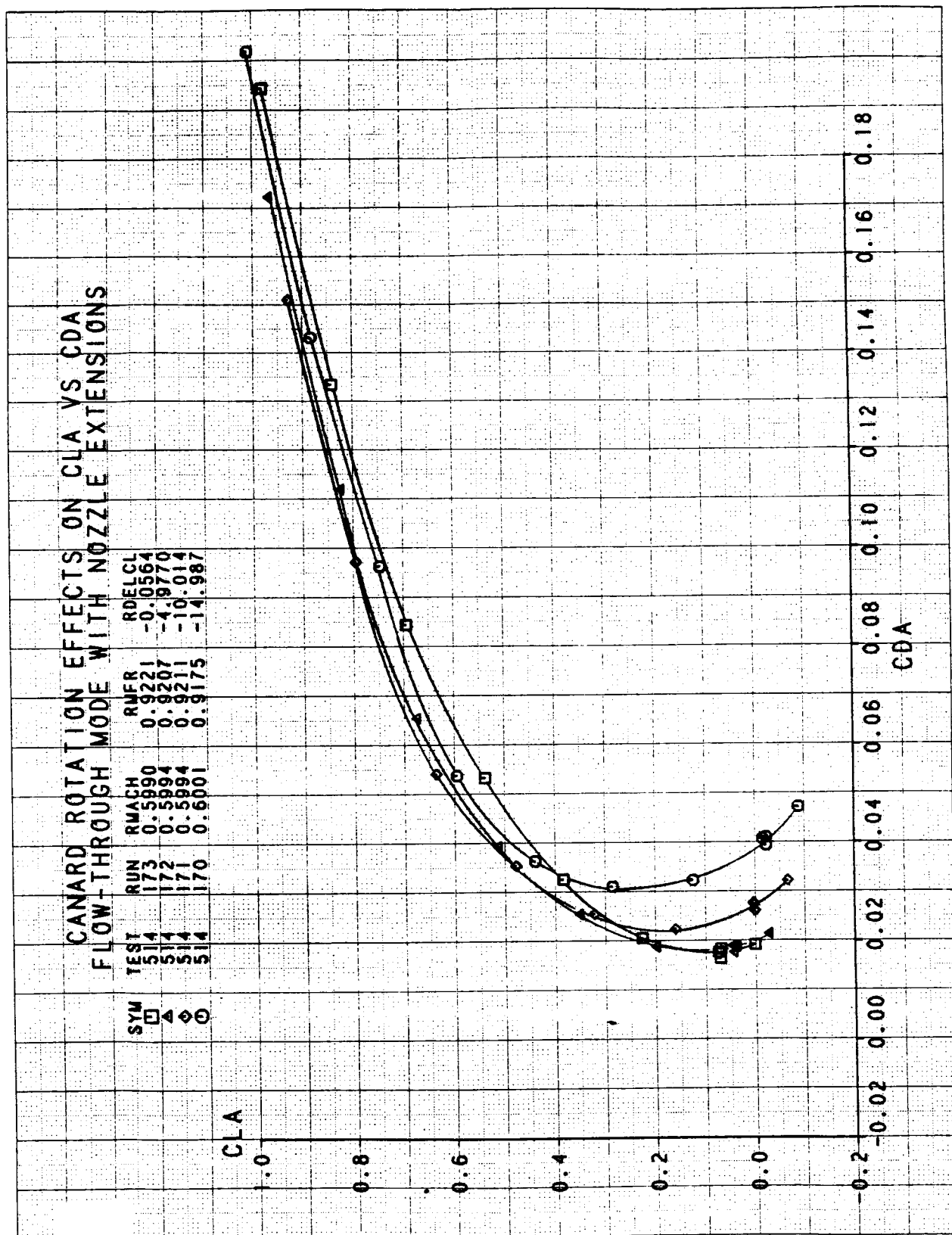
| SYM | TEST | RUN | RMACH | RMFR | RDELCL |
|-----|------|-----|--------|--------|---------|
| □ | 514 | 164 | 0.3996 | 1.1079 | 5.0449 |
| △ | 514 | 165 | 0.3989 | 1.2024 | -0.0455 |
| ◇ | 514 | 167 | 0.4016 | 1.1343 | -4.9956 |
| ○ | 514 | 168 | 0.3985 | 1.2163 | -10.002 |
| ⊗ | 514 | 169 | 0.3983 | 1.2087 | -15.006 |



CANARD ROTATION EFFECT ON CLA VS AOA AND CMA FLOW-THROUGH MODE WITH NOZZLE EXTENSIONS

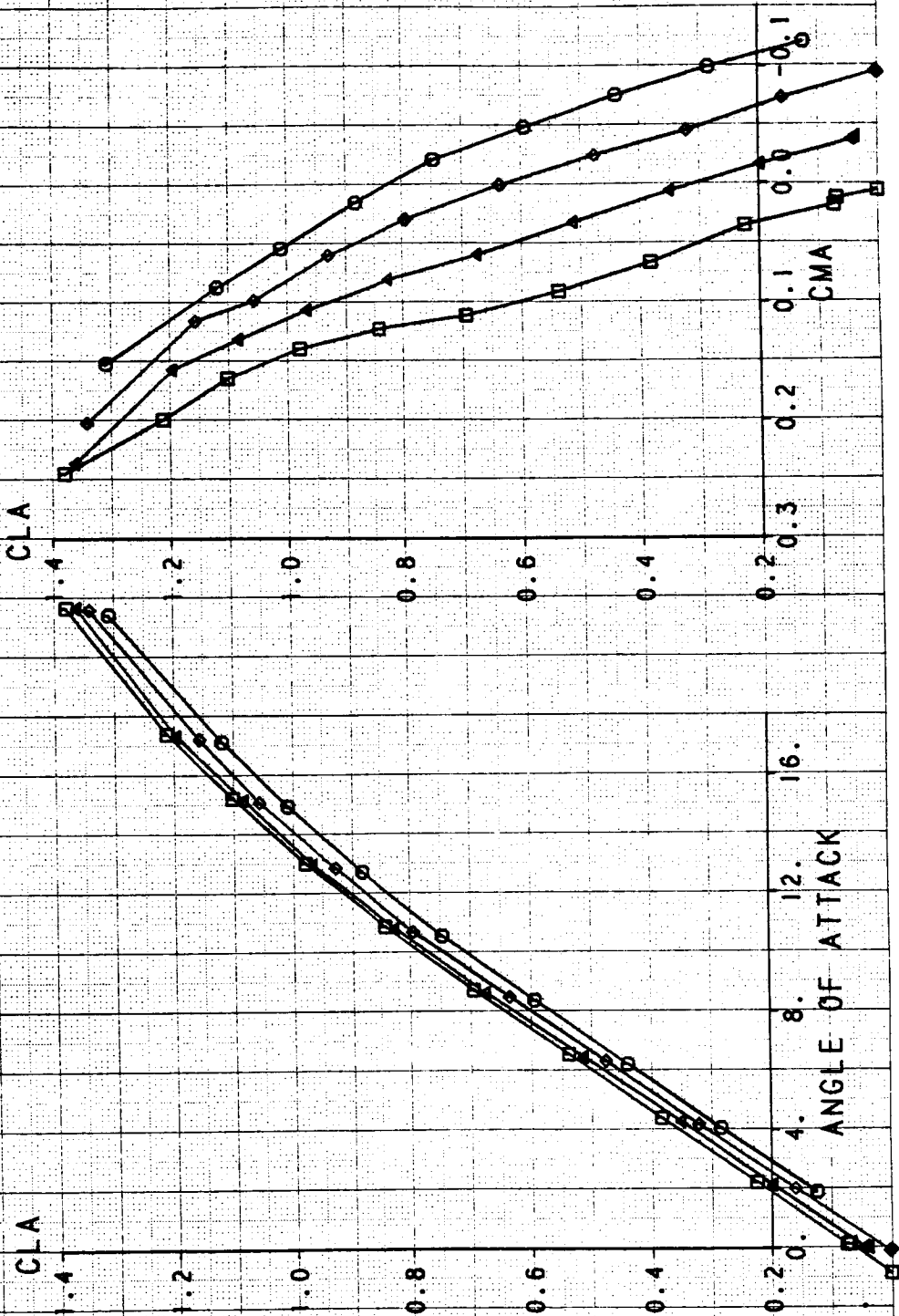
| SYM | TEST | RUN | RMACH | RMFR | RDELCL |
|-----|------|-----|--------|--------|---------|
| □ | 514 | 164 | 0.3996 | 1.1079 | 5.0449 |
| ◇ | 514 | 165 | 0.3989 | 1.2024 | -0.0455 |
| ◇ | 514 | 167 | 0.4016 | 1.1343 | -4.9956 |
| ◇ | 514 | 168 | 0.3985 | 1.2163 | -10.002 |
| ◆ | 514 | 169 | 0.3983 | 1.2087 | -15.005 |





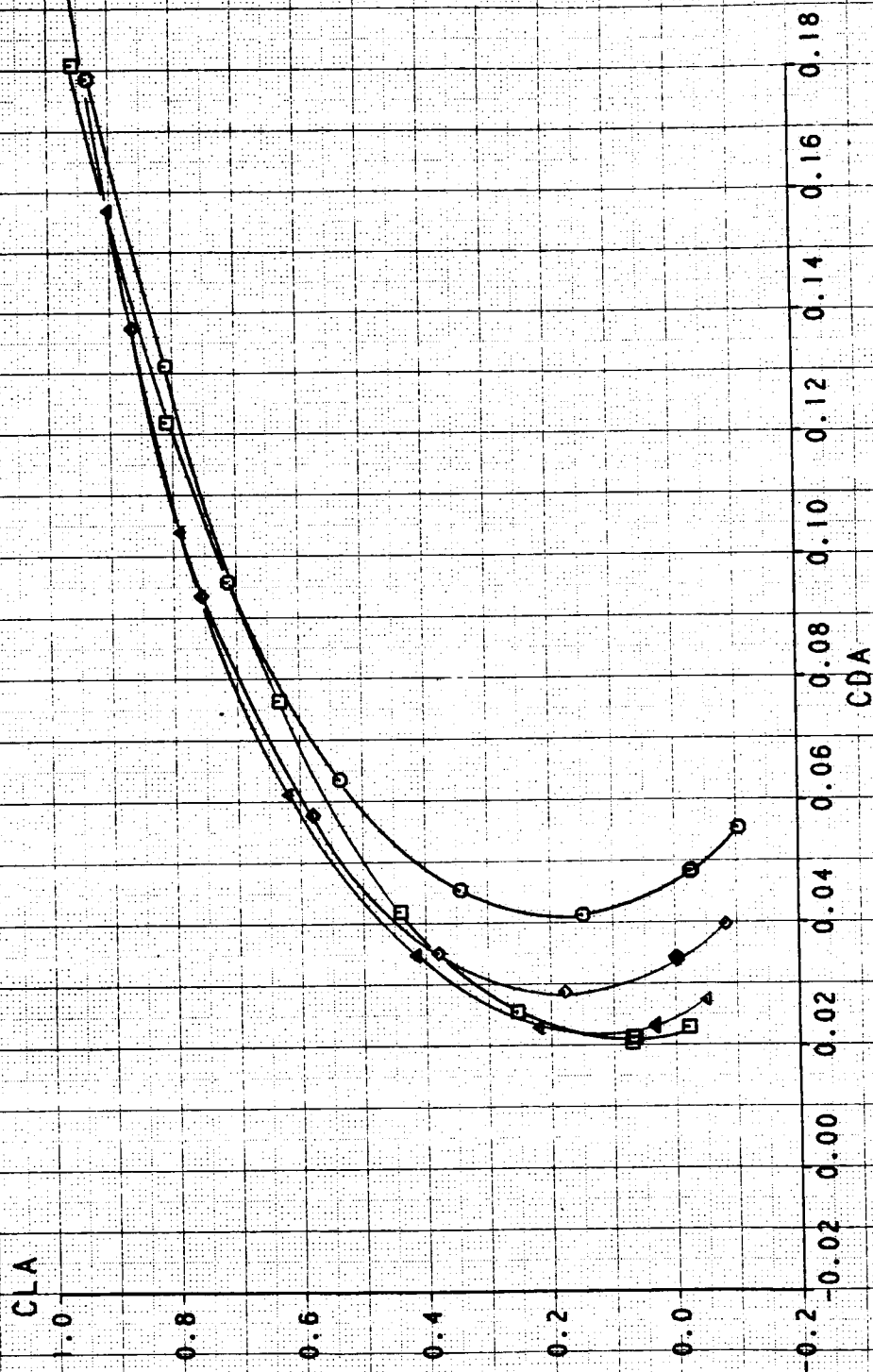
CANARD ROTATION EFFECT ON CLA VS AOA AND CMA FLOW-THROUGH MODE WITH NOZZLE EXTENSIONS

| SYM | TEST | RUN | RWACH | RWFR | RDELCL |
|-----|------|-----|--------|--------|---------|
| □ | 514 | 173 | 0.5890 | 0.9221 | -0.0564 |
| △ | 514 | 172 | 0.5894 | 0.9207 | -4.9770 |
| ◇ | 514 | 171 | 0.5894 | 0.9211 | -10.014 |
| ⊙ | 514 | 170 | 0.6001 | 0.9175 | -14.987 |



CANARD ROTATION EFFECTS ON CLA VS CDA FLOW-THROUGH MODE WITH NOZZLE EXTENSIONS

| SYM | TEST | RUN | RWACH | RWFR | RDELCL |
|-----|------|-----|--------|--------|---------|
| □ | 514 | 155 | 0.9018 | 0.8674 | -0.0601 |
| △ | 514 | 156 | 0.9022 | 0.8692 | -4.9921 |
| ◇ | 514 | 157 | 0.9020 | 0.8674 | -10.000 |
| ○ | 514 | 158 | 0.9020 | 0.8695 | -15.025 |

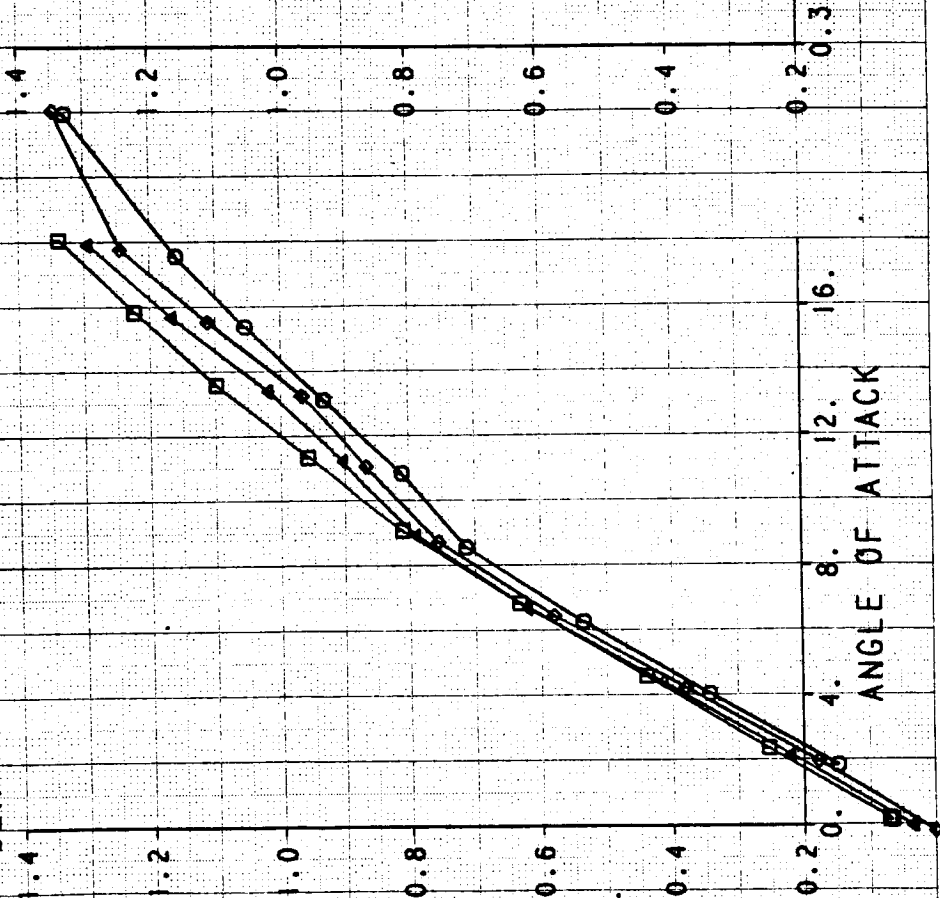


CANARD ROTATION EFFECT ON CLA VS AOA AND CMA FLOW-THROUGH MODE WITH NOZZLE EXTENSIONS

| SYM | TEST | RUN | RWACH | RWFR | RDELCL |
|-----|------|-----|--------|--------|---------|
| □ | 514 | 155 | 0.9018 | 0.8674 | -0.0601 |
| △ | 514 | 156 | 0.9022 | 0.8692 | -4.9921 |
| ◇ | 514 | 157 | 0.9020 | 0.8674 | -10.000 |
| ○ | 514 | 158 | 0.9020 | 0.8695 | -15.025 |

CLA

CLA



CMA

16.

12.

8.

4.

0.2

0.4

0.6

0.8

1.0

1.2

1.4

1.6

1.8

2.0

2.2

2.4

2.6

2.8

3.0

3.2

3.4

3.6

3.8

4.0

4.2

4.4

4.6

4.8

5.0

5.2

5.4

5.6

5.8

6.0

6.2

6.4

6.6

6.8

7.0

7.2

7.4

7.6

7.8

8.0

8.2

8.4

8.6

8.8

9.0

9.2

9.4

9.6

9.8

10.0

10.2

10.4

10.6

10.8

11.0

11.2

11.4

11.6

11.8

12.0

12.2

12.4

12.6

12.8

13.0

13.2

13.4

13.6

13.8

14.0

14.2

14.4

14.6

14.8

15.0

15.2

15.4

15.6

15.8

16.0

16.2

16.4

16.6

16.8

17.0

17.2

17.4

17.6

17.8

18.0

18.2

18.4

18.6

18.8

19.0

19.2

19.4

19.6

19.8

20.0

20.2

20.4

20.6

20.8

21.0

21.2

21.4

21.6

21.8

22.0

22.2

22.4

22.6

22.8

23.0

23.2

23.4

23.6

23.8

24.0

24.2

24.4

24.6

24.8

25.0

25.2

25.4

25.6

25.8

26.0

26.2

26.4

26.6

26.8

27.0

27.2

27.4

27.6

27.8

28.0

28.2

28.4

28.6

28.8

29.0

29.2

29.4

29.6

29.8

30.0

30.2

30.4

30.6

30.8

31.0

31.2

31.4

31.6

31.8

32.0

32.2

32.4

32.6

32.8

33.0

33.2

33.4

33.6

33.8

34.0

34.2

34.4

34.6

34.8

35.0

35.2

35.4

35.6

35.8

36.0

36.2

36.4

36.6

36.8

37.0

37.2

37.4

37.6

37.8

38.0

38.2

38.4

38.6

38.8

39.0

39.2

39.4

39.6

39.8

40.0

40.2

40.4

40.6

40.8

41.0

41.2

41.4

41.6

41.8

42.0

42.2

42.4

42.6

42.8

43.0

43.2

43.4

43.6

43.8

44.0

44.2

44.4

44.6

44.8

45.0

45.2

45.4

45.6

45.8

46.0

46.2

46.4

46.6

46.8

47.0

47.2

47.4

47.6

47.8

48.0

48.2

48.4

48.6

48.8

49.0

49.2

49.4

49.6

49.8

50.0

50.2

50.4

50.6

50.8

51.0

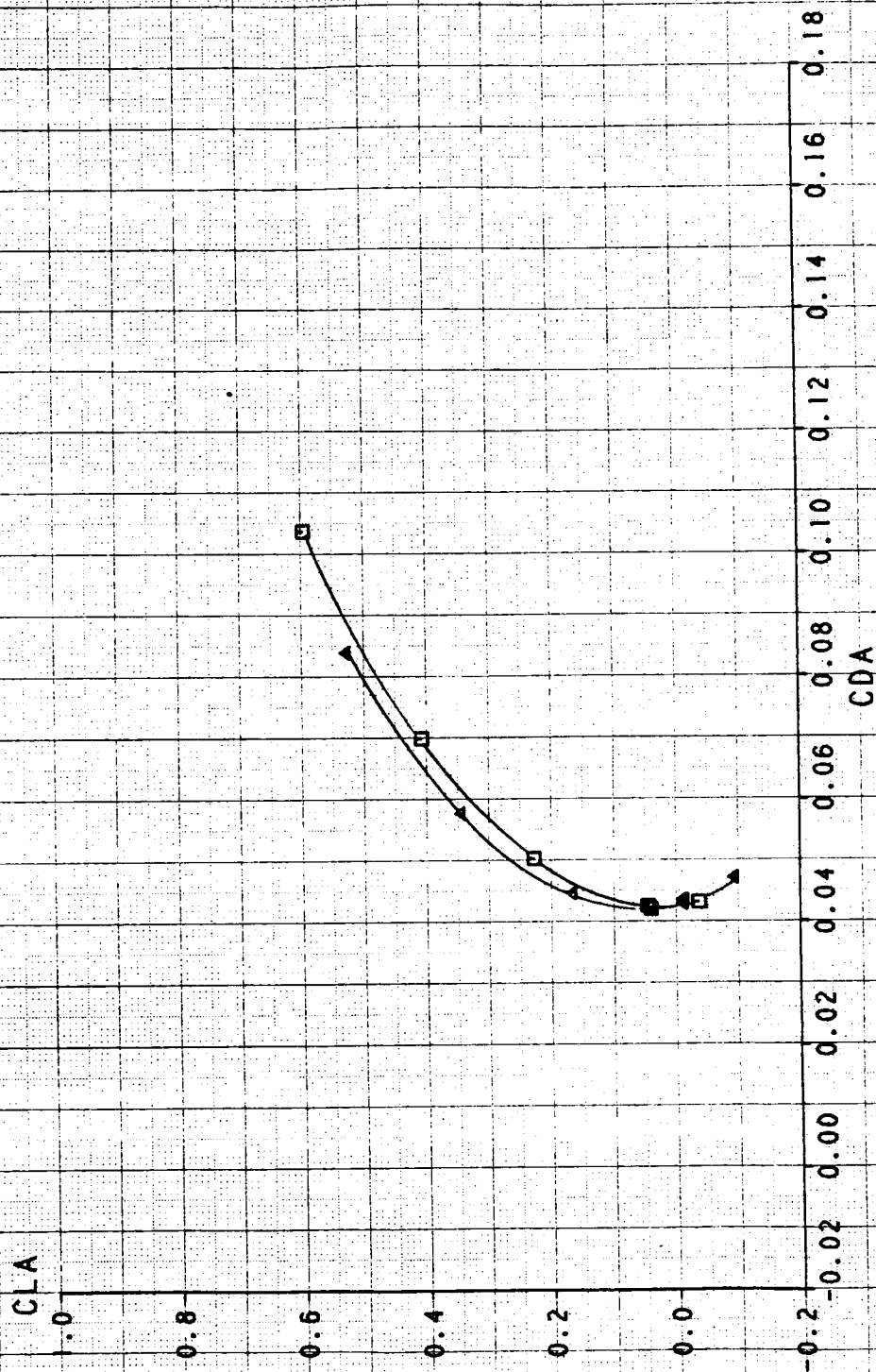
51.2

51.4

51.6

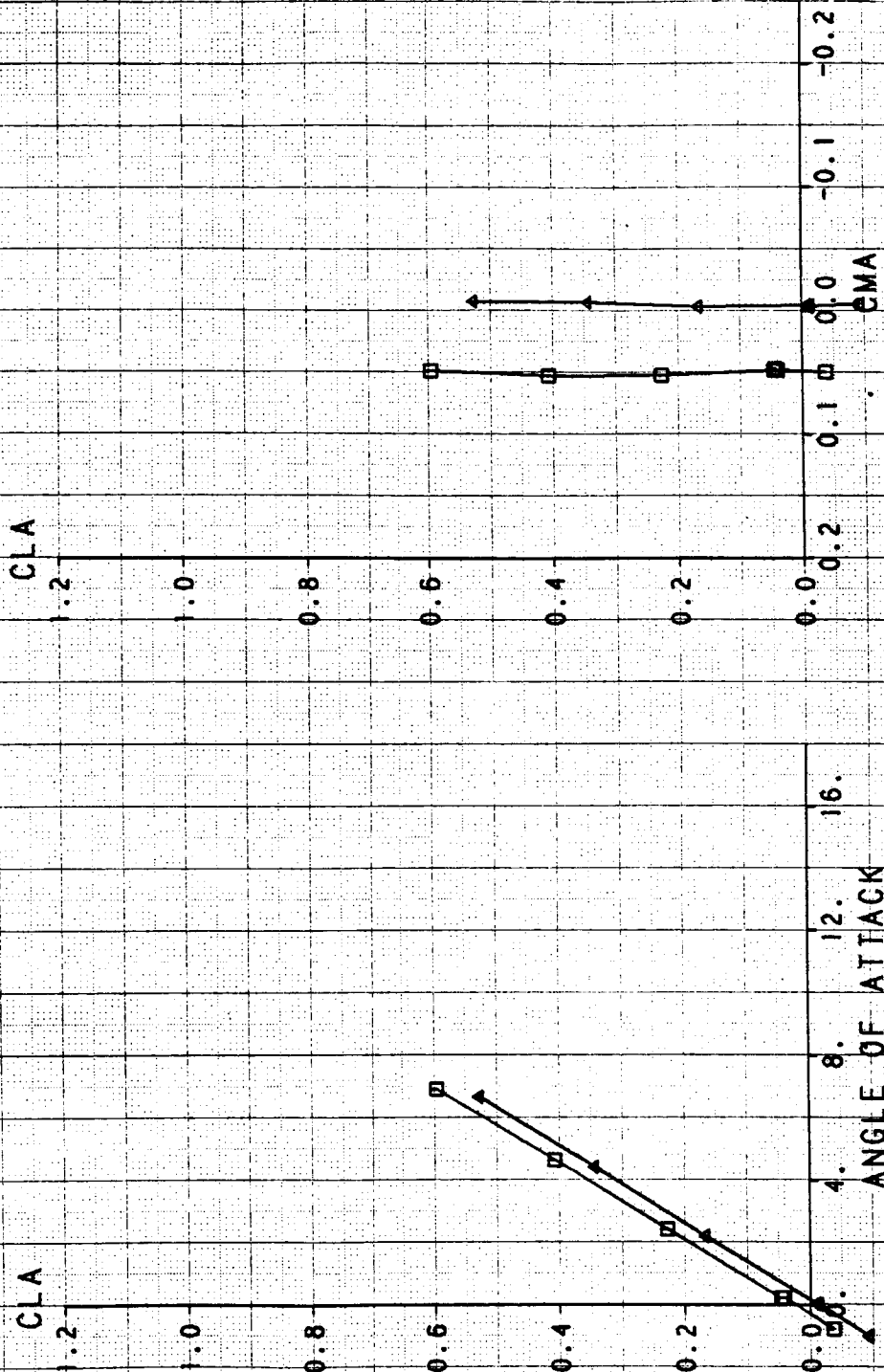
CANARD ROTATION EFFECTS ON CLA VS CDA FLOW-THROUGH MODE WITH NOZZLE EXTENSIONS

| SYM | TEST | RUN | RMACH | RMFR | RDELCL |
|-----|------|-----|--------|--------|---------|
| □ | 514 | 160 | 1.1972 | 0.8895 | -0.0539 |
| Δ | 514 | 159 | 1.1977 | 0.8895 | -4.9745 |



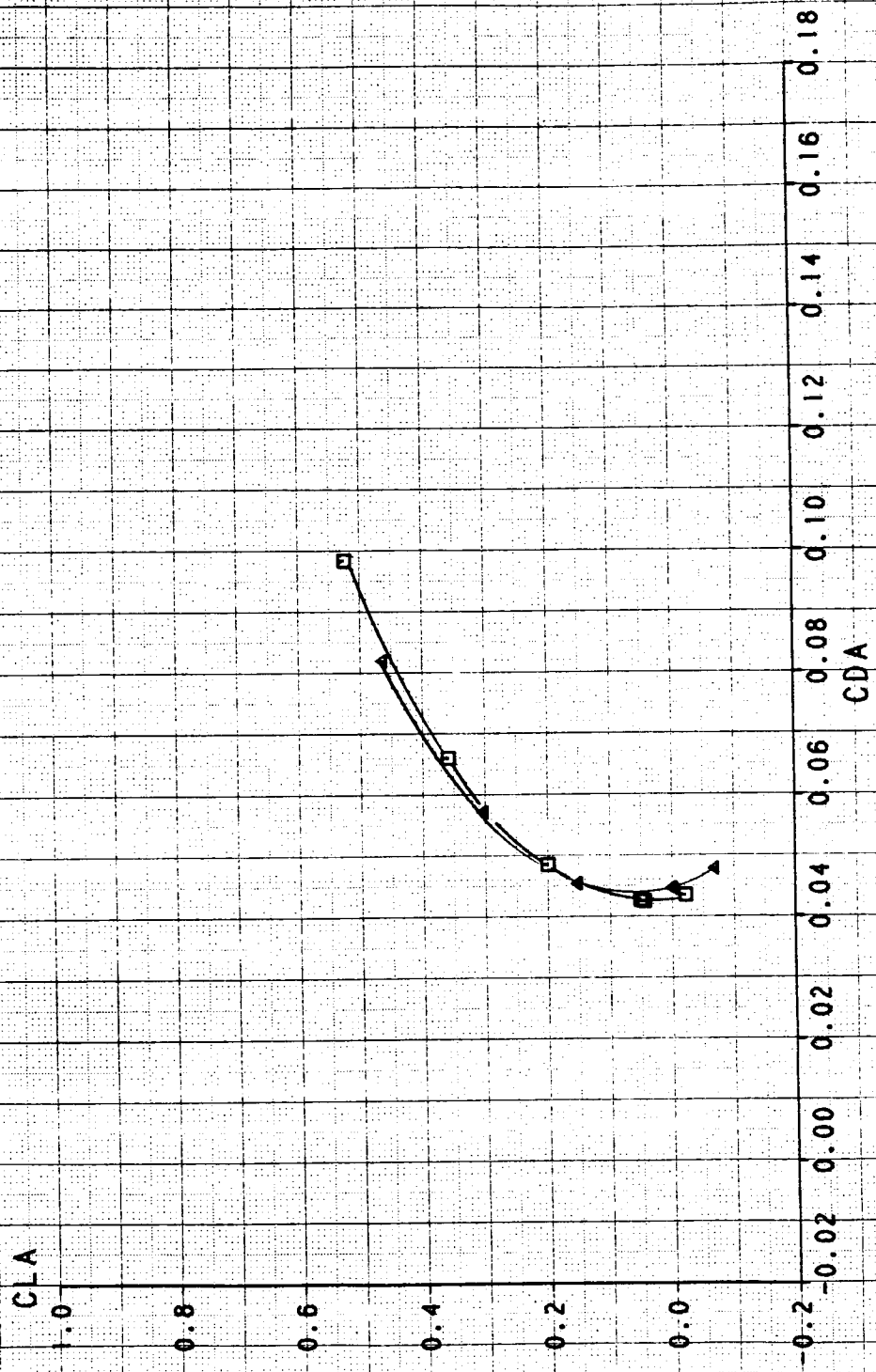
CANARD ROTATION EFFECT ON CLA VS AOA AND CMA

SYM TEST RUN RMACH RMFR RDELCL
 □ 514 160 1.1972 0.8895 -0.0539
 △ 514 159 1.1977 0.8895 -4.9745



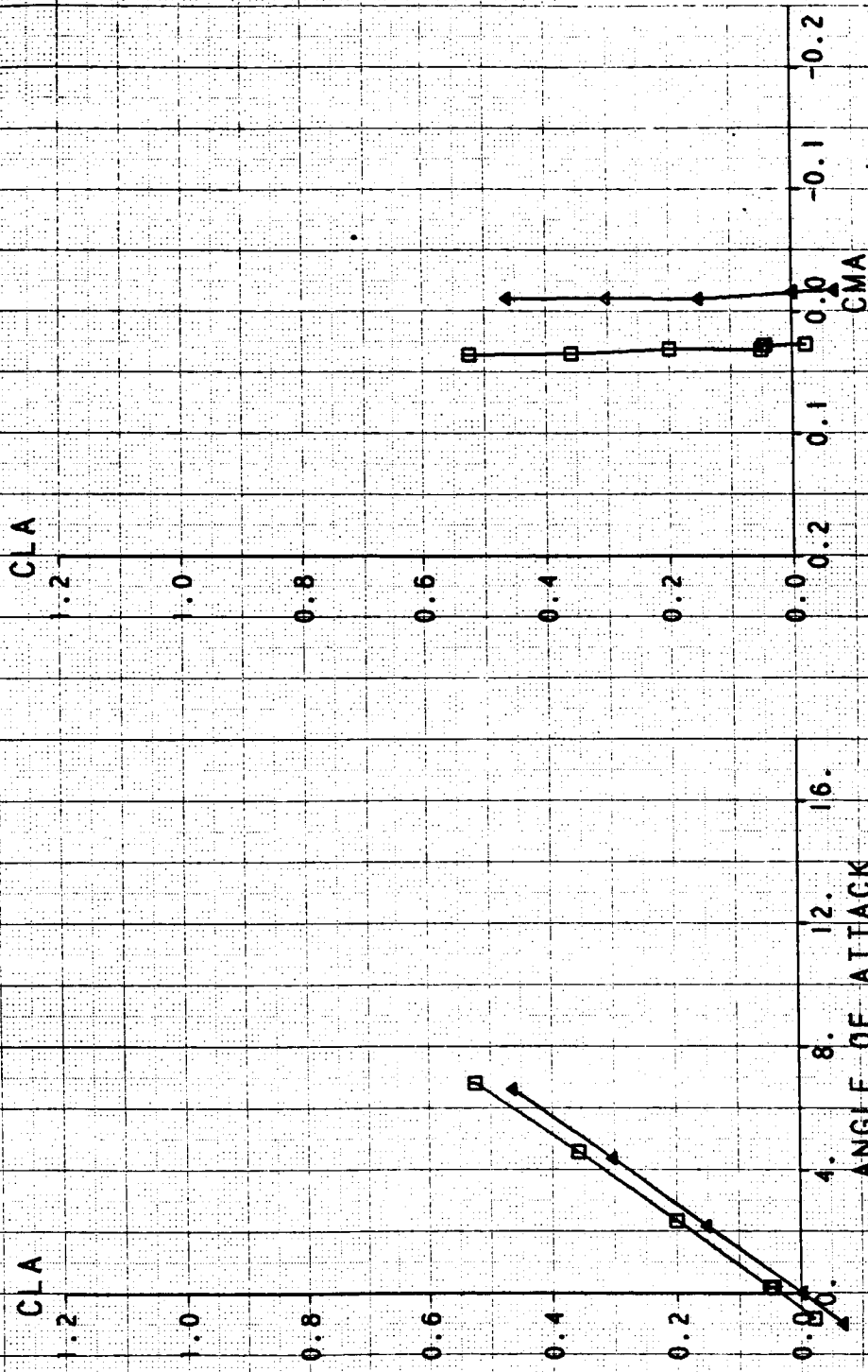
CANARD ROTATION EFFECTS ON CLA VS CDA FLOW-THROUGH MODE WITH NOZZLE EXTENSIONS

| SYM | TEST | RUN | RMACH | RWER | RDELCL |
|-----|------|-----|--------|--------|---------|
| □ | 514 | 161 | 1.3936 | 0.9250 | -0.0567 |
| Δ | 514 | 162 | 1.3939 | 0.9261 | -4.9931 |



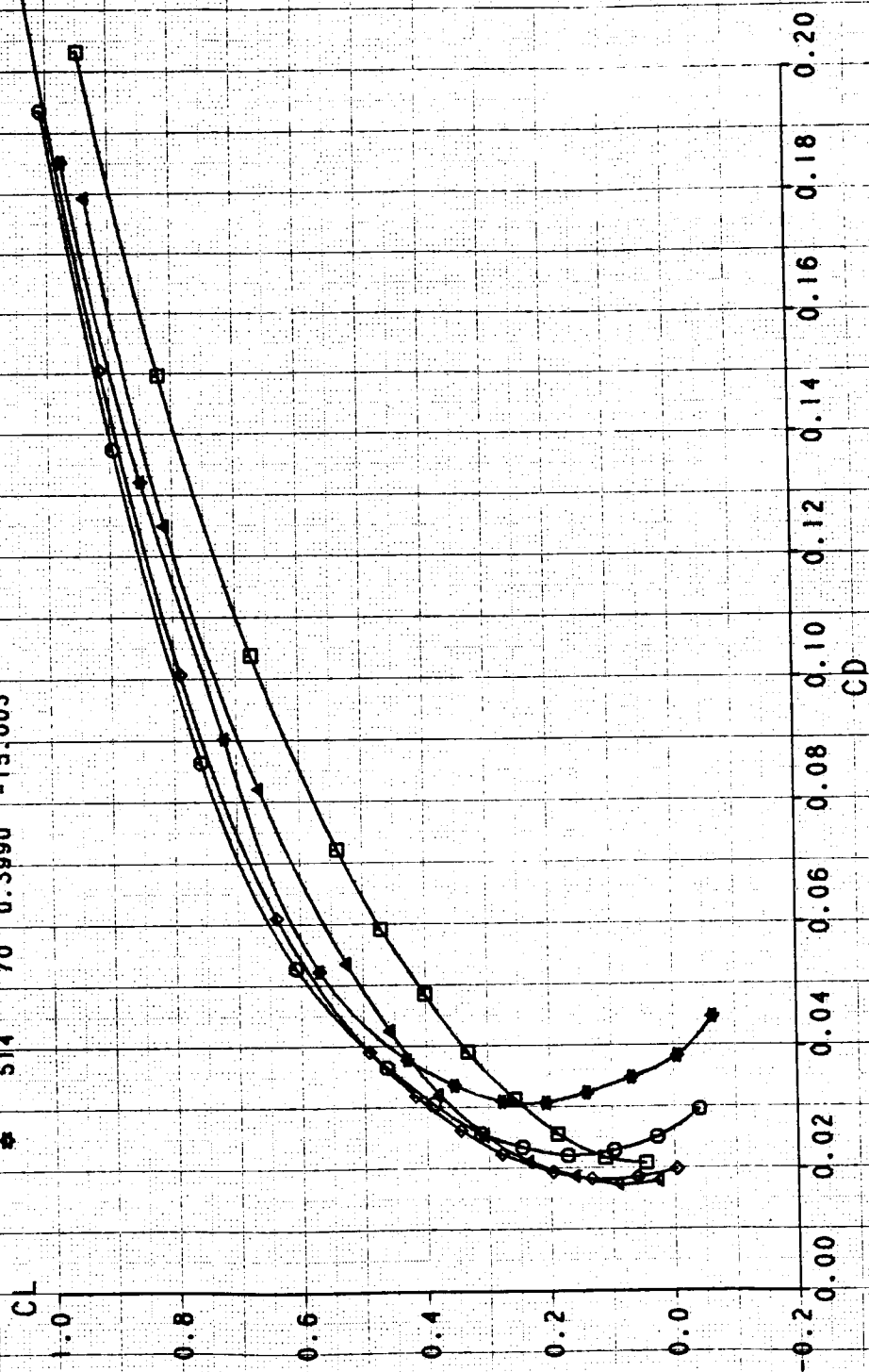
CANARD ROTATION EFFECT ON CLA VS AOA AND CMA FLOW-THROUGH MODE WITH NOZZLE EXTENSIONS

| SYM | TEST | RUN | RWACH | RWFR | RDELCL |
|-----|------|-----|--------|--------|---------|
| □ | 514 | 161 | 1.3936 | 0.9250 | -0.0567 |
| ▲ | 514 | 162 | 1.3939 | 0.9261 | -4.9931 |



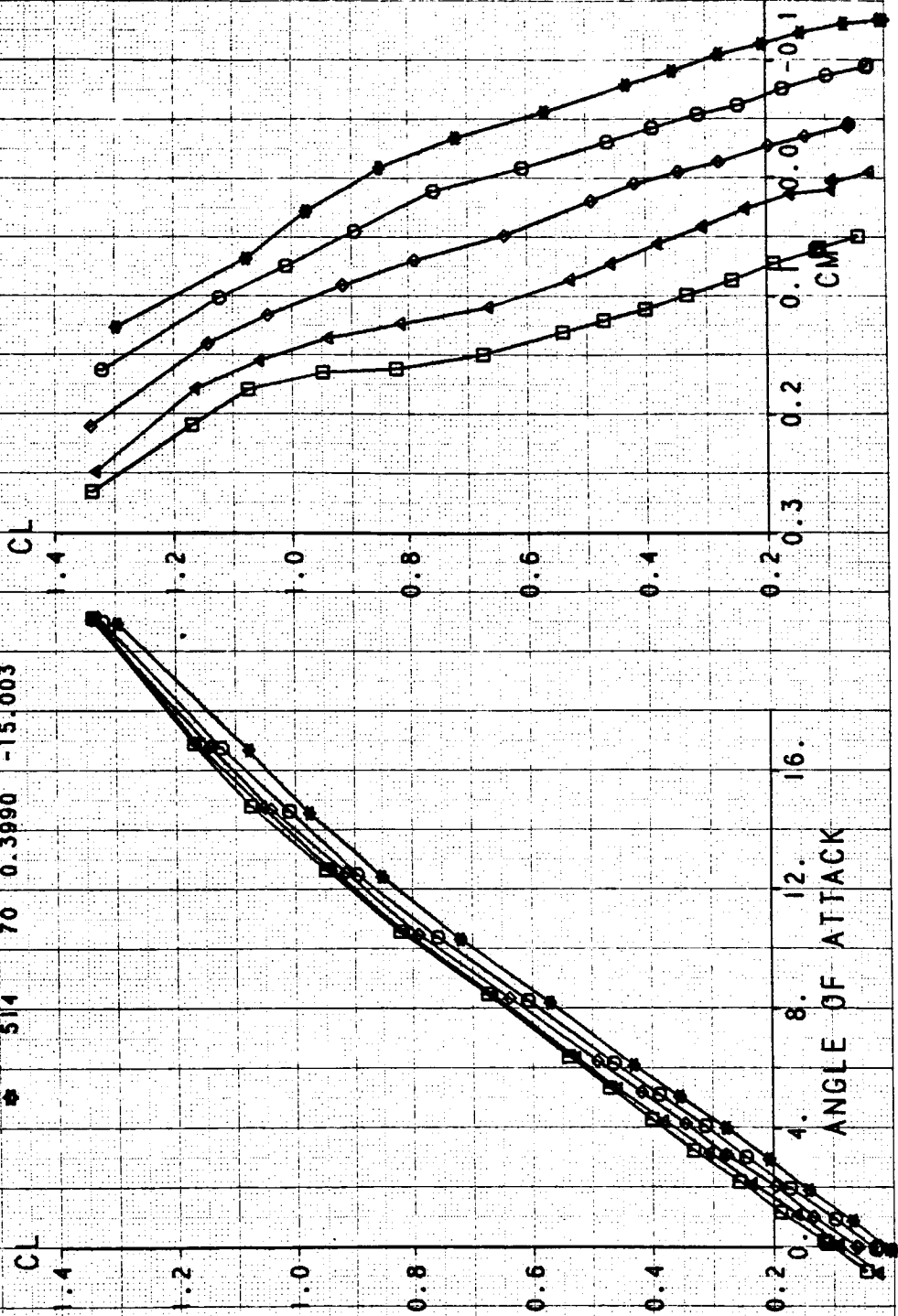
CANARD ROTATION EFFECT ON DRAG POLAR FT MODE IN COMMON BASELINE CONFIGURATION

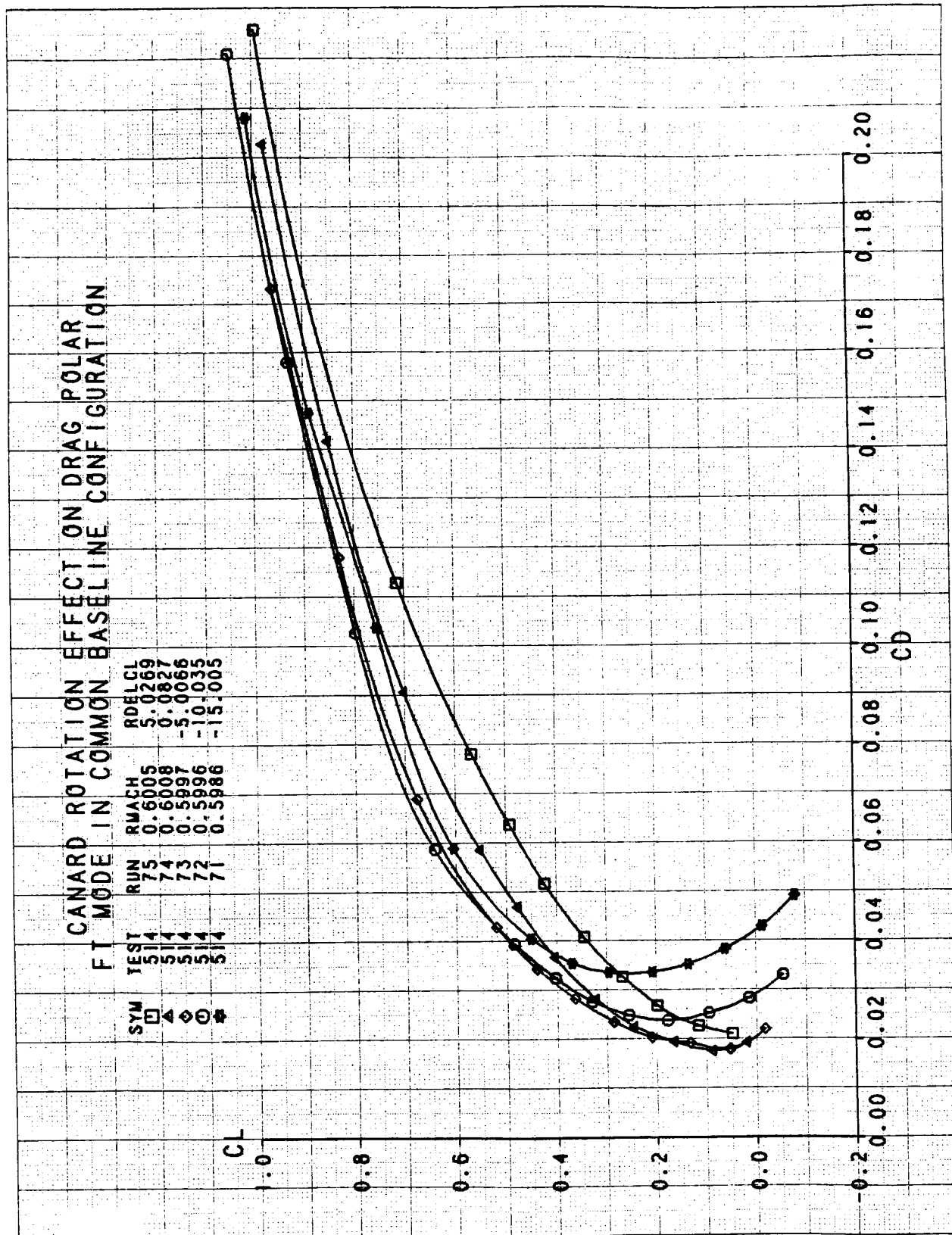
| SYM | TEST | RUN | RMACH | ROBLCL |
|-----|------|-----|--------|----------|
| □ | 514 | 66 | 0.3993 | 5.0293 |
| △ | 514 | 67 | 0.3989 | -0.0547 |
| ◇ | 514 | 68 | 0.3990 | -5.0061 |
| ○ | 514 | 69 | 0.3989 | -10.1026 |
| ✱ | 514 | 70 | 0.3990 | -15.1003 |



CANARD ROTATION EFFECT ON CL VS AOA AND CM

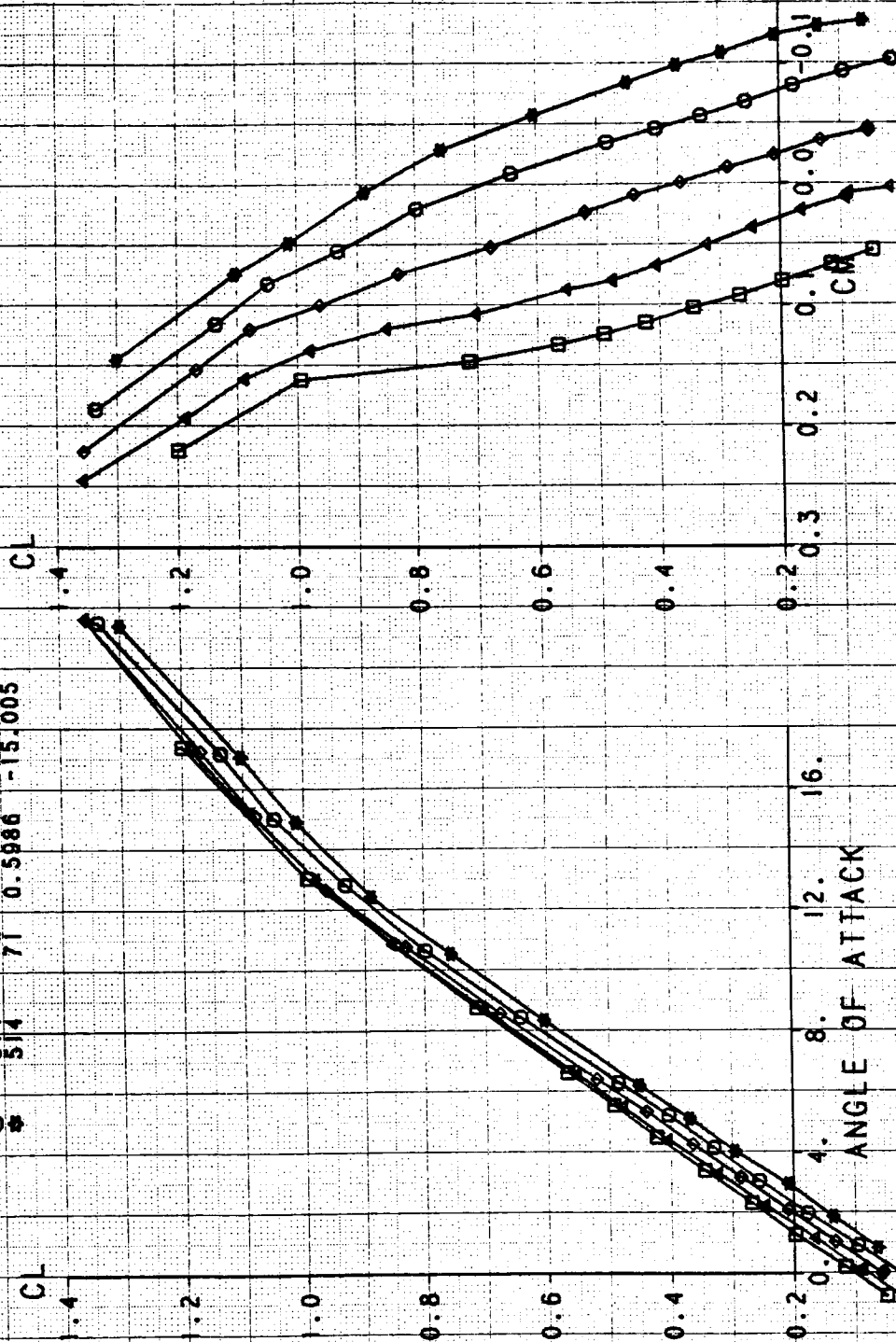
| SYM | TEST | RUN | RMACH | RDELCL |
|-----|------|-----|--------|---------|
| □ | 514 | 66 | 0.3993 | 5.0293 |
| △ | 514 | 67 | 0.3989 | -0.0547 |
| ◇ | 514 | 68 | 0.3990 | -5.0061 |
| ○ | 514 | 69 | 0.3989 | -10.026 |
| ● | 514 | 70 | 0.3990 | -15.003 |

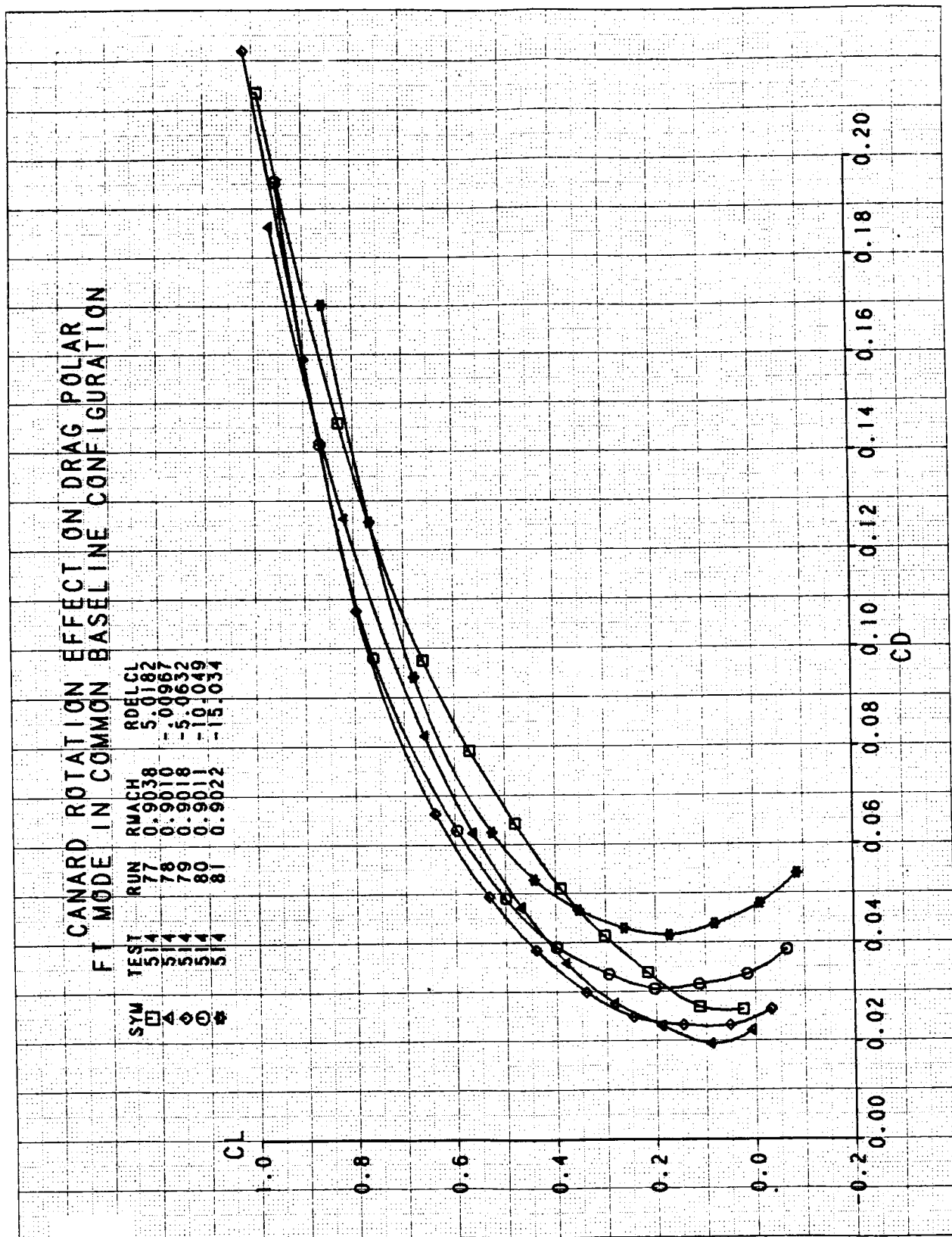


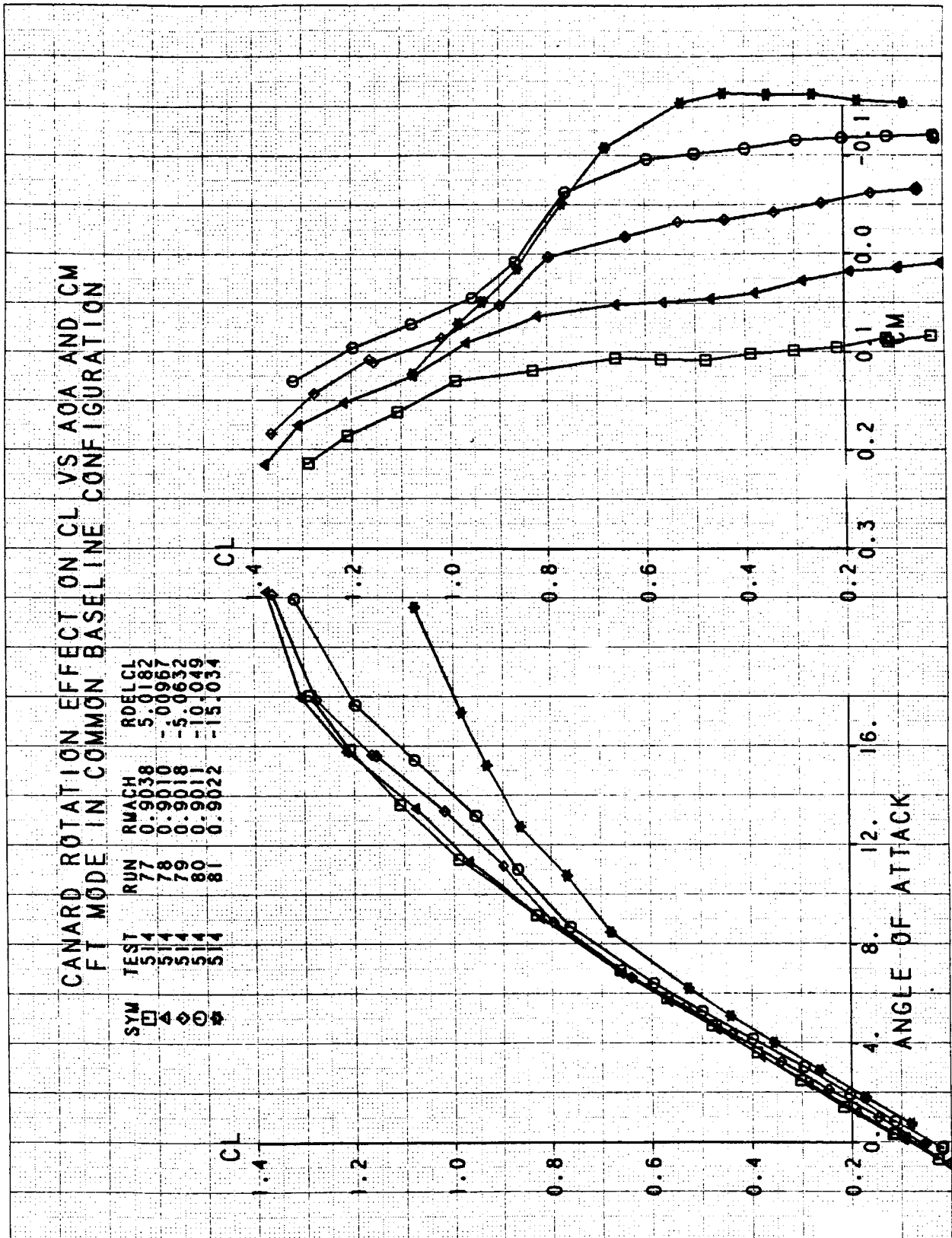


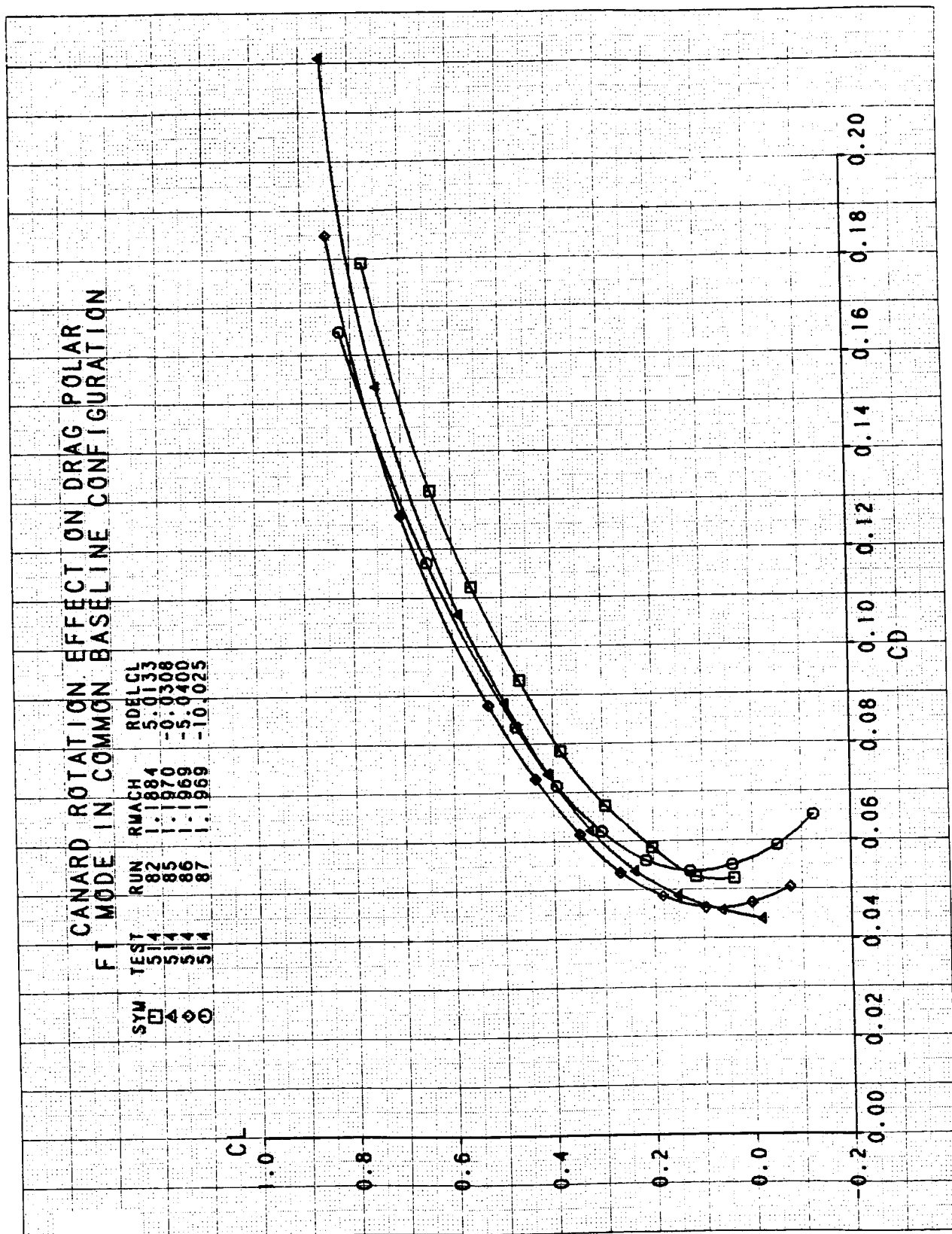
CANARD ROTATION EFFECT ON CL VS AOA AND CM

| SYM | TEST | RUN | RMACH | RDELCL |
|-----|------|-----|--------|---------|
| □ | 514 | 75 | 0.6005 | 5.0269 |
| △ | 514 | 74 | 0.6008 | 0.0827 |
| ◇ | 514 | 73 | 0.5997 | -5.0066 |
| ○ | 514 | 72 | 0.5996 | -10.035 |
| ● | 514 | 71 | 0.5986 | -15.005 |



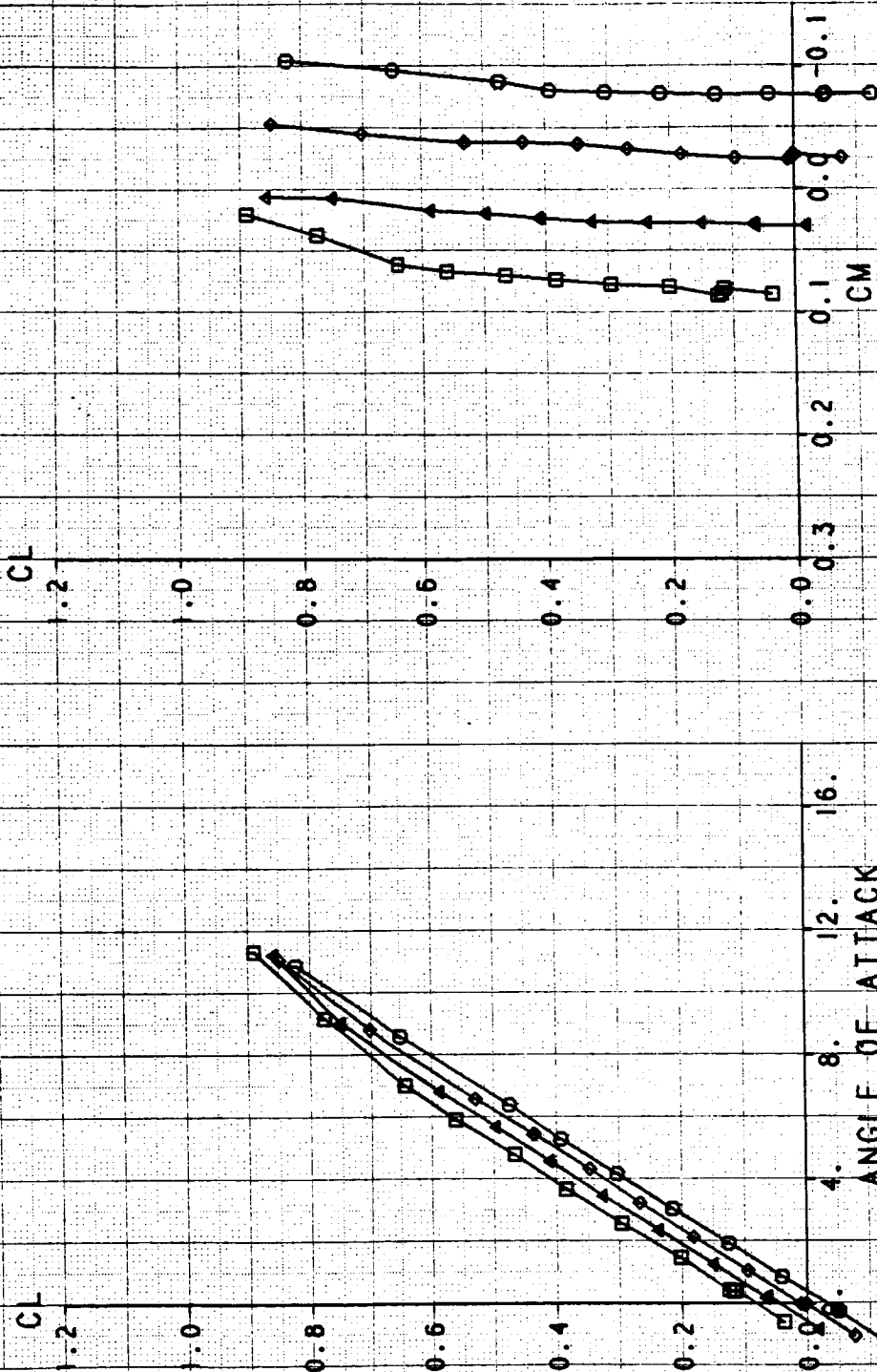






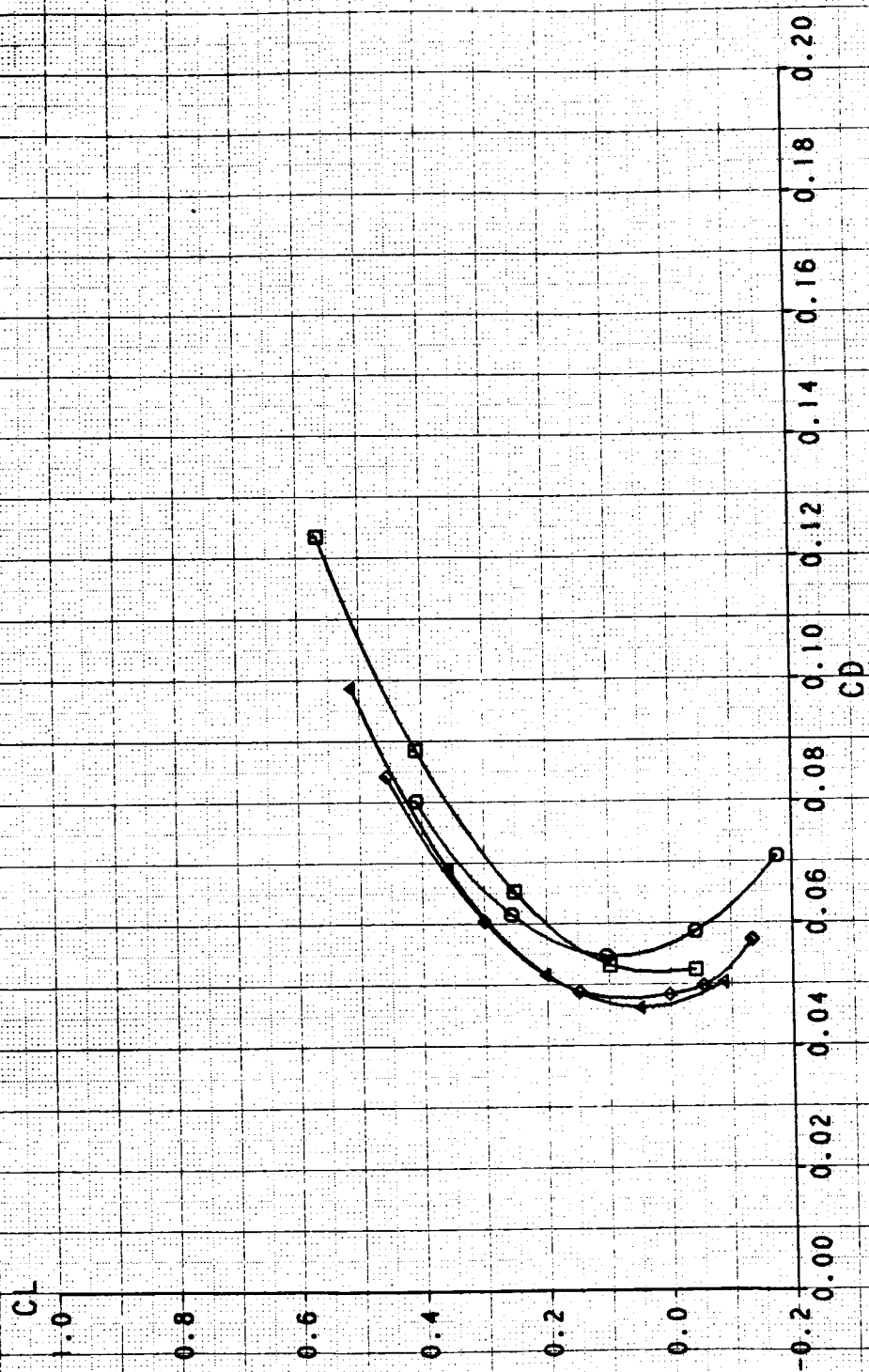
CANARD ROTATION EFFECT ON CL VS AOA AND CM

| SYM | TEST | RUN | RMACH | RDELCL |
|-----|------|-----|--------|---------|
| □ | 514 | 82 | 1.1884 | 5.0133 |
| △ | 514 | 85 | 1.1970 | -0.0308 |
| ◇ | 514 | 86 | 1.1969 | -5.0400 |
| ○ | 514 | 87 | 1.1969 | -10.025 |



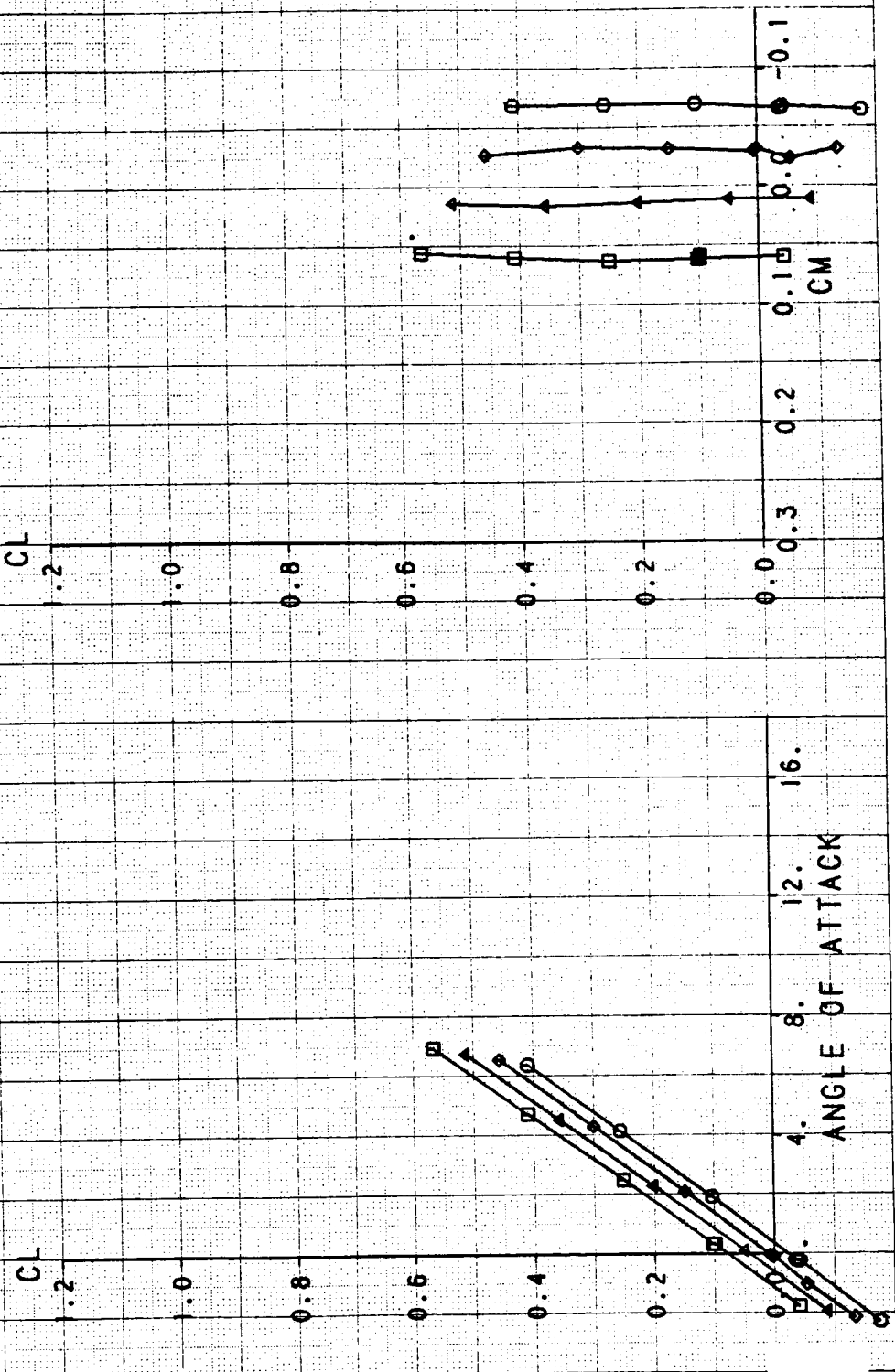
CANARD ROTATION EFFECT ON DRAG POLAR
 FT MODE IN COMMON BASELINE CONFIGURATION

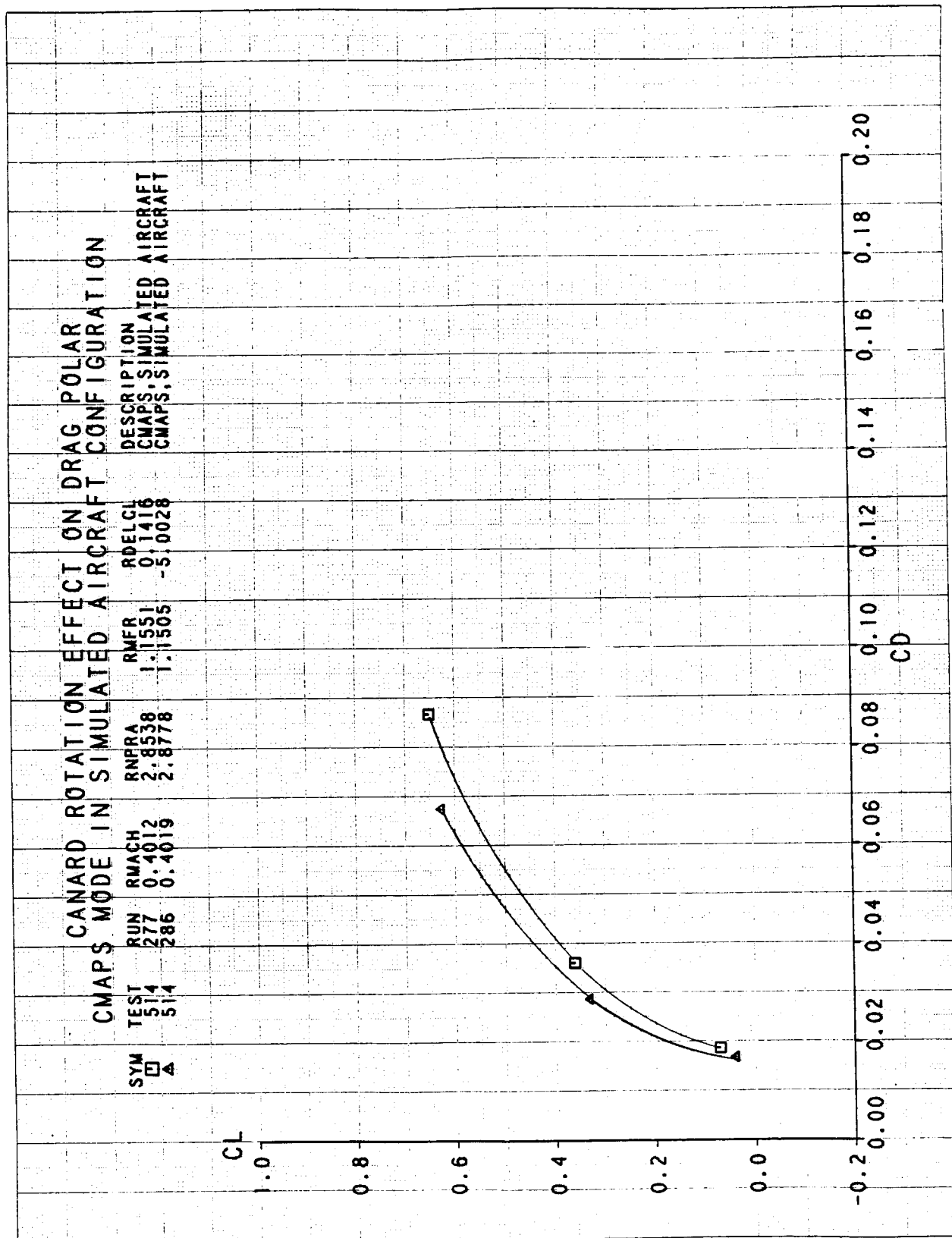
| SYM | TEST | RUN | RWACH | RDELCL |
|-----|------|-----|--------|---------|
| □ | 514 | 93 | 1.3899 | 5.1040 |
| △ | 514 | 92 | 1.3923 | -0.0318 |
| ◇ | 514 | 94 | 1.3917 | -4.9583 |
| ⊙ | 514 | 95 | 1.3908 | -10.046 |



CANARD ROTATION EFFECT ON CL VS AOA AND CM

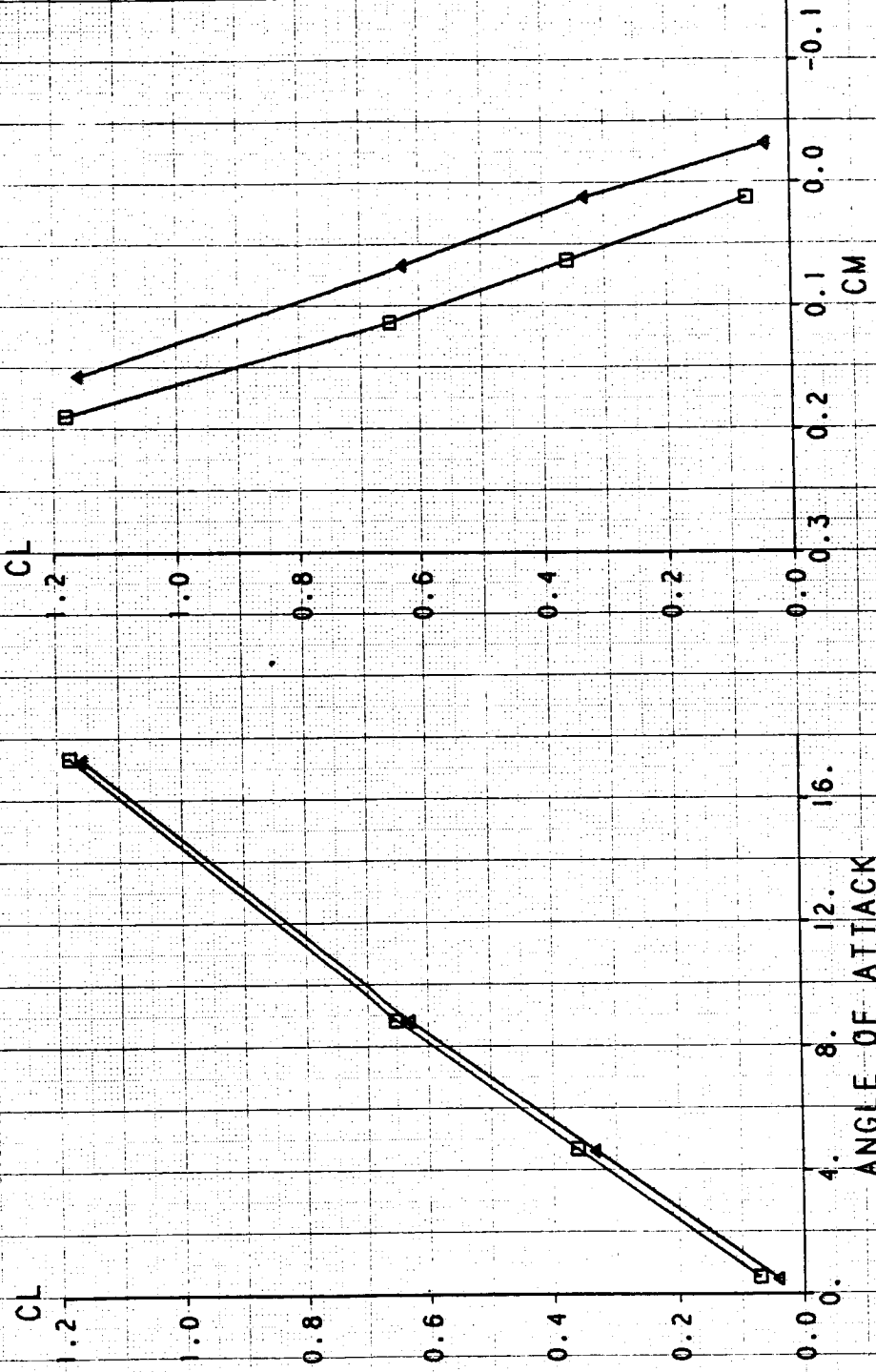
| SYM | TEST | RUN | RMACH | ROELCL |
|-----|------|-----|--------|----------|
| □ | 514 | 93 | 1.3899 | 5.1040 |
| △ | 514 | 92 | 1.3923 | -0.0318 |
| ◇ | 514 | 94 | 1.3917 | -4.9583 |
| ○ | 514 | 95 | 1.3908 | -10.1046 |





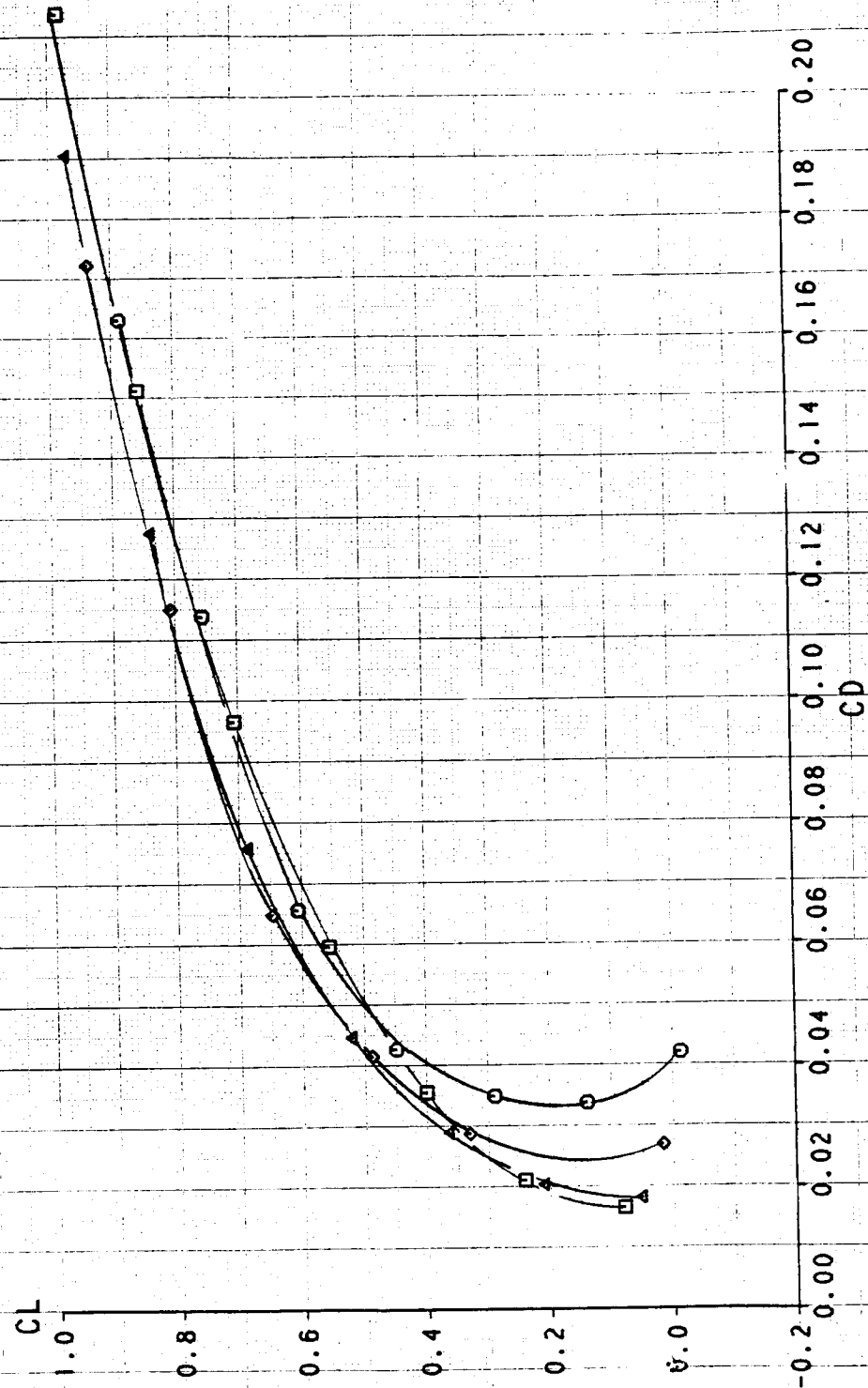
CANARD ROTATION EFFECT ON CL VS AOA AND CM CMAPS MODE IN SIMULATED AIRCRAFT CONFIGURATION

| SYM | TEST | RUN | RMACH | RNPRA | RMFR | RDELCL | DESCRIPTION |
|-----|------|-----|--------|--------|--------|---------|---------------------------|
| □ | 514 | 277 | 0.4012 | 2.8538 | 1.1551 | 0.1416 | CMAPS, SIMULATED AIRCRAFT |
| △ | 514 | 286 | 0.4019 | 2.8778 | 1.1505 | -5.0028 | CMAPS, SIMULATED AIRCRAFT |



CANARD ROTATION EFFECT ON DRAG POLAR CMAPS MODE IN SIMULATED AIRCRAFT CONFIGURATION

| SYM | TEST | RUN | RMACH | RNPRA | RMFR | RDELCL | DESCRIPTION |
|-----|------|-----|--------|--------|--------|---------|---------------------------|
| □ | 514 | 178 | 0.6009 | 3.8301 | 0.9161 | 0.1001 | CMAPS, SIMULATED AIRCRAFT |
| △ | 514 | 179 | 0.6010 | 3.8557 | 0.9158 | -4.9809 | CMAPS, SIMULATED AIRCRAFT |
| ◇ | 514 | 180 | 0.6010 | 3.8478 | 0.9169 | -10.081 | CMAPS, SIMULATED AIRCRAFT |
| ○ | 514 | 182 | 0.5994 | 3.8168 | 0.9215 | -14.883 | CMAPS, SIMULATED AIRCRAFT |



CANARD ROTATION EFFECT ON CL VS AOA AND CM CMAPS MODE IN SIMULATED AIRCRAFT CONFIGURATION

DESCRIPTION
CMAPS, SIMULATED AIRCRAFT
CMAPS, SIMULATED AIRCRAFT
CMAPS, SIMULATED AIRCRAFT
CMAPS, SIMULATED AIRCRAFT

RMFR 0.9161
0.9158
0.9169
0.9215

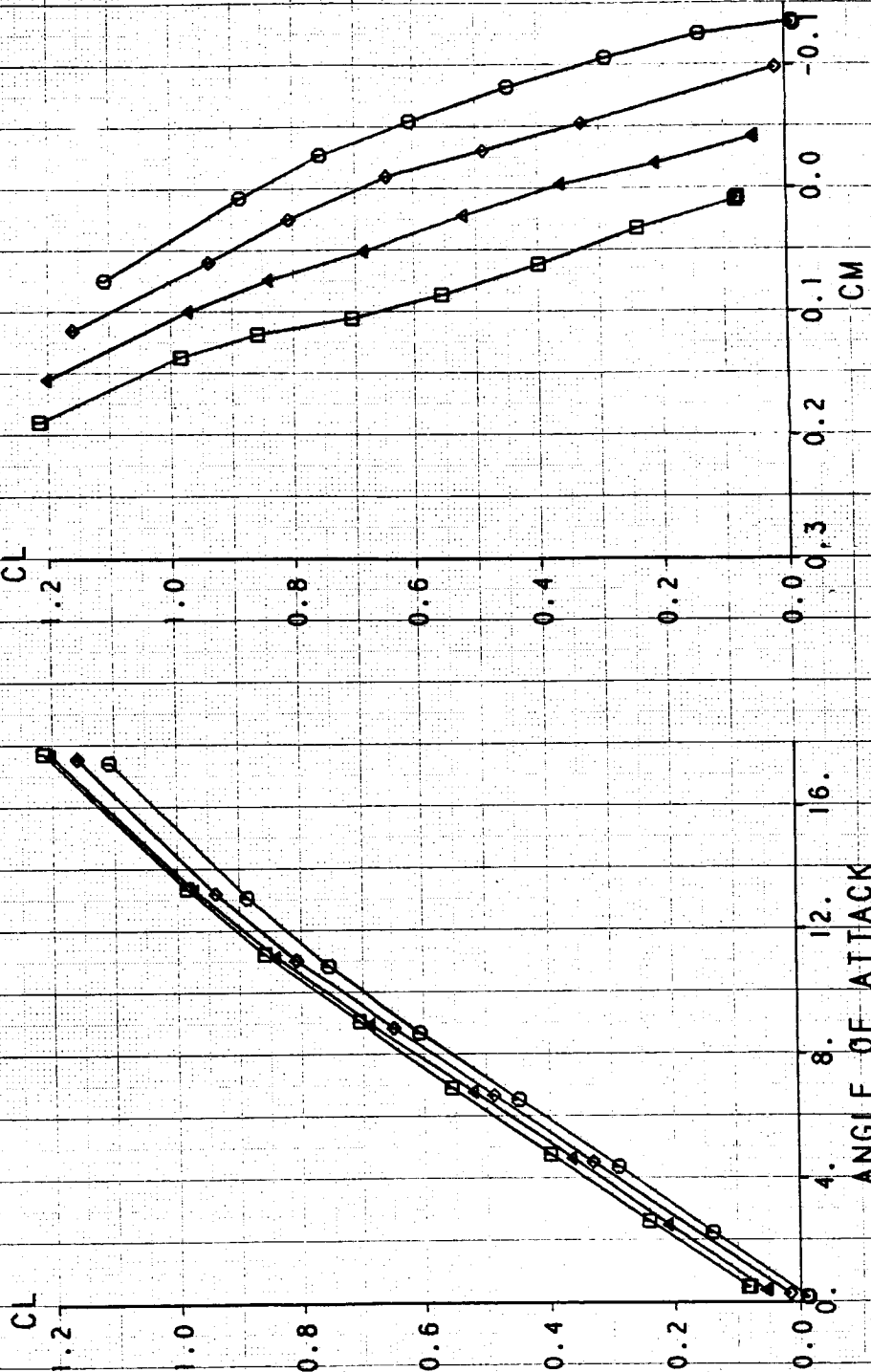
RMACH 0.6009
0.6010
0.6010
0.5994

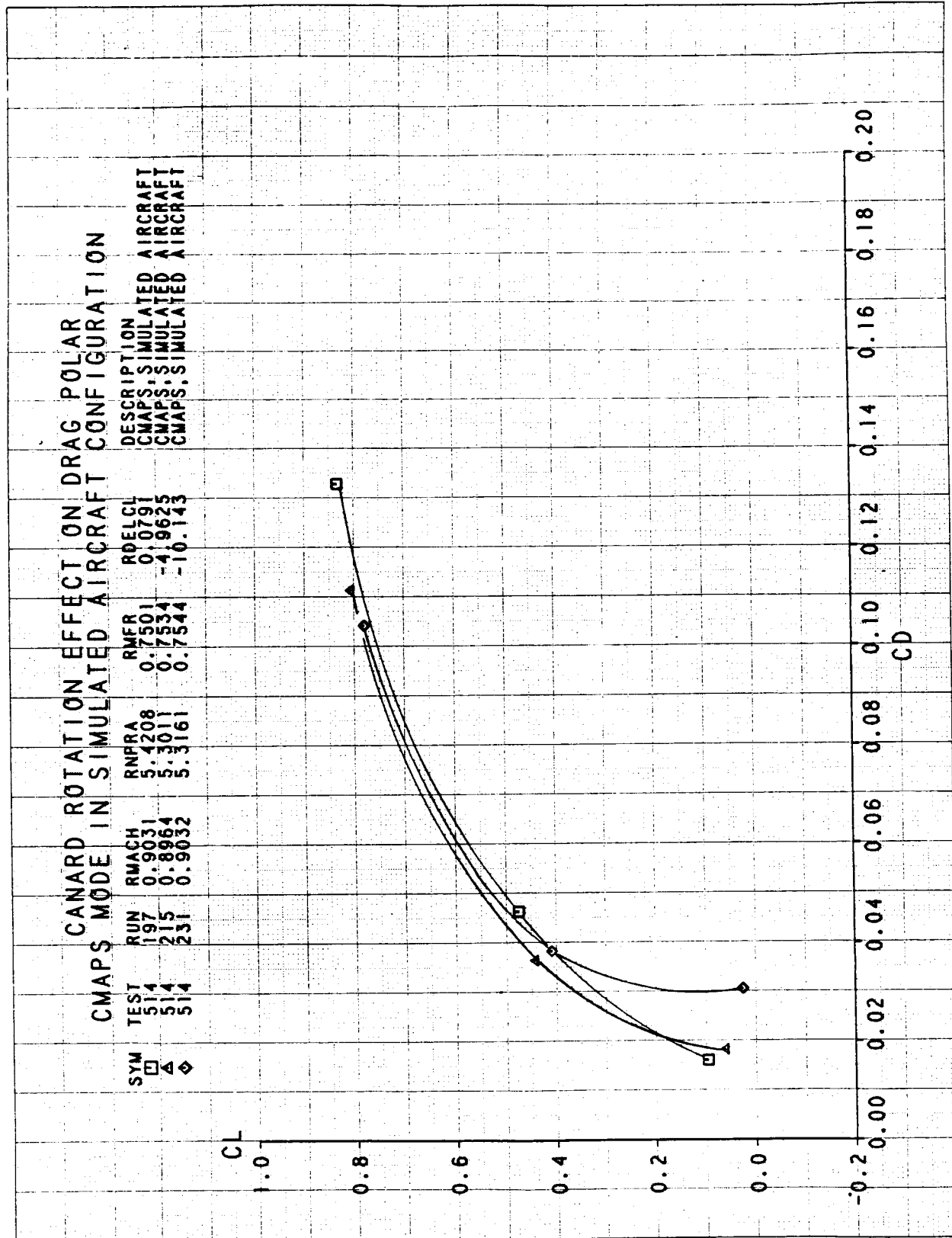
SYM □ ▲ ◆ ○

TEST RUN
514 178
514 179
514 180
514 182

RMFRA 3.8301
3.8357
3.8478
3.8168

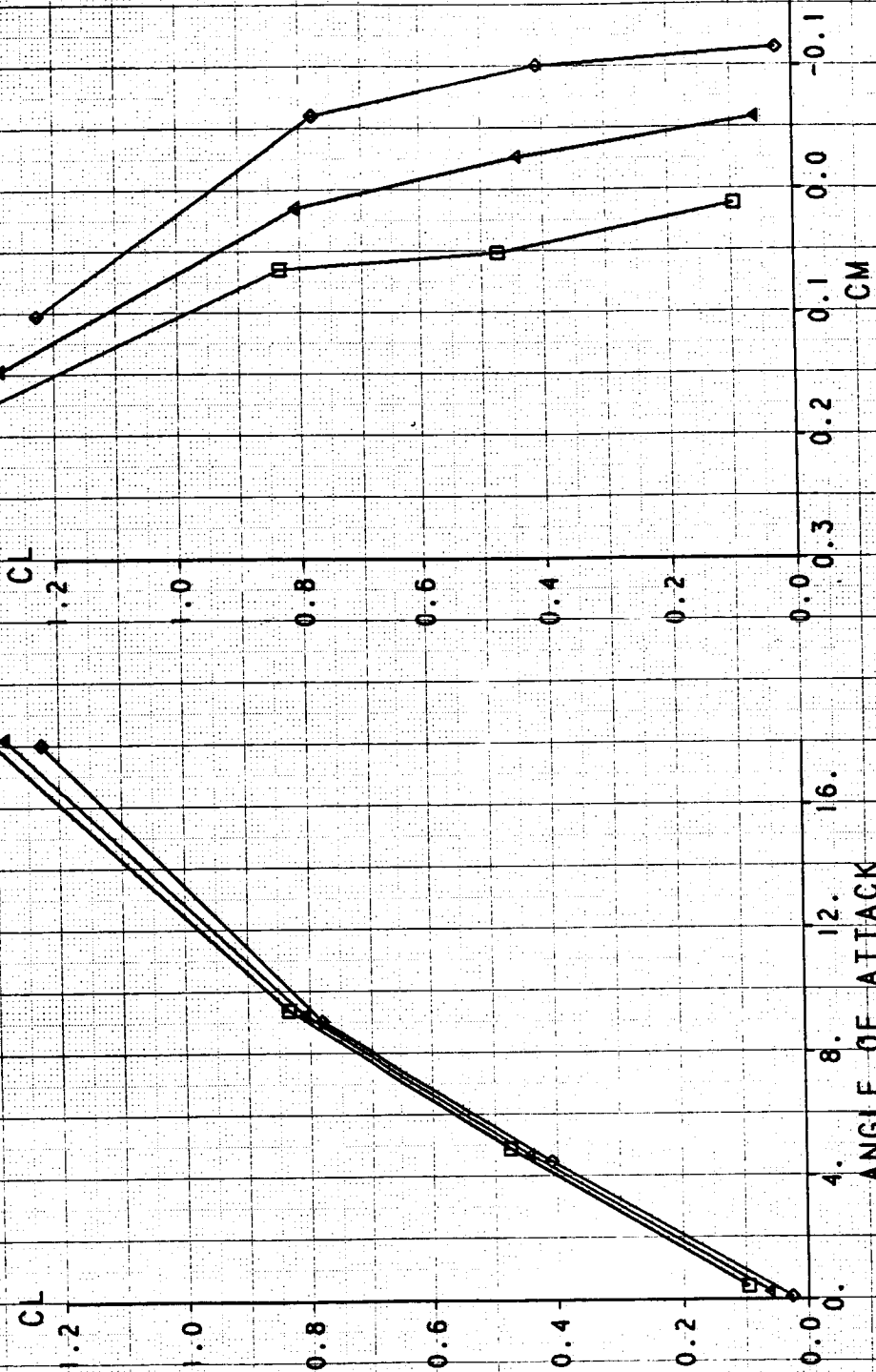
RDELCL 0.1001
-4.9809
-10.081
-14.883

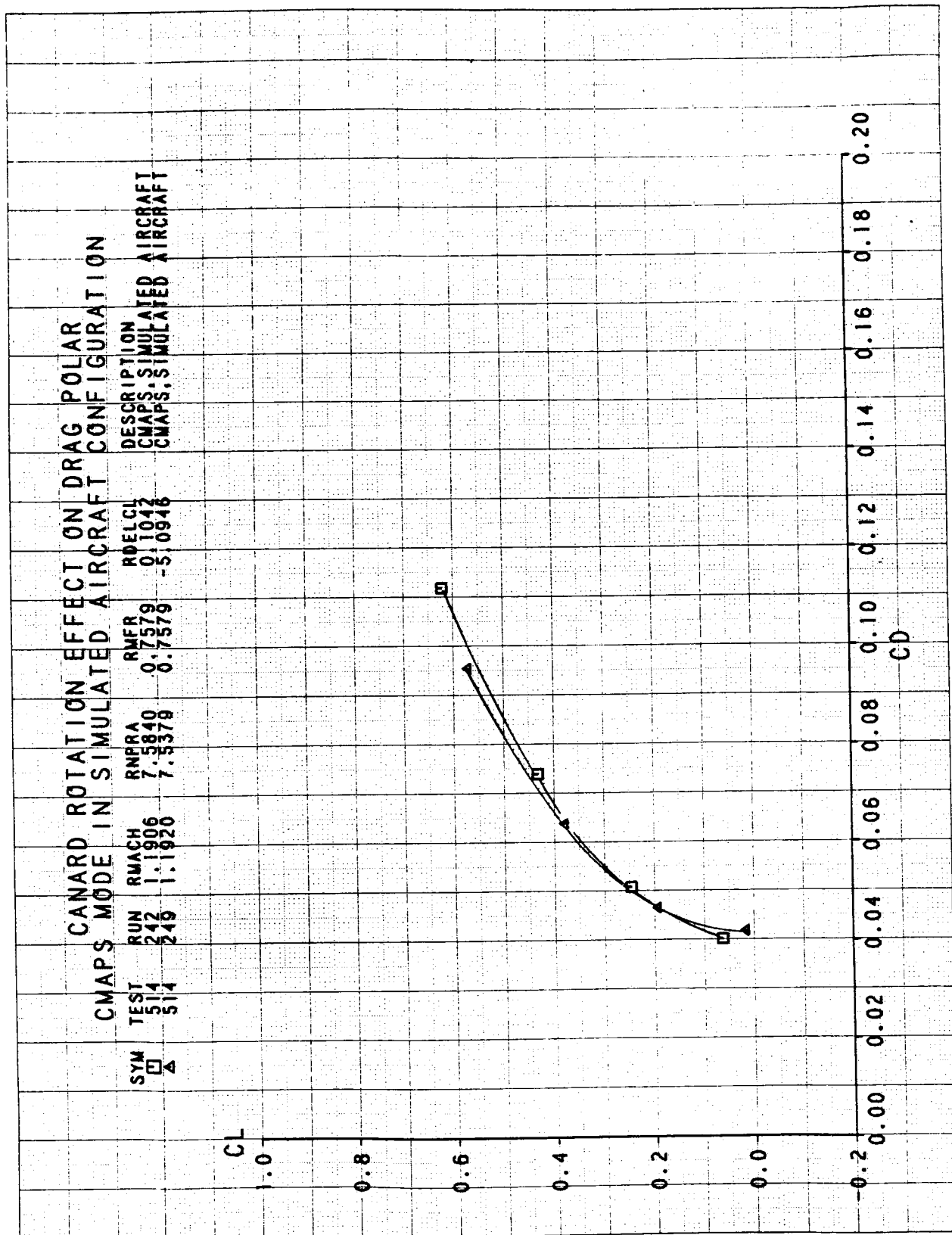




CANARD ROTATION EFFECT ON CL VS AOA AND CM CMAPS MODE IN SIMULATED AIRCRAFT CONFIGURATION

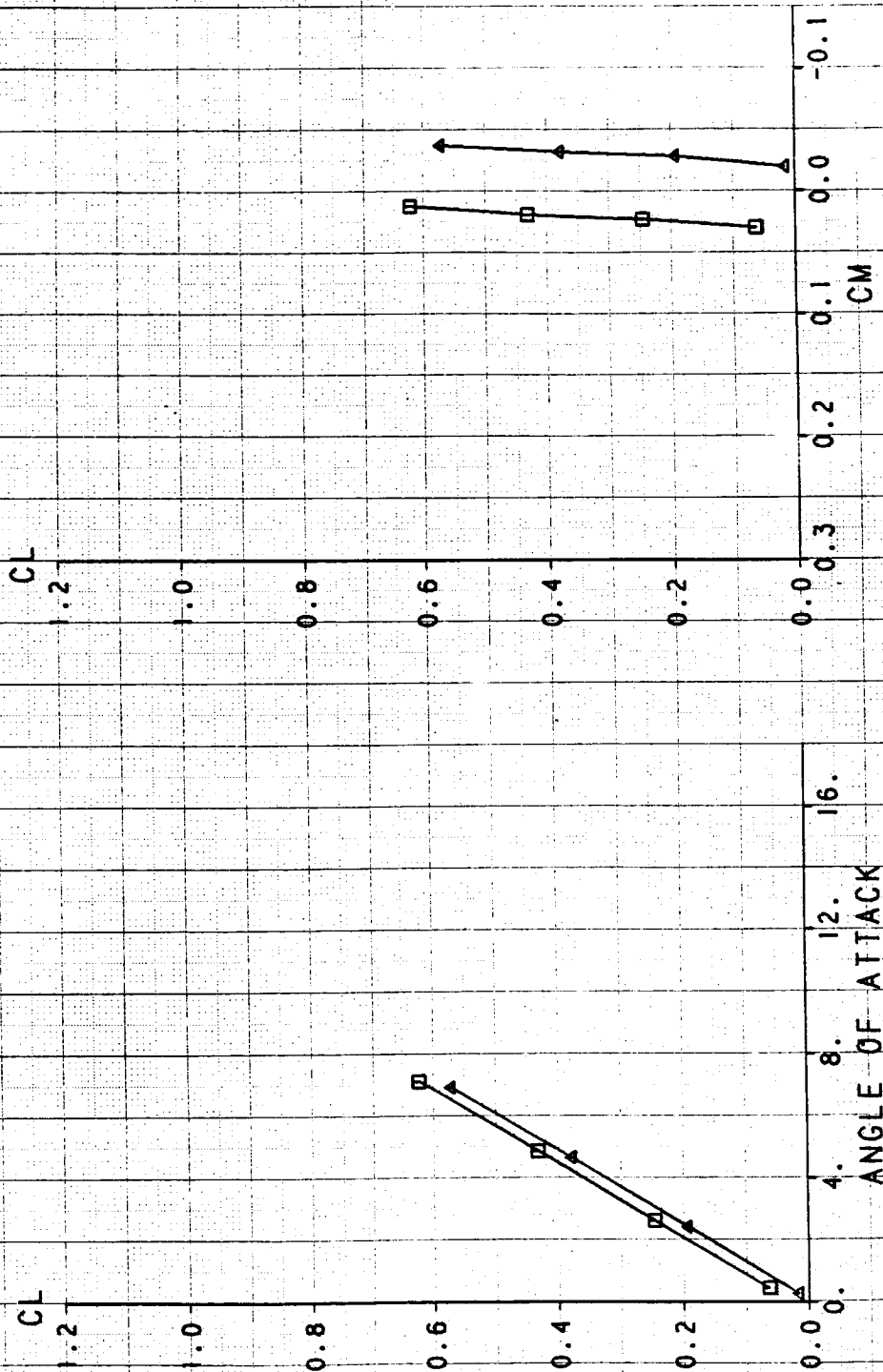
| SYM | TEST | RUN | RMACH | RNPRA | RMFR | RDELCL | DESCRIPTION |
|-----|------|-----|--------|--------|--------|---------|---------------------------|
| □ | 514 | 197 | 0.9031 | 5.4208 | 0.7501 | 0.0791 | CMAPS, SIMULATED AIRCRAFT |
| △ | 514 | 215 | 0.8964 | 5.3011 | 0.7534 | -4.9625 | CMAPS, SIMULATED AIRCRAFT |
| ◇ | 514 | 231 | 0.9032 | 5.3161 | 0.7544 | -10.143 | CMAPS, SIMULATED AIRCRAFT |

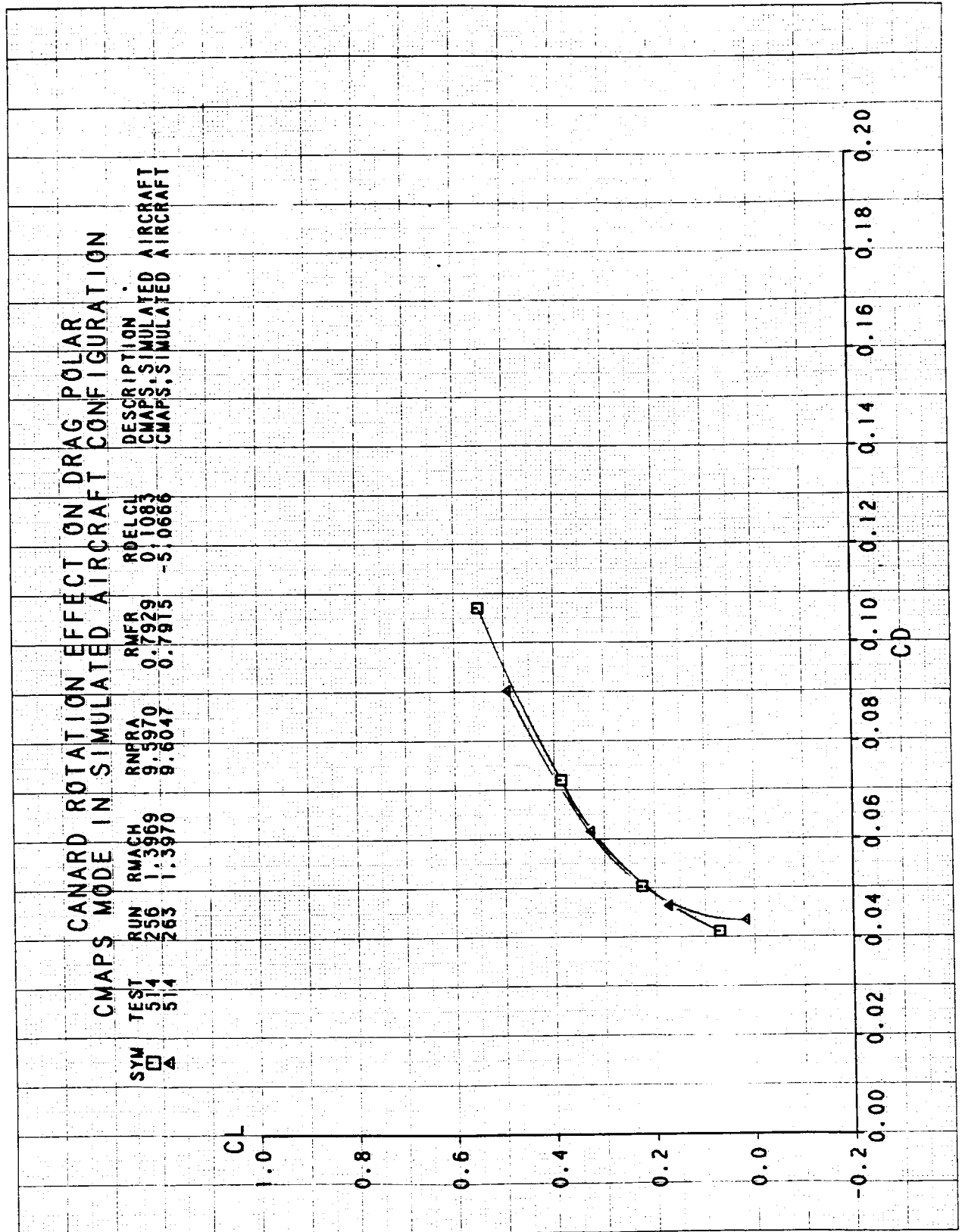




CANARD ROTATION EFFECT ON CL VS AOA AND CM CMAPS MODE IN SIMULATED AIRCRAFT CONFIGURATION

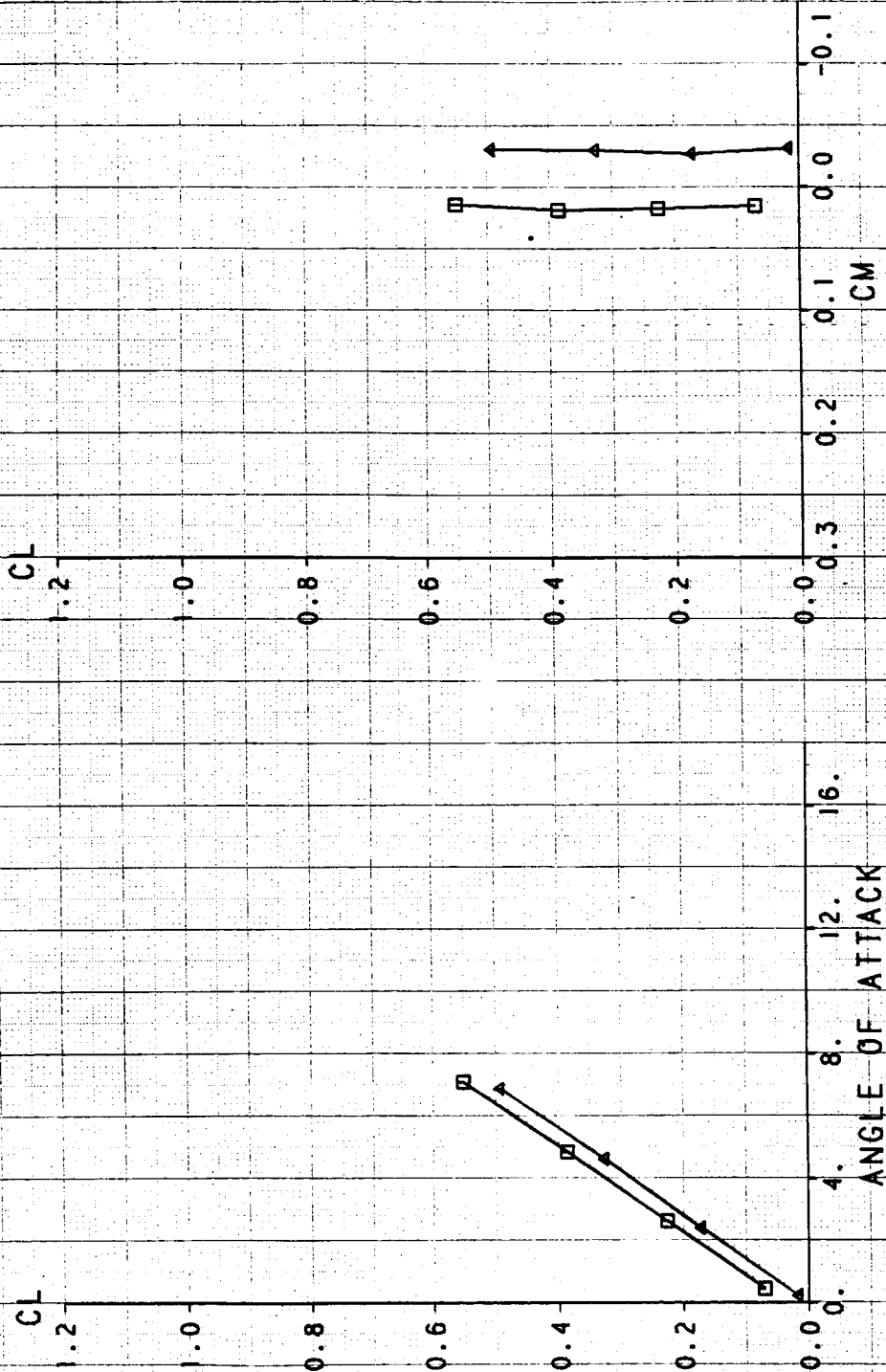
| SYM | TEST | RUN | RMACH | RNPRA | RMFR | RDELCL | DESCRIPTION |
|-----|------|-----|--------|--------|--------|---------|--------------------------|
| □ | 514 | 242 | 1.1906 | 7.5840 | 0.7579 | 0.1042 | CMAPS SIMULATED AIRCRAFT |
| △ | 514 | 249 | 1.1920 | 7.5379 | 0.7579 | -5.0946 | CMAPS SIMULATED AIRCRAFT |

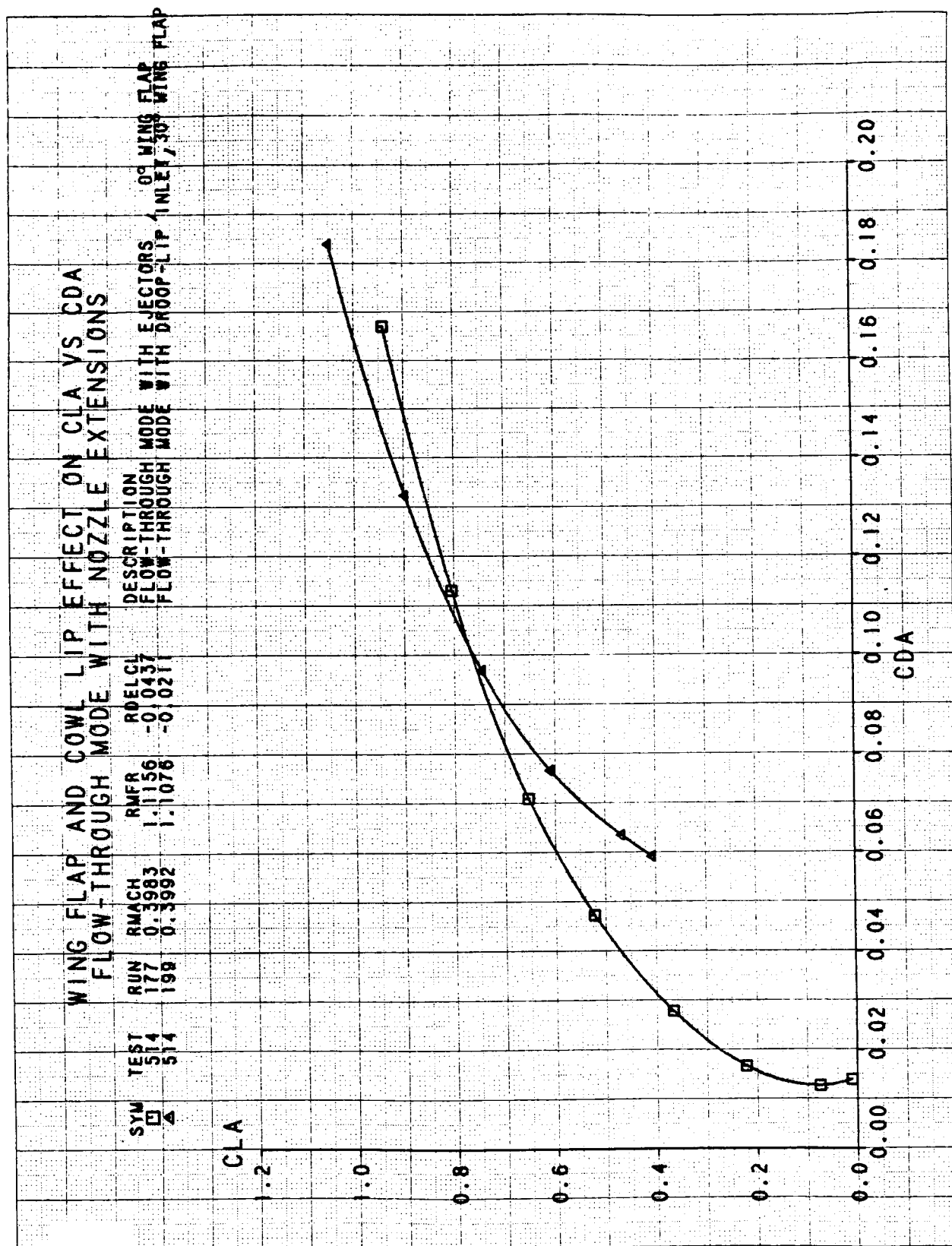


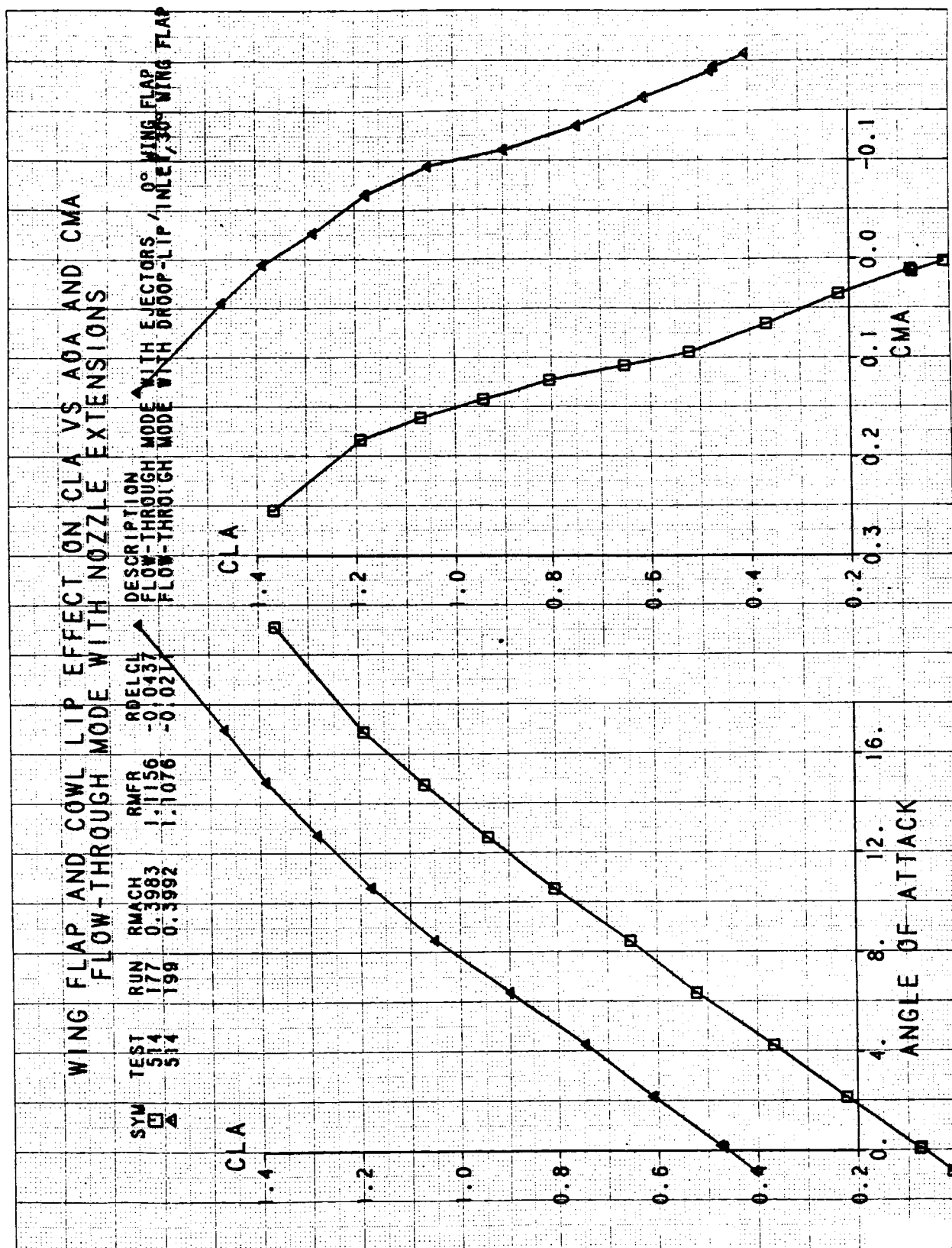


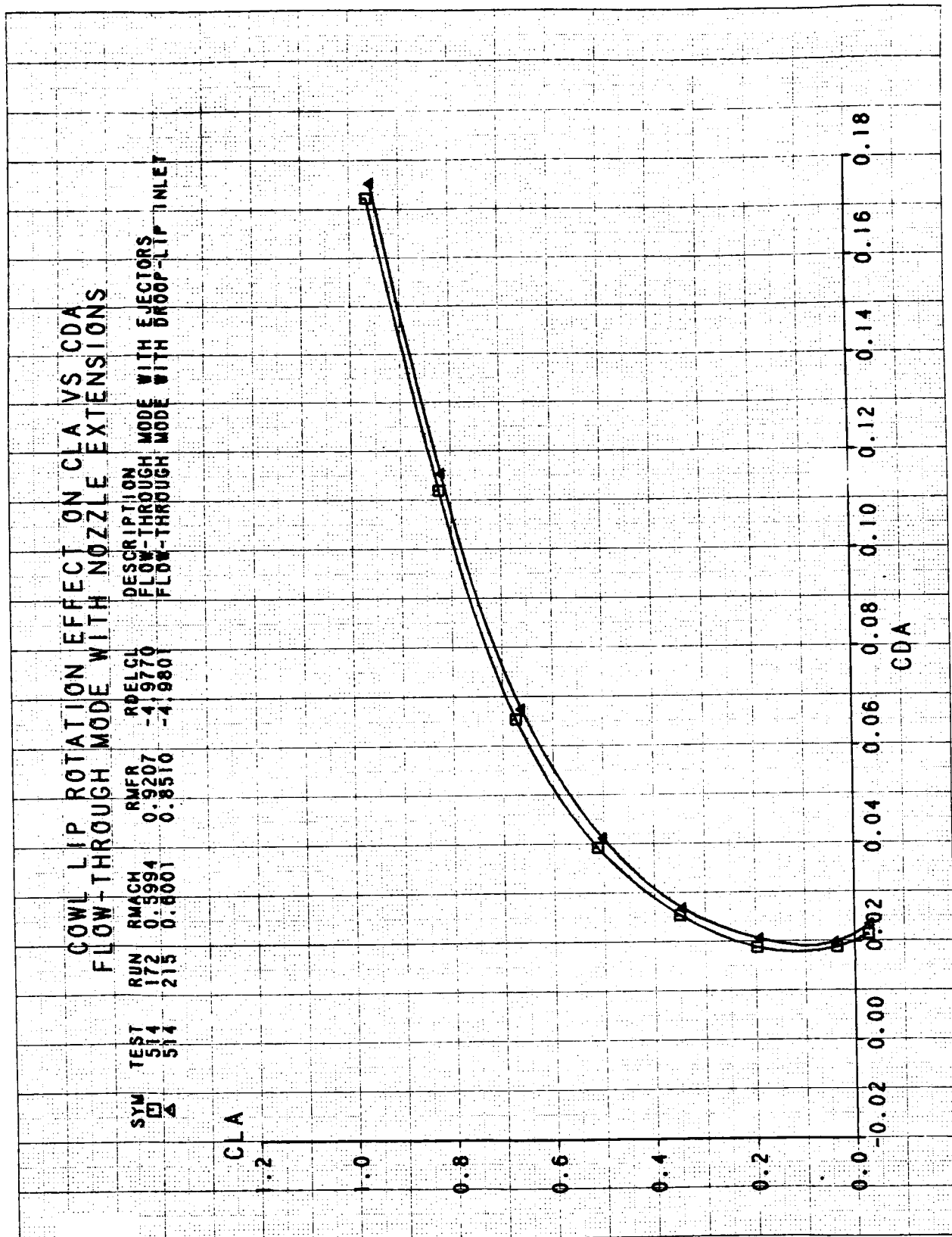
CANARD ROTATION EFFECT ON CL VS AOA AND CM

| SYM | TEST | RUN | RMACH | RNPR | RMFR | RDELCL | DESCRIPTION |
|-----|------|-----|--------|--------|--------|---------|---------------------------|
| □ | 514 | 256 | 1.3969 | 9.5970 | 0.7929 | 0.1083 | CMAPS, SIMULATED AIRCRAFT |
| △ | 514 | 263 | 1.3970 | 9.6047 | 0.7915 | -5.0666 | CMAPS, SIMULATED AIRCRAFT |

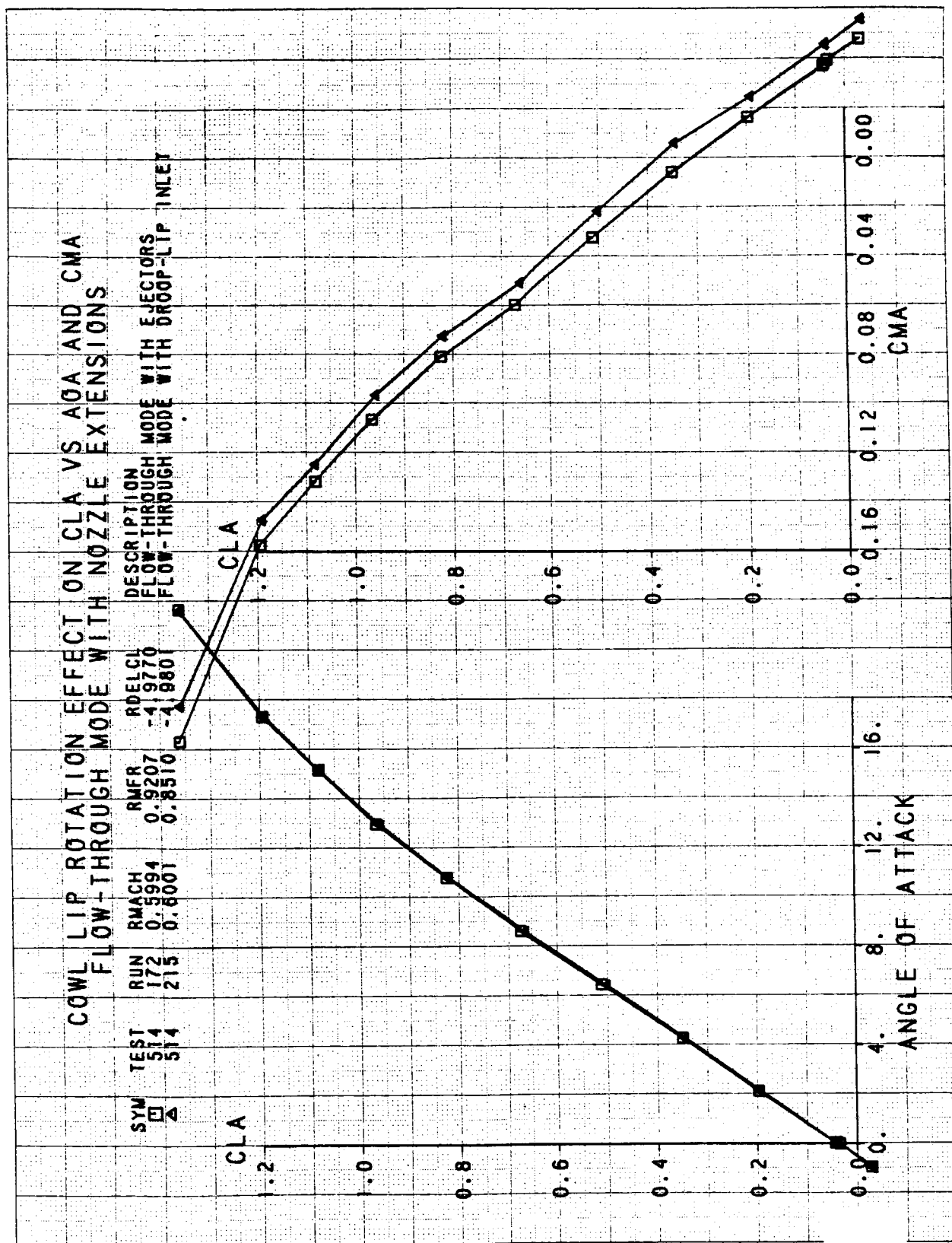


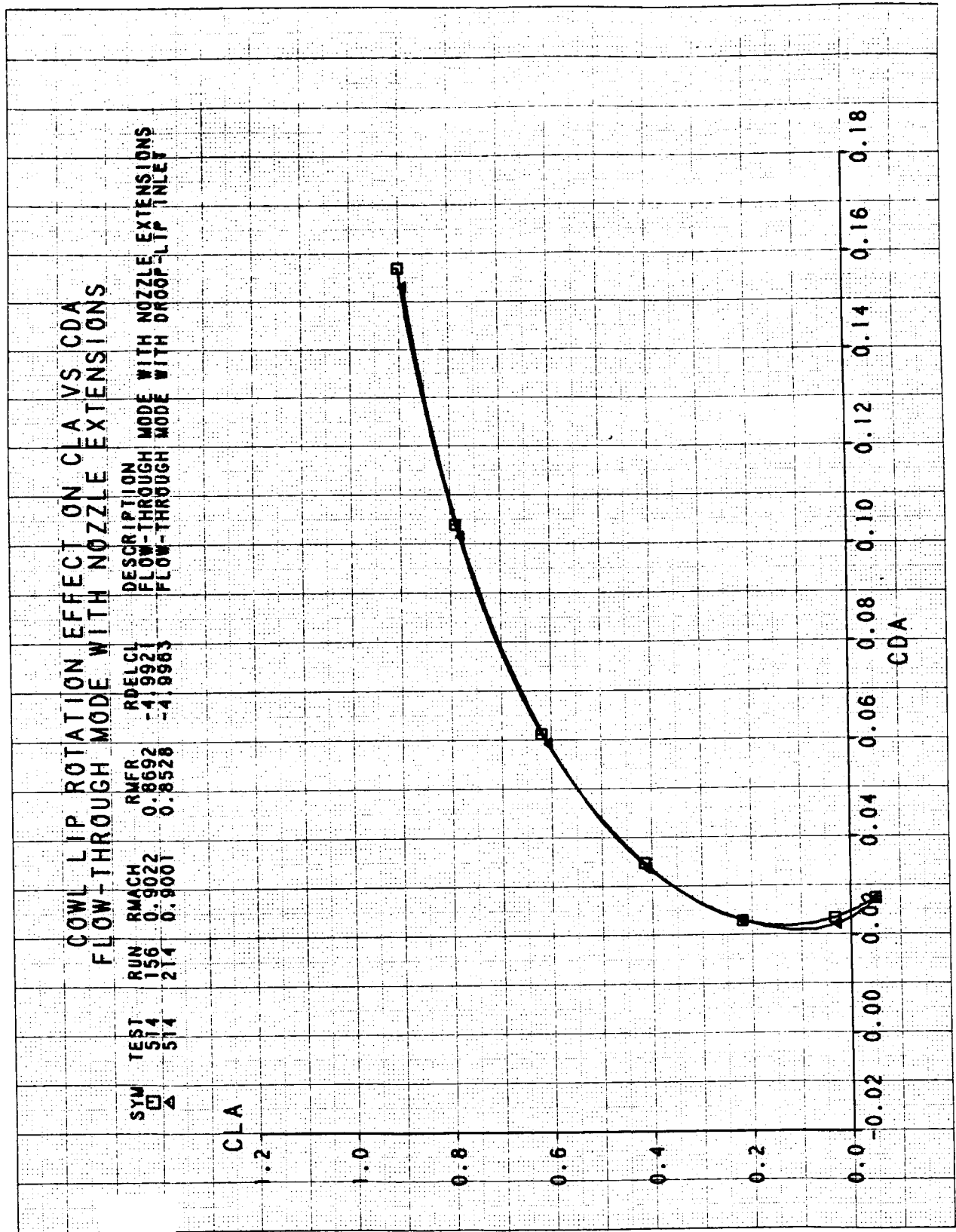


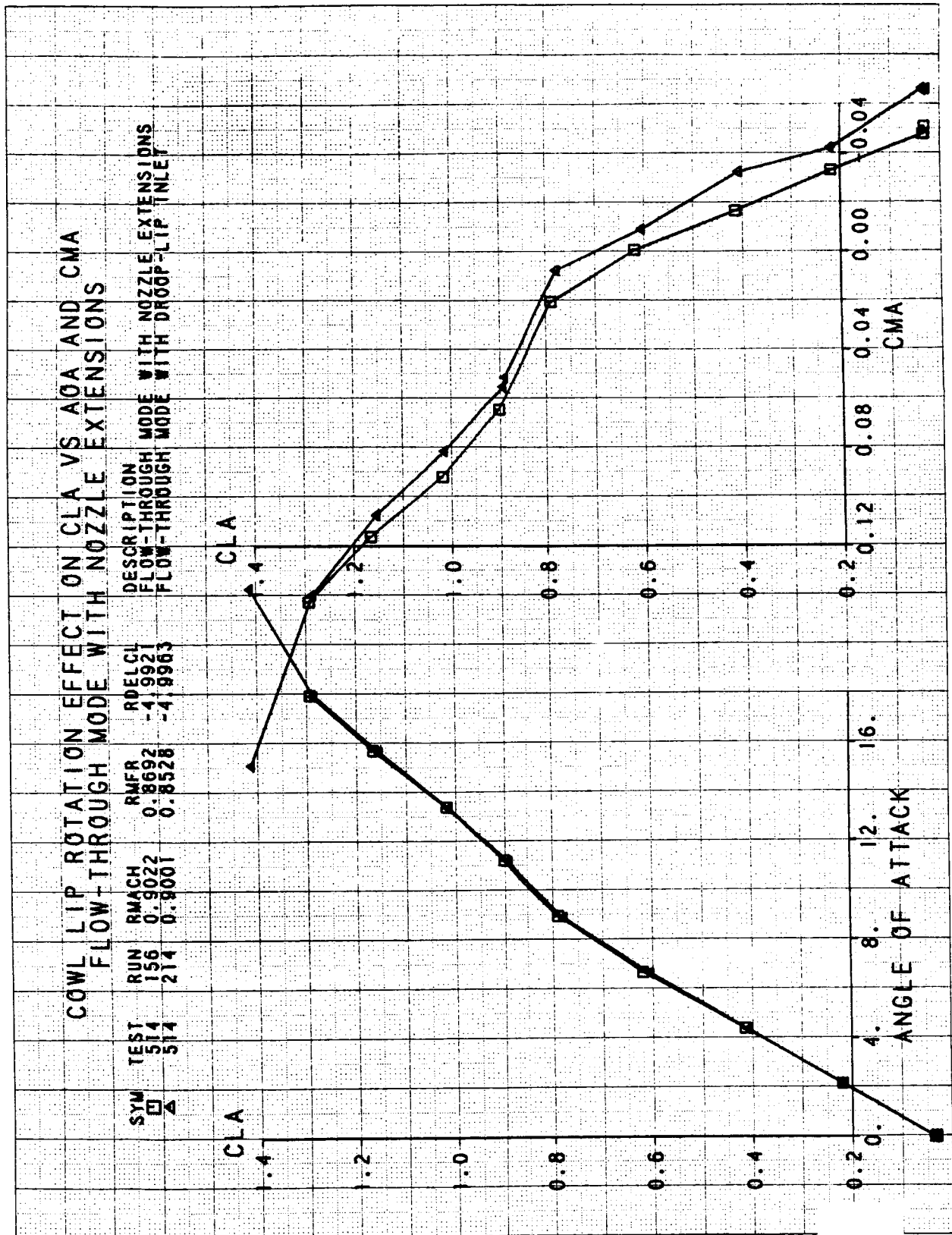


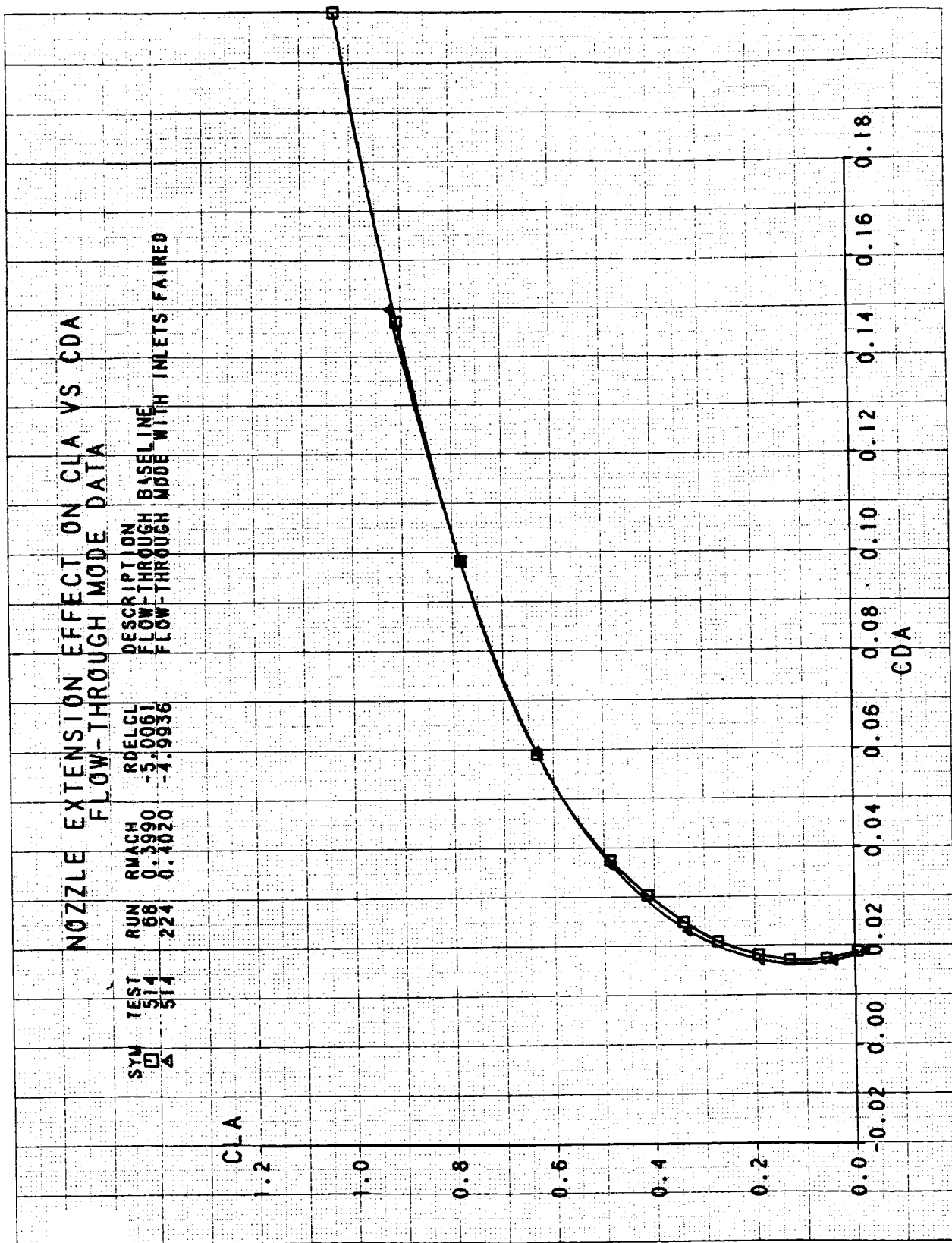


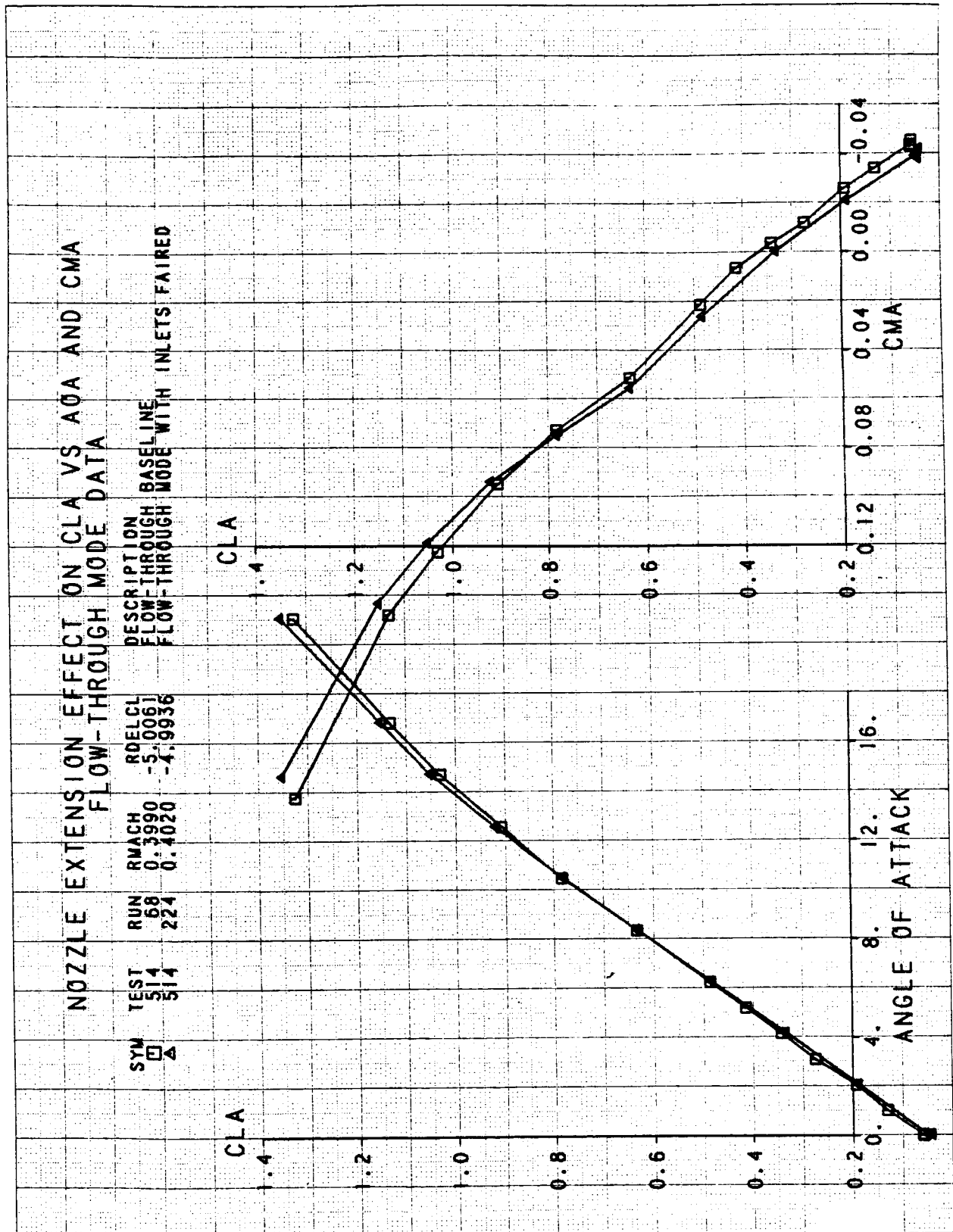
ORIGINAL PAGE IS
OF POOR QUALITY





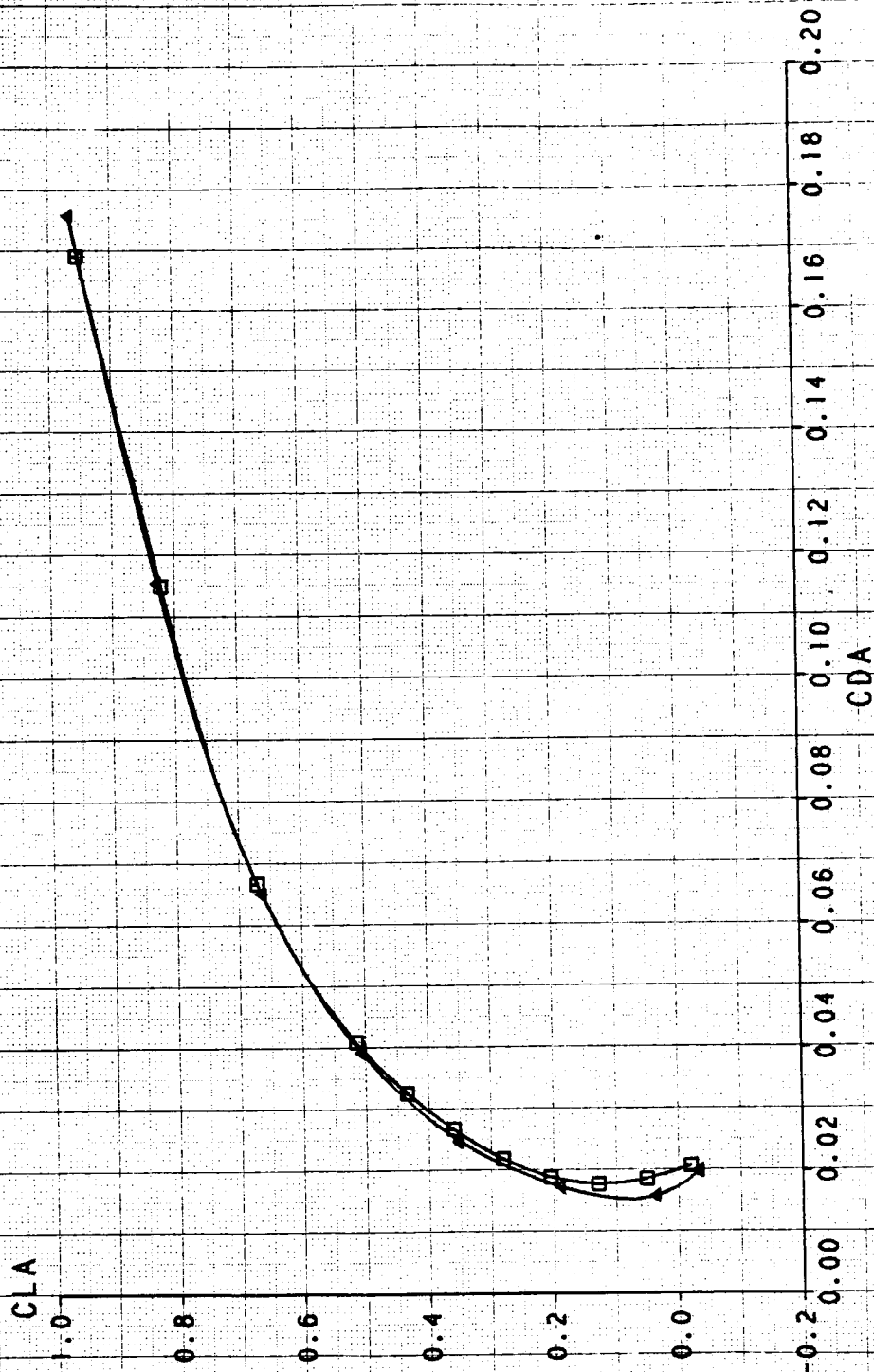


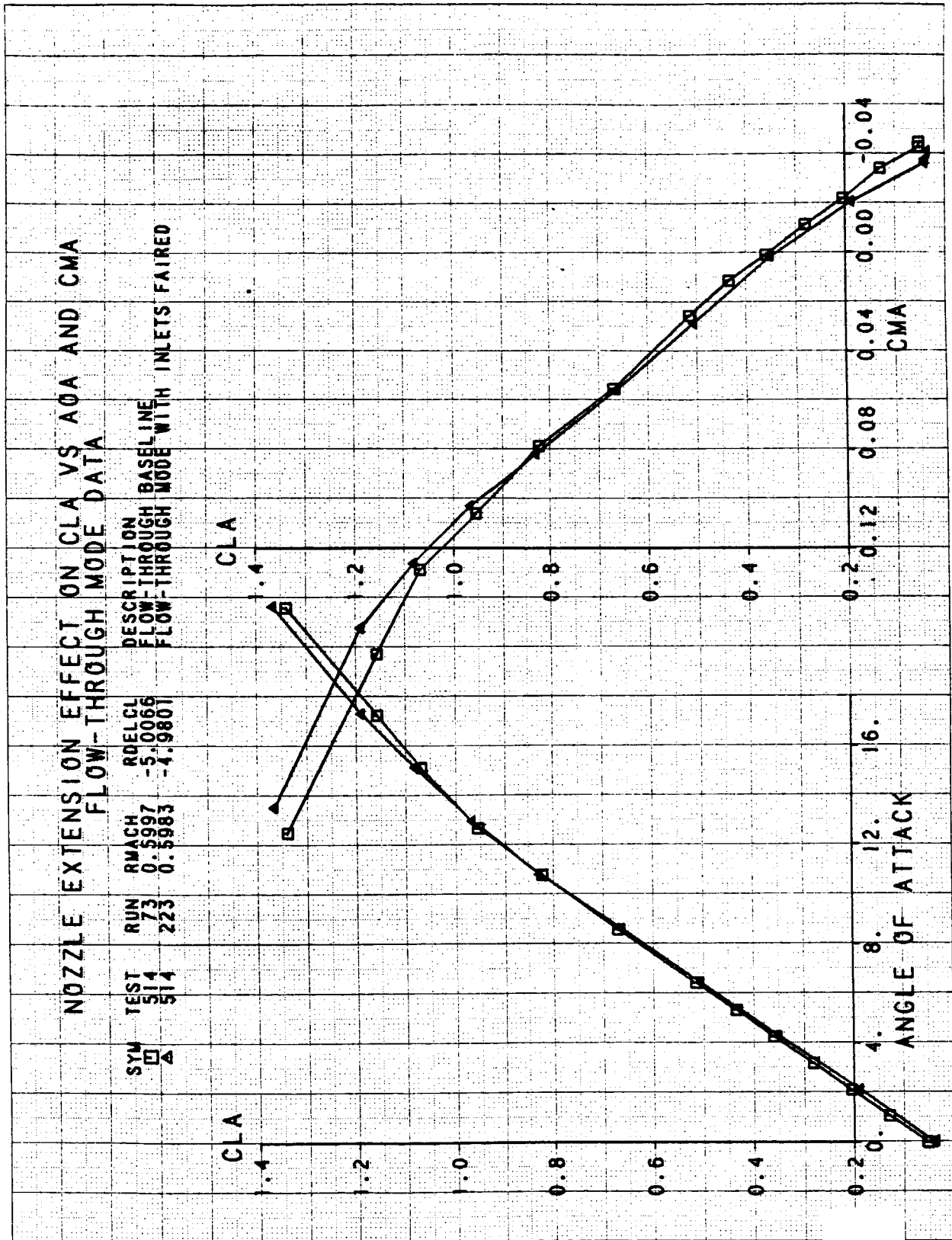


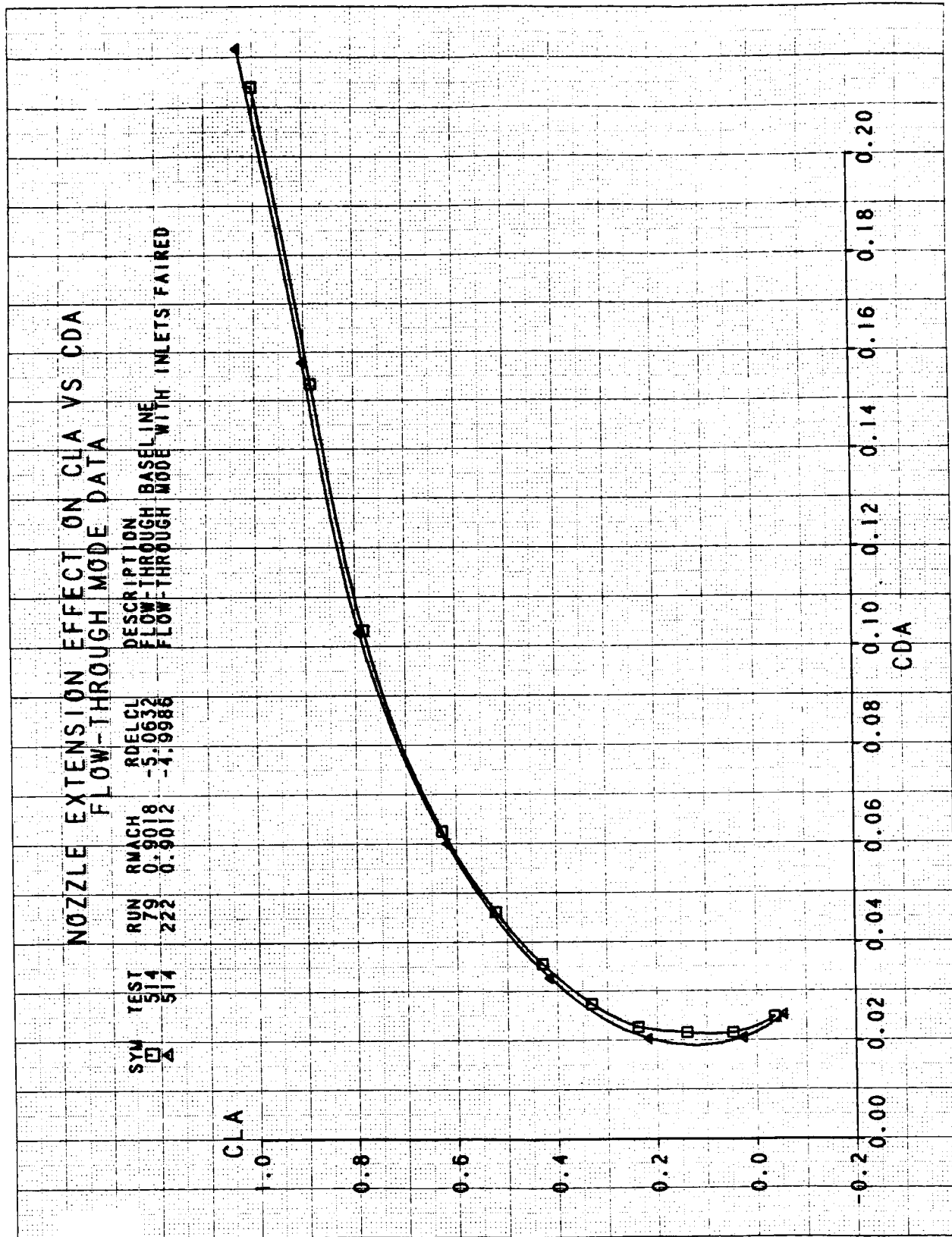


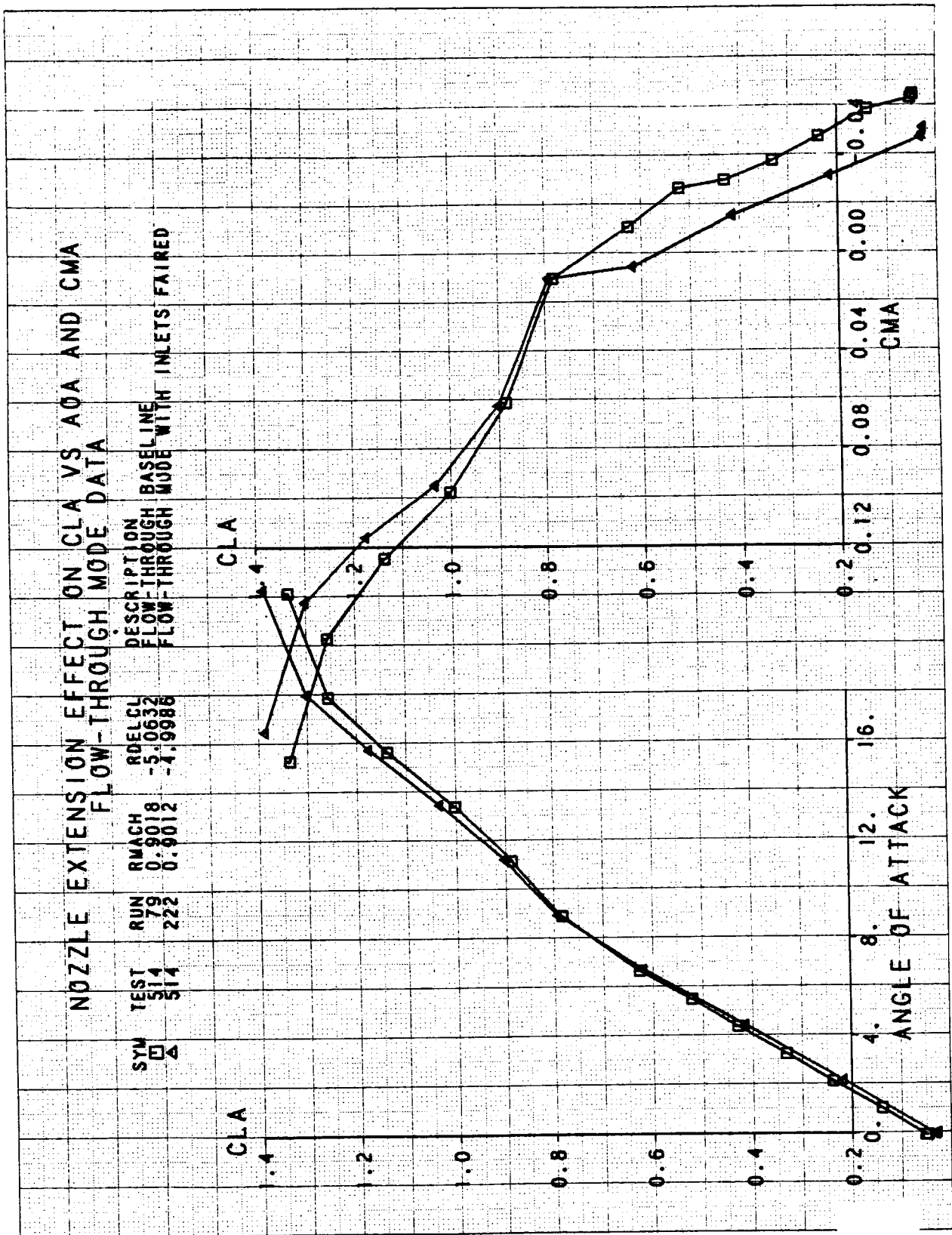
NOZZLE EXTENSION EFFECT ON CLA VS CDA

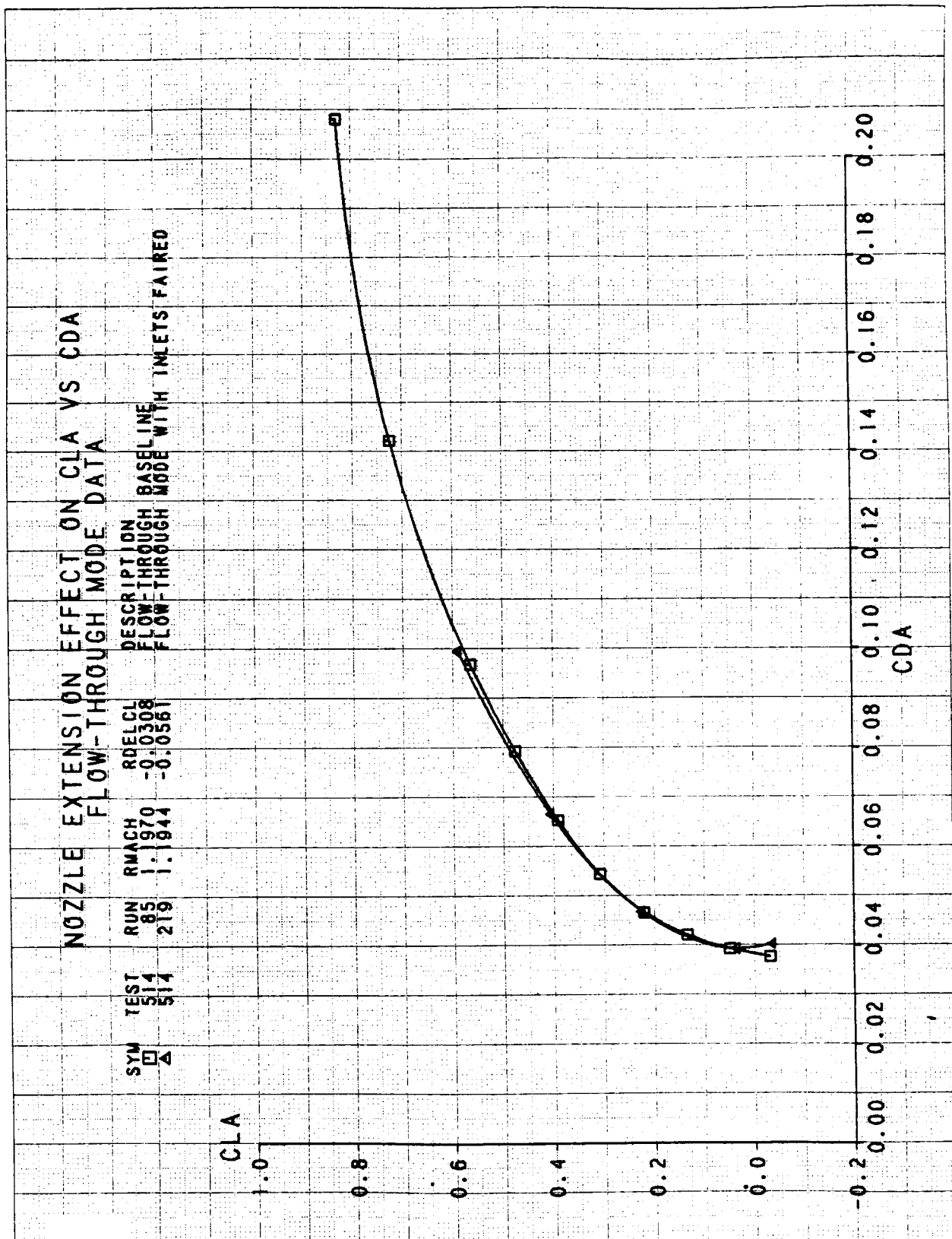
TEST 514
 SYM □
 RUN 73
 RMACH 0.5997
 RDELCL -5.0066
 DESCRIPTION FLOW-THROUGH MODE WITH INLETS FAIRED
 BASELINE
 -4.9801

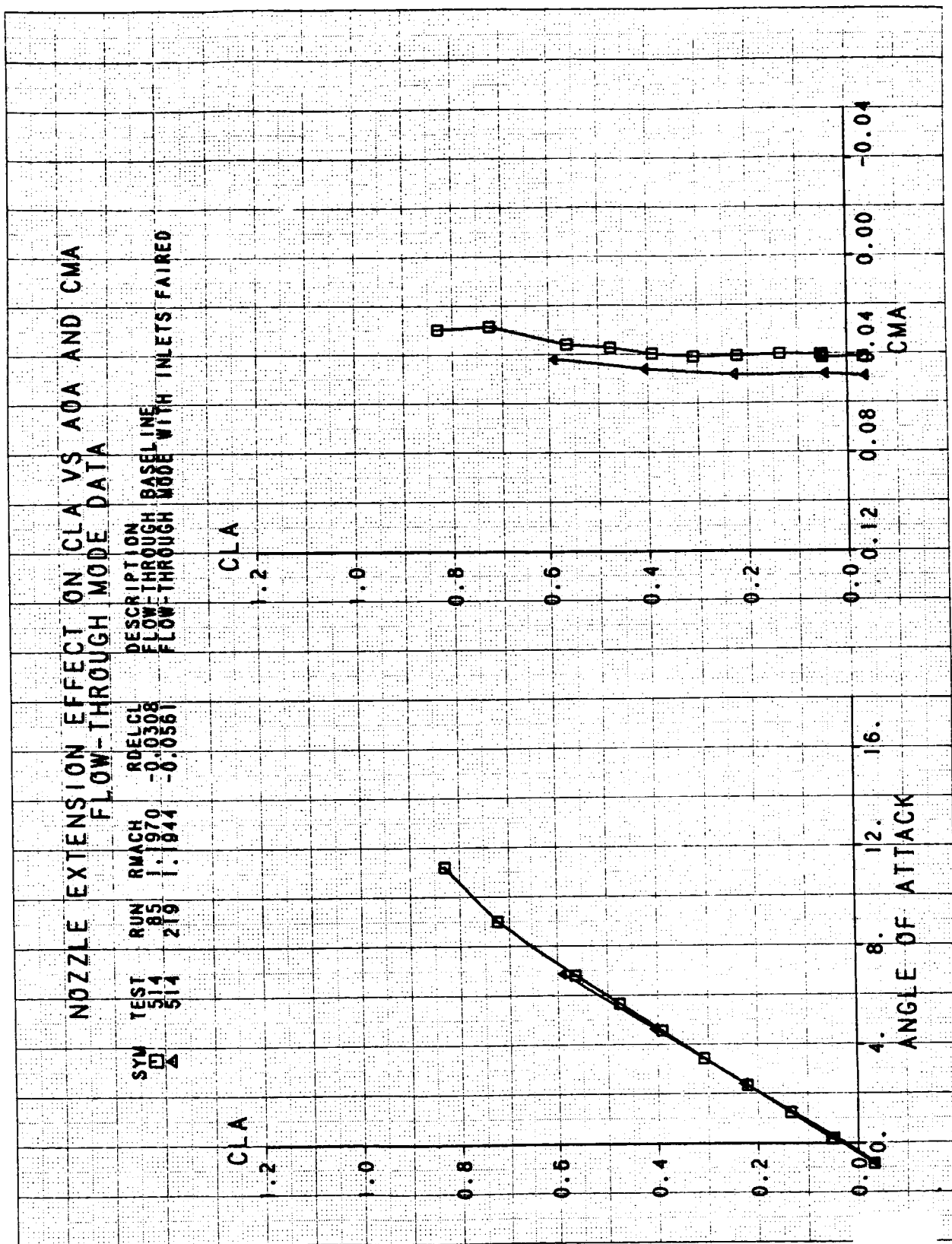


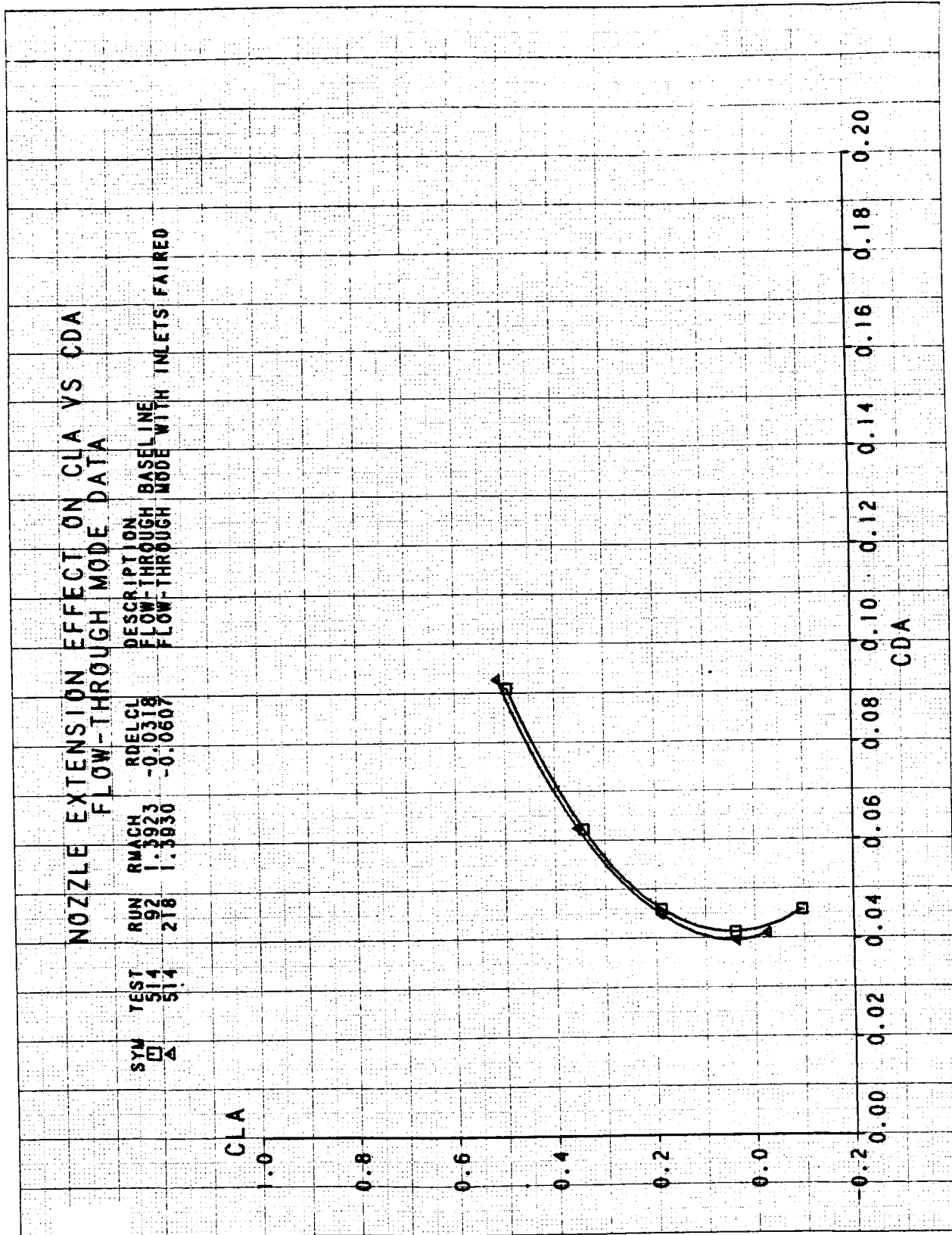








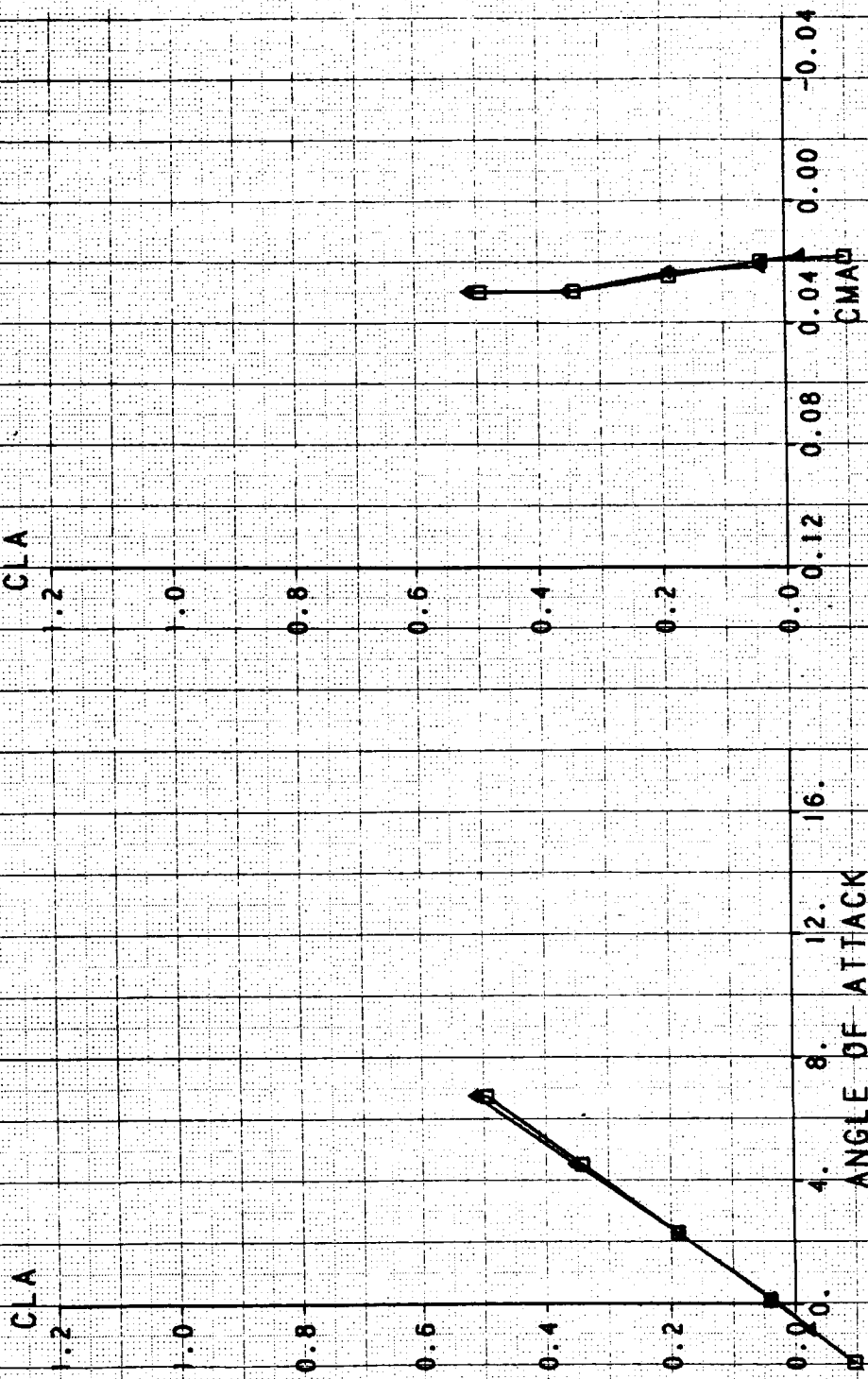




NOZZLE EXTENSION EFFECT ON CLA VS AOA AND CMA

FLOW-THROUGH MODE DATA

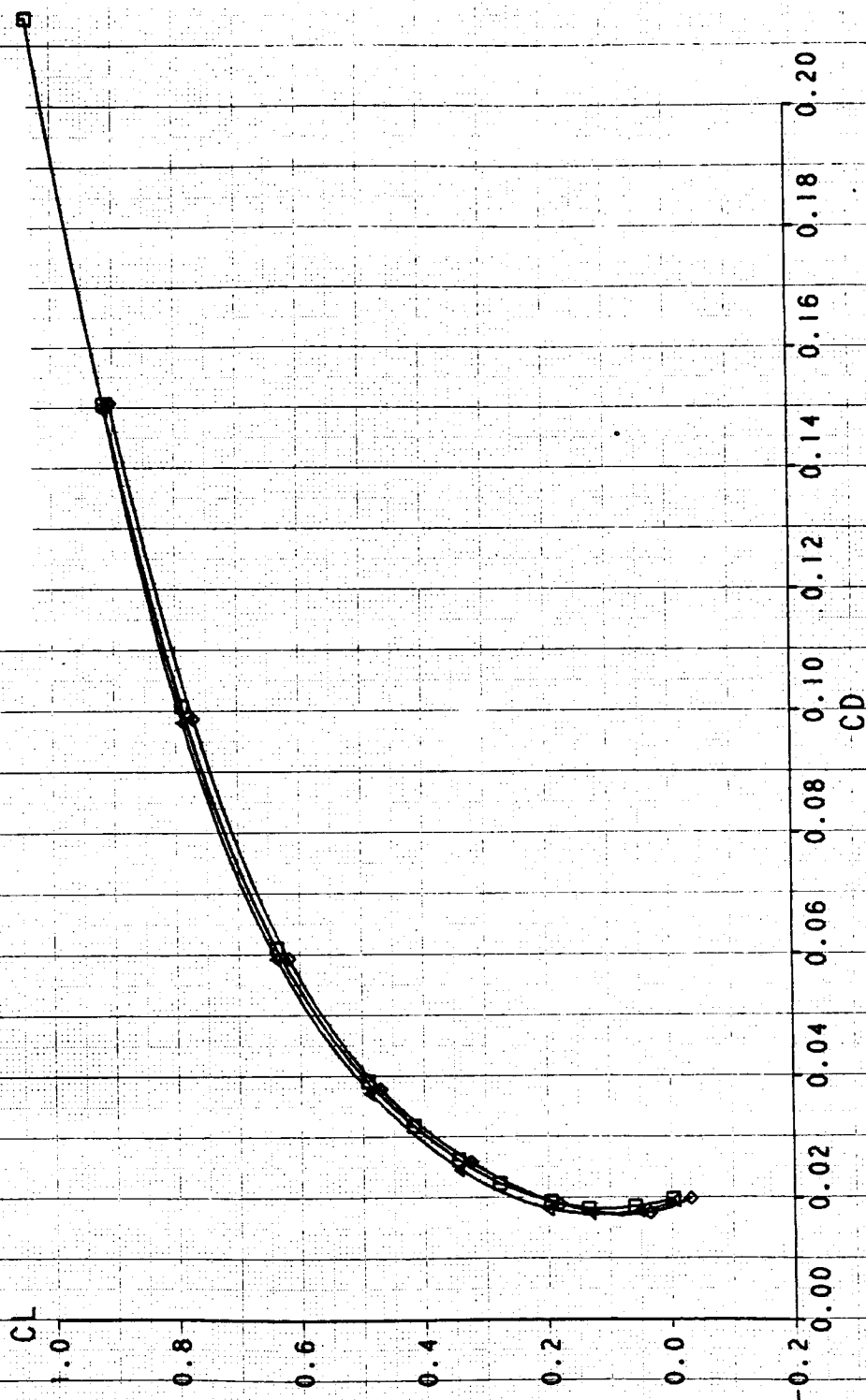
| SYM | TEST | RUN | RMACH | RDELCL | DESCRIPTION |
|-----|------|-----|--------|---------|--------------------------------------|
| □ | 514 | 92 | 1.3923 | -0.0318 | FLOW-THROUGH BASELINE |
| △ | 514 | 218 | 1.3930 | -0.0607 | FLOW-THROUGH MODE WITH INLETS FAIRED |

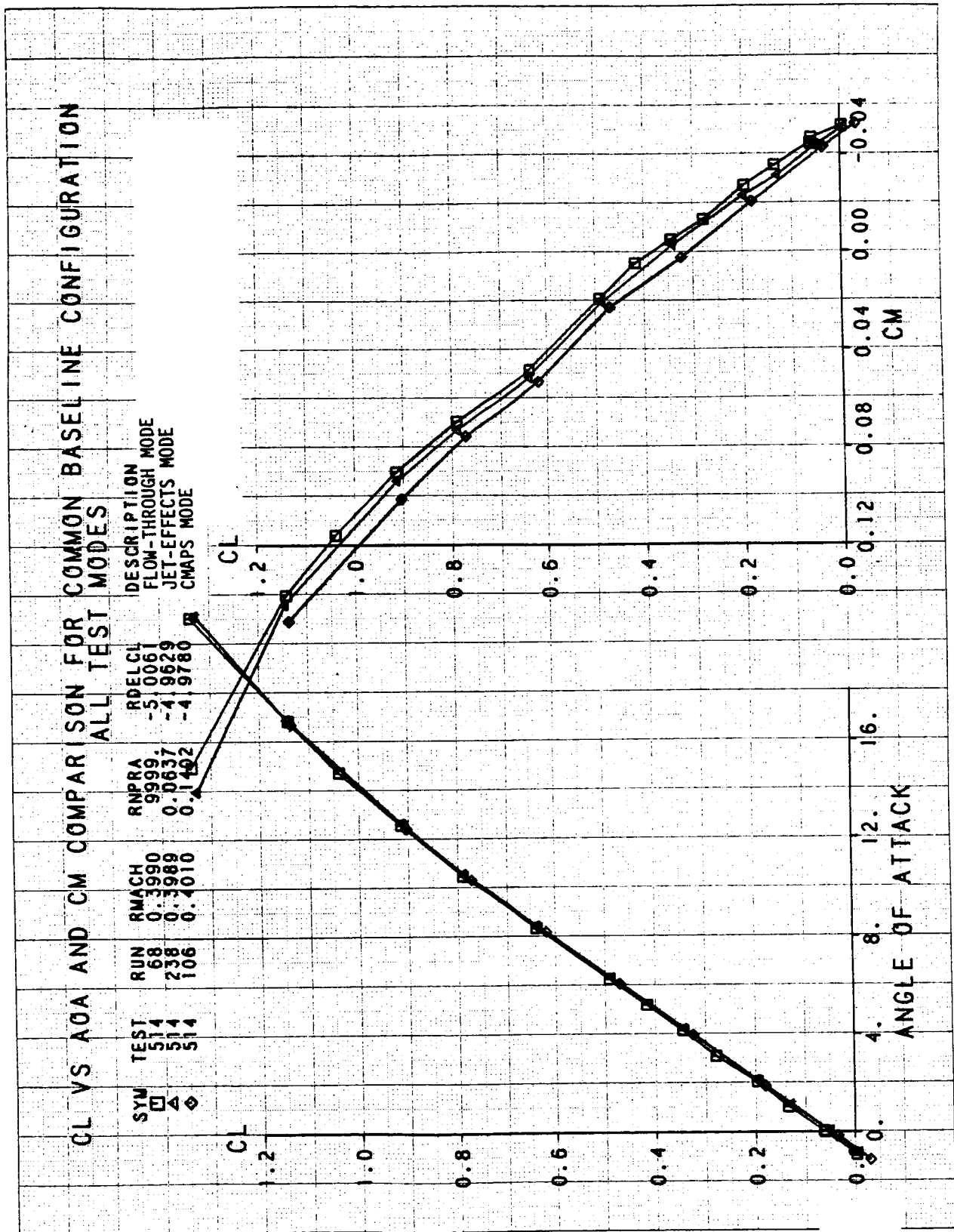


DRAG POLAR COMPARISON FOR COMMON BASELINE CONFIGURATION

ALL TEST MODES

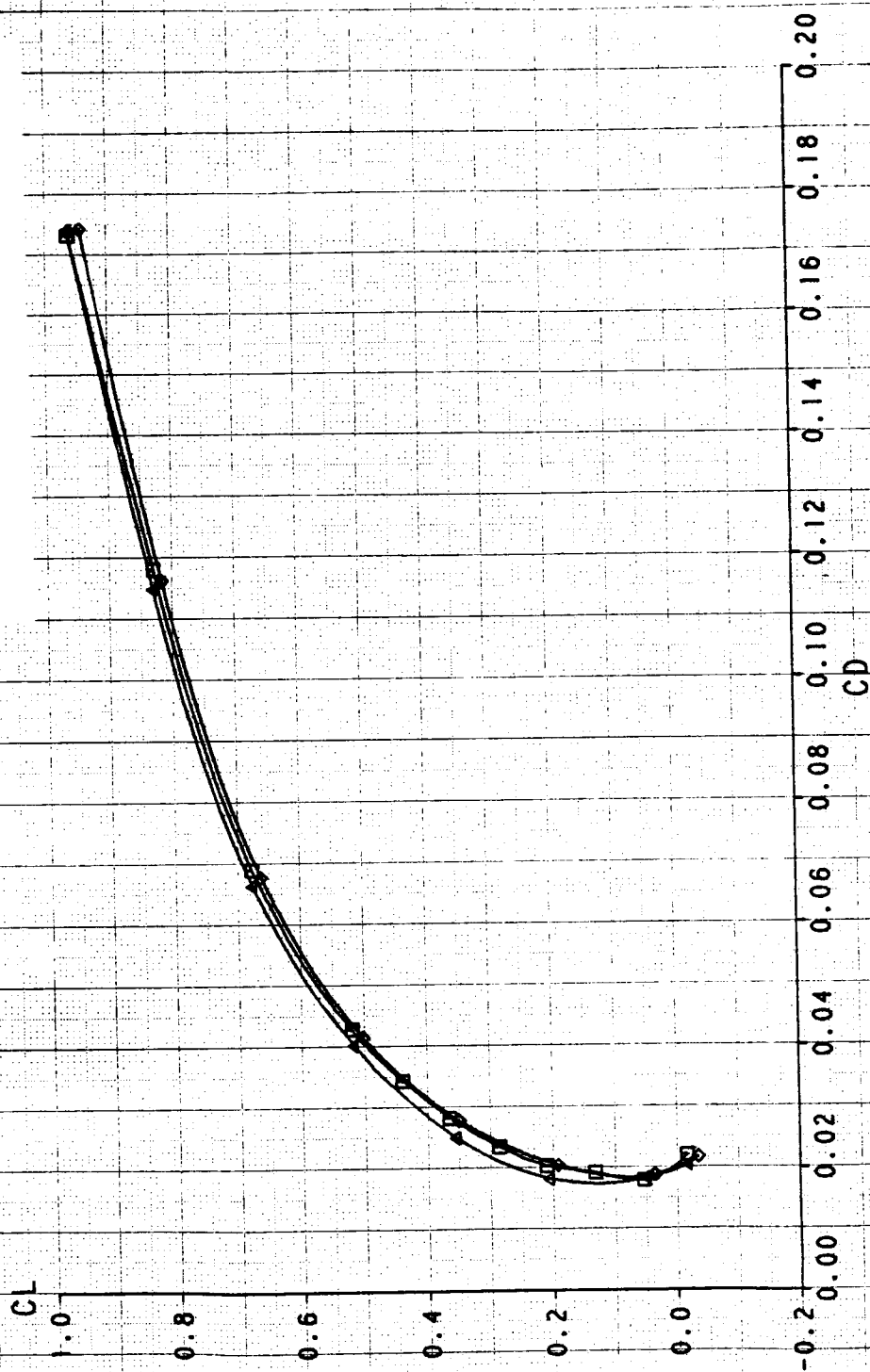
| SYM | TEST | RUN | RMACH | RNPRA | RDELCL | DESCRIPTION |
|-----|------|-----|--------|--------|---------|-------------------|
| □ | 514 | 68 | 0.3990 | 9999 | -5.0061 | FLOW-THROUGH MODE |
| △ | 514 | 238 | 0.3989 | 0.0637 | -4.9529 | JET-EFFECTS MODE |
| ◇ | 514 | 106 | 0.4010 | 0.1402 | -4.9780 | CWAPS MODE |



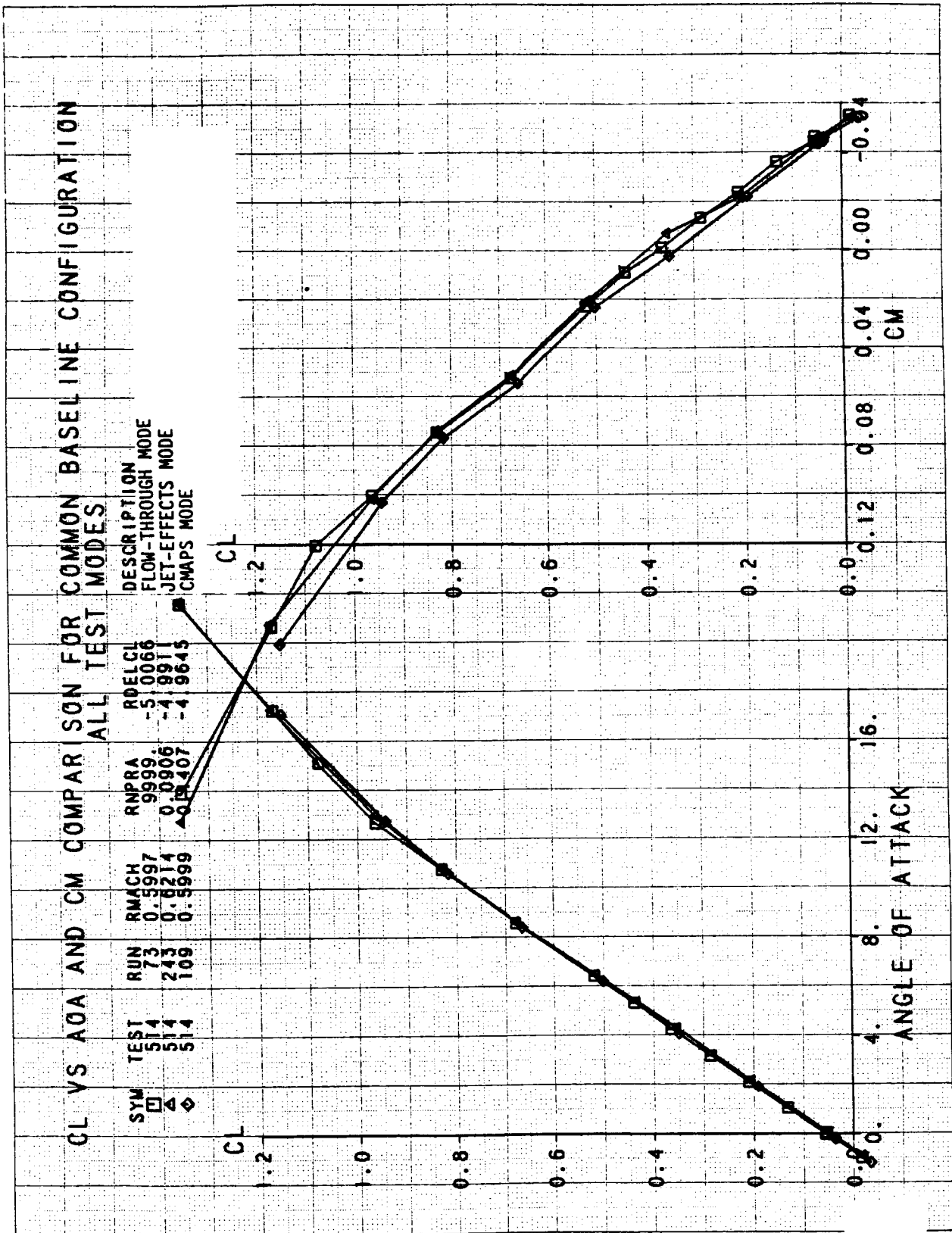


DRAG POLAR COMPARISON FOR COMMON BASELINE CONFIGURATION ALL TEST MODES

| SYM | TEST | RUN | RMACH | RNPRA | RDELCL | DESCRIPTION |
|-----|------|-----|--------|--------|---------|-------------------|
| □ | 514 | 73 | 0.5997 | 9999 | -5.0066 | FLOW-THROUGH MODE |
| △ | 514 | 243 | 0.6214 | 0.0906 | -4.9911 | JET-EFFECTS MODE |
| ◇ | 514 | 109 | 0.5999 | 0.1407 | -4.9645 | CWAPS MODE |



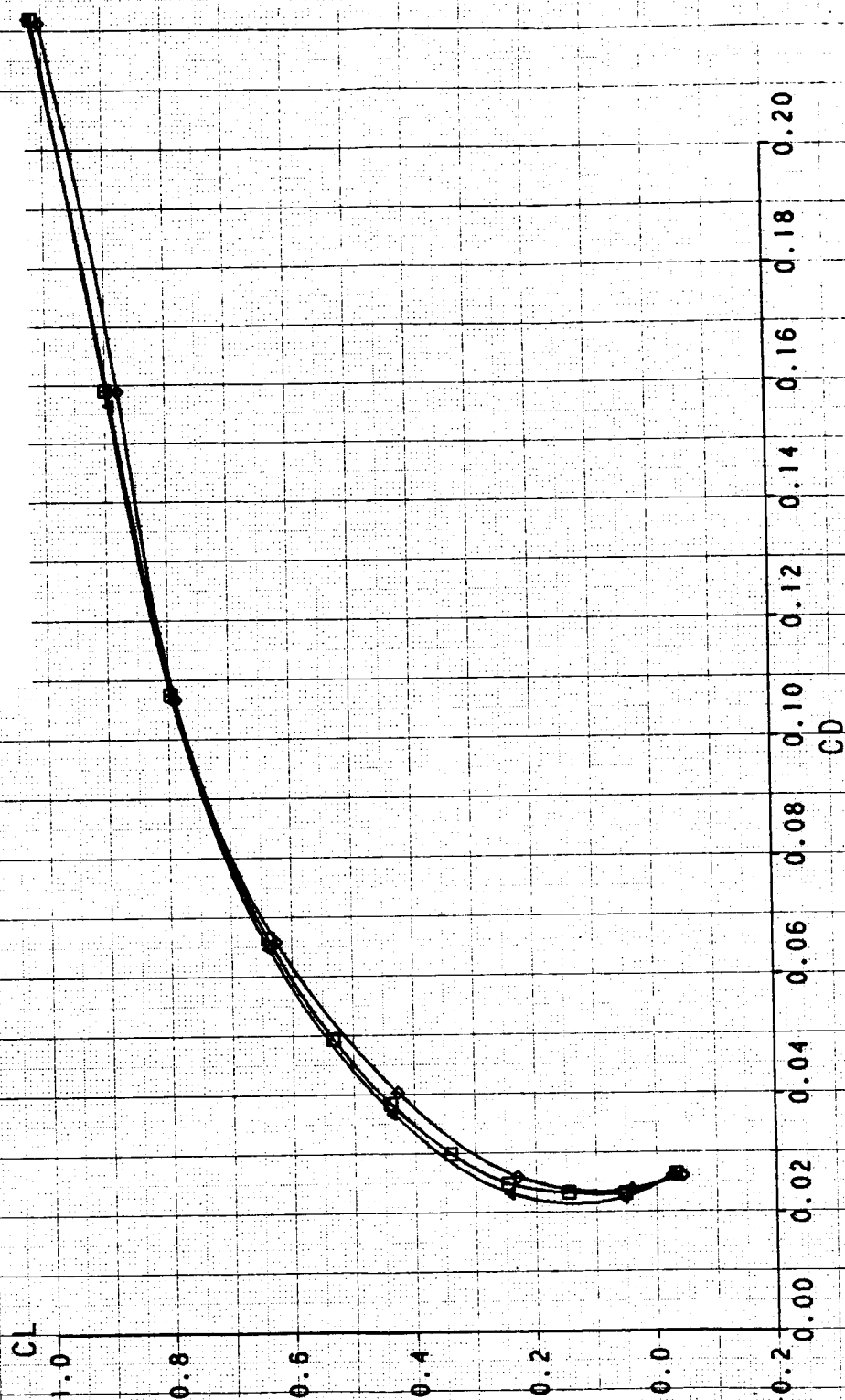
ORIGINAL PAGE IS
OF POOR QUALITY



DRAG POLAR COMPARISON FOR COMMON BASELINE CONFIGURATION

ALL TEST MODES

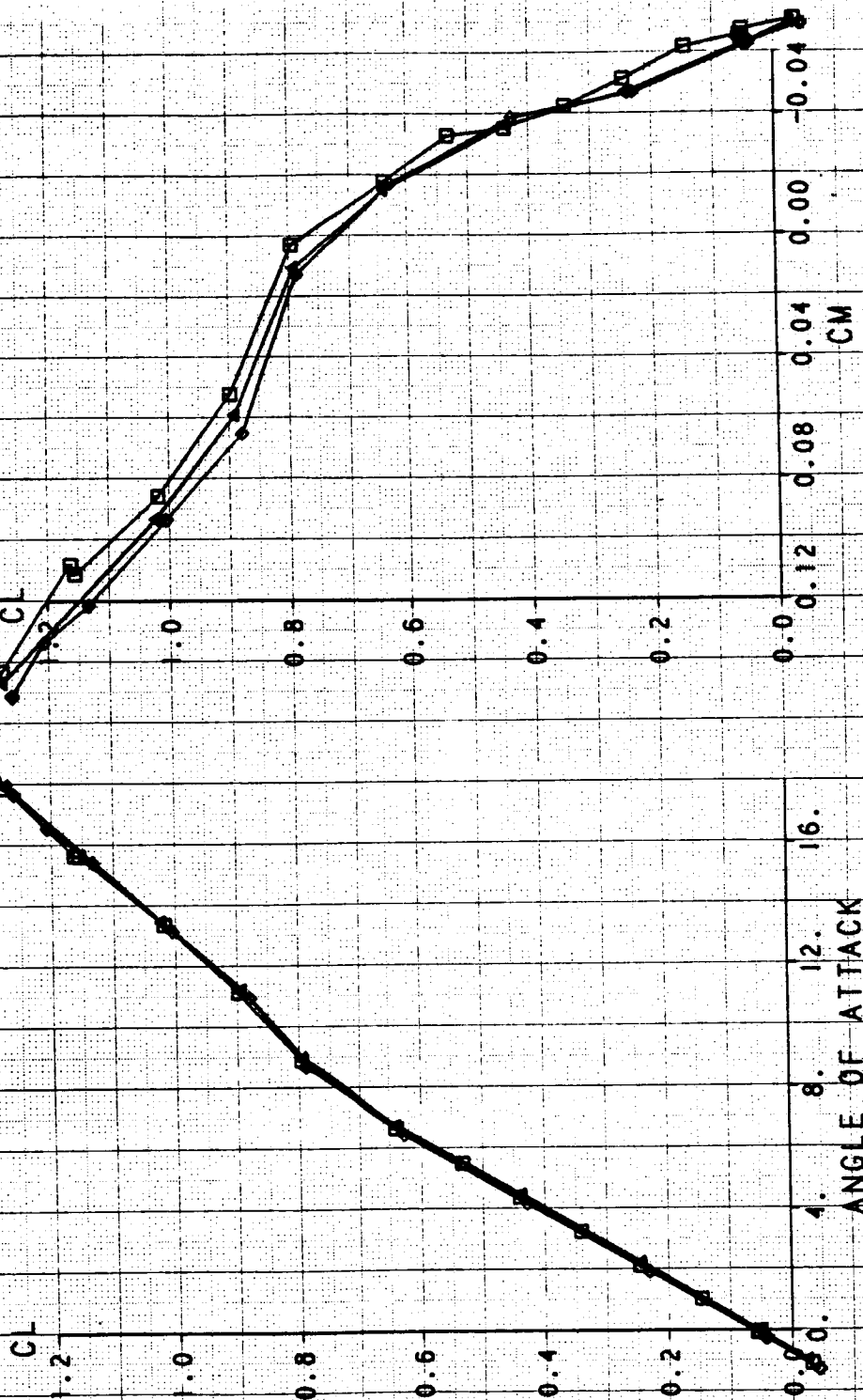
| SYM | TEST | RUN | RMACH | RNPRA | RDELCL | DESCRIPTION |
|-----|------|-----|--------|--------|---------|-------------------|
| □ | 514 | 79 | 0.9018 | 9999. | -5.0632 | FLOW-THROUGH MODE |
| △ | 514 | 244 | 0.9022 | 0.1384 | -4.9674 | JET-EFFECTS MODE |
| ◇ | 514 | 110 | 0.8980 | 0.1426 | -4.9715 | CMAPS MODE |



CL VS AOA AND CM COMPARISON FOR COMMON BASELINE CONFIGURATION

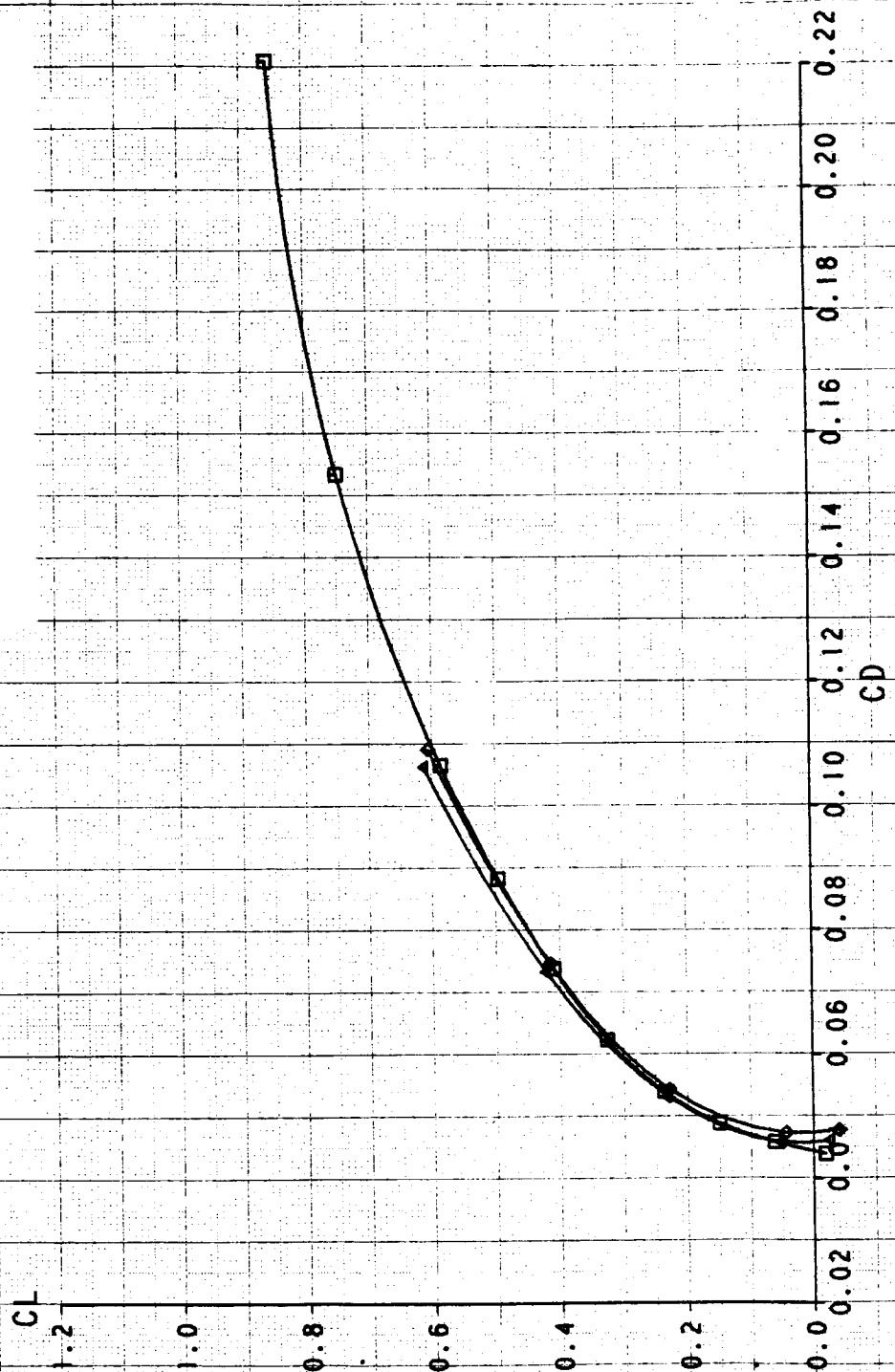
ALL TEST MODES

| SYM | TEST | RUN | RMACH | RNPRA | ROELCL | DESCRIPTION |
|-----|------|-----|--------|--------|---------|-------------------|
| □ | 514 | 79 | 0.9018 | 9999. | -5.0632 | FLOW-THROUGH MODE |
| △ | 514 | 244 | 0.9022 | 0.1384 | -4.8674 | JET-EFFECTS MODE |
| ◇ | 514 | 110 | 0.8980 | 0.1126 | -0.0715 | CHAPS MODE |



DRAG POLAR COMPARISON FOR COMMON BASELINE CONFIGURATION ALL TEST MODES

| SYM | TEST | RUN | RMACH | RNPRA | RDELCL | DESCRIPTION |
|-----|------|-----|--------|--------|---------|-------------------|
| □ | 514 | 85 | 1.1970 | 9999 | -0.0308 | FLOW-THROUGH MODE |
| △ | 514 | 245 | 1.1772 | 0.1893 | -0.1056 | JET-EFFECTS MODE |
| ◇ | 514 | 111 | 1.1659 | 0.1145 | 0.1546 | CNAPS MODE |

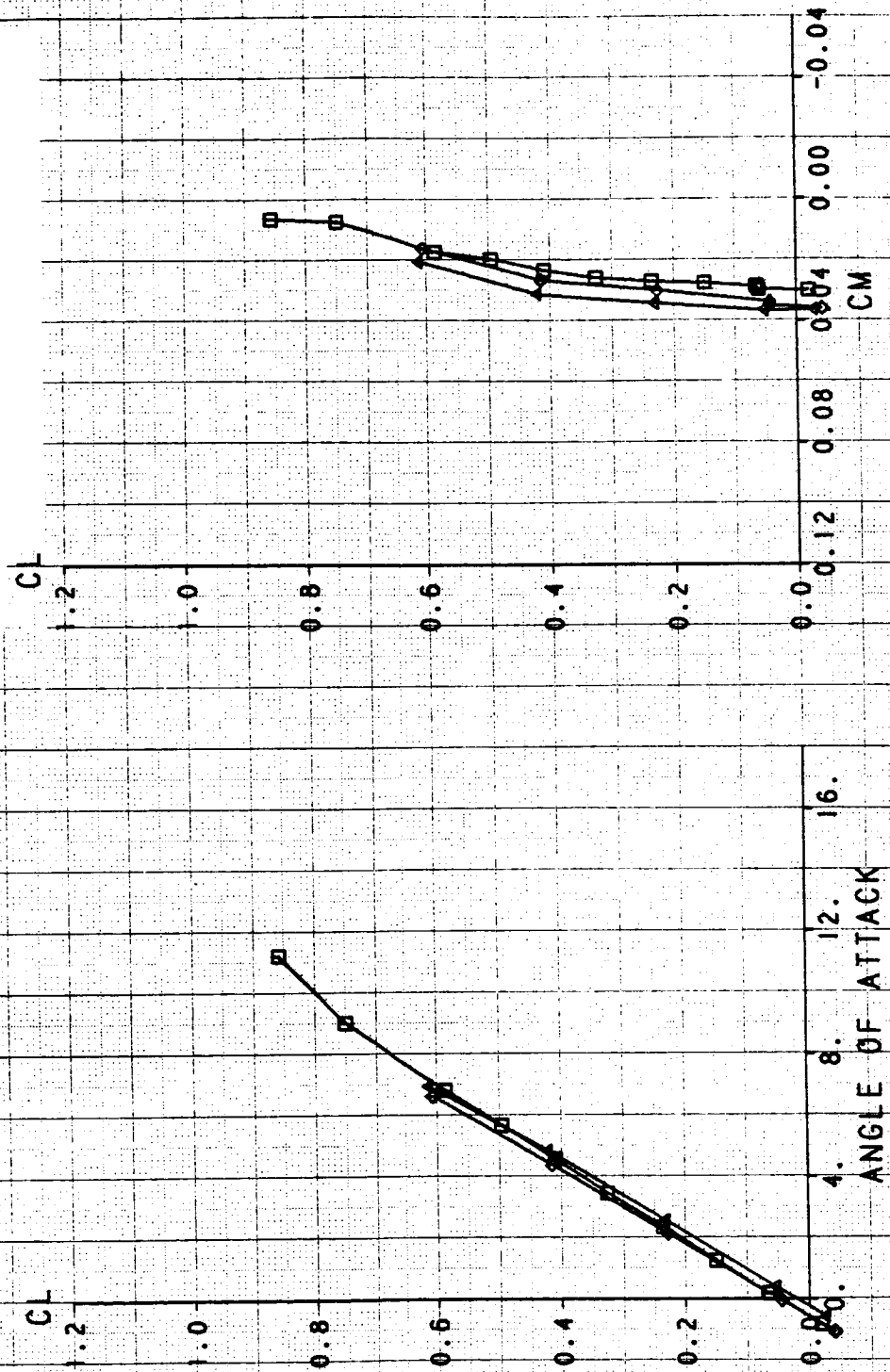


ORIGINAL PAGE IS
OF POOR QUALITY

CL VS AOA AND CM COMPARISON FOR COMMON BASELINE CONFIGURATION

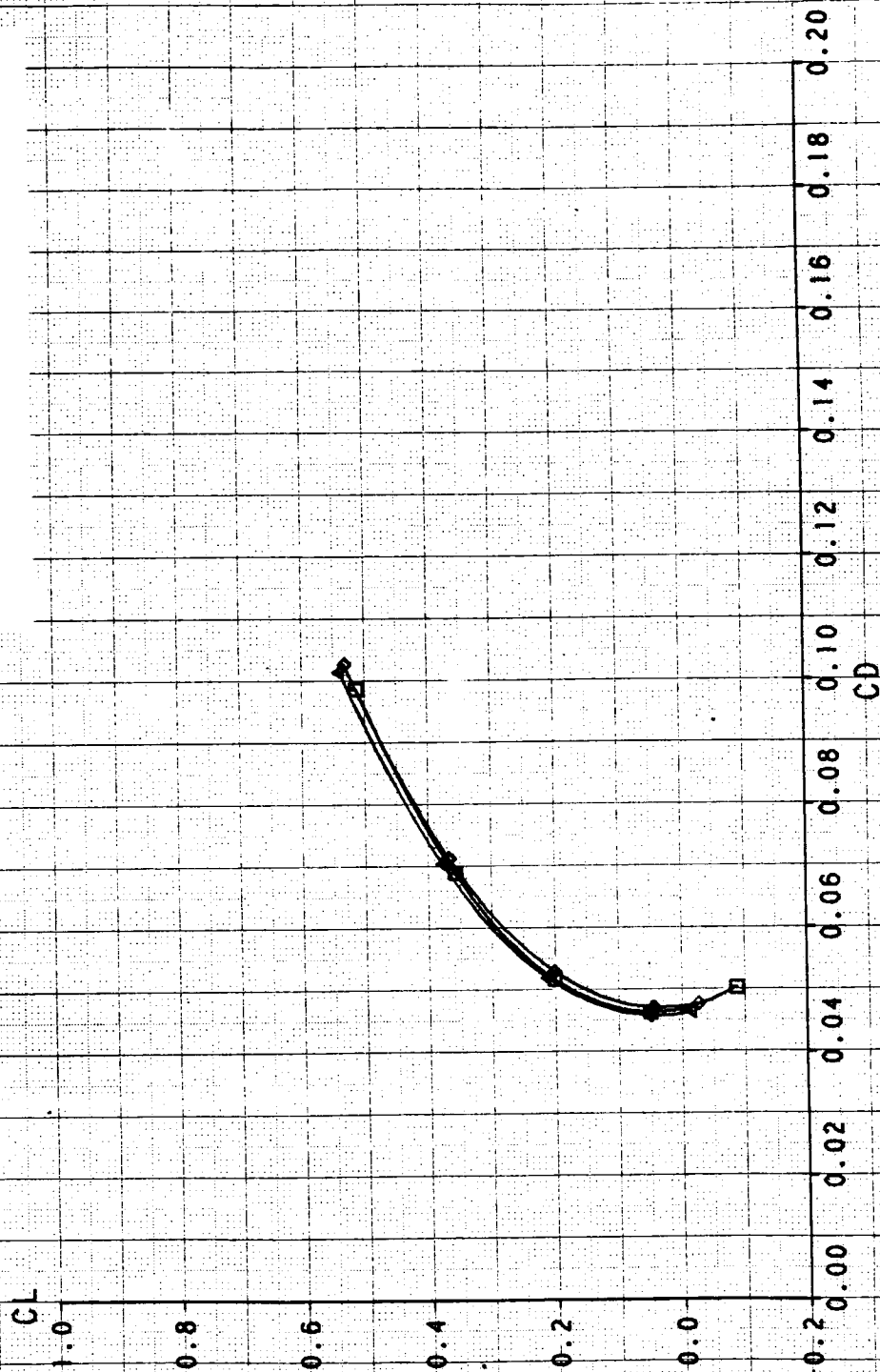
ALL TEST MODES

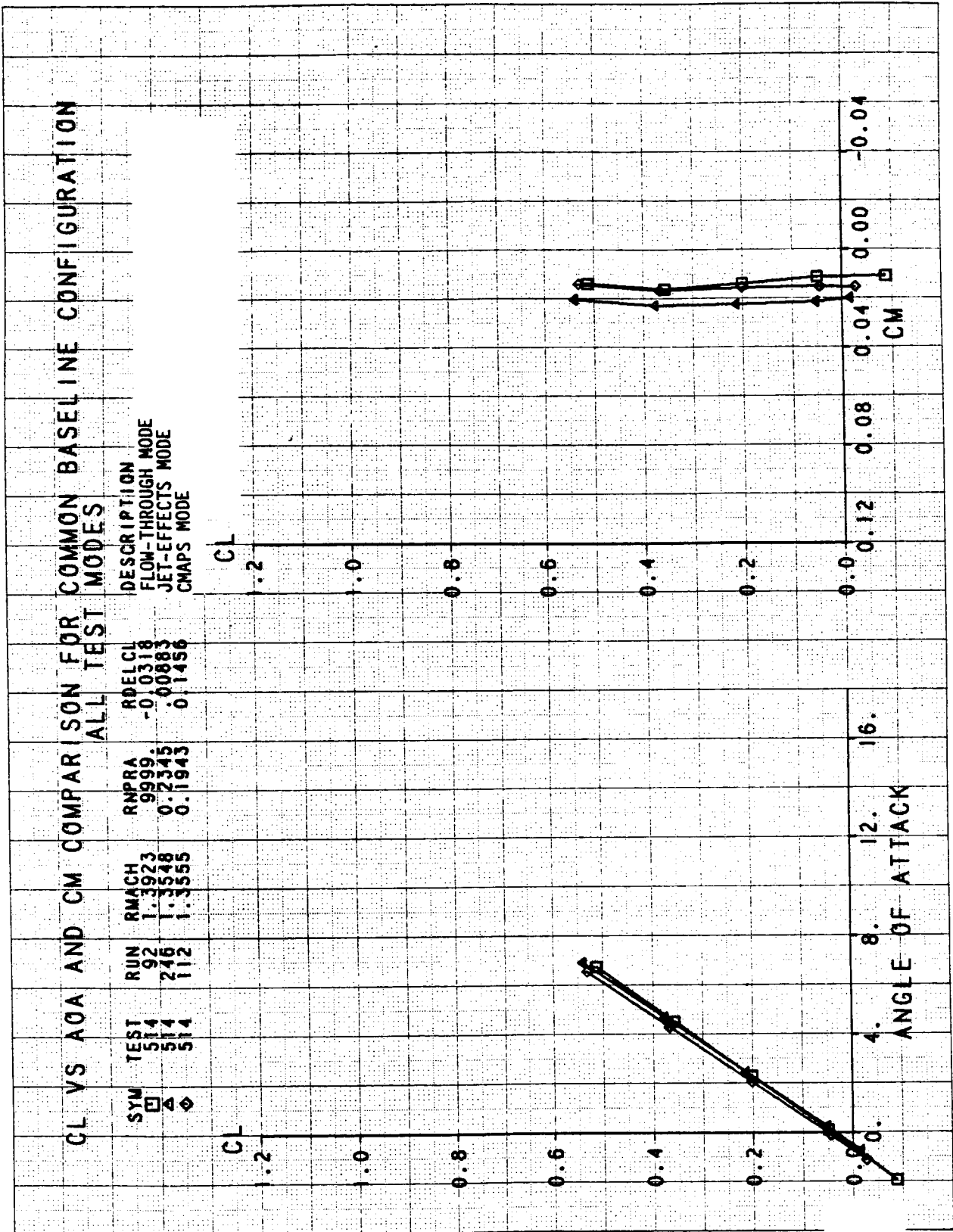
| SYM | TEST | RUN | RMACH | RNPRA | RDELCL | DESCRIPTION |
|-----|------|-----|--------|--------|----------|-------------------|
| □ | 514 | 85 | 1.1970 | 9999 | -0.10308 | FLOW-THROUGH MODE |
| △ | 514 | 245 | 1.1772 | 0.1893 | -0.1056 | JET-EFFECTS MODE |
| ◇ | 514 | 111 | 1.1659 | 0.1145 | 0.11546 | CMAPS MODE |

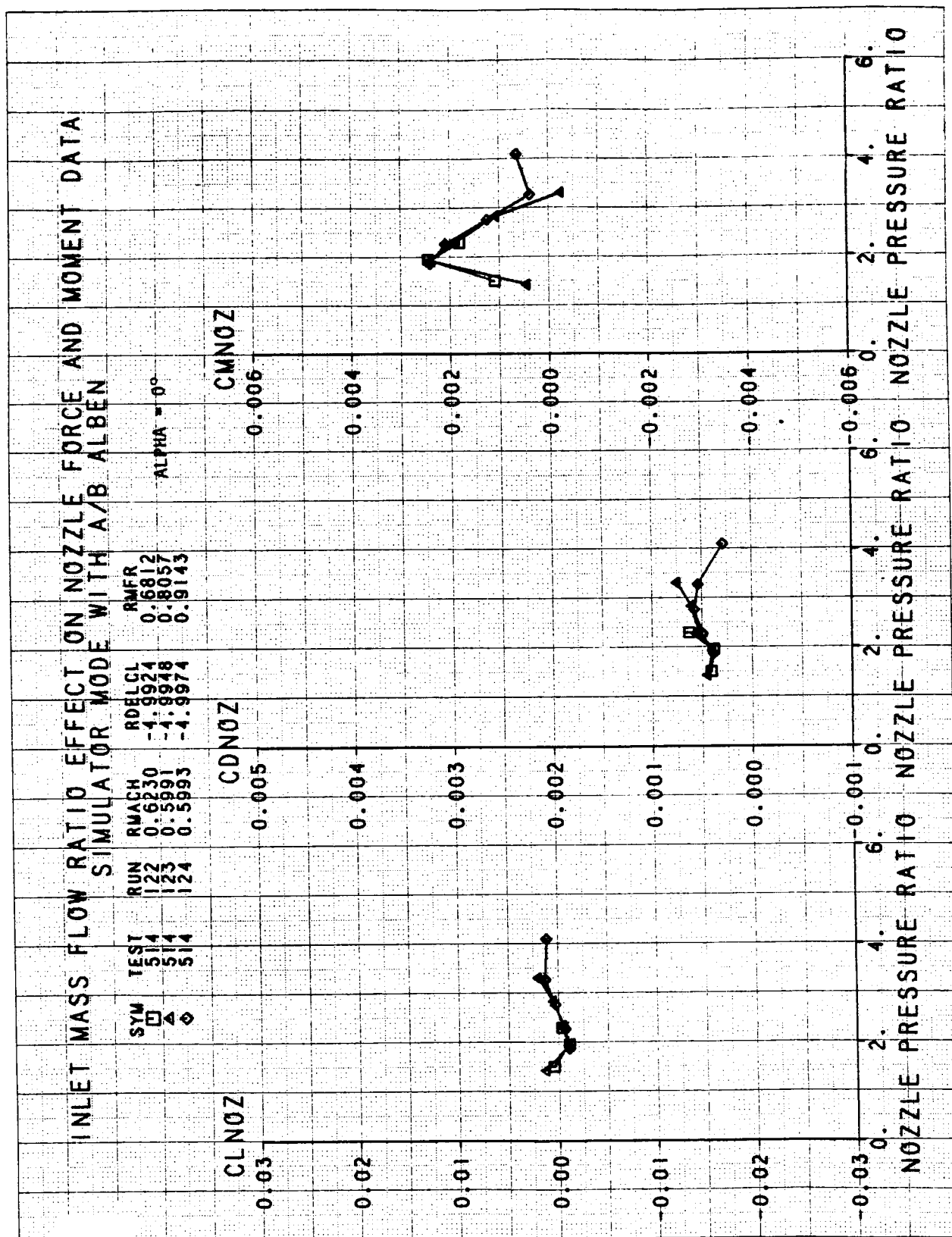


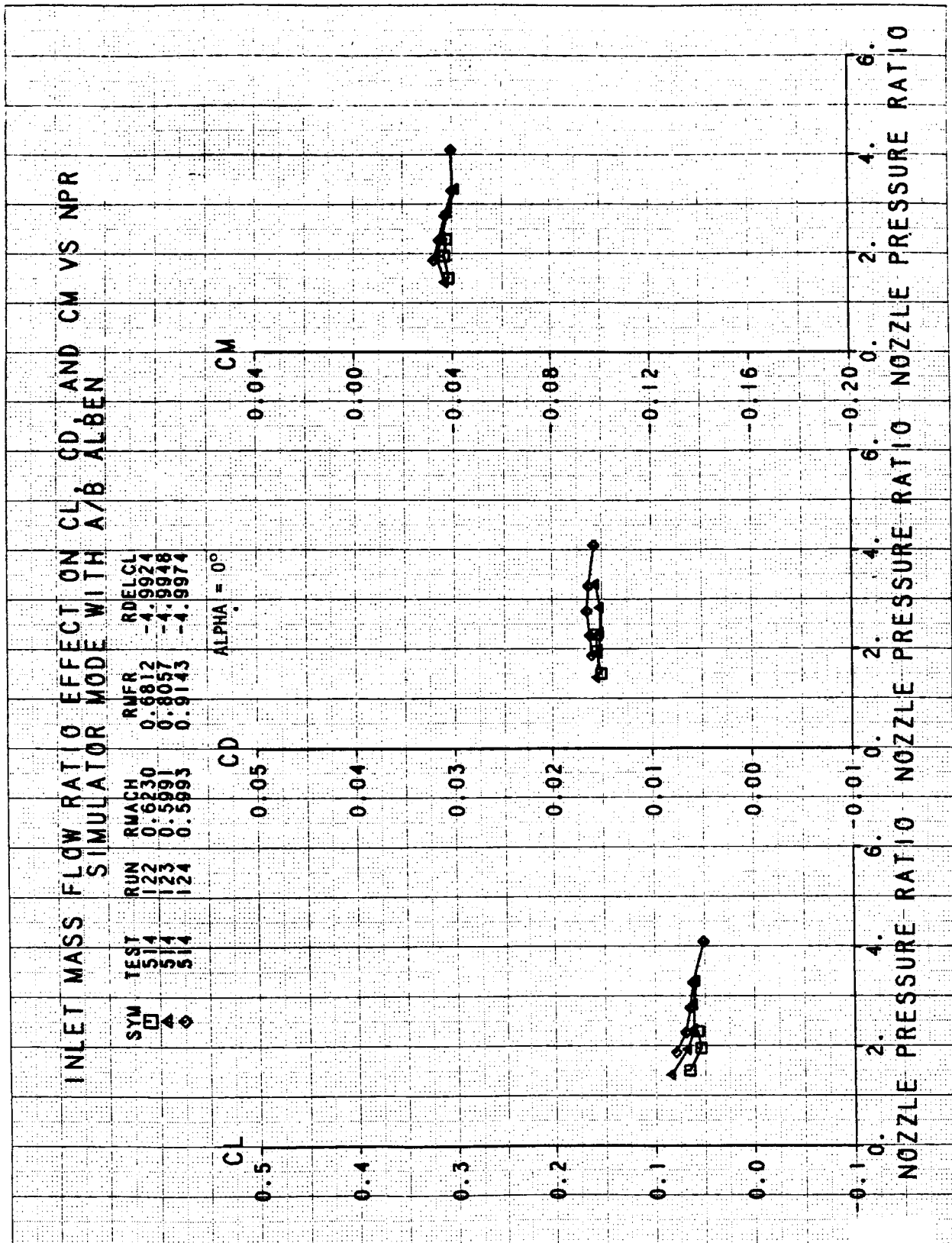
DRAG POLAR COMPARISON FOR COMMON BASELINE CONFIGURATION

| SYM | TEST | RUN | RMACH | RNPRA | RDELCL | DESCRIPTION |
|-----|------|-----|--------|--------|---------|-------------------|
| □ | 514 | 92 | 1.3923 | 9999 | -0.0318 | FLOW-THROUGH MODE |
| △ | 514 | 246 | 1.3518 | 0.2345 | -0.0883 | JET-EFFECTS MODE |
| ◇ | 514 | 112 | 1.3555 | 0.1943 | 0.1456 | CMAPS MODE |





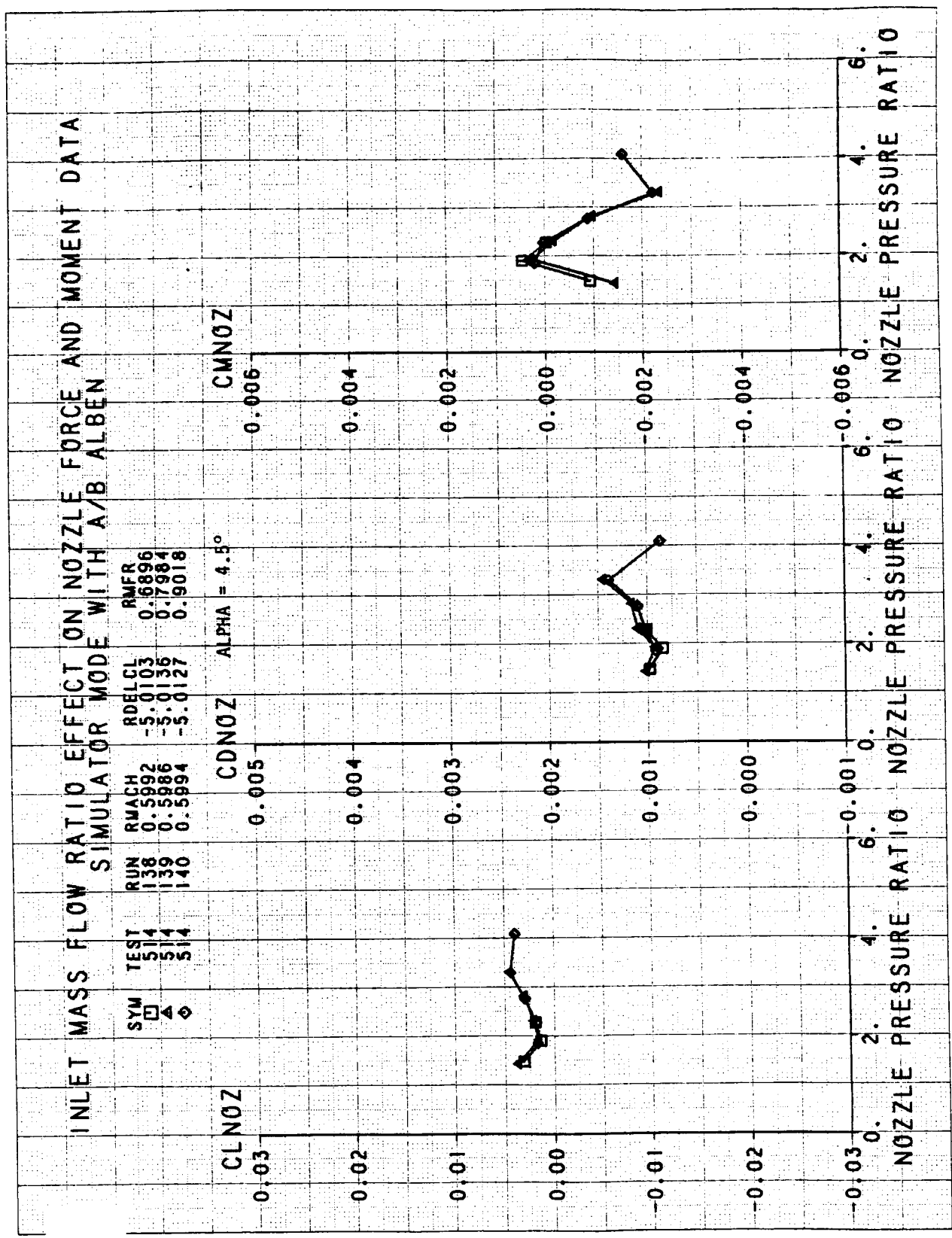


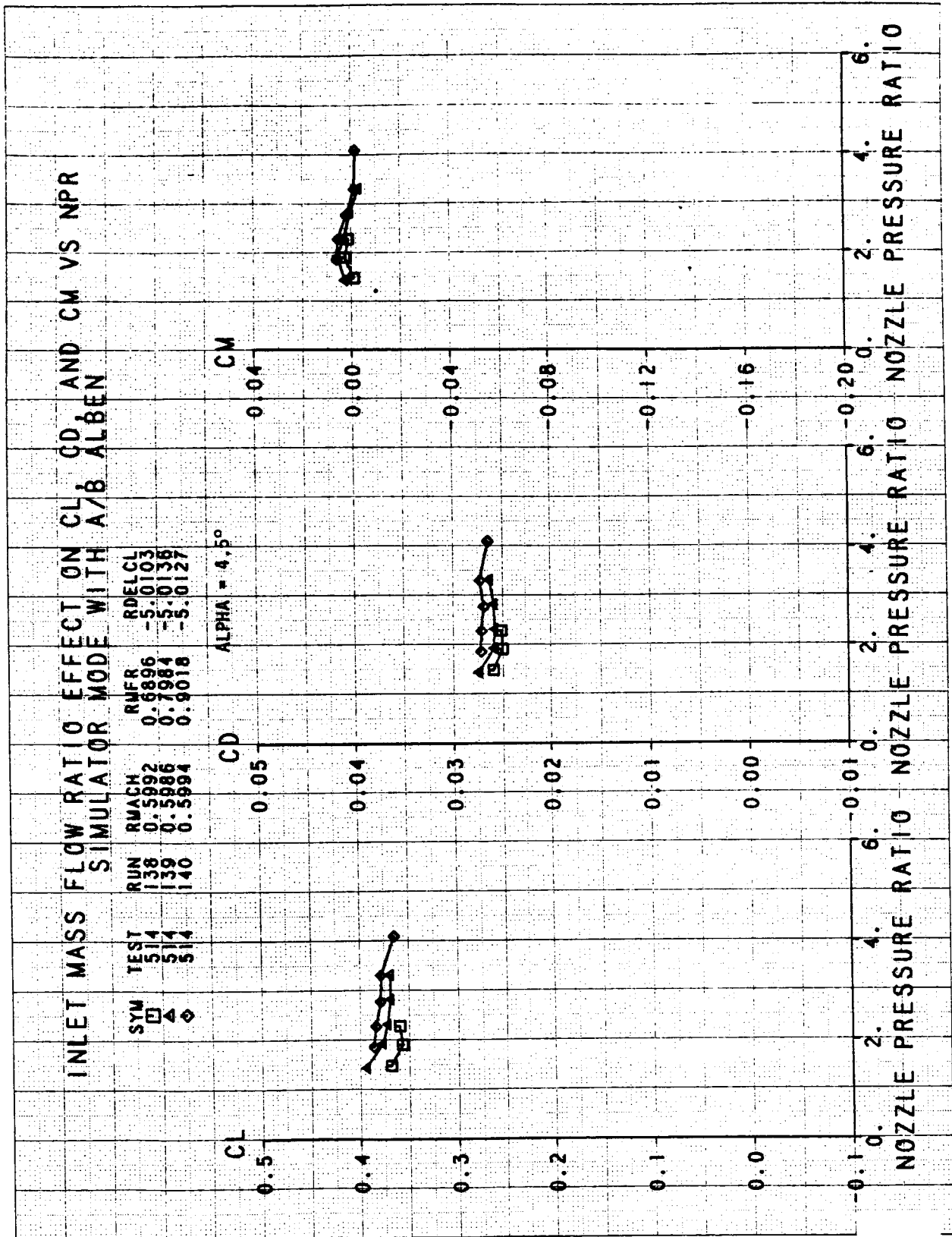


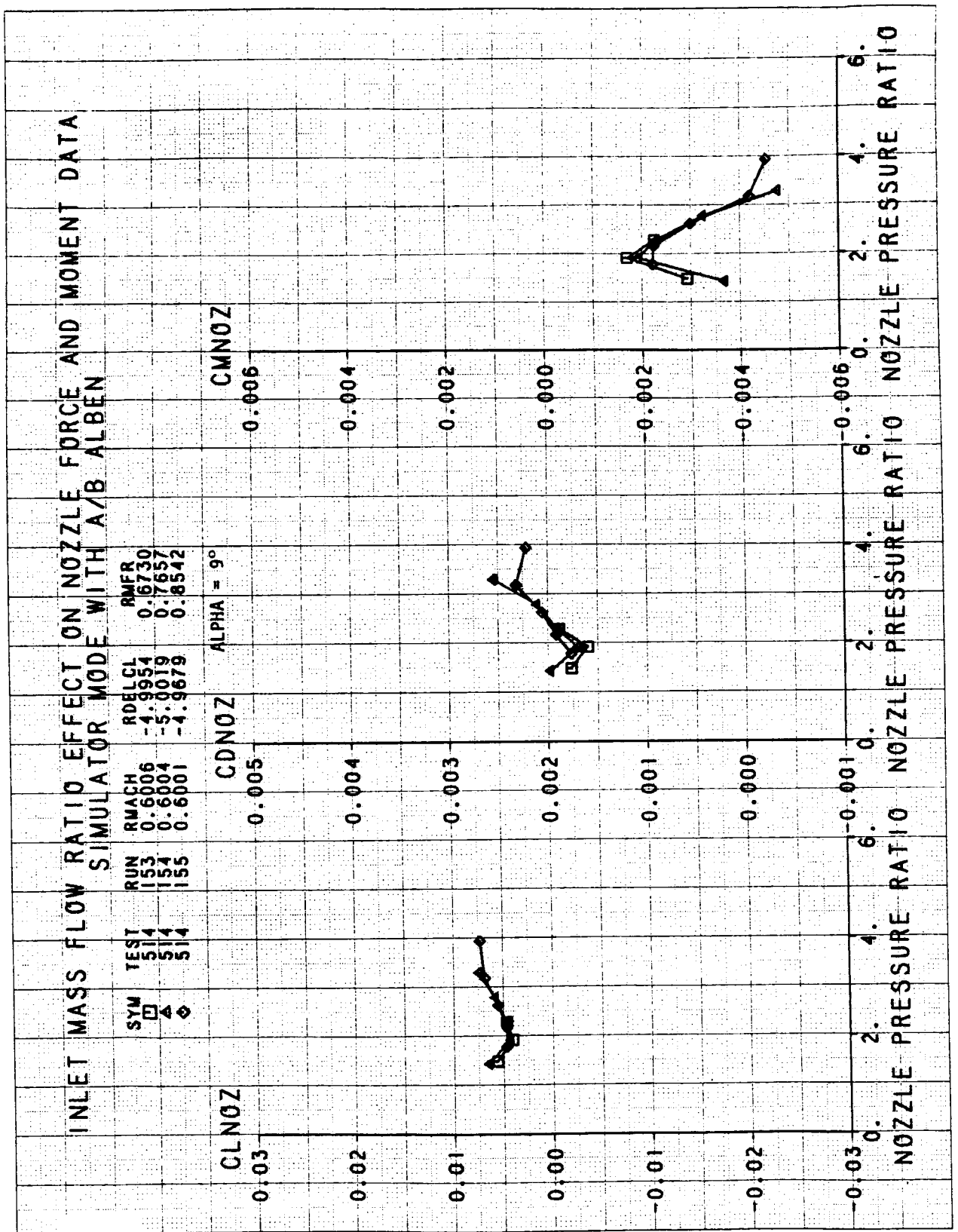
INLET MASS FLOW RATIO EFFECT ON NOZZLE FORCE AND MOMENT DATA SIMULATOR MODE WITH A/B ALBEN

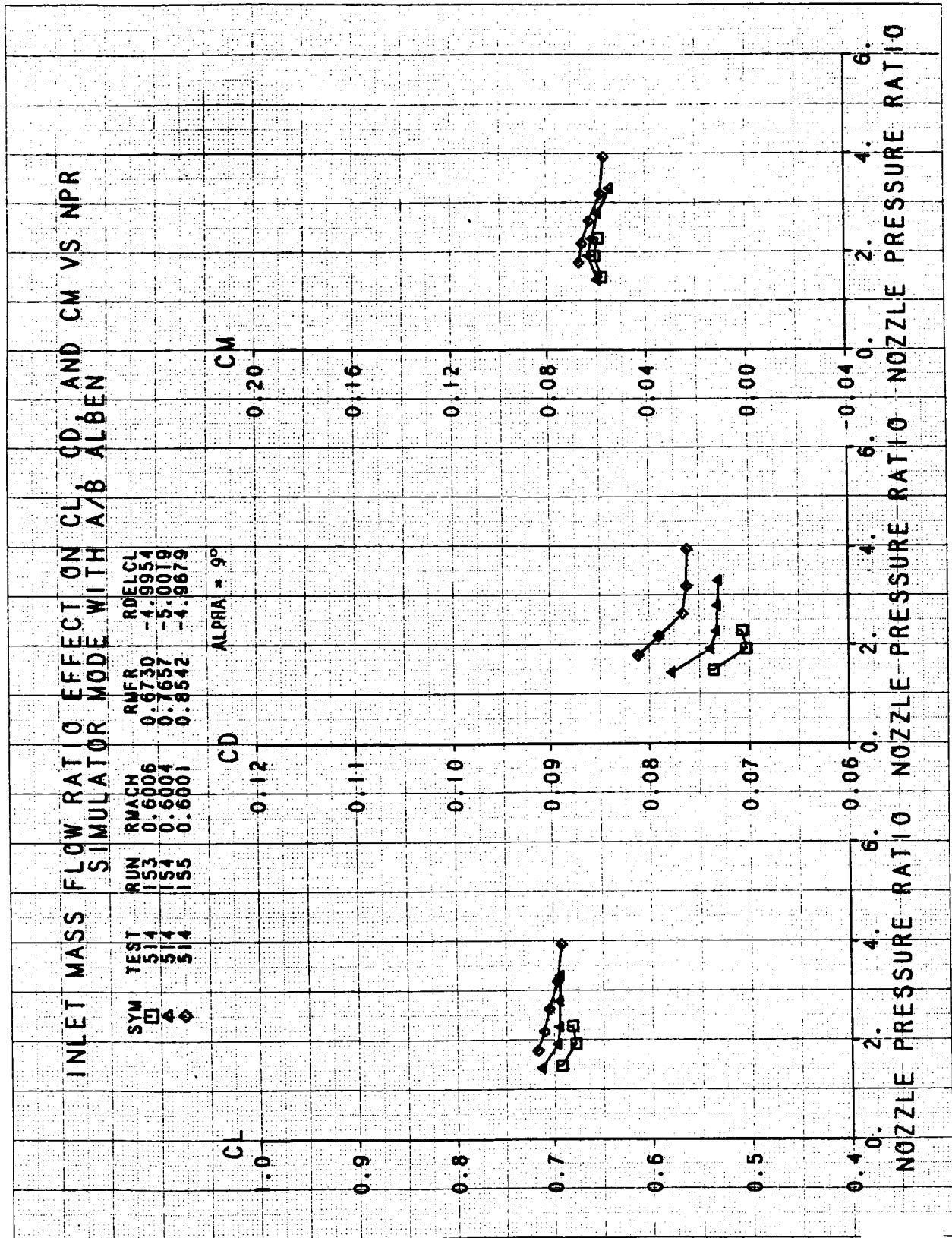
| SYM | TEST | RUN | RMACH | ROELCL | RMFR |
|-----|------|-----|--------|---------|--------|
| □ | 514 | 138 | 0.5992 | -5.0103 | 0.6896 |
| △ | 514 | 139 | 0.5986 | -5.0136 | 0.7984 |
| ◇ | 514 | 140 | 0.5994 | -5.0127 | 0.9018 |

CLNOZ CDNOZ CMNOZ ALPHA = 4.5°









INLET MASS FLOW RATIO EFFECT ON NOZZLE FORCE AND MOMENT DATA

SYMBOL TEST RUN RMACH RDELCL RMFR

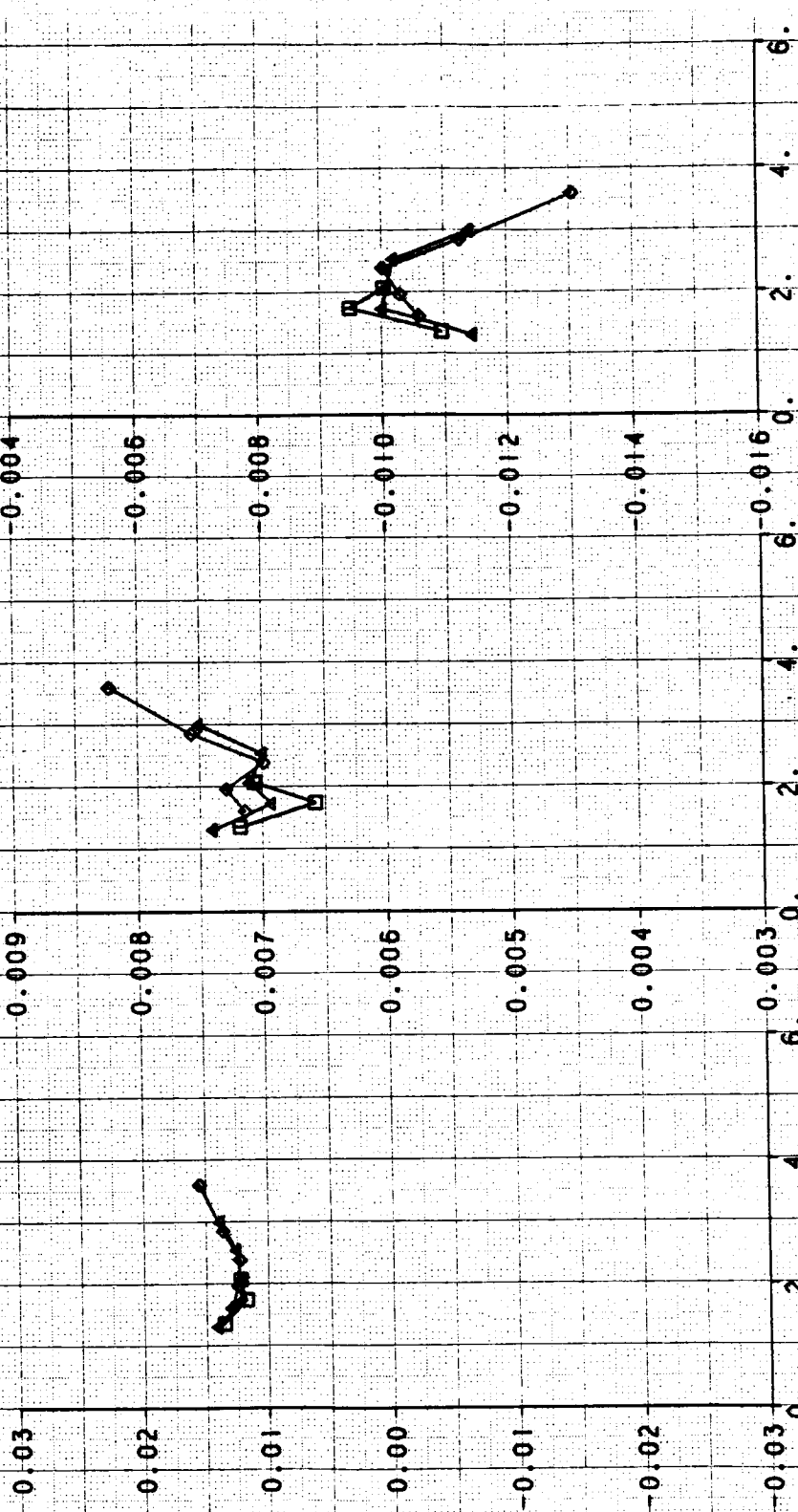
□ 514 167 0.6004 -4.9954 0.6097
 △ 514 168 0.6006 -4.9957 0.6843
 ◇ 514 169 0.6008 -5.0001 0.7554

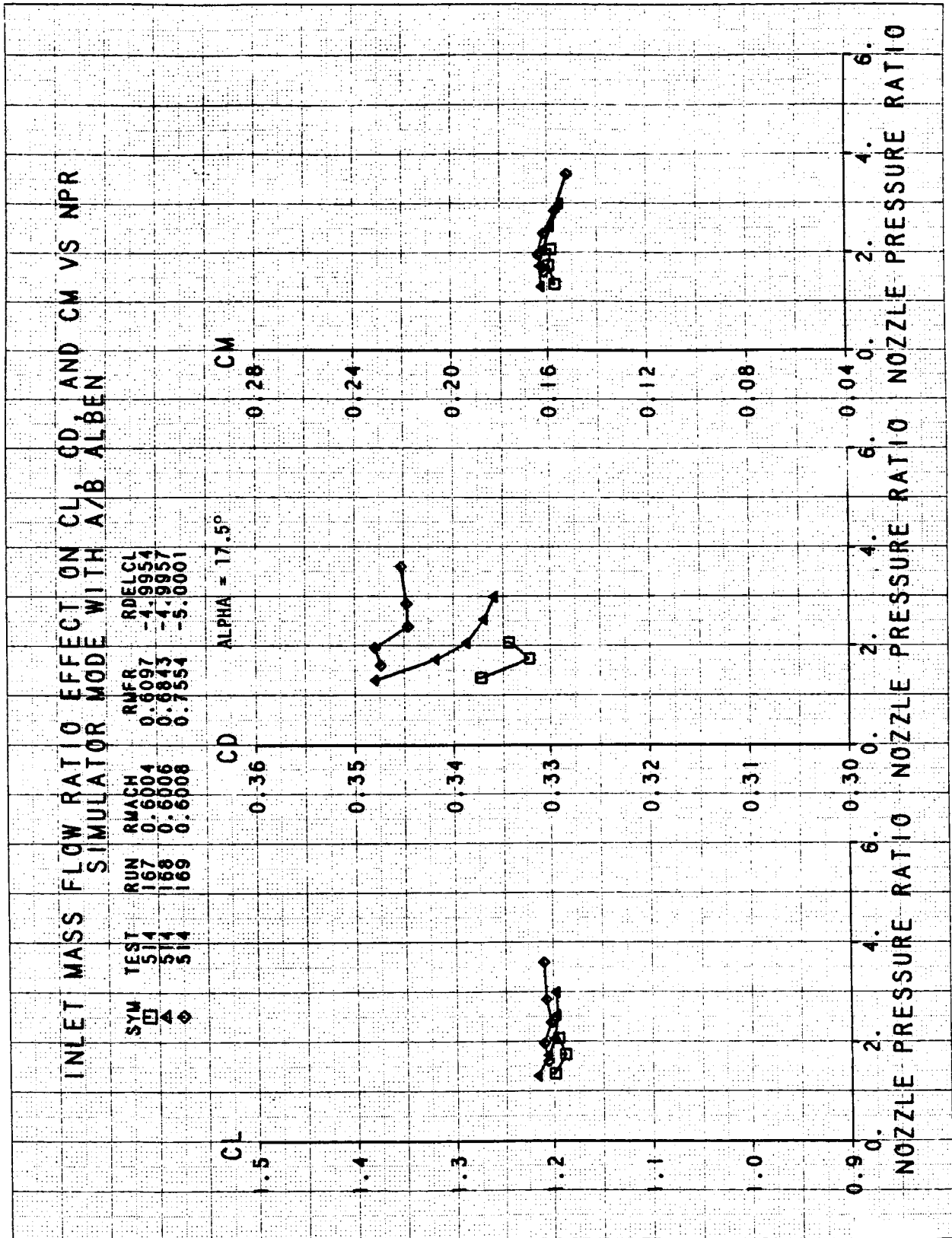
CLNOZ

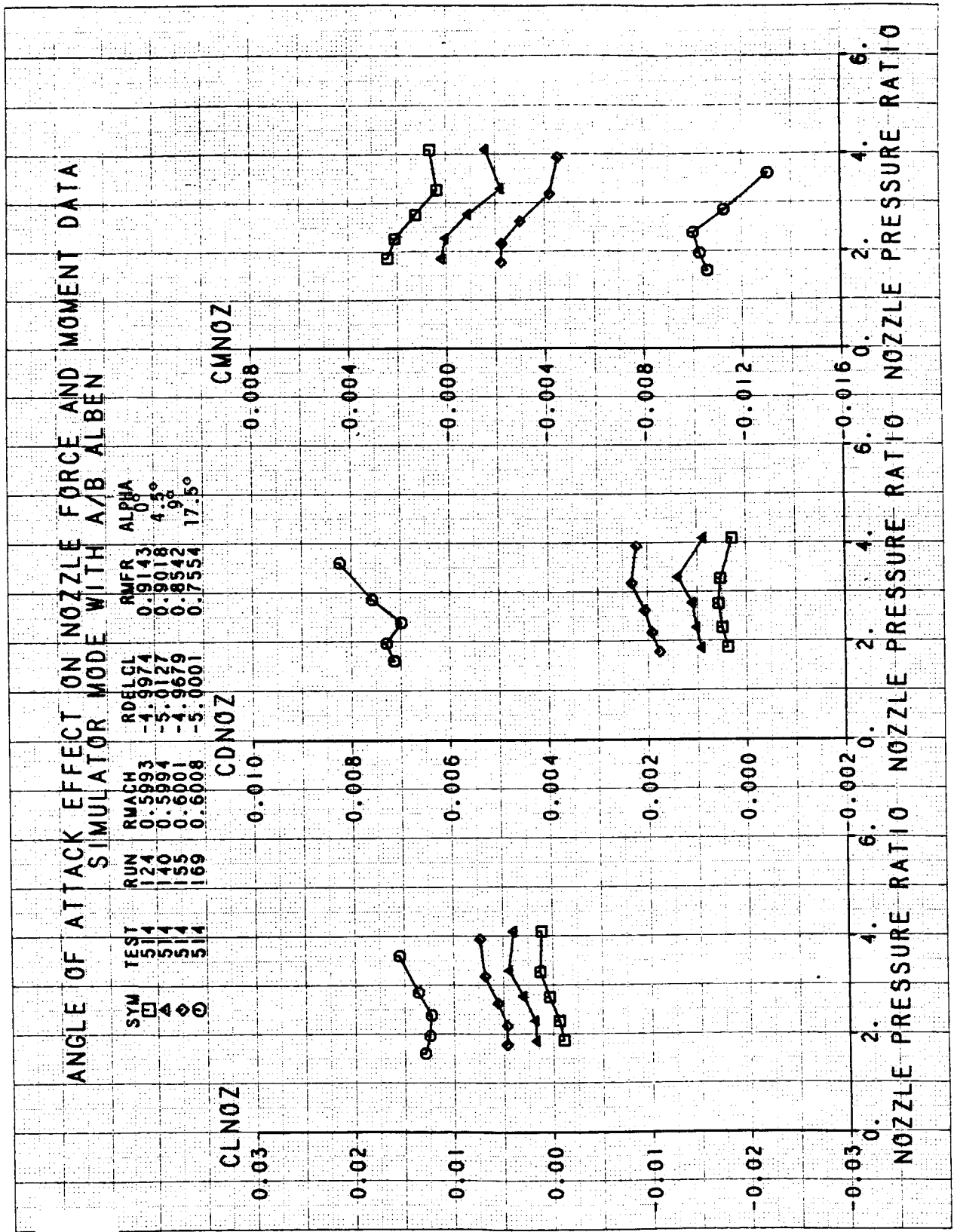
CDNOZ ALPHA = 17.5°

CMNOZ

NOZZLE PRESSURE RATIO

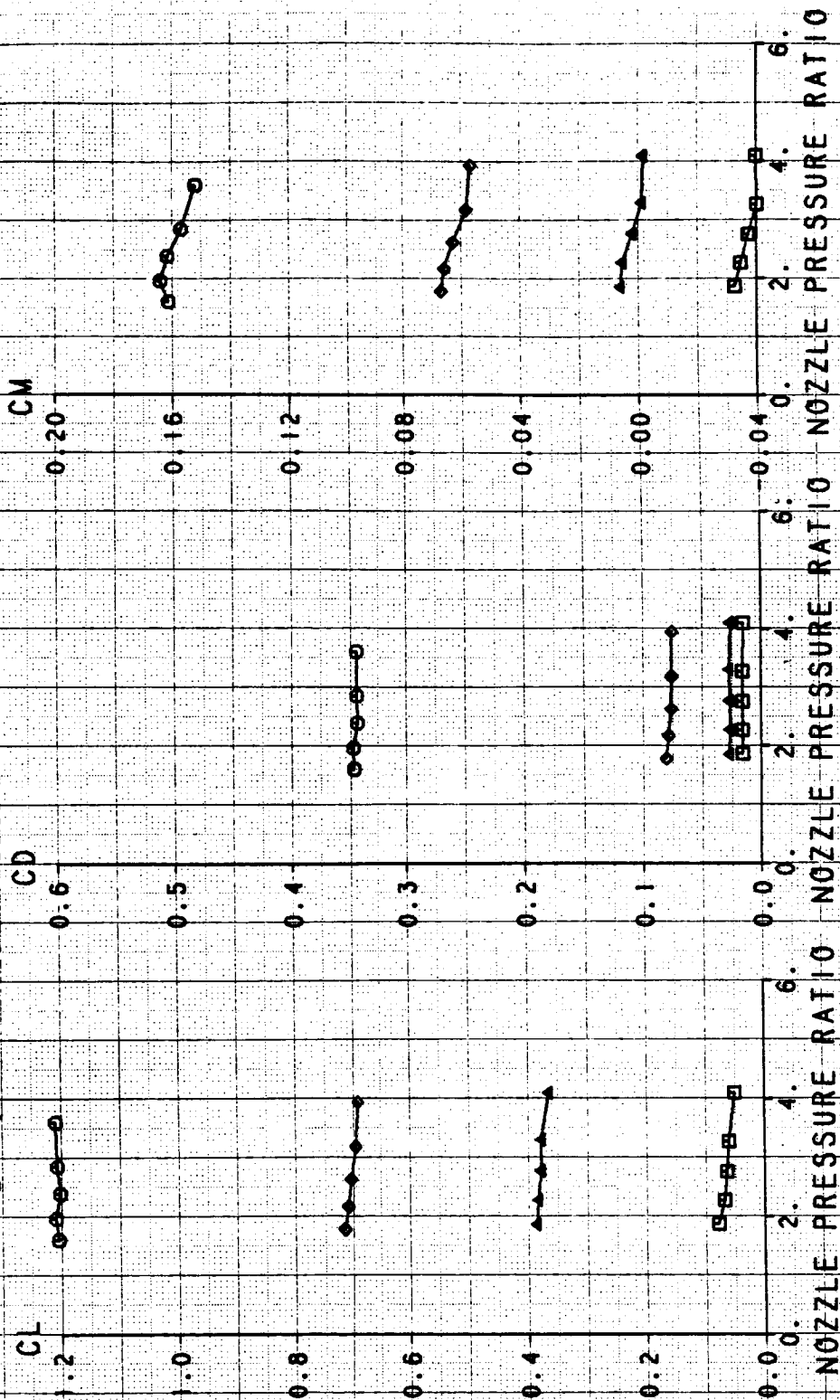






ANGLE OF ATTACK EFFECT ON CL, CD, AND CM VS NPR

| SYM | TEST | RUN | RMACH | RUFR | ROELCL | ALPHA |
|-----|------|-----|--------|--------|---------|-------|
| □ | 514 | 124 | 0.5993 | 0.9143 | -4.5974 | 0° |
| △ | 514 | 140 | 0.5994 | 0.9018 | -5.0127 | 4.5° |
| ◇ | 514 | 155 | 0.6001 | 0.8542 | -4.9679 | 9° |
| ○ | 514 | 169 | 0.6008 | 0.7554 | -5.0001 | 17.5° |



CANARD ROTATION EFFECT ON NOZZLE FORCE AND MOMENT DATA SIMULATOR MODE WITH A/B ALBEN

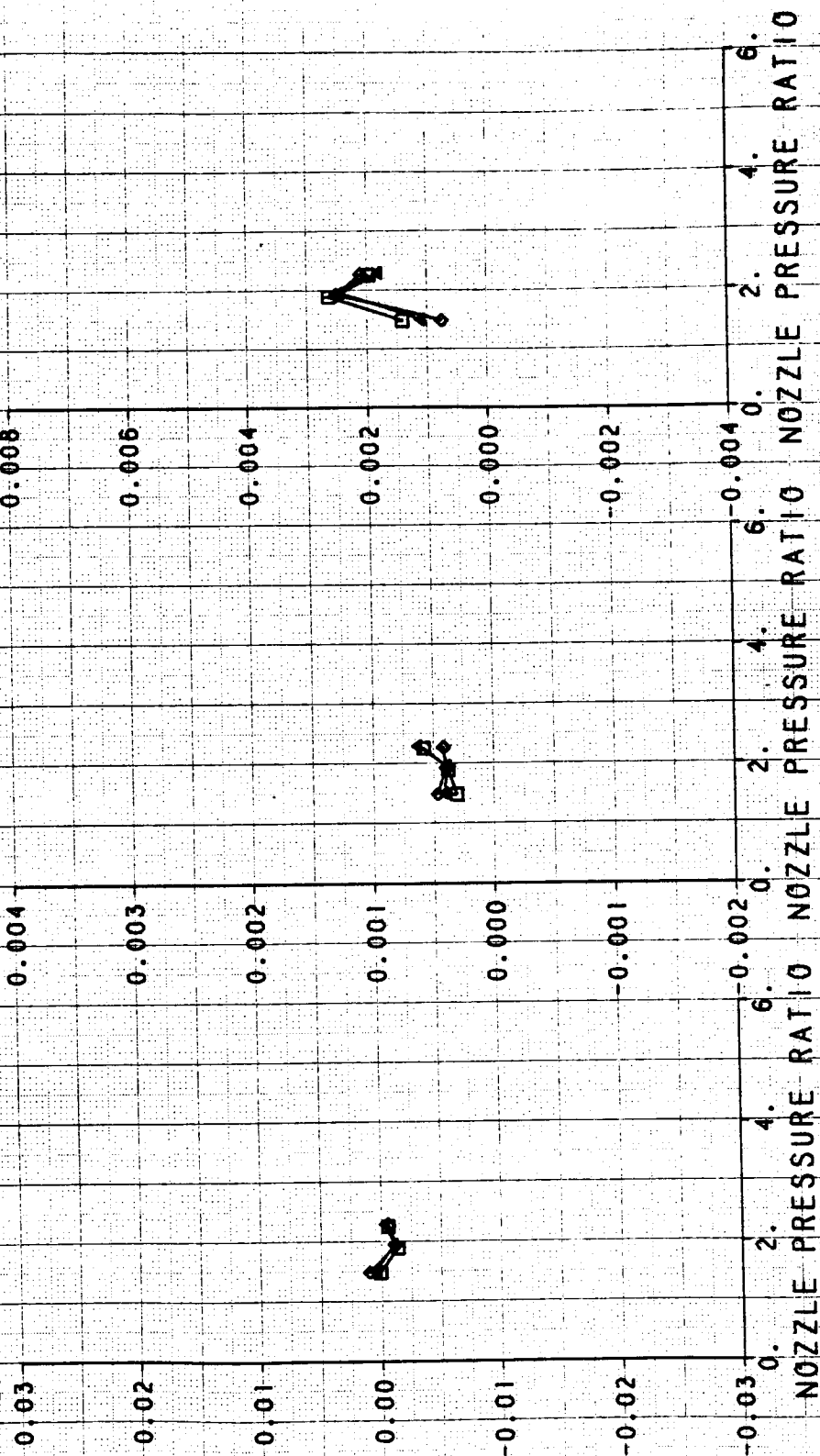
| SYM | TEST | RUN | RMACH | RDELCL | RMFR |
|-----|------|-----|--------|----------|--------|
| □ | 514 | 116 | 0.6003 | 0.1330 | 0.6905 |
| △ | 514 | 122 | 0.6230 | -4.9924 | 0.5812 |
| ◇ | 514 | 127 | 0.5991 | -10.1111 | 0.6886 |

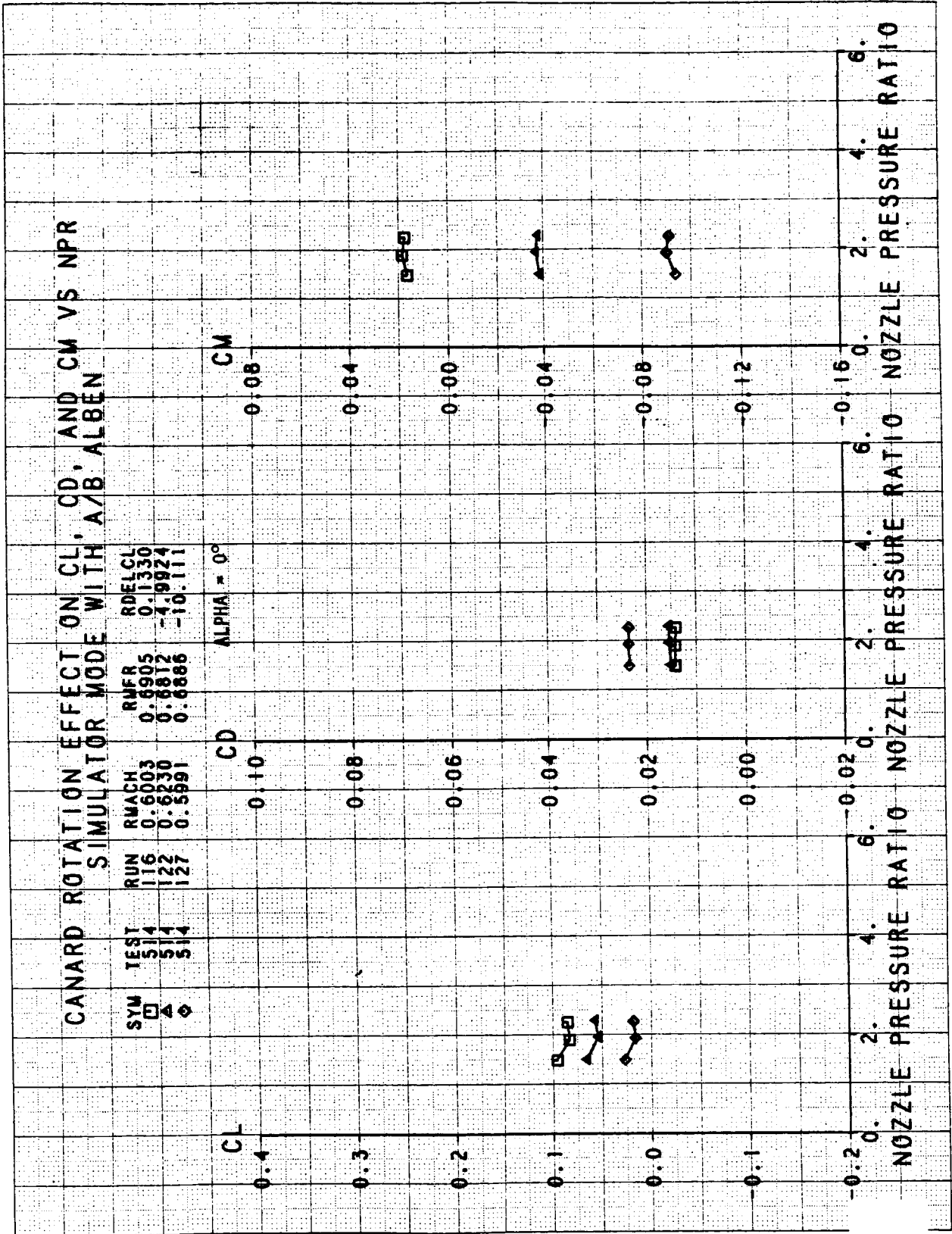
CMNOZ

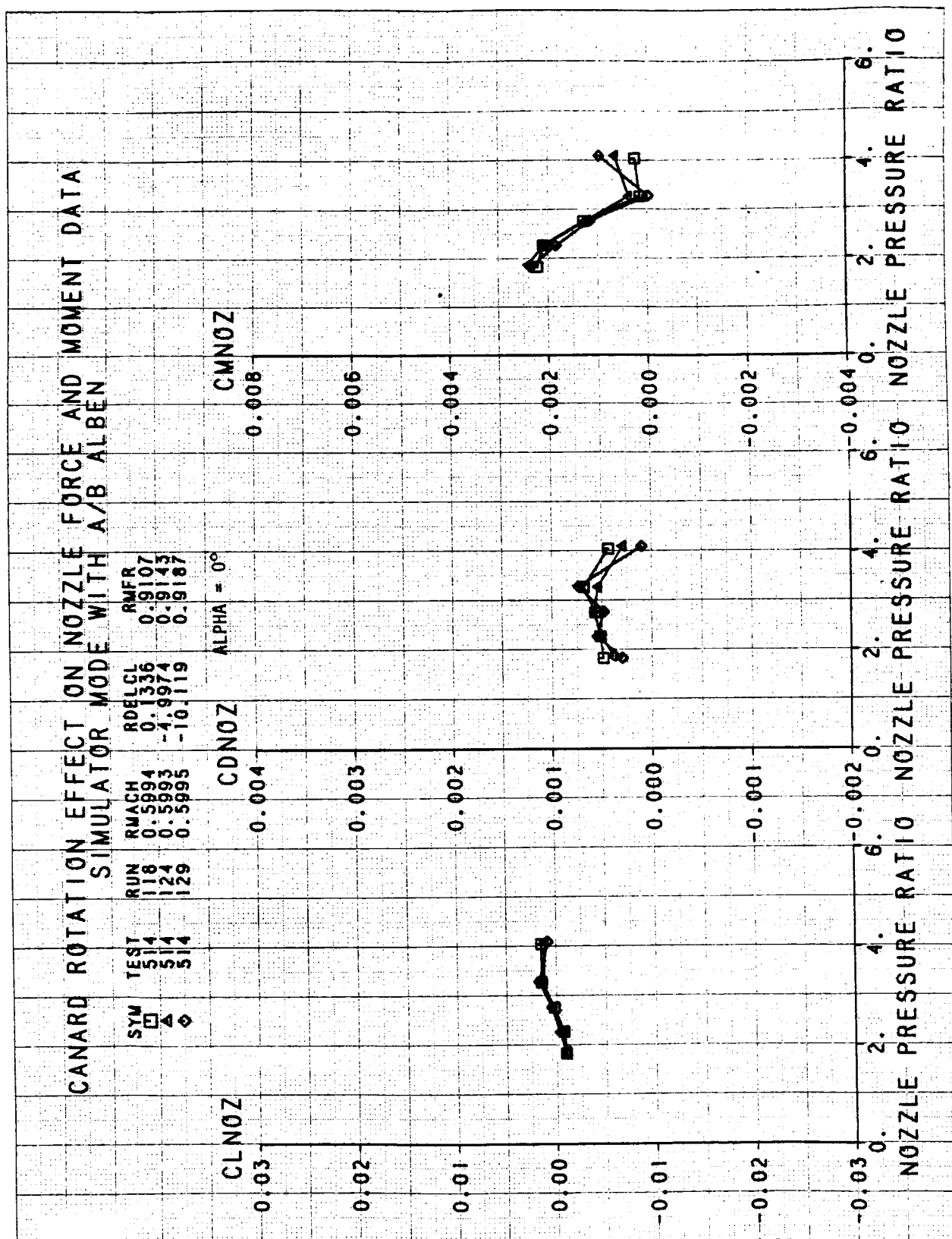
ALPHA = 0°

CDNOZ

CLNOZ



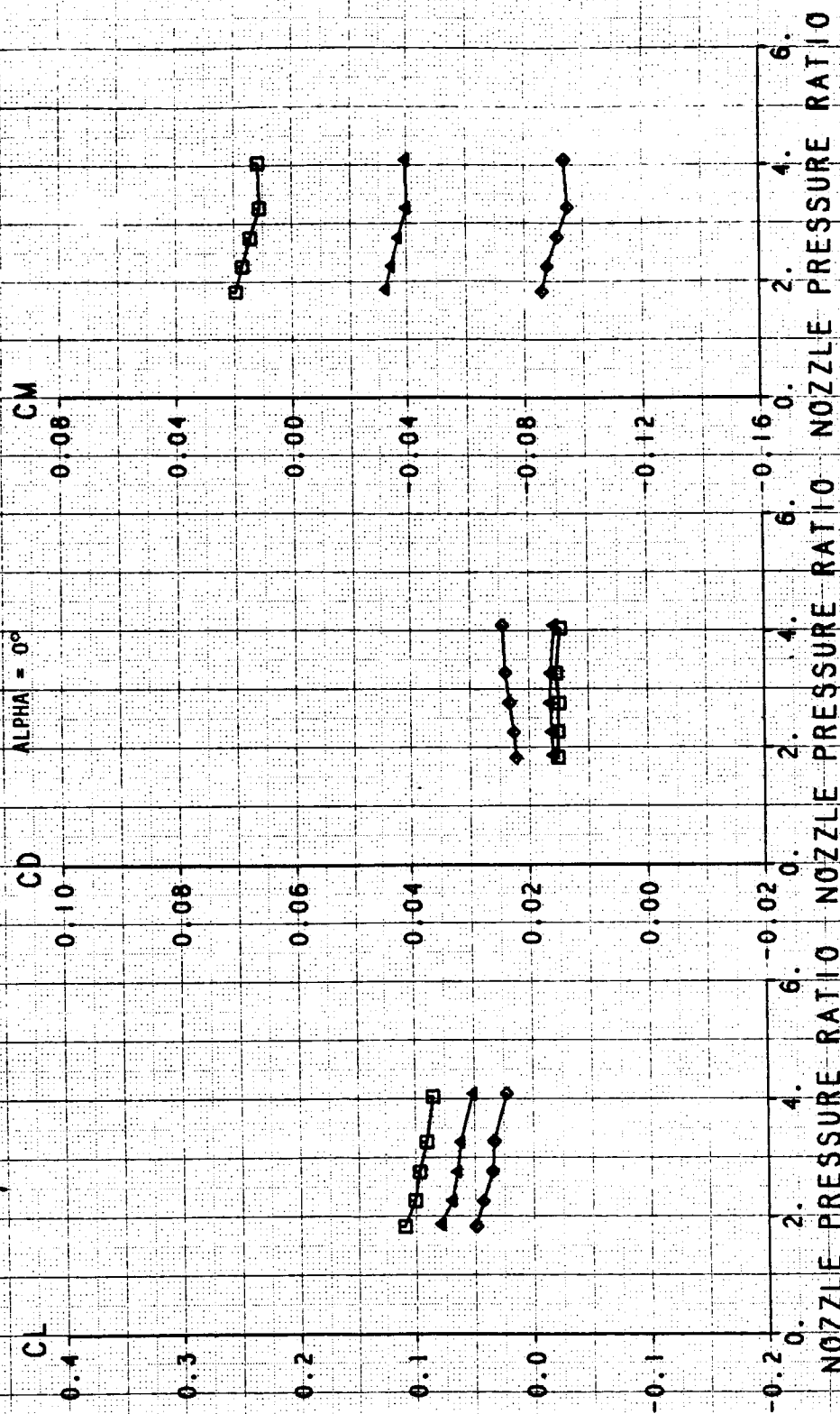


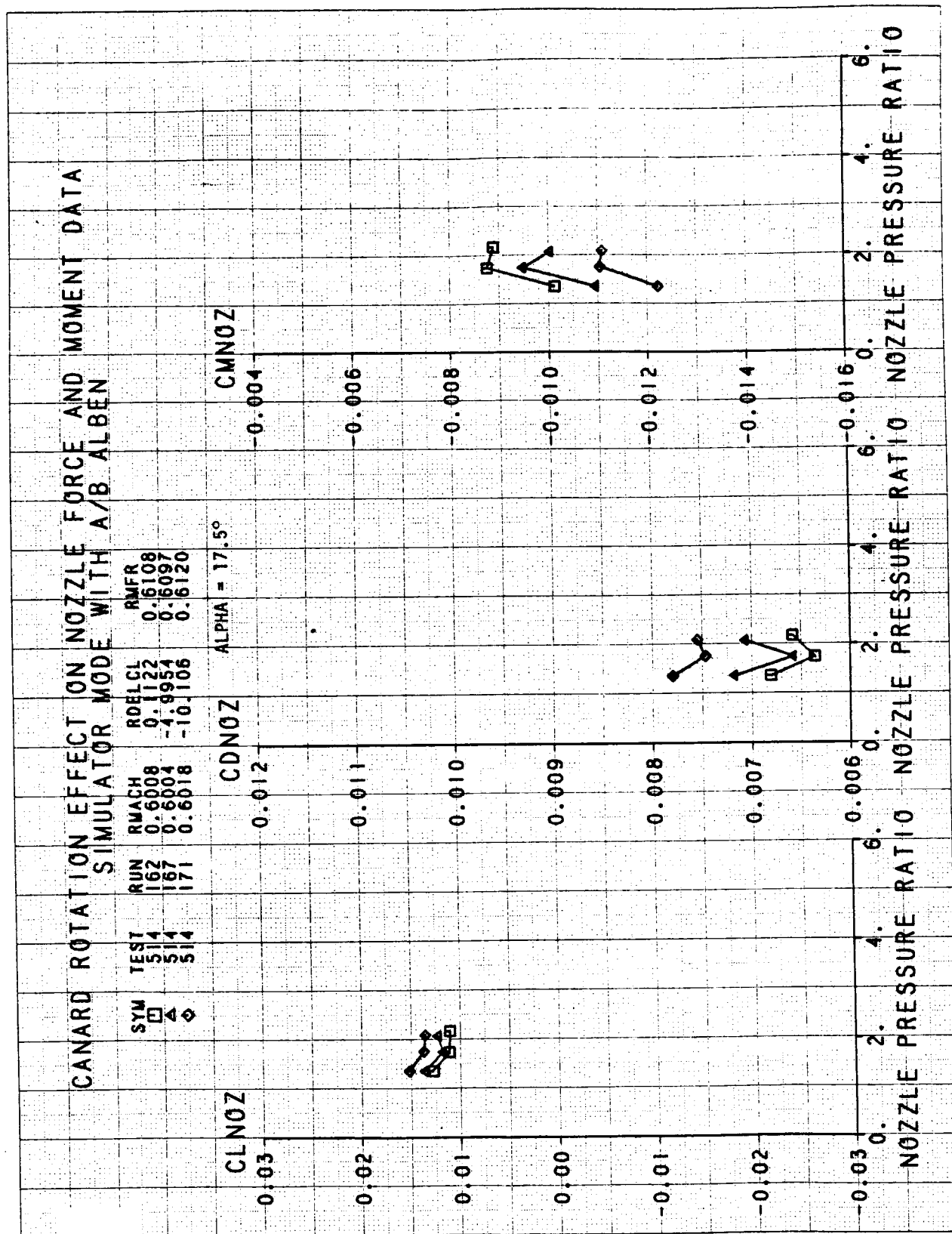


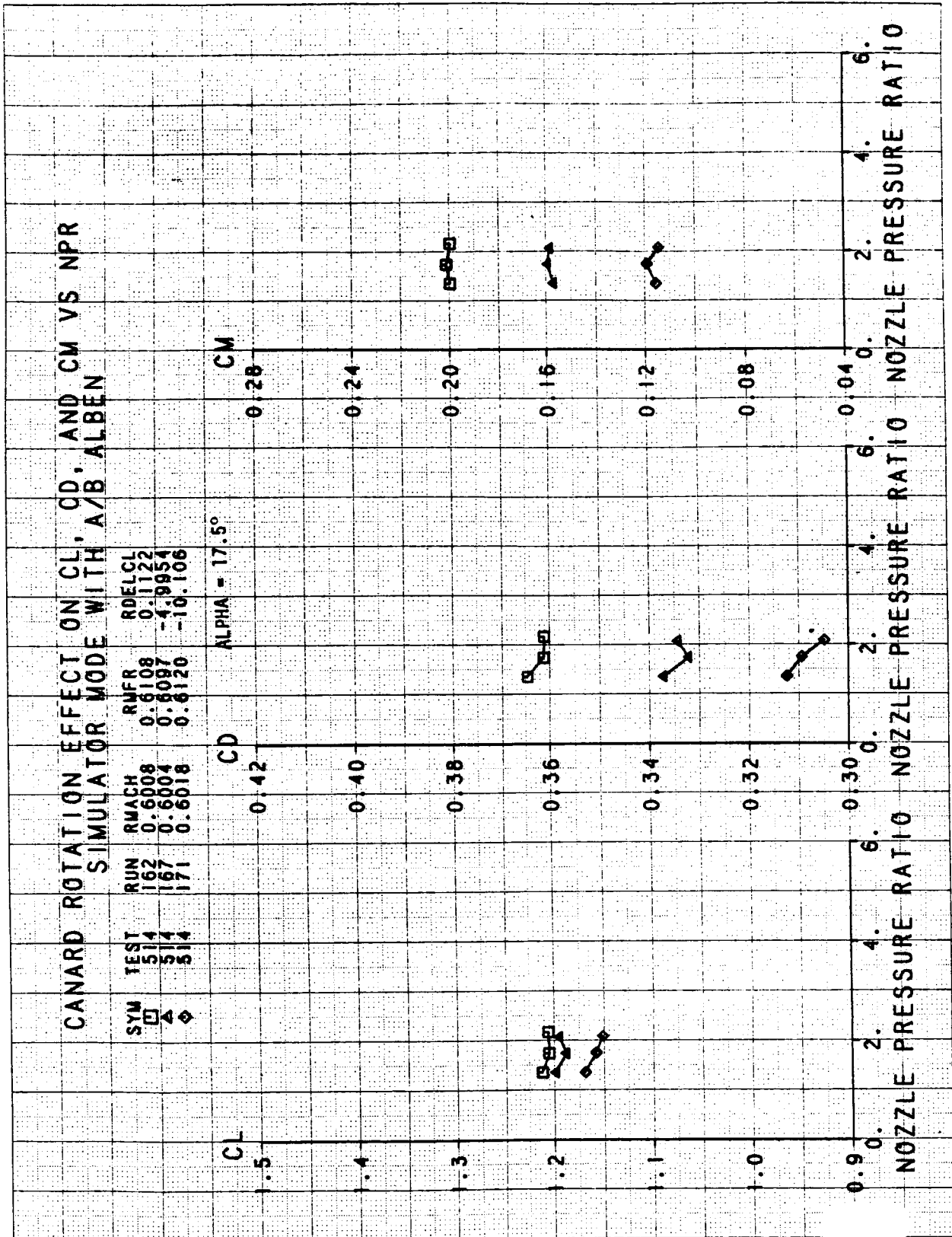
CANARD ROTATION EFFECT ON CL, CD, AND CM VS NPR

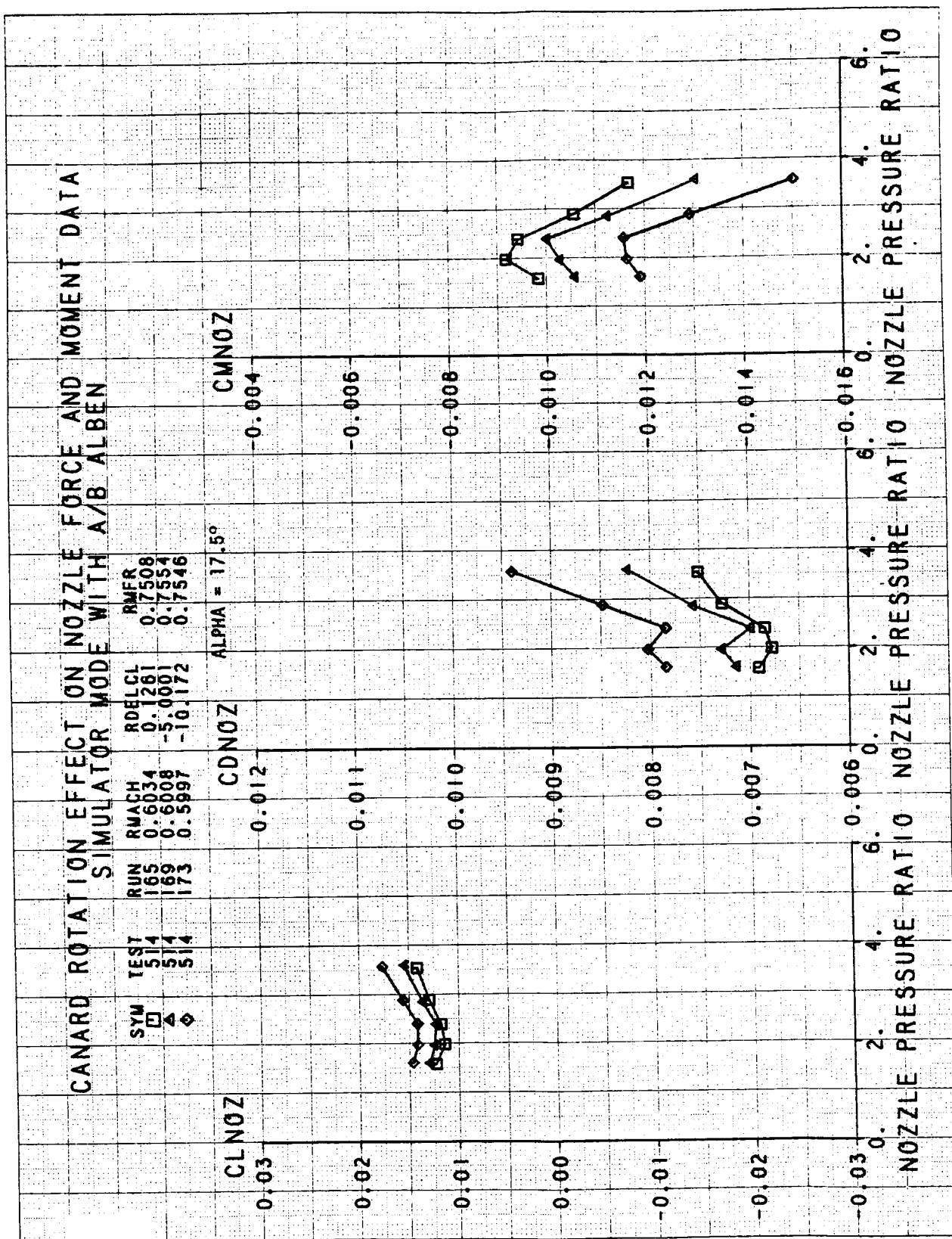
TEST RUN RMACH RUMR RDELCL
 514 118 0.5994 0.9107 0.1336
 514 124 0.5993 0.9143 -4.9974
 514 129 0.5995 0.9187 -10.119

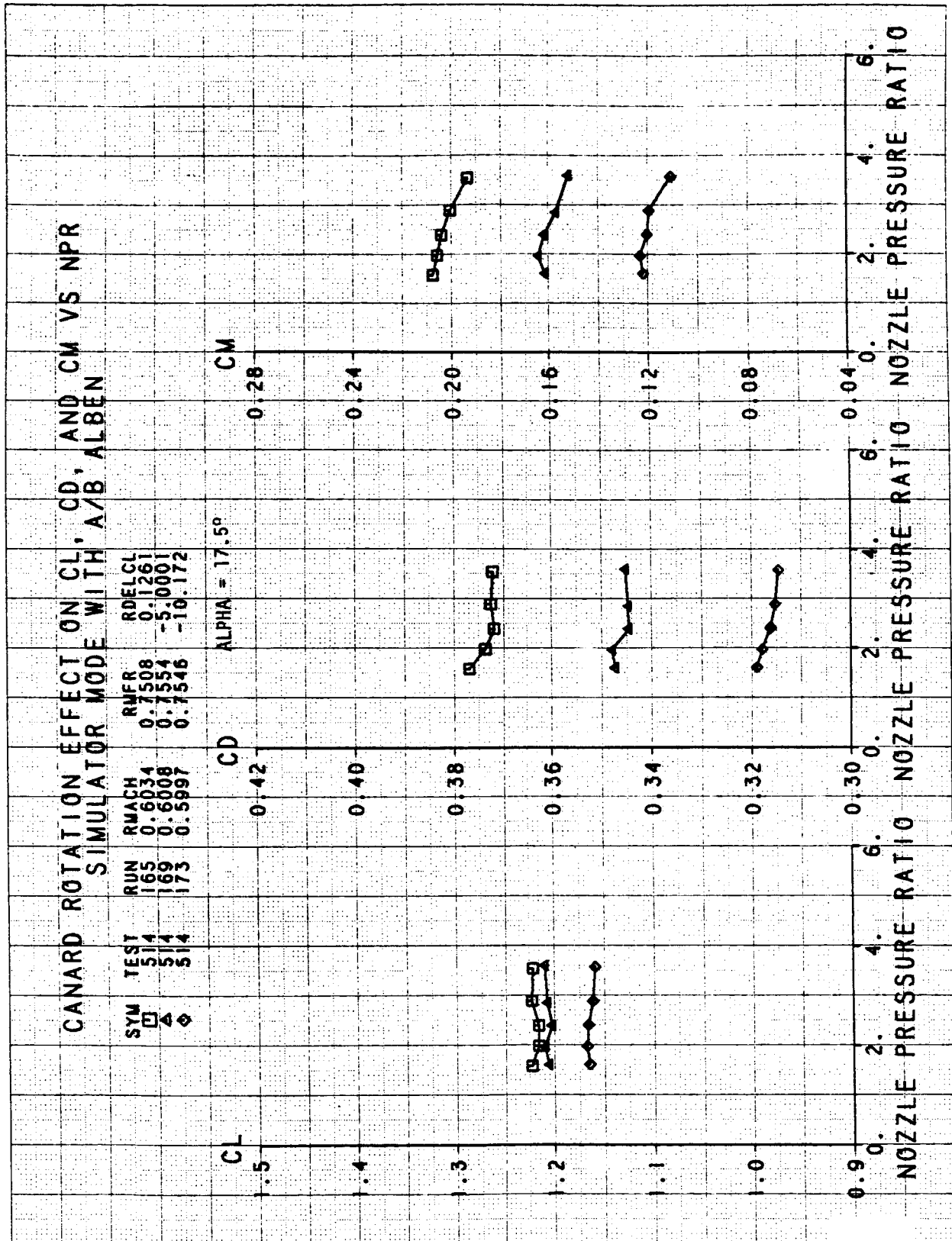
ALPHA = 0°

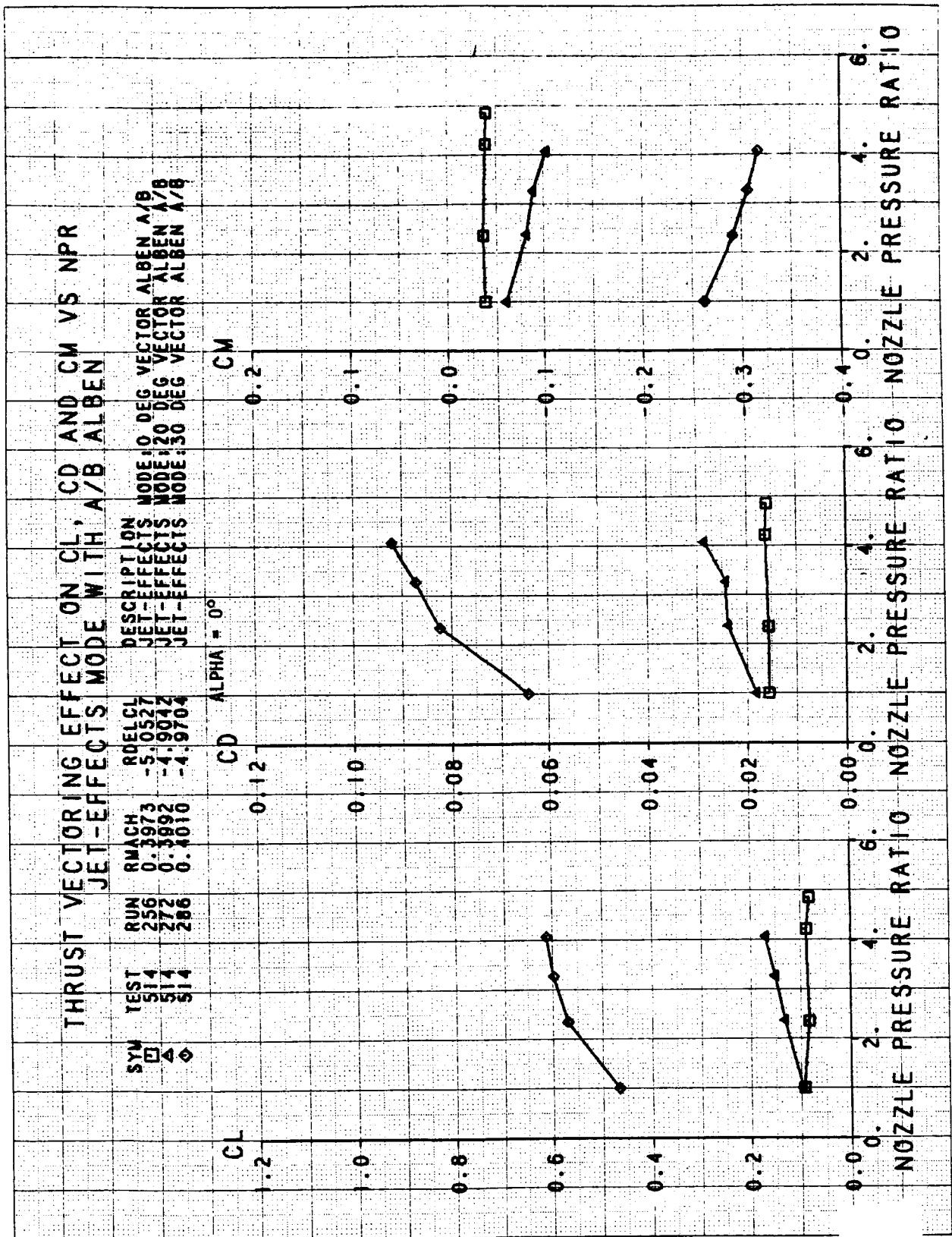


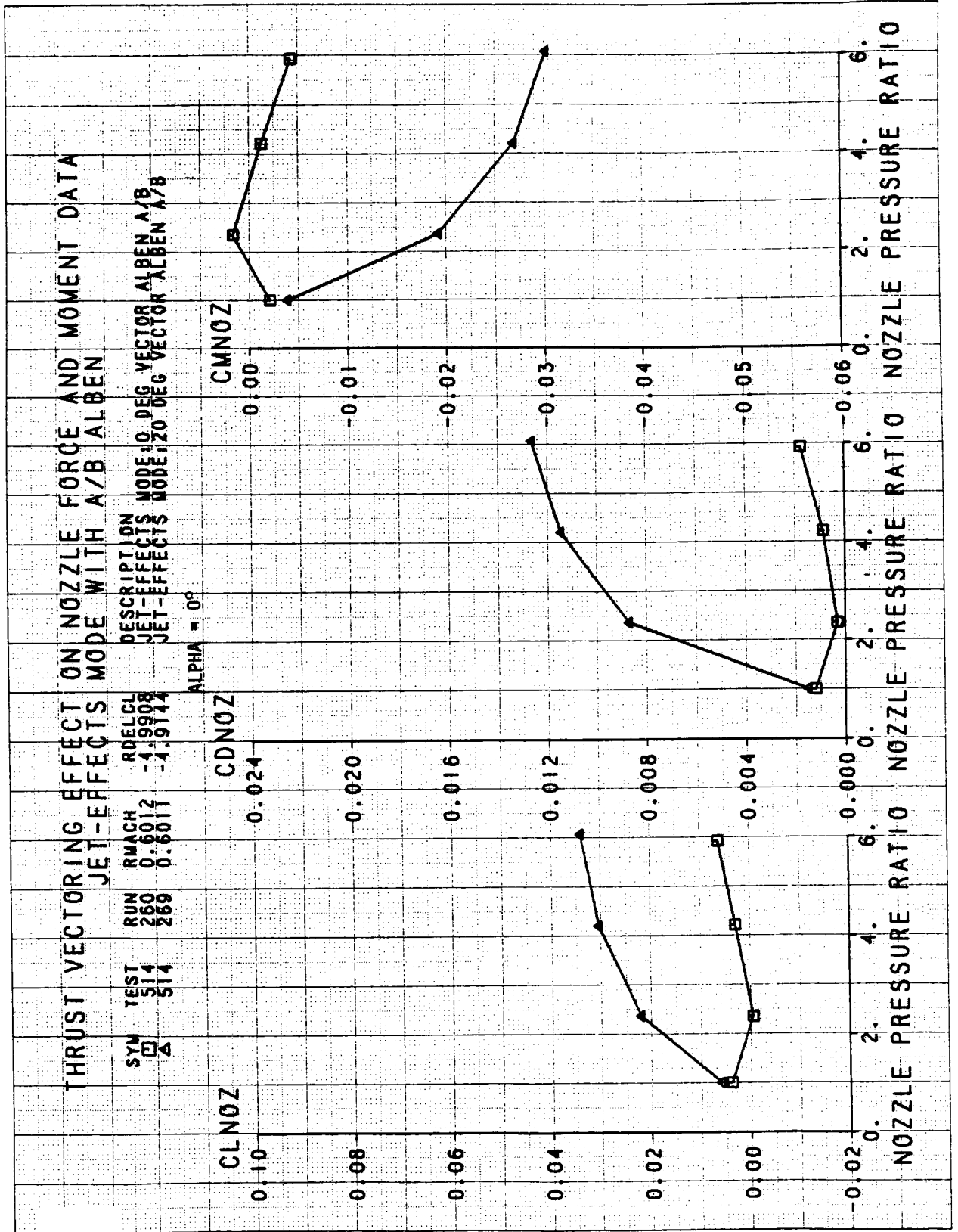


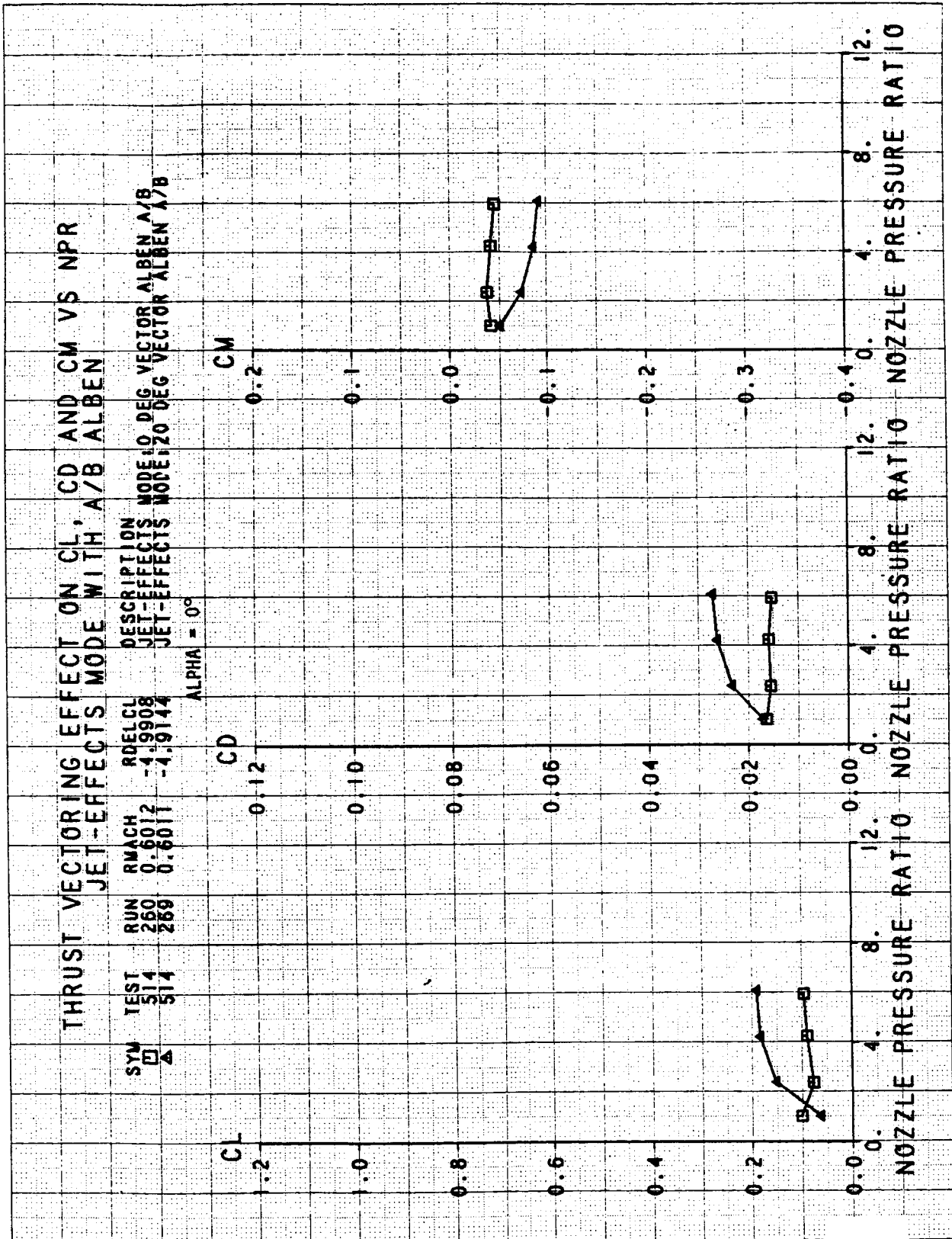








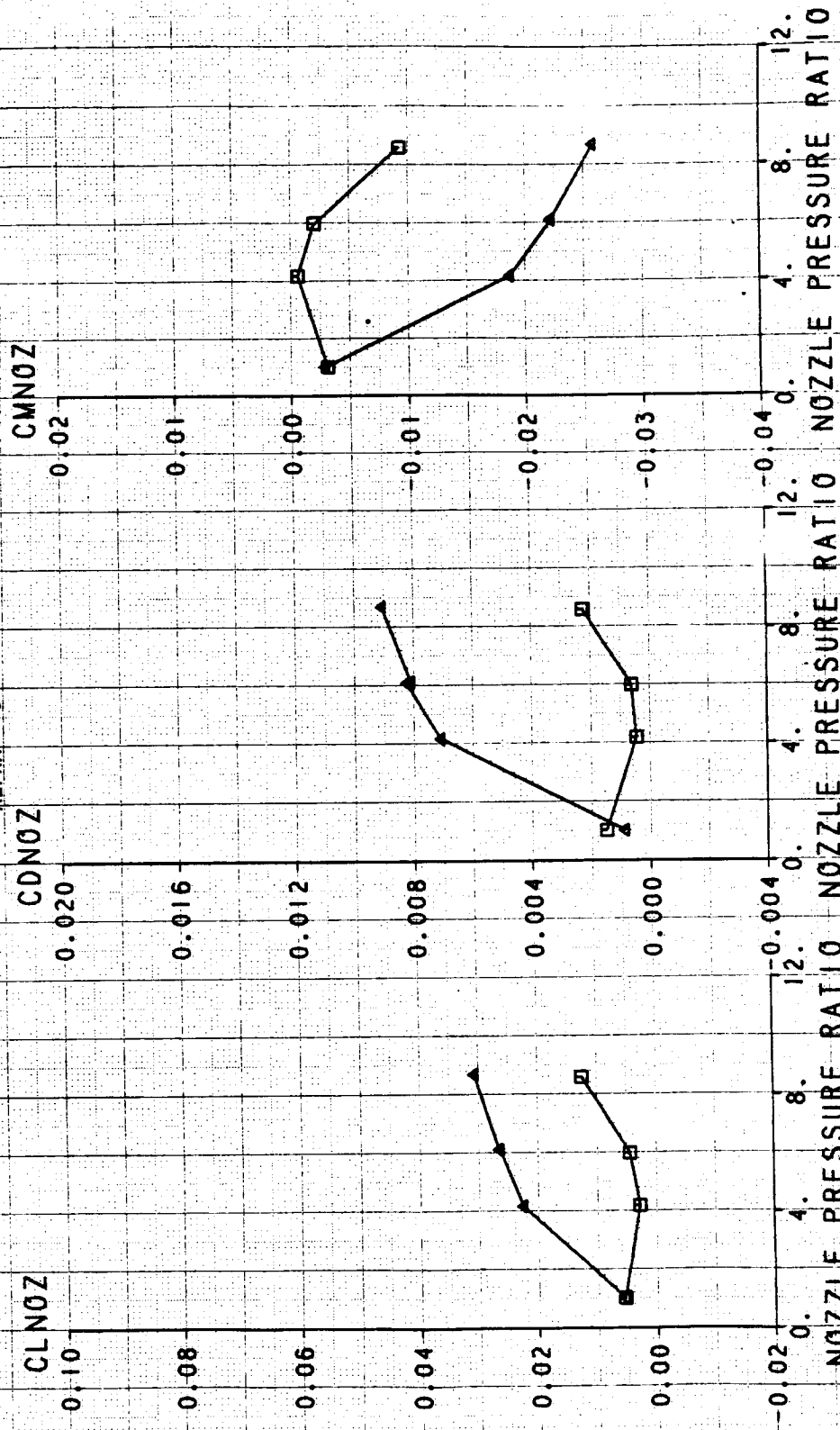


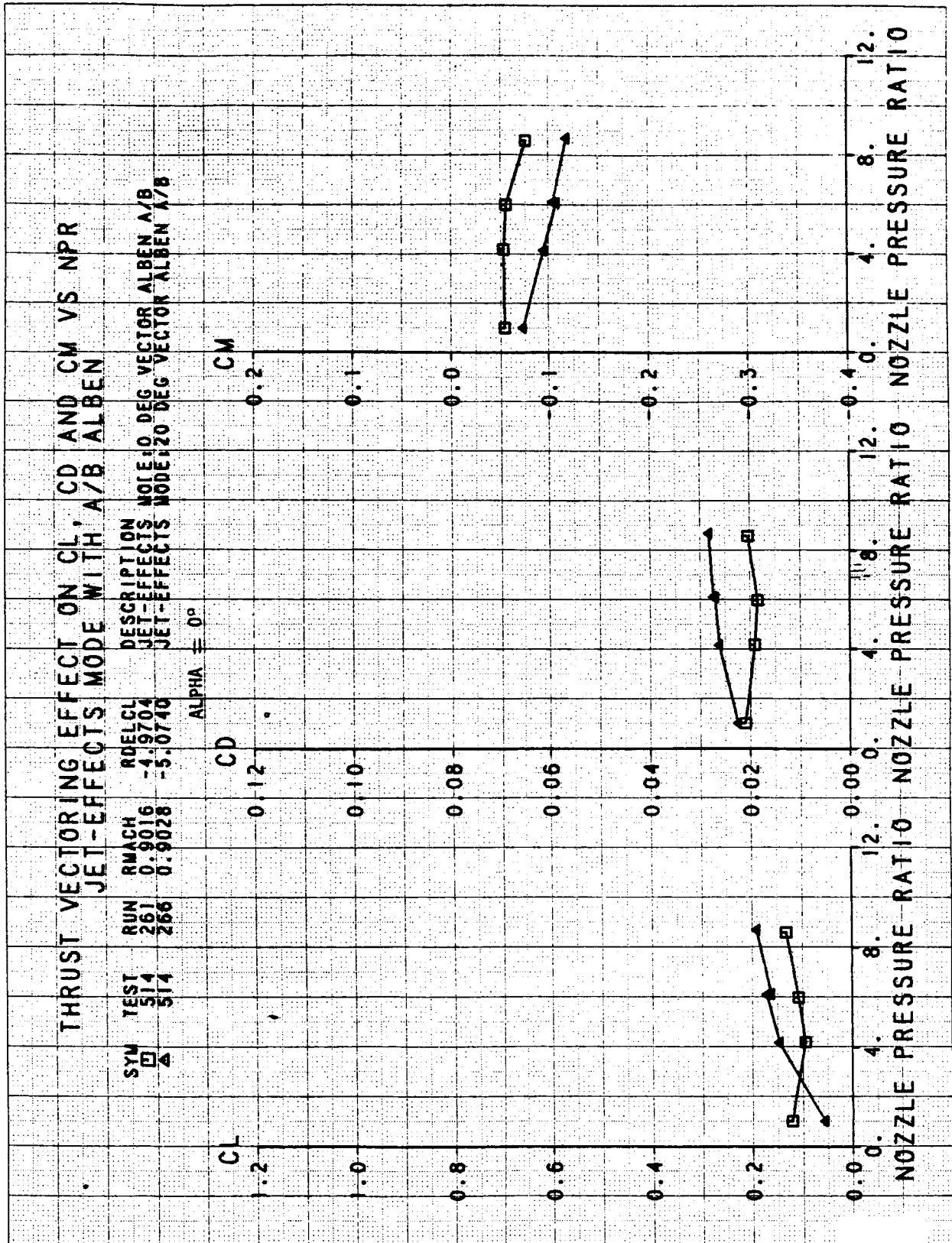


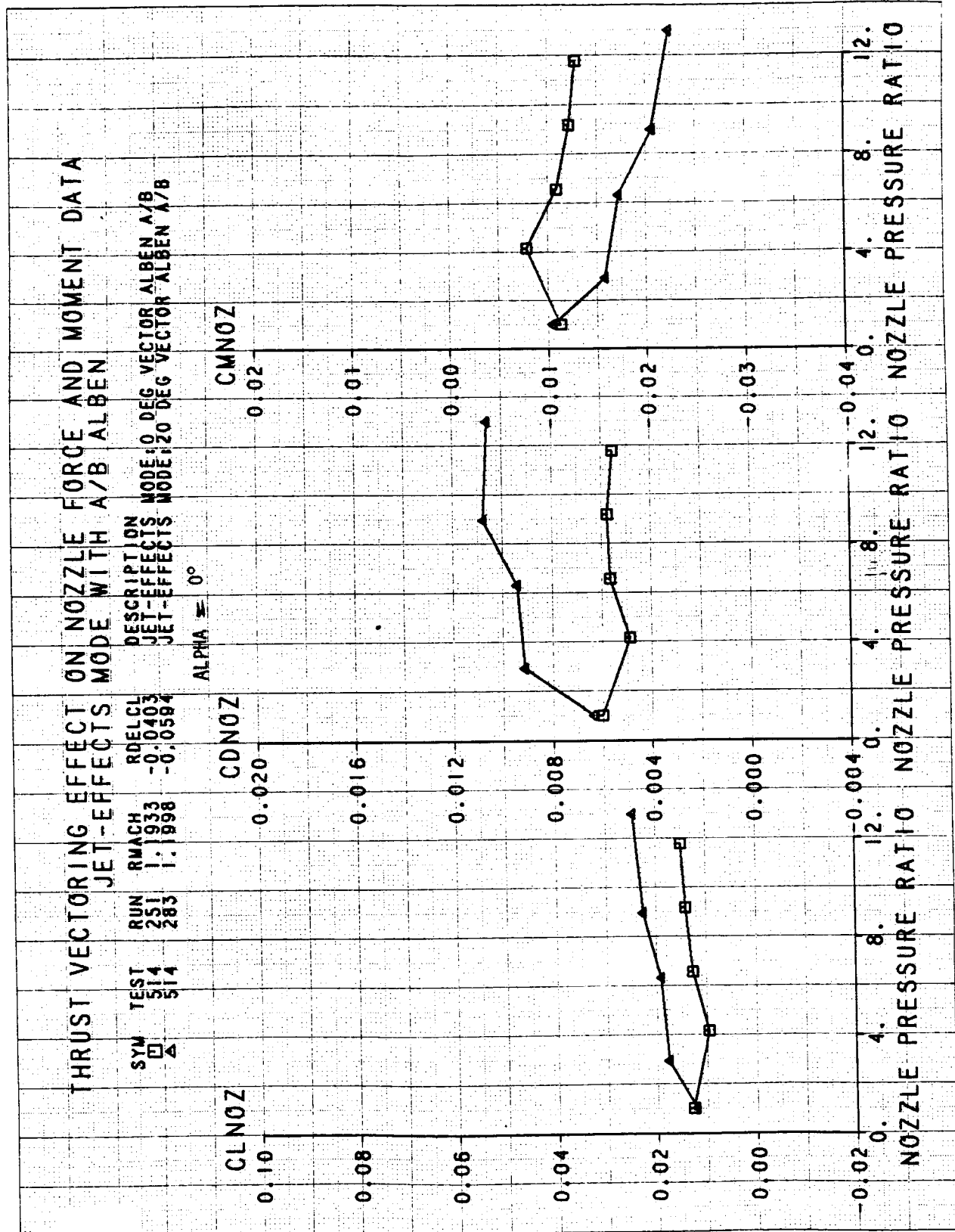
THRUST VECTORING EFFECT ON NOZZLE FORCE AND MOMENT DATA JET-EFFECTS MODE WITH A/B ALBEN

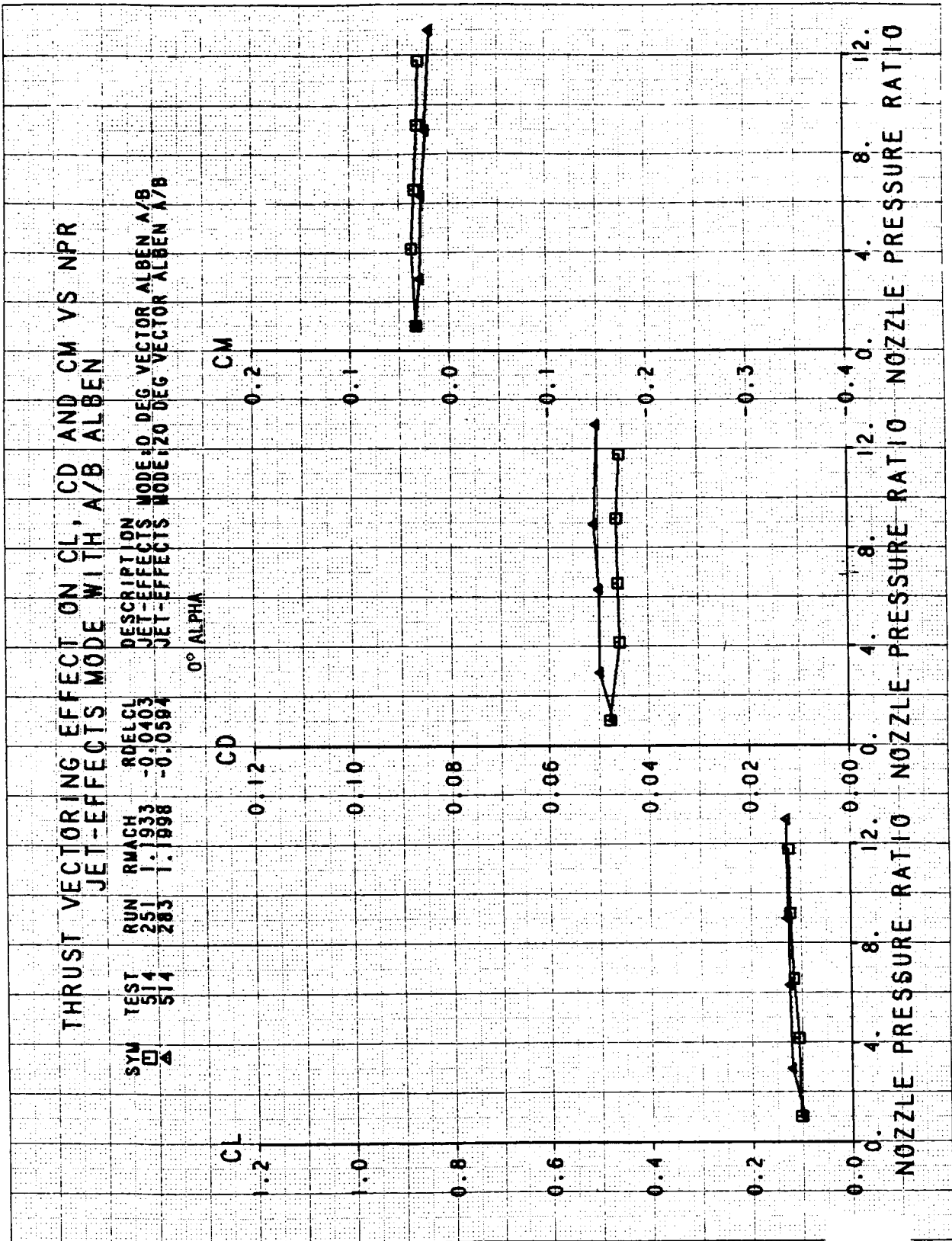
| SYM | TEST | RUN | RMACH | RDELCL | DESCRIPTION |
|-----|------|-----|--------|---------|---|
| □ | 514 | 261 | 0.9016 | -4.9704 | JET-EFFECTS MODE: 0 DEG VECTOR ALBEN A/B |
| △ | 514 | 266 | 0.9028 | -5.0740 | JET-EFFECTS MODE: 20 DEG VECTOR ALBEN A/B |

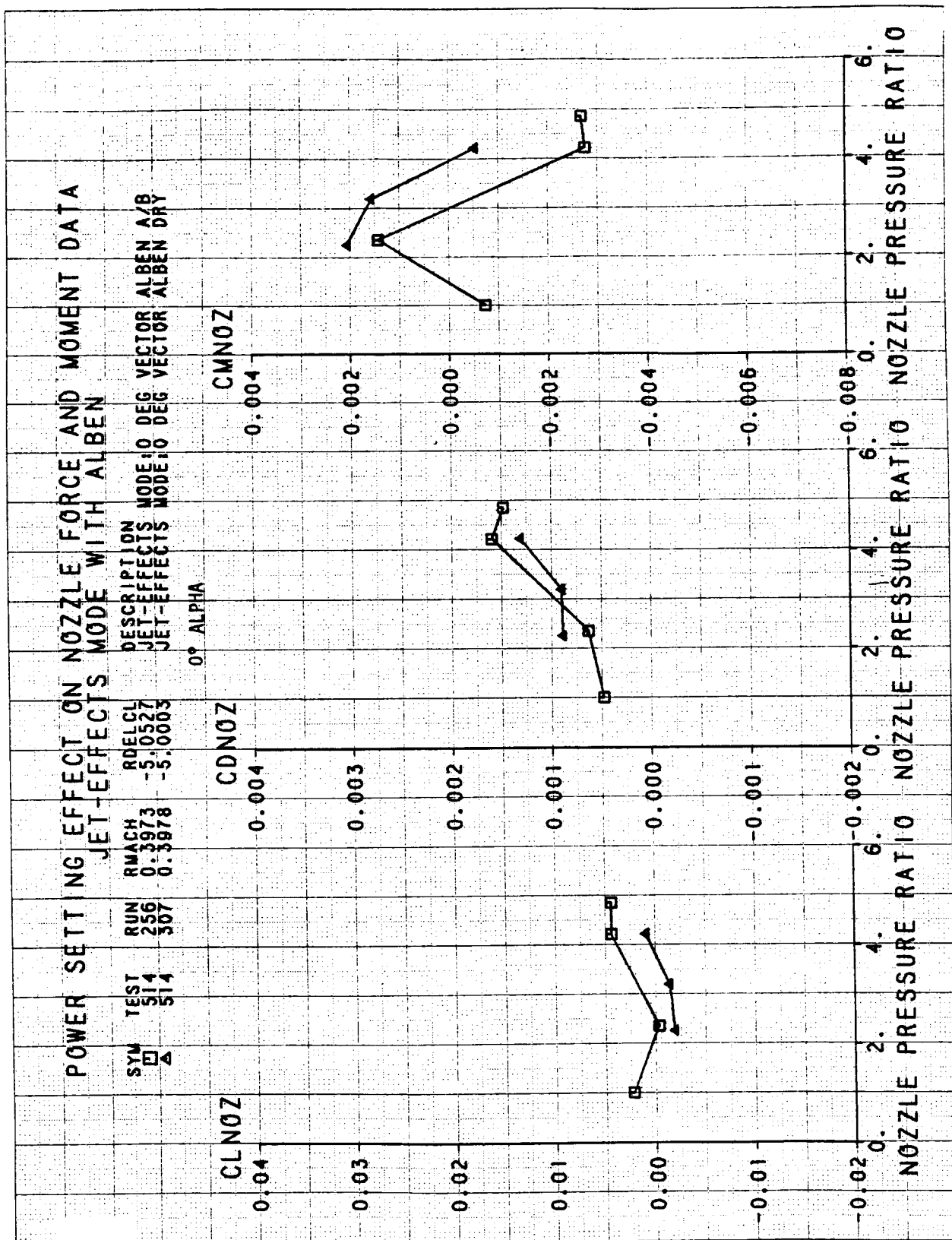
ALPHA = 0°



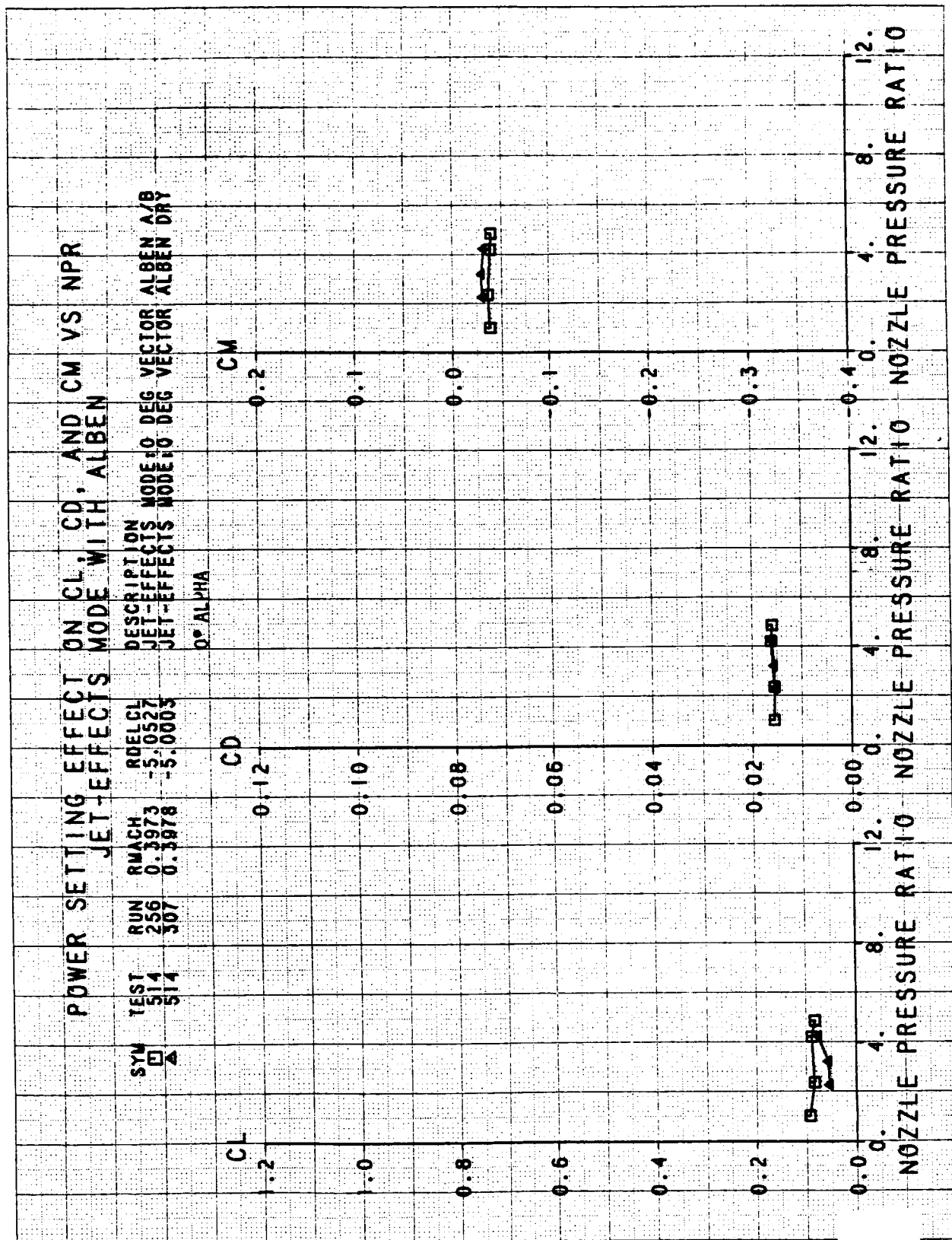


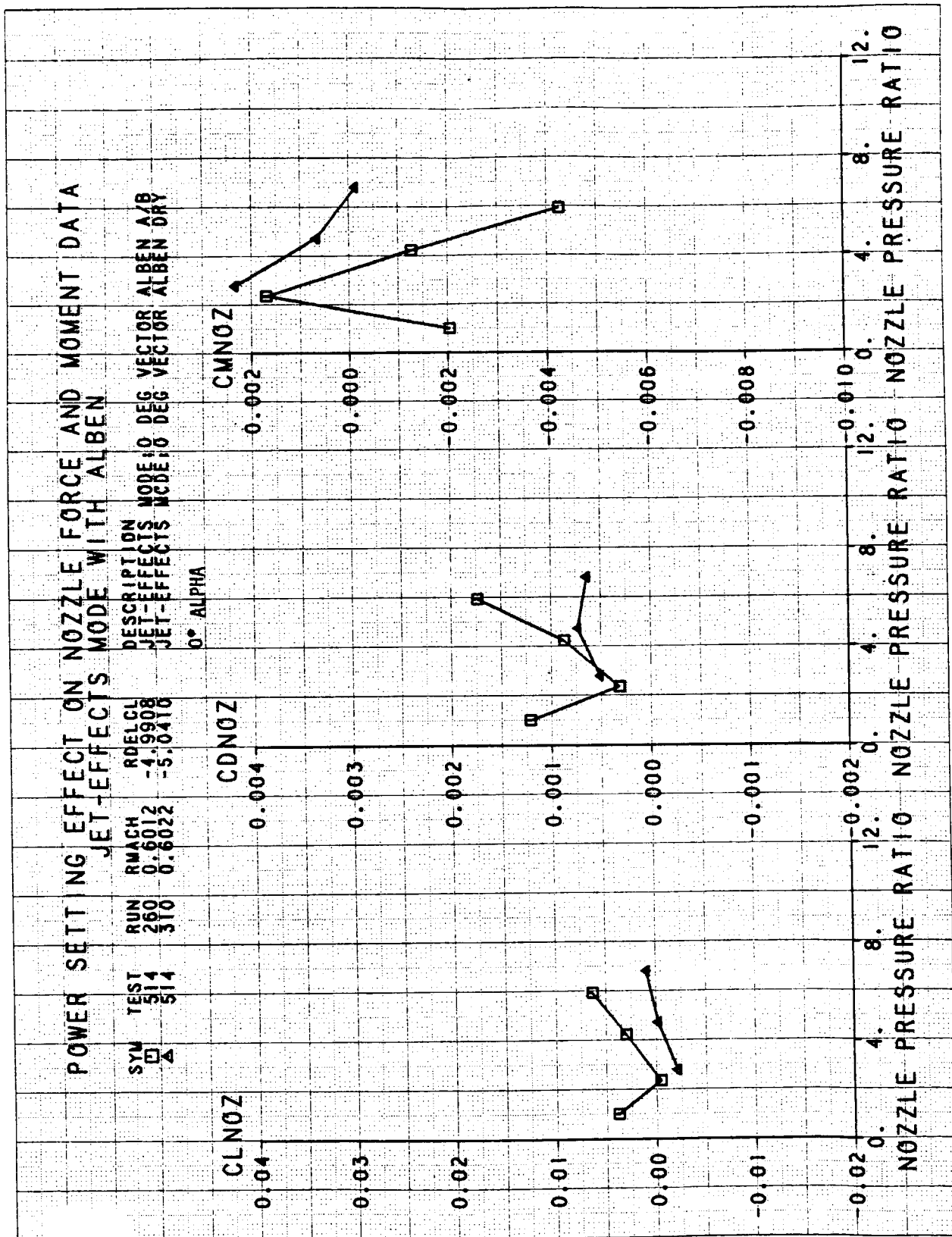


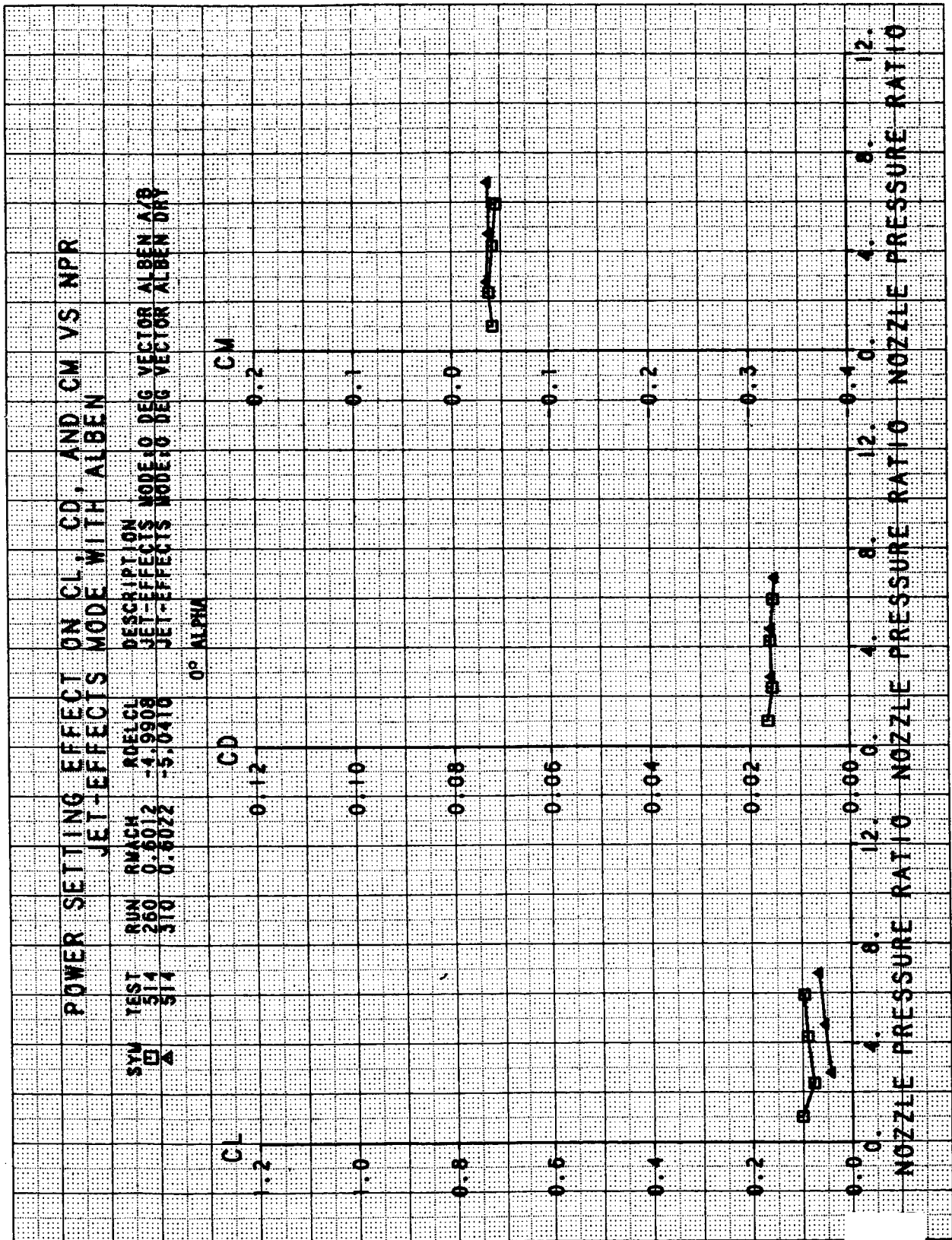


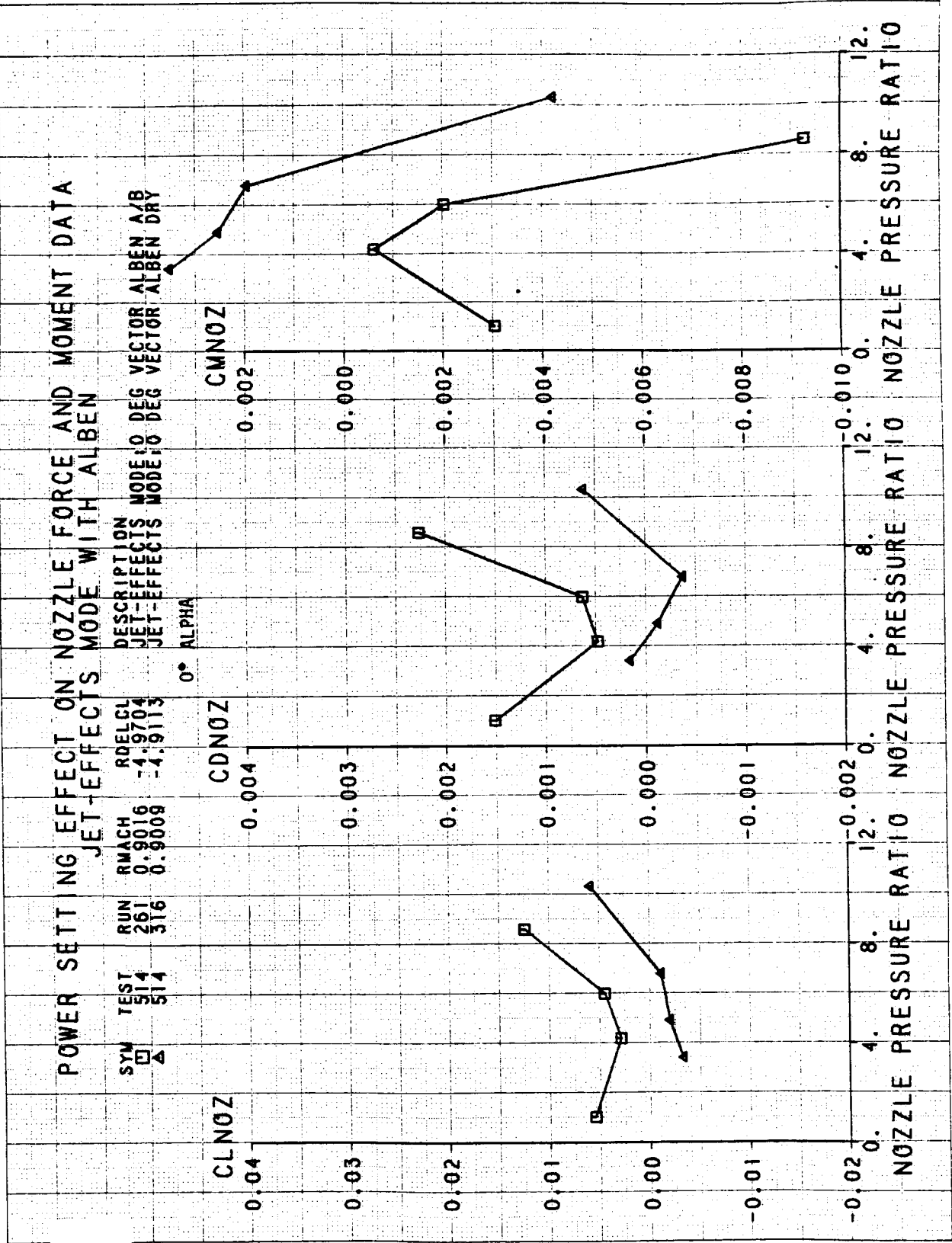


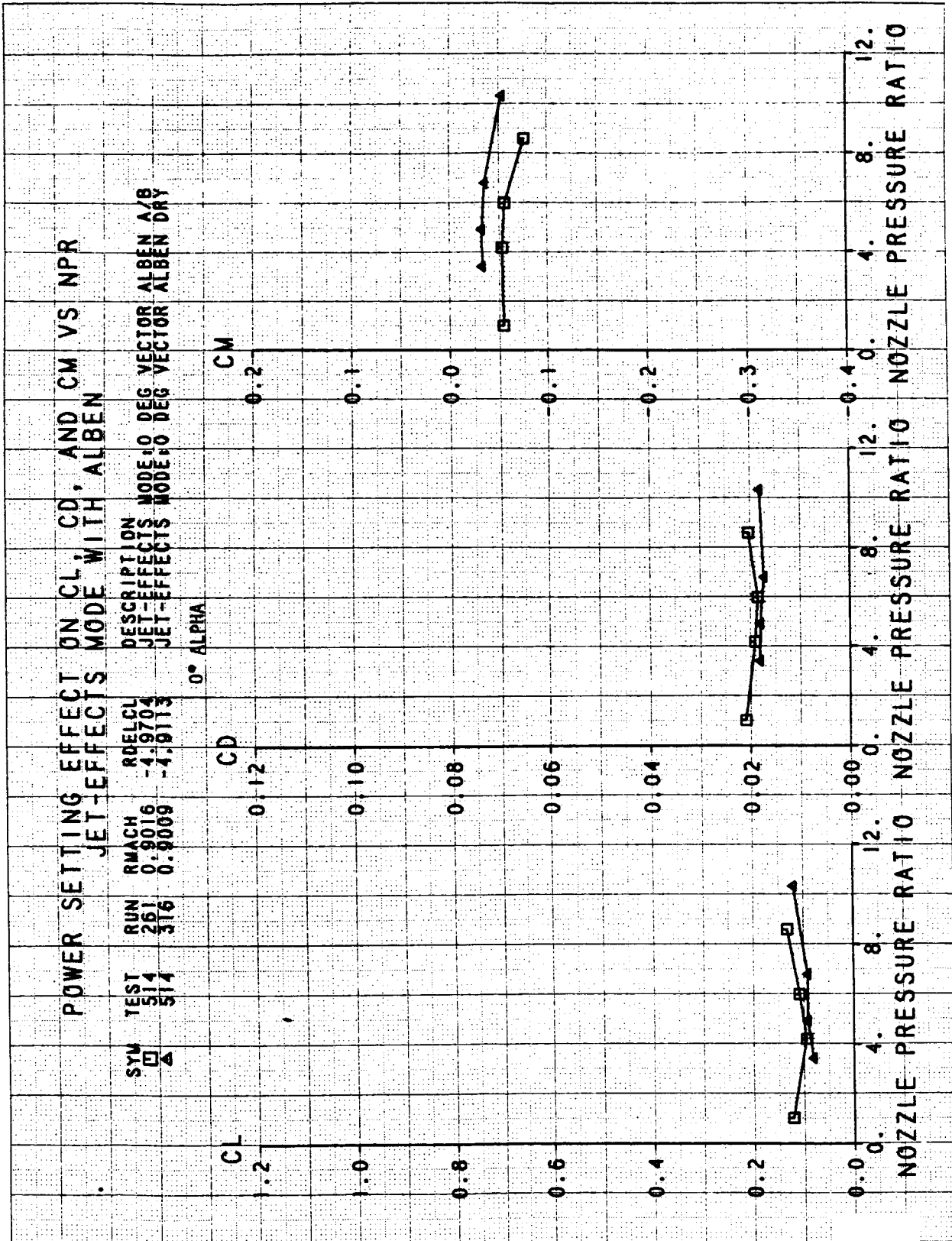
ORIGINAL PAGE IS
 OF POOR QUALITY





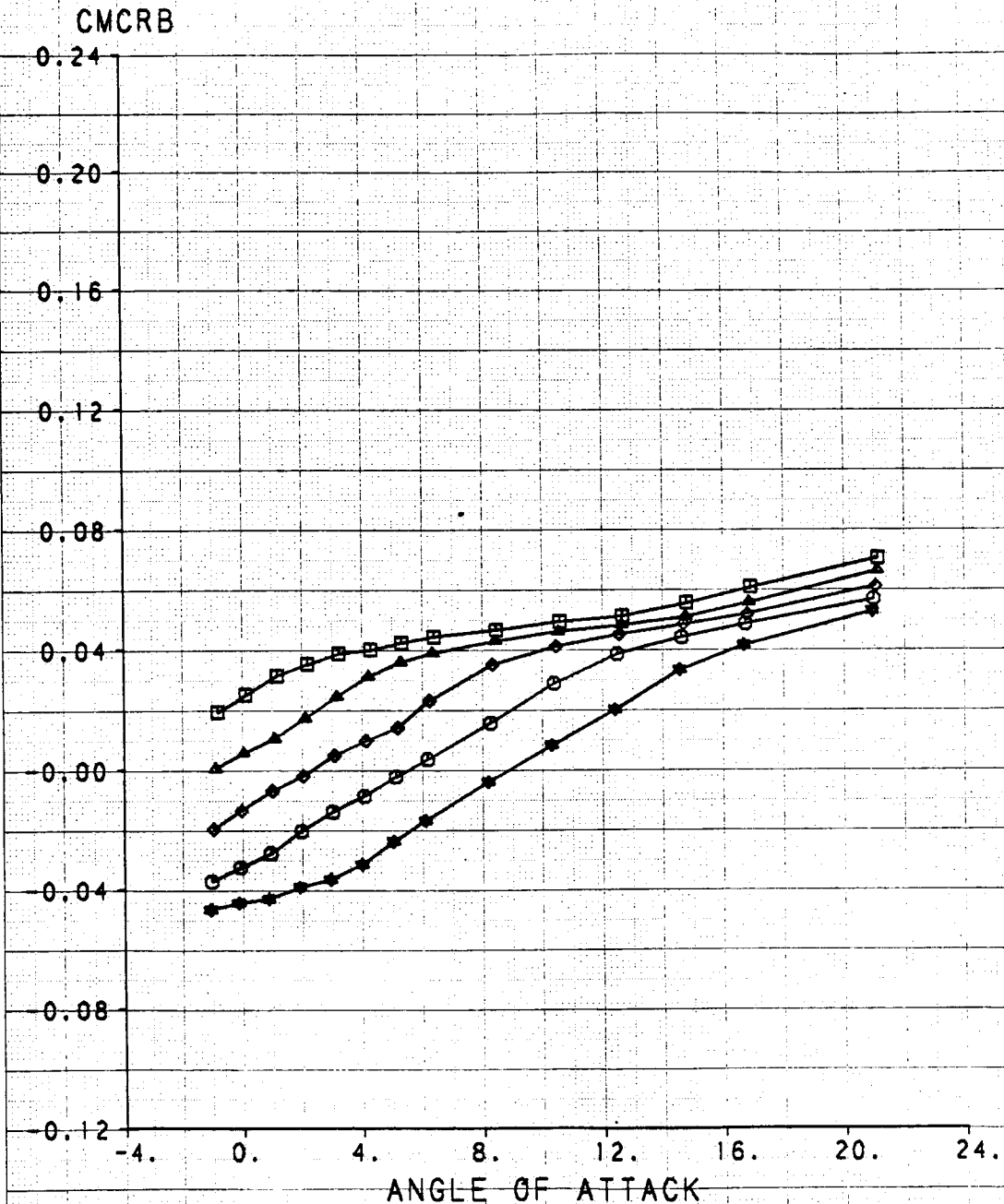






CANARD ROTATION EFFECTS ON CANARD ROOT BENDING MOMENT

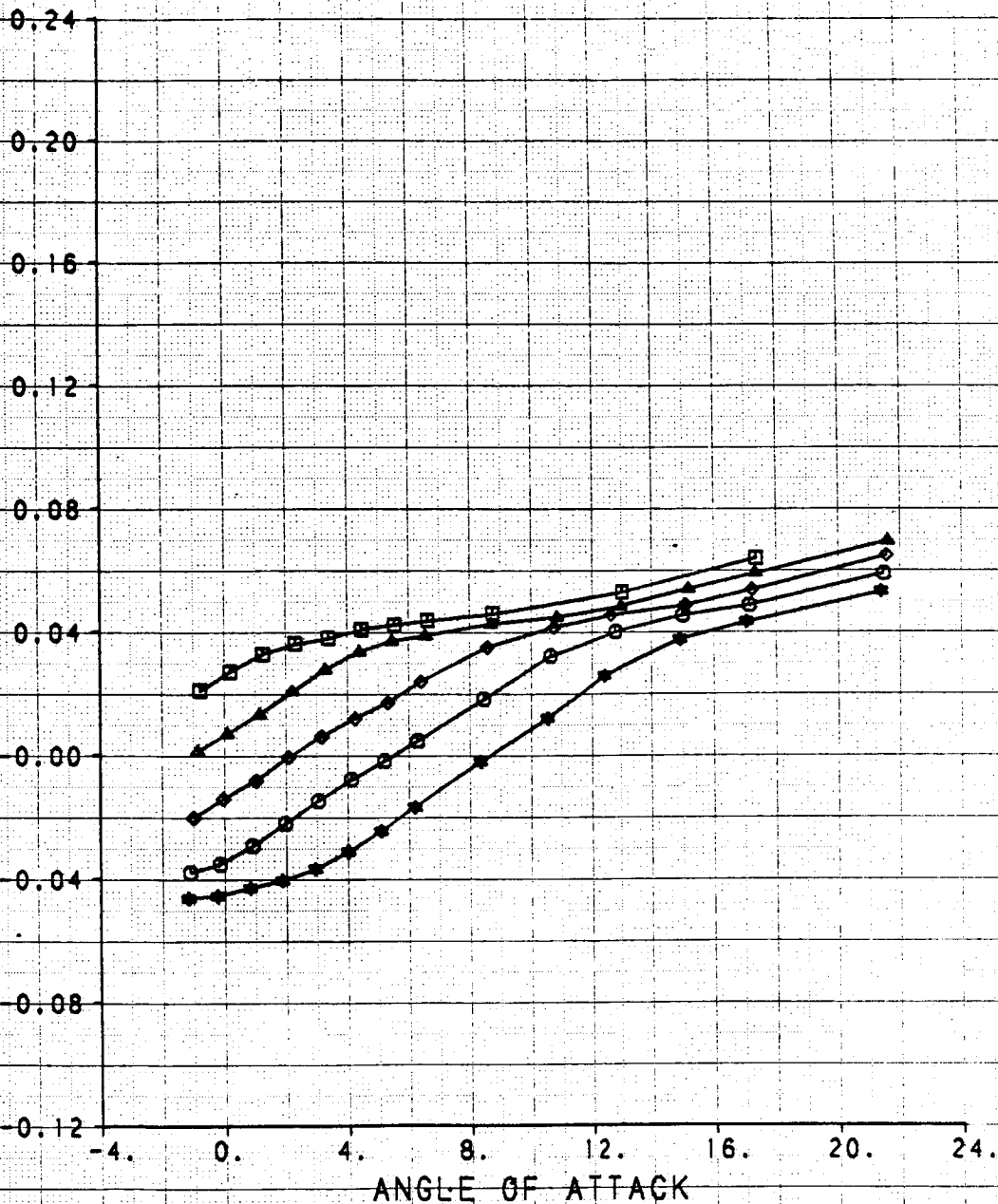
| SYM | TEST | RUN | RMACH | RDELCL | DESCRIPTION |
|-----|------|-----|--------|---------|----------------------|
| □ | 514 | 66 | 0.3993 | 5.0293 | F/T, COMMON BASELINE |
| ▲ | 514 | 67 | 0.3988 | -0.0547 | F/T, COMMON BASELINE |
| ◇ | 514 | 68 | 0.3990 | -5.0061 | F/T, COMMON BASELINE |
| ○ | 514 | 69 | 0.3989 | -10.026 | F/T, COMMON BASELINE |
| ★ | 514 | 70 | 0.3990 | -15.003 | F/T, COMMON BASELINE |



CANARD ROTATION EFFECTS ON CANARD ROOT BENDING MOMENT

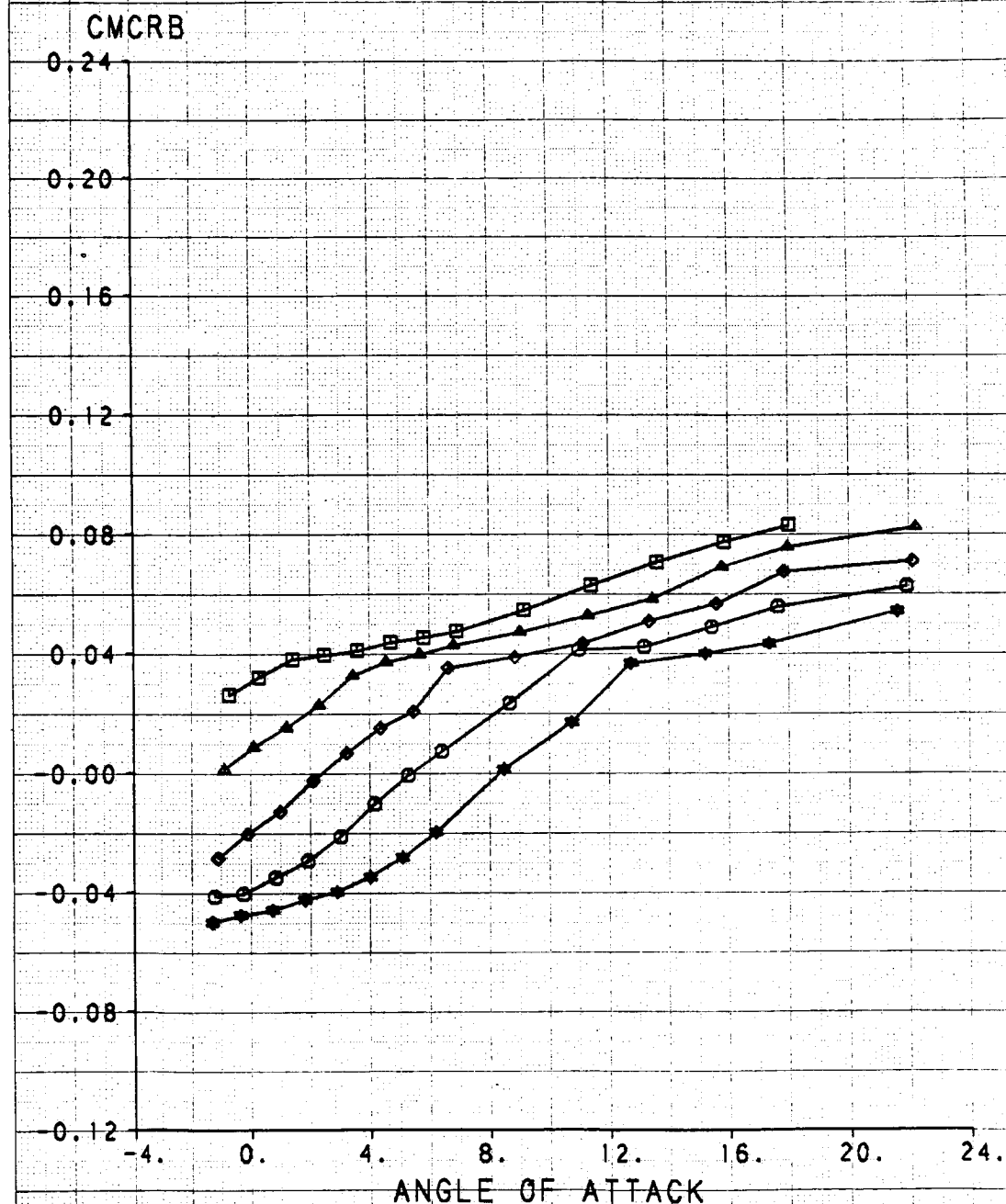
| SYM | TEST | RUN | RMACH | RDELCL | DESCRIPTION |
|-----|------|-----|--------|---------|----------------------|
| □ | 514 | 75 | 0.8005 | 5.0269 | F/T, COMMON BASELINE |
| ▲ | 514 | 74 | 0.8008 | 0.0827 | F/T, COMMON BASELINE |
| ◇ | 514 | 73 | 0.5997 | -5.0066 | F/T, COMMON BASELINE |
| ○ | 514 | 72 | 0.5996 | -10.035 | F/T, COMMON BASELINE |
| ★ | 514 | 71 | 0.5986 | -15.005 | F/T, COMMON BASELINE |

CMCRB



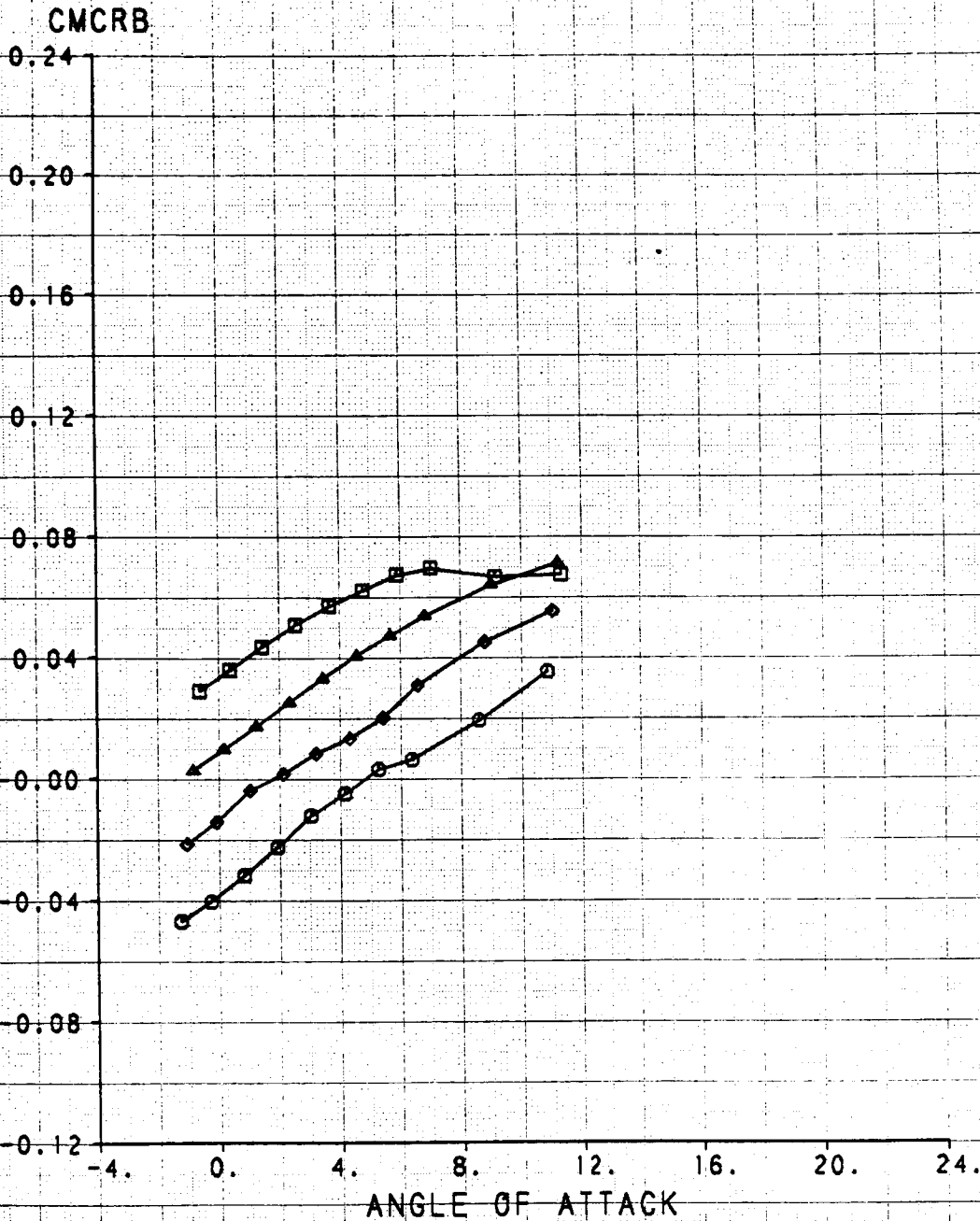
CANARD ROTATION EFFECTS ON CANARD ROOT BENDING MOMENT

| SYM | TEST | RUN | RMACH | RDELCL | DESCRIPTION |
|-----|------|-----|--------|----------|----------------------|
| □ | 514 | 77 | 0.9038 | 5.0182 | F/T, COMMON BASELINE |
| ▲ | 514 | 78 | 0.9010 | -0.00867 | F/T, COMMON BASELINE |
| ◇ | 514 | 79 | 0.9018 | -5.0632 | F/T, COMMON BASELINE |
| ○ | 514 | 80 | 0.9011 | -10.049 | F/T, COMMON BASELINE |
| ★ | 514 | 81 | 0.9022 | -15.034 | F/T, COMMON BASELINE |



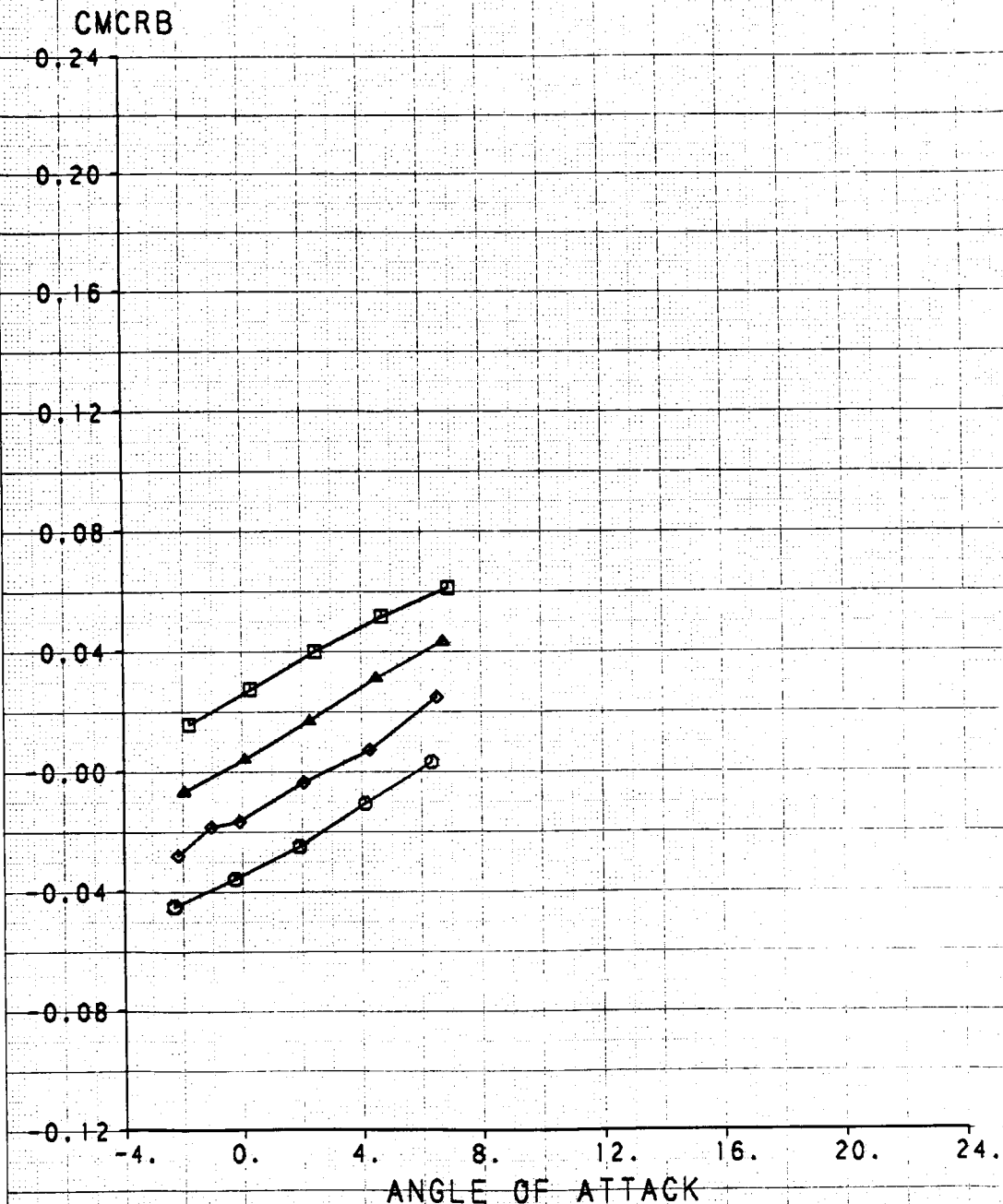
CANARD ROTATION EFFECTS ON CANARD ROOT BENDING MOMENT

| SYM | TEST | RUN | RMACH | RDELCL | DESCRIPTION |
|-----|------|-----|--------|---------|----------------------|
| □ | 514 | 82 | 1.1884 | 5.0133 | F/T, COMMON BASELINE |
| ▲ | 514 | 85 | 1.1970 | -0.0308 | F/T, COMMON BASELINE |
| ◇ | 514 | 86 | 1.1969 | -5.0400 | F/T, COMMON BASELINE |
| ○ | 514 | 87 | 1.1969 | -10.025 | F/T, COMMON BASELINE |



CANARD ROTATION EFFECTS ON CANARD ROOT BENDING MOMENT

| SYM | TEST | RUN | RMACH | RDELCL | DESCRIPTION |
|-----|------|-----|--------|---------|---------------------|
| □ | 514 | 93 | 1.3899 | 5.1040 | F/T,COMMON BASELINE |
| ▲ | 514 | 92 | 1.3923 | -0.0318 | F/T,COMMON BASELINE |
| ◇ | 514 | 94 | 1.3917 | -4.9583 | F/T,COMMON BASELINE |
| ○ | 514 | 95 | 1.3908 | -10.046 | F/T,COMMON BASELINE |

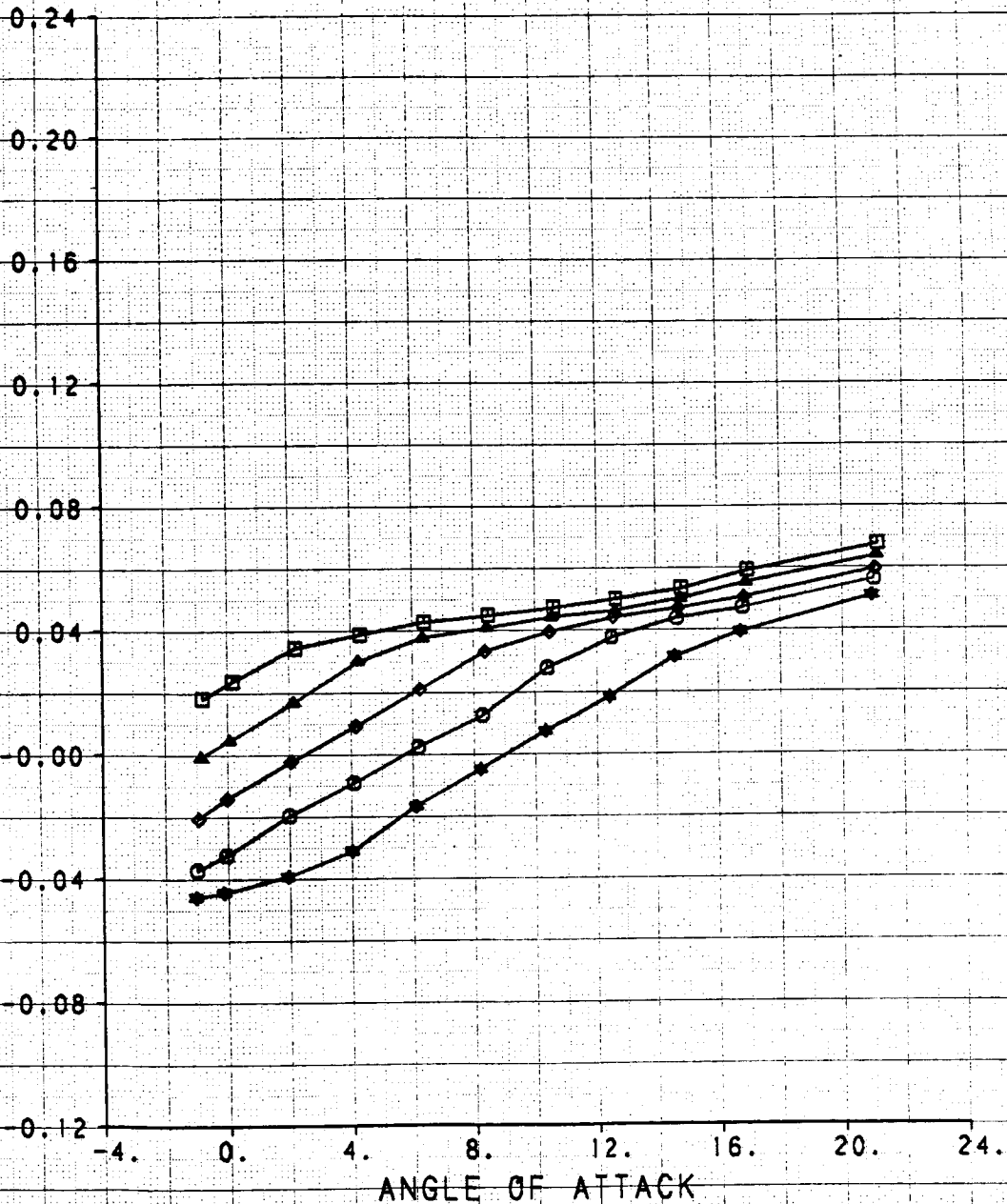


ORIGINAL PAGE IS
OF POOR QUALITY

CANARD ROTATION EFFECTS ON CANARD ROOT BENDING MOMENT

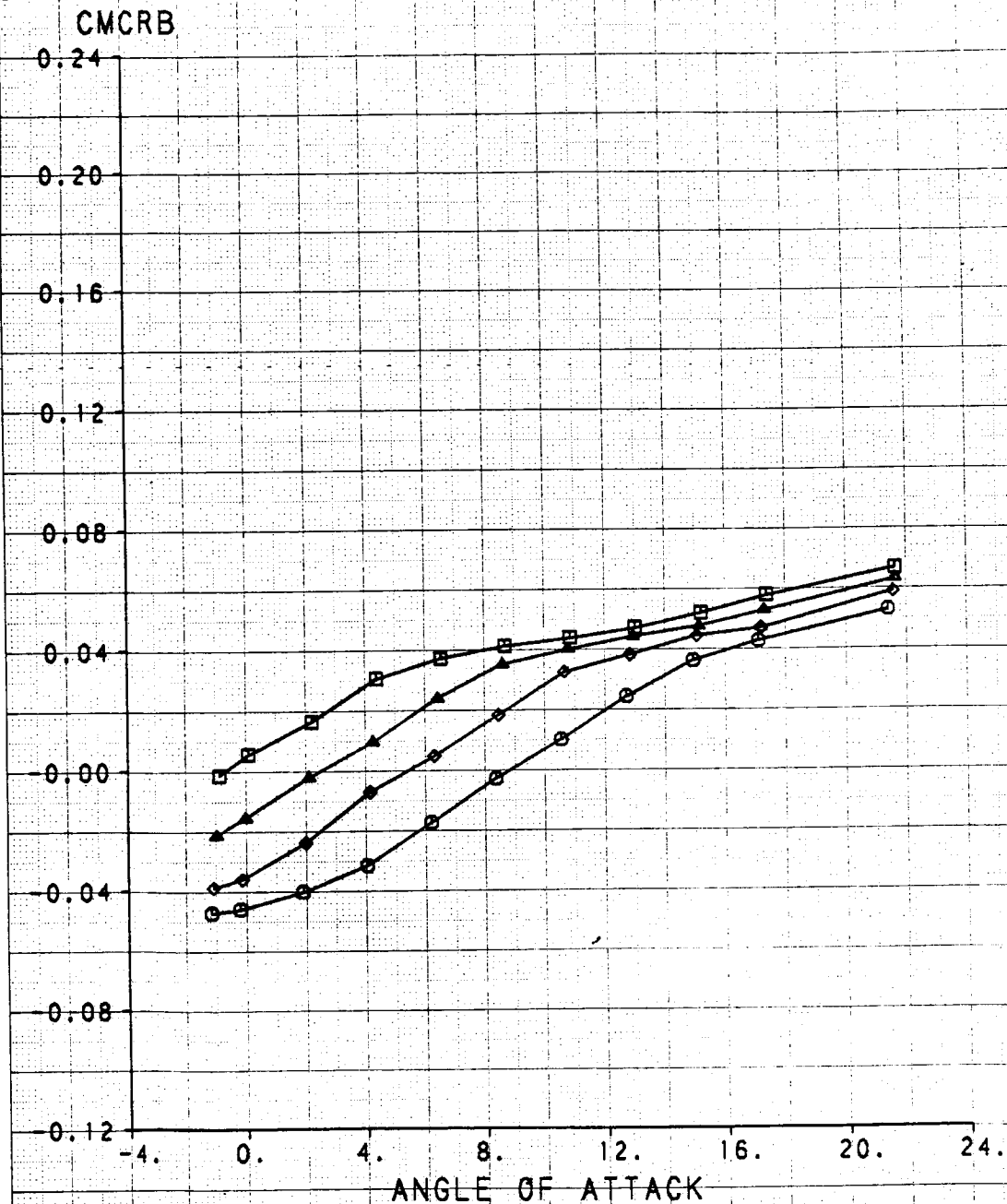
| SYM | TEST | RUN | RMACH | RDELCL | RMFR | DESCRIPTION |
|-----|------|-----|--------|---------|--------|-----------------------------------|
| □ | 514 | 164 | 0.3998 | 5.0449 | 1.1079 | F/T, NOZZLE EXTENSIONS W/EJECTORS |
| ▲ | 514 | 165 | 0.3988 | -0.0455 | 1.2024 | F/T, NOZZLE EXTENSIONS W/EJECTORS |
| ◆ | 514 | 167 | 0.4016 | -4.9958 | 1.1343 | F/T, NOZZLE EXTENSIONS W/EJECTORS |
| ○ | 514 | 168 | 0.3985 | -10.002 | 1.2163 | F/T, NOZZLE EXTENSIONS W/EJECTORS |
| ● | 514 | 169 | 0.3983 | -15.006 | 1.2087 | F/T, NOZZLE EXTENSIONS W/EJECTORS |

CMCRB



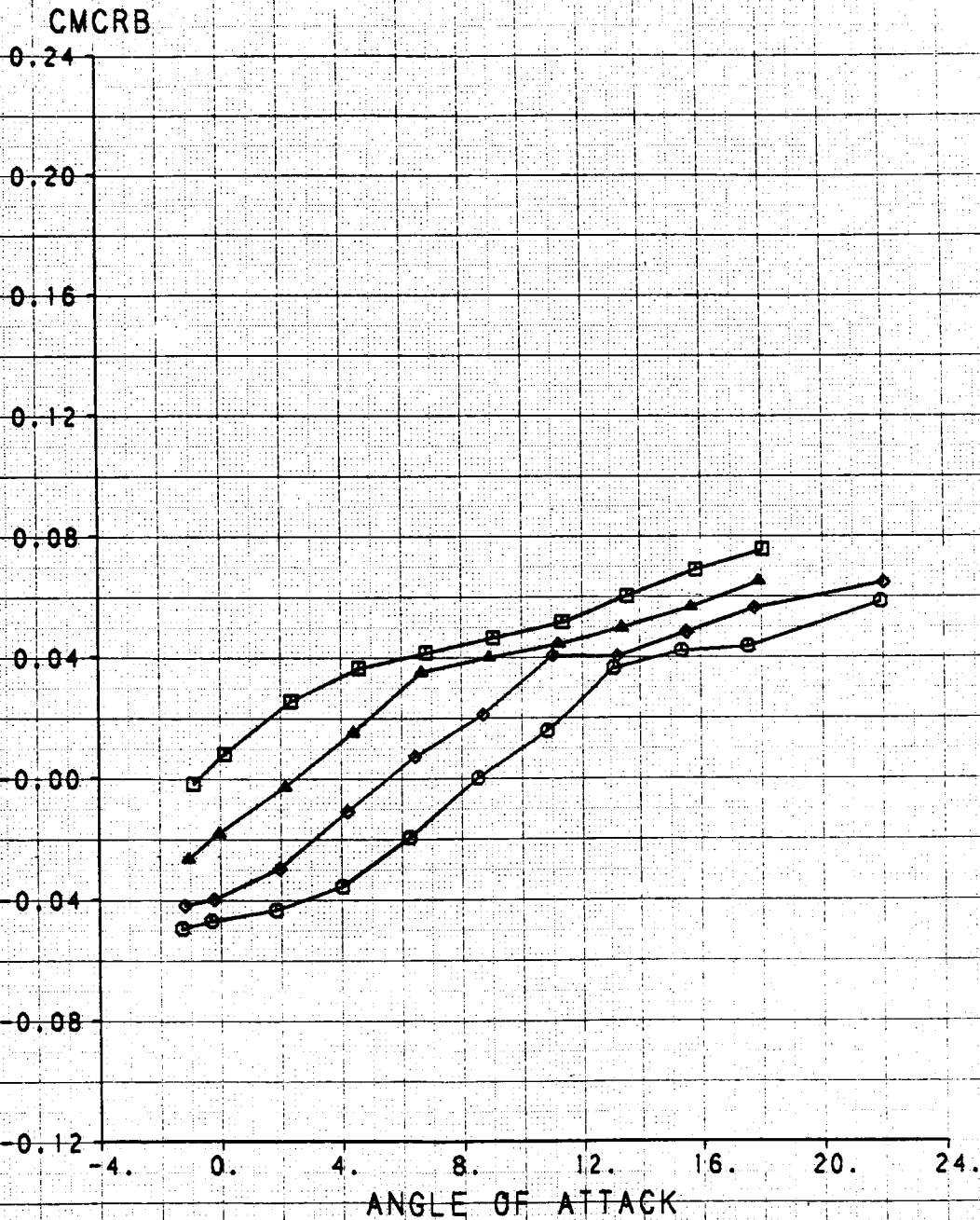
CANARD ROTATION EFFECTS ON CANARD ROOT BENDING MOMENT

| SYM | TEST | RUN | RMACH | RDELCL | RMFR | DESCRIPTION |
|-----|------|-----|--------|---------|--------|-----------------------------------|
| □ | 514 | 173 | 0.5990 | -0.0564 | 0.9221 | F/T, NOZZLE EXTENSIONS W/EJECTORS |
| ▲ | 514 | 172 | 0.5994 | -4.9770 | 0.9207 | F/T, NOZZLE EXTENSIONS W/EJECTORS |
| ◆ | 514 | 171 | 0.5994 | -10.014 | 0.9211 | F/T, NOZZLE EXTENSIONS W/EJECTORS |
| ○ | 514 | 170 | 0.6001 | -14.987 | 0.9175 | F/T, NOZZLE EXTENSIONS W/EJECTORS |



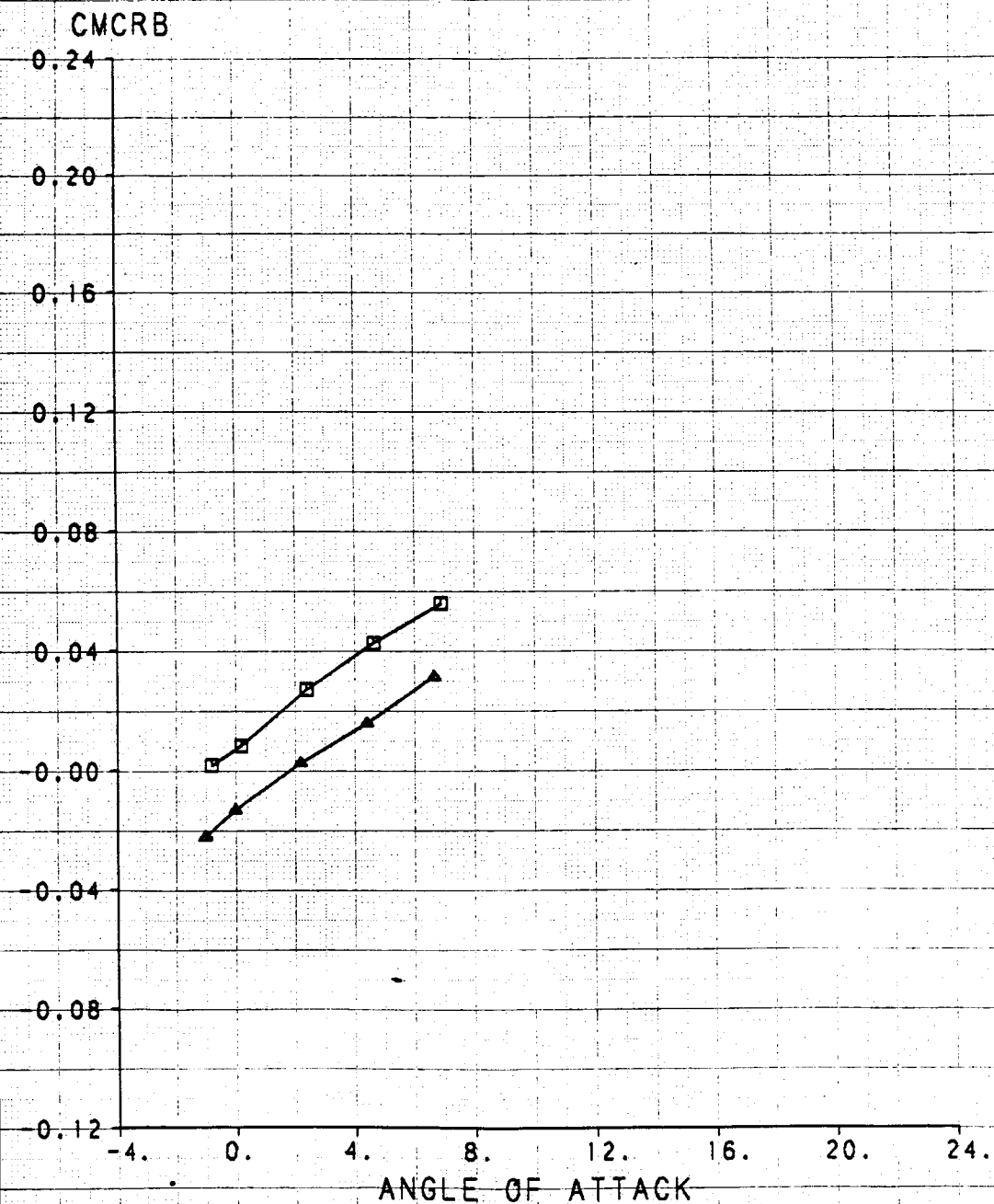
CANARD ROTATION EFFECTS ON CANARD ROOT BENDING MOMENT

| SYM | TEST | RUN | RMACH | HDELCL | RMFR | DESCRIPTION |
|-----|------|-----|--------|---------|--------|------------------------|
| □ | 514 | 155 | 0.9018 | -0.0601 | 0.8674 | F/T, NOZZLE EXTENSIONS |
| ▲ | 514 | 156 | 0.9022 | -4.8921 | 0.8692 | F/T, NOZZLE EXTENSIONS |
| ◆ | 514 | 157 | 0.9020 | -10.000 | 0.8674 | F/T, NOZZLE EXTENSIONS |
| ○ | 514 | 158 | 0.9020 | -15.025 | 0.8695 | F/T, NOZZLE EXTENSIONS |



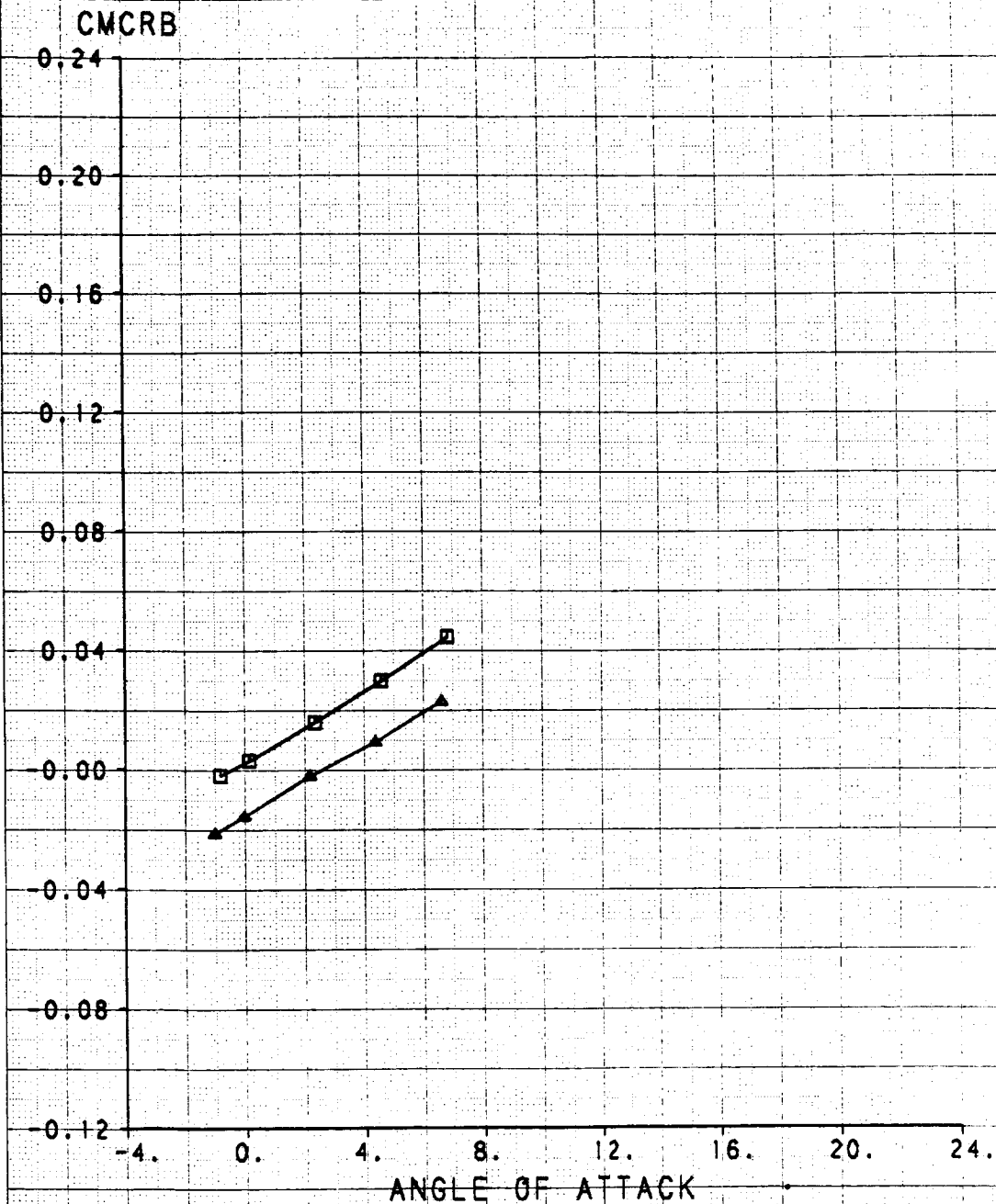
CANARD ROTATION EFFECTS ON CANARD ROOT BENDING MOMENT

| SYM | TEST | RUN | RMACH | RDELCL | RMFR | DESCRIPTION |
|-----|------|-----|--------|---------|--------|------------------------|
| □ | 514 | 180 | 1.1972 | -0.0539 | 0.8895 | F/T, NOZZLE EXTENSIONS |
| ▲ | 514 | 159 | 1.1977 | -4.9745 | 0.8895 | F/T, NOZZLE EXTENSIONS |



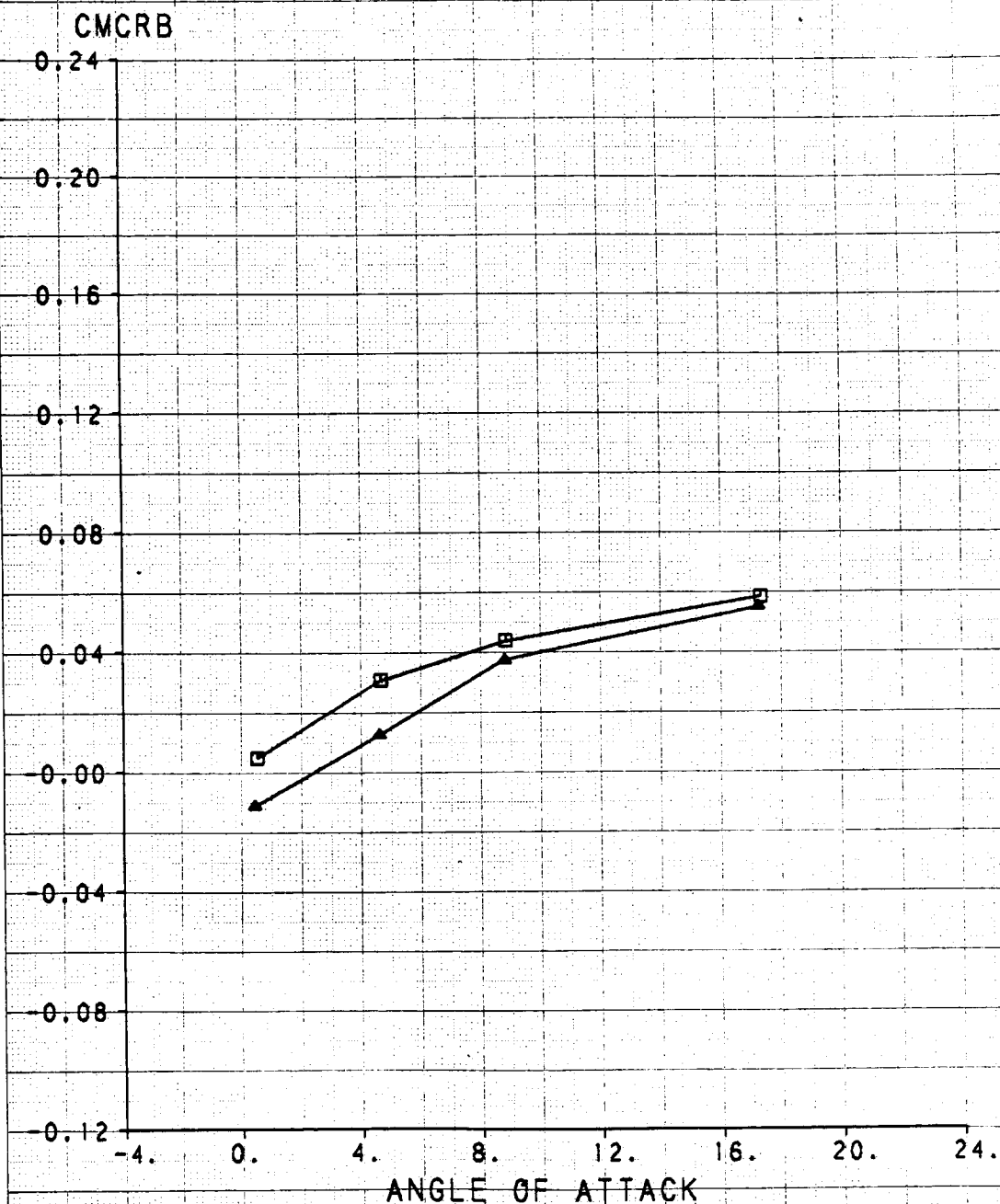
CANARD ROTATION EFFECTS ON CANARD ROOT BENDING MOMENT

| SYM | TEST | RUN | RMACH | RDELCL | RMFR | DESCRIPTION |
|-----|------|-----|--------|---------|--------|------------------------|
| □ | 514 | 161 | 1.3936 | -0.0567 | 0.9250 | F/T, NOZZLE EXTENSIONS |
| ▲ | 514 | 162 | 1.3939 | -4.8931 | 0.9281 | F/T, NOZZLE EXTENSIONS |



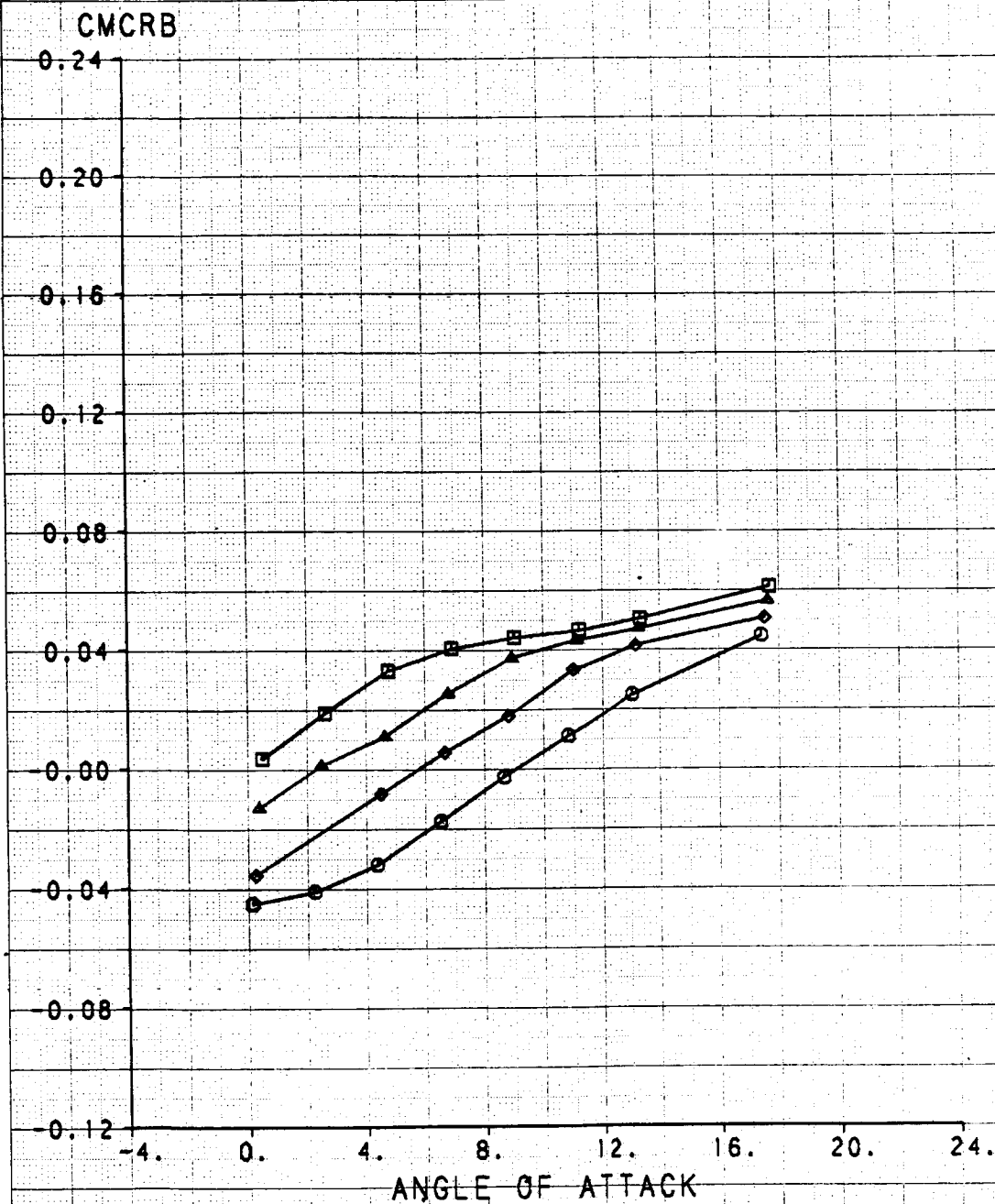
CANARD ROTATION EFFECTS ON CANARD ROOT BENDING MOMENT

| SYM | TEST | RUN | RMACH | ROELCL | RMFR | RNPRA | DESCRIPTION |
|-----|------|-----|--------|---------|--------|--------|---------------------------|
| □ | 514 | 277 | 0.4012 | 0.1416 | 1.1551 | 2.8538 | CMAPS, SIMULATED AIRCRAFT |
| ▲ | 514 | 288 | 0.4019 | -5.0028 | 1.1505 | 2.8778 | CMAPS, SIMULATED AIRCRAFT |



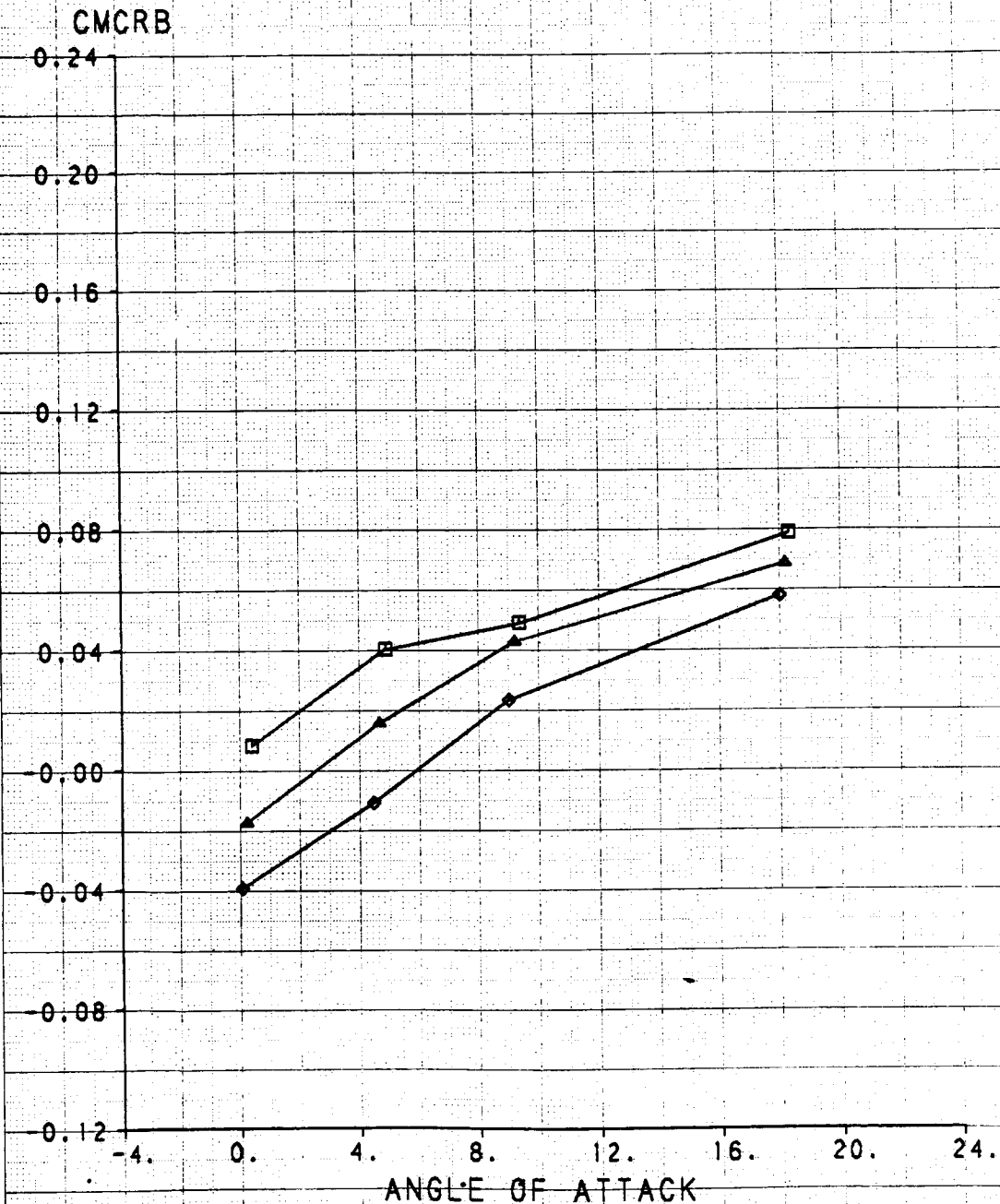
CANARD ROTATION EFFECTS ON CANARD ROOT BENDING MOMENT

| SYM | TEST | RUN | RMACH | RDELCL | RMFR | RNPRA | DESCRIPTION |
|-----|------|-----|--------|---------|--------|--------|---------------------------|
| □ | 514 | 178 | 0.8009 | 0.1001 | 0.9161 | 3.8301 | CMAPS, SIMULATED AIRCRAFT |
| ▲ | 514 | 179 | 0.8010 | -4.9809 | 0.9158 | 3.8557 | CMAPS, SIMULATED AIRCRAFT |
| ◇ | 514 | 180 | 0.8010 | -10.081 | 0.9169 | 3.8478 | CMAPS, SIMULATED AIRCRAFT |
| ○ | 514 | 182 | 0.5994 | -14.883 | 0.9215 | 3.8168 | CMAPS, SIMULATED AIRCRAFT |



CANARD ROTATION EFFECTS ON CANARD ROOT BENDING MOMENT

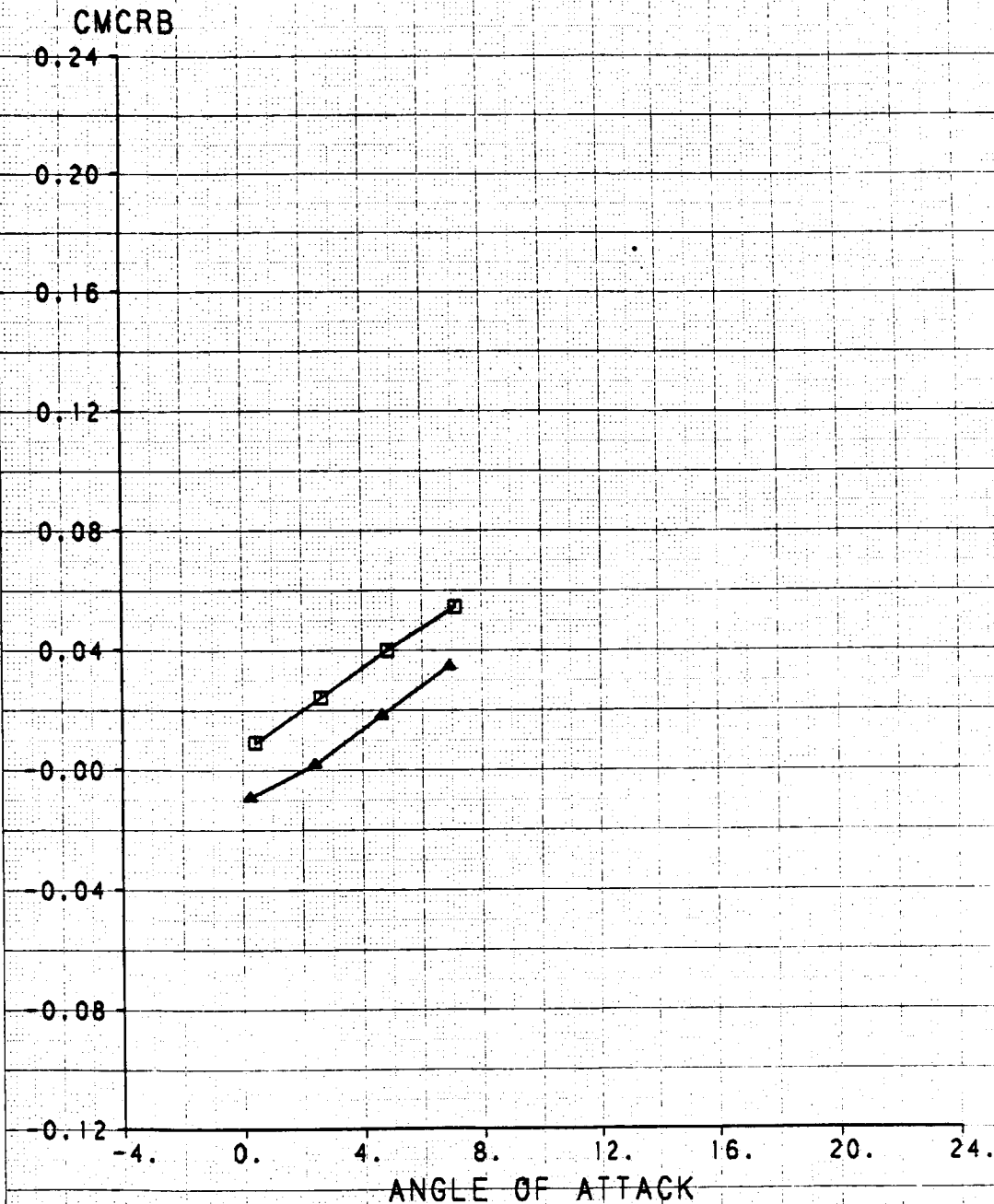
| SYM | TEST | RUN | RMACH | RDELCL | RMFR | RNPRA | DESCRIPTION |
|-----|------|-----|--------|---------|--------|--------|---------------------------|
| □ | 514 | 197 | 0.9031 | 0.0791 | 0.7501 | 5.4208 | CMAPS, SIMULATED AIRCRAFT |
| ▲ | 514 | 215 | 0.8984 | -4.9625 | 0.7534 | 5.3011 | CMAPS, SIMULATED AIRCRAFT |
| ◇ | 514 | 231 | 0.9032 | -10.143 | 0.7544 | 5.3161 | CMAPS, SIMULATED AIRCRAFT |



ORIGINAL PAGE IS
OF POOR QUALITY

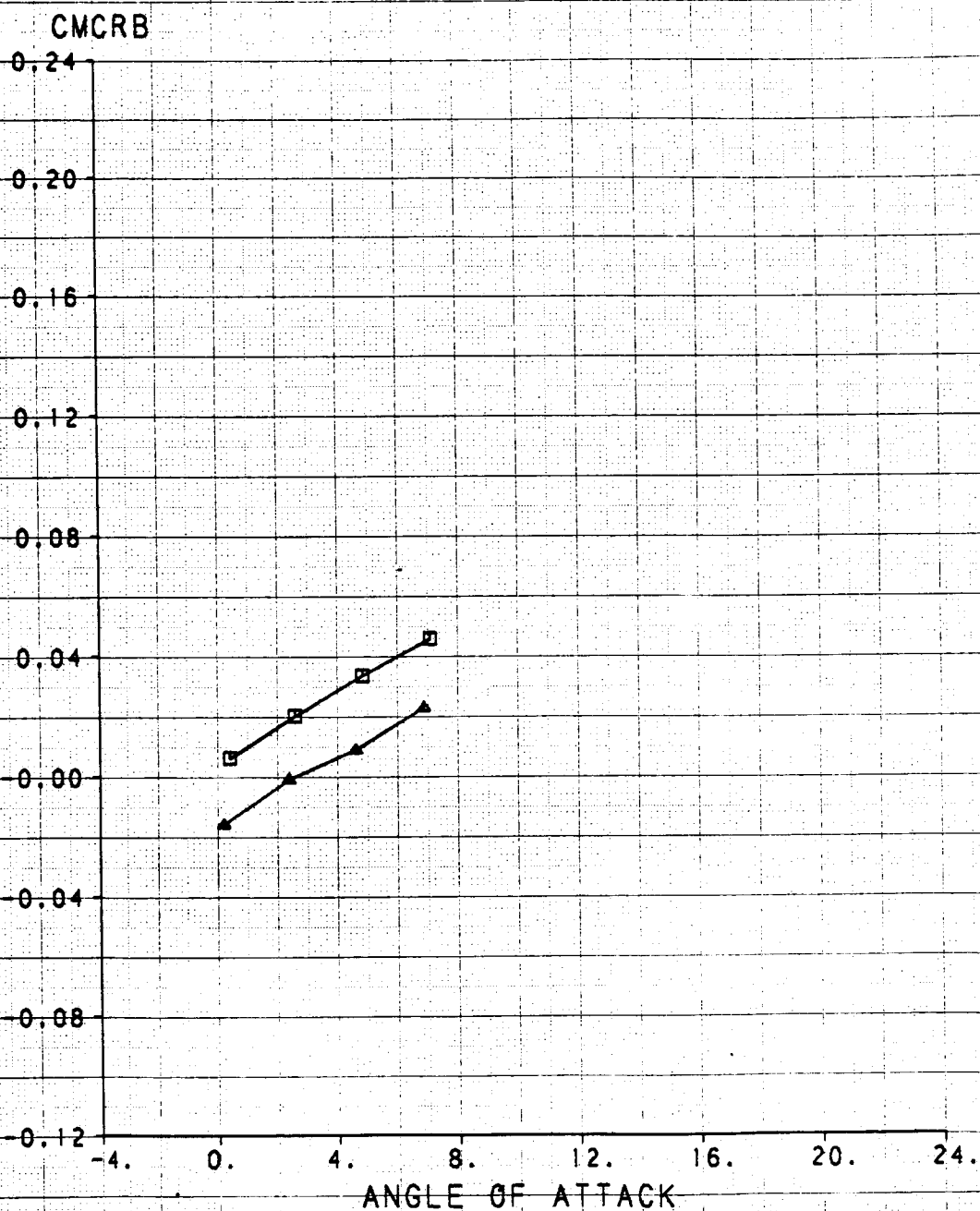
CANARD ROTATION EFFECTS ON CANARD ROOT BENDING MOMENT

| SYM | TEST | RUN | RMACH | RDELCL | RMFR | RNPRA | DESCRIPTION |
|-----|------|-----|--------|---------|--------|--------|---------------------------|
| □ | 514 | 242 | 1.1908 | 0.1042 | 0.7579 | 7.5840 | CMAPS, SIMULATED AIRCRAFT |
| ▲ | 514 | 249 | 1.1920 | -5.0946 | 0.7579 | 7.5379 | CMAPS, SIMULATED AIRCRAFT |



CANARD ROTATION EFFECTS ON CANARD ROOT BENDING MOMENT

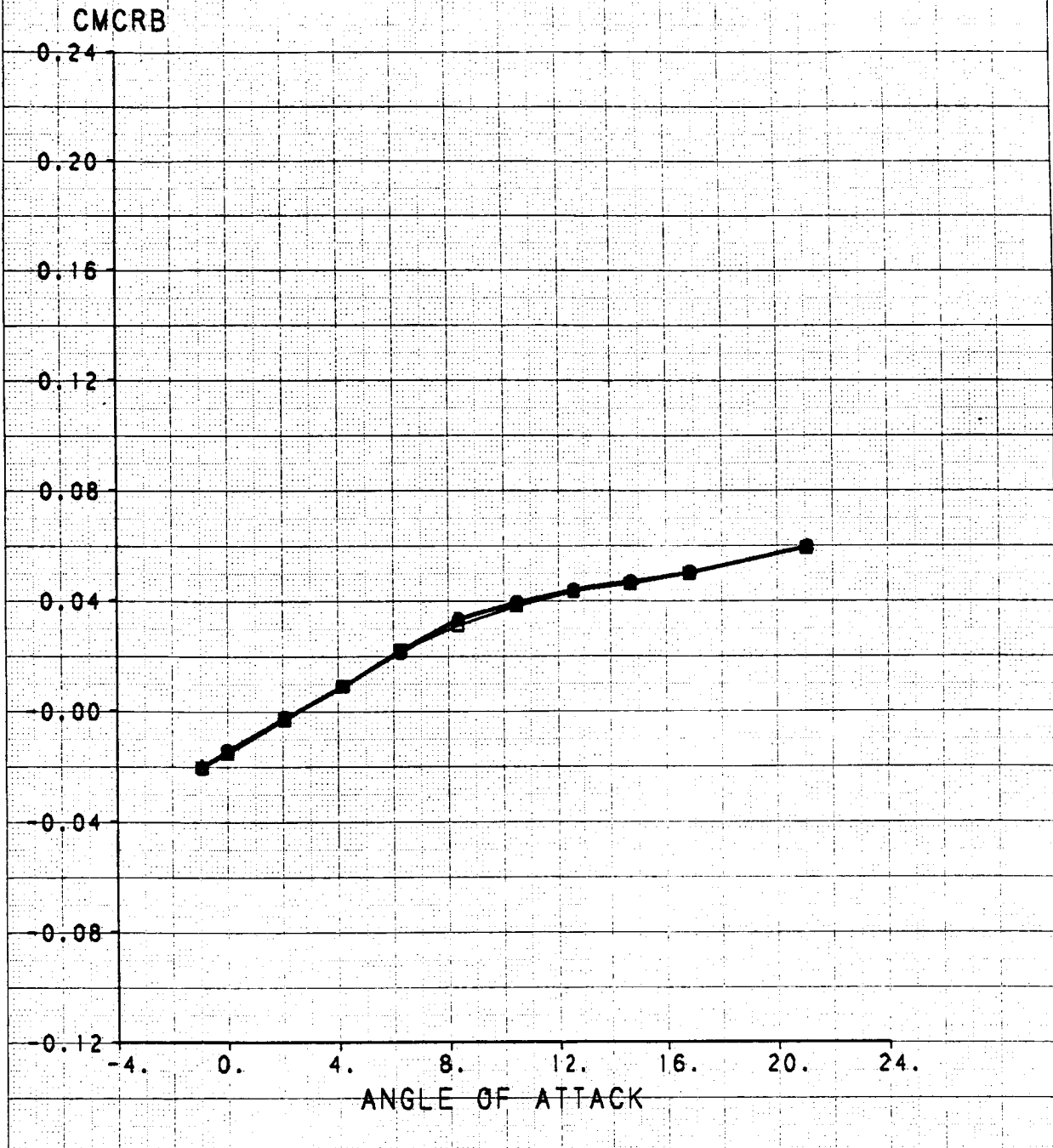
| SYM | TEST | RUN | RMACH | RDELCL | RMFR | RNPRA | DESCRIPTION |
|-----|------|-----|--------|---------|--------|--------|---------------------------|
| □ | 514 | 258 | 1.3989 | 0.1083 | 0.7929 | 9.5970 | CMAPS, SIMULATED AIRCRAFT |
| ▲ | 514 | 283 | 1.3970 | -5.0866 | 0.7915 | 9.6047 | CMAPS, SIMULATED AIRCRAFT |



ORIGINAL PAGE IS
OF POOR QUALITY

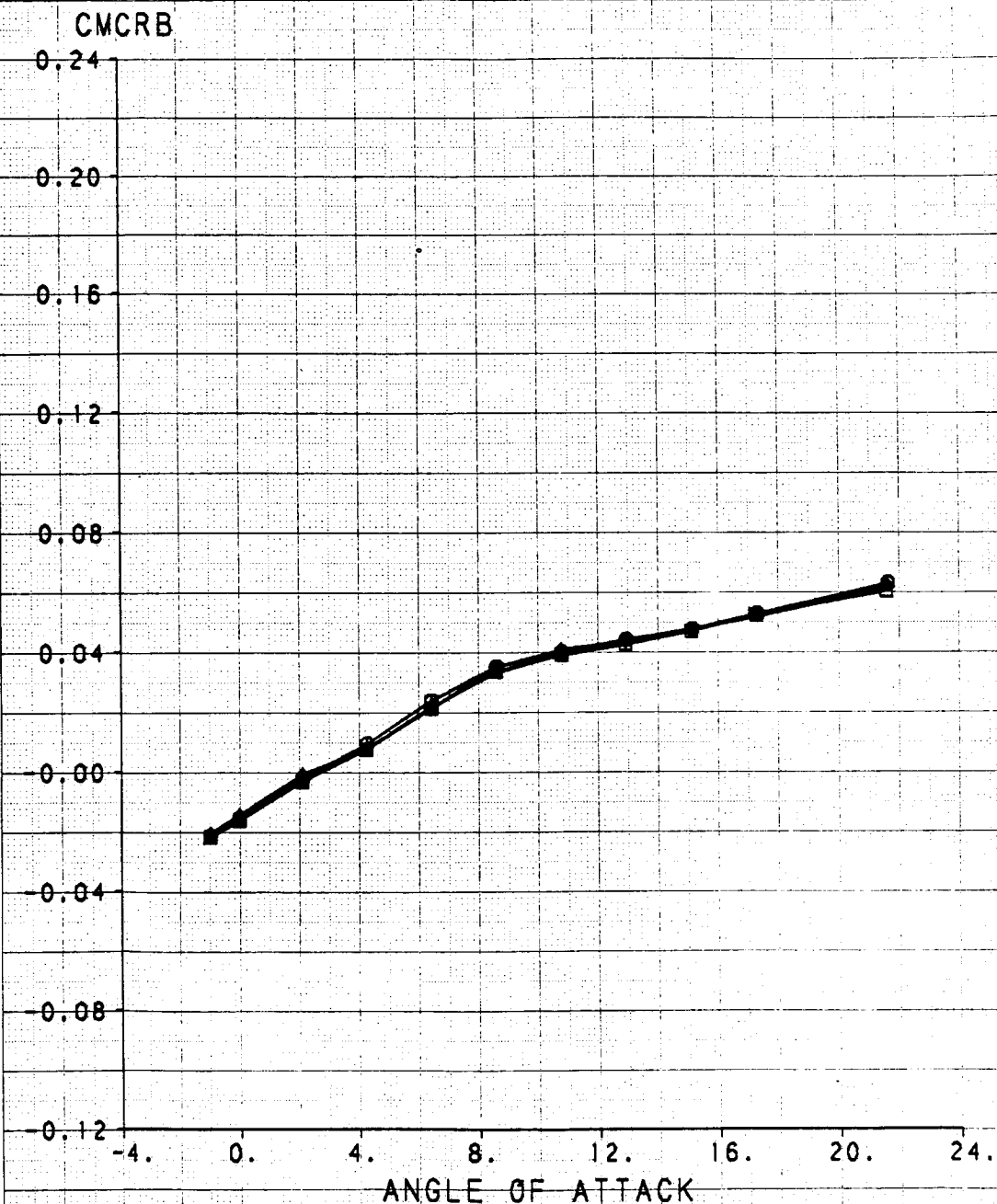
MASS FLOW RATIO EFFECTS ON CANARD ROOT BENDING MOMENT

| SYM | TEST | RUN | RMACH | RDELCL | RMFR | DESCRIPTION |
|-----|------|-----|--------|---------|--------|-----------------------------------|
| □ | 514 | 188 | 0.3999 | -4.9989 | 0.5548 | F/T, NOZZLE EXTENSIONS W/EJECTORS |
| △ | 514 | 288 | 0.3982 | -4.9948 | 0.8216 | F/T, NOZZLE EXTENSIONS W/EJECTORS |
| ◆ | 514 | 178 | 0.3988 | -4.9726 | 1.1164 | F/T, NOZZLE EXTENSIONS W/EJECTORS |
| ○ | 514 | 167 | 0.4016 | -4.8956 | 1.1343 | F/T, NOZZLE EXTENSIONS W/EJECTORS |



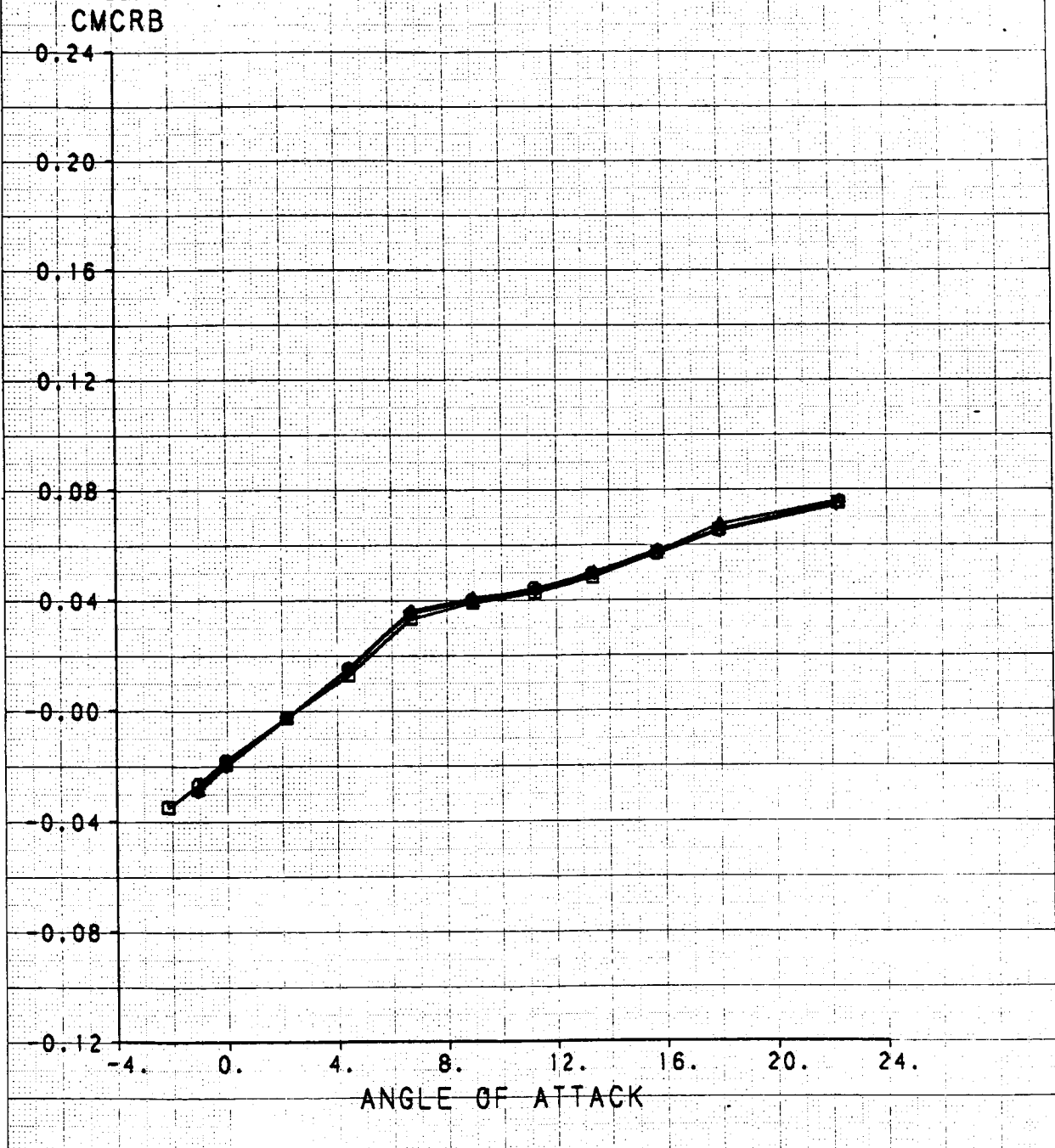
MASS FLOW RATIO EFFECTS ON CANARD ROOT BENDING MOMENT

| SYM | TEST | RUN | RMACH | RDELCL | RMFR | DESCRIPTION |
|-----|------|-----|--------|---------|--------|-----------------------------------|
| □ | 514 | 193 | 0.5980 | -4.9926 | 0.4112 | F/T, NOZZLE EXTENSIONS W/EJECTORS |
| ▲ | 514 | 211 | 0.5982 | -4.9896 | 0.6102 | F/T, NOZZLE EXTENSIONS W/EJECTORS |
| ◇ | 514 | 182 | 0.5987 | -4.9870 | 0.8311 | F/T, NOZZLE EXTENSIONS W/EJECTORS |
| ○ | 514 | 172 | 0.5984 | -4.9770 | 0.9207 | F/T, NOZZLE EXTENSIONS W/EJECTORS |



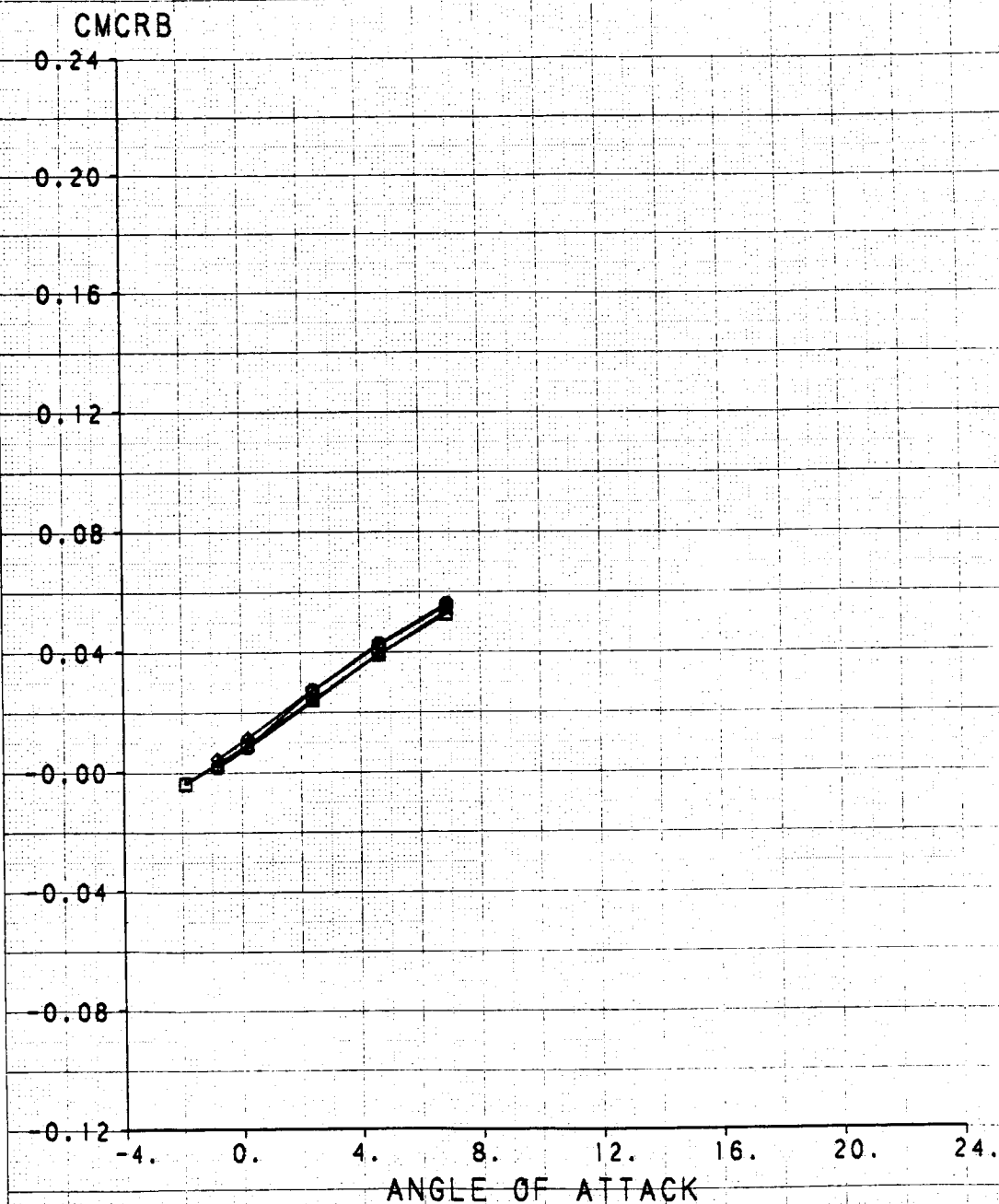
MASS FLOW RATIO EFFECTS ON CANARD ROOT BENDING MOMENT

| SYM | TEST | RUN | RMACH | RMELCL | RMFR | DESCRIPTION |
|-----|------|-----|--------|---------|--------|------------------------|
| □ | 514 | 117 | 0.9000 | -4.9149 | 0.3485 | F/T, NOZZLE EXTENSIONS |
| ▲ | 514 | 133 | 0.9018 | -4.9835 | 0.5176 | F/T, NOZZLE EXTENSIONS |
| ◆ | 514 | 147 | 0.9018 | -4.9854 | 0.7063 | F/T, NOZZLE EXTENSIONS |
| ○ | 514 | 156 | 0.9022 | -4.9921 | 0.8692 | F/T, NOZZLE EXTENSIONS |



MASS FLOW RATIO EFFECTS ON CANARD ROOT BENDING MOMENT

| SYM | TEST | RUN | RMACH | RDELCL | RMFR | DESCRIPTION |
|-----|------|-----|--------|---------|--------|------------------------|
| □ | 514 | 121 | 1.1999 | -0.0575 | 0.3523 | F/T, NOZZLE EXTENSIONS |
| ▲ | 514 | 129 | 1.1991 | -0.0409 | 0.5236 | F/T, NOZZLE EXTENSIONS |
| ◆ | 514 | 145 | 1.1963 | -0.0861 | 0.7123 | F/T, NOZZLE EXTENSIONS |
| ○ | 514 | 160 | 1.1972 | -0.0539 | 0.8895 | F/T, NOZZLE EXTENSIONS |

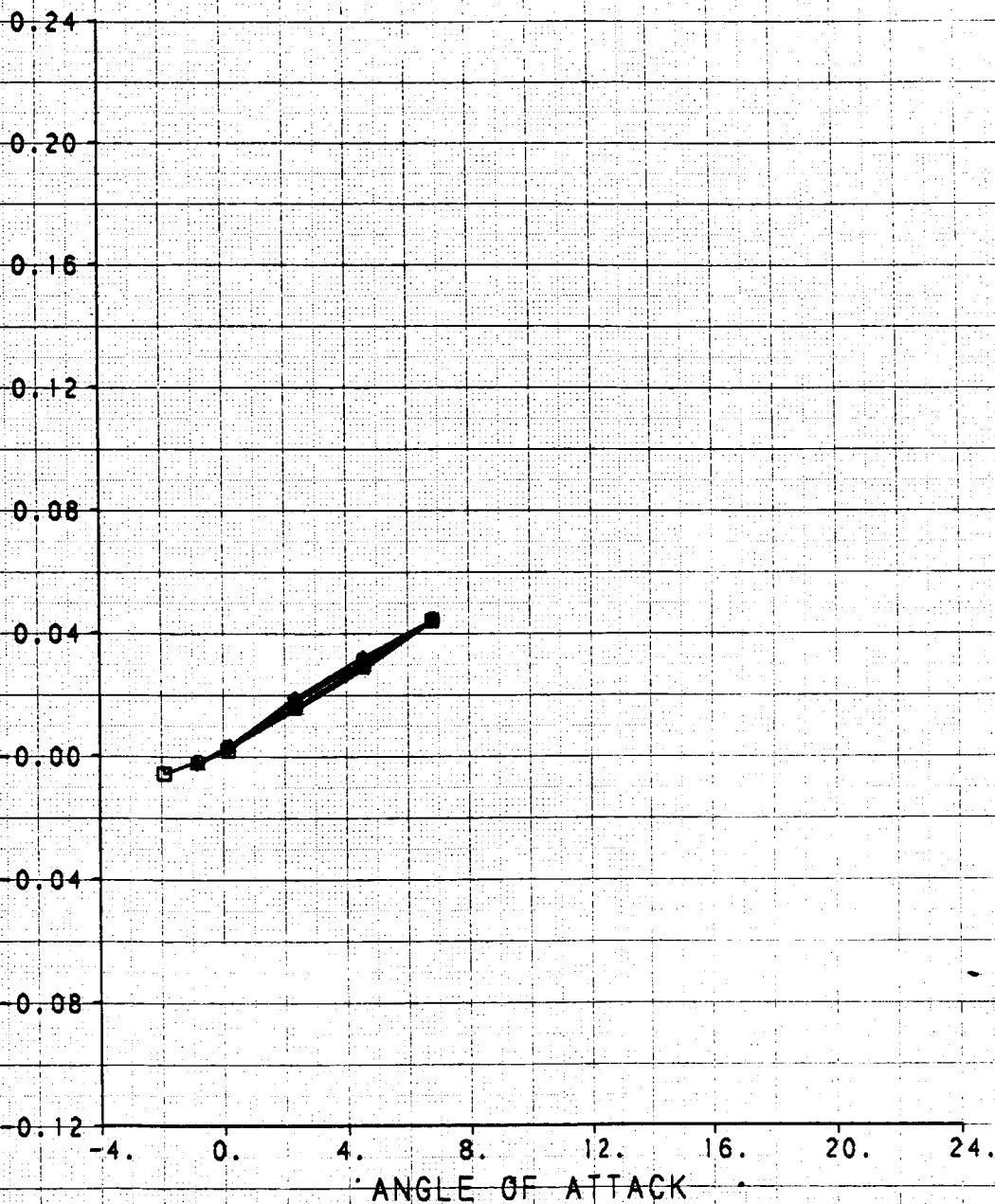


ORIGINAL PAGE IS
OF POOR QUALITY

MASS FLOW RATIO EFFECTS ON CANARD ROOT BENDING MOMENT

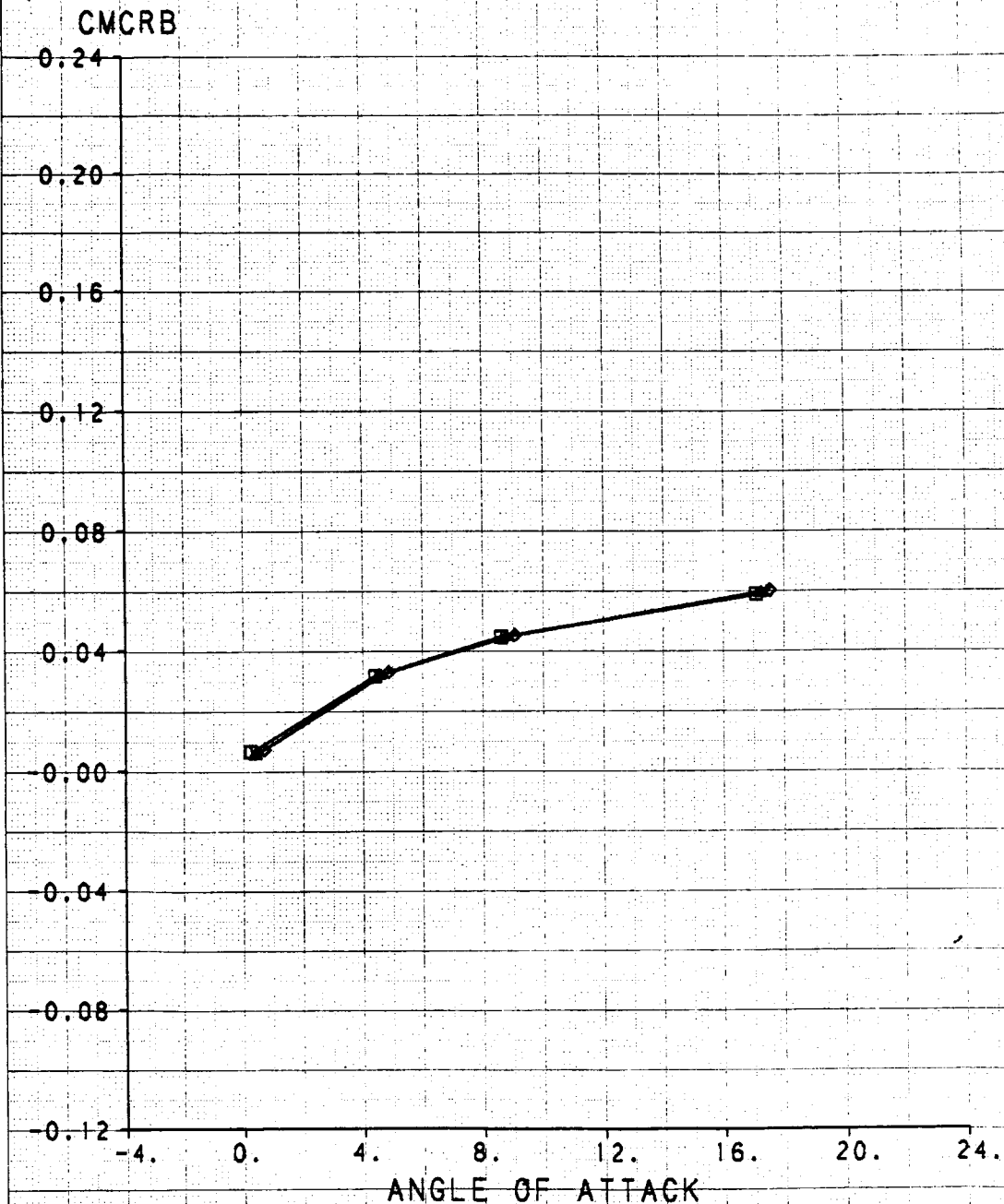
| SYM | TEST | RUN | RMACH | RDELCL | RMFR | DESCRIPTION |
|-----|------|-----|--------|----------|--------|------------------------|
| □ | 514 | 124 | 1.3871 | -0.00408 | 0.3654 | F/T, NOZZLE EXTENSIONS |
| ▲ | 514 | 128 | 1.3948 | -0.0234 | 0.5445 | F/T, NOZZLE EXTENSIONS |
| ◆ | 514 | 142 | 1.3972 | -0.0567 | 0.7423 | F/T, NOZZLE EXTENSIONS |
| ⊙ | 514 | 161 | 1.3936 | -0.0567 | 0.9250 | F/T, NOZZLE EXTENSIONS |

CMCRB



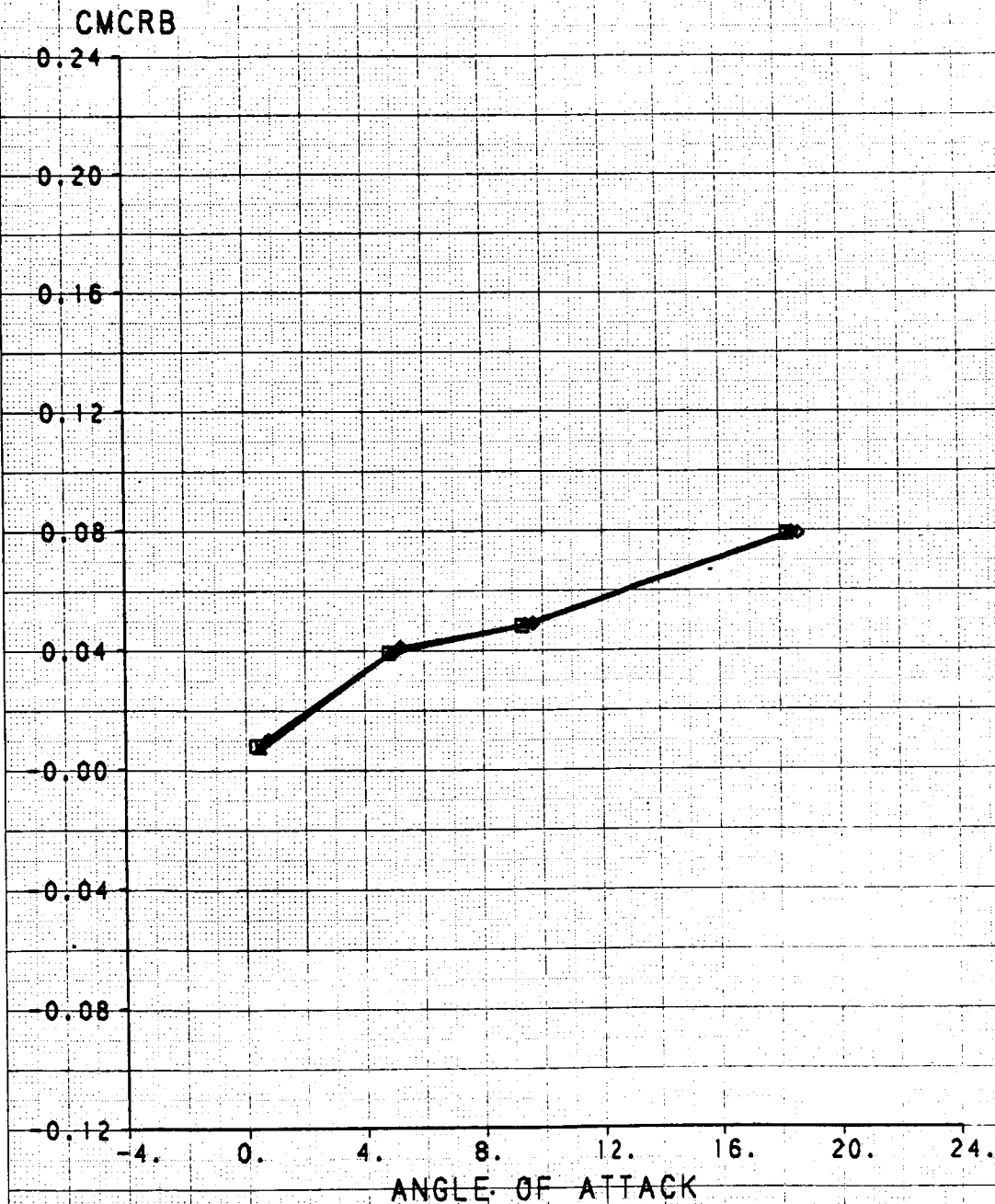
MASS FLOW RATIO EFFECTS ON CANARD ROOT BENDING MOMENT

| SYM | TEST | RUN | RMACH | RDELCL | RMFR | RNPRA | DESCRIPTION |
|-----|------|-----|--------|--------|--------|--------|---------------------------|
| □ | 514 | 265 | 0.4019 | 0.1531 | 0.7801 | 1.3322 | CMAPS, SIMULATED AIRCRAFT |
| ▲ | 514 | 266 | 0.4019 | 0.1562 | 0.9176 | 1.3145 | CMAPS, SIMULATED AIRCRAFT |
| ◇ | 514 | 269 | 0.4023 | 0.1520 | 1.0552 | 1.2816 | CMAPS, SIMULATED AIRCRAFT |



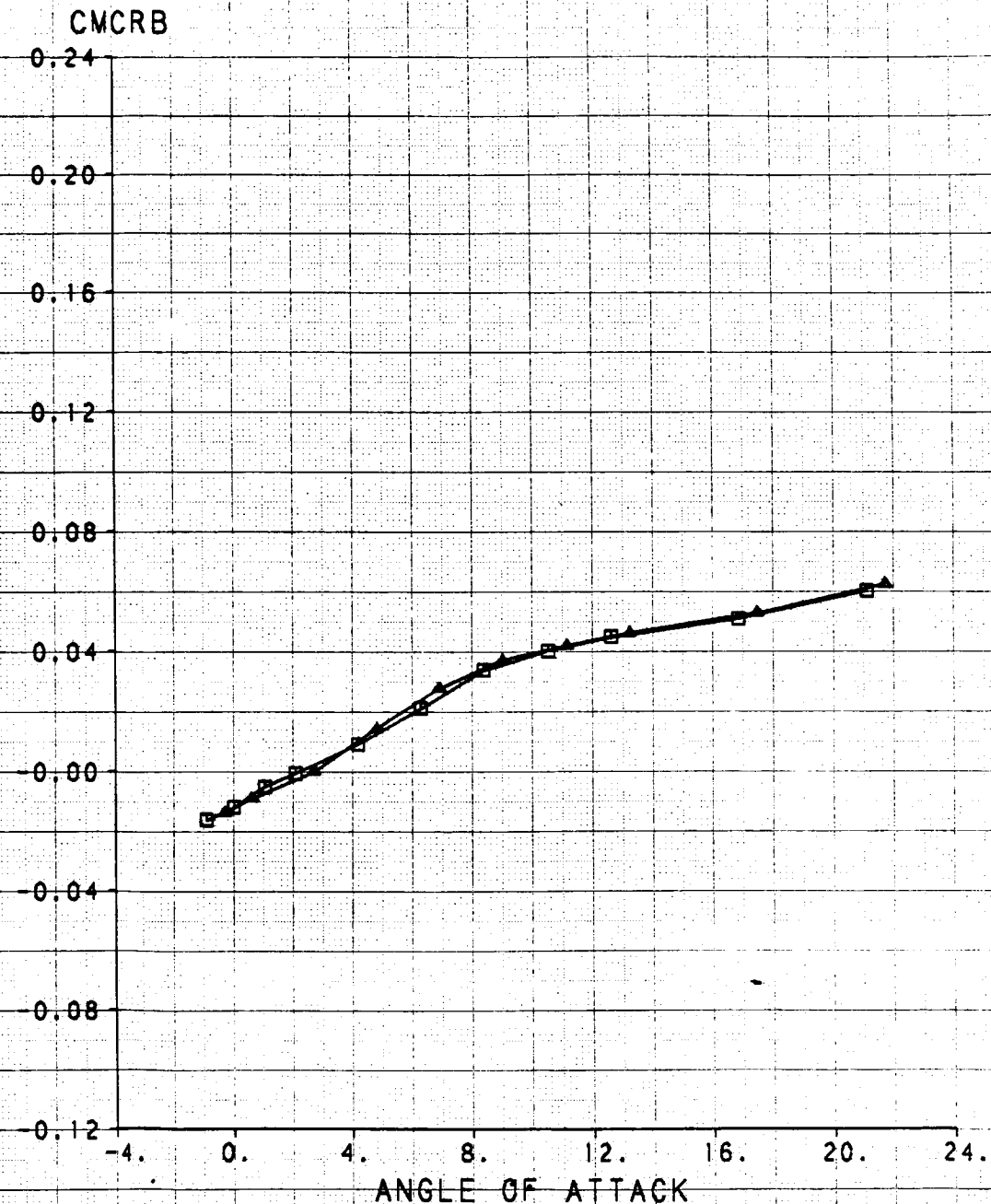
MASS FLOW RATIO EFFECTS ON CANARD ROOT BENDING MOMENT

| SYM | TEST | RUN | RMACH | RDELCL | RMFR | RNPRA | DESCRIPTION |
|-----|------|-----|--------|--------|--------|--------|---------------------------|
| □ | 514 | 192 | 0.9021 | 0.1239 | 0.6751 | 4.4266 | CMAPS, SIMULATED AIRCRAFT |
| △ | 514 | 198 | 0.9042 | 0.0938 | 0.7568 | 4.3951 | CMAPS, SIMULATED AIRCRAFT |
| ◇ | 514 | 200 | 0.9052 | 0.1250 | 0.8665 | 4.2850 | CMAPS, SIMULATED AIRCRAFT |



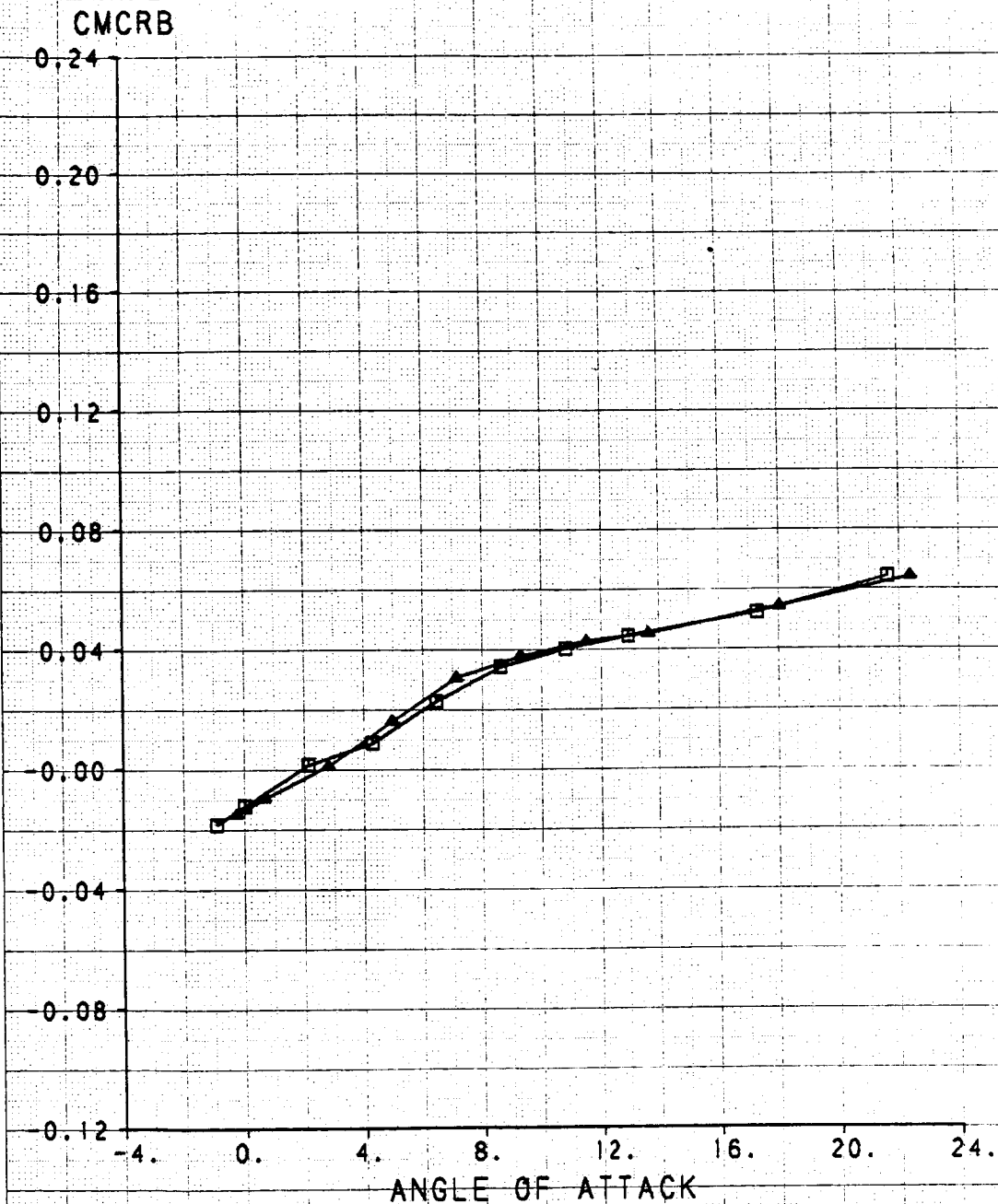
NOZZLE PRESSURE RATIO EFFECTS ON CANARD ROOT BENDING MOMENT

| SYM | TEST | RUN | RMACH | RDELCL | RNPRA | DESCRIPTION |
|-----|------|-----|--------|---------|--------|------------------------------|
| □ | 514 | 238 | 0.3989 | -4.9629 | 0.0637 | J/E, COMMON BASELINE JET-OFF |
| ▲ | 514 | 258 | 0.3992 | -5.0064 | 4.0334 | J/E, COMMON BASELINE JET-ON |



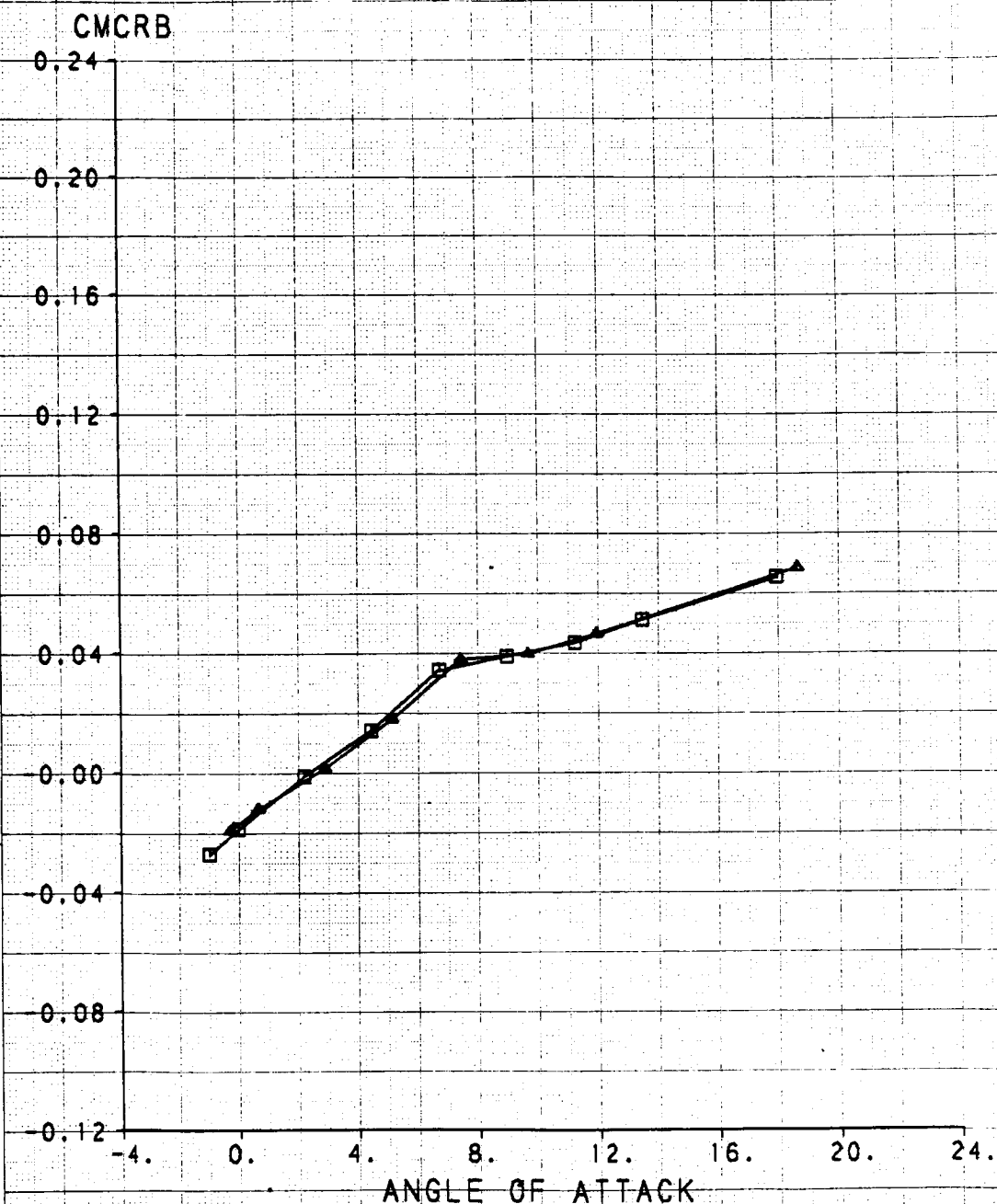
NOZZLE PRESSURE RATIO EFFECTS ON CANARD ROOT BENDING MOMENT

| SYM | TEST | RUN | RMACH | DELCL | RNPRA | DESCRIPTION |
|-----|------|-----|--------|---------|--------|------------------------------|
| □ | 514 | 243 | 0.8214 | -4.9911 | 0.0908 | J/E, COMMON BASELINE JET-OFF |
| ▲ | 514 | 259 | 0.8009 | -4.9783 | 4.1998 | J/E, COMMON BASELINE JET-ON |



NOZZLE PRESSURE RATIO EFFECTS ON CANARD ROOT BENDING MOMENT

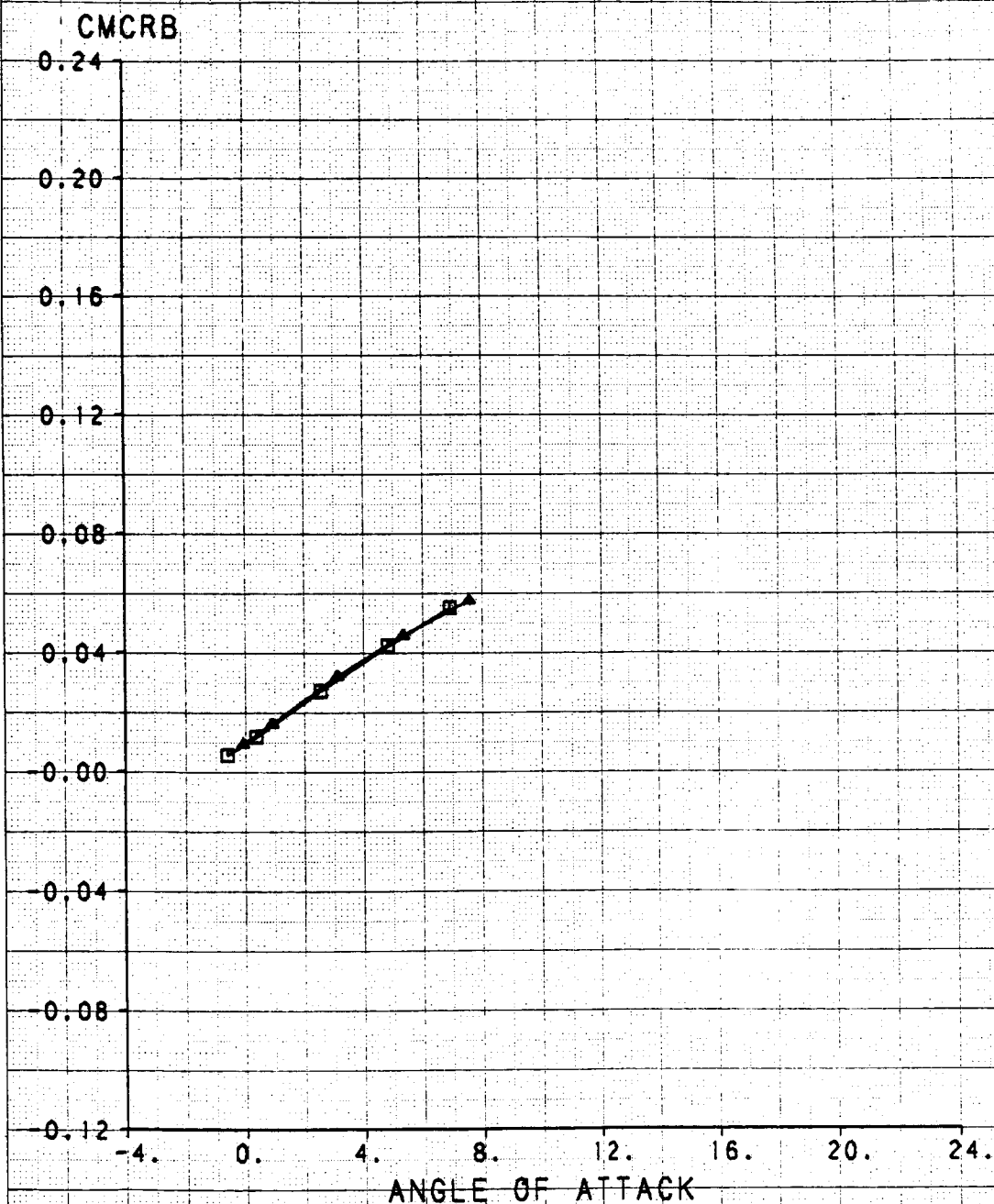
| SYM | TEST | RUN | RMACH | ROELCL | RNPRA | DESCRIPTION |
|-----|------|-----|--------|---------|--------|------------------------------|
| □ | 514 | 244 | 0.9022 | -4.9674 | 0.1384 | J/E, COMMON BASELINE JET-OFF |
| ▲ | 514 | 282 | 0.9019 | -4.9691 | 0.0982 | J/E, COMMON BASELINE JET-ON |



ORIGINAL PAGE IS
OF POOR QUALITY

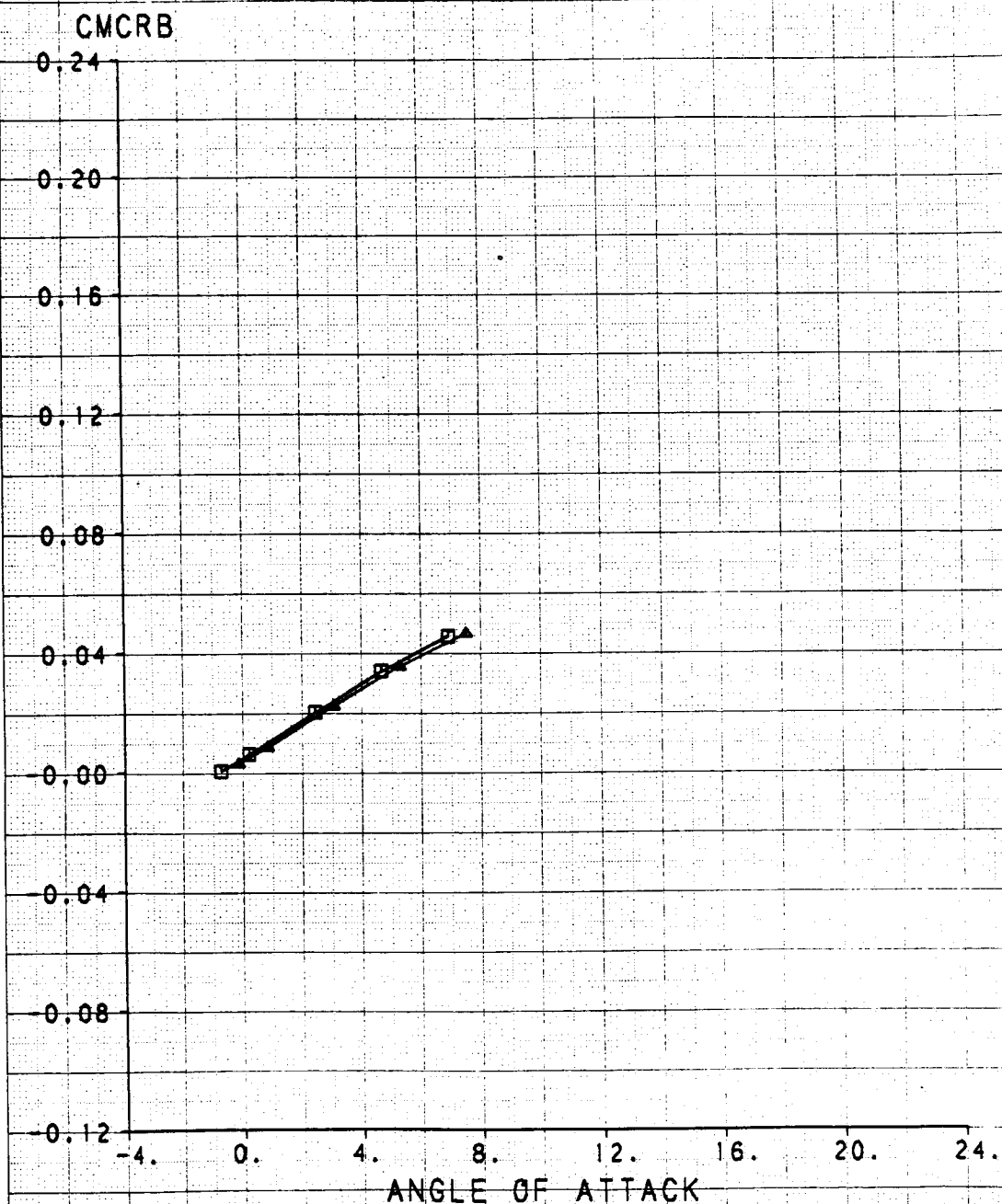
NOZZLE PRESSURE RATIO EFFECTS ON CANARD ROOT BENDING MOMENT

| SYM | TEST | RUN | RMACH | RDELCL | RNPRA | DESCRIPTION |
|-----|------|-----|--------|---------|--------|------------------------------|
| □ | 514 | 245 | 1.1772 | -0.1036 | 0.1893 | J/E, COMMON BASELINE JET-OFF |
| ▲ | 514 | 252 | 1.1846 | -0.0448 | 0.0806 | J/E, COMMON BASELINE JET-ON |



NOZZLE PRESSURE RATIO EFFECTS ON CANARD ROOT BENDING MOMENT

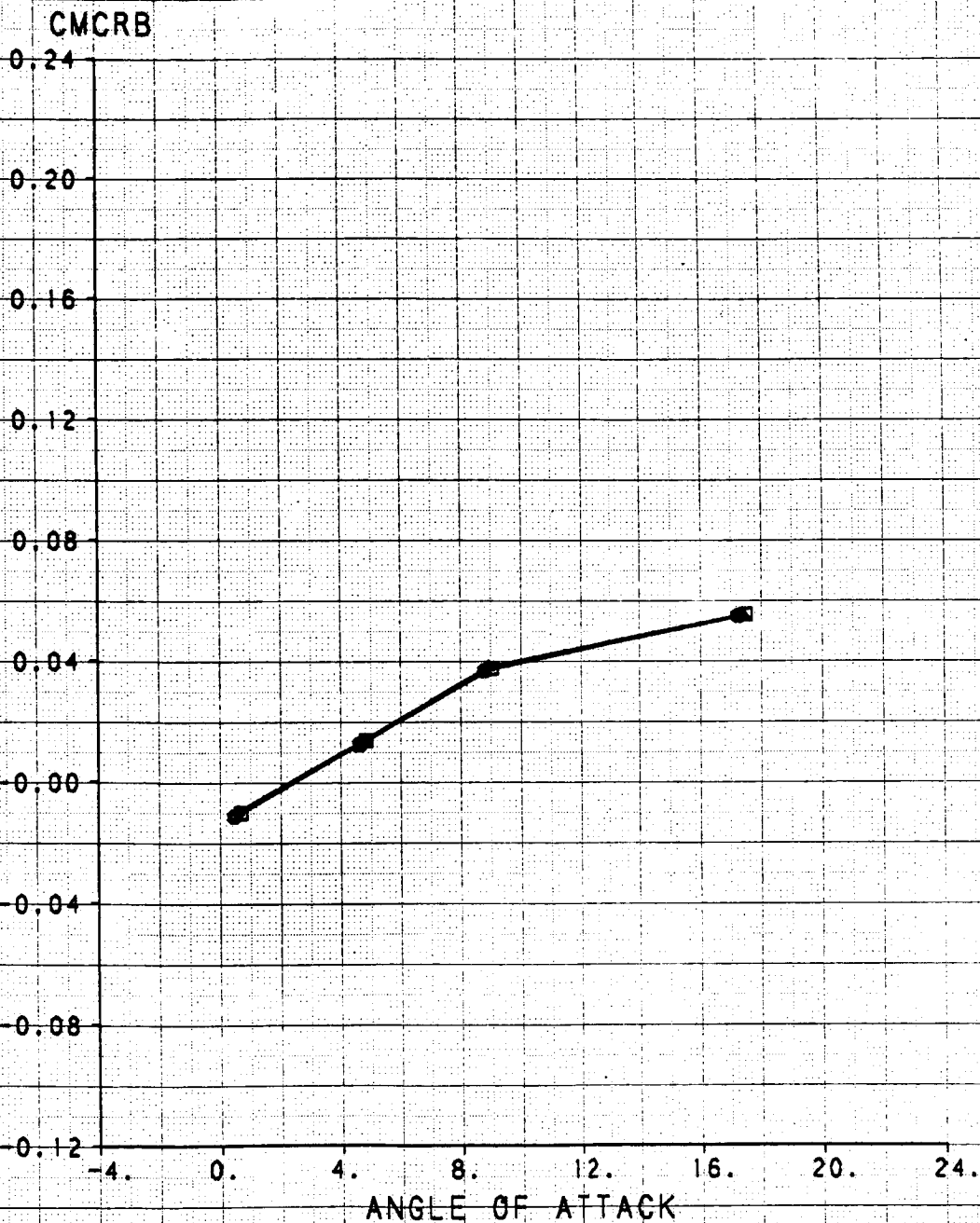
| SYM | TEST | RUN | RMACH | NDELCL | RNPRA | DESCRIPTION |
|-----|------|-----|--------|---------|--------|------------------------------|
| □ | 514 | 248 | 1.3548 | .00883 | 0.2345 | J/E, COMMON BASELINE JET-OFF |
| ▲ | 514 | 254 | 1.3839 | -0.0460 | 10.389 | J/E, COMMON BASELINE JET-ON |



ORIGINAL PAGE IS
OF POOR QUALITY

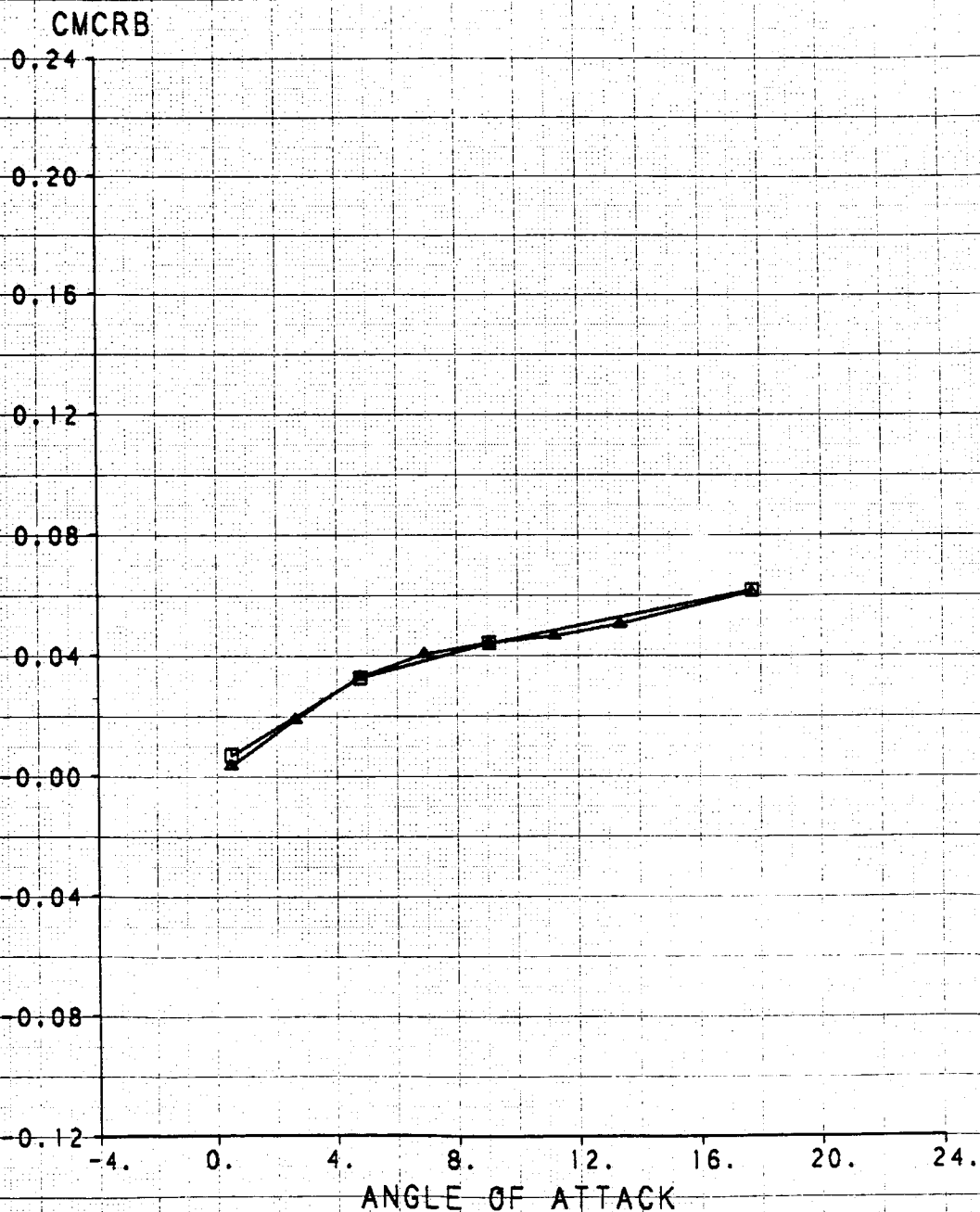
NOZZLE PRESSURE RATIO EFFECTS ON CANARD ROOT BENDING MOMENT

| SYM | TEST | RUN | RMACH | ROELCL | RMFR | RNPRA | DESCRIPTION |
|-----|------|-----|--------|---------|--------|--------|---------------------------|
| □ | 514 | 283 | 0.4017 | -5.0039 | 1.1604 | 1.6483 | CMAPS, SIMULATED AIRCRAFT |
| △ | 514 | 284 | 0.4014 | -5.0028 | 1.1603 | 1.9882 | CMAPS, SIMULATED AIRCRAFT |
| ◇ | 514 | 285 | 0.4019 | -4.9983 | 1.1571 | 2.4178 | CMAPS, SIMULATED AIRCRAFT |
| ○ | 514 | 286 | 0.4032 | -5.0263 | 1.1353 | 3.3566 | CMAPS, SIMULATED AIRCRAFT |



NOZZLE PRESSURE RATIO EFFECTS ON CANARD ROOT BENDING MOMENT

| SYM | TEST | RUN | RMACH | RDELCL | RMFR | RNPRA | DESCRIPTION |
|-----|------|-----|--------|--------|--------|--------|---------------------------|
| □ | 514 | 175 | 0.5992 | 0.1480 | 0.9202 | 3.2903 | CMAPS, SIMULATED AIRCRAFT |
| ▲ | 514 | 176 | 0.6009 | 0.1001 | 0.9161 | 3.8301 | CMAPS, SIMULATED AIRCRAFT |

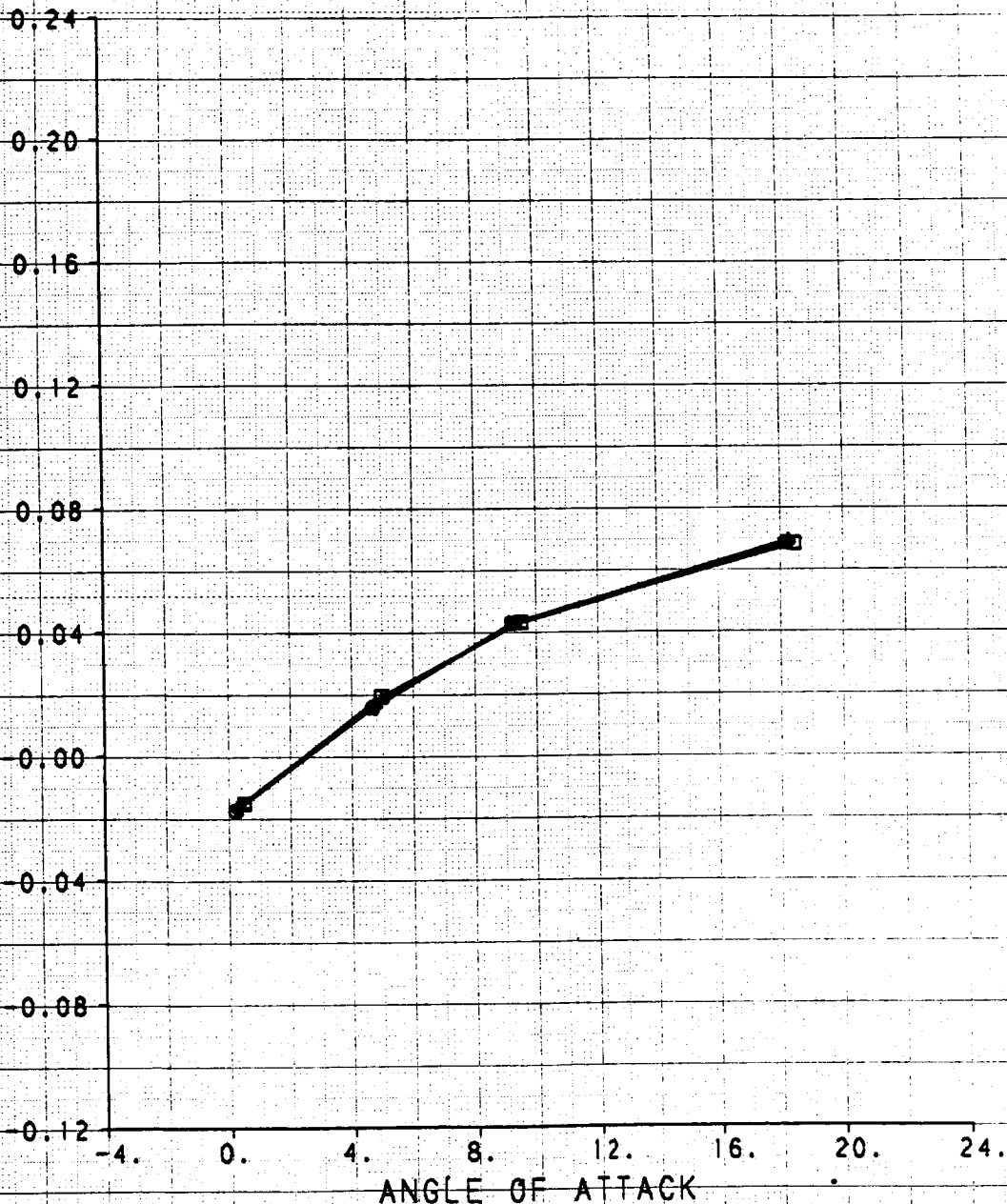


ORIGINAL PAGE IS
OF POOR QUALITY

NOZZLE PRESSURE RATIO EFFECTS ON CANARD ROOT BENDING MOMENT

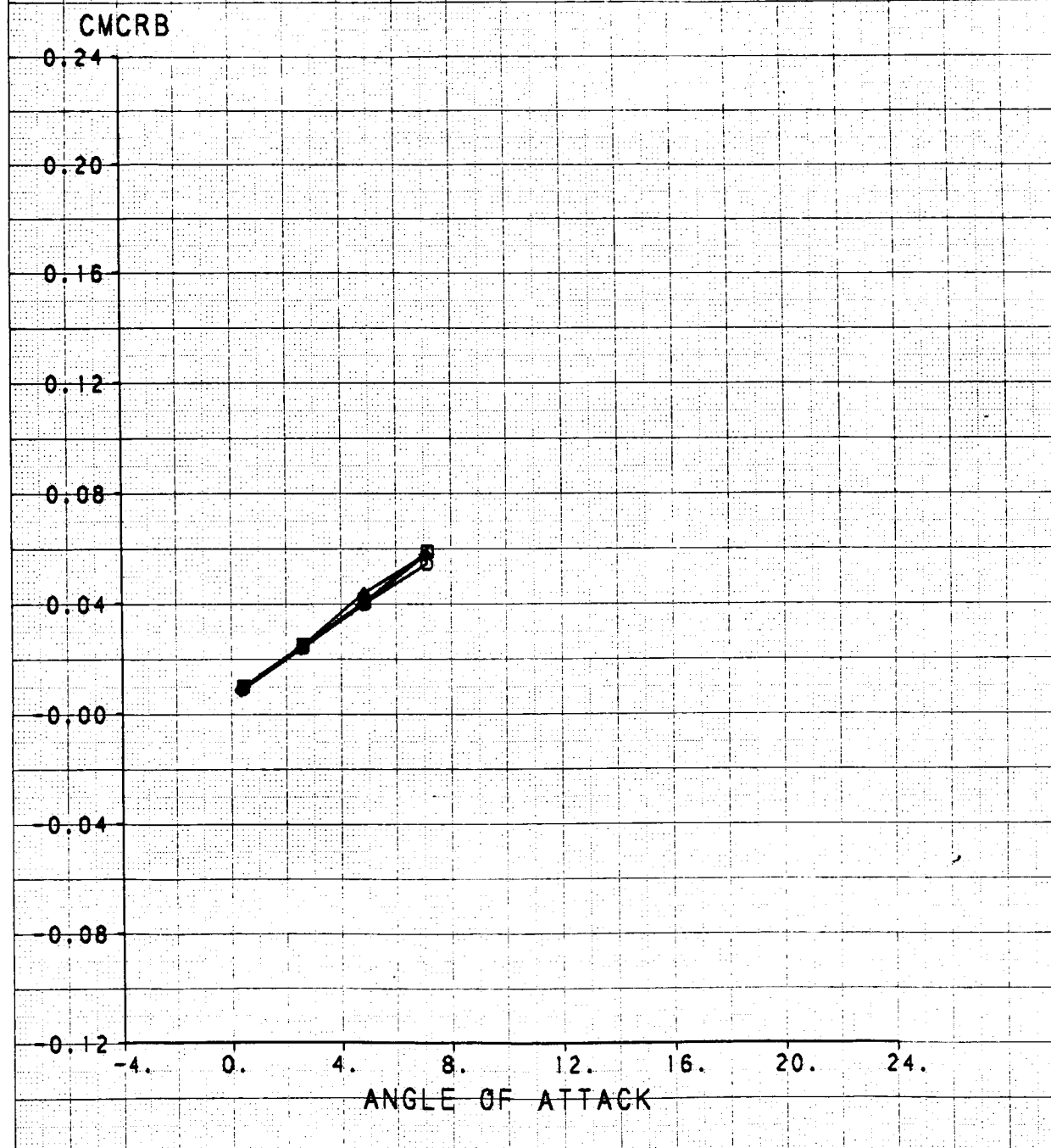
| SYM | TEST | RUN | RMACH | RDELCL | RMFR | RNPRA | DESCRIPTION |
|-----|------|-----|--------|---------|--------|--------|---------------------------|
| □ | 514 | 211 | 0.8966 | -4.9703 | 0.7627 | 2.4771 | CMAPS, SIMULATED AIRCRAFT |
| △ | 514 | 213 | 0.8953 | -4.9849 | 0.7638 | 3.6541 | CMAPS, SIMULATED AIRCRAFT |
| ◇ | 514 | 214 | 0.8987 | -4.9849 | 0.7595 | 4.3555 | CMAPS, SIMULATED AIRCRAFT |
| ○ | 514 | 215 | 0.8964 | -4.9625 | 0.7534 | 5.3011 | CMAPS, SIMULATED AIRCRAFT |

CMCRB



NOZZLE PRESSURE RATIO EFFECTS ON CANARD ROOT BENDING MOMENT

| SYM | TEST | RUN | RMACH | RDELCL | RMFR | RNPRA | DESCRIPTION |
|-----|------|-----|--------|--------|--------|--------|---------------------------|
| □ | 514 | 239 | 1.1834 | 0.1042 | 0.6863 | 4.2464 | CMAPS, SIMULATED AIRCRAFT |
| ▲ | 514 | 240 | 1.1896 | 0.1083 | 0.6841 | 5.2134 | CMAPS, SIMULATED AIRCRAFT |
| ◇ | 514 | 241 | 1.1903 | 0.1125 | 0.6803 | 6.1521 | CMAPS, SIMULATED AIRCRAFT |
| ○ | 514 | 242 | 1.1906 | 0.1042 | 0.7579 | 7.5840 | CMAPS, SIMULATED AIRCRAFT |

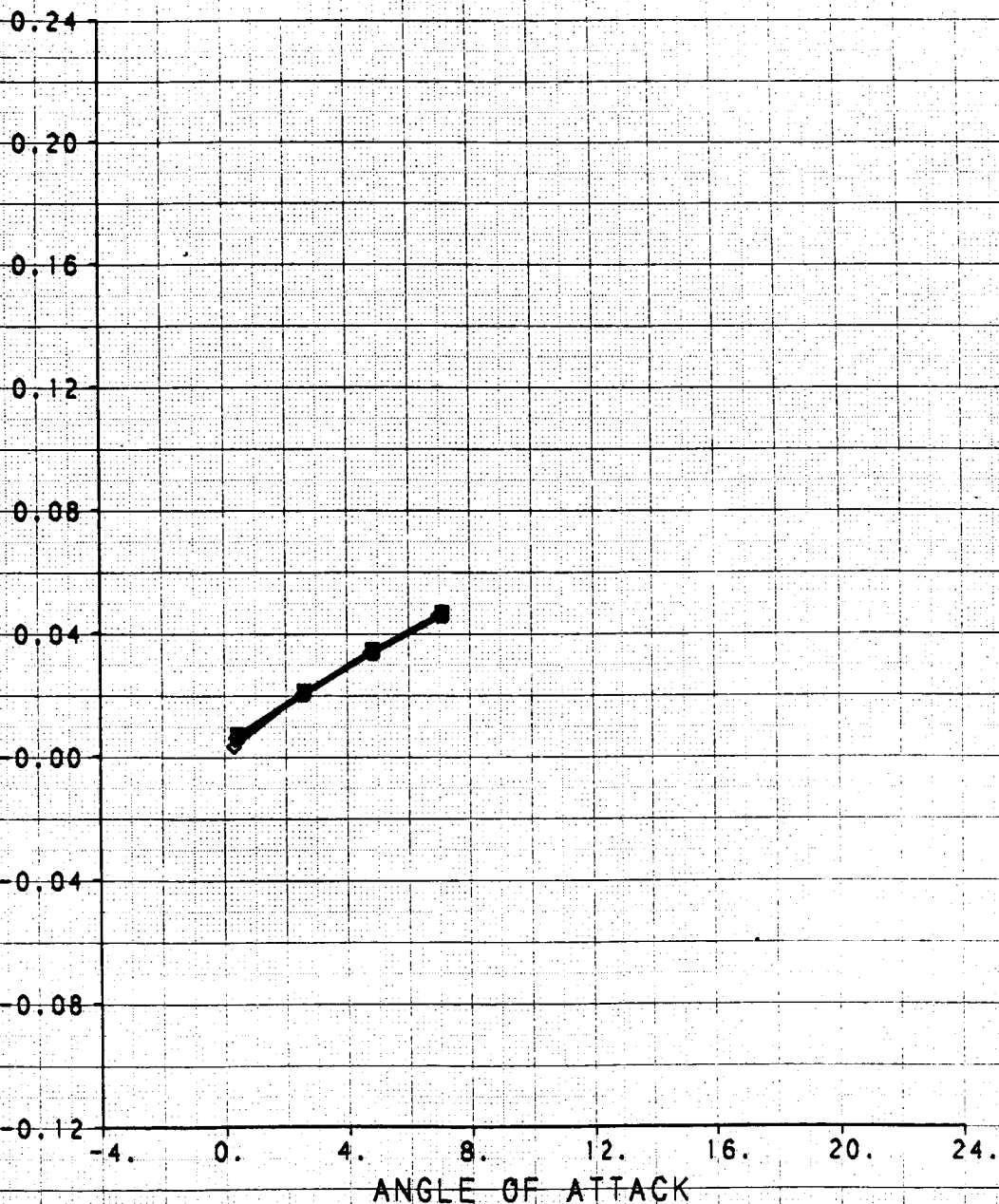


ORIGINAL PAGE IS
OF POOR QUALITY

NOZZLE PRESSURE RATIO EFFECTS ON CANARD ROOT BENDING MOMENT

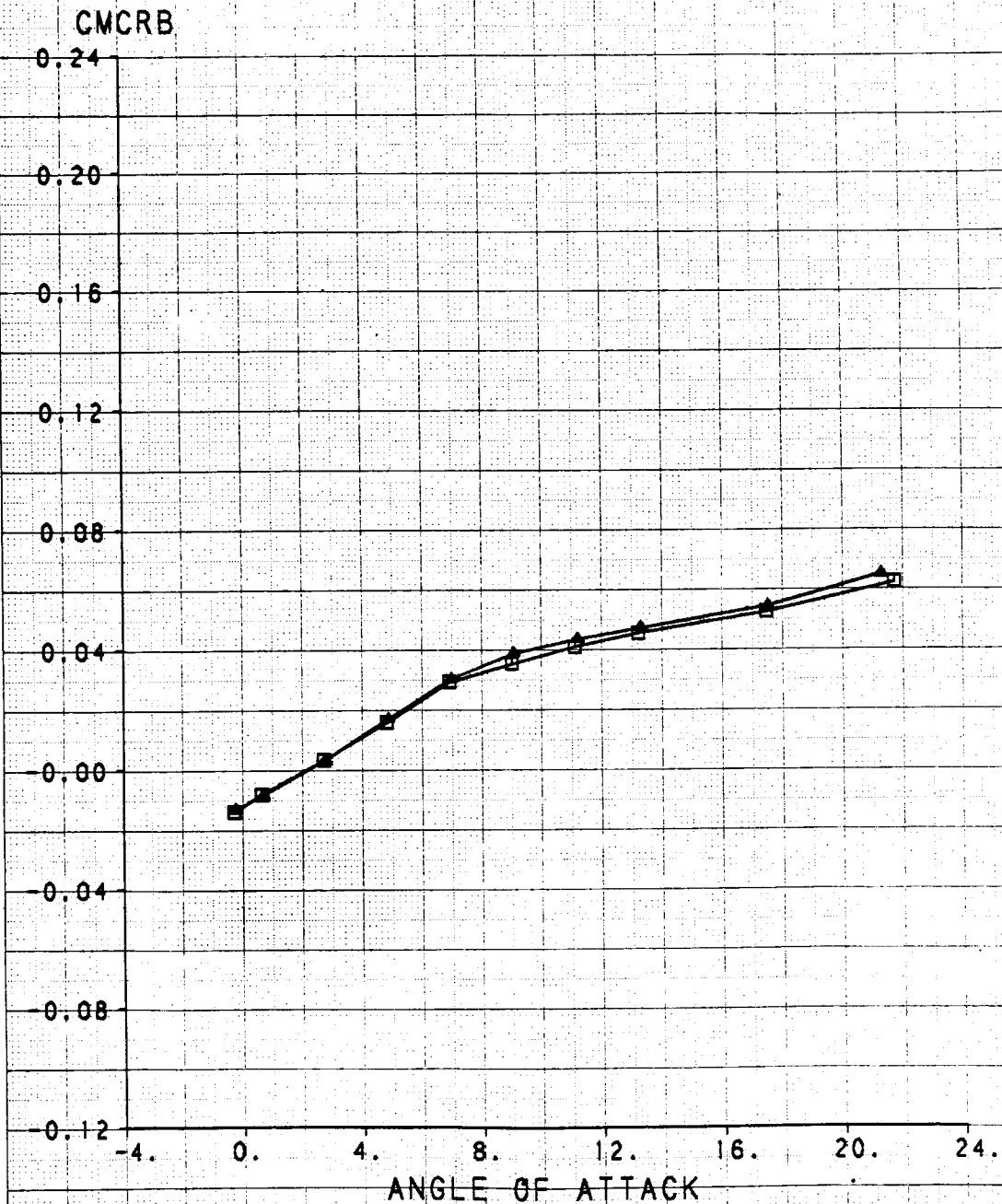
| SYM | TEST | RUN | RMACH | RDELCL | RMFR | RNPRA | DESCRIPTION |
|-----|------|-----|--------|--------|--------|--------|---------------------------|
| □ | 514 | 253 | 1.3938 | 0.1281 | 0.7198 | 5.4634 | CMAPS, SIMULATED AIRCRAFT |
| △ | 514 | 254 | 1.3978 | 0.1229 | 0.7203 | 6.6757 | CMAPS, SIMULATED AIRCRAFT |
| ◇ | 514 | 255 | 1.3966 | 0.1322 | 0.7118 | 7.8725 | CMAPS, SIMULATED AIRCRAFT |
| ○ | 514 | 256 | 1.3969 | 0.1083 | 0.7929 | 9.5970 | CMAPS, SIMULATED AIRCRAFT |

CMCRB



THRUST VECTORING EFFECTS ON CANARD ROOT BENDING MOMENT

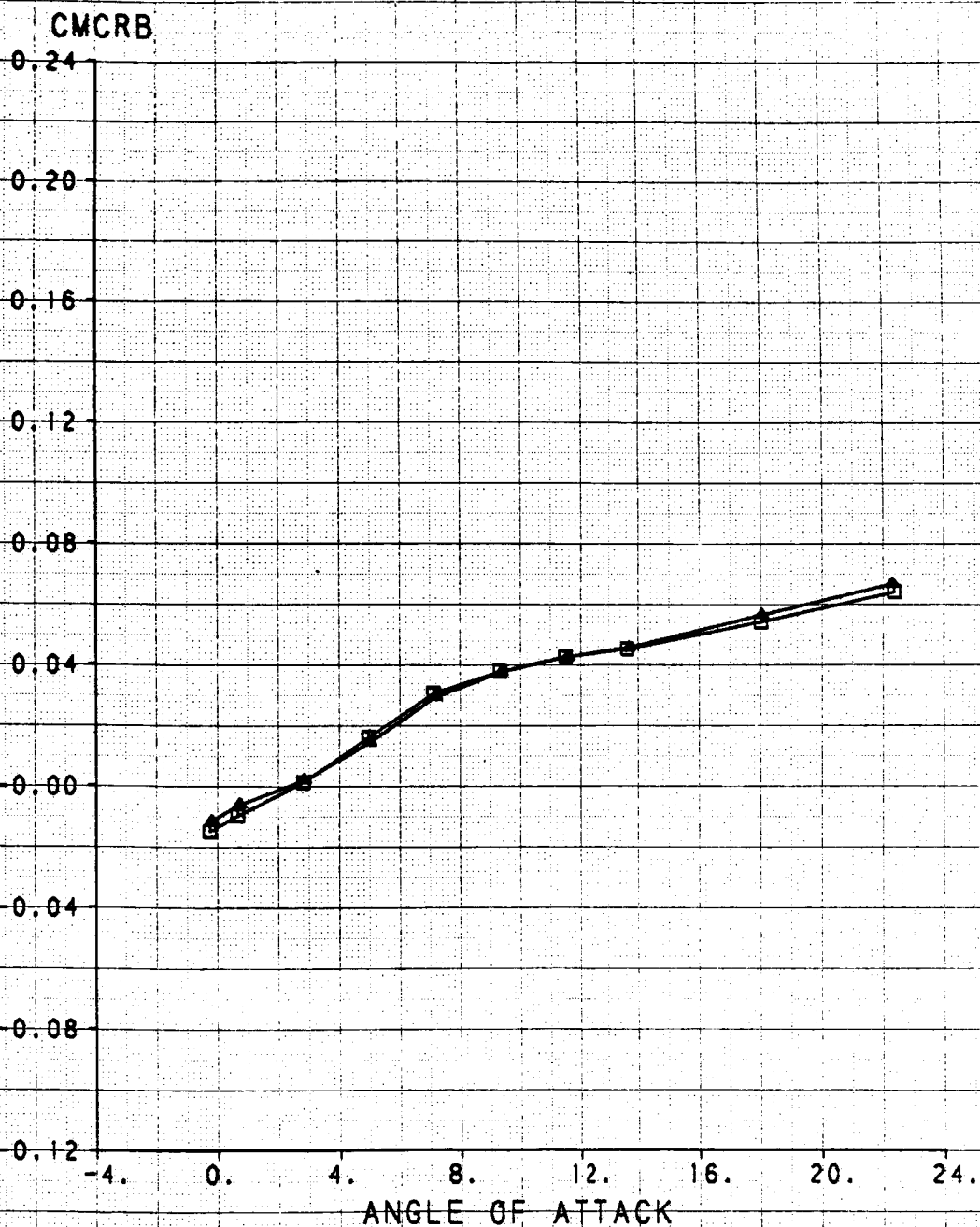
| SYM | TEST | RUN | RMACH | RDELCL | RNPRA | DESCRIPTION |
|-----|------|-----|--------|---------|--------|-----------------------------|
| □ | 514 | 257 | 0.3966 | -4.9911 | 4.0323 | J/E, COMMON BASELINE JET-ON |
| ▲ | 514 | 271 | 0.3987 | -4.9364 | 4.0129 | J/E, 20 DEG ALBEN A7B |



ORIGINAL PAGE IS
OF POOR QUALITY

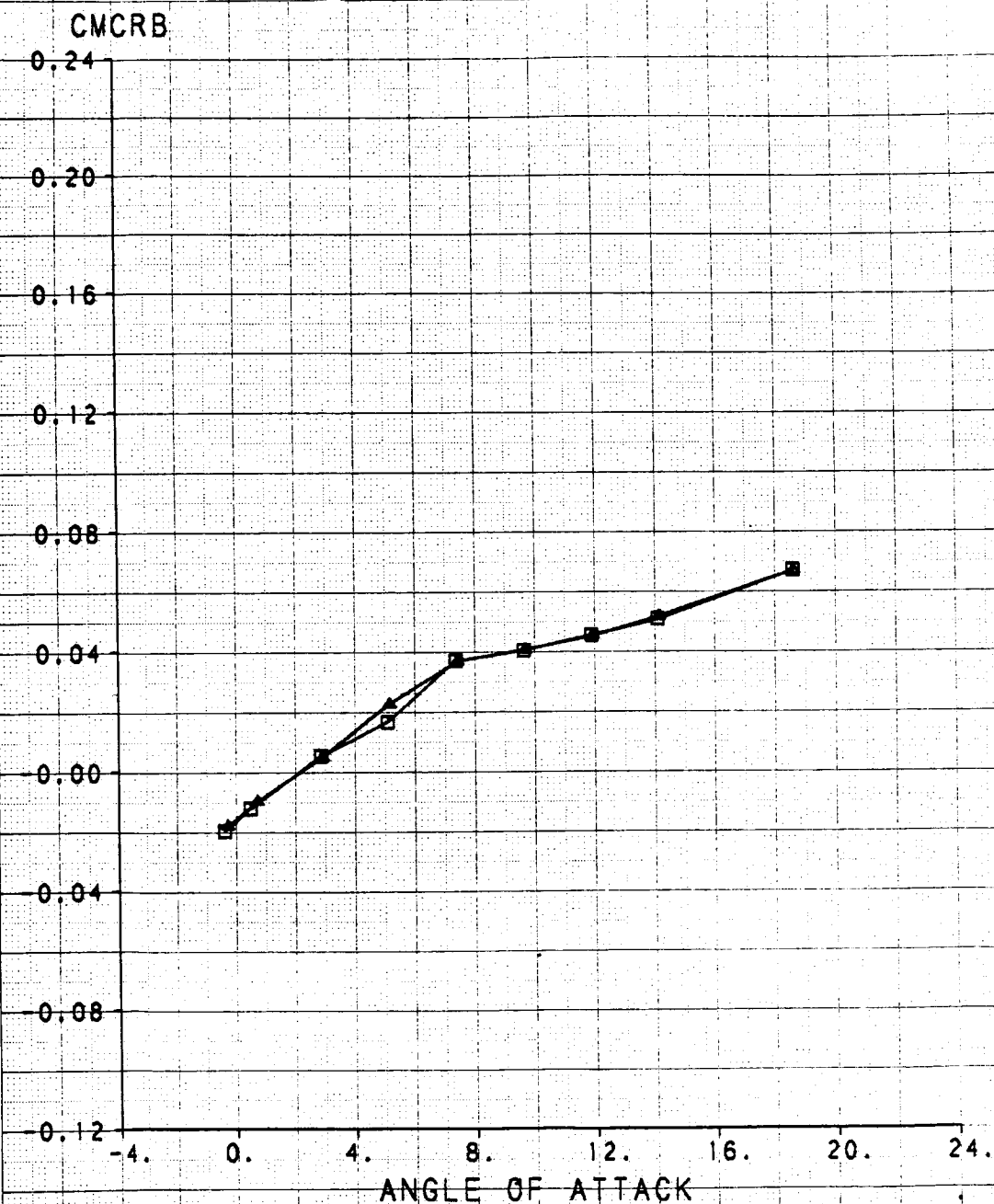
THRUST VECTORING EFFECTS ON CANARD ROOT BENDING MOMENT

| SYM | TEST | RUN | RMACH | RDELCL | RNPRA | DESCRIPTION |
|-----|------|-----|--------|---------|--------|-----------------------------|
| □ | 514 | 258 | 0.0000 | -4.9763 | 4.1998 | J/E, COMMON BASELINE JET-ON |
| △ | 514 | 276 | 0.5901 | -4.9460 | 4.2228 | J/E, 20 DEG ALBEN A/B |



THRUST VECTORING EFFECTS ON CANARD ROOT BENDING MOMENT

| SYM | TEST | RUN | RMACH | RDELCL | RNPRA | DESCRIPTION |
|-----|------|-----|--------|---------|--------|-----------------------------|
| □ | 514 | 250 | 0.8998 | -4.9737 | 6.2195 | J/E, COMMON BASELINE JET-ON |
| ▲ | 514 | 280 | 0.9061 | -4.9963 | 6.2122 | J/E, 20 DEG ALBEN A/B |



APPENDIX B

TEST MATRICES

The Phase 3 wind tunnel tests were performed over the range $M = 0.4-1.4$. Each run comprised either an Angle of Attack (α) sweep or a Nozzle Pressure Ratio (NPR) sweep. The run matrix for each test mode is presented in this appendix.

Flow-Through Test Mode

| Configuration | δ_c | 0.4 | 0.6 | 0.9 | 1.2 | 1.4 |
|--|------------|----------|----------|-----|-----|-----|
| Common Baseline A/B ALBEN $\delta_N = 0^\circ$ $\delta_F = 0^\circ$ | 5 | 66 | 75 | 77 | 82 | 93 |
| | 0 | 67 | 74 | 78 | 85 | 92 |
| | -5 | 68 | 73 | 79 | 86 | 94 |
| | -10 | 69 | 72 | 80 | 87 | 95 |
| | -15 | 70 | 71 | 81 | - | - |
| Nozzle Extension 2 $A_{choke} = 12.49 \text{ cm}^2$ (1.936 in ²) | | Ejectors | Ejectors | | | |
| | | | With W/O | | | |
| | 5 | 186 | - | - | - | - |
| | 0 | 187 | 111 194 | 118 | 121 | 124 |
| | -5 | 188 | 112 193 | 117 | 120 | 123 |
| $A_{choke} = 18.74 \text{ cm}^2$ (2.907 in ²) | -10 | 189 | 113 192 | 116 | 119 | 122 |
| | -15 | 190 | 114 191 | 115 | - | - |
| | 5 | 204 | - | - | - | - |
| | 0 | 205 | 136 212 | 132 | 129 | 126 |
| | -5 | 206 | 137 211 | 133 | 130 | 127 |
| $A_{choke} = 26.11 \text{ cm}^2$ (4.047 in ²) | -10 | 207 | 138 210 | 134 | 131 | 128 |
| | -15 | 208 | 139 209 | 135 | - | - |
| | 5 | 176 | - | - | - | - |
| | 0 | 177 | 153 181 | 146 | 145 | 142 |
| | -5 | 178 | 152 182 | 147 | 144 | 143 |
| $A_{choke} = 34.25 \text{ cm}^2$ (5.309 in ²) | -10 | 179 | 151 183 | 148 | - | - |
| | -15 | 180 | 150 184 | 149 | - | - |
| | 5 | 164 | - | - | - | - |
| | 0 | 165 | 170 - | 155 | 160 | 161 |
| | -5 | 167 | 171 - | 156 | 159 | 162 |
| | -10 | 168 | 172 - | 157 | - | - |
| | -15 | 169 | 173 - | 158 | - | - |

Flow-Through Test Mode

| Configuration | δ_c | 0.4 | 0.6 | 0.9 | 1.2 | 1.4 |
|---|----------------|------------------------|---------------|------------------------|---------------|-------------------|
| Nozzle Extension $\delta_F = 30^\circ$ Cowl Lip = 45° $A_{choke} = 12.49 \text{ cm}^2$ (1.936 in ²) | 5 0 | Ejectors 196 197 | | | | |
| $A_{choke} = 18.74 \text{ cm}^2$ (2.907 in ²) | 5 0 | 203 201 202 | | | | |
| $A_{choke} = 26.11 \text{ cm}^2$ (4.047 in ²) | 5 0 | 200 199 | | | | |
| Nozzle Extension $\delta_F = 0^\circ$ Cowl Lip = 45° $A_{choke} = 34.25 \text{ cm}^2$ (5.309 in ²) | -5 | | 215 | 214 | | |
| Nozzle Extension Baseline | 0 -5 -15 | - 224 - | - 223 - | - 220 222 221 | 219 - - | 217/218 - - |

ORIGINAL PAGE IS
OF POOR QUALITY

[illegible]

CMAPS MODE

| Configuration | δ_c | Alpha-Sweeps | | | | |
|---|----------------------------|---------------------------------|--------------------------|--------------------------|-------------------------|-------------------------|
| | | 0.4 | 0.6 | 0.9 | 1.2 | 1.4 |
| Common Baseline A/B ALBEN $\delta_F = 0^\circ$ $\delta_N = 0^\circ$ | 5 0 -5 -10 -15 | 104 105 106 107 108 | 109 | 110 | 111 | 112 |
| Nozzle Extensions *Percent Design Corrected Flow Rate: 38% | 5 0 -5 -10 -15 | 26 30 34 38 42 | - 47 51 55 - | - 59 63 67 - | - 71 75 - - | - 79 83 - - |
| 58% | 5 0 -5 -10 -15 | 27 31 35 39 43 | - 52 48 56 - | - 60 64 68 - | - 72 76 - - | - 80 84 - - |
| 84% | 5 0 -5 -10 -15 | 28 32 36 40 44 | - 53 49 57 - | - 61 65 69 - | - 73 77 - - | - 81 85 - - |
| 96% @ M = 0.4, 0.6 106% @ M = 0.9, 1.2, 1.4 | 5 0 -5 -10 -15 | 29 33 37 41 45 | - 54 50 57 - | - 62 66 70 - | - 74 78 - - | - 82 86 - - |

*Design Corrected Flow Rate:

0.7049 kg/sec

(1.554 lb/sec)

Simulator Mode
 Mach = 0.6
 ALBEN A/B $\delta_N = 0^\circ$

EPR - Sweeps

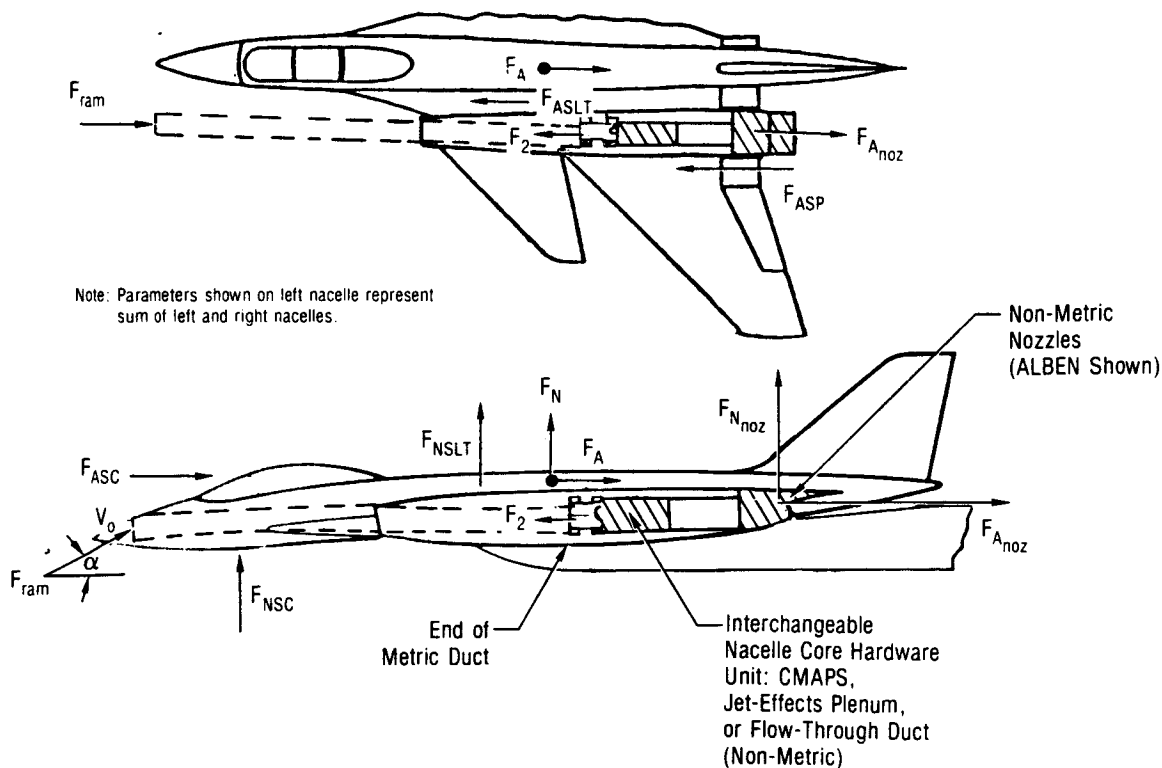
| *Percent Design Corrected Flowrate | δ_c | AOA | | | |
|------------------------------------|------------|-----------|-----------|-----------|------------|
| | | 0° | 4° | 8° | 16° |
| 38% | 0 | 114 | 131 | 146 | - |
| | -5 | 120 | 136 | 151 | - |
| | -10 | 125 | 141 | 156 | - |
| 58% | 0 | 115 | 132 | 147 | 161 |
| | -5 | 121 | 137 | 152 | 166 |
| | -10 | 126 | 142 | 157 | 170 |
| 71% | 0 | 116 | 133 | 148 | 162 |
| | -5 | 122 | 138 | 153 | 167 |
| | -10 | 127 | 143 | 158 | 171 |
| 84% | 0 | 117 | 134 | 149 | 163 |
| | -5 | 123 | 139 | 154 | 168 |
| | -10 | 128 | 144 | 159 | 172 |
| 97% | 0 | 118 | 135 | 150 | 164/165 |
| | -5 | 124 | 140 | 155 | 169 |
| | -10 | 129 | 145 | 160 | 173 |

*Design Corrected Flow Rate =

0.7049 kg/sec
 (1.554 lb/sec)

APPENDIX C
DATA REDUCTION PROCEDURE

The overall model commonality between the three test modes (Jet-Effects, Flow-Through, and CMAPS) allowed a single force and moment data reduction procedure to be applied to all configurations. The balance outputs were corrected for seal, cavity, base, stream thrust, and ram drag tares, as summarized in Figure C-1. Typical values of the data reduction terms presented in Figure C-1 are shown in Figure C-2 for the CMAPS mode. A listing of the data reduction equations is also provided in this appendix.



- Total Drag = $(F_A + F_{A_{noz}} + F_2 + F_{ASLT} - F_{ASC} + F_{ASP}) \cos \alpha + (F_N + F_{N_{noz}} - F_{NSC} - F_{NSLT}) \sin \alpha + F_{ram}$
- Total Lift = $-(F_A + F_{A_{noz}} + F_2 + F_{ASLT} - F_{ASC} + F_{ASP}) \sin \alpha + (F_N + F_{N_{noz}} - F_{NSC} - F_{NSLT}) \cos \alpha$

Note: With inlets faired: $F_2 = F_{ram} = 0$

Where: F_A = Total Airframe Balance Axial Force
 F_N = Total Airframe Balance Normal Force
 $F_{A_{noz}}$ = Pressure-Integrated Nozzle Axial Force
 $F_{N_{noz}}$ = Pressure-Integrated Nozzle Normal Force
 F_2 = Compressor Face Stream Thrust
 F_{ram} = Inlet Ram Drag
 F_{ASLT} = Inlet Duct Seal Axial Tare (Slope + Intercept Correction)
 F_{NSLT} = Inlet Duct Seal Normal Tare (Slope + Intercept Correction)
 F_{ASC} = Model Internal Cavity Axial Tare
 F_{NSC} = Model Internal Cavity Normal Tare
 F_{ASP} = Aft Metric Break Seal Axial Tare

GP53-0666-95-R

Figure C-1. Total Lift and Drag Data Reduction Summary

| | Mach 0.9 | | Mach 1.4 | |
|-----------------|-------------------------------|-------------------------------|-------------------------------|-------------------------------|
| Term | $\alpha = 0.22^\circ$ (lb) | $\alpha = 9.20^\circ$ (lb) | $\alpha = 0.43^\circ$ (lb) | $\alpha = 7.08^\circ$ (lb) |
| $F_A =$ | 21.32 | - 60.82 | 67.76 | 46.48 |
| $F_N =$ | 144.71 | 1,759.01 | 212.93 | 1,526.10 |
| $F_{A_{noz}} =$ | 0.15 | 1.31 | 5.11 | 6.64 |
| $F_{N_{noz}} =$ | 3.57 | 13.20 | 11.28 | 24.69 |
| $F_2 =$ | 57.72 | 50.37 | 83.59 | 83.58 |
| $R_{ram} =$ | - 47.30 | - 44.59 | - 62.58 | - 62.52 |
| $R_{ASLT} =$ | 3.29 | 7.03 | 0.44 | 9.81 |
| $R_{NSLT} =$ | 1.19 | - 5.17 | - 1.95 | - 7.66 |
| $F_{ASC} =$ | - 4.42 | - 4.97 | - 10.45 | - 12.46 |
| $F_{NSC} =$ | 18.31 | 20.59 | 43.30 | 51.63 |
| $F_{ASP} =$ | - 0.02 | - 0.73 | 1.33 | 1.27 |

$$\text{Axial force} = F_A + F_{A_{noz}} + F_2 + F_{ASLT} - F_{ASC} + F_{ASP}$$

$$\text{Normal Force} = F_N + F_{N_{noz}} - F_{NSC} - F_{NSLT}$$

GP53-0814-50-T

**Figure C-2. Typical Data Reduction Terms for Axial and Normal Force
Simulated Aircraft Configuration**

DATA REDUCTION EQUATIONS

The following is a listing of the FORTRAN equations used for all of the data reduction. Comment cards are included to indicate which equations are unique to a particular test mode. Some of the flags and logic control statements have been omitted for clarity. Some of the calls to table look-ups and calls to subroutines have also been omitted. This list is intended to apply to all three test modes unless noted otherwise as comment cards.

```

C *** CALCULATE THE FOLLOWING STANDARD PARAMETERS FROM TUNNEL MEASUREMENTS
C *** OF PRESSURE AND TEMPERATURE:
C ***
C *** PF=FREESTREAM STATIC PRESSURE (PSF)
C *** PT=FREESTREAM TOTAL PRESSURE (PSF)
C *** TT=FREESTREAM TOTAL TEMPERATURE (DEG F)
C *** XMO=FREESTREAM MACH NUMBER
C *** Q=FREESTREAM DYNAMIC PRESSURE (PSF)
C *** VO=FREESTREAM VELOCITY (FPS)
C
      TTR=TT+459.7
      PTO=PT/144
      PO=PF/144
      XMO=SQRT(((PT/PF)**0.2857-1)*5)
      Q=0.7*PF*XMO**2
      QO=Q/144
      VO=XMO*(2403.076*(TTR/(1+0.2*XMO**2))**0.5)
C
C *** PRESSURE MEASUREMENTS ***
C
C *** THE PRESSURES (K=2 TO 47) MEASURED AT THE SCANIVALVES (J=1 TO 7)
C *** IN PSF ARE CONVERTED TO PSI, CODED GOOD OR BAD, AND STORED IN
C *** THE ARRAY P(J,K)
C
      DO 110 J=1,7
      DO 100 K=2,47
      P(J,K)=PRESSSV(J,K)*C(J,K)/144
100    CONTINUE
110    CONTINUE
C
C *** C(J,K)=1 FOR GOOD PRESSURE
C          0 FOR BAD PRESSURE
C
C *** CALCULATE PRESSURE COEFFICIENTS ***
C
      DO 210 J=1,7
      DO 200 K=2,47
      CP(J,K)=(PRESSSV(J,K)-PF)/Q
200    CONTINUE

```

ORIGINAL PAGE IS
OF POOR QUALITY

```

210  CONTINUE
C
C *** CALCULATE INLET AVERAGE TOTAL AND STATIC PRESSURES;
C ***      I=1 FOR LEFT HAND SIDE
C ***      I=2 FOR RIGHT HAND SIDE
C
      CSUM=0
      PSUM=0
      DO 300 K=28,38
        J=4
        PSUM=PSUM+P(J,K)
        CSUM=CSUM+C(J,K)
        PT2(1)=PSUM/CSUM
300  CONTINUE
C
      CSUM=0
      PSUM=0
      DO 400 K=12,13
        J=4
        PSUM=PSUM+P(J,K)
        CSUM=CSUM+C(J,K)
        PS2(1)=PSUM/CSUM
400  CONTINUE
C
      CSUM=0
      PSUM=0
      DO 500 K=19,45
        J=3
        PSUM=PSUM+P(J,K)
        CSUM=CSUM+C(J,K)
        PT2(2)=PSUM/CSUM
500  CONTINUE
C
      CSUM=0
      PSUM=0
      DO 600 K=12,16
        J=3
        PSUM=PSUM+P(J,K)
        CSUM=CSUM+C(J,K)
        PS2(2)=PSUM/CSUM
600  CONTINUE
C
C *** AVERAGE COMPRESSOR INLET STATIC PRESSURE
C
      PIDS=(PS2(1)+PS2(2))/2
C
C *** NOTE: IF PRESSURES ARE BAD CODED SUCH THAT EITHER PS2(1) OR PS2(2)
C ***      IS EQUAL TO ZERO, THEN ELIMINATE THE DIVISION BY TWO IN
C ***      PRECEDING EQUATION.

```

```

C
C *** CAVITY PRESSELTE
C
      CSUM=0
      PSUM=0
      J=1
      DO 700 K=45,46
      PSUM=PSUM+P(J,K)
700    CSUM=CSUM+C(J,K)
      J=2
      DO 710 K=8,8
      PSUM=PSUM+P(J,K)
710    CSUM=CSUM+C(J,K)
      J=2
      DO 720 K=32,34
      PSUM=PSUM+P(J,K)
720    CSUM=CSUM+C(J,K)
      J=2
      DO 730 K=36,38
      PSUM=PSUM+P(J,K)
730    CSUM=CSUM+C(J,K)
      J=4
      DO 740 K=16,18
      PSUM=PSUM+P(J,K)
740    CSUM=CSUM+C(J,K)
C
      PCAV=PSUM/CSUM
C
C *** CAVITY PRESSURE COEFFICIENT
C
      CPCAVA=(PCAV-P0)/Q0
C
C *** INLET DUCT SEAL PRESSURE DIFFERENTIAL
C
      DPDS=PIDS-PCAV
C
C *** CALCULATE EXIT CHOKE AVERAGE TOTAL AND STATIC PRESSURES;
C ***      I=1 FOR LEFT HAND SIDE
C ***      I=2 FOR RIGHT HAND SIDE
C
      CSUM=0
      PSUM=0
      DO 800 K=20,21
      J=5
      PSUM=PSUM+P(J,K)
800    CSUM=CSUM+C(J,K)
      DO 810 K=28,34
      J=5
      PSUM=PSUM+P(J,K)
810    CSUM=CSUM+C(J,K)

```

```

C      PTNC(1)=PSUM/CSUM
C
      CSUM=0
      PSUM=0
      DO 900 K=33,37
      J=5
      PSUM=PSUM+P(J,K)
900    CSUM=CSUM+C(J,K)
C
      PSNC(1)=PSUM/CSUM
C
      CSUM=0
      PSUM=0
      DO 1000 K=5,8
      J=6
      PSUM=PSUM+P(J,K)
1000   CSUM=CSUM+C(J,K)
      DO 1010 K=10,11
      J=6
      PSUM=PSUM+P(J,K)
1010   CSUM=CSUM+C(J,K)
      PSUM=PSUM+P(6,13)+P(6,16)+P(6,22)
      CSUM=CSUM+C(6,13)+C(6,16)+C(6,22)
C
      PTNC(2)=PSUM/CSUM
C
      PSUM=0
      CSUM=0
      PSUM=P(6,12)+P(6,17)+P(6,20)+P(6,21)
      CSUM=C(6,12)+C(6,17)+C(6,20)+C(6,21)
C
      PSNC(2)=PSUM/CSUM
C *** CALCULATE ALBEN AVERAGE TOTAL PRESSURES;
C                                     I=1 FOR LEFT HAND SIDE
C                                     I=2 FOR RIGHT HAND SIDE
C
      PSUM=0
      CSUM=0
      DO 1100 K=5,8
      J=7
      PSUM=PSUM+P(J,K)
1100   CSUM=CSUM+C(J,K)
C
      PTNA(1)=PSUM/CSUM
C
      PSUM=0
      CSUM=0
      DO 1110 K=5,8
      J=7

```

```

        PSUM=PSUM+P(J,K)
1110    CSUM=CSUM+C(J,K)
C
        PTNA(2)=PSUM/CSUM
C
C *** ALBEN STATIC PRESSURE FROM VEER MEASUREMENTS
C
        PSUM=0
        CSUM=0
        DO 1200 K=2,4
            J=7
            PSUM=PSUM+P(J,K)
1110    CSUM=CSUM+C(J,K)
C
        PVEERA=PSUM/CSUM
C
C
C *** TEMPERATURE MEASUREMENTS
C
C
C *** DRIVE AND BLEED LINE TEMPS. (CMAPS MODE ONLY)
C
        TTRDV=TTDV+459.7
        TTRBV=TTBV+459.7
C
C *** AVERAGE NOZZLE TEMPERATURES (DEG F)
C
C             I=1,L/H SIDE    I=1,R/H SIDE
C
        T7(1)=(T711+T712)/2
        T7(2)=(T721+T722)/2
C
C *** CONVERSION TO RANKINE
C
        TT7(1)=T7(1)+459.7
        TT7(2)=T7(2)+459.7
C
C *** CORRECTION FACTOR TO STANDARD DAY TEMPERATURE
C
        THETA=SQRT(TTR/518.69)
C
C *** ANGLE MEASUREMENTS ***
C
C *** NOTE:  THE MODEL NOZZLES ARE NON-METRIC (I.E. NOT ATTACHED TO THE
C ***          AIRCRAFT BALANCE, BUT GROUNDED TO THE STING).  IN ORDER TO
C ***          RESOLVE NOZZLE FORCES FROM PRESSURE INTEGRATION, THE NOZZLE
C ***          OR STING ANGLE MUST BE COMPUTED, IN ADDITION TO THE MODEL OR
C ***          BALANCE ANGLE:
C
C                      NOZZLE ALPHA = BALALPHA(1)
C                      MODEL ALPHA = BALALPHA(2)

```

```

C ***      BALALPHA(1 AND 2) ARE CALCULATED FROM THE NASA-AMES STANDARD
C ***      DATA REDUCTION EQUATIONS AND INCLUDE STING AND BALANCE
C ***      DEFLECTIONS DUE TO ELASTIC BENDING.  A CORRECTION TERM WAS
C ***      ADDED TO EACH OF THESE ANGLES TO ACCOUNT FOR STING THERMAL
C ***      BENDING.  THIS CORRECTION TERM IS DENOTED "THRM".
C
C *** MODEL ANGLE OF ATTACK
C
C      ALPHAM=BALALPHA(2)+THRM
C
C *** NOZZLE ANGLE OF ATTACK
C
C      ALPHAN=BALALPHA(1)+THRM
C
C *** NOTE: THRM IS DEFINED SEPARATELY FOR EACH TEST MODE
C
C *** FLOW-THROUGH MODE:
C
C      THRM=0.0
C
C *** JET-EFFECTS MODE:
C
C      THRM=0.490140754+4.17191423E-3*(TTDV(1))-7.65960224E-3*(TTBV(1))
C
C *** CMAPS MODE:
C
C      THRM=-4.533611E-2+3.007169E-3*(TTDV(1))-4.558083E-3*(TTBV(1))
C      +3.152366E-2*(WDV(1))+0.37941*(WBV(1))+2.637508E-7*(NC(1))
C
C *** WHERE:  WDV(1)=LEFT HAND SIDE DRIVE LINE AIRFLOW (LB/SEC)
C             WBV(1)=LEFT HAND SIDE BLEED LINE AIRFLOW (LB/SEC)
C             NC(1)=LEFT HAND SIDE CORRECTED CMAPS ROTOR SPEED (RPM)
C
C *** THESE TERMS ARE CALCULATED LATER FOR THE CMAPS MODE
C
C
C *** BALANCE CORRECTIONS ***
C
C *** MODEL CAVITY CORRECTION
C
C      NAFSC=CPCAVA*Q0*ACAVN
C
C      AFASC=CPCAVA*Q0*ACAVA
C
C      PMASC=NAFSC*XCAV+AFASC*ZCAV
C
C *** WHERE:  ACAVN=44.569 SQ.IN.
C             ACAVA=10.548 SQ.IN. FOR CMAPS AND FLOW-THROUGH MODES
C             =24.892 SQ.IN. FOR JET-EFFECTS MODE

```

```

C          XCAV =0.29167 FT.
C          ZCAV =-0.15 FT.
C
C *** INLET DUCT SEAL CORRECTION
C
C          FSEALN=0.0
C          FSEALA=TABLE LOOK UP FUNCTION OF DPDS
C          MSEALA=TABLE LOOK UP FUNCTION OF DPDS
C
C *** SEE FIGURES 3-18 AND 3-19 IN TEXT FOR DEFINITION OF TABLES
C
C *** INLET DUCT SEAL CORRECTION - A FUNCTION OF PRESSURE AND LOADS
C
C          AFNSLT=KST28*NF+KST29*PM+KST30*AF
C          AFASLT=KST31*NF+KST32*PM+KST33*AF
C          APMSLT=KST34*NF+KST35*PM+KST36*AF
C
C *** WHERE: THE COEFFICIENTS KST28 THROUGH KST36 ARE TABLE LOOK-UP
C ***          VALUES AS A FUNCTION OF THE BALANCE OUTPUTS (NF, PM, AF)
C ***          AND THE INLET DUCT SEAL PRESSURE DIFFERENTIAL (DPDS). (SEE
C ***          FIGURE 3-20 IN TEXT)
C
C *** NOTE: ALL PITCHING MOMENT CORRECTIONS AND INPUTS IN FT-LBS.
C
C
C *** AFT SEAL CORRECTION
C
C          DO 3000 I=1,5
C          DO 3000 K=40,44
C          J=1
C 3000    CP(I)=CP(J,K)
C
C          DO 3010 I=6,8
C          DO 3010 K=40,42
C          J=2
C 3010    CP(I)=CP(J,K)
C
C          CPSUM=0.0
C          CPSUM1=0.0
C          DO 3100 I=1,8
C          CPSUM=CPSUM+CP(I)*ALA1(I)
C 3100    CPSUM1=CPSUM1+CP(I)*ALA1(I)*RPMA1(I)
C
C          AFASP=Q0*CPSUM
C          PMASP=Q0*CPSUM1
C
C
C *** WHERE: ALA1 AND RPMA1 ARE THE AFT FACING AREA AND THE MOMENT ARM
C ***          ASSOCIATED WITH THE PRESSURE TAPS AT THE AFT SEAL

```



```

C
C ***          ALA1(1)=0.662 SQ.IN.          RPMA1(1)=-0.15 FT.
C              (2)=1.466                    (2)=-0.030417
C              (3)=0.732                    (3)=0.019167
C              (4)=1.466                    (4)=-0.030417
C              (5)=0.894                    (5)=-0.15
C              (6)=0.368                    (6)=-0.269583
C              (7)=0.368                    (7)=-0.319167
C              (8)=0.368                    (8)=-0.269583
C
C
C *** TOTAL CAVITY CORRECTION ***
C
C      ACAV(2)=AFASC+FSEALA+AFASP+AFASLT
C      NCAV(2)=NAFSC+FSEALN+AFNSLT
C      PMCAV(2)=PMASC+MSEALA+APMSLT+PMASP
C
C *** CONVERT TO COEFFICIENT FORM
C
C      ACAVN=ACAV(2)/(Q*5.221 SQ.FT.)
C      NCAVN=NCAV(2)/(Q*5.221 SQ.FT.)
C      PMCAVN=PMCAV(2)/(Q*5.221 SQ.FT. * 1.368 FT.)
C
C
C *** NOTE: THE BALANCE CORRECTIONS DUE TO STREAM THRUST AND RAM DRAG ARE
C           CALCULATED LATER FOLLOWING THE CALCULATIONS OF AIRFLOW THROUGH
C           THE MODEL AND THE PRESSURE-AREA INTEGRATIONS OF NOZZLE FORCES
C           WHICH IMMEDIATELY FOLLOW HERE.
C
C *** NOZZLE PRESSURE-AREA INTEGRATED FORCES ***
C
C      ASSIGN THE VALUES OF NOZZLE PRESSURES FROM THE LARGE CP(J,K) ARRAY
C      TO A SMALLER ARRAY LABELED CPNOZ(I)
C
C      DO 4000 I=1,19
C      DO 4000 K=4,22
C      J=5
C 4000  CPNOZ(I)=CP(J,K)
C
C      DO 4010 I=20,31
C      DO 4010 K=16,37
C      J=5
C 4010  CPNOZ(I)=CP(J,K)
C
C      DO 4020 I=32,51
C      DO 4010 K=4,23
C      J=6
C 4020  CPNOZ(I)=CP(J,K)
C
C      CALCULATE NORMAL FORCE AND AXIAL FORCE ON THE UPPER AND LOWER

```

```

C      HALVES OF THE ALBEN BY PERFORMING A PRESSURE AREA INTEGRATION
C
      NFNU=0.0
      DO 5000 I=1,31
      NFNU=NFNU+CPNOZ(I)*ALN(I)*Q0
5000  CONTINUE
C
      NFNL=0.0
      DO 5010 I=32,51
      NFNL=NFNL+CPNOZ(I)*ALN(I)*Q0
5010  CONTINUE
C
      AFNU=0.0
      DO 5020 I=1,31
      AFNU=AFNU+CPNOZ(I)*ALA(I)*Q0
5020  CONTINUE
C
      AFNL=0.0
      DO 5030 I=32,51
      AFNL=AFNL+CPNOZ(I)*ALA(I)*Q0
5030  CONTINUE
C
      CALCULATE THE PITCHING MOMENT ON THE NOZZLE
C
      PMN=0.0
      DO 5040 I=1,51
      PMN=PMN+(CPNOZ(I)*ALN(I)*RPMN(I)*Q0+CPNOZ(I)*ALA(I)*RPMA(I))
5040  CONTINUE
C
C
C      *** NOZZLE FORCE COEFFICIENTS - BODY AXIS ***
C
      CNNU=2*NFNU/Q*5.221
      CNNL=2*NFNL/Q*5.221
      CANU=2*AFNU/Q*5.221
      CANL=2*AFNL/Q*5.221
C
      CNN=CNNU+CNNL
      CAN=CANU+CANL
C
      CPMN=2*PMN/12*5.221*1.368
C
C *** NOTE: MULTIPLICATION BY TWO IN EACH CASE IS TO GENERATE THE FORCE OR
C           MOMENT FOR TWO NOZZLES (THE PRESSURE INTEGRATION IS PERFORMED
C           ONLY ON ONE NOZZLE). THE DIVISION BY TWELVE IN THE PITCHING
C           MOMENT COEFFICIENT EQUATION IS TO CONVERT THE NOZZLE PITCHING
C           MOMENT (PMN) TO THE UNITS OF FT-LB.
C
C *** NOZZLE FORCE COEFFICIENTS - STABILITY AXIS ***
C

```

```

C
C      CLN=CNM*COS(ALPHAN)-CAN*SIN(ALPHAN)
C      CDN=CNM*SIN(ALPHAN)+CAN*COS(ALPHAN)
C
C      CALCULATE APPROXIMATION FOR NOZZLE SKIN FRICTION
C
C      NUM=0.455*(1+.2*XMO**2)**-0.467
C      DEN(I)=(LOG((RN*10**6)*X(I)))*2.58
C      CFN(I)=NUM/DEN(I)
C
C *** NOTE: I=1 FOR LOWER SURFACE OF ALBEN
C           I=2 FOR UPPER SURFACE OF ALBEN
C
C      NSF=Q*(CFN(2)*AWET(2)-CFN(1)*AWET(1))
C
C ***      X(1)=2.614 FT (CHARACTERISTIC LENGTH FOR LOWER SURFACE OF 2
C                   NOZZLES)
C           X(2)=3.297 FT (CHARACTERISTIC LENGTH FOR UPPER SURFACES)
C           AWET(1)=4.145 SQ.FT. (LOWER SURFACE WETTED AREA, 2 NOZZLES)
C           AWET(2)=5.202 SQ.FT. (UPPER SURFACE WETTED AREA, 2 NOZZLES)
C
C      CDNSF=NSF/Q*5.221
C
C *** TOTAL NOZZLE DRAG INCLUDING SKIN FRICTION
C
C      CDARONF=CDN+CDNSF
C
C
C
C
C *** AIRFLOW CALCULATIONS ***
C
C
C      CALCULATE THE AIRFLOW THROUGH DRIVE AND BLEED LINES FOR CMAPS AND
C      JET-EFFECTS MODES. NO FLOW WAS DELIVERED TO THE MODEL FOR THE FLOW-
C      THROUGH TEST MODE.
C
C *** DRIVE LINE - CMAPS AND JET-EFFECTS MODES ***
C
C      NOTE: I=1 FOR LEFT HAND SIDE
C           I=2 FOR RIGHT HAND SIDE
C
C           PDV(I)=STATIC PRESSURE MEASURED IN DRIVE VENTURI
C           TTRDV(I)=TOTAL TEMPERATURE MEASURED IN DRIVE VENTURI
C
C           GAMMA=TABLE LOOK UP AS FUNCTION OF PDV(I) AND TTRDV(I)
C
C      PERFORM FOLLOWING ITERATION TO FIND MACH NUMBER IN VENTURI
C
C      100      J=0

```

```

M(1)=0.01
SUF=2/(GAMMA+1)
TOP=(GAMMA+1)/2*(GAMMA-1)
TOP1=(3-GAMMA)/2*(GAMMA-1)
200 J=J+1
CORE=1+((GAMMA-1)/2)*M(J)**2
NUMBER=((SUF*CORE)**TOP)/M(J))-AOAS(I)
C
C NOTE: AOAS(I)=AOASD(1)=AOASD(2)=7 FOR DRIVE VENTURI
C          =AOASB(1)=AOASB(2)=3 FOR BLEED VENTURI
C AOAS=AREA RATIO OF VENTURI
C
DENOM=((SUF*CORE)**TOP1)-((SUF*CORE)**TOP/M(J)**2)
M(J+1)=M(J)-NUMBER/DENOM
TEST=ABS((M(J+1)-M(J))/M(J+1))
IF TEST.LT.0.001 GOTO 300
GO TO 200
300 MACH=M(J+1)
C
PTDV(I)=PDV(I)*(1+((GAMMA-1)/2)*MACH**2)**(GAMMA/(GAMMA-1))
C
GAMMA2=TABLE LOOK UP AS A FUNCTION OF PTDV(I) AND TTRDV(I)
TEST2=ABS(GAMMA2-GAMMA)
IF TEST2.LT.0.0005 GOTO 400
GAMMA=GAMMA2
GOTO 100
400 MACHV(I)=MACH
C *** END OF ITERATION
C
C *** NOTE: THIS ITERATION IS BASED ON THE ISENTROPIC FLOW EQUATION FOR
C          "A" OVER "A-STAR" AS A FUNCTION OF LOCAL MACH NUMBER AND
C          GAMMA. THE TABLE LOOK-UPS FOR GAMMA ARE BASED ON A STANDARD
C          GAS TABLE.
C
C *** DRIVE VENTURI AIRFLOW
C
TRDV(I)=TTRDV(I)/(1+0.2*MACHV(I)**2)
C
CORRECTED VENTURI AREA
C
ADV(I)=(0.11 SQ.IN.)*(1+9.6E-6*(TRDV(I)-518.7))**2
C
CORRECTED VENTURI DIAMETER
C
DDV(I)=SQRT(4*ADV(I)/PI)
C
INDICATED AIRFLOW
C
CSTD(I)=TABLE LOOK-UP AS FUNCTION OF PDV(I) AND TTRDV(I)

```

```

C      WDI(I)=(CSTD(I)*32.174*PTDV(I)*ADV(I))/SQRT(1716.5*TTRDV(I))
C
C      STATIC TEMPERATURE
C
C      TSTD(I)=0.833333*TTRDV(I)
C
C      VISCOSITY
C
C      VISCD(I)=(2.27E-8*TSTD(I)**1.5)/(TSTD(I)+198.6)
C
C      REYNOLDS NUMBER
C
C      RNDVOT(I)=(4.74883E-6*WDI(I))/(DDV(I)*VISCD(I)*TTRDV(I)**4)
C
C      ACTUAL AIRFLOW
C
C      CDDV(I)=TABLE LOOK-UP BASED ON VENTURI CALIBRATION
C
C      WDV(I)=CDDV(I)*WDI(I)
C
C
C      *** BLEED LINE -CMAPS MODE ONLY ***
C
C      PBV(I)=STATIC PRESSURE MEASURED IN BLEED VENTURI
C      TTRBV(I)=TOTAL TEMPERATURE MEASURED IN BLEED VENTURI
C
C      GAMMA=TABLE LOOK UP AS FUNCTION OF PBV(I) AND TTRBV(I)
C
C      PERFORM FOLLOWING ITERATION TO FIND MACH NUMBER IN VENTURI.
C      THIS IS THE SAME ITERATION USED FOR THE DRIVE LINE.
C
100    J=0
        M(1)=0.01
        SUF=2/(GAMMA+1)
        TOP=(GAMMA+1)/2*(GAMMA-1)
        TOP1=(3-GAMMA)/2*(GAMMA-1)
200    J=J+1
        CORE=1+((GAMMA-1)/2)*M(J)**2
        NUMER=((SUF*CORE)**TOP)/M(J)-ADAS(I)
C
C      NOTE: ADAS(I)=ADASD(1)=ADASD(2)=7 FOR DRIVE VENTURI
C              =AOASB(1)=AOASB(2)=3 FOR BLEED VENTURI
C      ADAS=AREA RATIO OF VENTURI
C
C      DENOM=((SUF*CORE)**TOP1)-((SUF*CORE)**TOP/M(J)**2)
C      M(J+1)=M(J)-NUMER/DENOM
C      TEST=ABS((M(J+1)-M(J))/M(J+1))
C      IF TEST.LT.0.001 GOTO 300

```

```

      GO TO 200
300   MACH=M(J+1)
      C
      PTBV(I)=PBV(I)*(1+((GAMMA-1)/2)*MACH**2)**(GAMMA/(GAMMA-1))
      C
      GAMMA2=TABLE LOOK UP AS A FUNCTION OF PTBV(I) AND TTRBV(I)
      TEST2=ABS(GAMMA2-GAMMA)
      IF TEST2.LT.0.0005 GOTO 400
      GAMMA=GAMMA2
      GOTO 100
400   MACHB(I)=MACH
      C *** END OF ITERATION
      C
      C *** NOTE: THIS ITERATION IS BASED ON THE ISENTROPIC FLOW EQUATION FOR
      C              "A" OVER "A-STAR" AS A FUNCTION OF LOCAL MACH NUMBER AND
      C              GAMMA. THE TABLE LOOK-UPS FOR GAMMA ARE BASED ON A STANDARD
      C              GAS TABLE.
      C
      C *** BLEED VENTURI AIRFLOW - CMAPS MODE ONLY***
      C
      TRBV(I)=TTRBV(I)/(1+0.2*MACHB(I)**2)
      C
      CORRECTED VENTURI AREA
      C
      ABV(I)=(0.11 SQ.IN.)*(1+9.6E-6*(TRBV(I)-518.7))**2
      C
      CORRECTED VENTURI DIAMETER
      C
      DBV(I)=SQRT(4*ABV(I)/PI)
      C
      INDICATED AIRFLOW
      C
      CSTB(I)=TABLE LOOK-UP AS FUNCTION OF PBV(I) AND TTRBV(I)
      C
      WBI(I)=(CSTB(I)*32.174*PTBV(I)*ABV(I))/SQRT(1716.5*TTRBV(I))
      C
      STATIC TEMPERATURE
      C
      TSTB(I)=0.833333*TTRBV(I)
      C
      VISCOSITY
      C
      VISCB(I)=(2.27E-8*TSTB(I)**1.5)/(TSTB(I)+198.6)
      C
      REYNOLDS NUMBER
      C
      RNBV(I)=(4.74883E+10*WBI(I))/(DBV(I)*VISCB(I))
      C
      C ACTUAL BLEED LINE AIRFLOW - INCLUDING SUBCRITICAL CONDITIONS

```

```

C
PTBVQ(I)=PTBV(I)/P0
C
BVP(I)=BLEED VALVE POSITION AS INPUT FROM CMAPS CONTROLLER
C
IF BVP(I).GE.13.5 .AND. PTBVQ(I).GE.1.17 GO TO 100
GOTO 200
CDBV(I)=TABLE LOOK-UP BASED ON VENTURI CALIBRATION
C
100 WBV(I)=CDBV(I)*WBI(I)
GO TO 500
200 IF BVP(I).GE.13.5 .AND. PTBVQ(I).LT.1.17 GO TO 300
GO TO 400
300 PTEXP=PTBVQ(I)**(2/7)
WBV(I)=((2.05464*ABV(I)*P0)/SQRT(TTRBV(I)))*PTEXP*SQRT(1-(1/PTEXP))
GO TO 500
400 IF BVP(I).LT.13.5 .OR. PTBVQ(I).LT.1.0 WBV(I)=0.0
500 CONTINUE
C
C
C
C *** BLEED LINE AIRFLOW FOR JET-EFFECTS MODE ONLY ***
C
C
IF PTBM(I).LT.100 GO TO 100
GO TO 200
100 KMIX(I)=0.0035*PTBM(I)+0.75
GO TO 500
200 IF PTBM(I).GE.100 .AND. .LE.400 GO TO 300
GO TO 400
300 KMIX(I)=-2.357E-6*PTBM(I)**2+0.00165*PTBM(I)+0.9512
GO TO 500
400 IF PTBM(I).GT.400 KMIX(I)=1.26
500 CONTINUE
C
WMIX(I)=(KMIX(I)*0.1395*PTBM(I))/SQRT(TTRBV(I))
C
NOTE: THE AREA TERM (0.1395 SQ.IN.) WHICH IS USED ABOVE, IS THE AREA
C IN THE MIXER CORRECTED FOR THE MIXER FLOW COEFFICIENT AND THE
C FLOW RATE CONSTANT FOR CHOKED FLOW:
C 0.1395=CDMIXER*AMIXER*0.5315
C
WBV(I)=WMIX(I)
C
C
C
C *** THE CALCULATIONS FOR COMPRESSOR INLET AIRFLOW BEGIN ON THE NEXT PAGE
C

```

```

C *** COMPRESSOR INLET AIRFLOW CALCULATIONS ***
C
C FLOW THROUGH MODE - IN THIS MODE, INLET AIRFLOW CALCULATIONS WERE
C BASED ON MEASUREMENTS AT THE SIMULATED COMPRESSOR FACE AND AT THE
C CHOKE NOZZLES ON THE EXTENSION DUCTS. THESE ARE REFERRED TO AS THE
C PLANE 2 AND PLANE 8 METHODS RESPECTIVELY.
C
C PLANE 2 METHOD
C
C   PRAT=PS2(I)/PT2(I)
C   PREX=PRAT**(6/7)
C   PREX2=(1/PRAT)**(2/7)
C   W2(I)=((0.91886*7.07*PT2(I))/SQRT(TTR))*PREX*SQRT(5*(PREX2-1))
C
C AVERAGE INLET AIRFLOW
C
C   WAF2=(W2(1)+W2(1))/2
C
C CORRECTED INLET AIRFLOW
C
C   SEA-LEVEL STANDARD DAY PRESSURE CORRECTION
C
C   DEL(I)=PT2(I)/14.697
C
C   W2R(I)=(W2(I)*THETA)/DEL(I)
C
C PLANE 8 METHOD - USED WITH EXIT CHOKES
C
C   PRCH(I)=PTNC(I)/PSNC(I)
C   WTAP(I)=A+B*PRCH(I)+C*PRCH(I)**2+D*PRCH(I)**3
C   IF PRCH(I).GT.PRMAXC WTAP(I)=WLIMC
C   IF PRCH(I).LT.PRMINC WTAP(I)=0
C
C NOTE: THE FOLLOWING CONSTANTS ARE OBTAINED IN A TABLE LOOK-UP.
C       THESE TABLES WERE GENERATED IN STATIC CALIBRATIONS OF THE
C       CHOKES. SEE REFERENCE 7 FOR A LISTING OF THESE TABLES.
C       A, B, C, D, WLIMC, PRMAXC, PRMINC, ATC=CHOKE AREA
C
C   WB(I)=(WTAP(I)*PTNC(I)*ATC)/SQRT(TTR)
C
C CORRECTED INLET AIRFLOW
C
C   WBR(I)=(WB(I)*THETA)/DEL(I)
C
C ***CMAPS AIRFLOW CALCULATIONS BEGIN NEXT PAGE ***
C
C

```



```

C  CMAPS MODE - IN THIS MODE, INLET AIRFLOW CALCULATIONS WERE
C  BASED ON MEASUREMENTS AT THE SIMULATED COMPRESSOR FACE, THE
C  CHOKE NOZZLES ON THE EXTENSION DUCTS, THE COMPRESSOR DISCHARGE PLANE,
C  AND THE TURBINE DISCHARGE PLANE. THESE ARE REFERRED TO AS THE
C  PLANE 2, PLANE 8, PLANE 15, AND PLANE 57 METHODS RESPECTIVELY.
C
C  PLANE 2 METHOD - THIS METHOD IS IDENTICAL TO THE FLOW-THROUGH MODE
C
C      PRAT=PS2(I)/PT2(I)
C      PREX=PRAT**(6/7)
C      PREX2=(1/PRAT)**(2/7)
C      W2(I)=((0.91886*7.07*PT2(I))/SQRT(TTR))*PREX*SQRT(5*(PREX2-1))
C
C  AVERAGE INLET AIRFLOW
C
C      WAF2=(W2(1)+W2(2))/2
C
C  CORRECTED INLET AIRFLOW
C
C      W2R(I)=(W2(I)*THETA)/DEL(I)
C
C  PLANE 8 METHOD - INSTRUMENTATION FAILURES PROHIBITED THE USE OF THIS
C                  METHOD THROUGHOUT THE CMAPS MODE. THEREFORE, THE
C                  EQUATIONS ARE NOT LISTED HERE. THE METHOD IS FULLY
C                  DESCRIBED IN THE TEXT.
C
C  PLANE 15 METHOD - BASED ON PRESSURE AND TEMPERATURE MEASUREMENTS MADE
C                  AT THE CMAPS COMPRESSOR DISCHARGE STATION.
C
C      PRAT15(I)=PS15(I)/PT15(I)
C      PREX15(I)=PRAT15(I)**(6/7)
C      PREX25(I)=SQRT(5*((1/PRAT15(I))**(2/7)-1))
C      DENOM(I)=SQRT(TT15(I)+459.7)
C      W15I(I)=((0.91886*(3.4 SQ.IN.)*PT15(I))/DENOM(I))
C      *PREX15(I)*PREX25(I)
C
C      W15(I)=W15I(I)*CD15(I)
C
C      CD15(I)=TABLE LOOK-UP AS A FUNCTION OF NCP(I) AND BVPOS(I)
C
C      NOTE:  NCP(I)=PERCENT CORRECTED ROTOR SPEED
C            BVPOS(I)=BLEED VALVE POSITION
C
C  PLANE 57 METHOD - THIS METHOD IS BASED ON A CORRELATION OF THE TURBINE
C                  DISCHARGE PRESSURE AND PERCENT CORRECTED ROTOR SPEED
C                  AS MEASURED DURING THE STATIC AIRFLOW CALIBRATIONS
C                  IN THE NASA-AMES 9X7 FT WIND TUNNEL.
C
C  *** NOTE: PLANE 57 METHOD CONTINUED ON NEXT PAGE
C

```

```

C   LEFT HAND CMAPS
C
C       PSQDELL=PS57L/DEL(1)
C
C   NOTE: PS57L (TURBINE DISCHARGE STATIC PRESSURE) IS INPUT FROM THE CMAPS
C   CONTROLLER.
C
C       NRPL=(NCPL/78185)*100
C
C       DATA (XCDEFL(I),I=1,3)/.3875,-47.575,1601.25/
C       DATA (YCDEFL(I),I=1,6)/3.9714795E-9,-1.7028217E-6,2.8122667E-4,
1       -2.2420302E-2,8.8135679E-1,-12.957557/
C
C       A=-2.2E-7
C
C       X1=0.0
C       DO 20 J=1,3
C       X1=X1*NRPL+XCDEFL(J)
20      CONTINUE
C
C       Y=0.0
C       DO 30 N=1,6
C       Y=Y*NRPL+YCDEFL(N)
30      CONTINUE
C
C       IF (PSQDELL.GT.X1) GO TO 40
C
C       W57LC=Y
C       GO TO 45
C
C       40  W57LC=A*(PSQDELL-X1)**2.+Y
C       45  W57LX=W57LC*DEL(1)/THETA
C
C   *** NOTE: THIS CORRELATION GENERATES THE SEA-LEVEL REFERENCED (I.E.
C   CORRECTED) AIRFLOW. THEREFOR, THE LAST EQUATION ABOVE IS
C   USED TO GENERATED THE PHYSICAL AIRFLOW AT THE COMPRESSOR
C   INLET BASED ON MEASUREMENTS MADE AT PLANE 57.
C
C   RIGHT HAND CMAPS
C
C       PSQDELR=PS57R/DEL(2)
C
C   NOTE: PS57R (TURBINE DISCHARGE STATIC PRESSURE) IS INPUT FROM THE CMAPS
C   CONTROLLER.
C
C       NRPR=(NCPR/78185)*100
C
C       DATA (XCDEFR(I),I=1,4)/.2041667E-1,-4.4142857,321.74405,-7651.5714/
C       DATA (YCDEFR(I),I=1,6)/4.3672014E-9,-1.9017866E-6,3.20077316E-4,

```

```

1      -2.6095576E-2,1.0498427,-15.96689/
C
C      A=-8.1E-7
C
C      X1=0.0
C      DO 20 J=1,4
C      X1=X1*NRPR+XCDEFR(J)
20     CONTINUE
C
C      Y=0.0
C      DO 30 N=1,6
C      Y=Y*NRPR+YCOEFR(N)
30     CONTINUE
C
C      IF (PSQDEL.R.GT.X1) GO TO 40
C
C      W57RC=Y
C      GO TO 45
C
C      40 W57RC=A*(PSQDEL.R-X1)**2.+Y
C      45 W57RX=W57RC*DEL(2)/THETA
C
C      *** NOTE: THIS CORRELATION GENERATES THE SEA-LEVEL REFERENCED (I.E.
C      CORRECTED) AIRFLOW. THEREFORE, THE LAST EQUATION ABOVE IS
C      USED TO GENERATED THE PHYSICAL AIRFLOW AT THE COMPRESSOR
C      INLET BASED ON MEASUREMENTS MADE AT PLANE 57.
C
C      W57(1)=W57LX
C      W57R(1)=W57LC
C      W57(2)=W57RX
C      W57R(2)=W57RC
C
C      STREAM THRUST AND RAM DRAG CORRECTIONS TO BALANCE OUTPUTS
C
C      *** CALCULATE INLET STREAM THRUST AND RAM DRAG USING THE AIRFLOWS
C      CALCULATED FROM THE PLANE 2, PLANE 8, PLANE 15, AND PLANE 57
C      METHODS.
C
C      INLET MACH NUMBER ITERATION SCHEME
C      (GENERIC VERSION FOR ALL FOUR AIRFLOW CALCULATION METHODS)
C
C      INPUTS: COMPRESSOR INLET PHYSICAL AIRFLOW: WX
C      COMPRESSOR FACE AVERAGE TOTAL PRESSURE: PT2X
C      (LEFT OR RIGHT AS APPROPRIATE)
C
C      CTR=0
C      NX=1.88045*SQRT(TTR)/7.07*(WX/PT2X)
C      IF (NX.GT.1.0) GO TO 50
C      IF (NX.LT.0.0) GO TO 70
C

```

```

C      XM5=1-SQRT(1-NX)
5      NXPRM=1.728*XM5*(1+0.2*(XM5)**2)**-3
      ERROR=NX-NXPRM
10     XM2=1-(1-XM5)*SQRT((1-XN)/(1-NXPRM))
      CTR=CTR+1
      IF (ERROR.LT.0.0001) GO TO 100
      IF (CTR.GT.50) GO TO 100
      XM5=XM2
      GO TO 5
50     XM2=1.0
      GO TO 100
70     XM2=0.0
      GO TO 100

C
100    M=XM2
C
C *** THIS ENDS THE INLET MACH ITERATION ROUTINE ***
C
C      CALCULATE INLET MACH NUMBER FOR EACH OF THE FOUR INLET AIRFLOWS
C      CALCULATED.
C
C      INLET MACH: PLANE 2 METHOD
C
C *** NOTE:  I=1 FOR LEFT HAND INLET
C             I=2 FOR RIGHT HAND INLET
C
C      WX=W2(I)
C      PT2X=PT2(I)
C
C      APPLY ITERATION ROUTINE
C
C      M2(I)=MX
C
C      INLET MACH: PLANE 8 METHOD
C
C *** NOTE:  I=1 FOR LEFT HAND INLET
C             I=2 FOR RIGHT HAND INLET
C
C      WX=W8(I)
C      PT2X=PT2(I)
C
C      APPLY ITERATION ROUTINE
C
C      M8(I)=MX
C

```

```

C  INLET MACH: PLANE 15 METHOD
C
C  *** NOTE:  I=1 FOR LEFT HAND INLET
C              I=2 FOR RIGHT HAND INLET
C
C      WX=W15(I)
C      PT2X=PT2(I)
C
C  APPLY ITERATION ROUTINE
C
C      M15(I)=MX
C
C  INLET MACH: PLANE 57 METHOD
C
C  *** NOTE:  I=1 FOR LEFT HAND INLET
C              I=2 FOR RIGHT HAND INLET
C
C      WX=W57(I)
C      PT2X=PT2(I)
C
C  APPLY ITERATION ROUTINE
C
C      M57(I)=MX
C
C  CALCULATE INLET STATIC PRESSURE BASED ON THE CALCULATED INLET MACH
C
C  INLET STATIC PRESSURE: PLANE 2 METHOD
C
C      PS2C(I)=PT2(I)*(1+0.2*(M2(I)**2))**-3.5
C
C  INLET STATIC PRESSURE: PLANE 8 METHOD
C
C      PS2C8(I)=PT2(I)*(1+0.2*(M8(I)**2))**-3.5
C
C  INLET STATIC PRESSURE: PLANE 15 METHOD
C
C      PS2C15(I)=PT2(I)*(1+0.2*(M15(I)**2))**-3.5
C
C  INLET STATIC PRESSURE: PLANE 57 METHOD
C
C      PS2C57(I)=PT2(I)*(1+0.2*(M57(I)**2))**-3.5
C
C  COMPRESSOR STREAM THRUST CALCULATION
C
C  PLANE 2 METHOD
C
C      F22=7.07*(PS2C(1)*(1+1.4*M2(1)**2)+PS2C(2)*(1+1.4*M2(2)**2)-2*P0)
C

```

```

C     PLANE 8 METHOD
C
C     F28=7.07*(PS2C8(1)*(1+1.4*M8(1)**2)+PS2C8(2)*(1+1.4*M8(2)**2)-2*P0)
C
C     PLANE 15 METHOD
C
C     F215=7.07*(PS2C15(1)*(1+1.4*M15(1)**2)+PS2C15(2)*(1+1.4*M15(2)**2)
1     -2*P0)
C
C     PLANE 57 METHOD
C
C     F257=7.07*(PS2C57(1)*(1+1.4*M57(1)**2)+PS2C57(2)*(1+1.4*M57(2)**2)
1     -2*P0)
C
C
C *** AVERAGE INLET AIRFLOW ***
C
C     W2A=(W2(1)+W2(2))/2
C
C     W8A=(W8(1)+W8(2))/2
C
C     W15A=(W15(1)+W15(2))/2
C
C     W57A=(W57(1)+W57(2))/2
C
C
C *** RAM DRAG ***
C
C     FRAM2=(-2/32.174)*W2A*V0
C
C     FRAM8=(-2/32.174)*W8A*V0
C
C     FRAM15=(-2/32.174)*W15A*V0
C
C     FRAM57=(-2/32.174)*W57A*V0
C
C *** BALANCE OUTPUT CORRECTION TERMS FOR RAM DRAG AND STREAM THRUST ***
C
C     PLANE 2 METHOD:
C
C     AXIAL FORCE CORRECTION
C
C     ABASE2=F22+FRAM2*COS(ALPHAM)
C
C     NORMAL FORCE CORRECTION
C
C     NBASE2=FRAM2*SIN(ALPHAM)
C

```

```

C PLANE 8 METHOD:
C
C AXIAL FORCE CORRECTION
C
C   ABASE8=F28+FRAM8*COS(ALPHAM)
C
C NORMAL FORCE CORRECTION
C
C   NBASE8=FRAM8*SIN(ALPHAM)
C
C PLANE 15 METHOD:
C
C AXIAL FORCE CORRECTION
C
C   ABASE15=F215+FRAM15*COS(ALPHAM)
C
C NORMAL FORCE CORRECTION
C
C   NBASE15=FRAM15*SIN(ALPHAM)
C
C PLANE 57 METHOD:
C
C AXIAL FORCE CORRECTION
C
C   ABASE57=F257+FRAM57*COS(ALPHAM)
C
C NORMAL FORCE CORRECTION
C
C   NBASE57=FRAM57*SIN(ALPHAM)
C
C *** FLOW CORRECTION COEFFICIENTS ***
C
C AXIAL FORCE COEFFICIENT
C
C   CDIA2=ABASE2/(Q*5.221)
C
C   CDIA8=ABASE8/(Q*5.221)
C
C   CDIA15=ABASE15/(Q*5.221)
C
C   CDIA57=ABASE57/(Q*5.221)
C
C NORMAL FORCE COEFFICIENT
C
C   CDIN2=NBASE2/(Q*5.221)
C
C   CDIN8=NBASE8/(Q*5.221)
C
C   CDIN15=NBASE15/(Q*5.221)
C
C   CDIN57=NBASE57/(Q*5.221)

```

```

C *** WEIGHT TARE CORRECTIONS ***
C
C   NWT=-212*(1-COS(ALPHAM))
C
C   AWT=-212*(SIN(ALPHAM))
C
C   PMWT=-X1*AWT+X2*NWT
C
C *** WHERE X1 AND X2 ARE THE MOMENT ARM LENGTHS FROM MODEL C.G. TO A/C
C   REFERENCE C.G. IN THE AXIAL AND NORMAL DIRECTIONS ***
C
C   BALANCE OUTPUT COEFFICIENTS WITH WEIGHT TARES - BODY AXIS
C
C   **** NOTE: THE FOLLOWING TERMS ARE THE DESIGNATIONS USED BY THE NASA
C   AMES DATA REDUCTION PROGRAM FOR THE BALANCE OUTPUTS OF
C   NORMAL FORCE, AXIAL FORCE, AND PITCHING MOMENT:
C       .EX-TARE.N(1)
C       .EX-TARE.A(1)
C       .EX-TARE.PM(1)
C
C   CNUC=((.EX-TARE.N(1))+NWT)/(Q*5.221)
C
C   CAUC=((.EX-TARE.A(1))+AWT)/(Q*5.221)
C
C   CMUC=((.EX-TARE.PM(1))+PMWT)/(Q*5.221*1.368)
C
C   BALANCE OUTPUT COEFFICIENTS WITH WEIGHT TARES - STABILITY AXIS
C
C   CLUC=CNUC*COS(ALPHAM)-CAUC*SIN(ALPHAM)
C
C   CDUC=CAUC*COS(ALPHAM)+CNUC*SIN(ALPHAM)
C
C   AIRFRAME COEFFICIENTS - BODY AXIS
C
C   WITH FLOW CORRECTIONS BASED ON PLANE 2 METHOD
C
C   CNFA2=CNUC+NCAVN+CDIN2
C
C   CAFA2=CAUC+ACAVN+CDIA2
C
C   CMNA2=CMUC+PMCAVN
C
C   WITH FLOW CORRECTIONS BASED ON PLANE 8 METHOD
C
C   CNFAB=CNUC+NCAVN+CDIN8
C
C   CAFAB=CAUC+ACAVN+CDIAB
C
C   CMNAB=CMUC+PMCAVN
C

```



```

C      WITH FLOW CORRECTIONS BASED ON PLANE 15 METHOD
C
C      CNFA15=CNUC+NCAVN+CDIN15
C
C      CAFA15=CAUC+ACAVN+CDIA15
C
C      CMNA15=CMUC+PMCAVN
C
C      WITH FLOW CORRECTIONS BASED ON PLANE 57 METHOD
C
C      CNFA57=CNUC+NCAVN+CDIN57
C
C      CAFA57=CAUC+ACAVN+CDIA57
C
C      CMNA57=CMUC+PMCAVN
C
C      AIRFRAME COEFFICIENTS - STABILITY AXIS
C
C      WITH FLOW CORRECTIONS BASED ON PLANE 2 METHOD
C
C      CLA2=CNFA2*COS(ALPHAM)-CAFA2*SIN(ALPHAM)
C
C      CDA2=CAFA2*COS(ALPHAM)+CNFA2*SIN(ALPHAM)
C
C      CLASQ2=CLA2*ABS(CLA2)
C
C      WITH FLOW CORRECTIONS BASED ON PLANE 8 METHOD
C
C      CLAB=CNFA8*COS(ALPHAM)-CAFA8*SIN(ALPHAM)
C
C      CDA8=CAFA8*COS(ALPHAM)+CNFA8*SIN(ALPHAM)
C
C      CLASQ8=CLAB*ABS(CLAB)
C
C      WITH FLOW CORRECTIONS BASED ON PLANE 15 METHOD
C
C      CLA15=CNFA15*COS(ALPHAM)-CAFA15*SIN(ALPHAM)
C
C      CDA15=CAFA15*COS(ALPHAM)+CNFA15*SIN(ALPHAM)
C
C      CLASQ15=CLA15*ABS(CLA15)
C
C      WITH FLOW CORRECTIONS BASED ON PLANE 57 METHOD
C
C      CLA57=CNFA57*COS(ALPHAM)-CAFA57*SIN(ALPHAM)
C
C      CDA57=CAFA57*COS(ALPHAM)+CNFA57*SIN(ALPHAM)
C
C      CLASQ57=CLA57*ABS(CLA57)
C

```

```

C  TOTAL AIRCRAFT (AIRFRAME+NOZZLES) STABILITY AXIS COEFFICIENTS
C
C  PLANE 2 METHOD
C
C  CL2=CLA2+CLN
C
C  CD2=CDA2+CDN
C
C  CDAROTF2=CDA2+CDARONF
C
C  CM2=CMNA2+CPMN
C
C  CLSQ2=CL2*ABS(CL2)
C
C  PLANE 8 METHOD
C
C  CL8=CLA8+CLN
C
C  CD8=CDA8+CDN
C
C  CDAROTF8=CDA8+CDARONF
C
C  CM8=CMNA8+CPMN
C
C  CLSQ8=CL8*ABS(CL8)
C
C  PLANE 15 METHOD
C
C  CL15=CLA15+CLN
C
C  CD15=CDA15+CDN
C
C  CDAROTF15=CDA15+CDARONF
C
C  CM15=CMNA15+CPMN
C
C  CLSQ15=CL15*ABS(CL15)
C
C  PLANE 57 METHOD
C
C  CL57=CLA57+CLN
C
C  CD57=CDA57+CDN
C
C  CDAROTF57=CDA57+CDARONF
C
C  CM57=CMNA57+CPMN
C
C  CLSQ57=CL57*ABS(CL57)
C
C  *** NOTE: THE COEFFICIENTS FROM THE PLANE 8 METHOD WERE CHOSEN AS THE

```

```

C          PRIMARY PARAMETERS IN THE CONVENTIONAL MODE ANALYSIS. THE
C          PLANE 57 COEFFICIENTS WERE USED IN THE CMAPS ANALYSIS.
C
C *** CAPTURE AREA RATIO (MASS FLOW RATIO) ***
C
C          MDOT=SQRT(0.9443*XMO**2+0.1688*XMO**4)
C
C          NOTE:  I=1 FOR LEFT HAND INLET
C                  I=2 FOR RIGHT HAND INLET
C
C          A02(I)=(W2(I)*SQRT(TTR))/(P0*MDOT)
C
C          A08(I)=(W8(I)*SQRT(TTR))/(P0*MDOT)
C
C          A015(I)=(W15(I)*SQRT(TTR))/(P0*MDOT)
C
C          A057(I)=(W57(I)*SQRT(TTR))/(P0*MDOT)
C
C CAPTURE AREA RATIO CALCULATION
C
C          CAP2(I)=A02(I)/5.46
C
C          CAP8(I)=A08(I)/5.46
C
C          CAP15(I)=A015(I)/5.46
C
C          CAP57(I)=A057(I)/5.46
C
C *** NOTE: THE PLANE 8 MFR WAS THE PARAMETER USED FOR THE FLOW-THROUGH
C          MODE. THE PLANE 57 MFR WAS USED FOR THE CMAPS ANALYSIS.
C
C *** NOZZLE PRESSURE RATIO CALCULATION ***
C
C NOZZLE TOTAL PRESSURE INSTRUMENTATION FAILURES DURING THE JET-EFFECTS
C AND CMAPS MODES TESTING NECESSITATED THE FOLLOWING SCHEME OF
C CALCULATING NOZZLE TOTAL PRESSURE FROM THE TOTAL AIRFLOW THROUGH THE
C NOZZLE. THE TEXT IN SECTION 3.0 OF THIS REPORT FURTHER DESCRIBES THE
C PROCESS.
C
C *** JET-EFFECTS MODE ***
C
C          WB(I)=WDV(I)+WMIX(I)
C
C          NPR(I)=(WB(I)*SQRT(TT7(I)))/(P0*ALL*0.505)
C
C          ALL=THROAT AREA OF THE ALBEN DEPENDING ON POWER SETTING AND VECTOR
C          ANGLE
C

```

```

C *** CMAPS MODE ONLY ***
C
      WJF(I)=W57(I)+WDV(I)-WBV(I)
C
C   THE FOLLOWING ITERATION SCHEME IS USED TO CALCULATE NPR BASED ON WJF
C
      TERM=(WJF(I)*SQRT(TT7))/(P0*5.151)
      NPRX(1)=TERM/0.5150
      J=0
05   J=J+1
C
      IF (NPRX(J).LT.1.01) GO TO 10
      IF (NPRX(J).LE.1.50) GO TO 30
C
      TAP(J)=0.5150
      GO TO 50
C
10   TAP(J)=0.3000
      GO TO 50
C
30   TAP(J)=-7.7494+16.7138*NPRX(J)-11.2561*NPRX(J)**2+2.5231*NPRX(J)**3
C
50   NPRX(J+1)=TERM/TAP(J)
C
      TEST=ABS((NPRX(J+1)-NPRX(J))/NPRX(J+1))
C
      IF (TEST.LT.0.001) GO TO 100
      GO TO 05
C
100  NPR(I)=NPRX(J+1)
C
      NPRA=(NPR(1)+NPR(2))/2
C
      EPR(I)=NPR(I)*P0/PT2(I)
C

```

This concludes the list of data reduction equations for the three test modes.

| | | | | | |
|--|--|--|---|--|--|
| 1. Report No. NASA CR-177343-VOL-2 | | 2. Government Accession No. | | 3. Recipient's Catalog No. | |
| 4. Title and Subtitle PROPULSION AND AIRFRAME AERODYNAMIC INTERACTIONS OF SUPERSONIC V/STOL CONFIGURATIONS VOLUME II: WIND TUNNEL TEST FORCE AND MOMENT DATA REPORT | | | | 5. Report Date Sept 85 | |
| | | | | 6. Performing Organization Code | |
| 7. Author(s) D. E. Zilz | | | | 8. Performing Organization Report No. | |
| 9. Performing Organization Name and Address McDonnell Aircraft Company P.O. Box 516 St. Louis, Missouri 63166 | | | | 10. Work Unit No. T-3288Y | |
| | | | | 11. Contract or Grant No. NAS2-10791 | |
| 12. Sponsoring Agency Name and Address National Aeronautics and Space Administration Washington, D.C. 20546 | | | | 13. Type of Report and Period Covered Contractor Report | |
| | | | | 14. Sponsoring Agency Code 505-43-01 | |
| 15. Supplementary Notes Point of Contact: Technical Monitor, Rodney O. Bailey (415) 694-6265 Ames Research Center, Moffett Field, CA 94035 | | | | | |
| 16. Abstract A wind tunnel model of a supersonic V/STOL fighter configuration has been tested to measure the aerodynamic interaction effects which can result from geometrically close-coupled propulsion system/airframe components. The approach was to configure the model to represent two different test techniques. One was a conventional test technique composed of two test modes. In the Flow-Through mode, absolute configuration aerodynamics are measured, including inlet/airframe interactions. In the Jet-Effects mode, incremental nozzle/airframe interactions are measured. The other test technique is a propulsion simulator approach, where a sub-scale, externally powered engine is mounted in the model. This allows proper measurement of inlet/airframe and nozzle/airframe interactions simultaneously. | | | | | |
| 17. Key Words (Suggested by Author(s)) Flowfield Interactions Propulsion Simulators Supersonic V/STOL | | | 18. Distribution Statement [REDACTED] Until August 1987 Star Category 02 | | |
| 19. Security Classif. (of this report) Unclassified | | 20. Security Classif. (of this page) Unclassified | | 21. No. of Pages 312 | |
| 22. Price* | | | | | |